**Report Title**

Basin Analysis and Petroleum System Characterization and Modeling, Interior Salt Basins, Central and Eastern Gulf of Mexico

**Type of Report**

Final Report

**Reporting Period Start Date**

May 1, 2003

**Reporting Period End Date**

April 30, 2008

**Principal Author**

Ernest A. Mancini (205/348-4319)
Department of Geological Sciences
Box 870338
202 Bevill Building
University of Alabama
Tuscaloosa, AL 35487-0338

**Date Report was Issued**

June 30, 2008

**DOE Award Number**

DE-FC26-03NT15395

**Name and Address of Participants**

Ernest A. Mancini
Paul Aharon
Dept. of Geological Sciences
Box 870338
Univ. of Alabama
Tuscaloosa, AL 35487-0338

Donald A. Goddard
Marty Horn
Roger Barnaby
Center for Energy Studies
Louisiana State Univ.
Baton Rouge, LA 70803

## Disclaimer

## Abstract

The project consisted of two phases: Concept Development and Concept Demonstration. The principal research effort for Phase 1 (Concept Development) of the project has been data compilation; determination of the tectonic, depositional, burial, and thermal maturation histories of the North Louisiana Salt Basin; basin modeling (geohistory, thermal maturation, hydrocarbon expulsion); petroleum system identification; comparative basin evaluation; and initial assessment of undiscovered and undeveloped reservoirs in the North Louisiana Salt Basin. Existing information on the North Louisiana Salt Basin has been evaluated, an electronic database has been developed, and regional cross sections have been prepared. Structure, isopach and formation lithology maps have been constructed, and burial history, thermal maturation history, and hydrocarbon expulsion profiles have been prepared. Seismic data, cross sections, subsurface maps and burial history, thermal maturation history, and hydrocarbon expulsion profiles have been used in evaluating the tectonic, depositional, burial and thermal maturation histories of the basin. The principal research effort for Phase 2 (Concept Demonstration) of the project has been characterization of the Smackover petroleum system in the North Louisiana Salt Basin, characterization of the Upper Jurassic to Lower Cretaceous Bossier petroleum system, hydrocarbon flow pathway modeling in the North Louisiana Salt Basin, and refined assessment of the undiscovered and underdeveloped reservoirs in the North Louisiana Salt Basin. Presentations on the results of this work have been made at the annual meetings of the American Association of Petroleum Geologists and Gulf Coast Association of Geological Societies. Technology transfer workshops have been conducted in Shreveport, Louisiana, Jackson, Mississippi, and Tuscaloosa, Alabama.

## Table of Contents

**Basin Analysis and Petroleum System Characterization and Modeling,**
**Interior Salt Basins, Central and Eastern Gulf of Mexico**
**Final Report**
**May 1, 2003—April 30, 2008**

## INTRODUCTION

The University of Alabama and Louisiana State University have undertaken a cooperative 5-year, fundamental research project involving sedimentary basin analysis and petroleum system characterization and modeling of the North Louisiana Salt Basin and Mississippi Interior Salt Basin. According to the USGS, the hydrocarbon volume of these basins ranks them in the top 8% of the most petroliferous basins of the world.

## EXECUTIVE SUMMARY

The principal research efforts of the project have been the determination of the tectonic, depositional, burial and thermal maturation histories of the North Louisiana Salt Basin, basin modeling (geohistory, thermal maturation, hydrocarbon expulsion, hydrocarbon flow pathway), petroleum system study (identification, characterization, modeling), comparative basin evaluation, and assessment of the undiscovered and underdeveloped reservoirs in the North Louisiana Salt Basin.

Existing information, including 2-D seismic sections, on the North Louisiana Salt Basin has been evaluated and an electronic database has been developed. Regional cross sections have been prepared. Structure, isopach, and formation lithology maps have been constructed on key surfaces and of key intervals, respectively. Seismic data, well logs, cross sections, subsurface maps and burial history, thermal maturation history and hydrocarbon expulsion profiles have

been used in evaluating the tectonic history, depositional history, burial history and thermal maturation history of the basin.

The origin of the North Louisiana Salt Basin is comparable to the origin of the Mississippi Interior Salt Basin. The geohistory of these basins is directly linked to the evolution of the Gulf of Mexico. The timing of tectonic events and the nature of the structural styles control the type and size of petroleum traps formed and the volume of hydrocarbons contained within these traps. The dominant structural styles are salt-supported anticlines, normal faults, and combination structural-stratigraphic features. Combination structural-stratigraphic features include large regional domal structures, such as the Sabine and Monroe Uplifts.

The main difference in the geohistories of the North Louisiana Salt Basin and the Mississippi Interior Salt Basin is the elevated heat flow the strata in the North Louisiana Salt Basin experienced in the Cretaceous due primarily to reactivation upward movement, igneous activity, and erosion associated with the Monroe and Sabine Uplifts. The Jackson Dome in the Mississippi Interior Salt Basin is a similar phenomenon, but the effects of this igneous intrusion are on a much lower level geographically.

The Upper Jurassic Smackover petroleum system is the principal petroleum system in these basins. The underburden, source, overburden, reservoir, and seal rocks associated with this petroleum system are a result of the rift-related geohistory. The generation of oil and gas from Smackover lime mudstone was initiated during the Early Cretaceous in the southern part of the basins and continued into the Tertiary. Hydrocarbon expulsion and migration commenced during the Early Cretaceous and continued into the Tertiary. Vertical and lateral migration is important to the productivity of these basins. In the North Louisiana Salt Basin, petroleum reservoirs include continental, coastal, and marine sandstone facies and nearshore marine, shelf, ramp, and

reef carbonate facies. Seal rocks include Upper Jurassic and Lower Cretaceous anhydrite and shale, Upper Cretaceous chalk and shale, and lower Tertiary shale.

The Upper Jurassic to Lower Cretaceous Bossier petroleum system had the potential to generate gas from thermally mature shale containing Type III kerogen giving the Bossier high potential as a shale gas reservoir in the North Louisiana Salt Basin.

Potential undiscovered reservoirs in the North Louisiana Salt Basin are subsalt Triassic Eagle Mills sandstone and Upper Jurassic to Lower Cretaceous sandstone, shale, and limestone. Potential underdeveloped reservoirs include Lower Cretaceous sandstone and limestone and Upper Cretaceous sandstone.

Knowledge of basin geohistory and of the concepts of sequence stratigraphy and petroleum systems facilitates the design of new exploration strategies for the targeting of combination structural and stratigraphic traps and specific reservoir facies in a transgressive-regressive sequence. In the North Louisiana Salt Basin, Upper Cretaceous sandstone reservoirs are recognized as transgressive backstepping facies in transgressive-regressive sequences that onlap onto the Monroe Uplift that serves as a combination structural and stratigraphic trap, thermogenic gas is predicted to occur in Upper Jurassic to Lower Cretaceous transgressive and regressive deeply buried (>20,000 ft) porous sandstone and carbonate facies, and the Bossier Formation is identified as a potential shale gas reservoir as a result of petroleum system study.

## PROJECT OBJECTIVES

The principal objectives of the project are to develop through basin analysis and modeling the concept that petroleum systems acting in a basin can be identified through basin modeling and to demonstrate that the information and analysis resulting from characterizing and modeling of these petroleum systems in the North Louisiana Salt Basin and the Mississippi Interior Salt

Basin can be used in providing a more reliable and advanced approach for targeting stratigraphic traps and specific reservoir facies within a geologic system and in providing a refined assessment of undiscovered and underdeveloped reservoirs and associated oil and gas resources.

## EXPERIMENTAL

### Work Accomplished

#### *Data Compilation*

Existing information on the North Louisiana Salt Basin (Fig. 1) has been evaluated and an electronic database has been developed. Representative oil and gas well logs (141) were utilized in the construction of 11 regional stratigraphic cross sections (Fig. 2). The digitized logs have been used to construct cross sections (Figs. 3-13) for the basin using PETRA software. Seismic reflection data have been studied for the basin. The well logs, cross sections and seismic profiles were used in making interpretations regarding the tectonic history and depositional history of the basin. Structure maps (Figs. 14-16), isopach maps (Figs. 17-19), an erosional thickness map for the Lower Cretaceous section (Fig. 20), and formation lithology maps (Figs. 21-40) have been constructed on key surfaces and of key intervals, respectively. Cores from wells that penetrate Jurassic strata have been studied to assist with the interpretations of the tectonic and depositional histories of the basin. Samples taken from these cores were used in the characterization of the petroleum source rocks in the basin to assist with the determination as to the source rocks that generated the oil and gas occurring in the North Louisiana Salt Basin (Table 1).

Seismic profiles and well log data have been used in constructing the cross sections (Figs. 3-13) and burial history (Figs. 41-82) profiles. Present day heat flow values (Fig. 83), lithospheric stretching beta factors (Fig. 84), measured and calculated vitrinite reflectance values, and a transient heat flow model (Figs. 85-86) were using in preparing the thermal maturation history

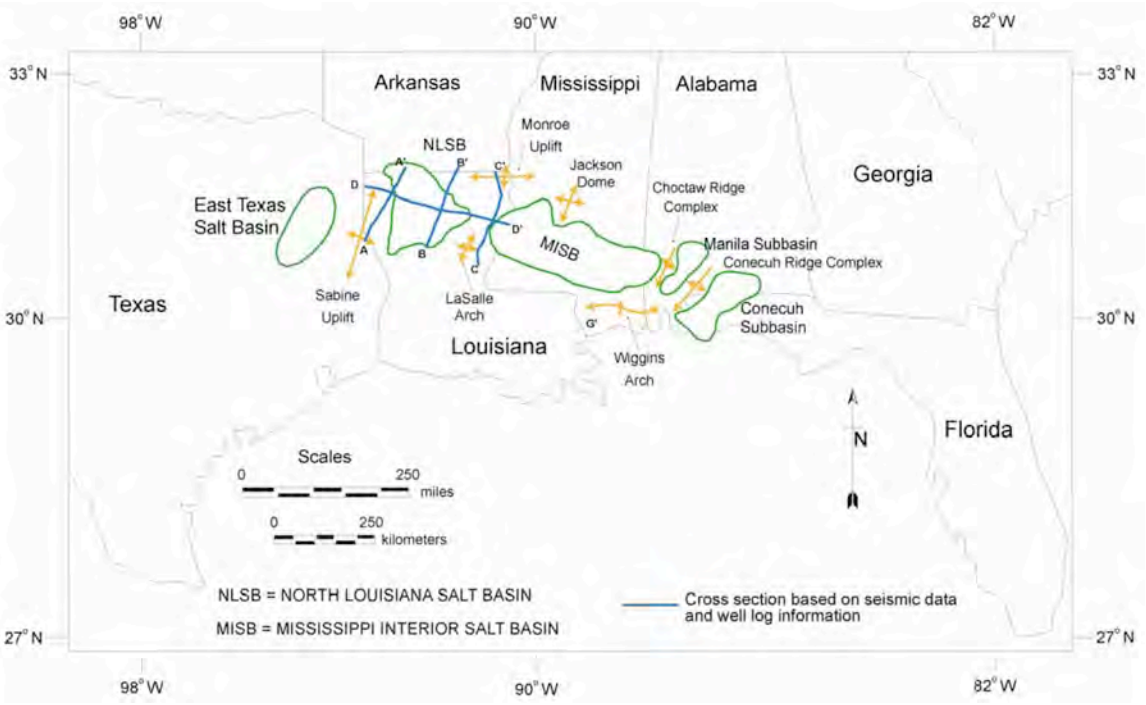


Figure 1. Location map of interior salt basins and subbasins in the north central and northeastern Gulf of Mexico area and regional seismic lines studied.

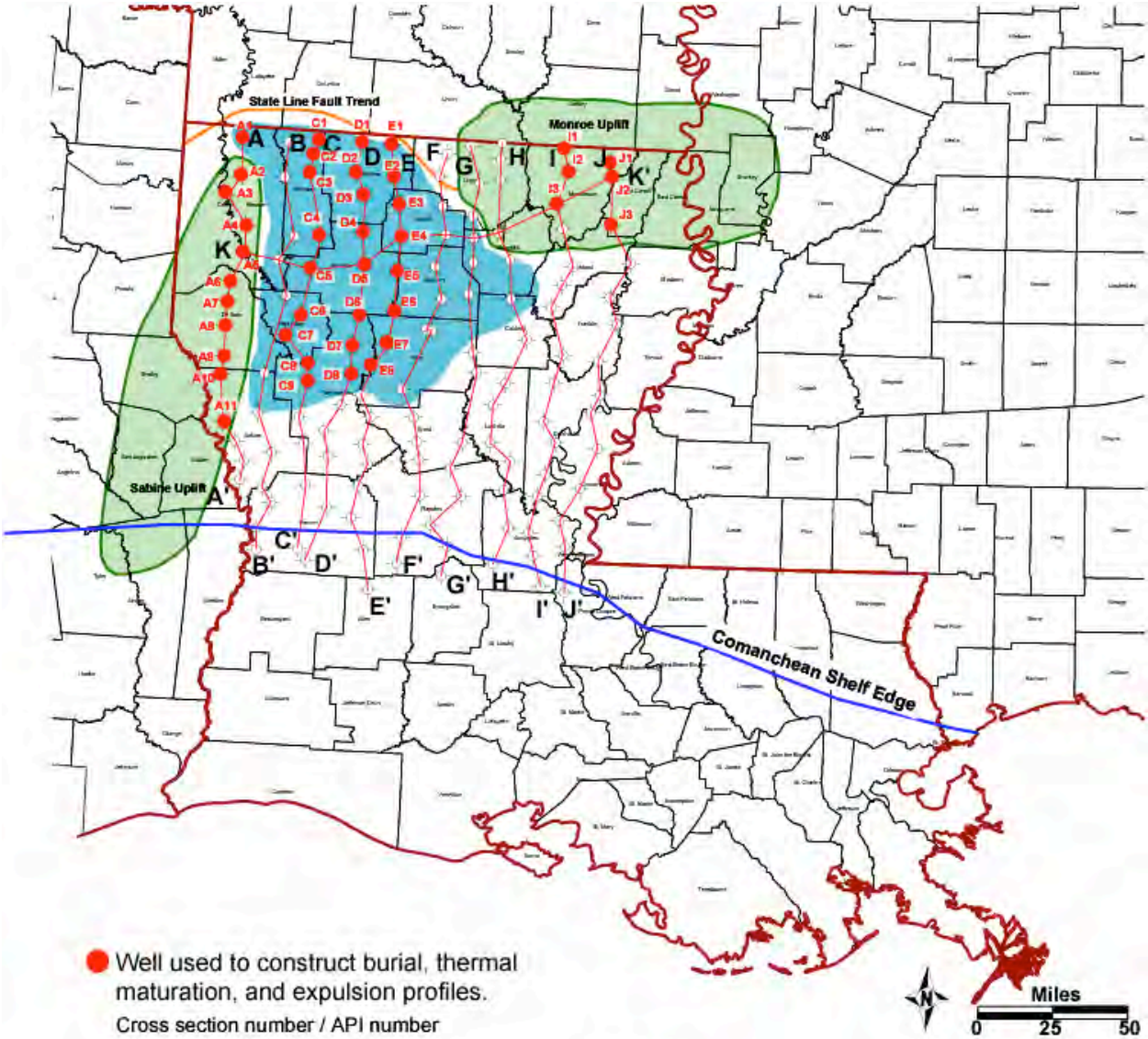


● Well used to construct burial, thermal maturation, and expulsion profiles.

Cross section number / API number

| | | | | | |
|---|---|---|---|---|---|
| A1 | 1701521100 | C4 | 1711961517 | E1 | 1702720242 |
| A2 | 1701500464 | C5 | 1701320275 | E2 | 1702700522 |
| A3 | 1701521099 | C6 | 1708120147 | E3 | 1706100051 |
| A4 | 1701500977 | C7 | 1708120267 | E4 | 1706100091 |
| A5 | 1701501689 | C8 | 1708100714 | E5 | 1701300138 |
| A6 | 1703120488 | C9 | 1706920034 | E6 | 1704920029 |
| A7 | 1703120378 | D1 | 1702701875 | E7 | 1712720324 |
| A8 | 1703100304 | D2 | 1702701974 | E8 | 1712701324 |
| A9 | 1703100117 | D3 | 1702720557 | I1 | 1706700012 |
| A10 | 1708520238 | D4 | 1701320349 | I2 | 1706700043 |
| A11 | 1708520177 | D5 | 1701320054 | I3 | 1706700182 |
| C1 | 1711920068 | D6 | 1706920079 | J1 | 1706700008 |
| C2 | 1711900502 | D7 | 1706900047 | J2 | 1706700061 |
| C3 | 1711920195 | D8 | 1706900174 | J3 | 1712300011 |

Figure 2. Index map showing line of cross sections and location of selected wells for the North Louisiana Salt Basin.

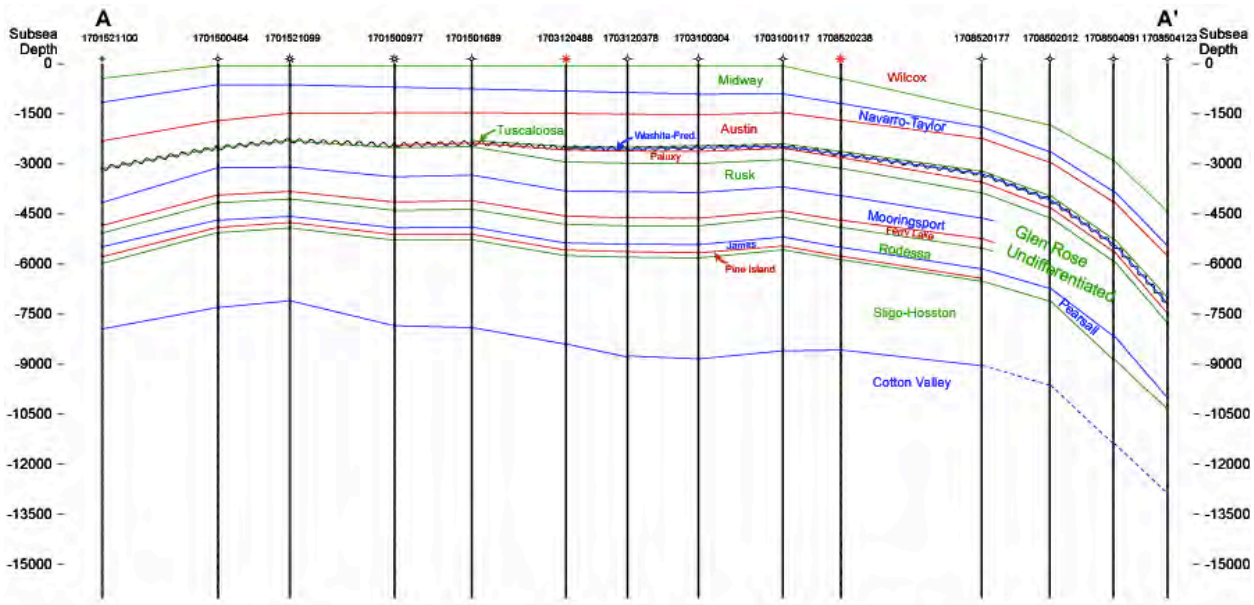


Figure 3. Cross section A-A' for the North Louisiana Salt Basin. See Figure 2 for location of cross section.

**VE:22X**

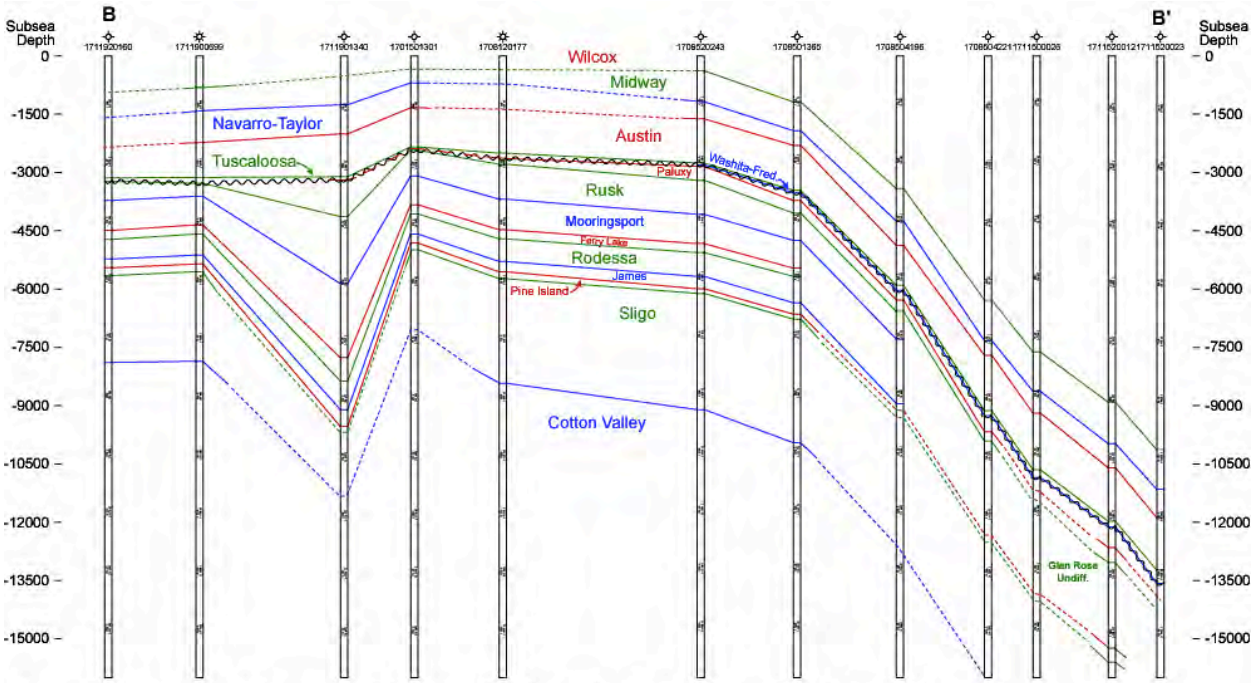


Figure 4. Cross section B-B' for the North Louisiana Salt Basin. See Figure 2 for location of cross section.

**VE:30X**

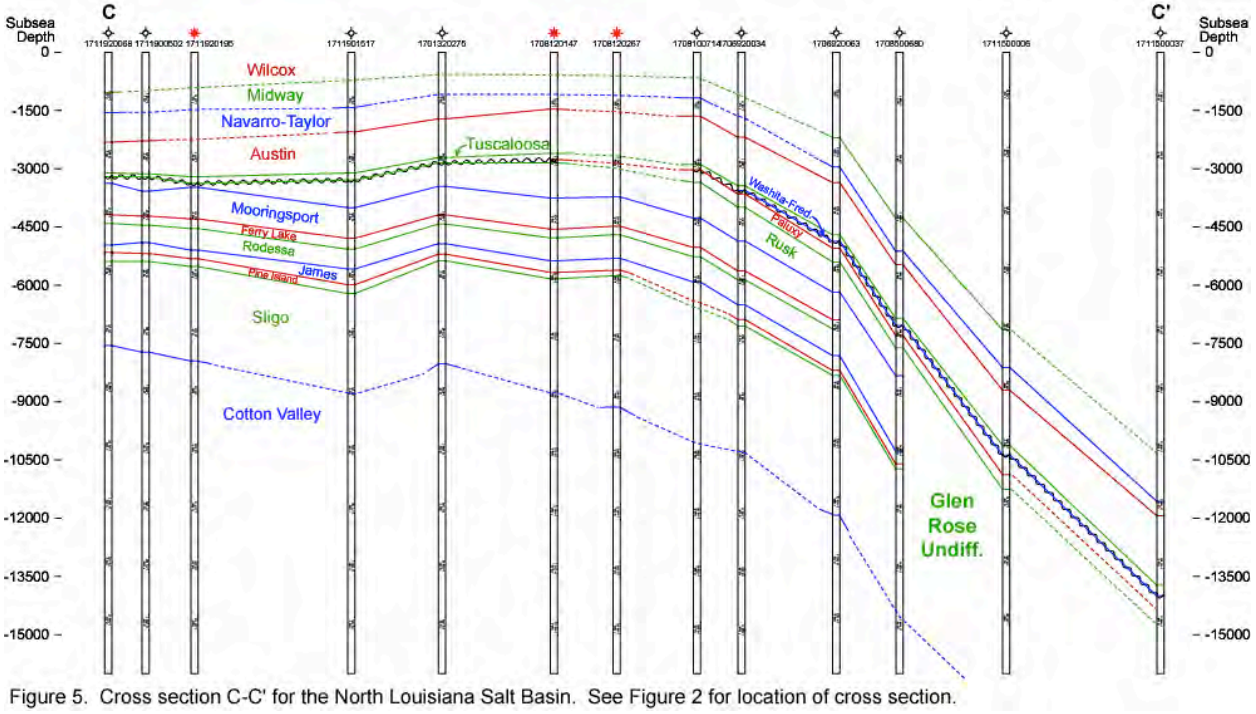


Figure 5. Cross section C-C' for the North Louisiana Salt Basin. See Figure 2 for location of cross section.

**VE:29X**

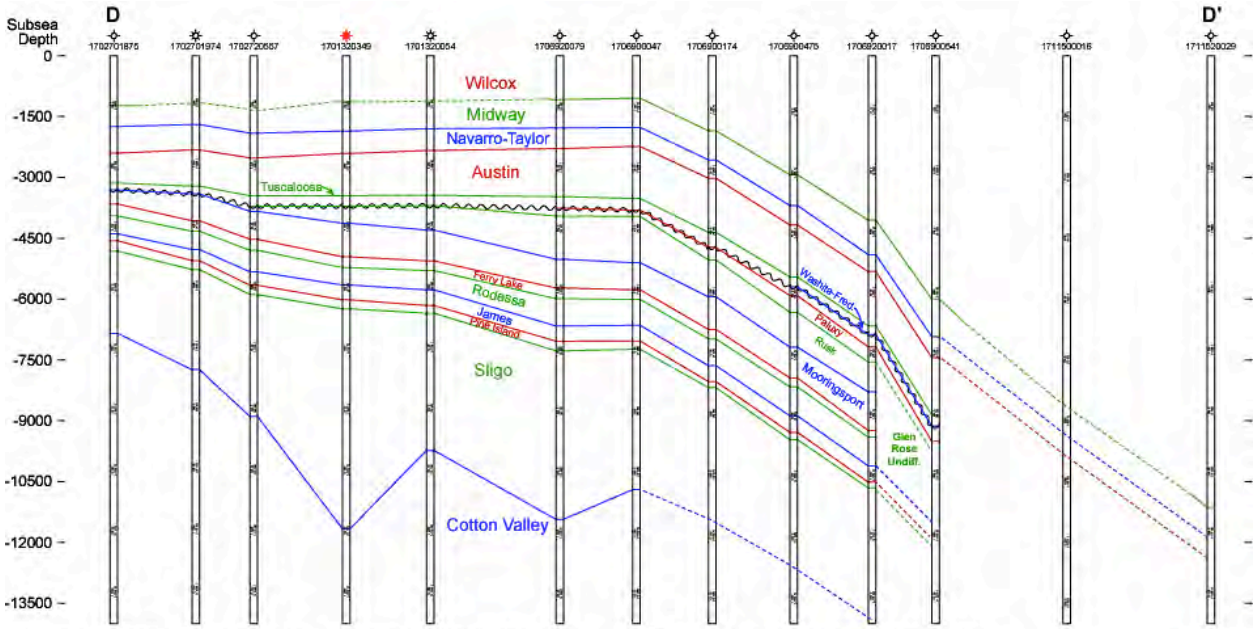


Figure 6. Cross section D-D' for the North Louisiana Salt Basin. See Figure 2 for location of cross section.

**VE:32X**

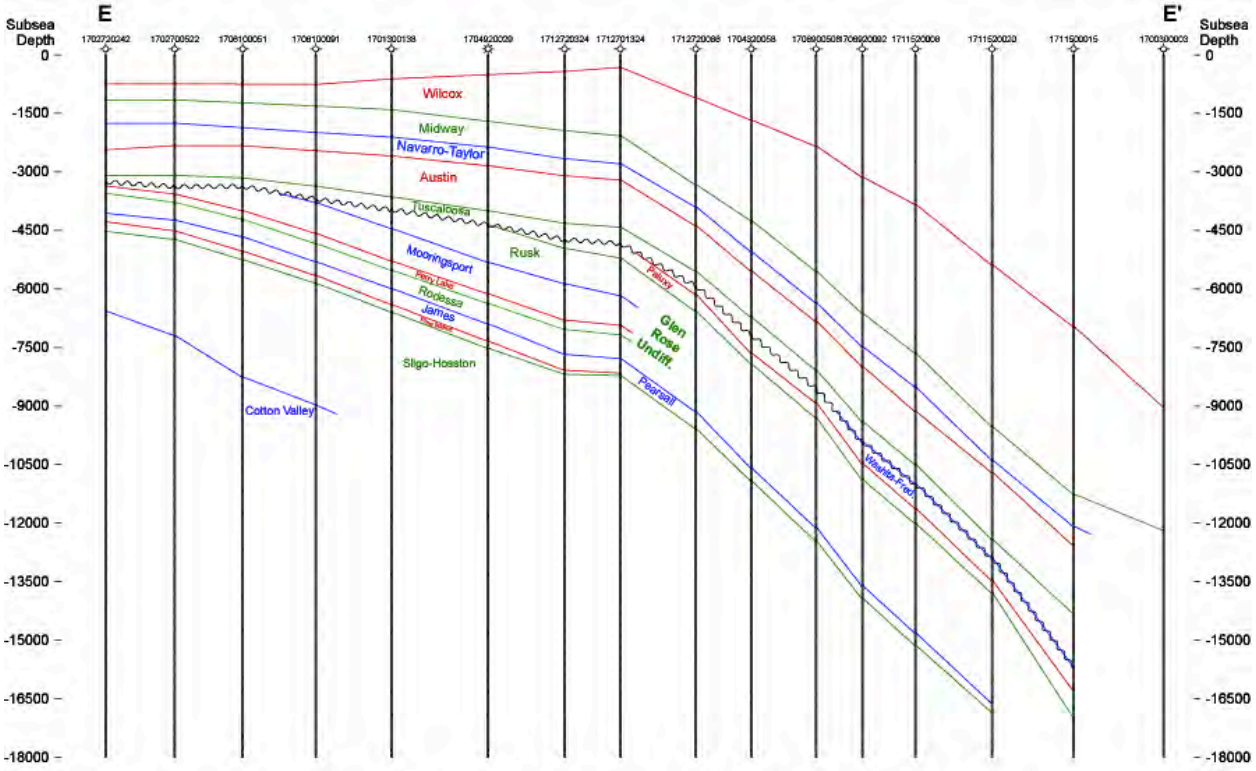


Figure 7. Cross section E-E' for the North Louisiana Salt Basin. See Figure 2 for location of cross section.

**VE:34X**

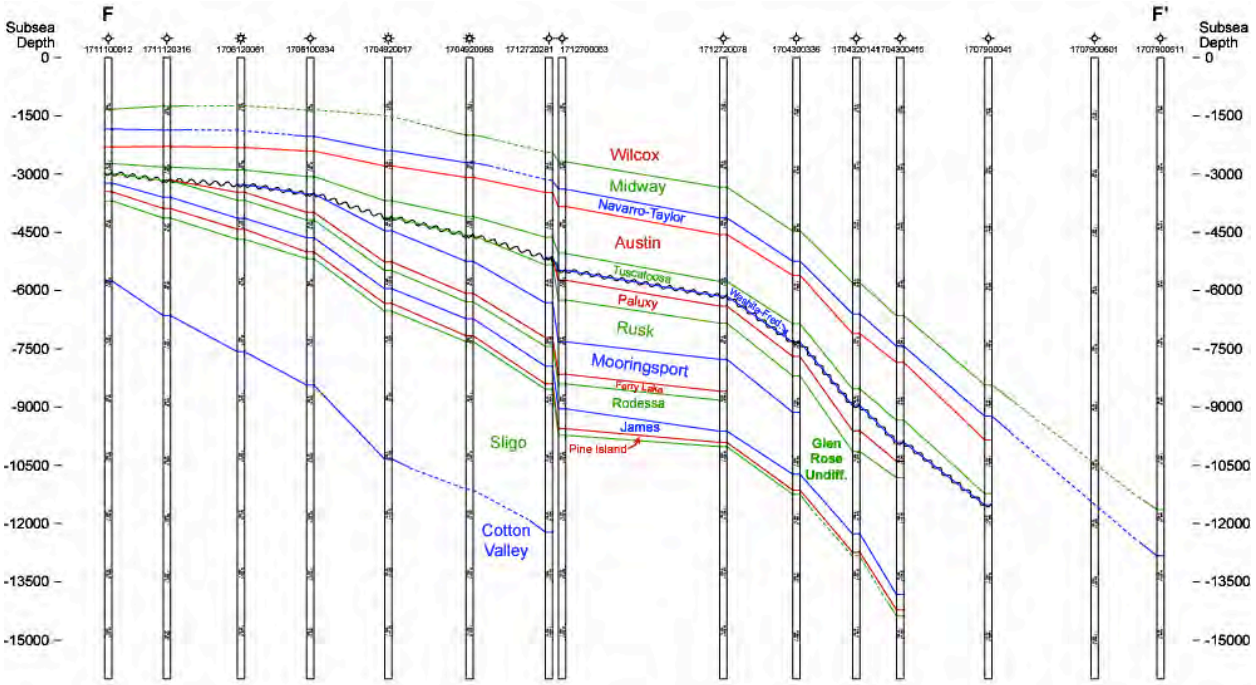


Figure 8. Cross section F-F' for the North Louisiana Salt Basin. See Figure 2 for location of cross section.

**VE:32X**

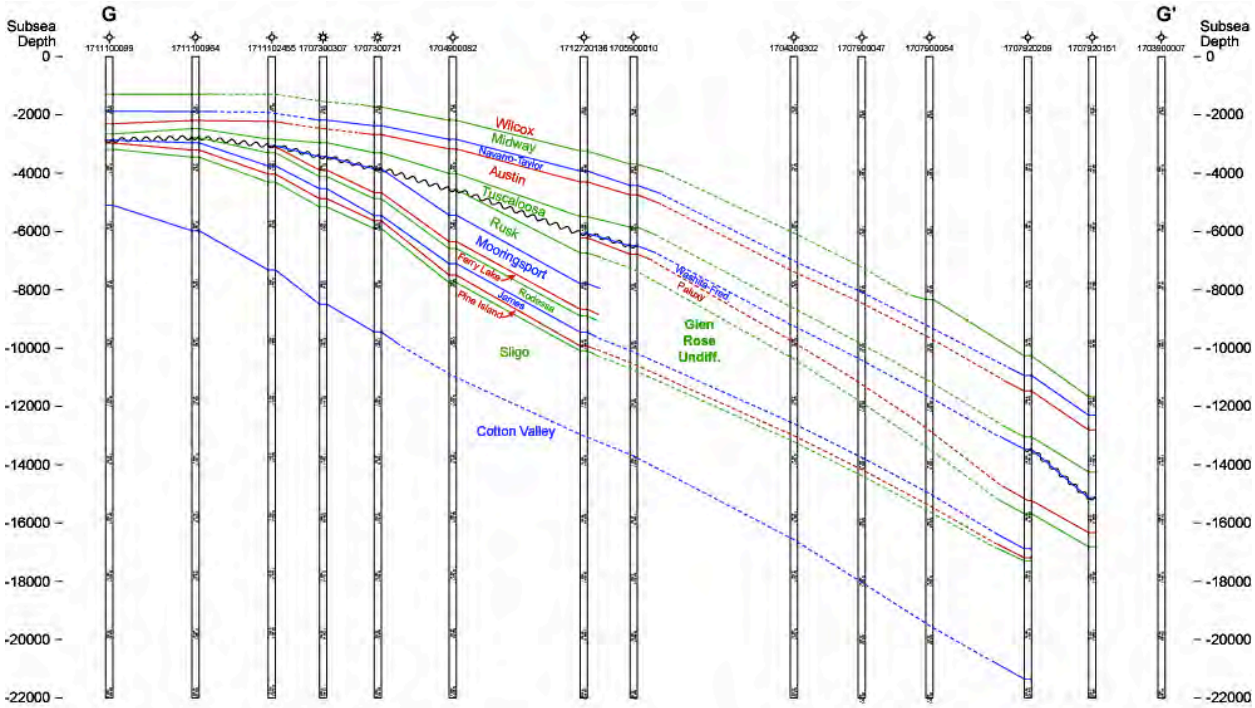


Figure 9. Cross section G-G' for the North Louisiana Salt Basin. See Figure 2 for location of cross section.

**VE:25X**

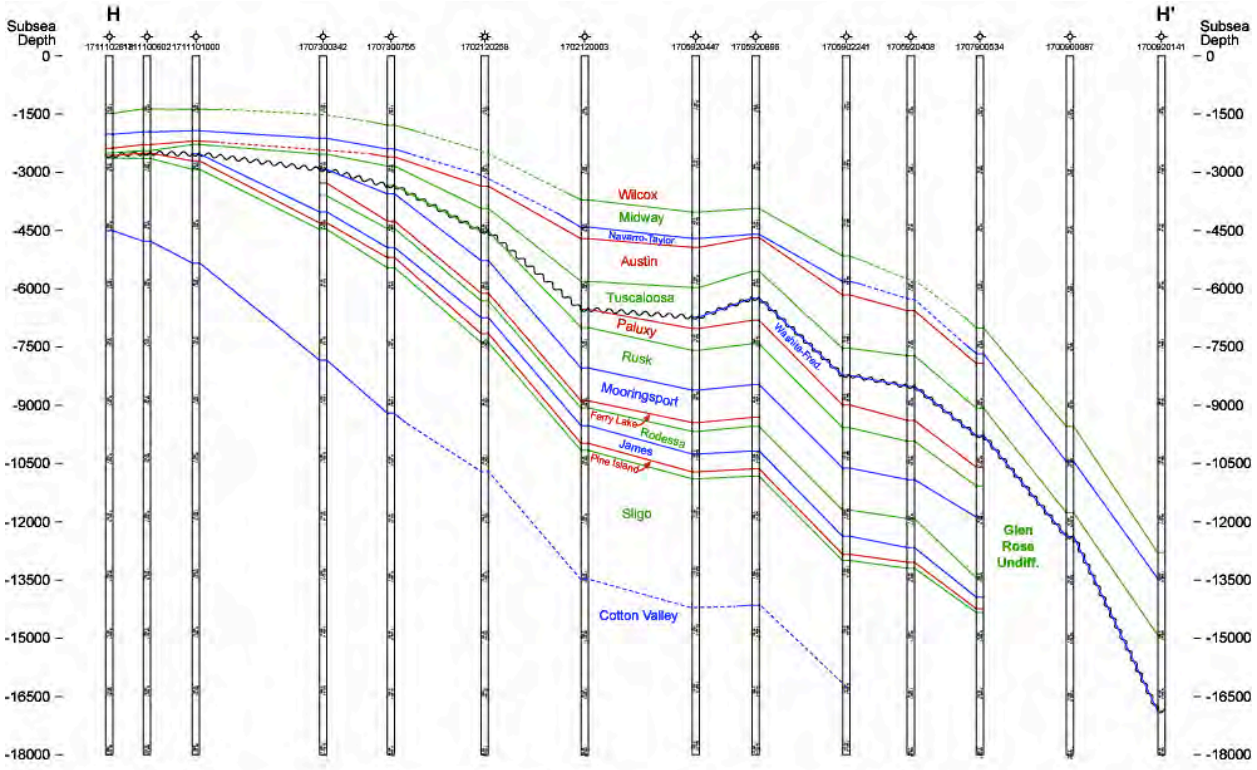


Figure 10. Cross section H-H' for the North Louisiana Salt Basin. See Figure 2 for location of cross section.

**VE:35X**

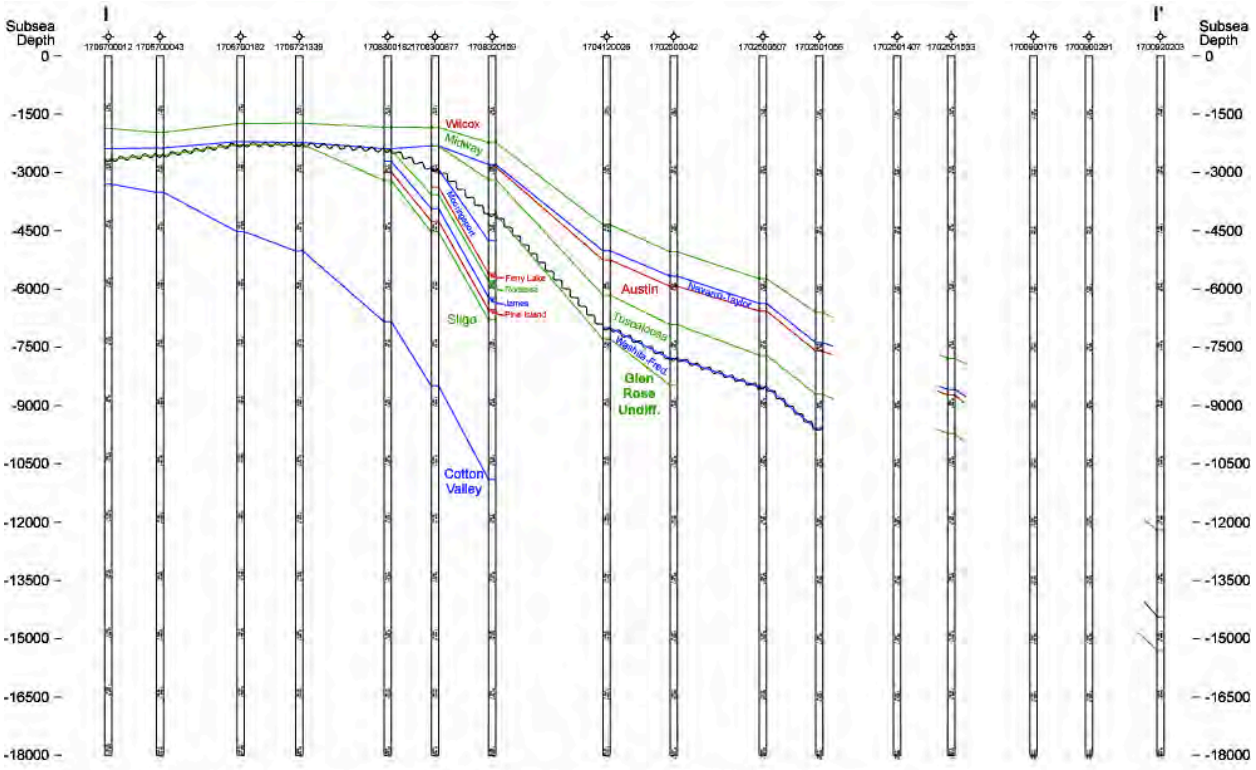


Figure 11. Cross section I-I' for the North Louisiana Salt Basin. See Figure 2 for location of cross section.

**VE:31X**

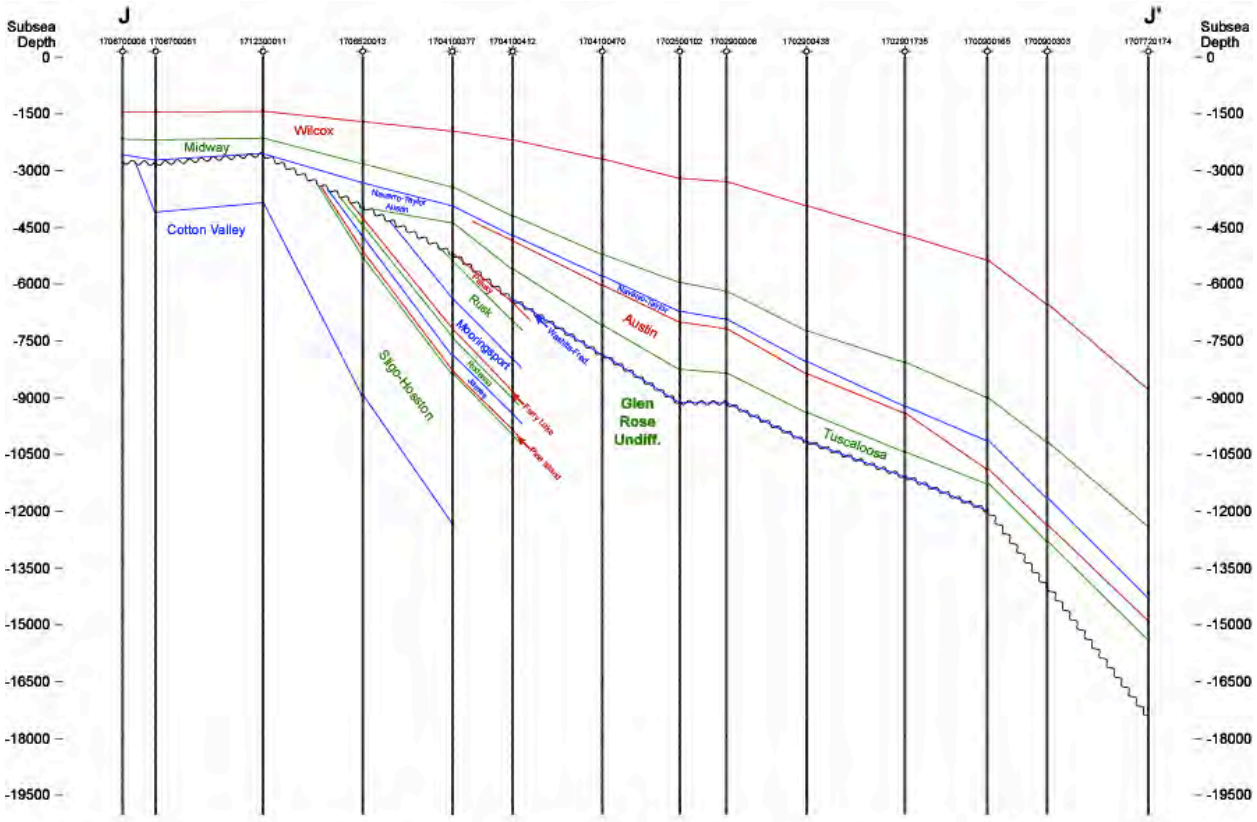


Figure 12. Cross section J-J' for the North Louisiana Salt Basin. See Figure 2 for location of cross section.

**VE:30X**

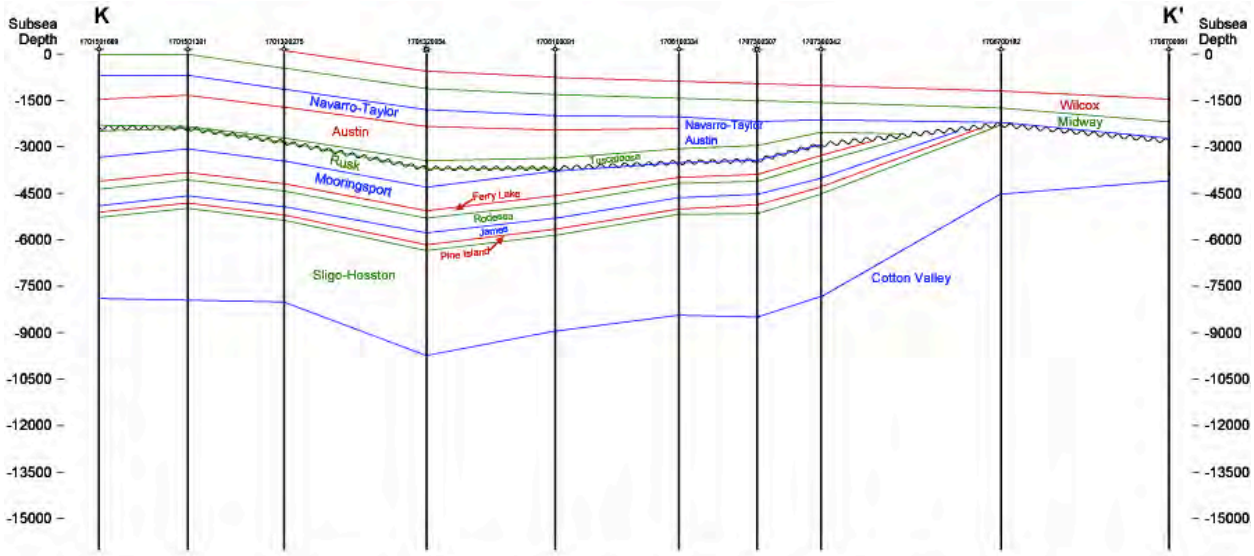


Figure 13. Cross section K-K' for the North Louisiana Salt Basin. See Figure 2 for location of cross section.

**VE:22X**

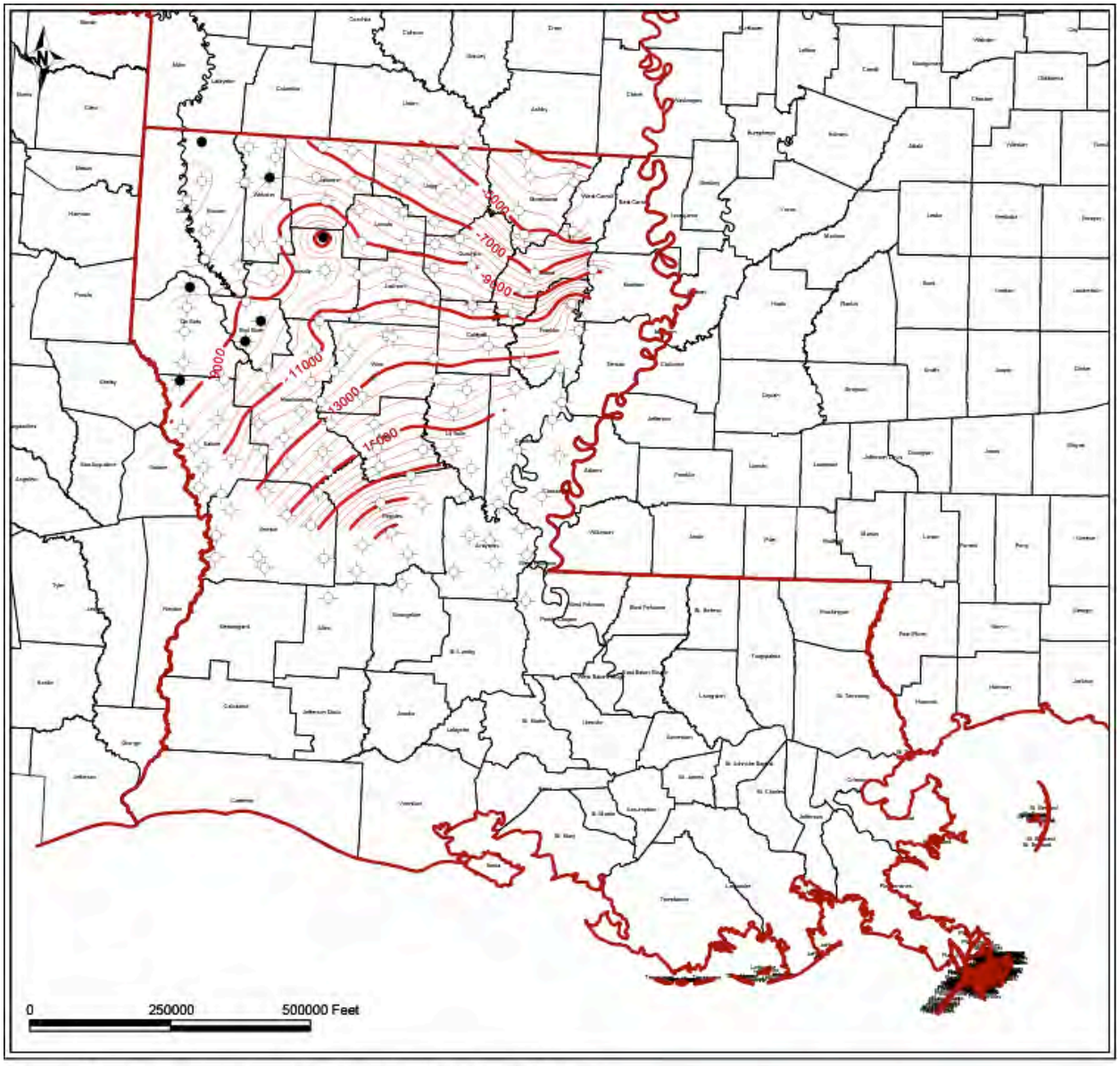


Figure 14. Structure map on the top of the Cotton Valley.
Contour interval = 500 feet

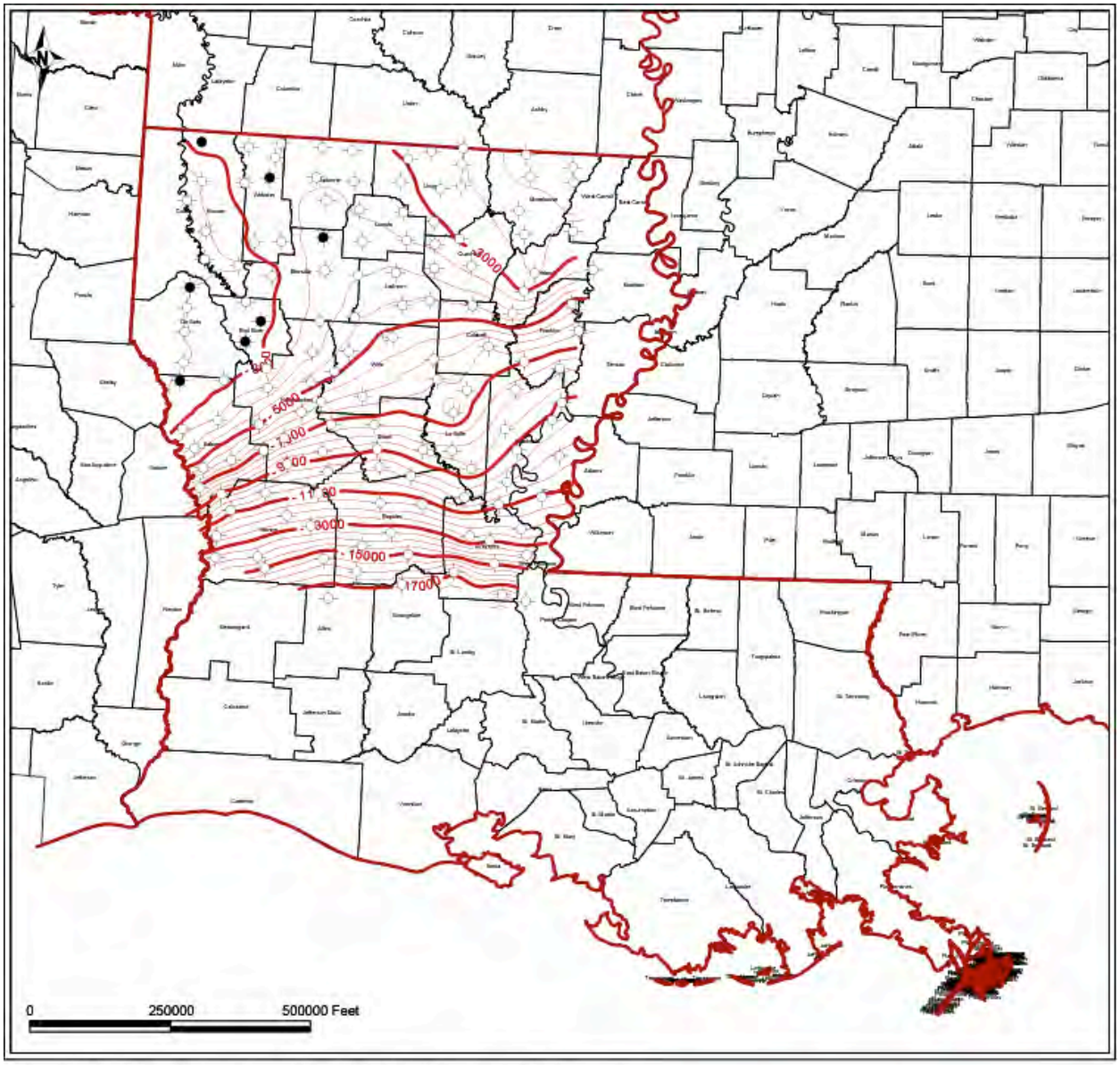


Figure 15. Structure map on the top of the Lower Cretaceous.
Contour interval = 500 feet

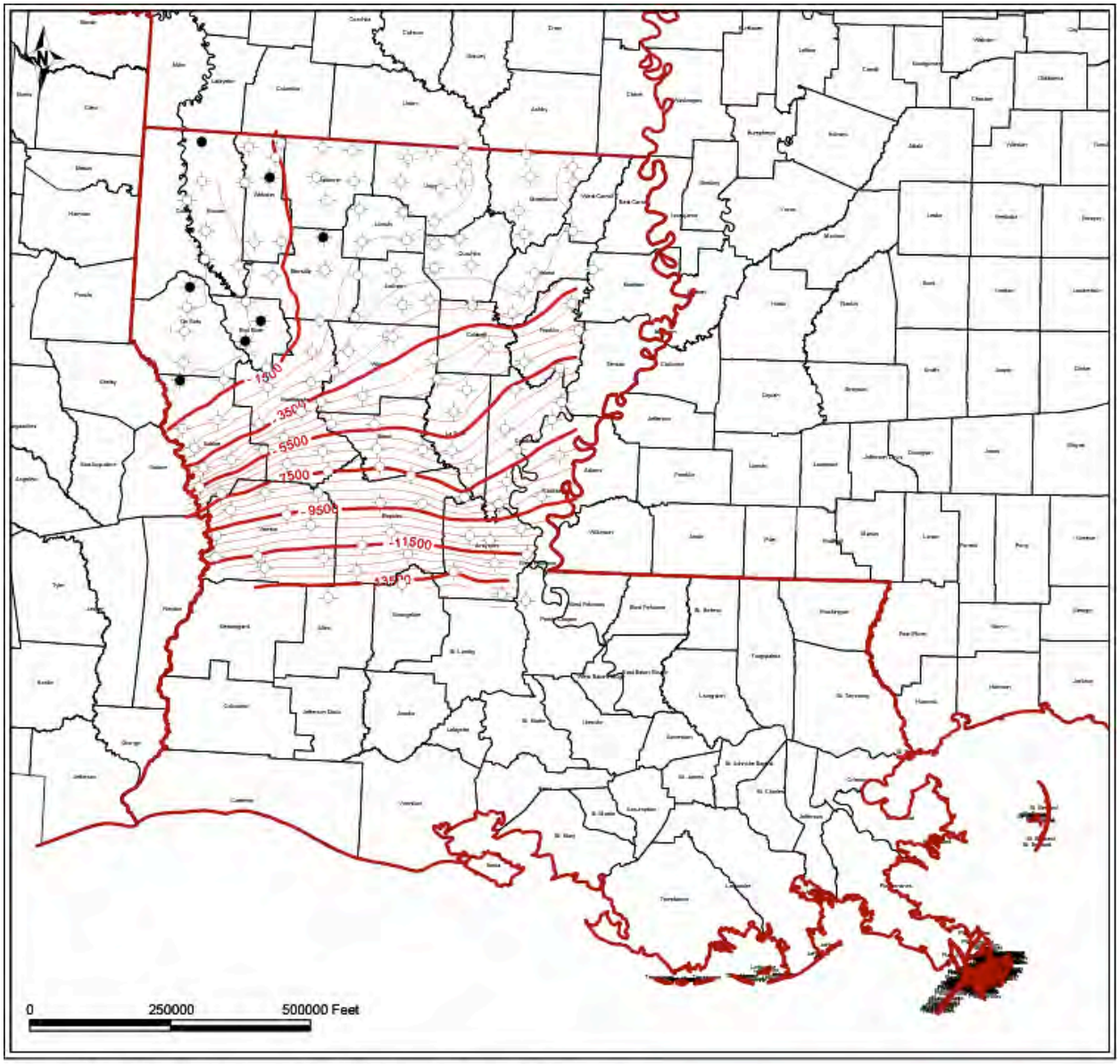


Figure 16. Structure map on the top of the Upper Cretaceous.
Contour interval = 500 feet

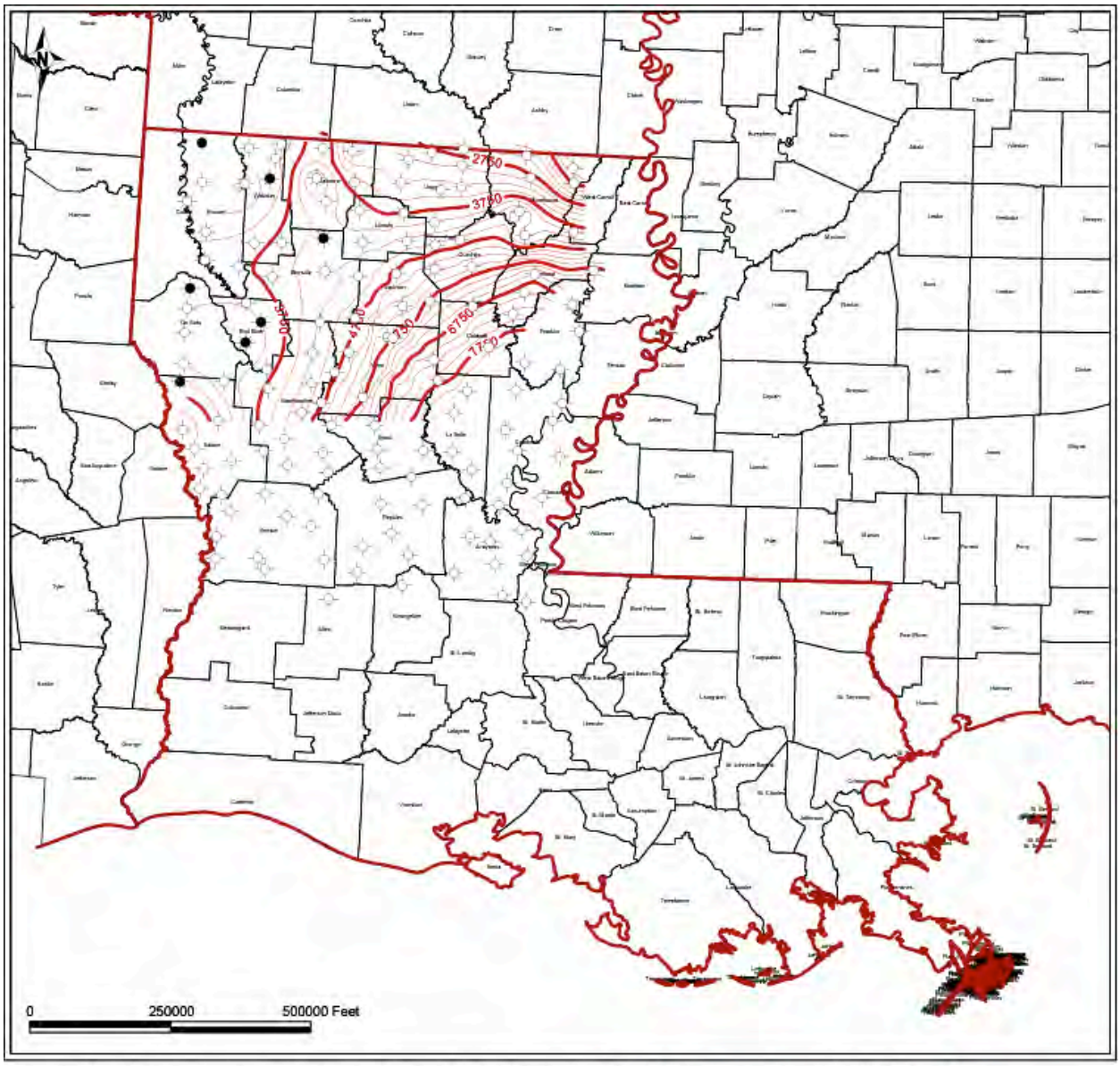


Figure 17. Isopach map of Cotton Valley strata, from the top of the Smackover to the top of the Cotton Valley.

Contour Interval = 250 feet

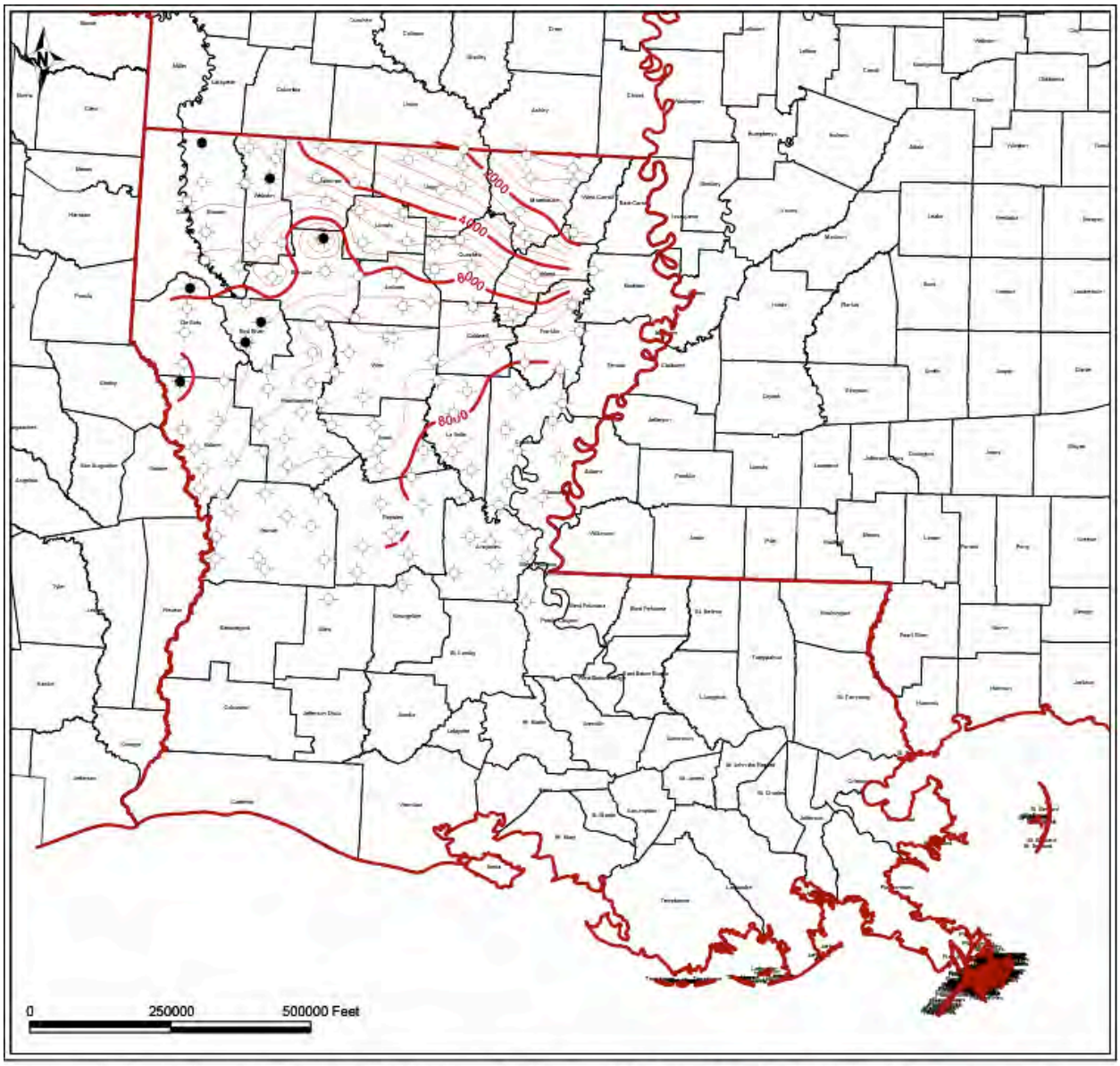


Figure 18. Isopach map of Lower Cretaceous strata, from the top of the Cotton Valley to the top of the Lower Cretaceous.

Contour Interval = 500 feet

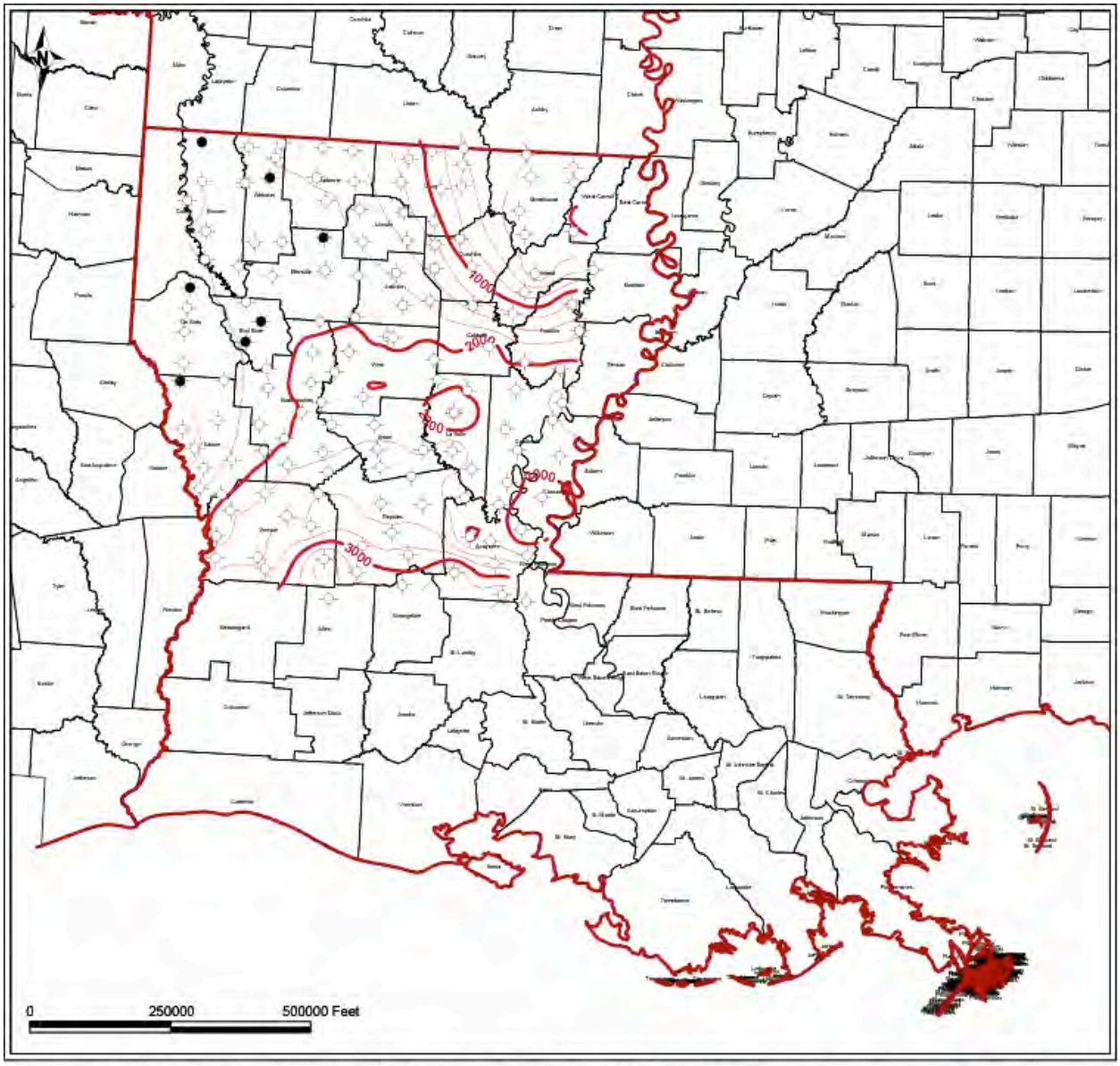


Figure 19. Isopach map of Upper Cretaceous strata, from the top of the Lower Cretaceous to the top of the Upper Cretaceous.

Contour Interval = 250 feet

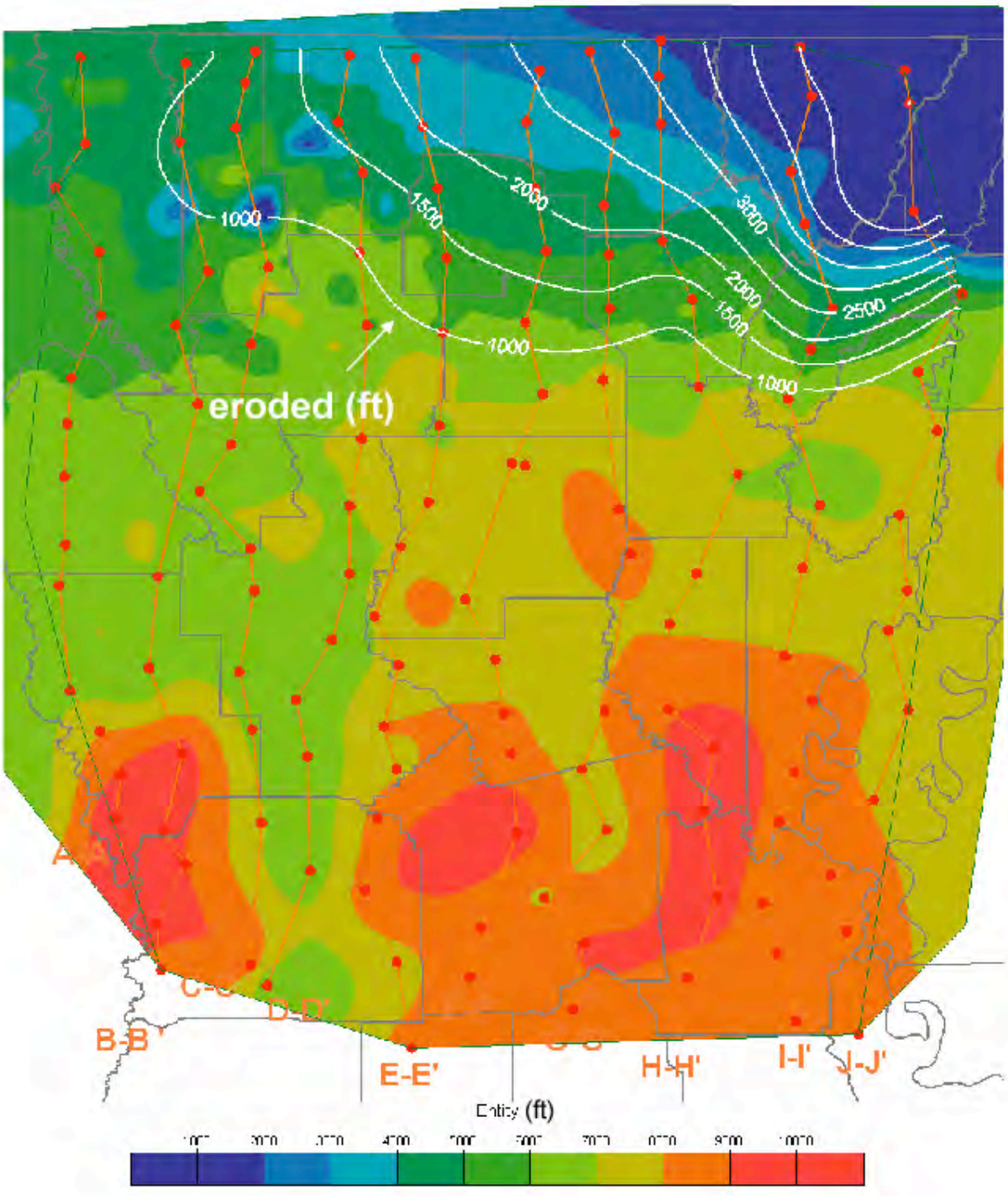


Figure 20. Erosion thickness of total Lower Cretaceous section. Prepared by Roger Barnaby.

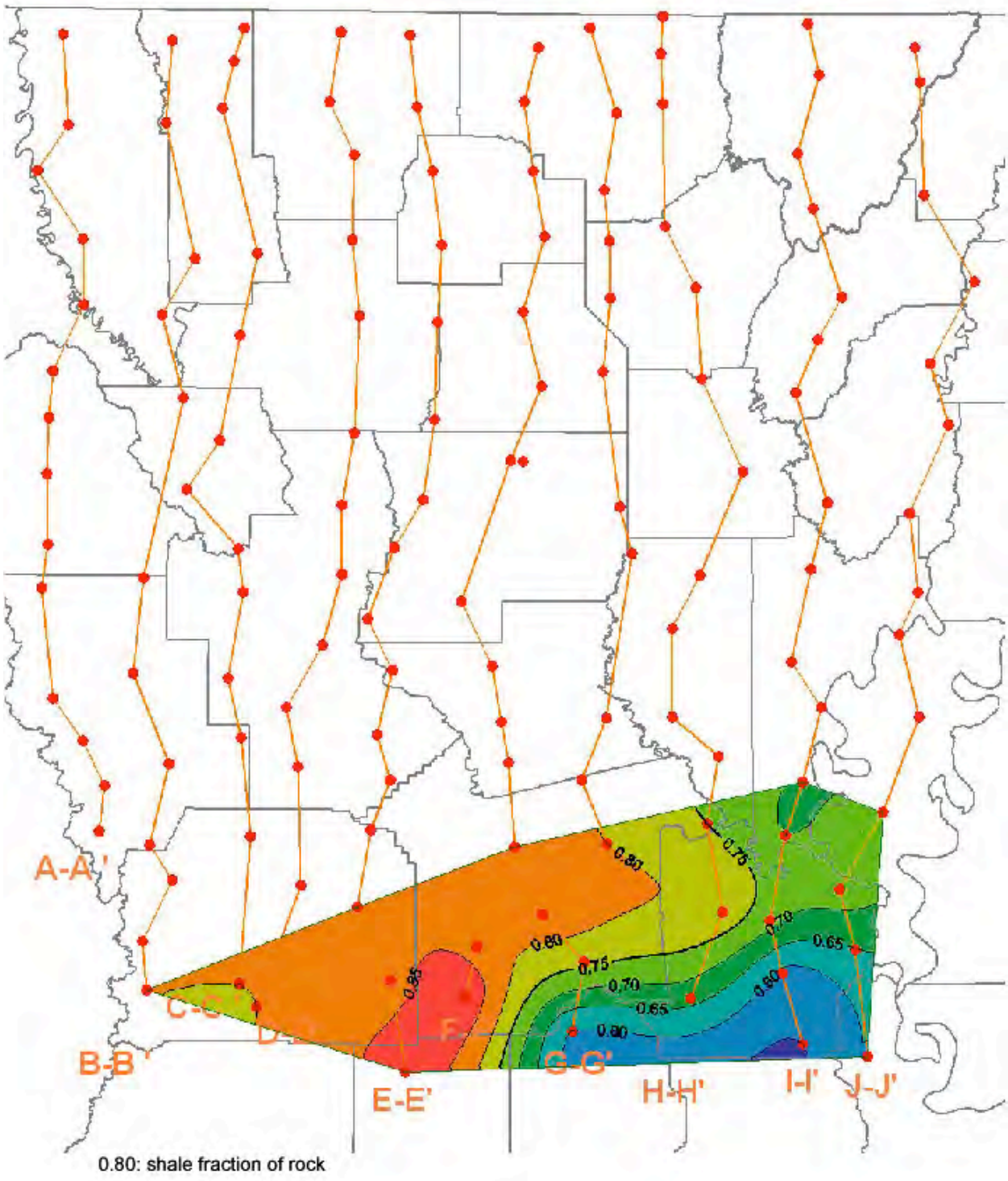


Figure 21. Lithology map of Miocene strata. Prepared by Roger Barnaby.

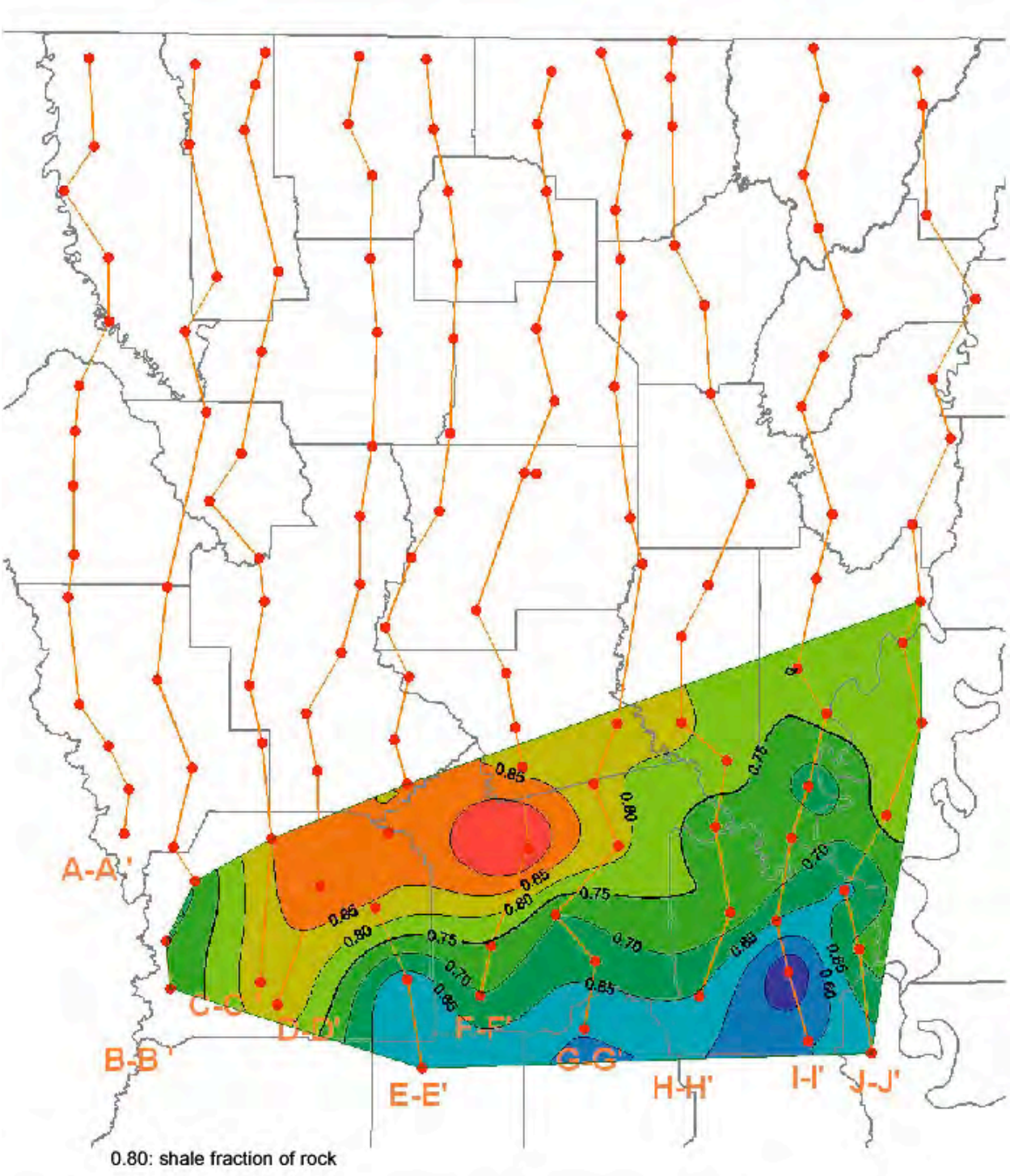


Figure 22. Lithology map of Oligocene strata. Prepared by Roger Barnaby.

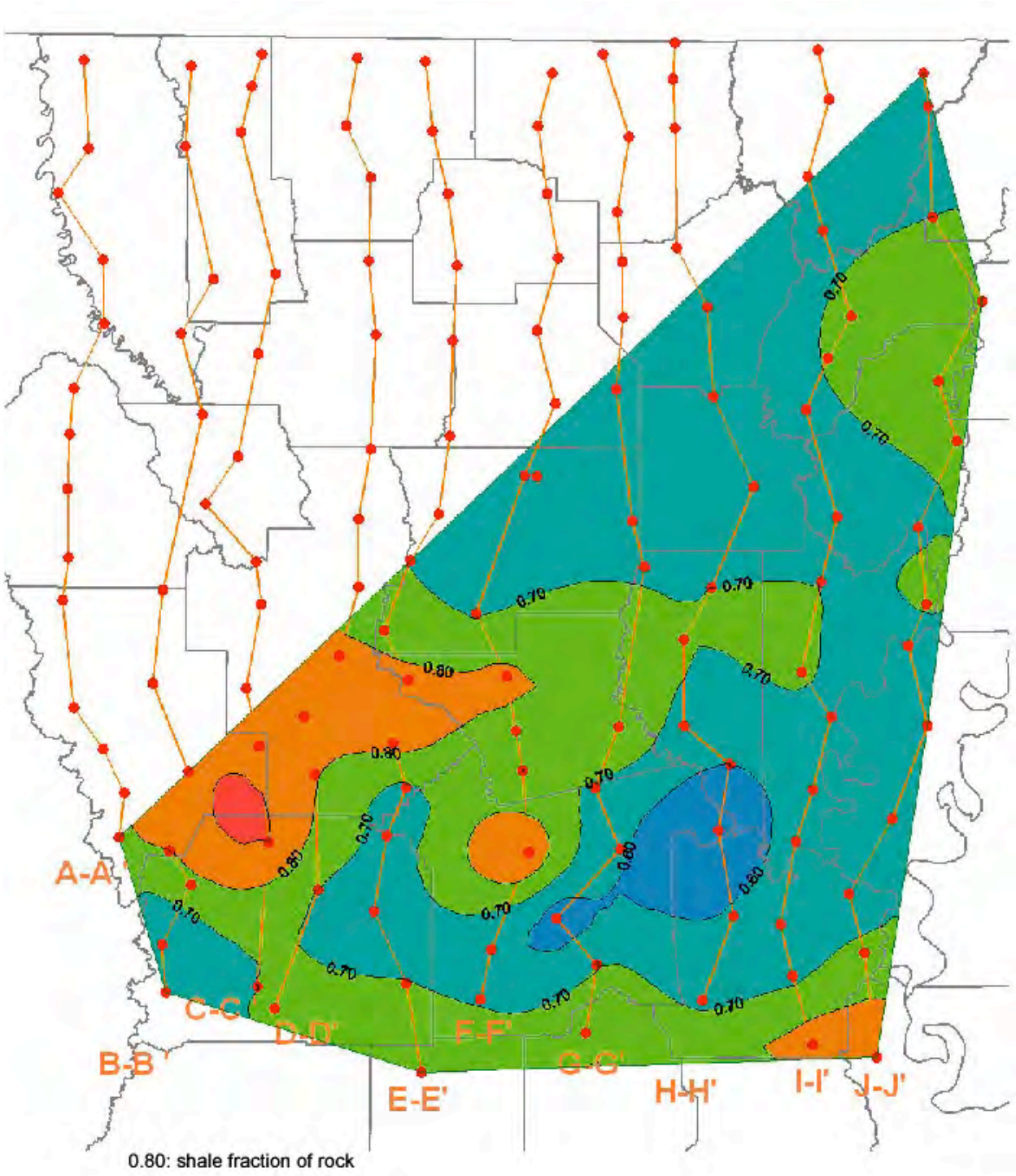


Figure 23. Lithology map of Cockfield. Prepared by Roger Barnaby.

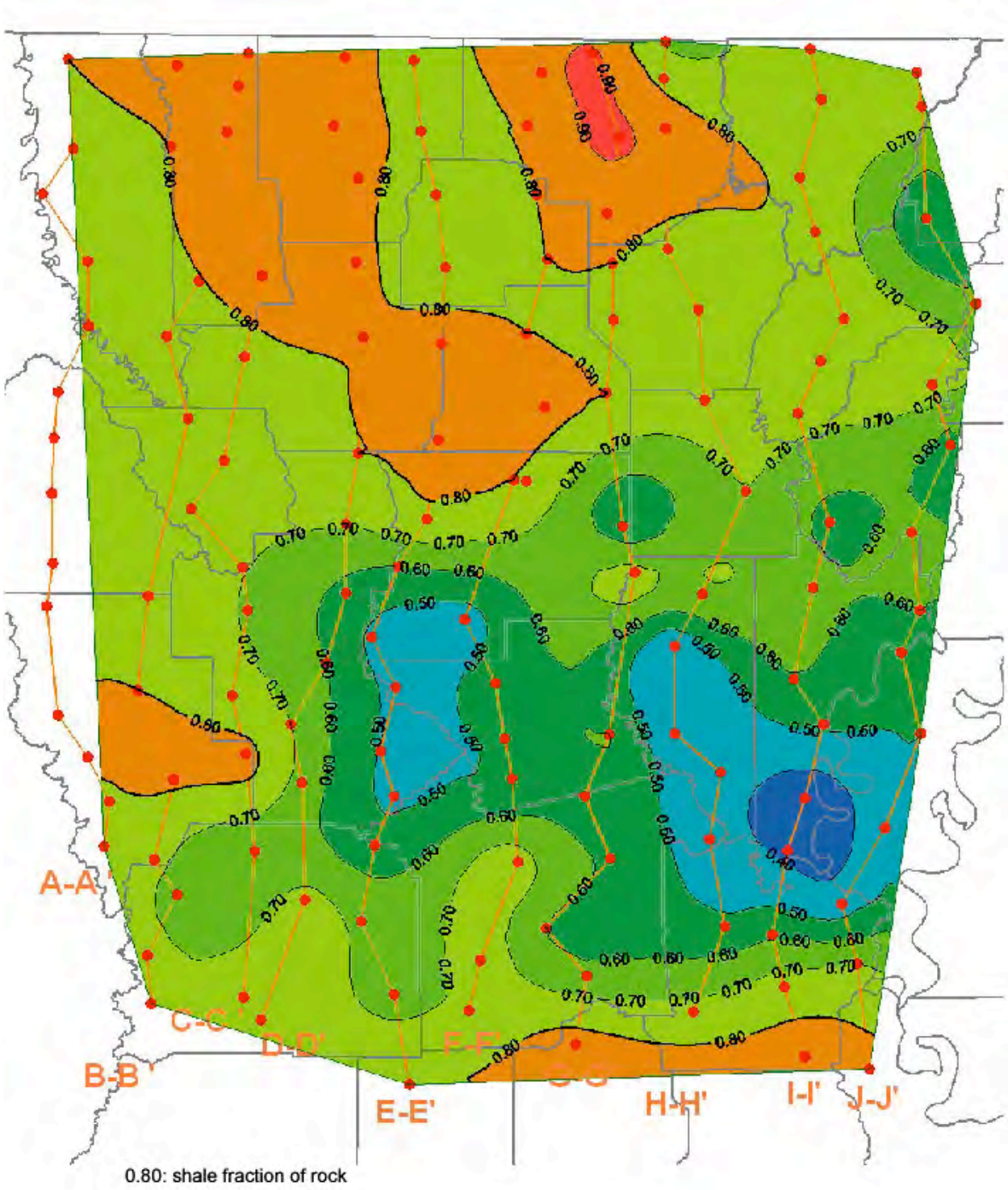


Figure 24. Lithology map of Sparta. Prepared by Roger Barnaby.

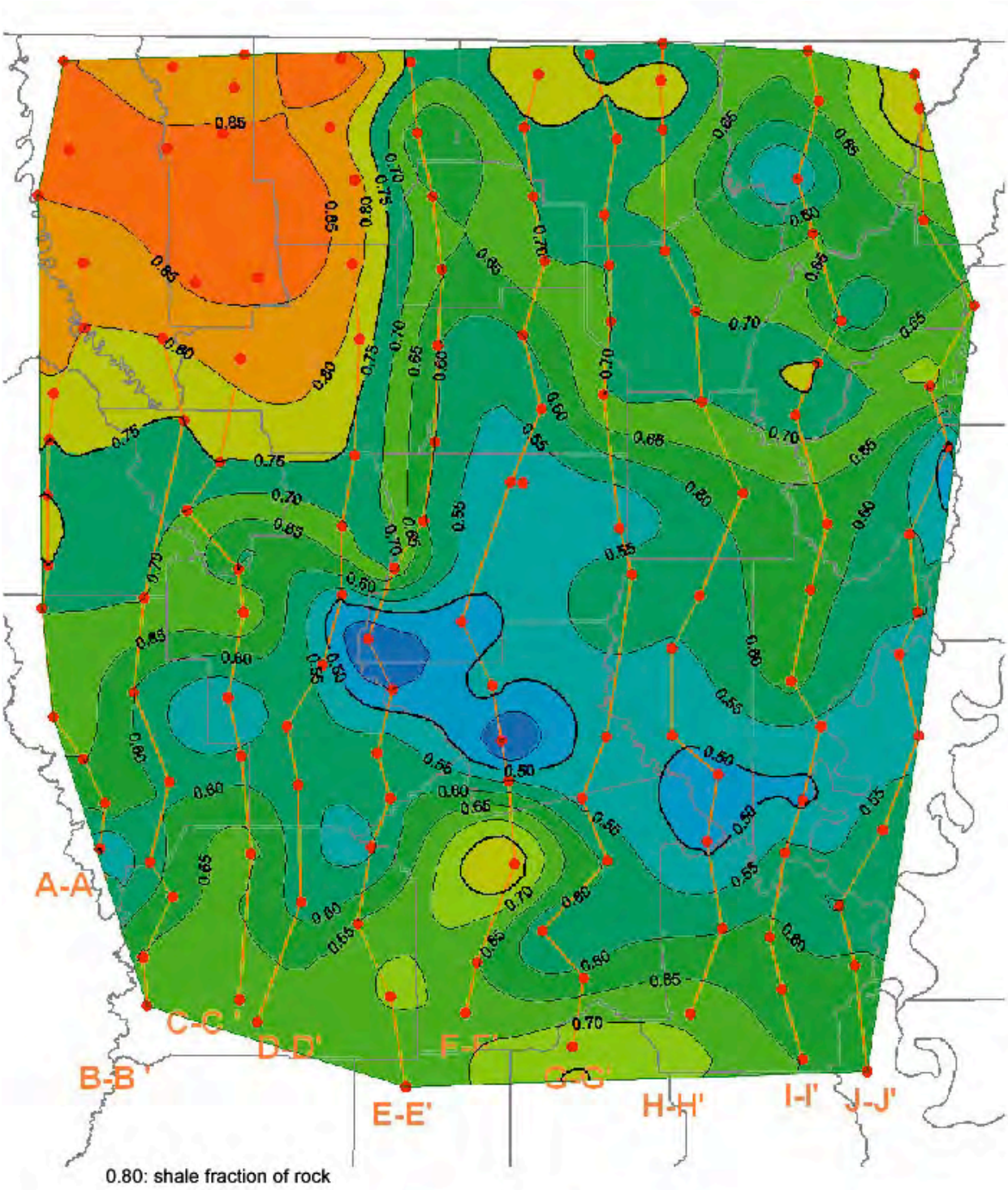


Figure 25. Lithology map of Wilcox. Prepared by Roger Barnaby.

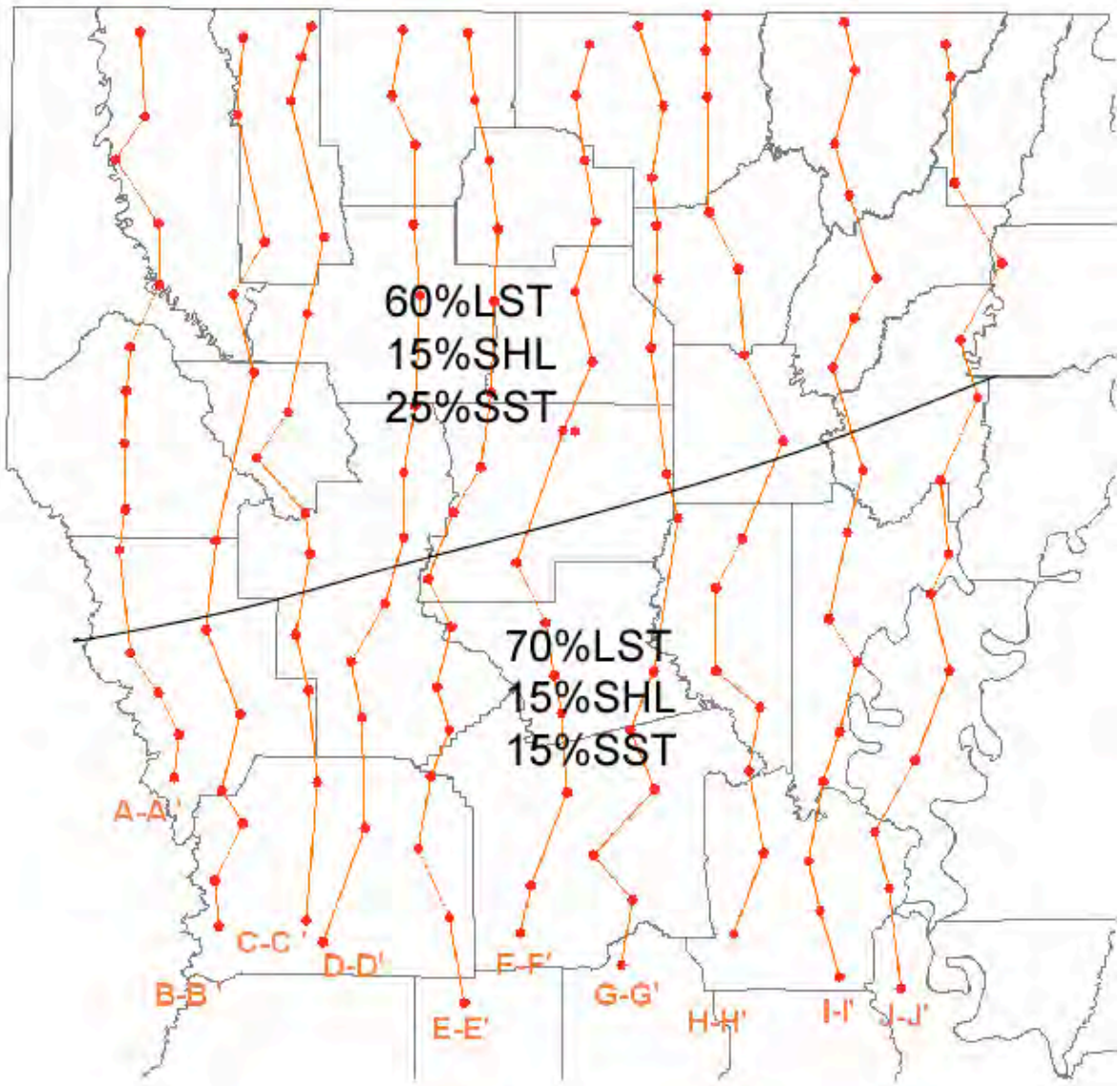


Figure 26. Lithology map of Upper Cretaceous strata. Prepared by Roger Barnaby.

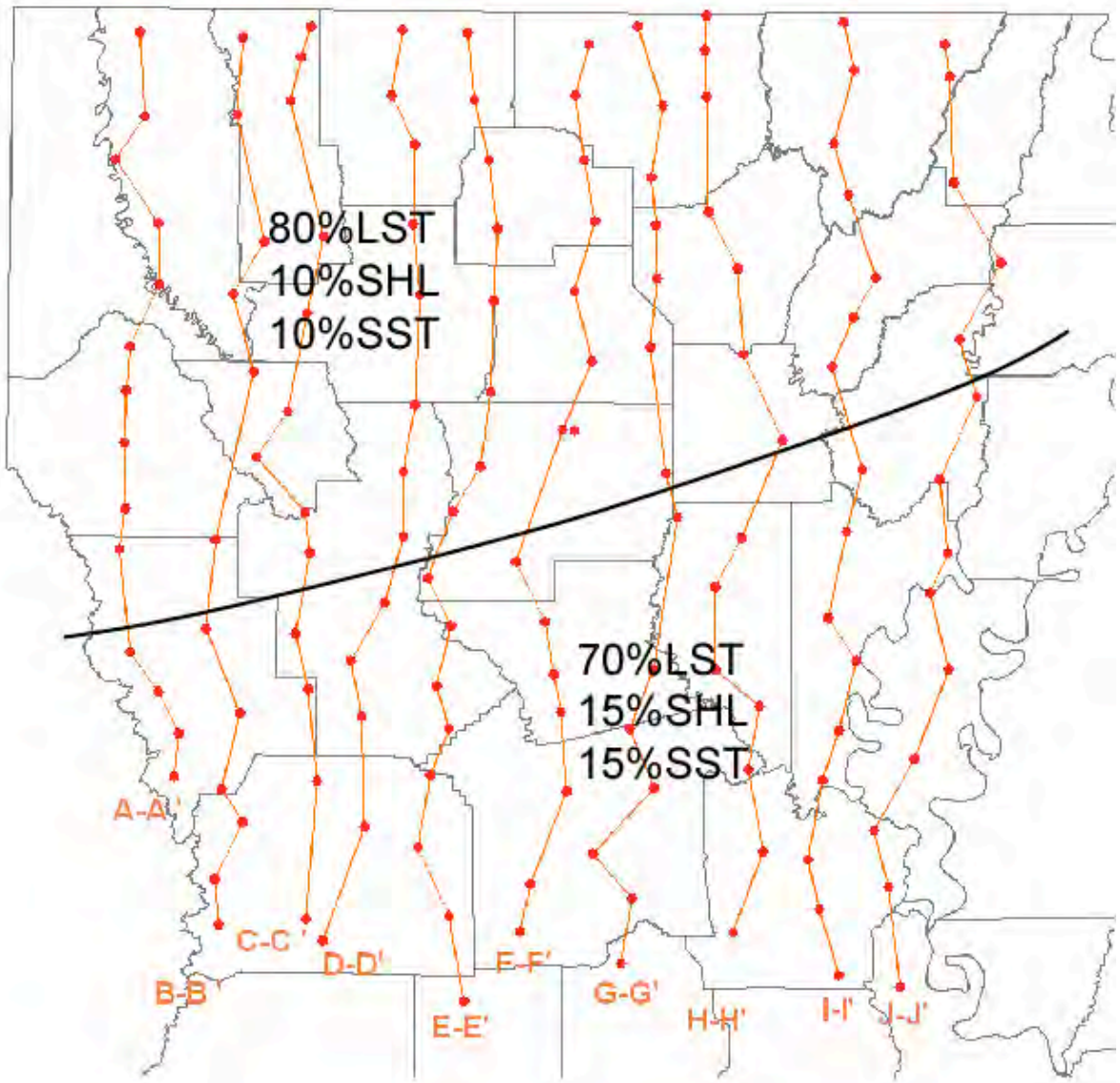


Figure 27. Lithology map of Austin. Prepared by Roger Barnaby.

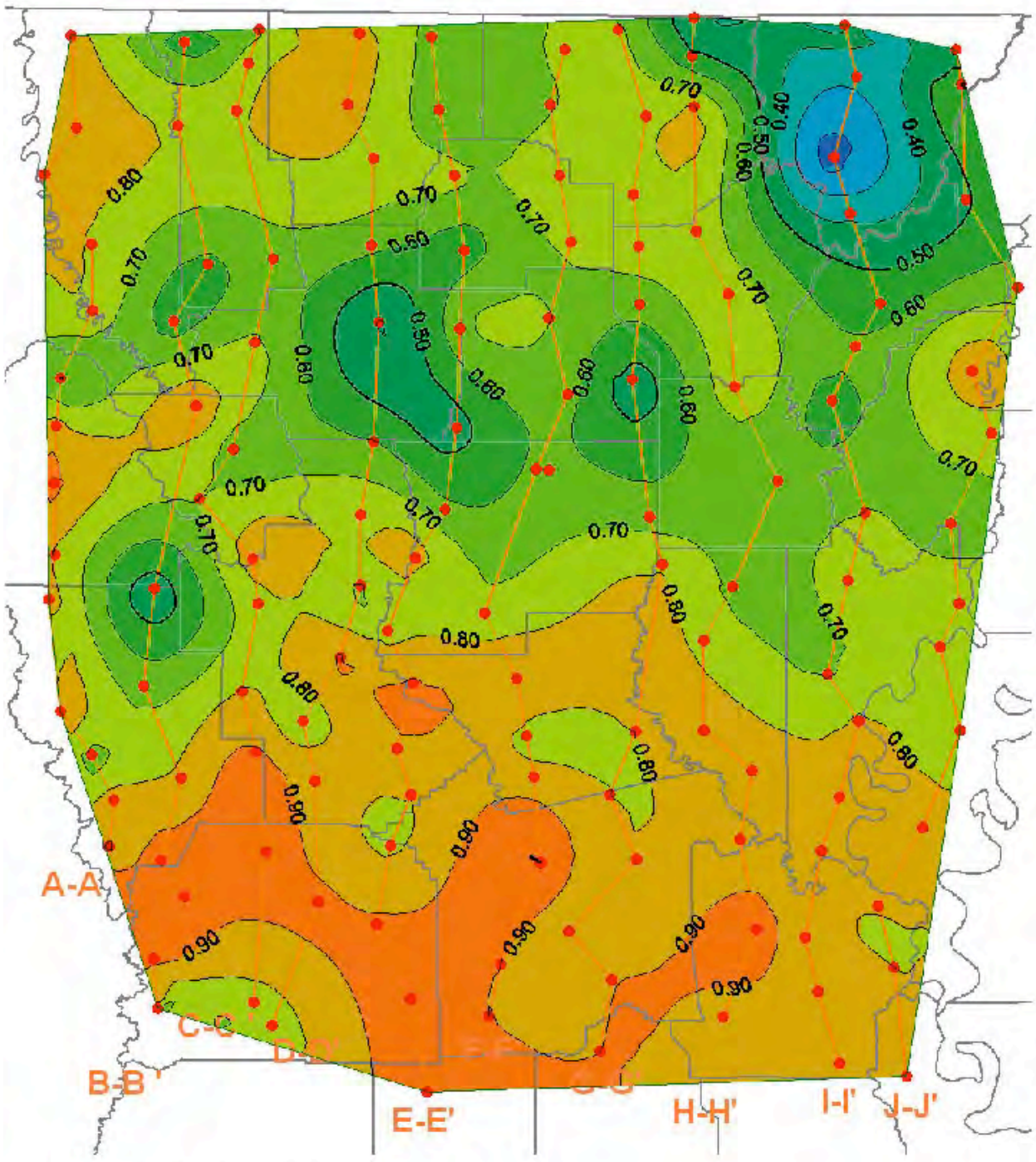


Figure 28. Lithology map of Tuscaloosa. Prepared by Roger Barnaby.

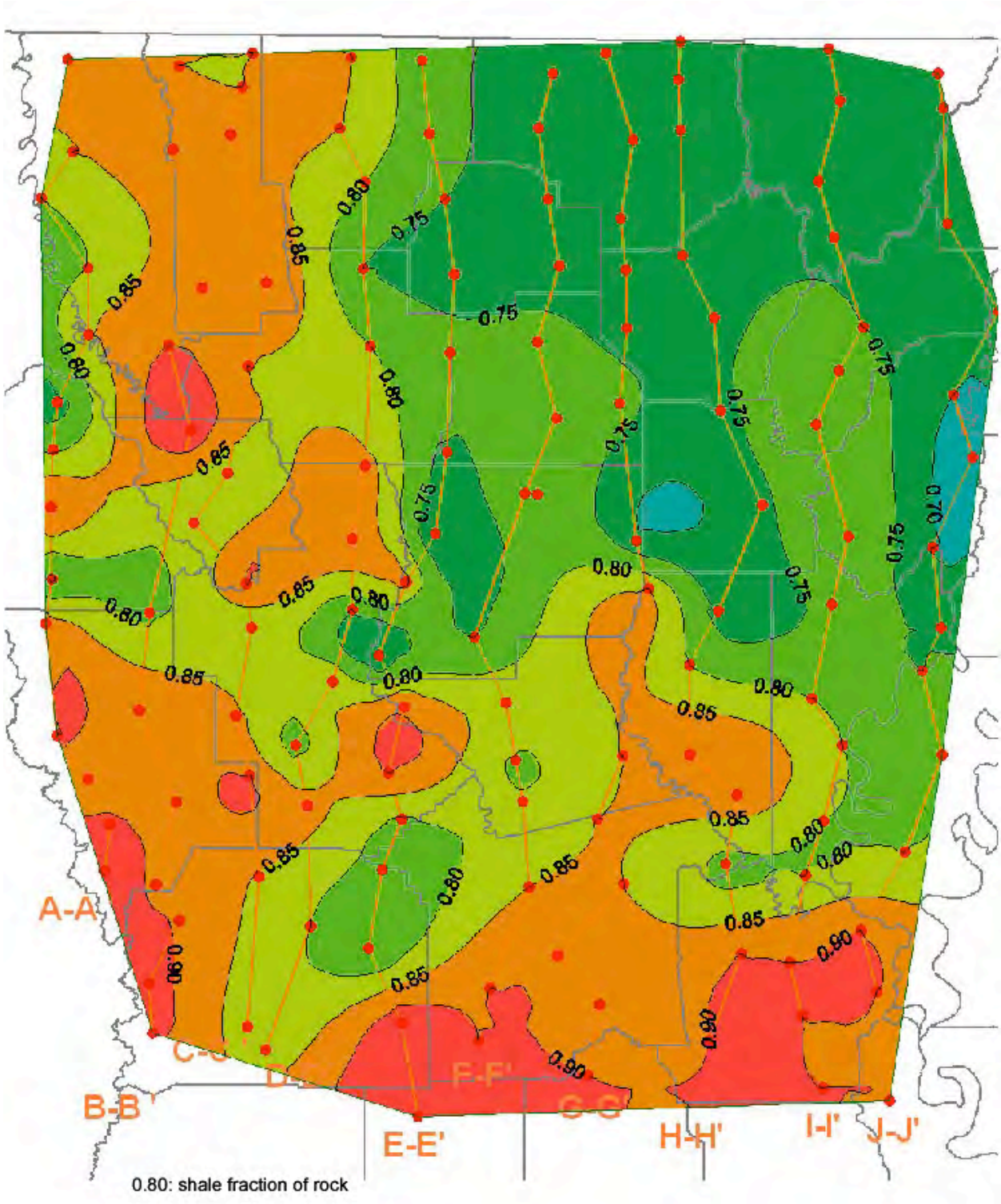


Figure 29. Lithology map of Paluxy. Prepared by Roger Barnaby.

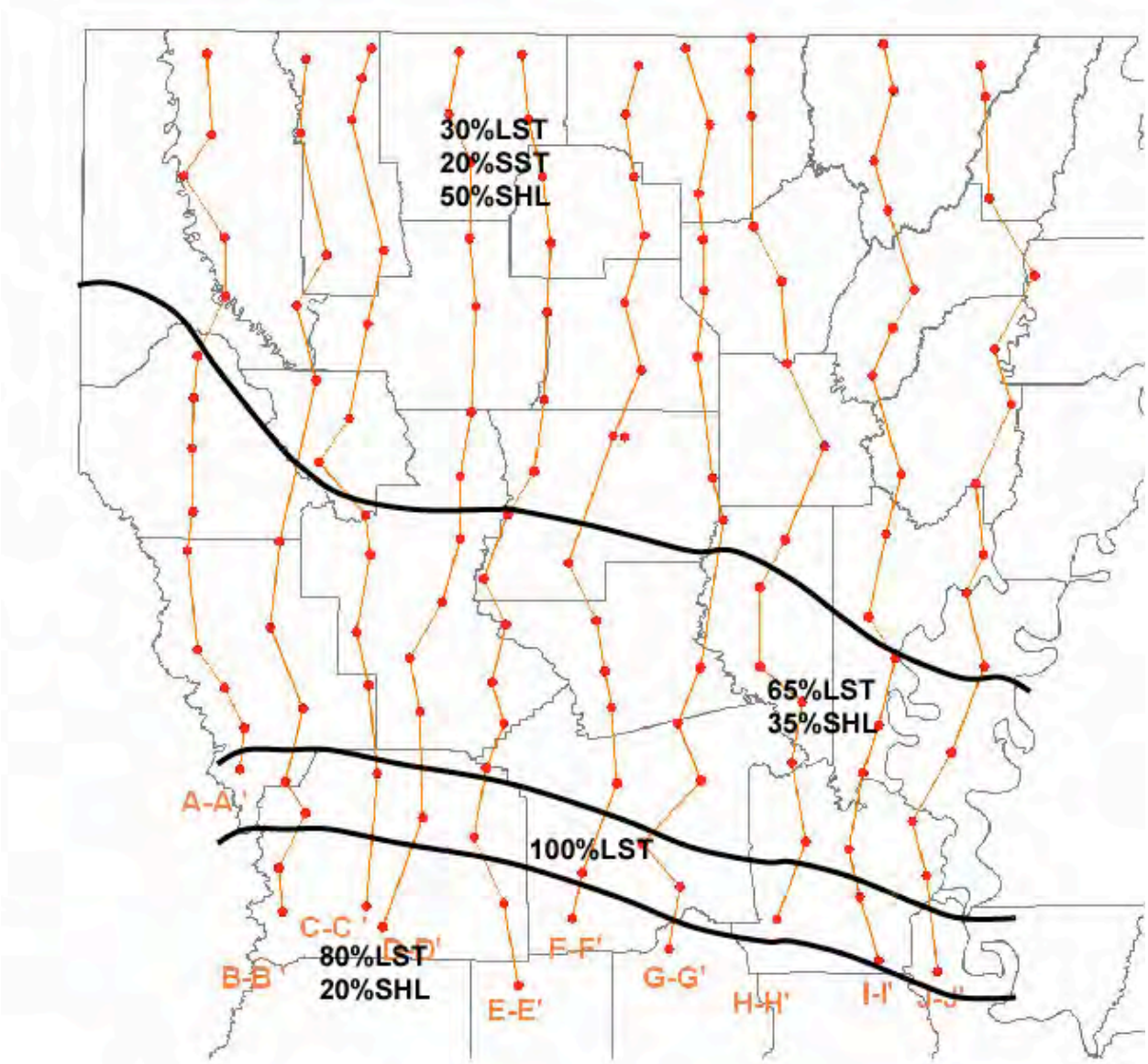


Figure 30. Lithology map of Upper Glen Rose. Prepared by Roger Barnaby.

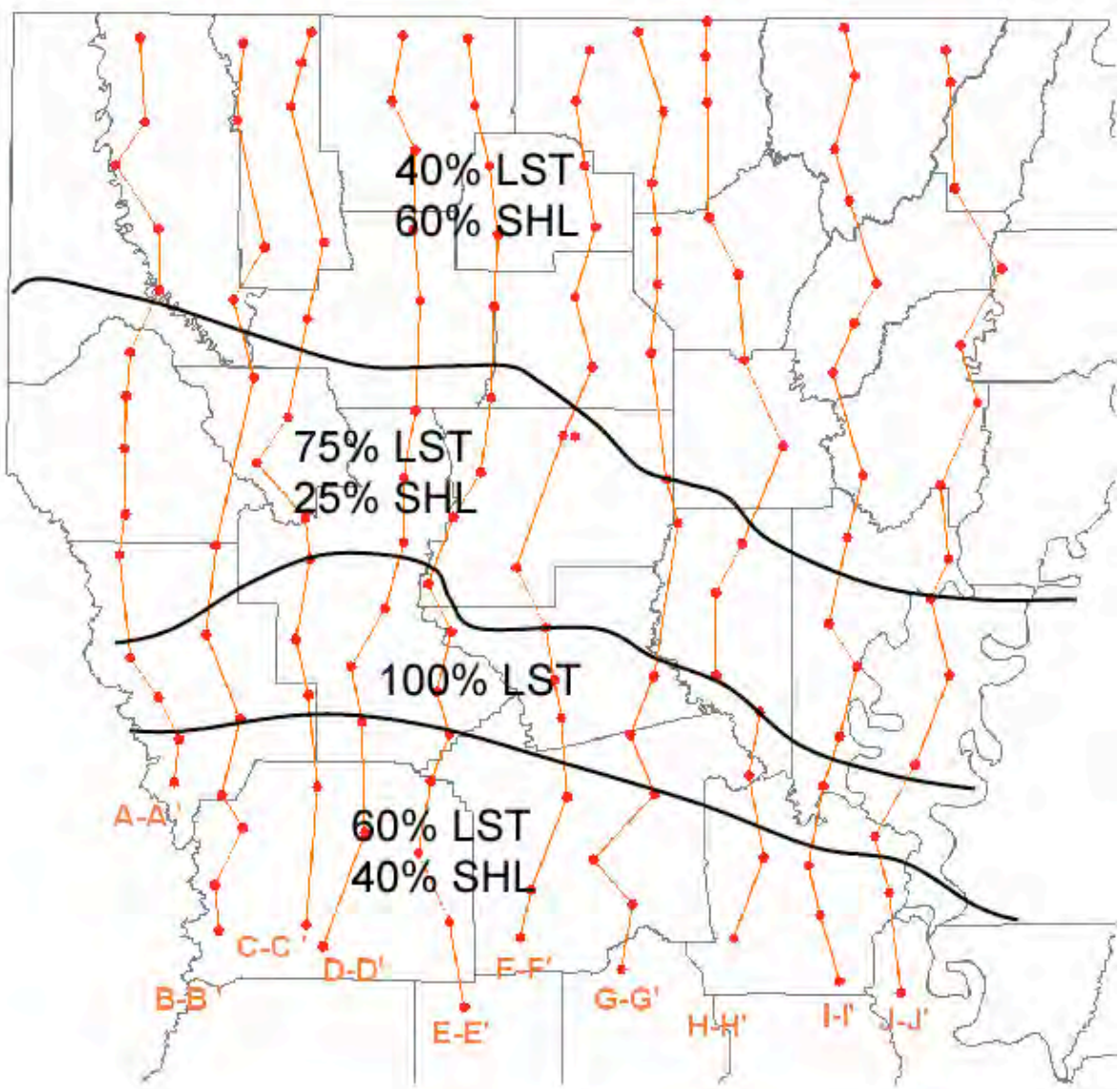


Figure 31. Lithology map of Mooringsport. Prepared by Roger Barnaby.

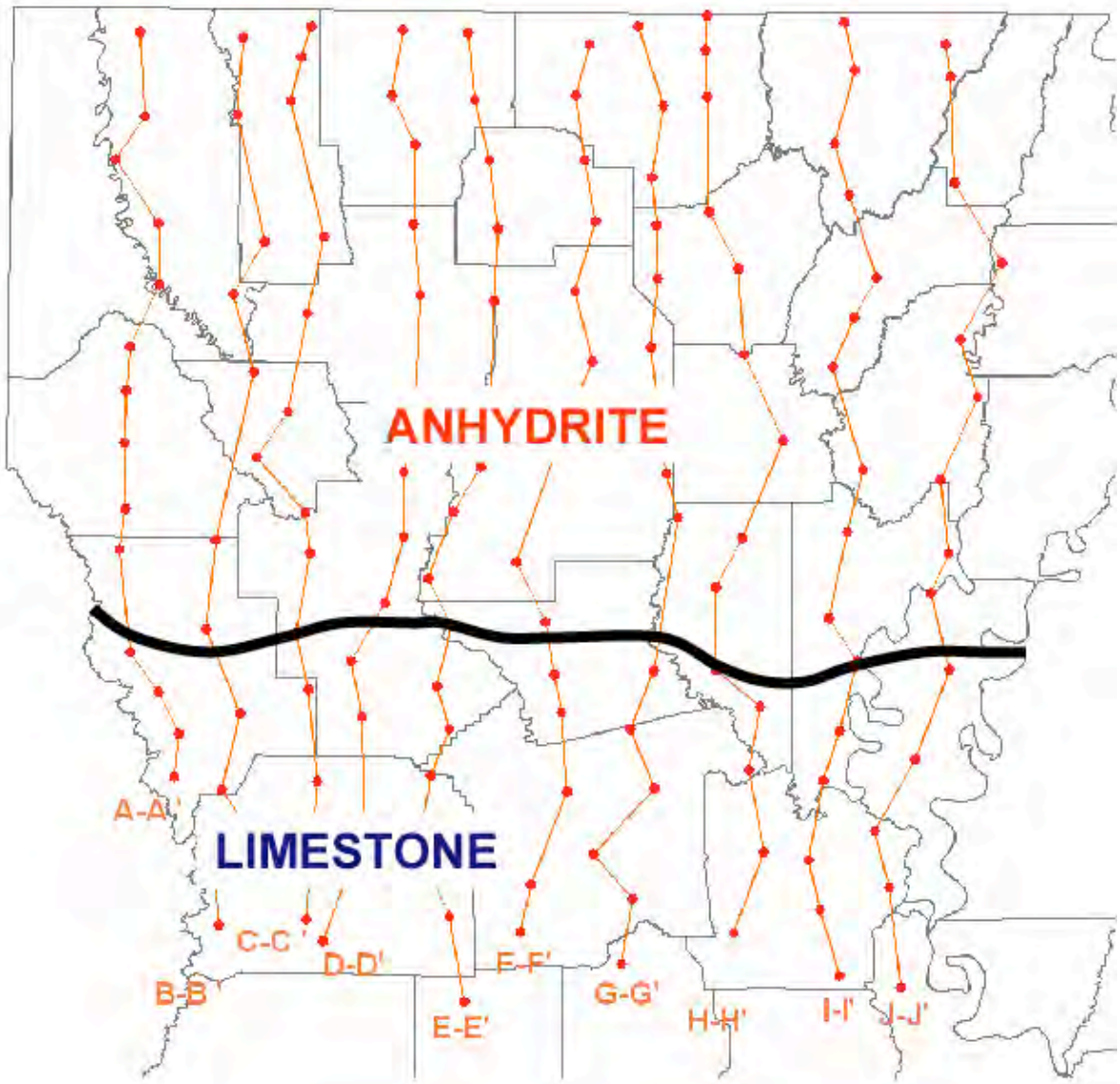


Figure 32. Lithology map of Ferry Lake. Prepared by Roger Barnaby.

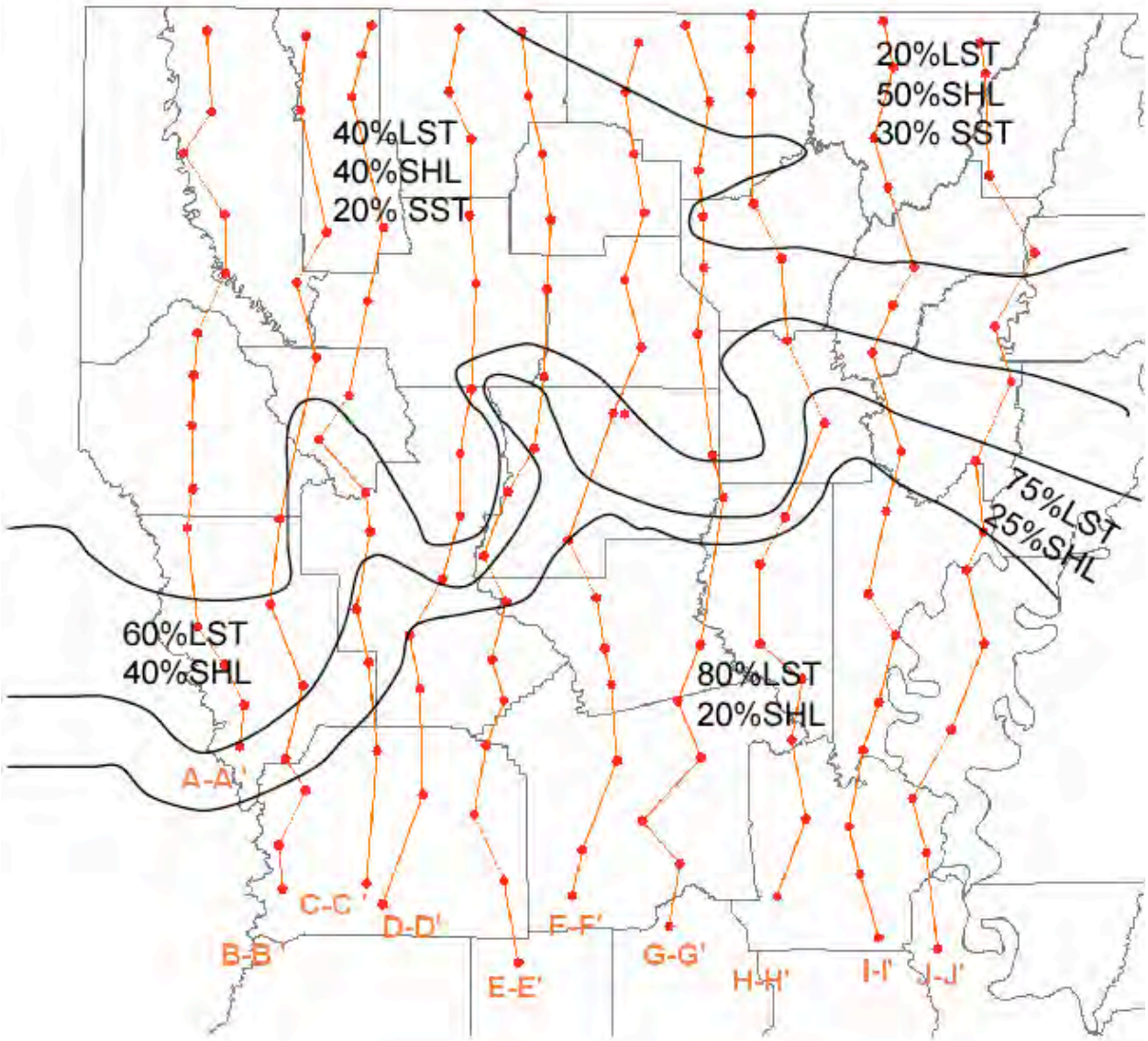


Figure 33. Lithology map of Rodessa. Prepared by Roger Barnaby.

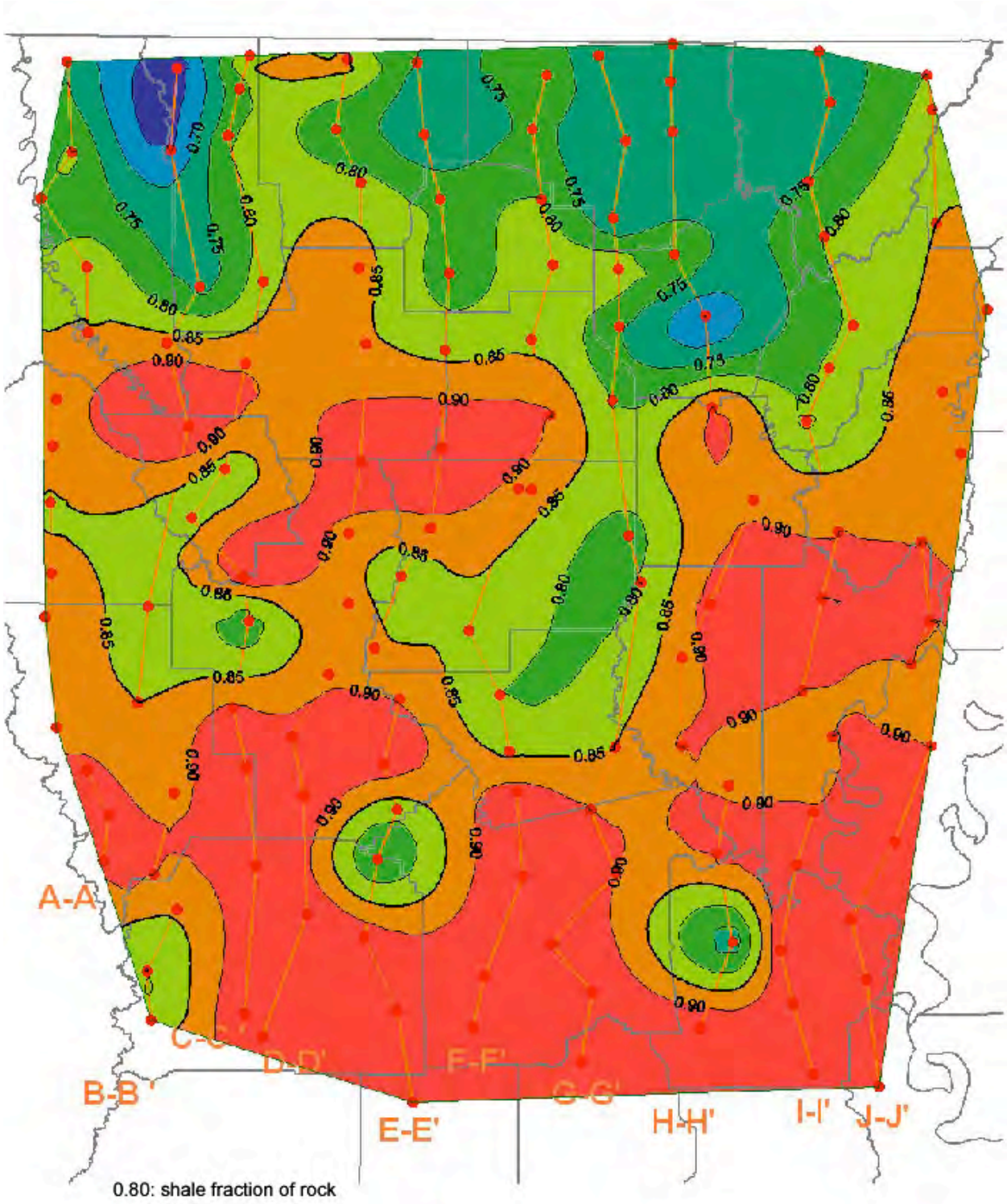


Figure 34. Lithology map of Bexar. Prepared by Roger Barnaby.

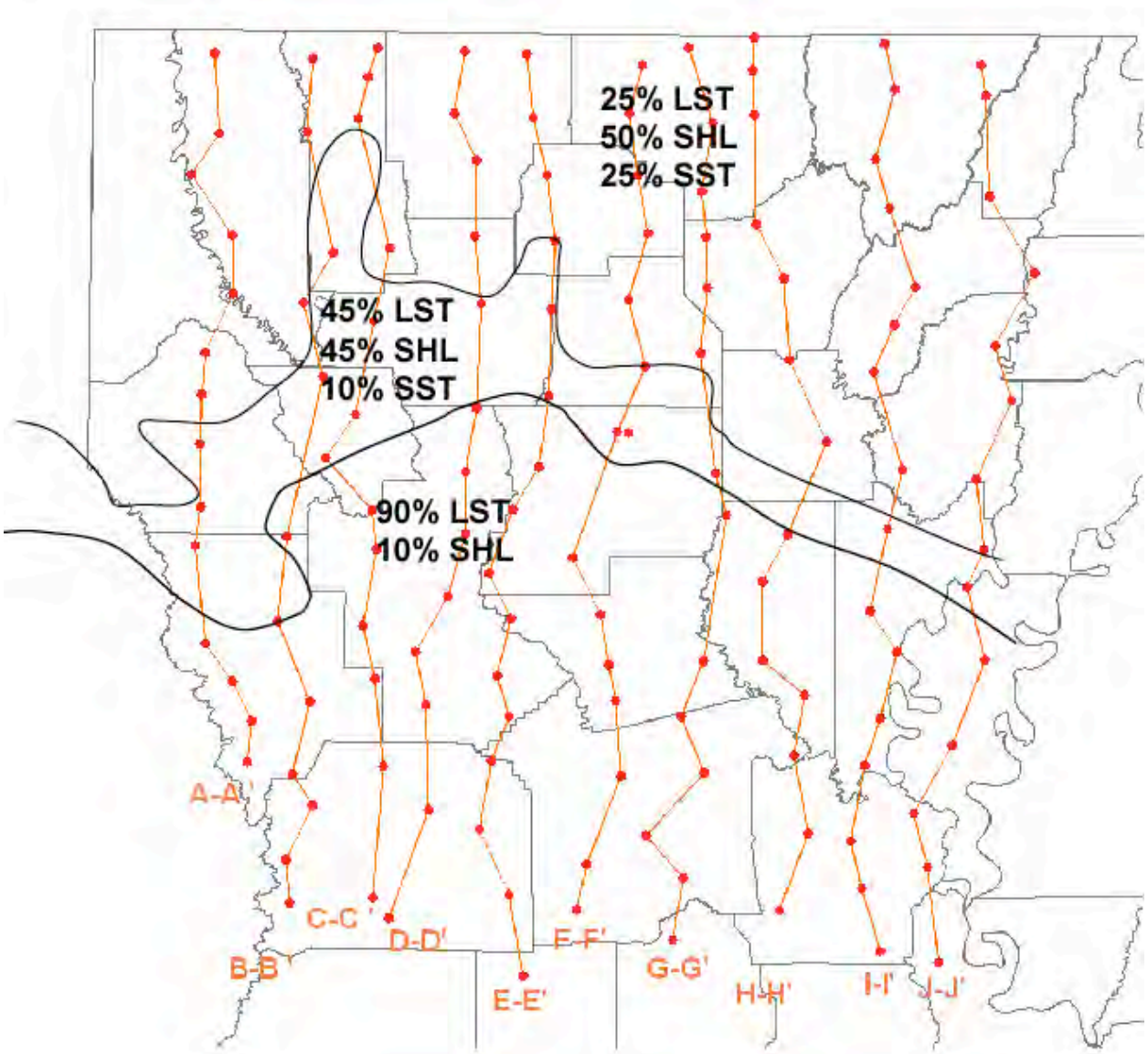


Figure 35. Lithology map of James. Prepared by Roger Barnaby.

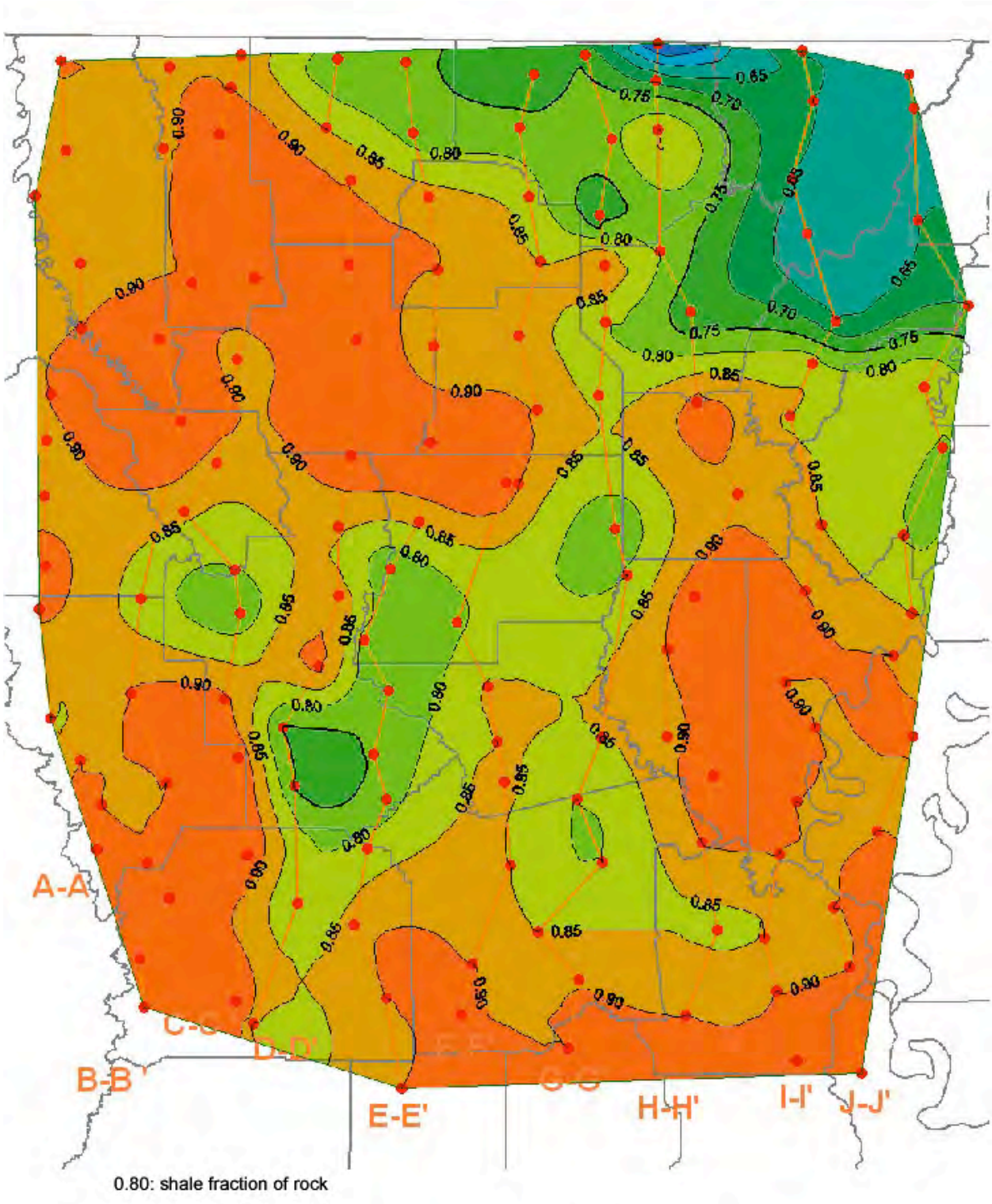


Figure 36. Lithology map of Pine Island. Prepared by Roger Barnaby.

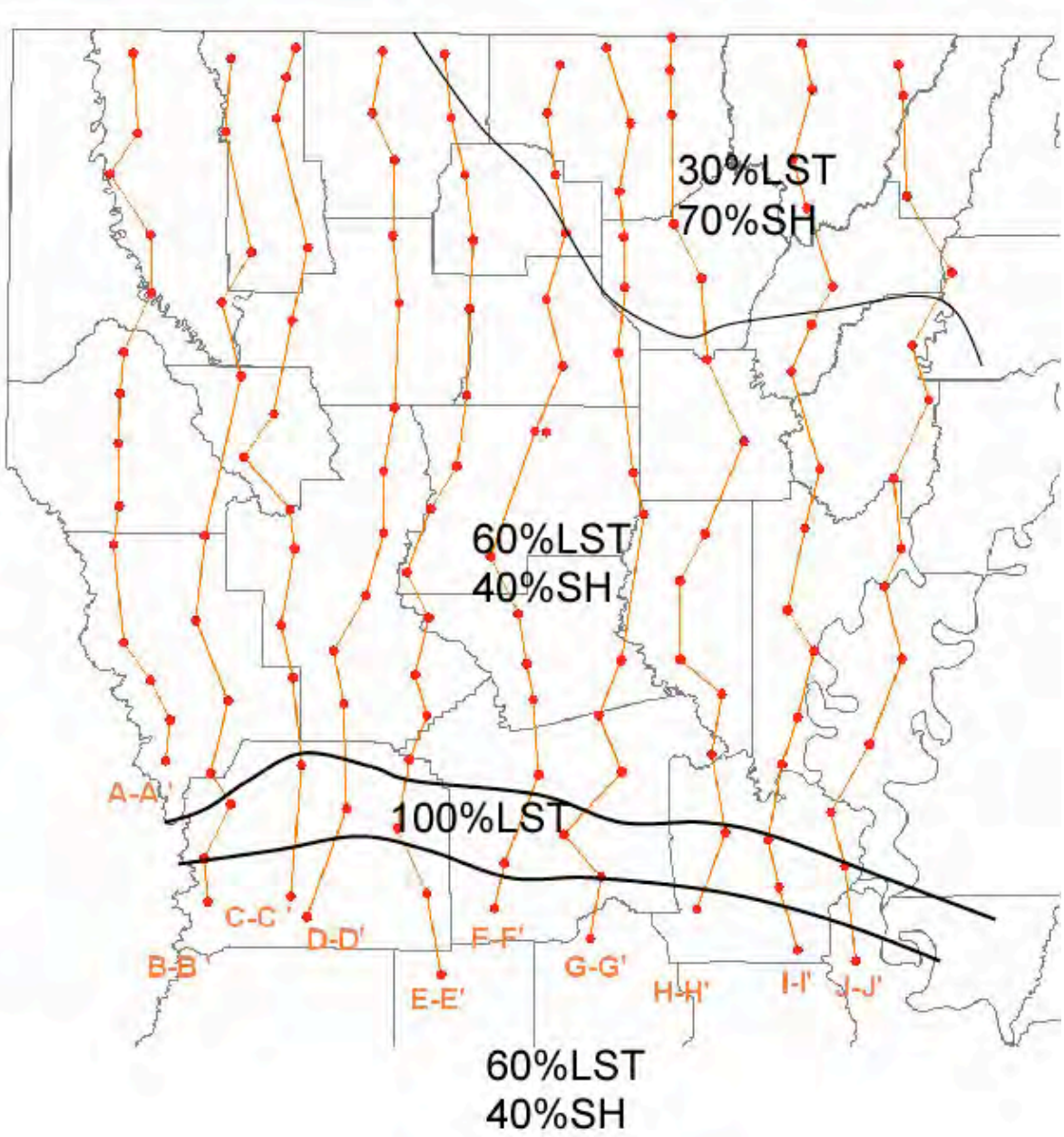


Figure 37. Lithology map of Sligo. Prepared by Roger Barnaby.

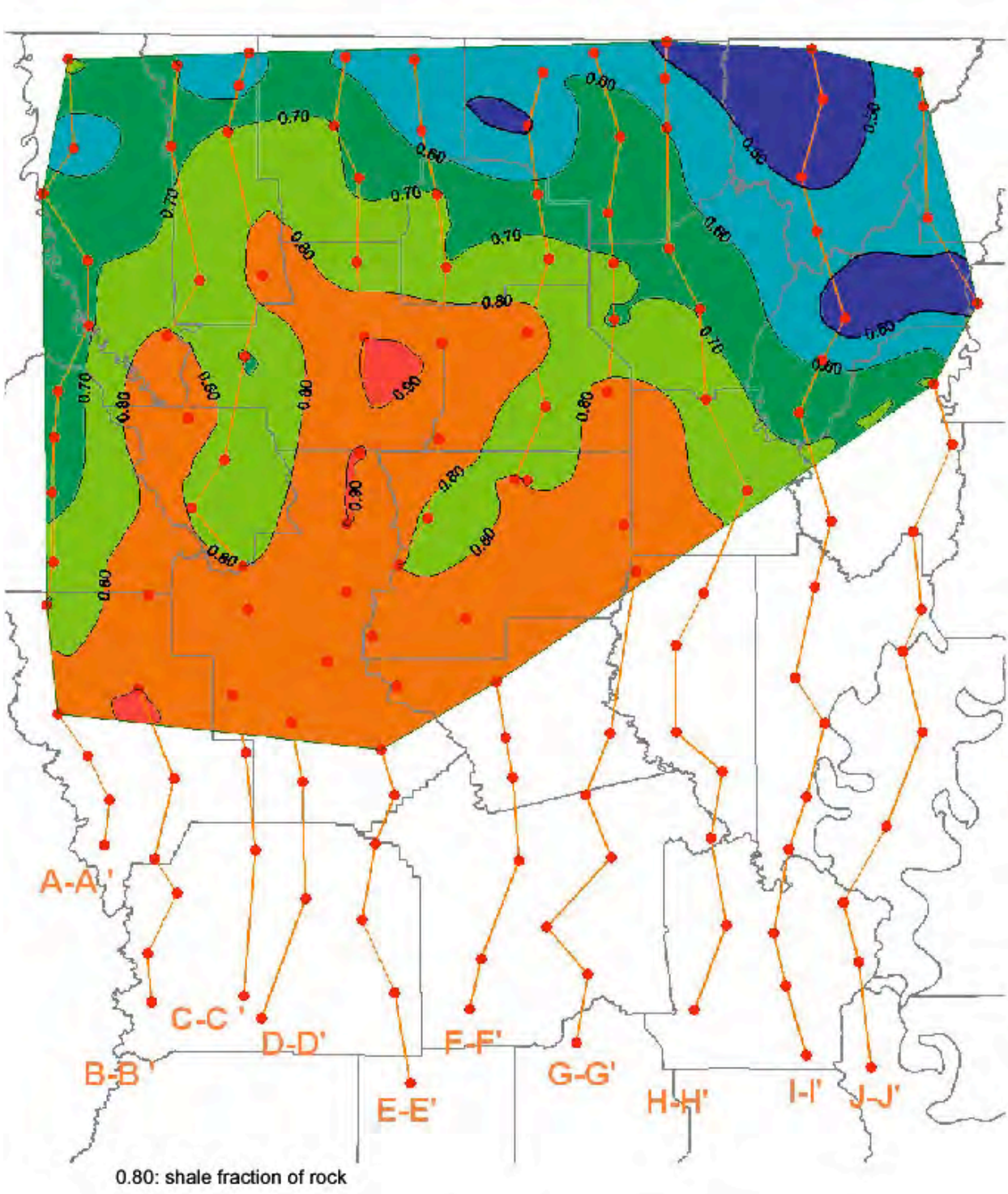


Figure 38. Lithology map of Hosston. Prepared by Roger Barnaby.

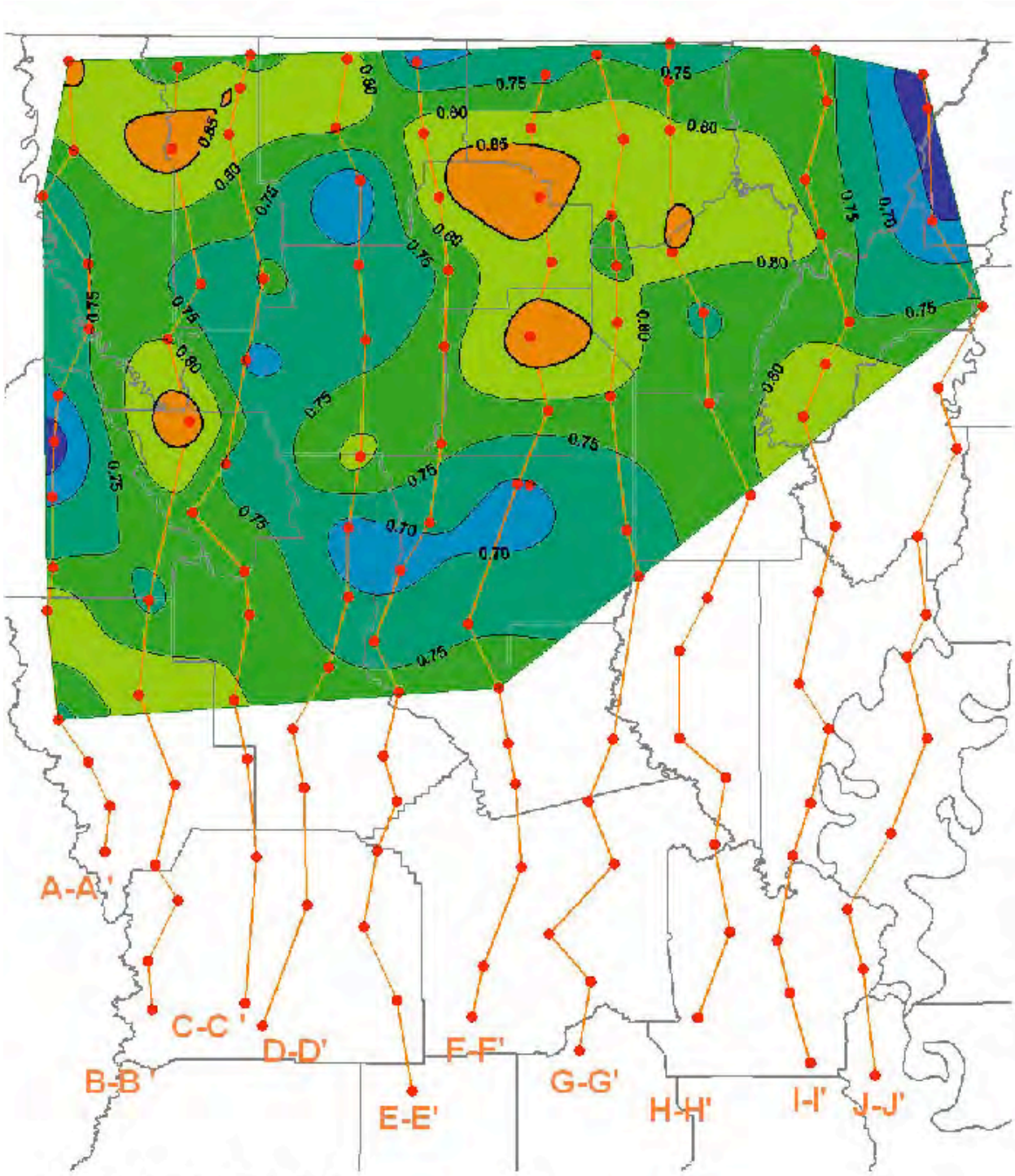


Figure 39. Lithology map of Cotton Valley. Prepared by Roger Barnaby.

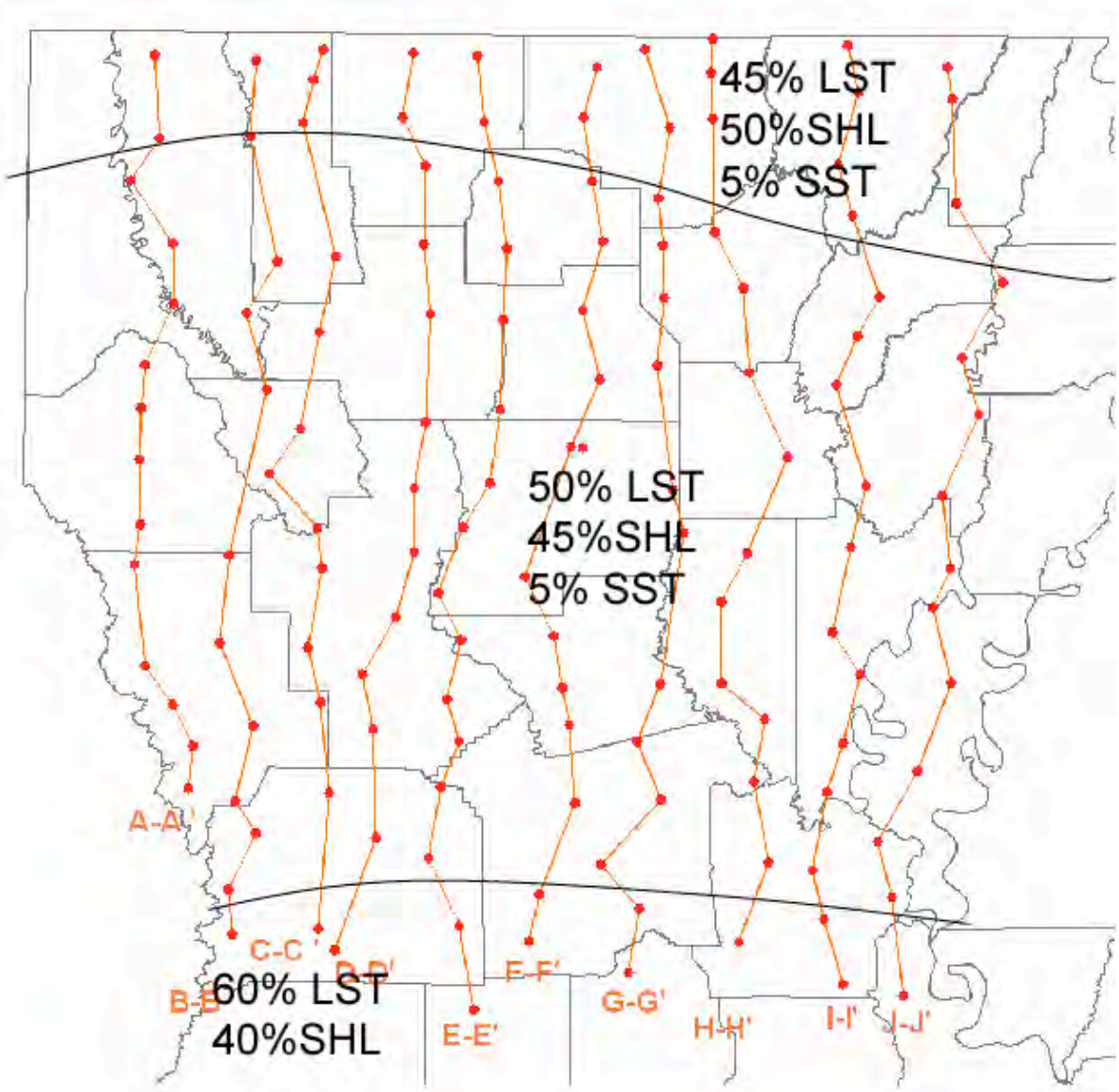


Figure 40. Lithology map of Smackover. Prepared by Roger Barnaby.

Table 1. Comparison of North Louisiana Salt Basin and Mississippi Interior Salt Basin.

| Petroleum system characteristics (Smackover) | North Louisiana Salt Basin | | | | Mississippi Interior Salt Basin | |
|---|---|---|---|---|---|---|
| Thickness (m) | 396 | | | | 116 | |
| Kerogen type | Type IIS (Microbial/Amorphous) | | | | Type IIS (Microbial/Amorphous) | |
| TOC (wt%) range | 0.06 – 8.42 | | | | 0.24 – 4.55 | |
| TOC (wt%) average | 0.58 (measured) - 1.0 (calculated for modeling) | | | | 0.85 (measured) – 1.5 (calculated for modeling) | |
| Depth to generate oil, m (ft) | 1829 – 2591 (6,000-8,500) | | | | 2438 – 3353 (8,000-11,000) | |
| Depth to generate gas, m (ft) | 3658 – 4877 (12,000-16,000) | | | | 5029 – 6401 (16,500-21,000) | |
| | Basin proper | | Monroe Uplift | Sabine Uplift | Updip/Margin | Downdip/Center |
| | Updip/Margin | Downdip/Center | | | | |
| Maturity ($R_o$%) | 0.8-1.3 | 1.3->2.6 | <0.5-1.3 | 0.8-1.5 | <0.5-1 | 1-2.5 |
| Time to generate oil (Ma) | 115-135 | 125-140 | 105-125 | 115-125 | 35-90 | 90-135 |
| Time to generate gas (Ma) | Present-50 | 50-105 | No gas | 20-50 | No gas | 12-80 |
| Time of expulsion (Ma) | 50-110 | 100-125 | 100–120* | 90-105 | 30-50 | 60-110 |
| Time of peak expulsion (Ma) | 40-105 | 80-120 | 90-110* | 60-100 | Present-45 | 50-100 |
| Heat flow (HFU) | 1.25 | | | | 1.09 | |

* Only in the southwest portion of Monroe Uplift

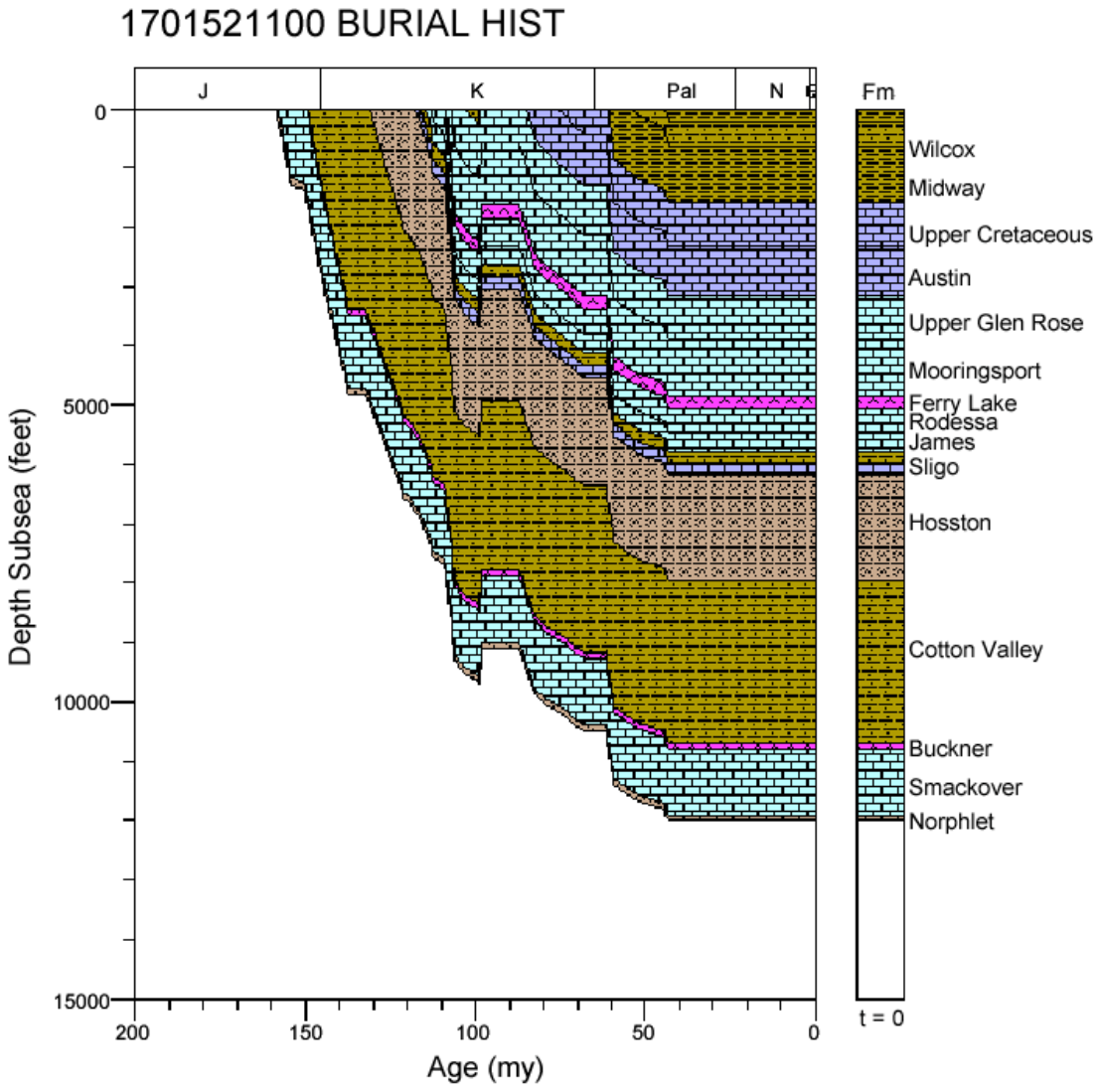


Figure 41. Burial history for well 1701521100, North Louisiana Salt Basin.

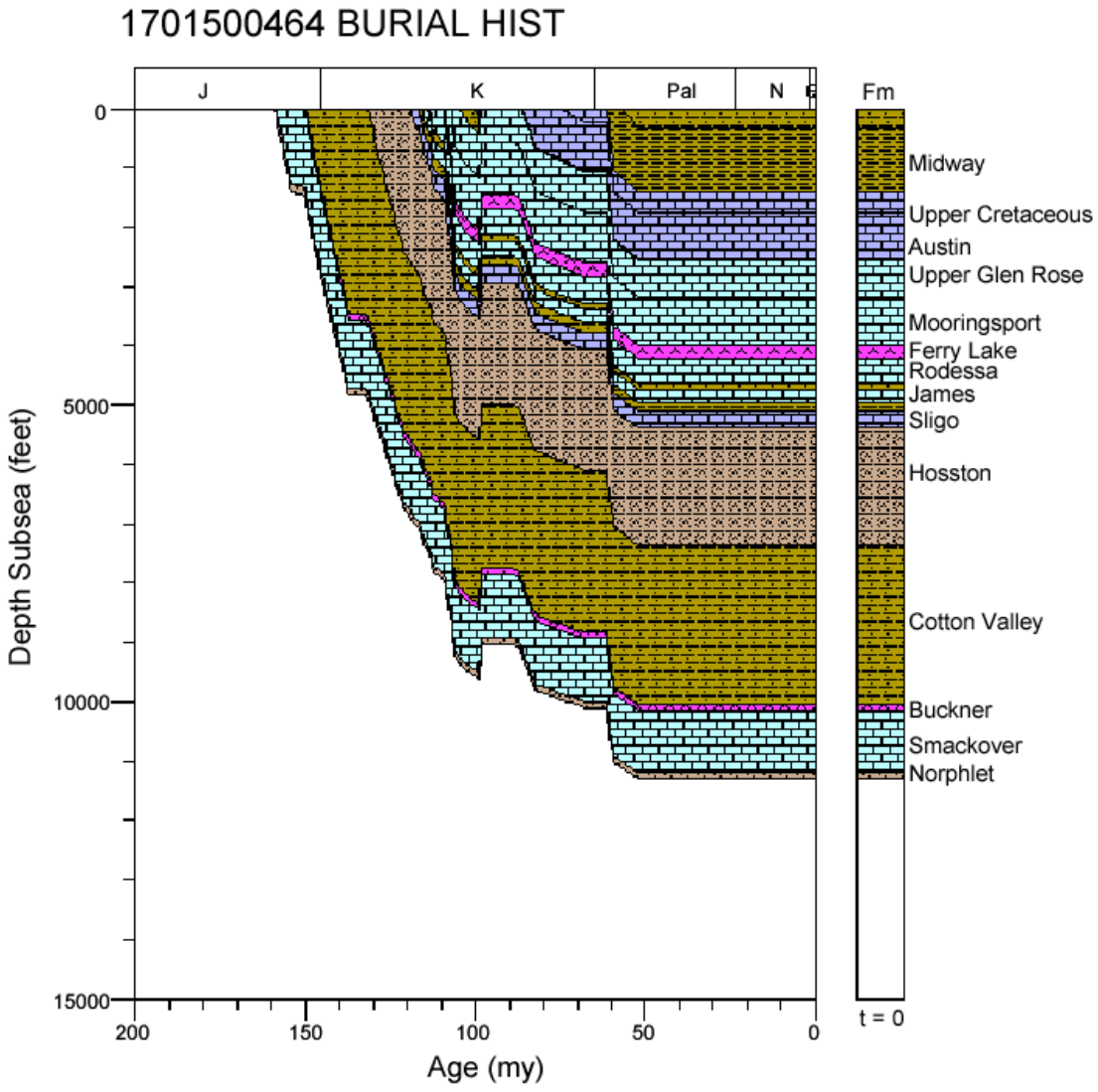


Figure 42. Burial history for well 1701500464, North Louisiana Salt Basin.

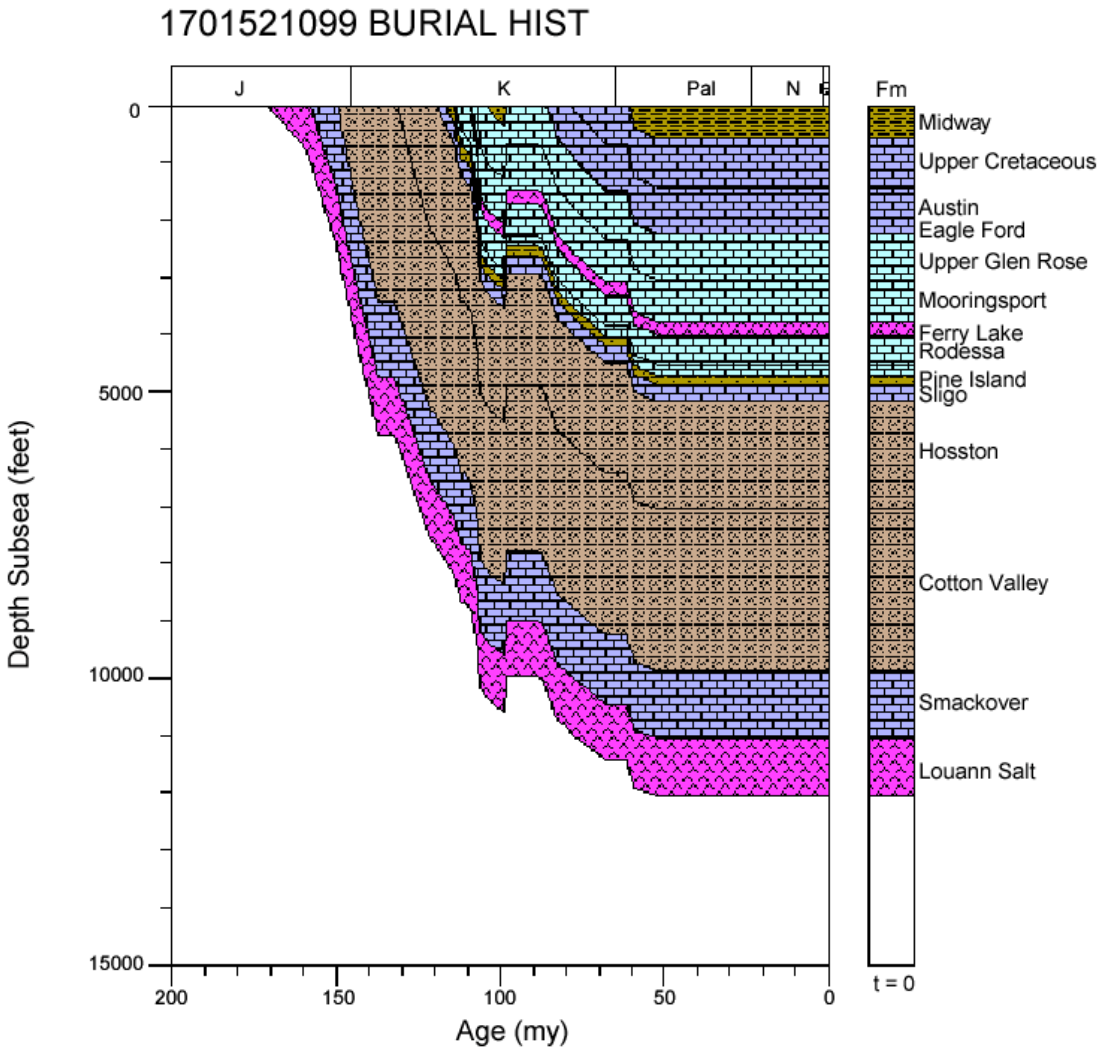


Figure 43. Burial history for well 1701521099, North Louisiana Salt Basin.

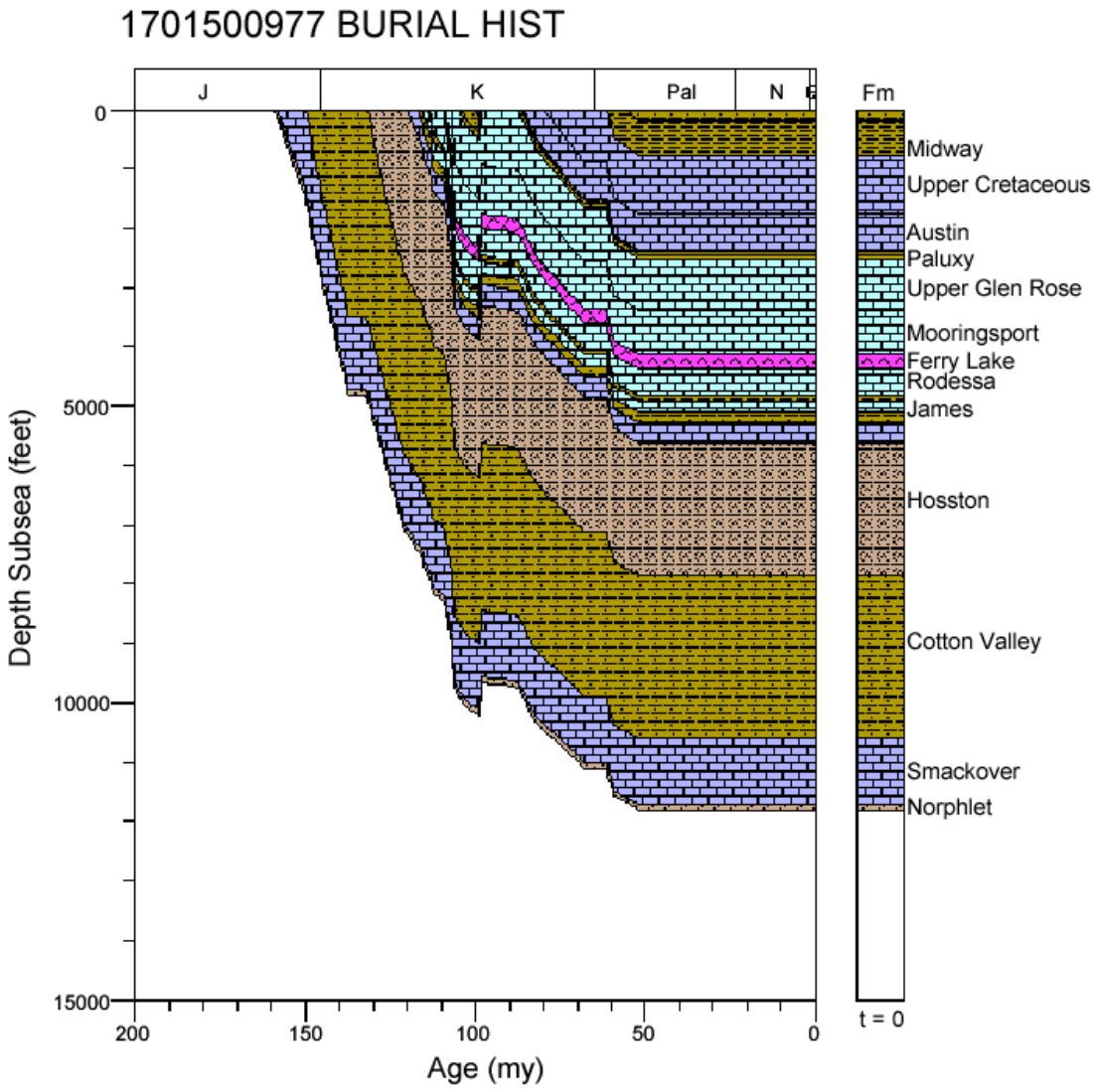


Figure 44. Burial history for well 1701500977, North Louisiana Salt Basin.

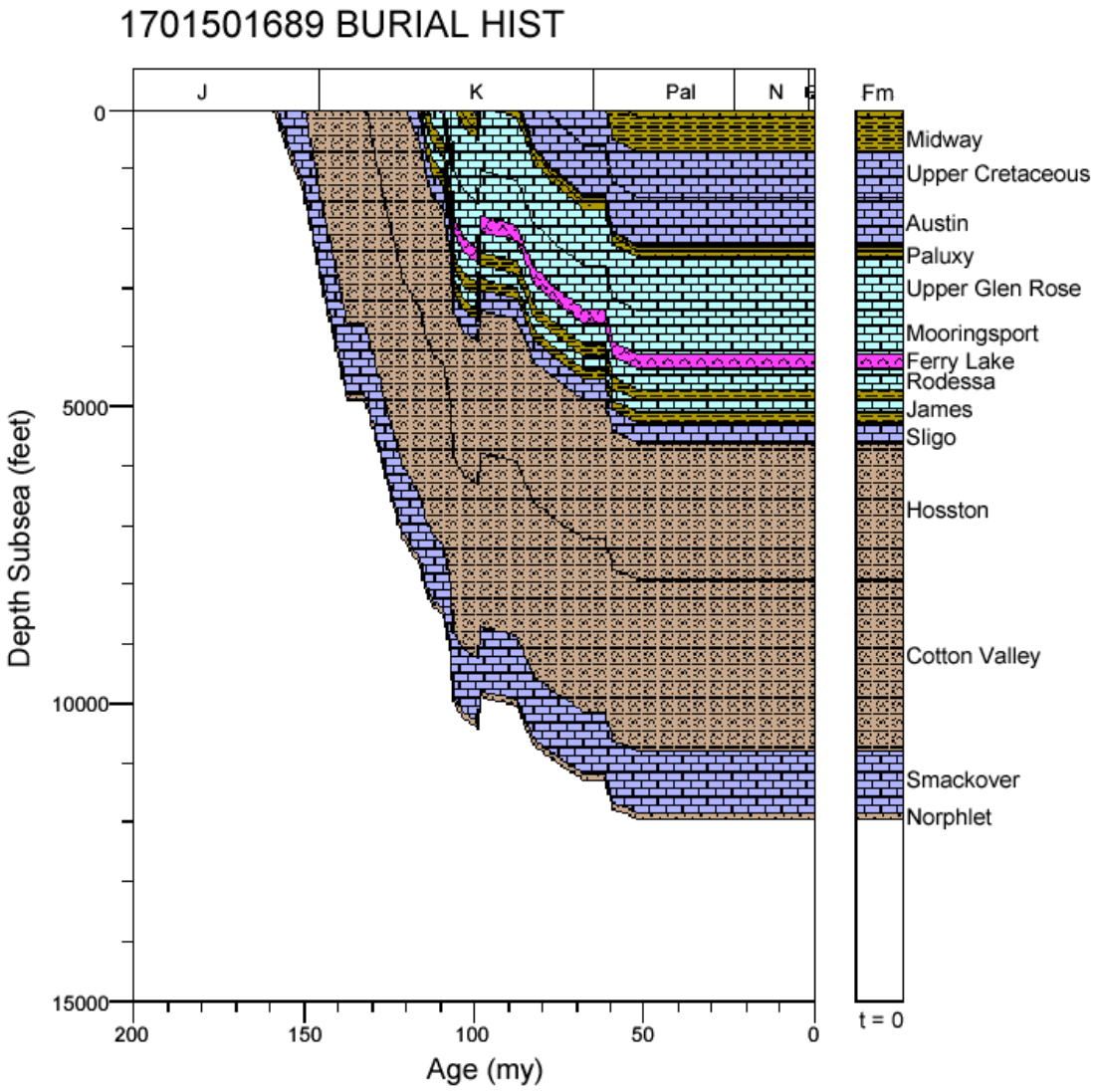


Figure 45. Burial history for well 1701501689, North Louisiana Salt Basin.

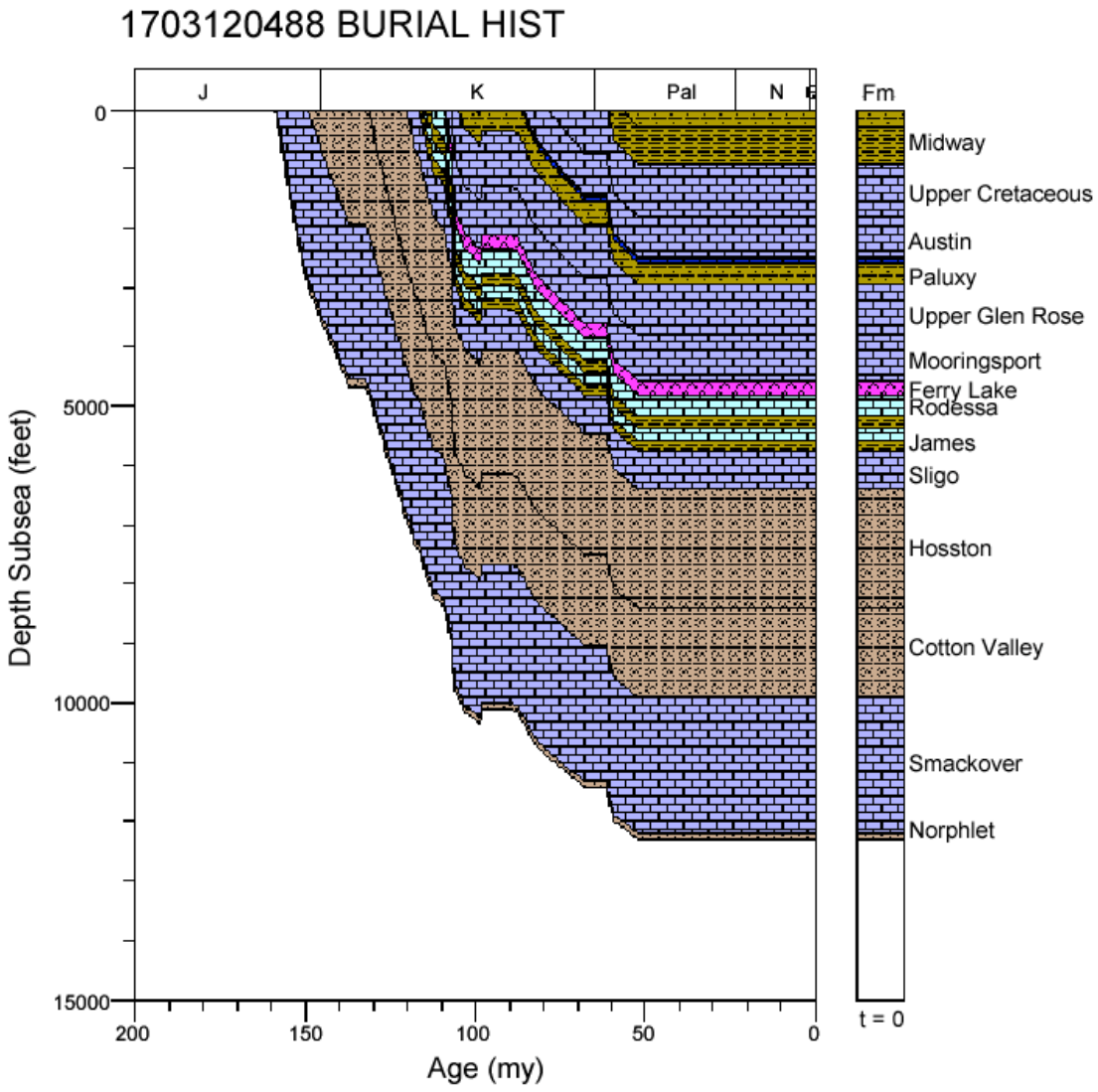


Figure 46. Burial history for well 1703120488, North Louisiana Salt Basin.

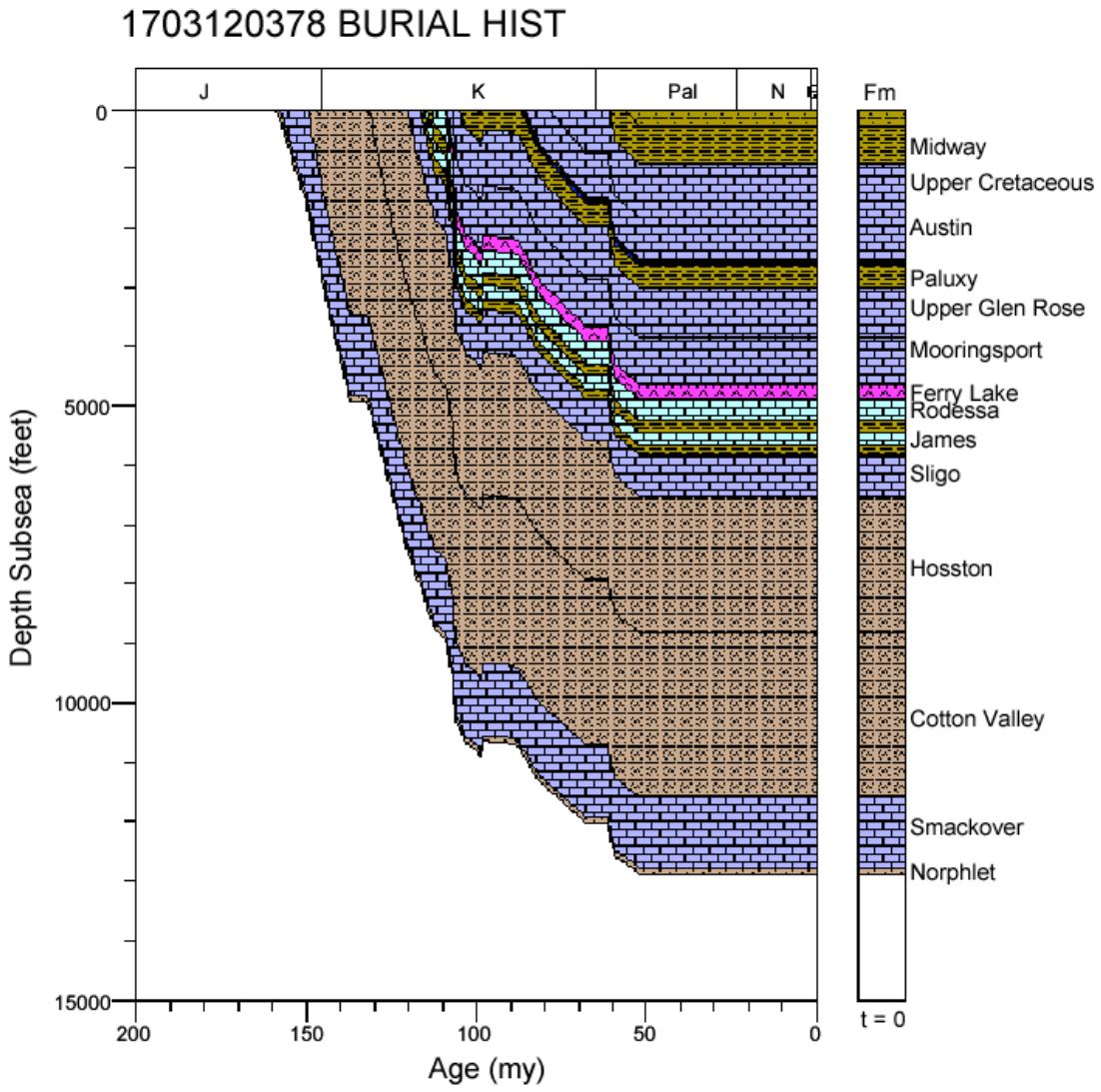


Figure 47. Burial history for well 1703120378, North Louisiana Salt Basin.

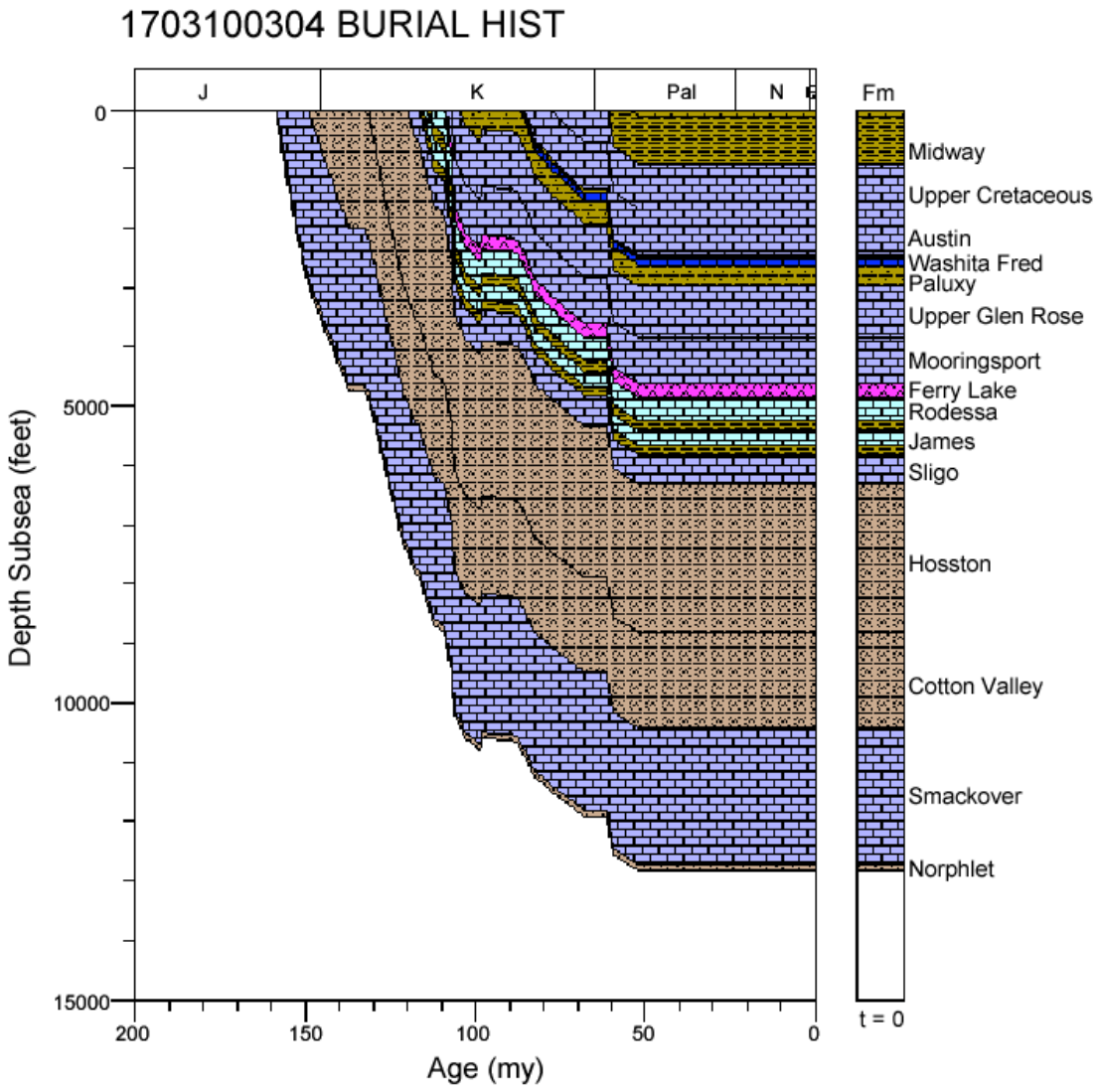


Figure 48. Burial history for well 1703100304, North Louisiana Salt Basin.

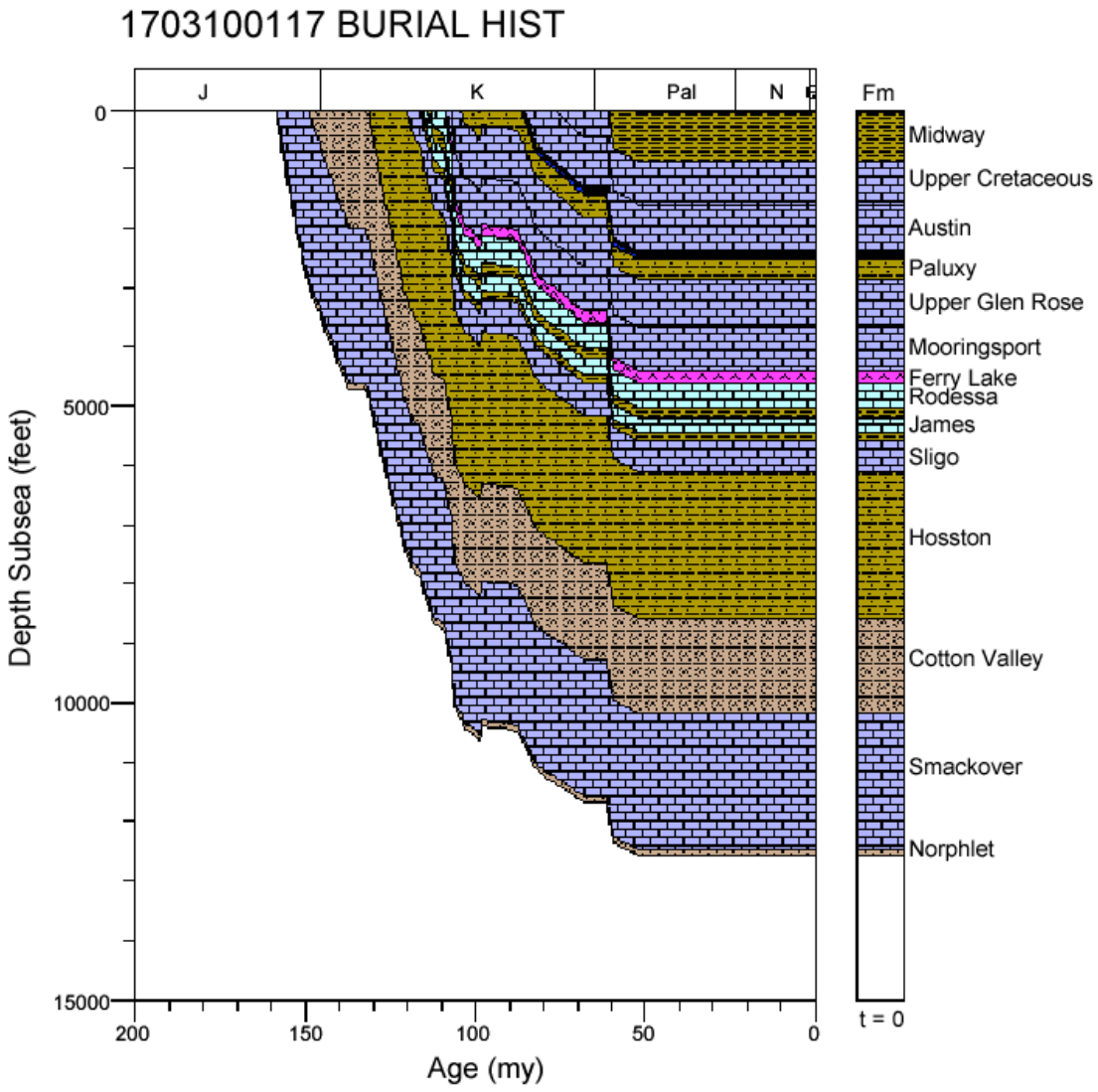


Figure 49. Burial history for well 1703100117, North Louisiana Salt Basin.

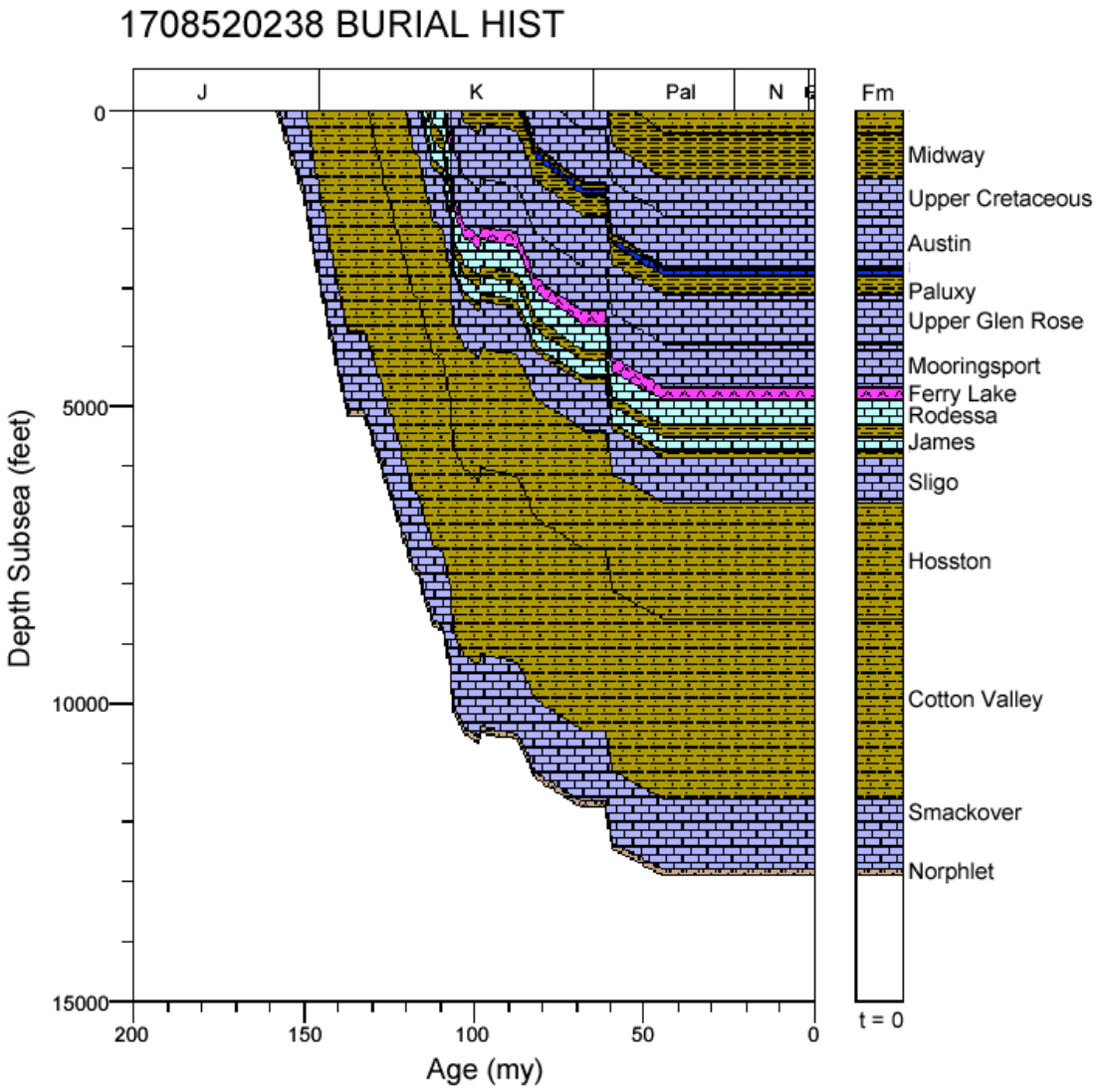


Figure 50. Burial history for well 1708520238, North Louisiana Salt Basin.

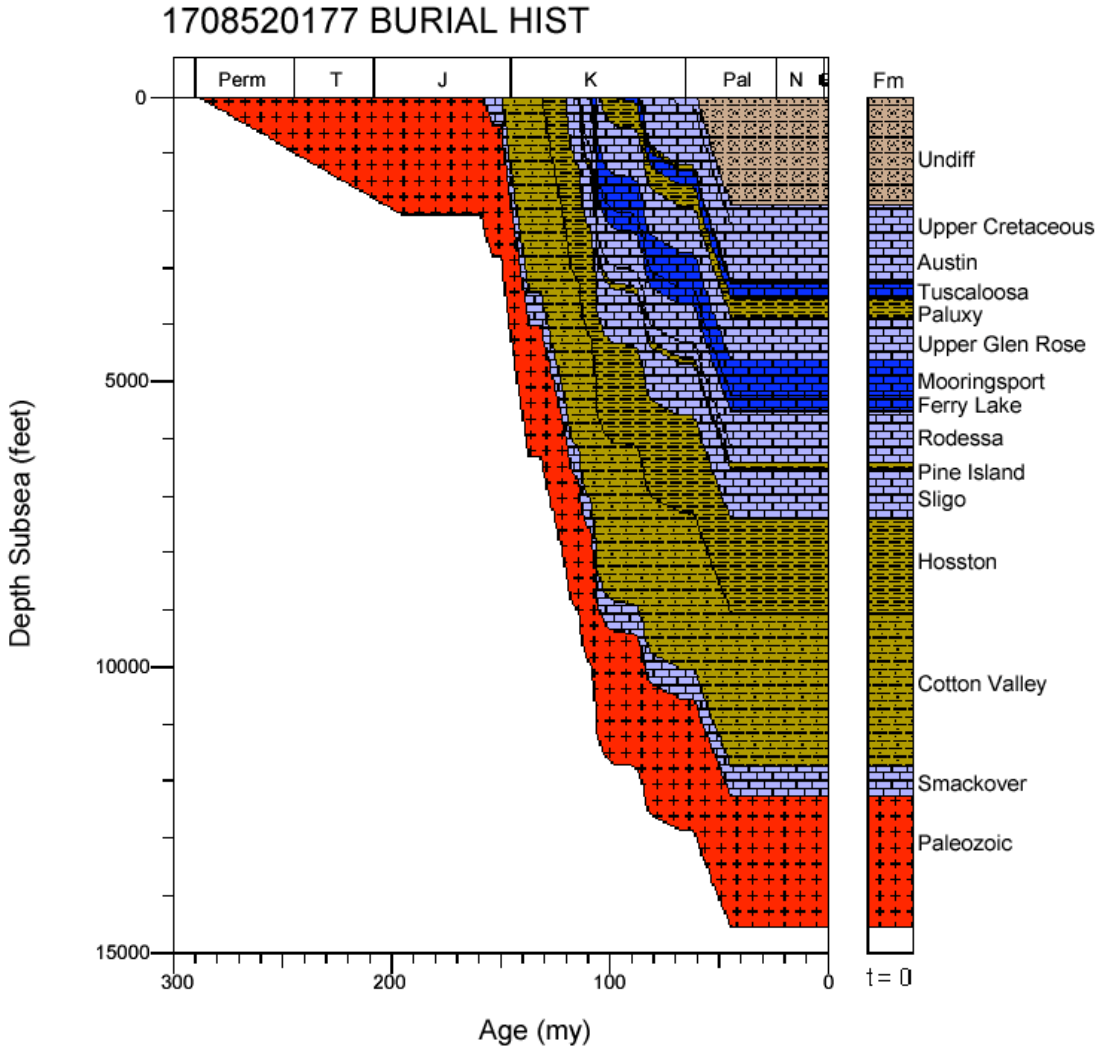


Figure 51. Burial history for well 1708520177, North Louisiana Salt Basin.

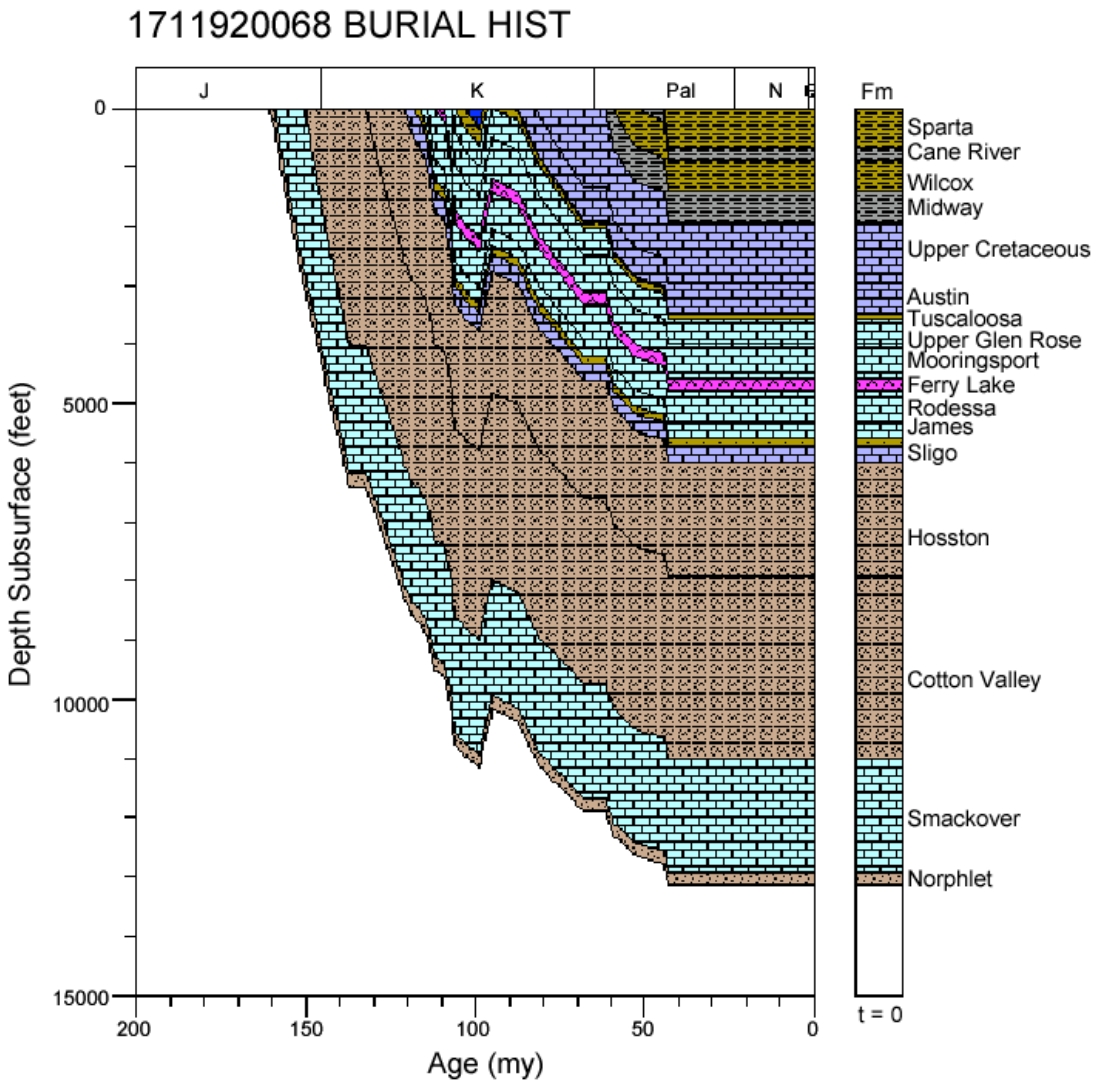


Figure 52. Burial history for well 1711920068, North Louisiana Salt Basin.

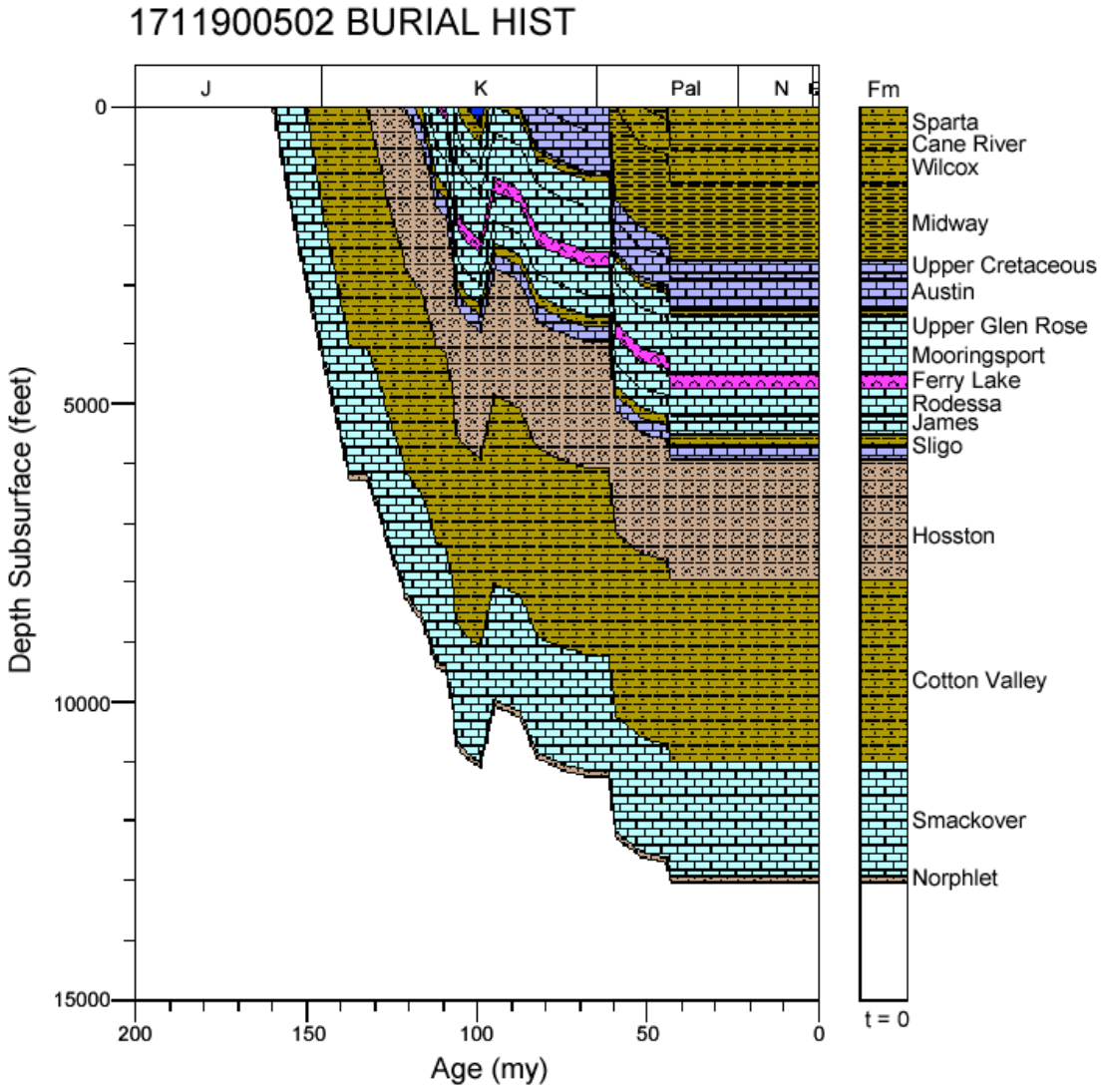


Figure 53. Burial history for well 1711900502, North Louisiana Salt Basin.

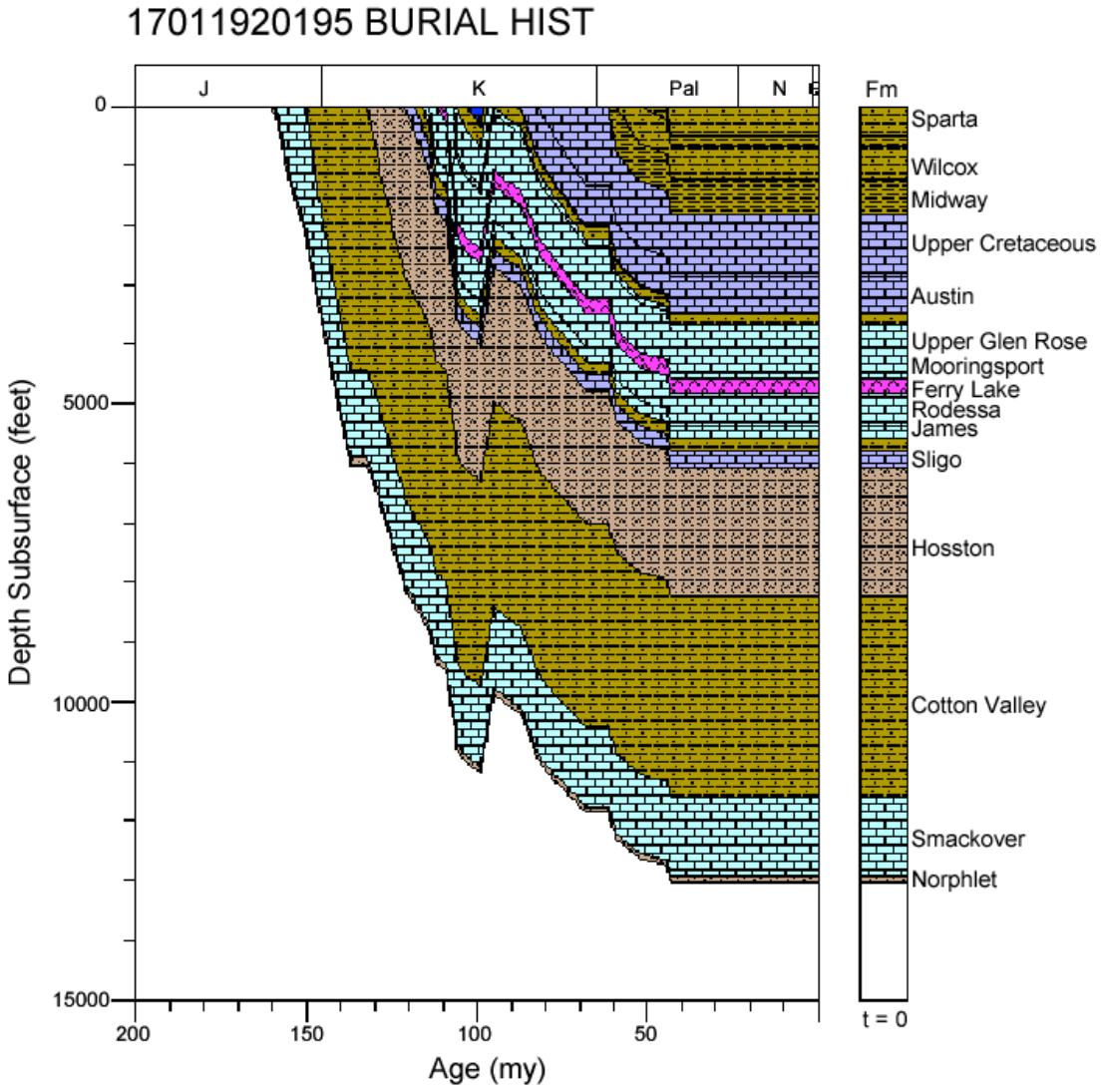


Figure 54. Burial history for well 1711920195, North Louisiana Salt Basin.

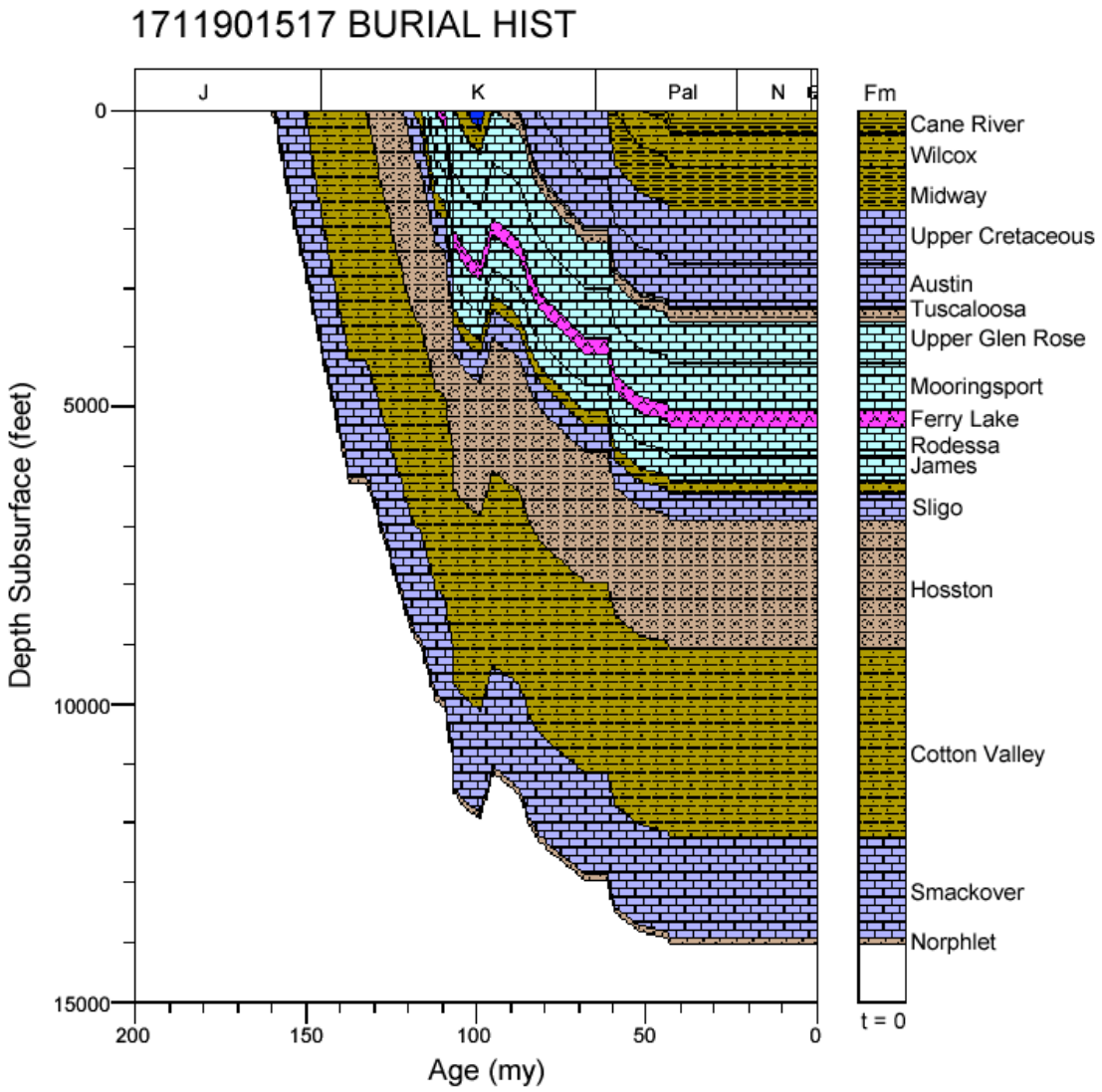


Figure 55. Burial history for well 1711901517, North Louisiana Salt Basin.

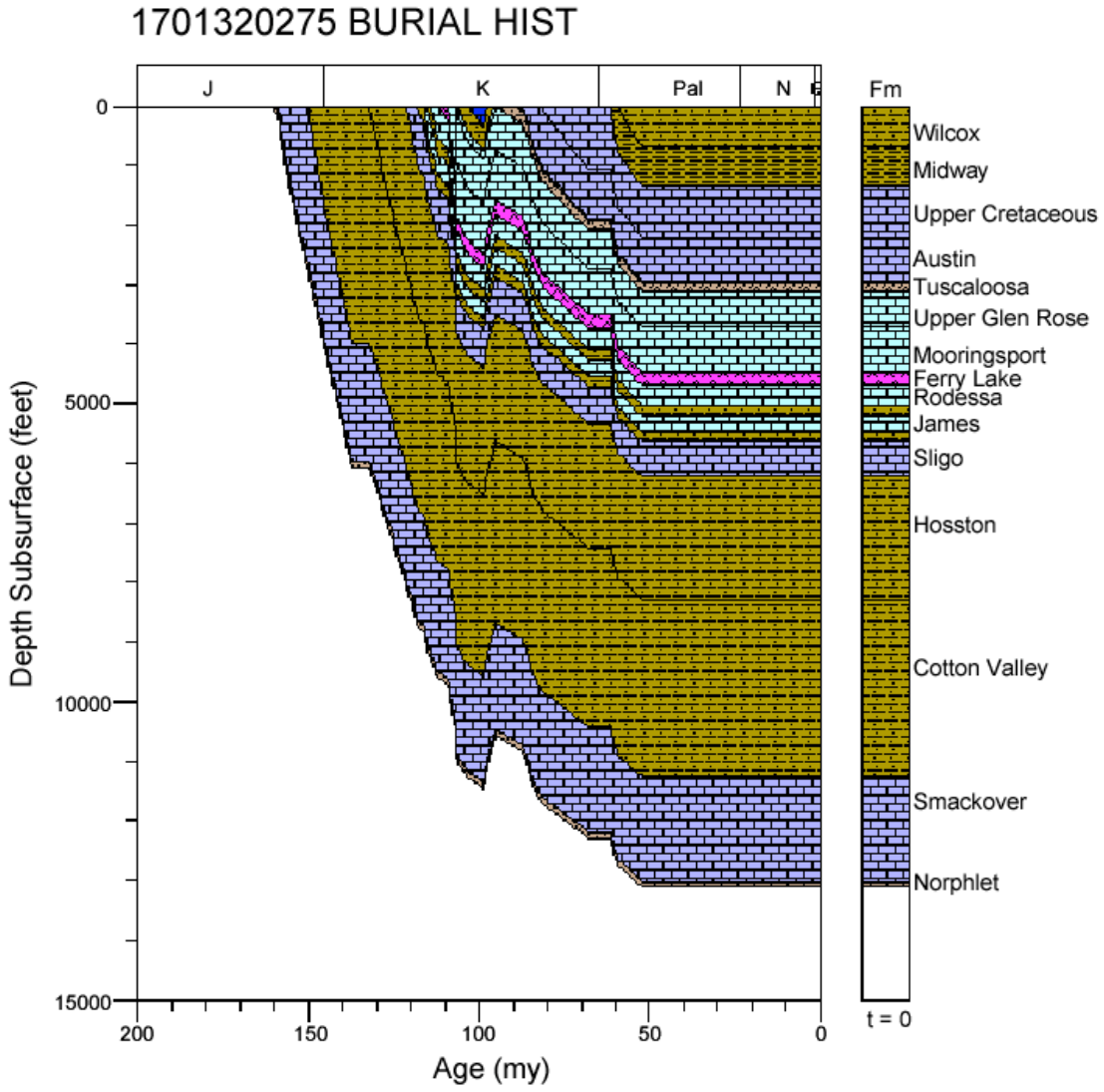


Figure 56. Burial history for well 1701320275, North Louisiana Salt Basin.

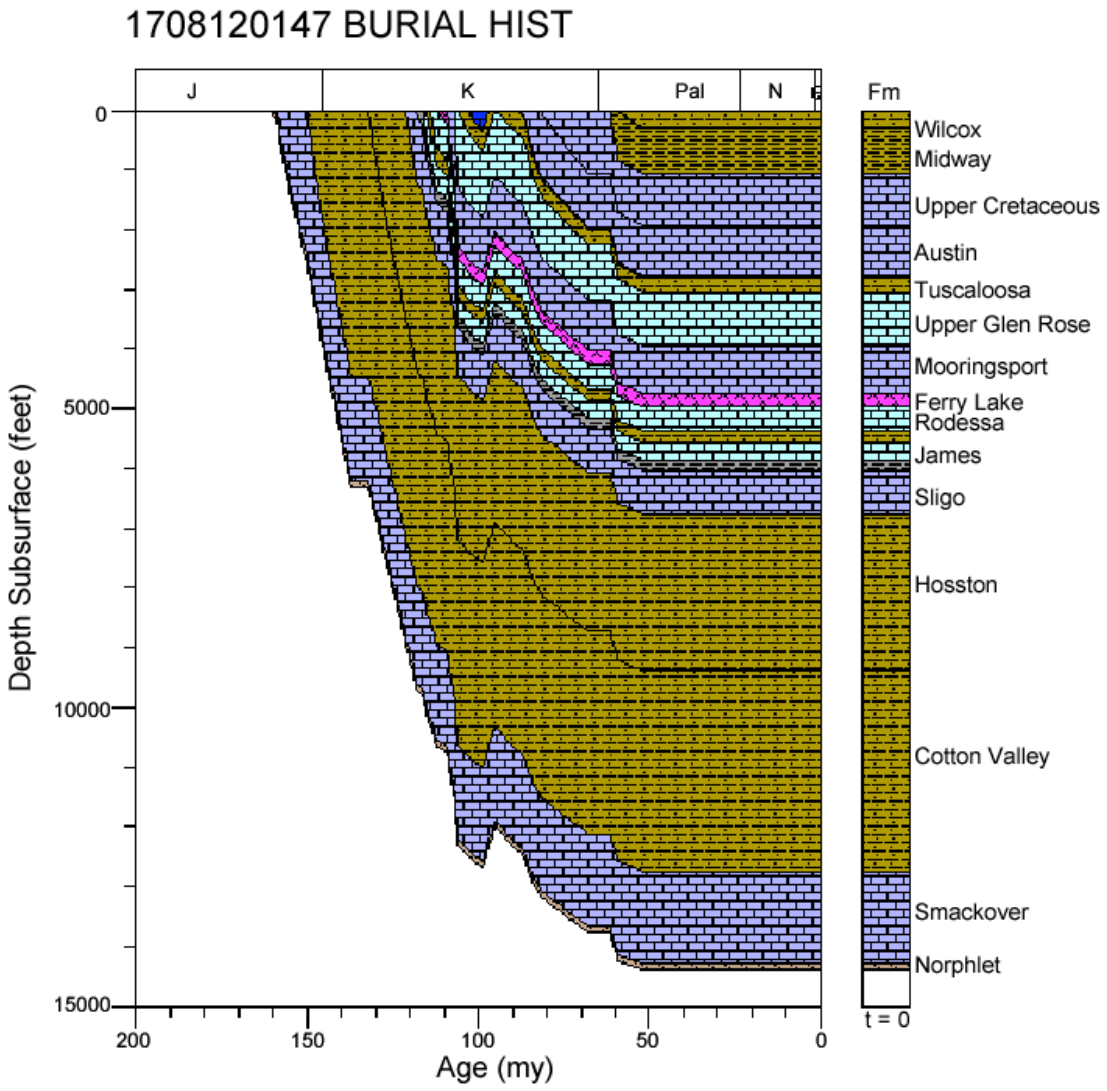


Figure 57. Burial history for well 1708120147, North Louisiana Salt Basin.

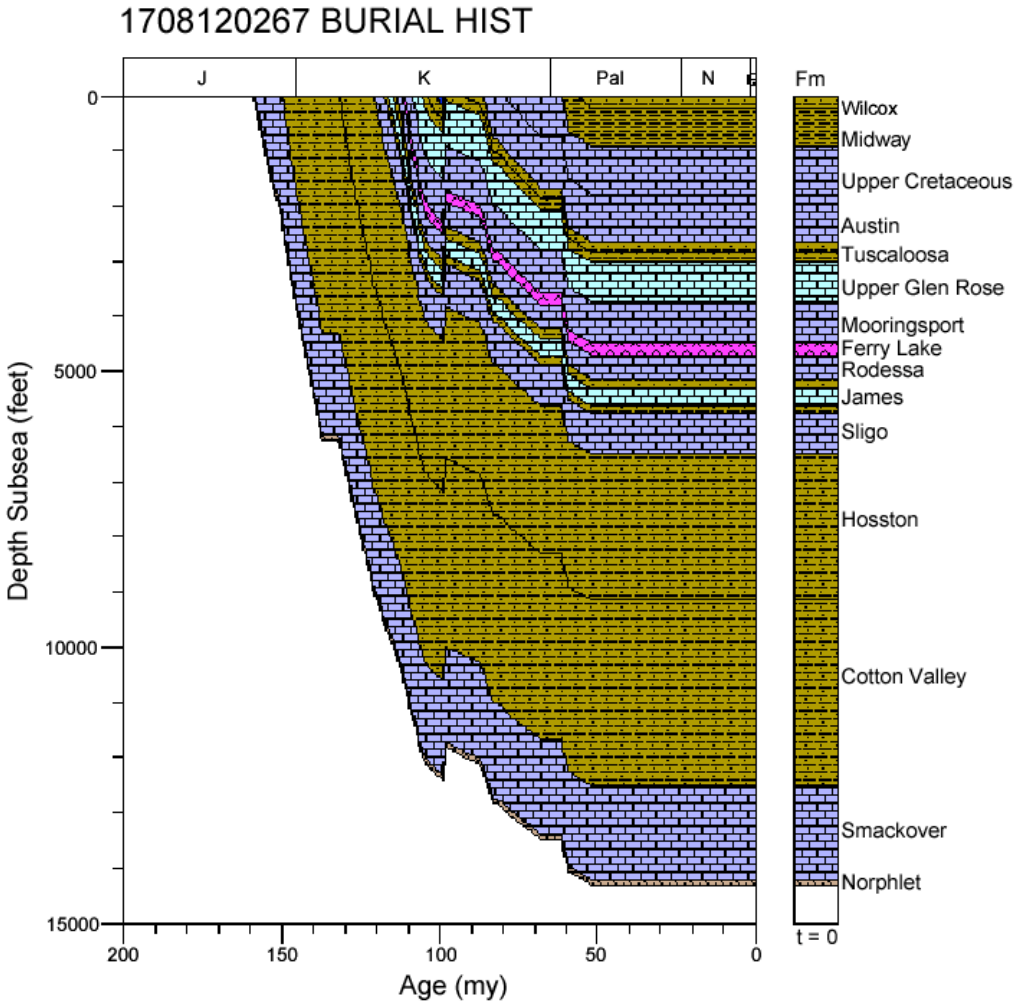


Figure 58. Burial history for well 1708120267, North Louisiana Salt Basin.

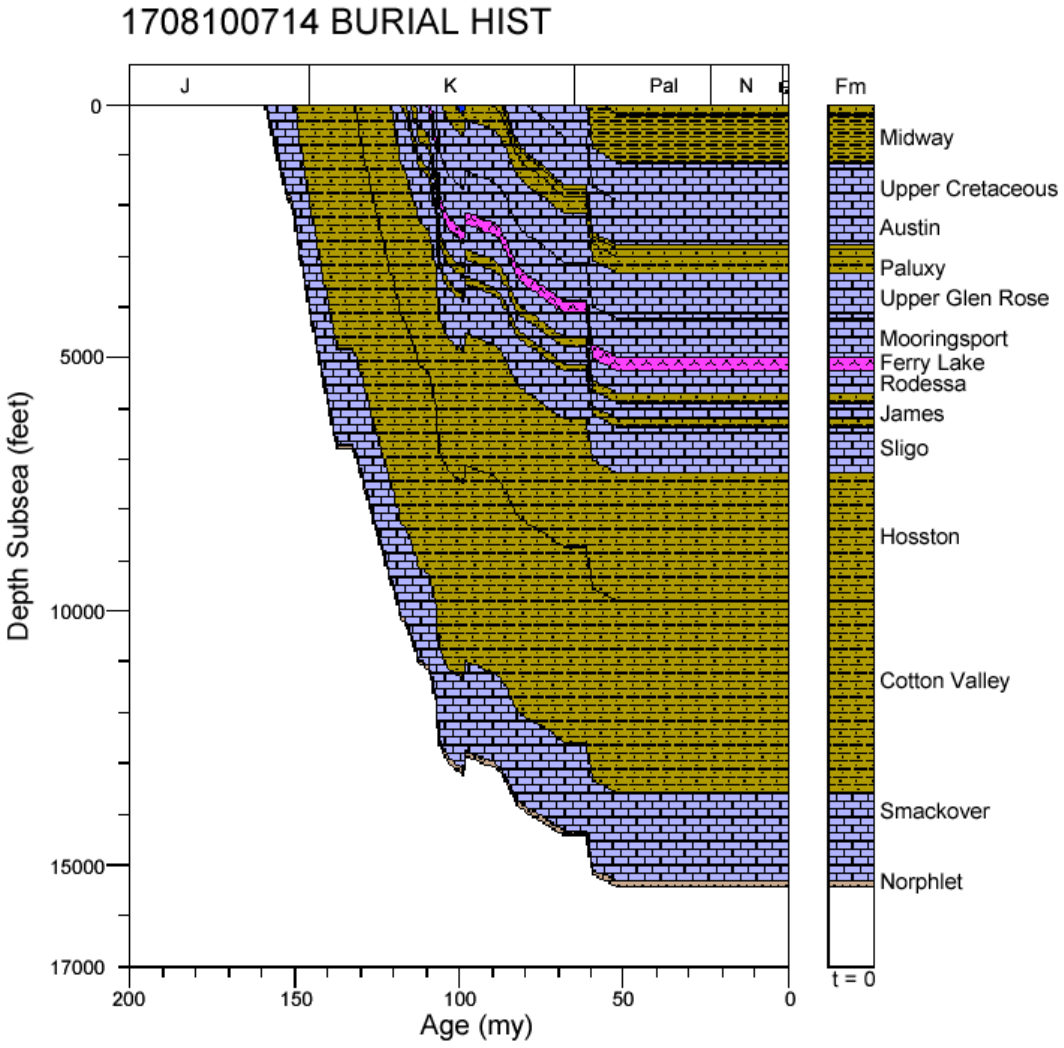


Figure 59. Burial history for well 1708100714, North Louisiana Salt Basin.

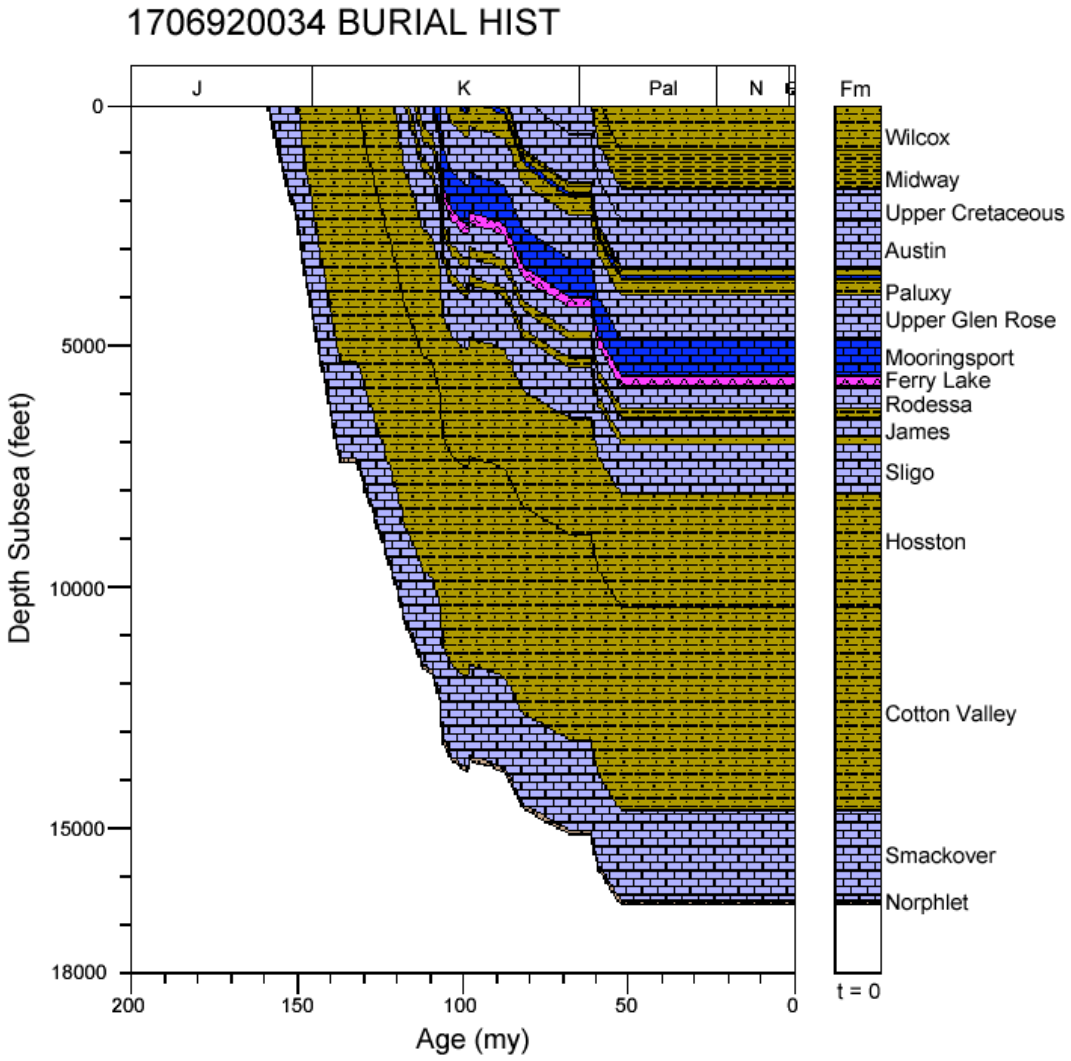


Figure 60. Burial history for well 1706920034, North Louisiana Salt Basin.

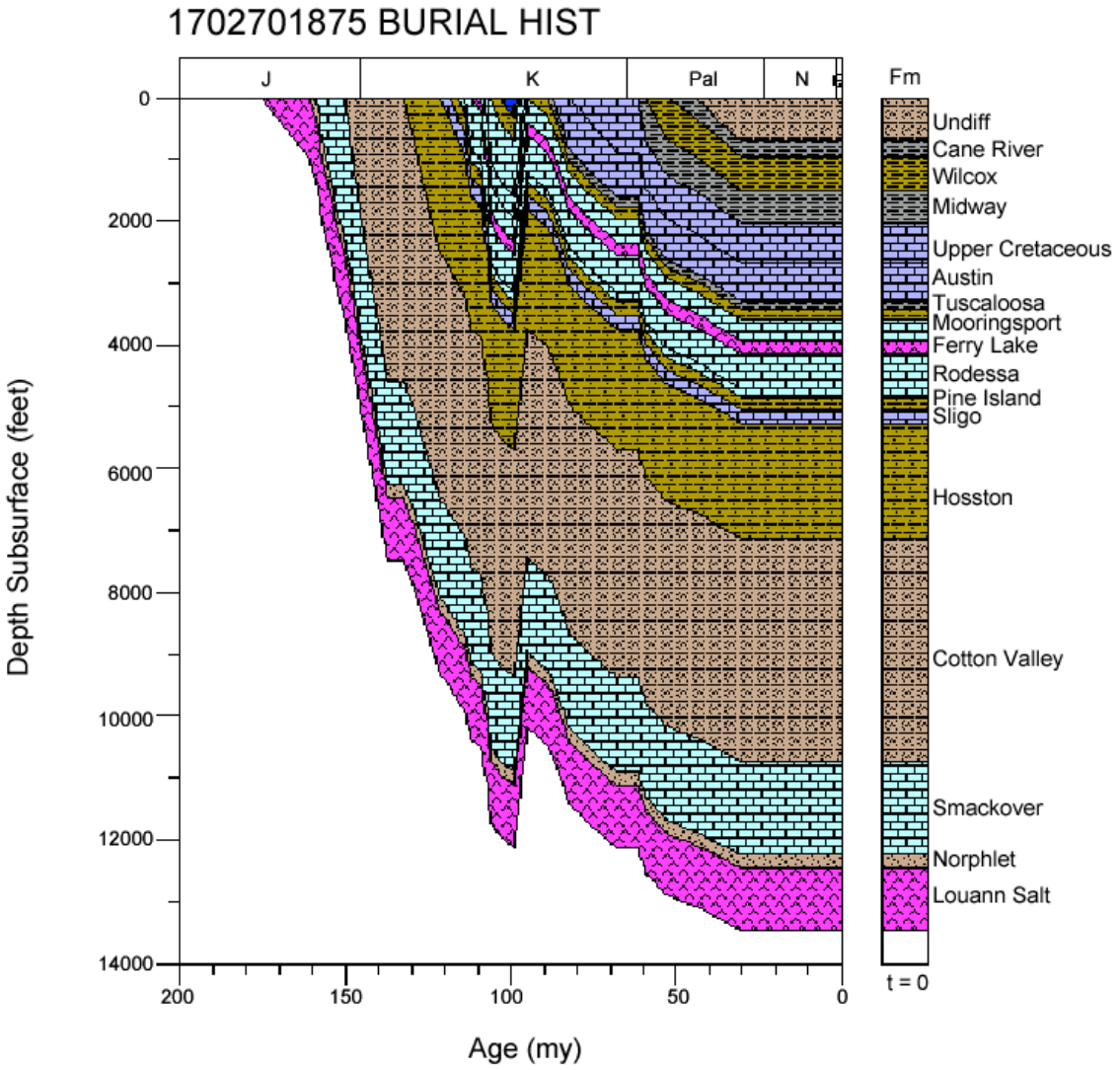


Figure 61. Burial history for well 1702701875, North Louisiana Salt Basin.

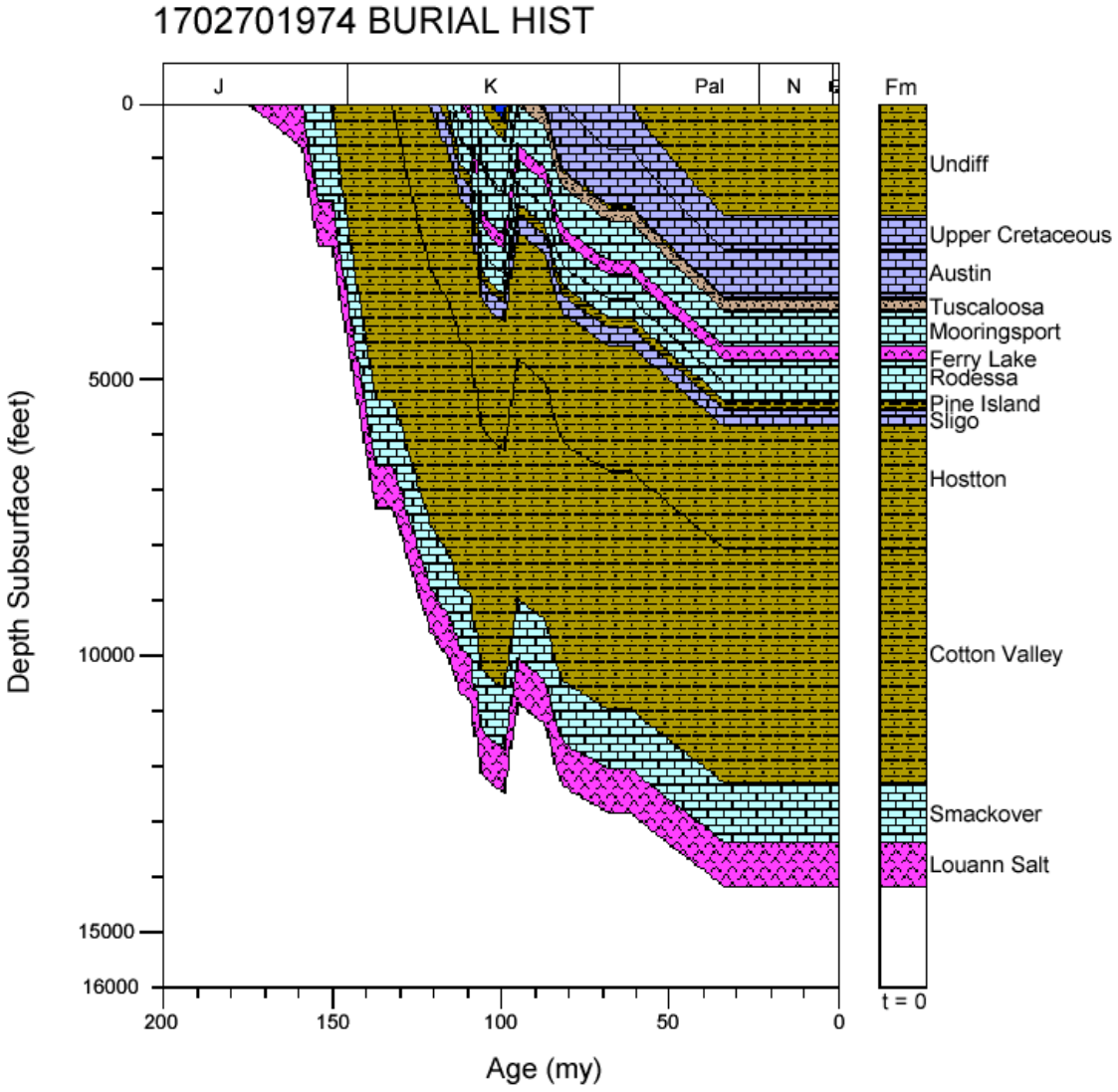


Figure 62. Burial history for well 1702701974, North Louisiana Salt Basin.

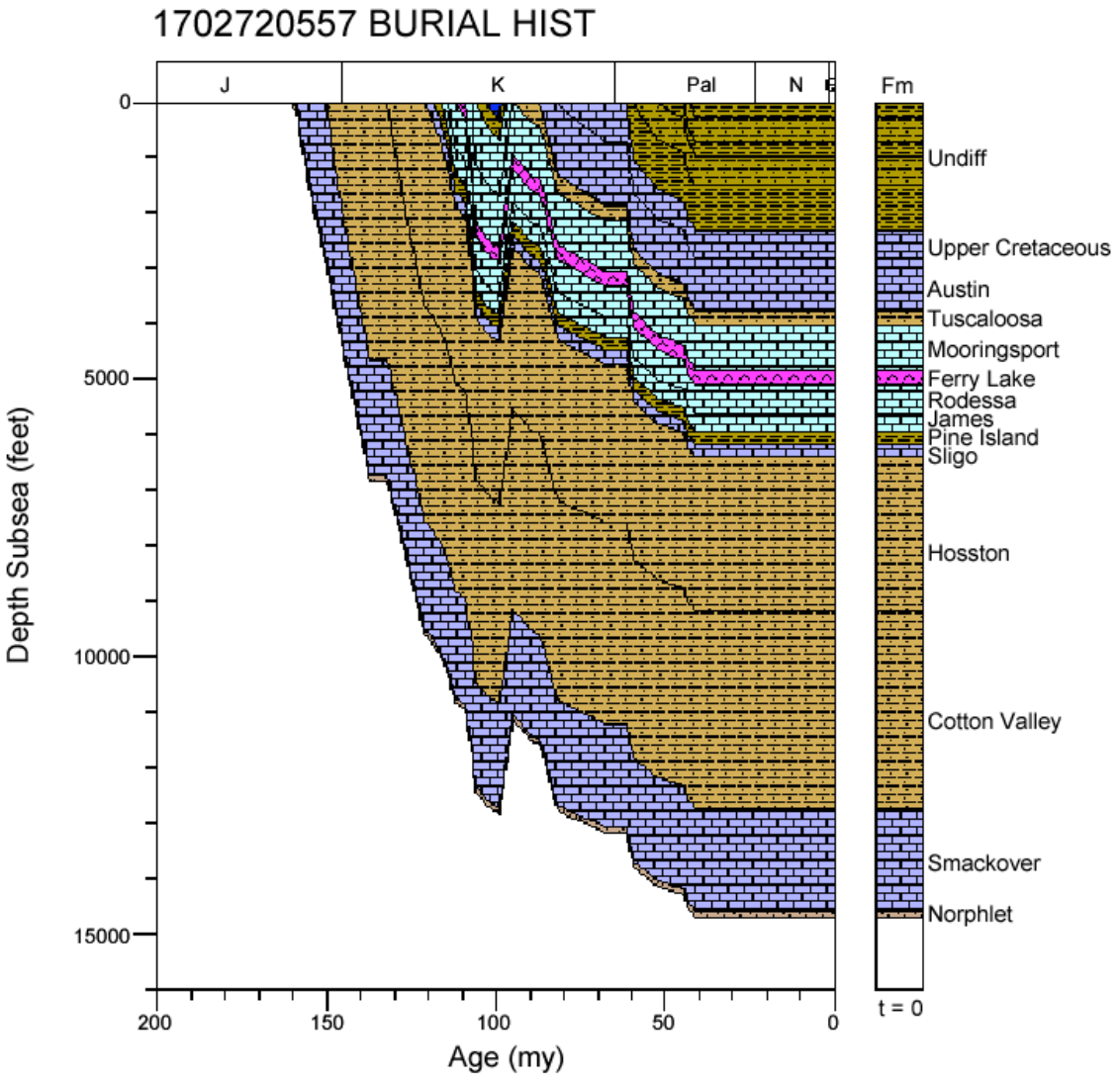


Figure 63. Burial history for well 1702720557, North Louisiana Salt Basin.

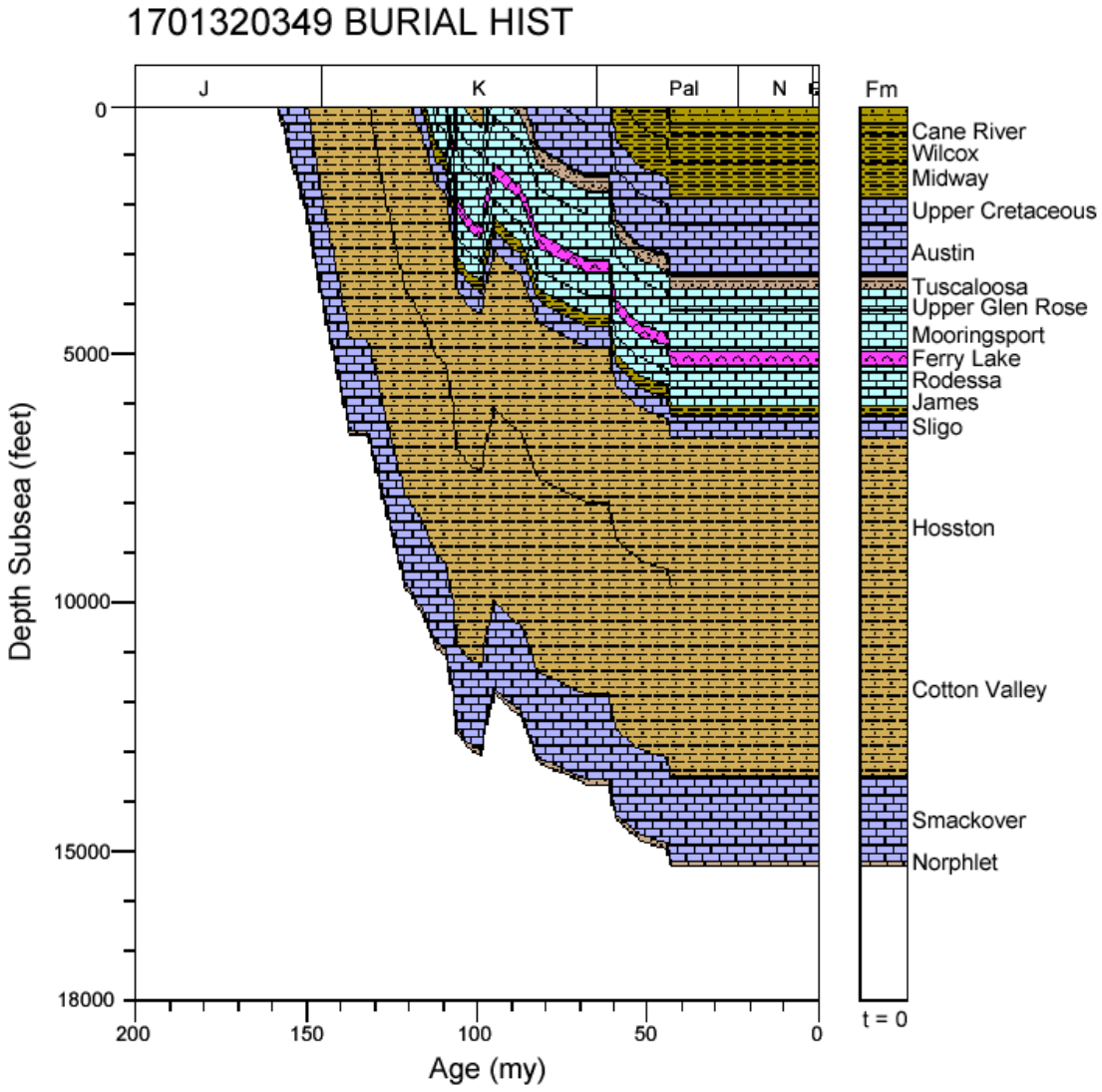


Figure 64. Burial history for well 1701320349, North Louisiana Salt Basin.

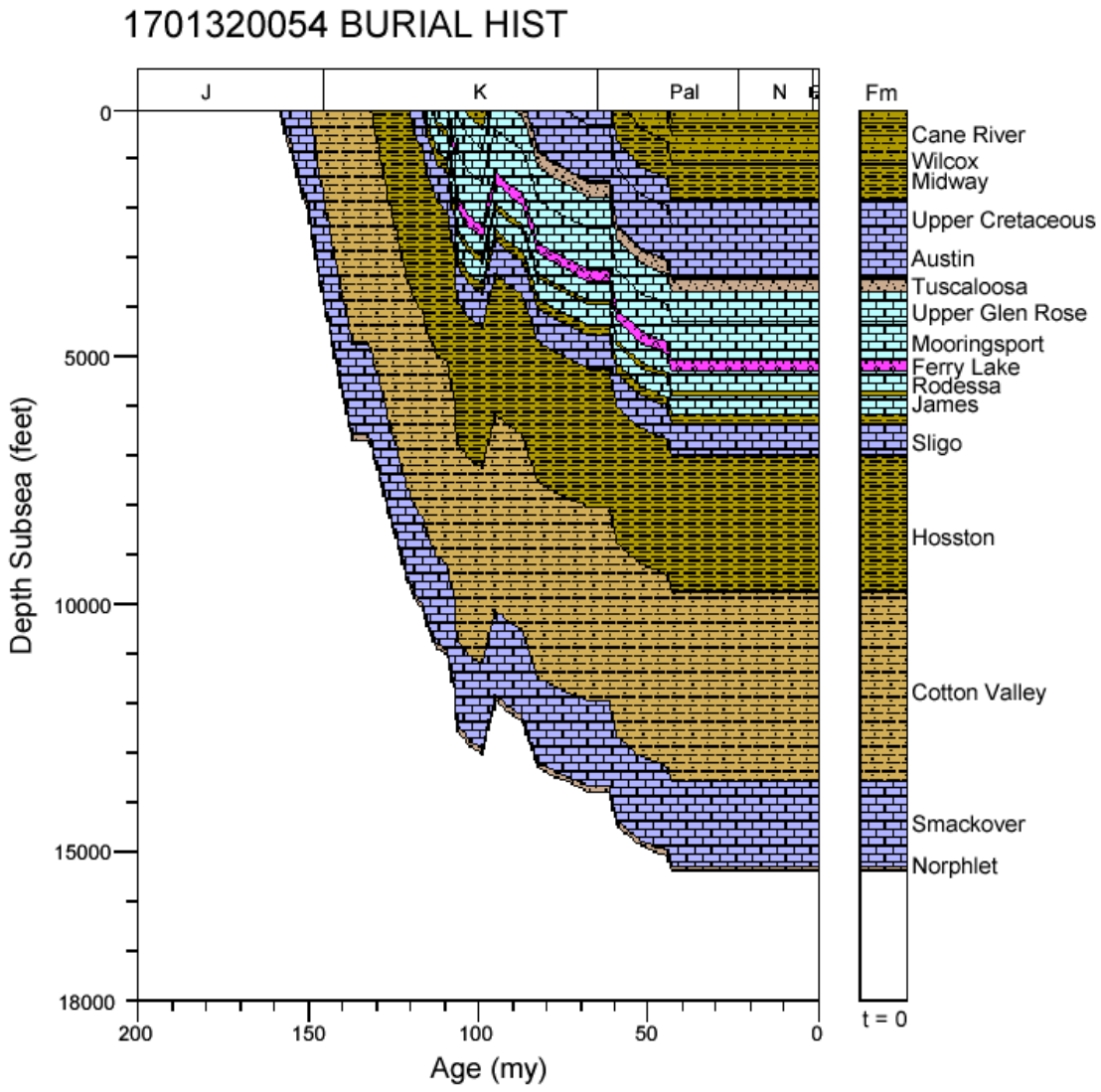


Figure 65. Burial history for well 1701320054, North Louisiana Salt Basin.

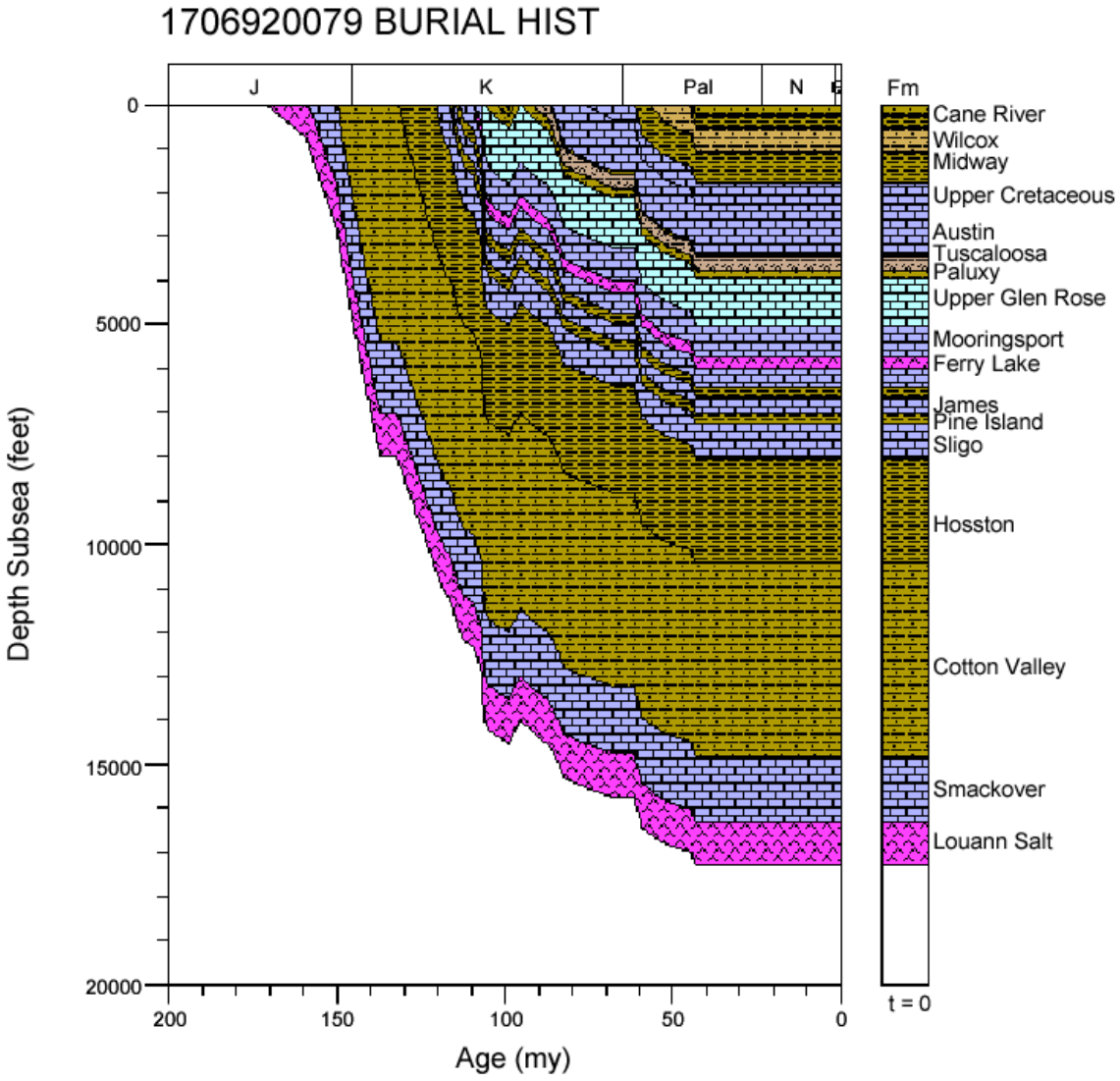


Figure 66. Burial history for well 1706920079, North Louisiana Salt Basin.

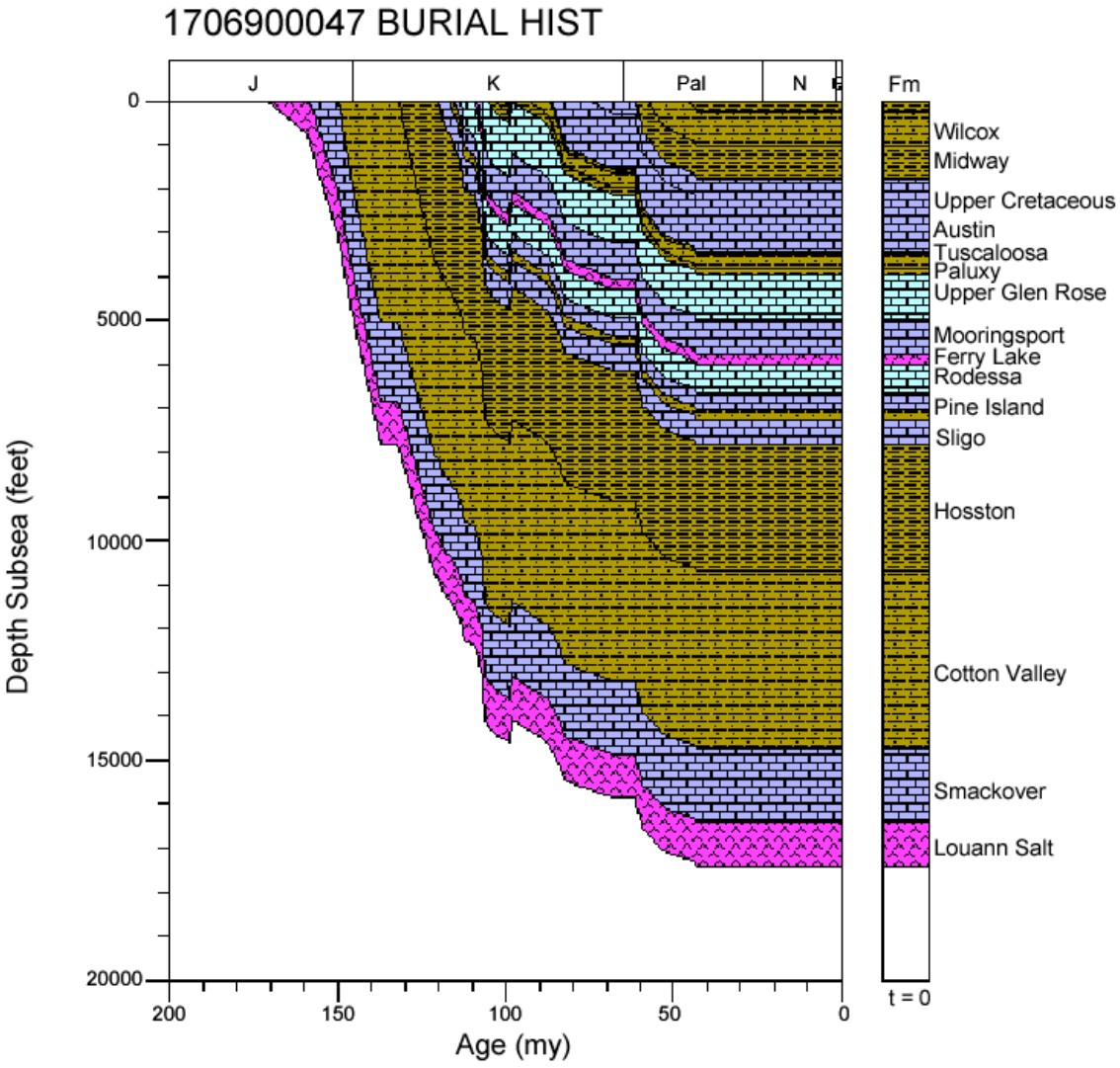


Figure 67. Burial history for well 1706900047, North Louisiana Salt Basin.

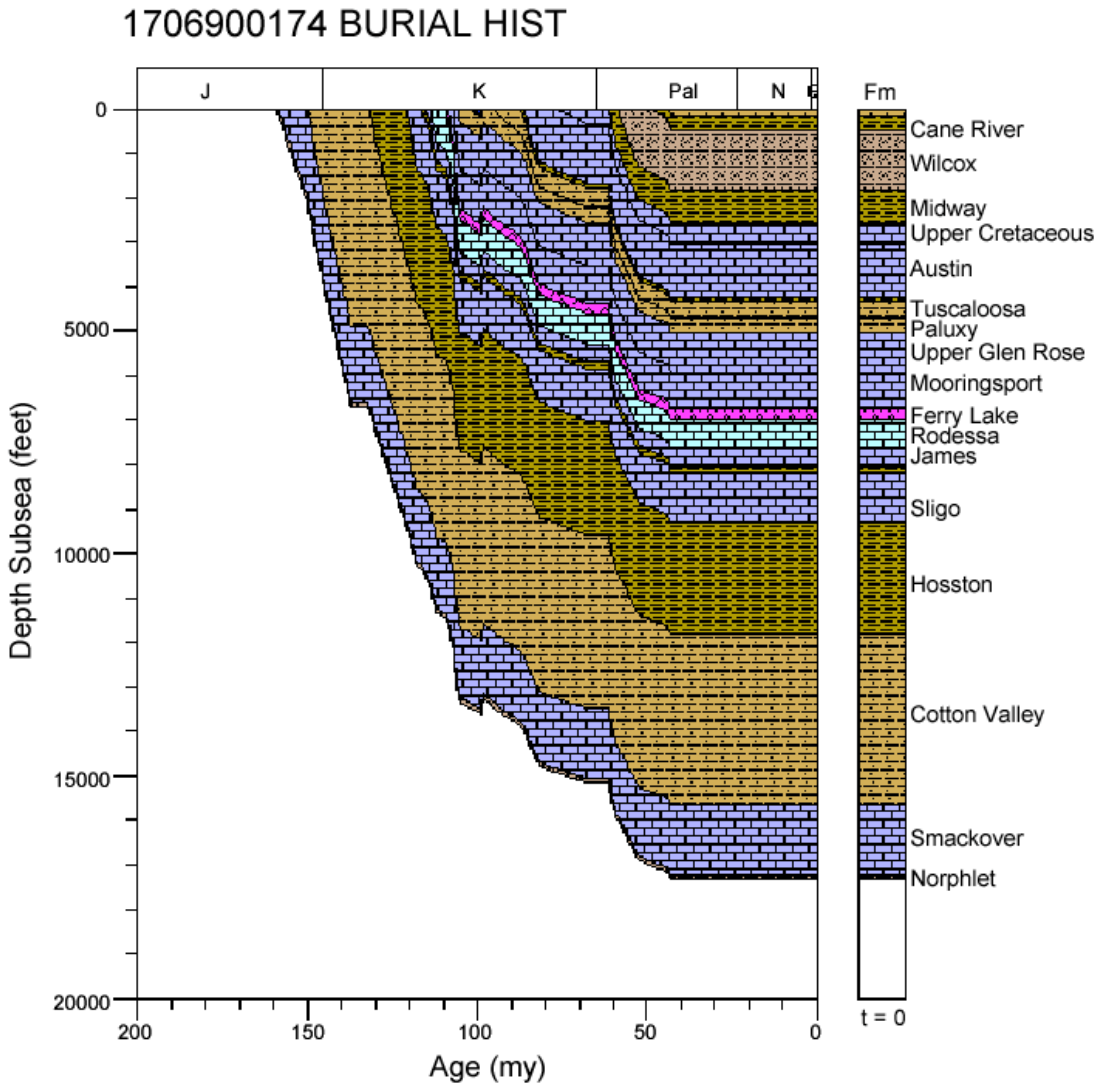


Figure 68. Burial history for well 1706900174, North Louisiana Salt Basin.

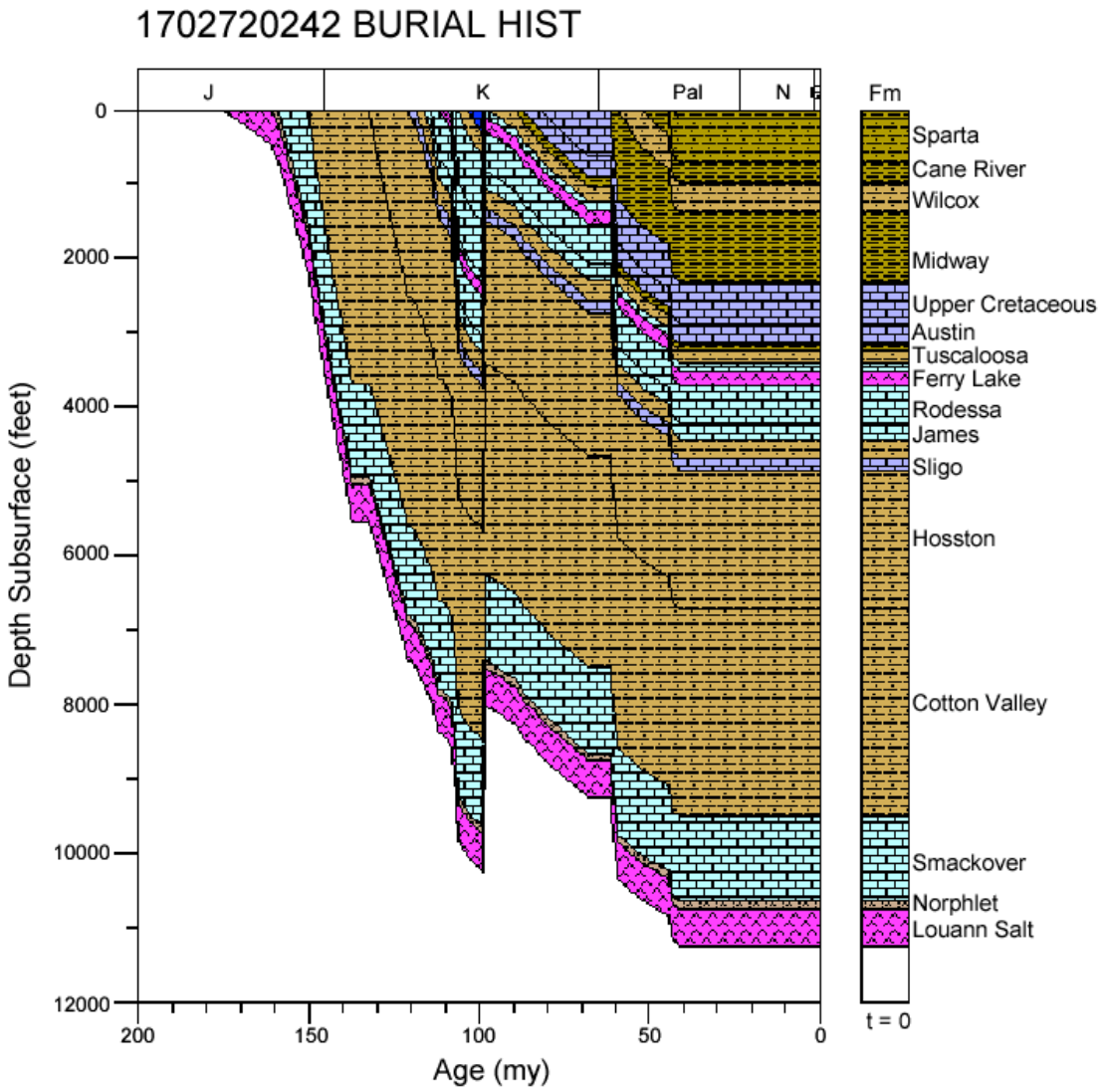


Figure 69. Burial history for well 1702720242, North Louisiana Salt Basin.

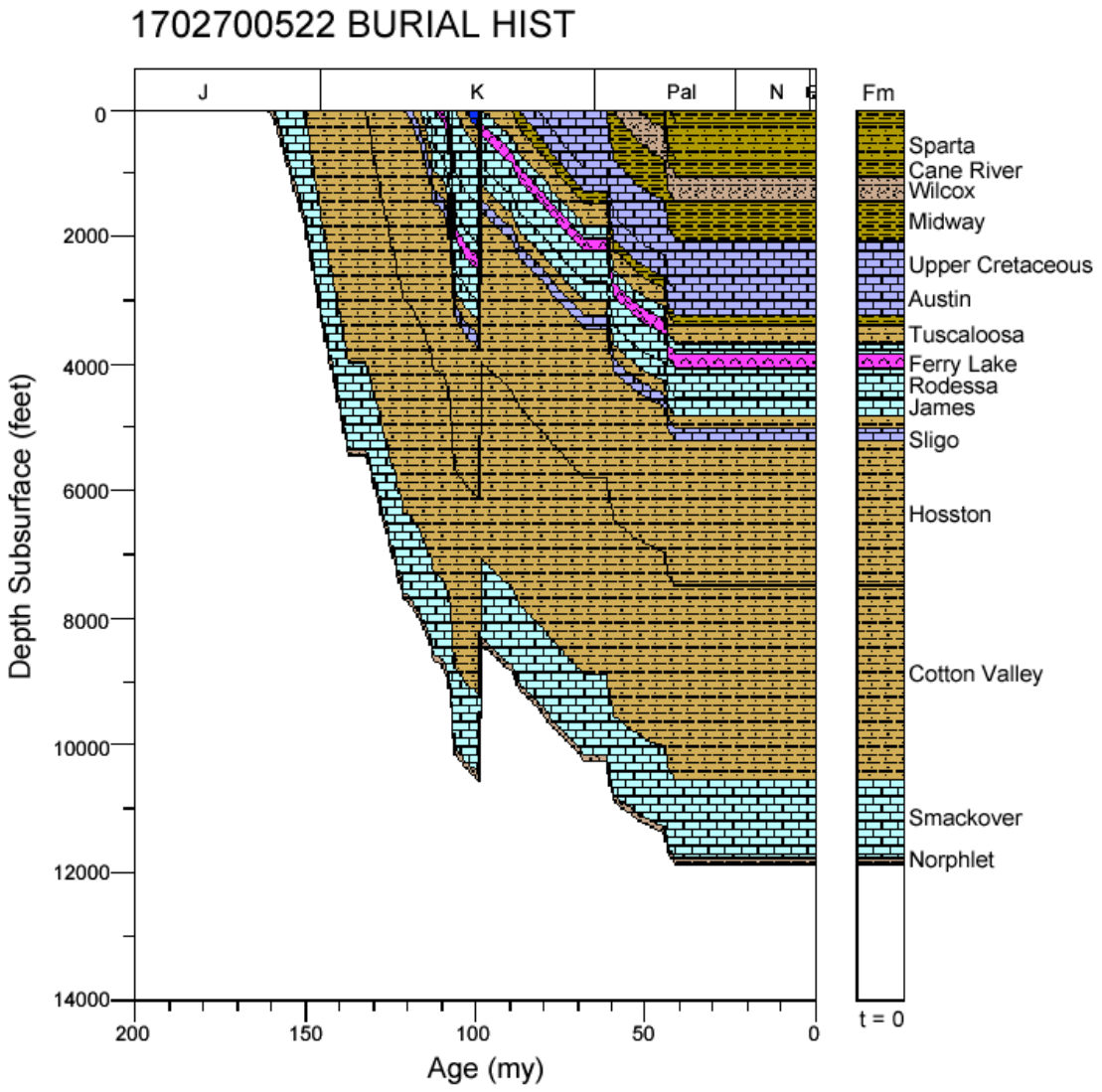


Figure 70. Burial history for well 1702700522, North Louisiana Salt Basin.

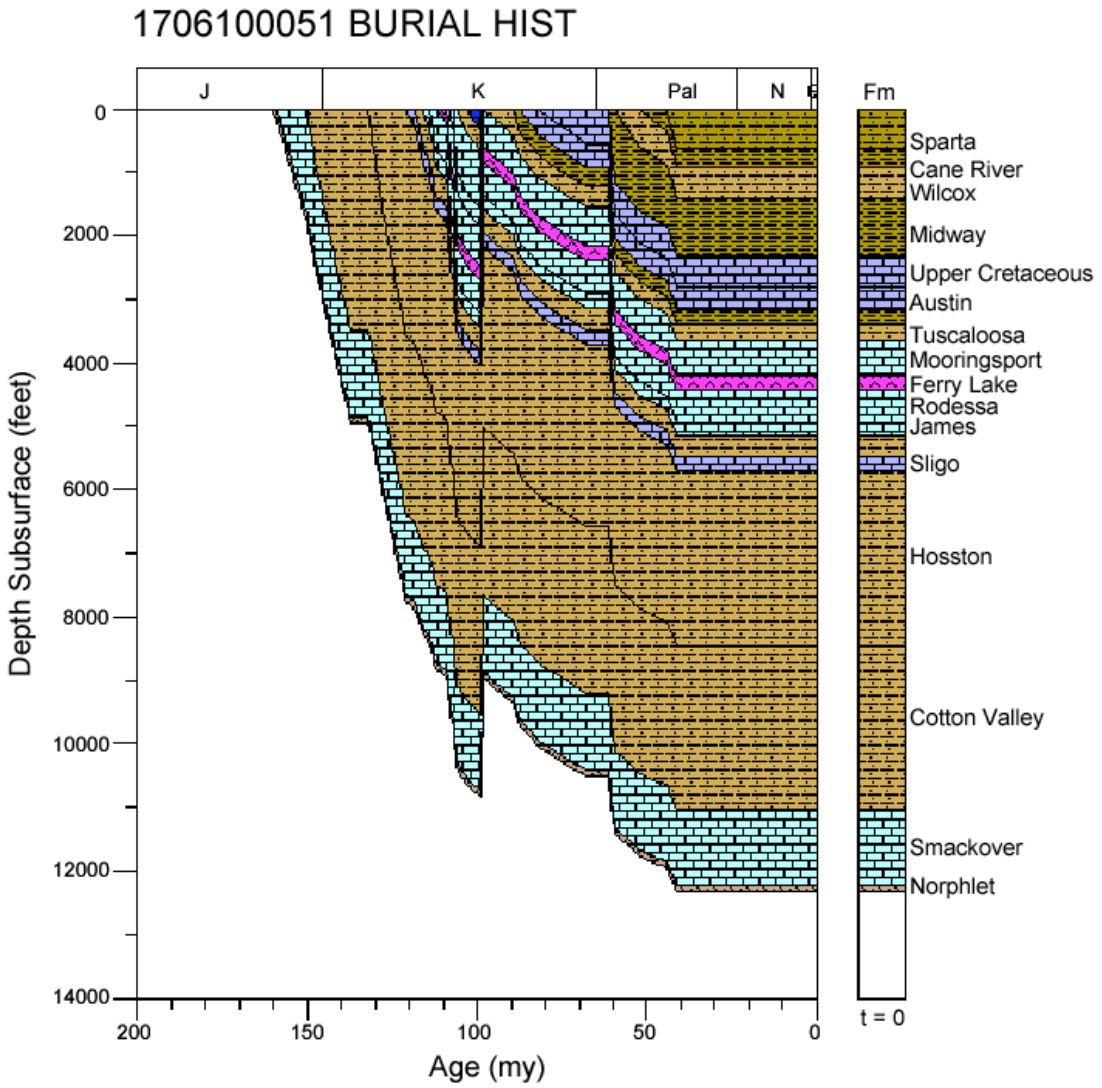


Figure 71. Burial history for well 1706100051, North Louisiana Salt Basin.

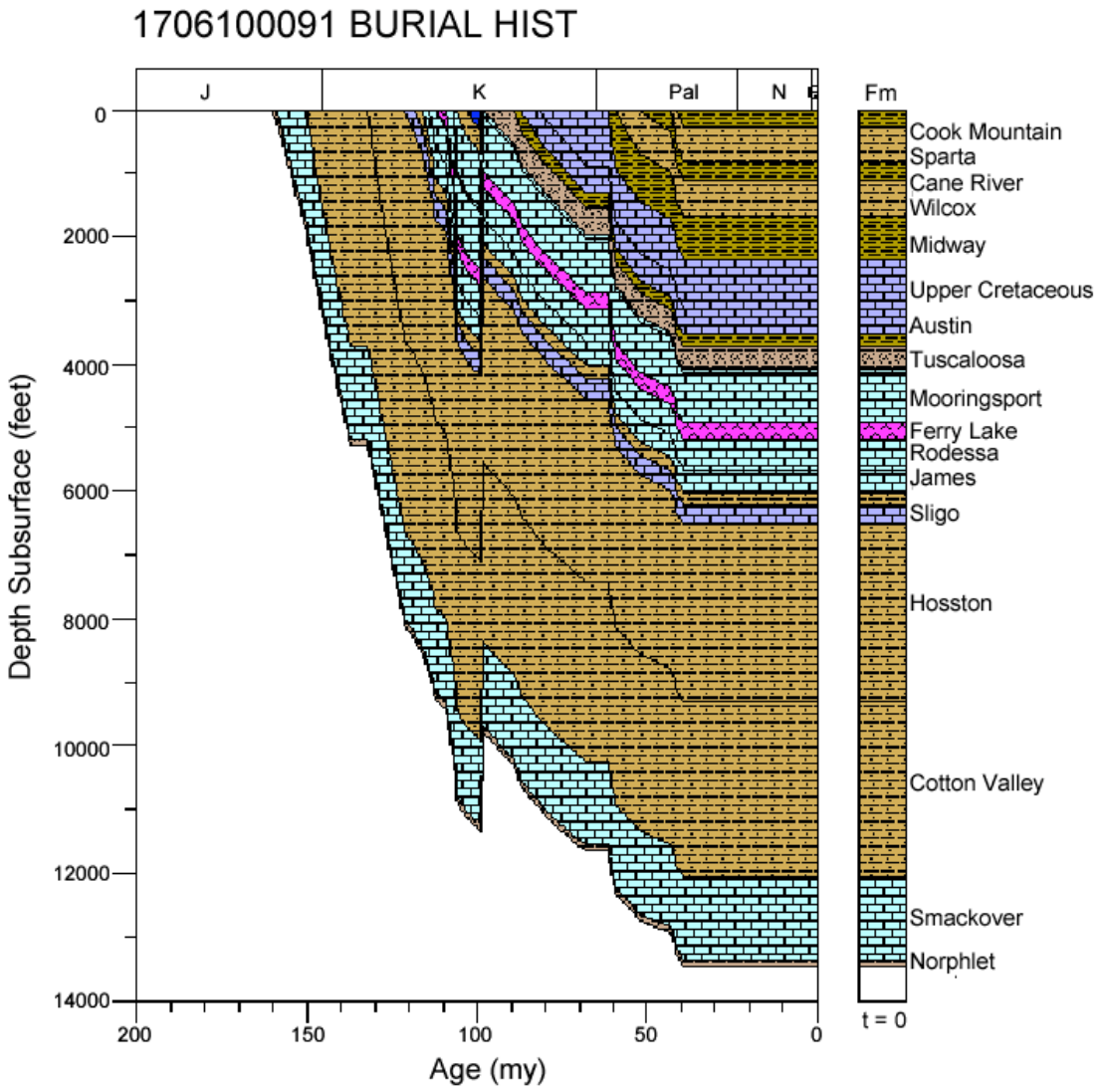


Figure 72. Burial history for well 1706100091, North Louisiana Salt Basin.

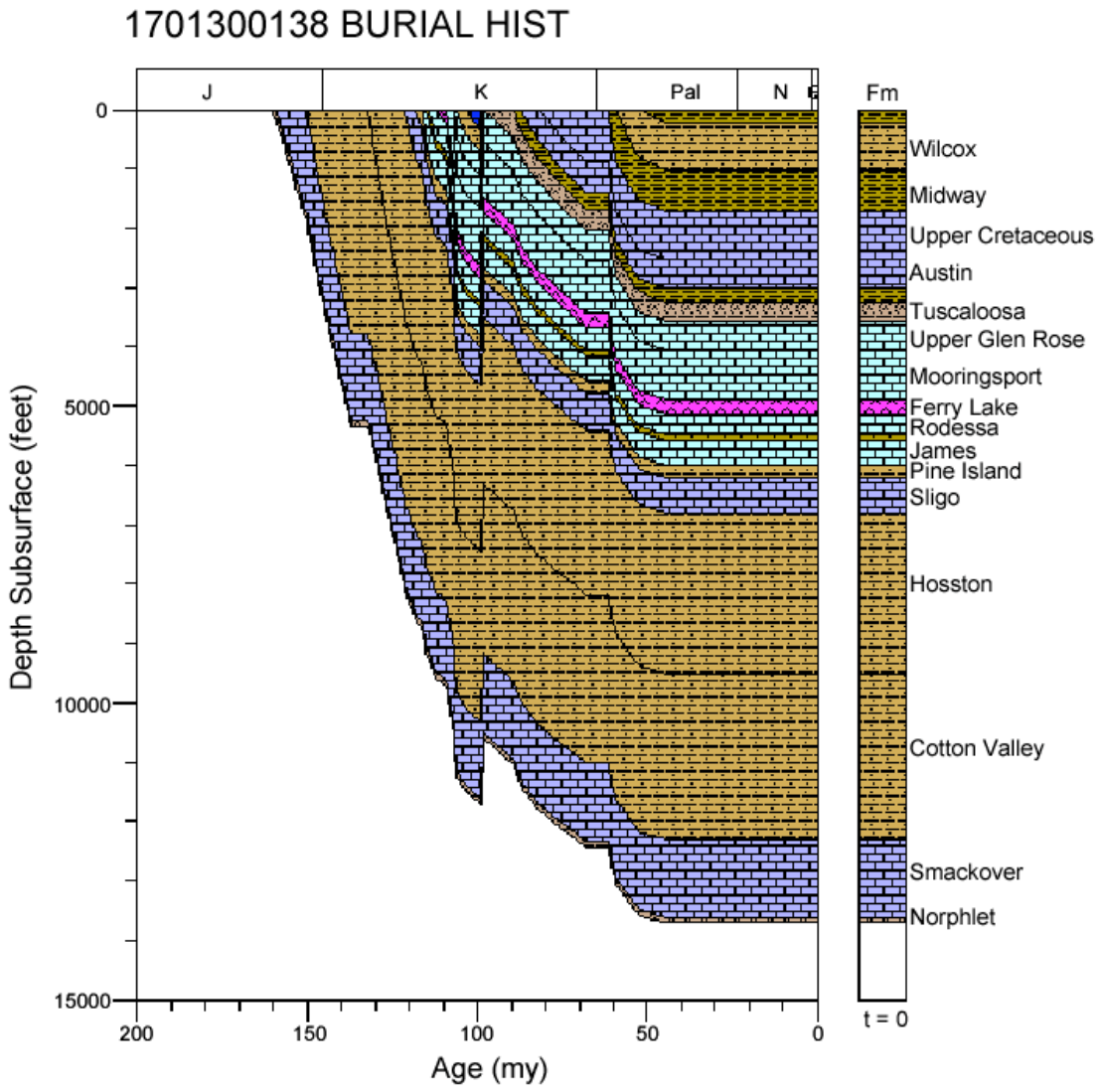


Figure 73. Burial history for well 1701300138, North Louisiana Salt Basin.

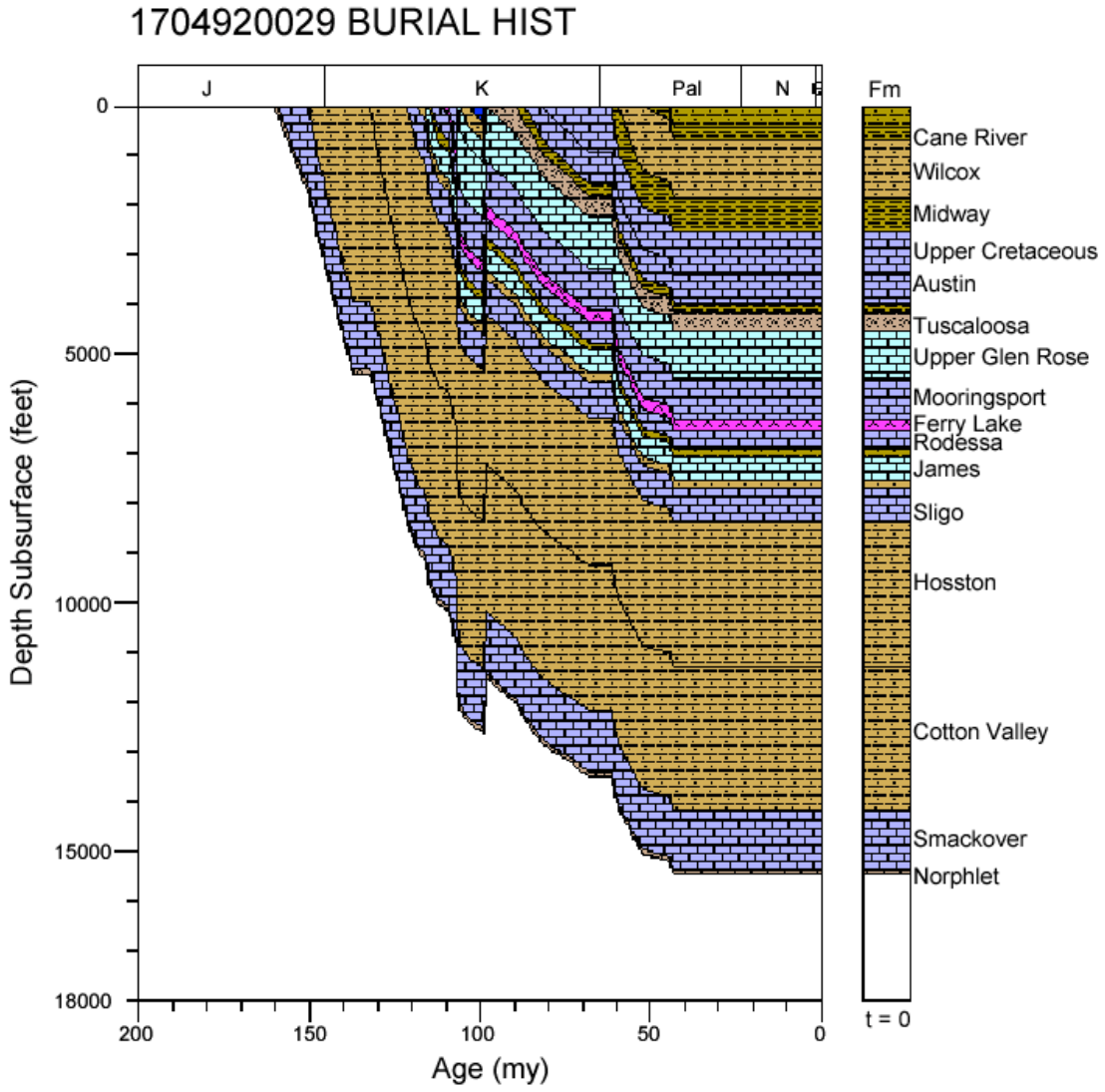


Figure 74. Burial history for well 1704920029, North Louisiana Salt Basin.

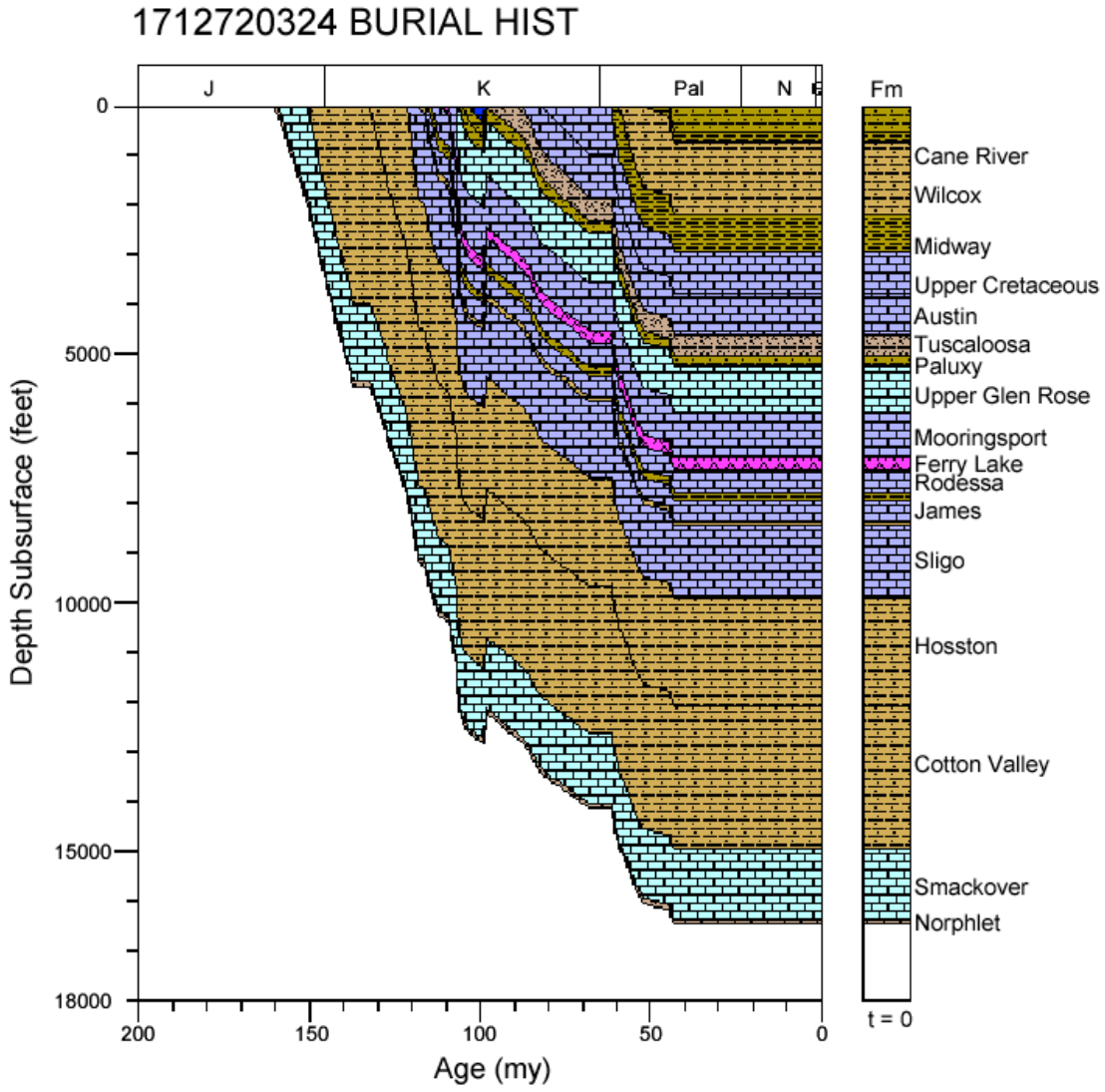


Figure 75. Burial history for well 1712720324, North Louisiana Salt Basin.

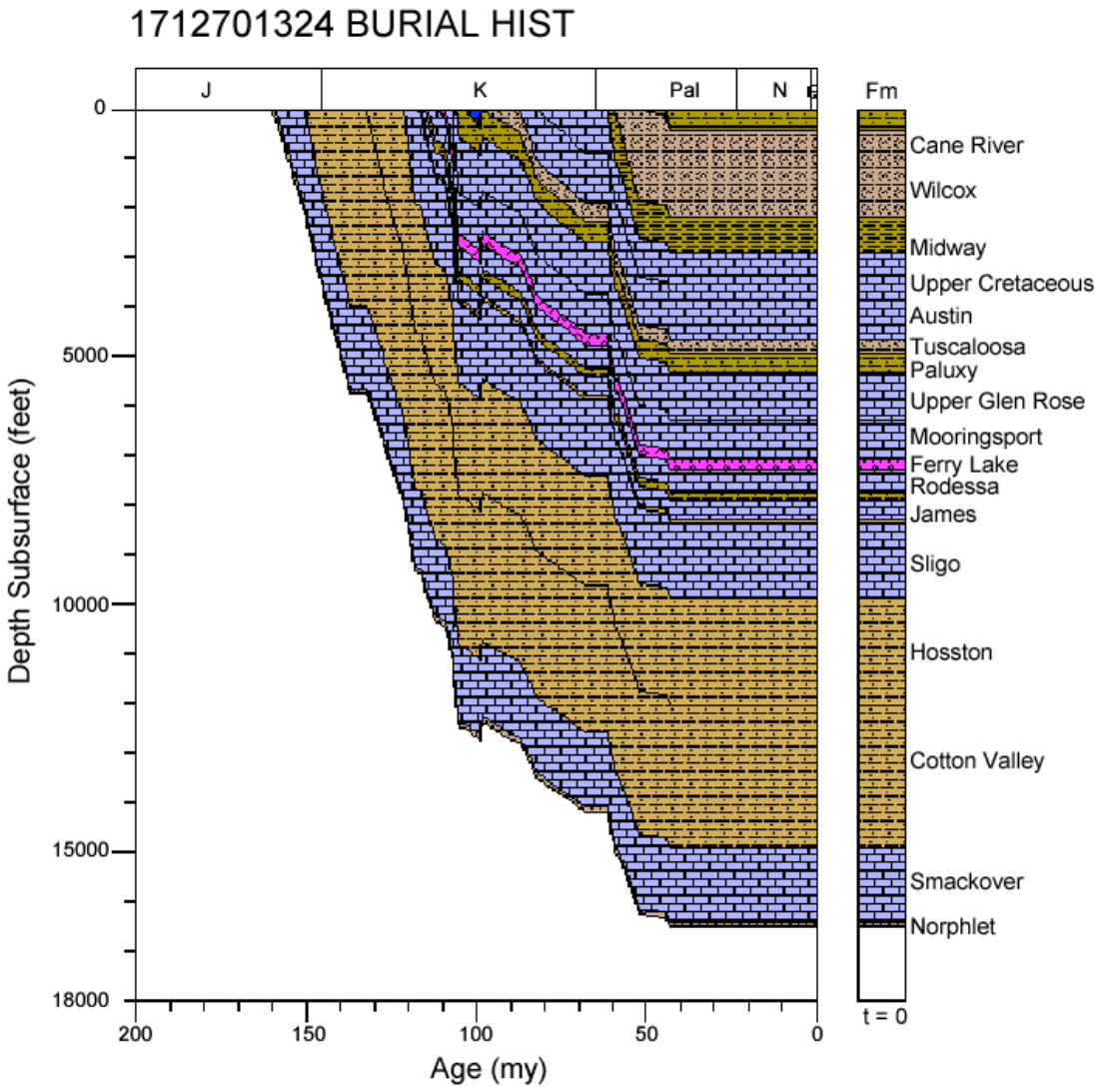


Figure 76. Burial history for well 1712701324, North Louisiana Salt Basin.

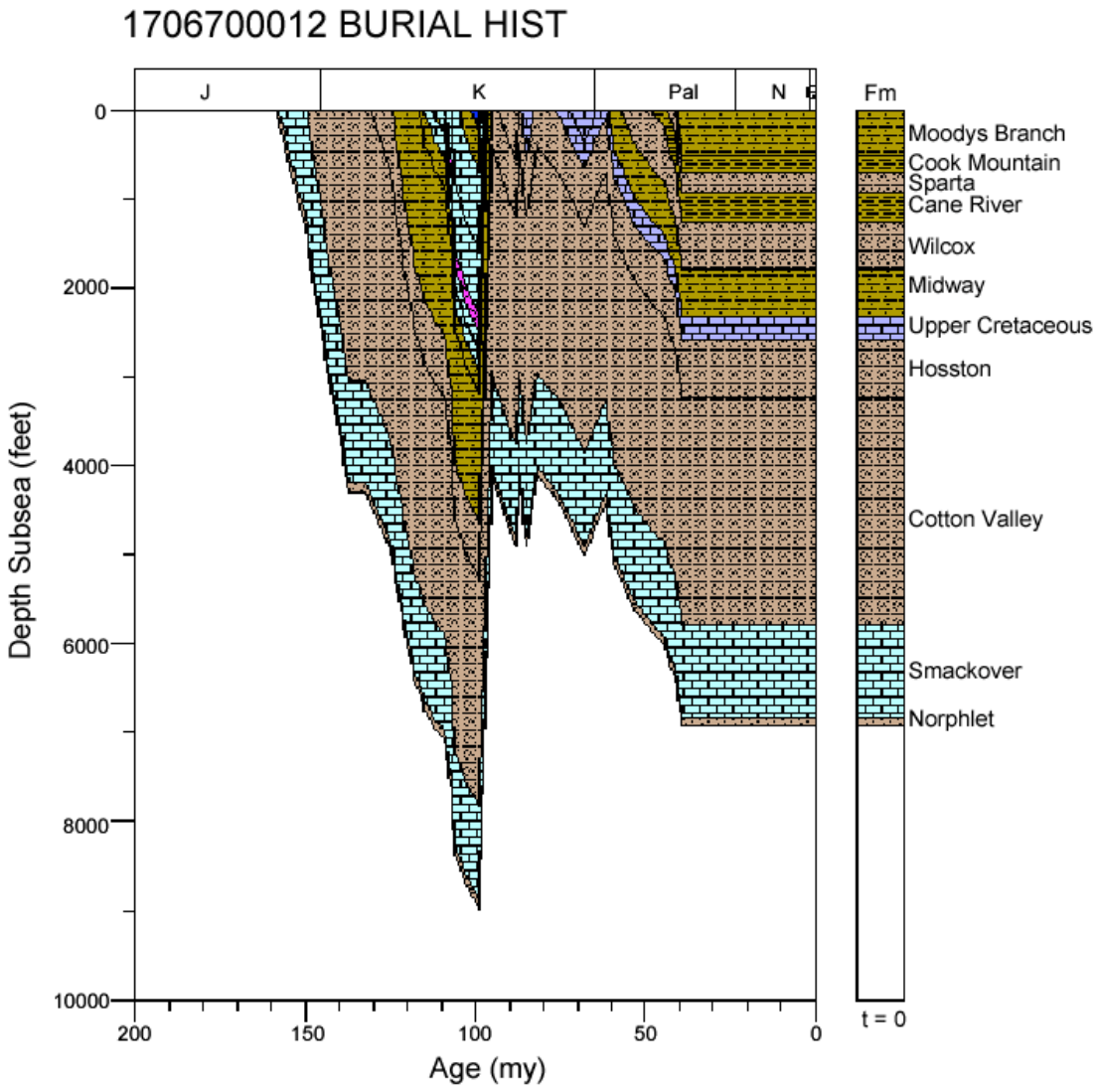


Figure 77. Burial history for well 1706700012, North Louisiana Salt Basin.

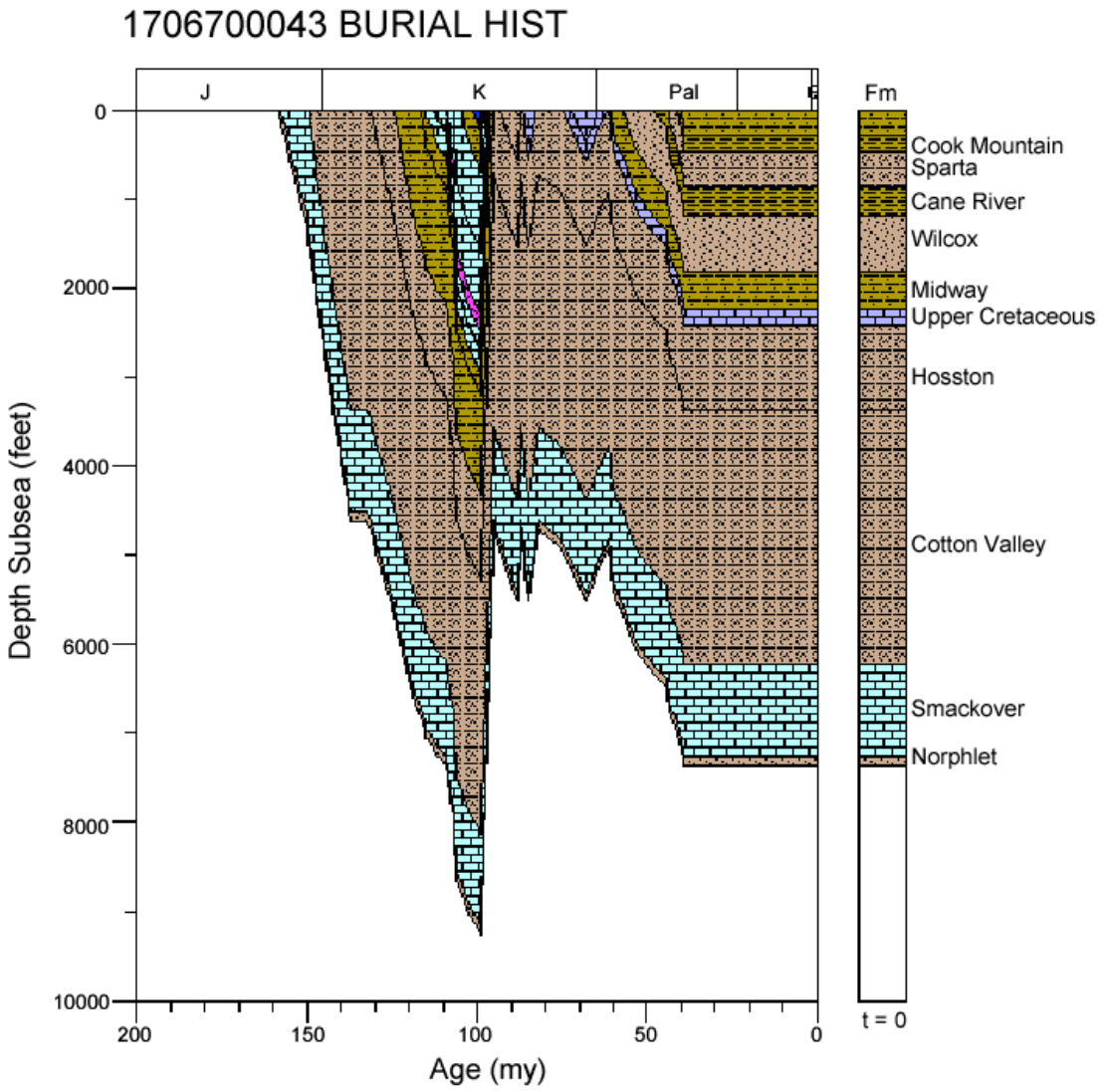


Figure 78. Burial history for well 1706700043, North Louisiana Salt Basin.

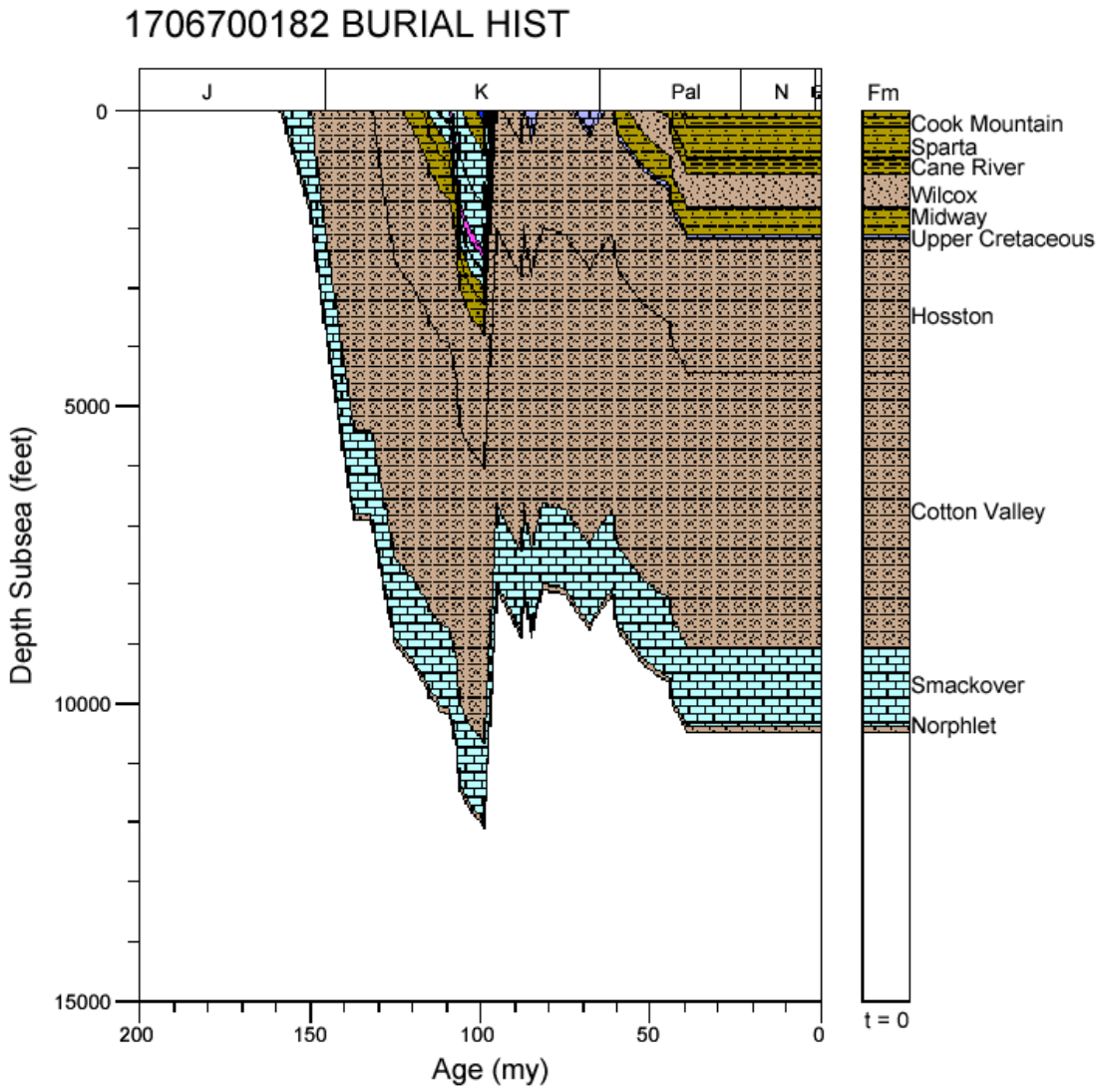


Figure 79. Burial history for well 1706700182, North Louisiana Salt Basin.

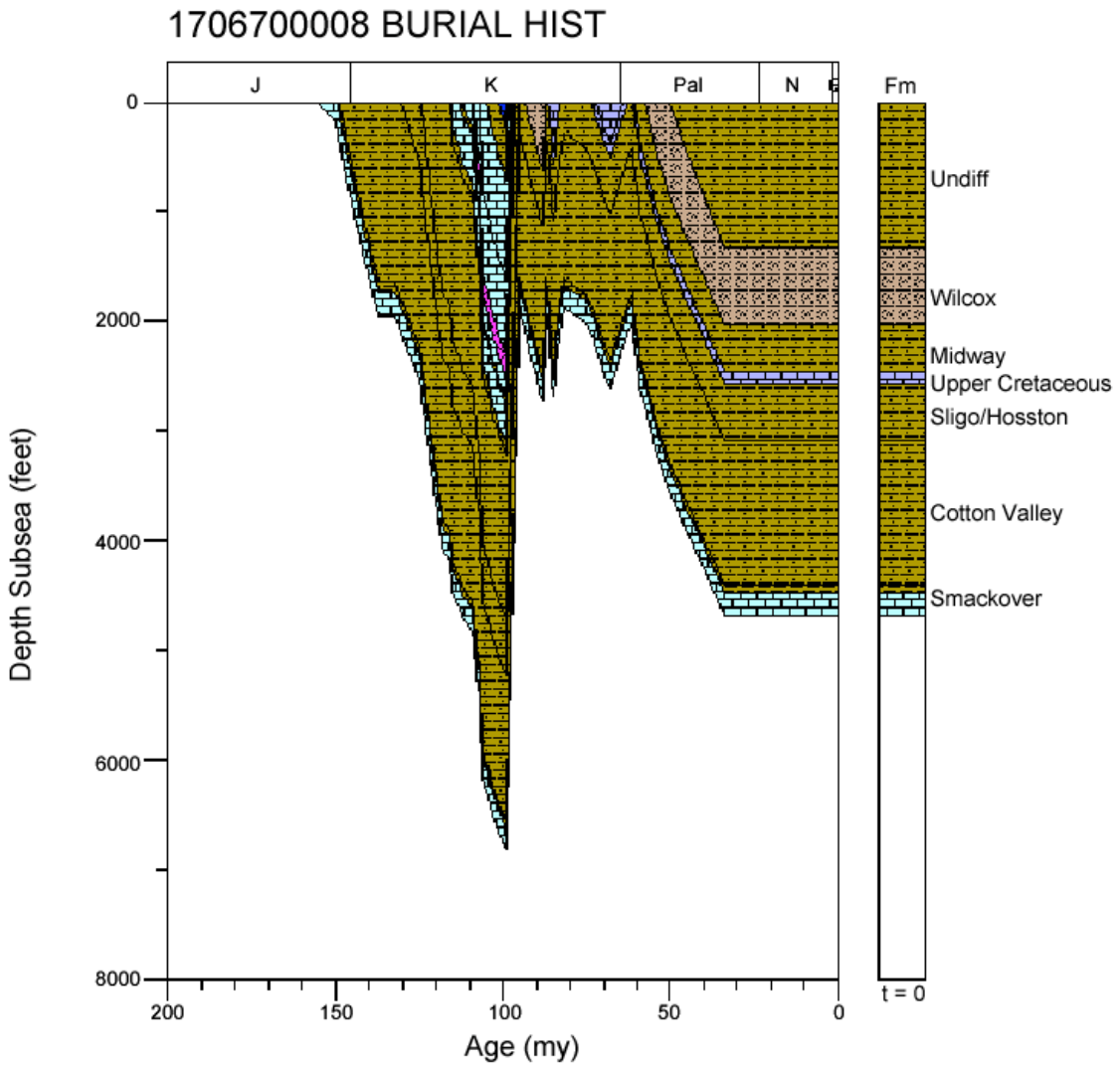


Figure 80. Burial history for well 1706700008, North Louisiana Salt Basin.

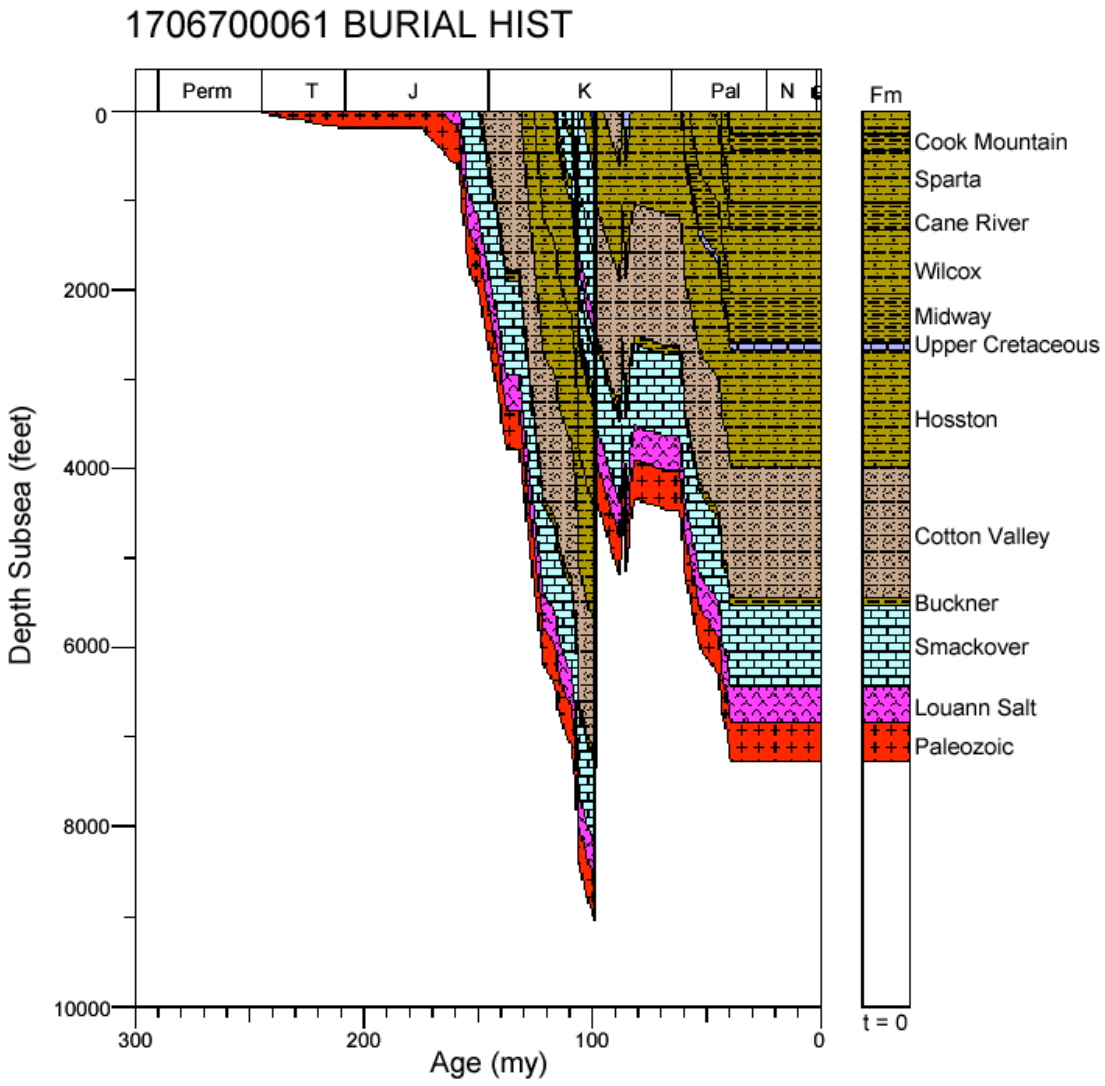


Figure 81. Burial history for well 1706700061, North Louisiana Salt Basin.

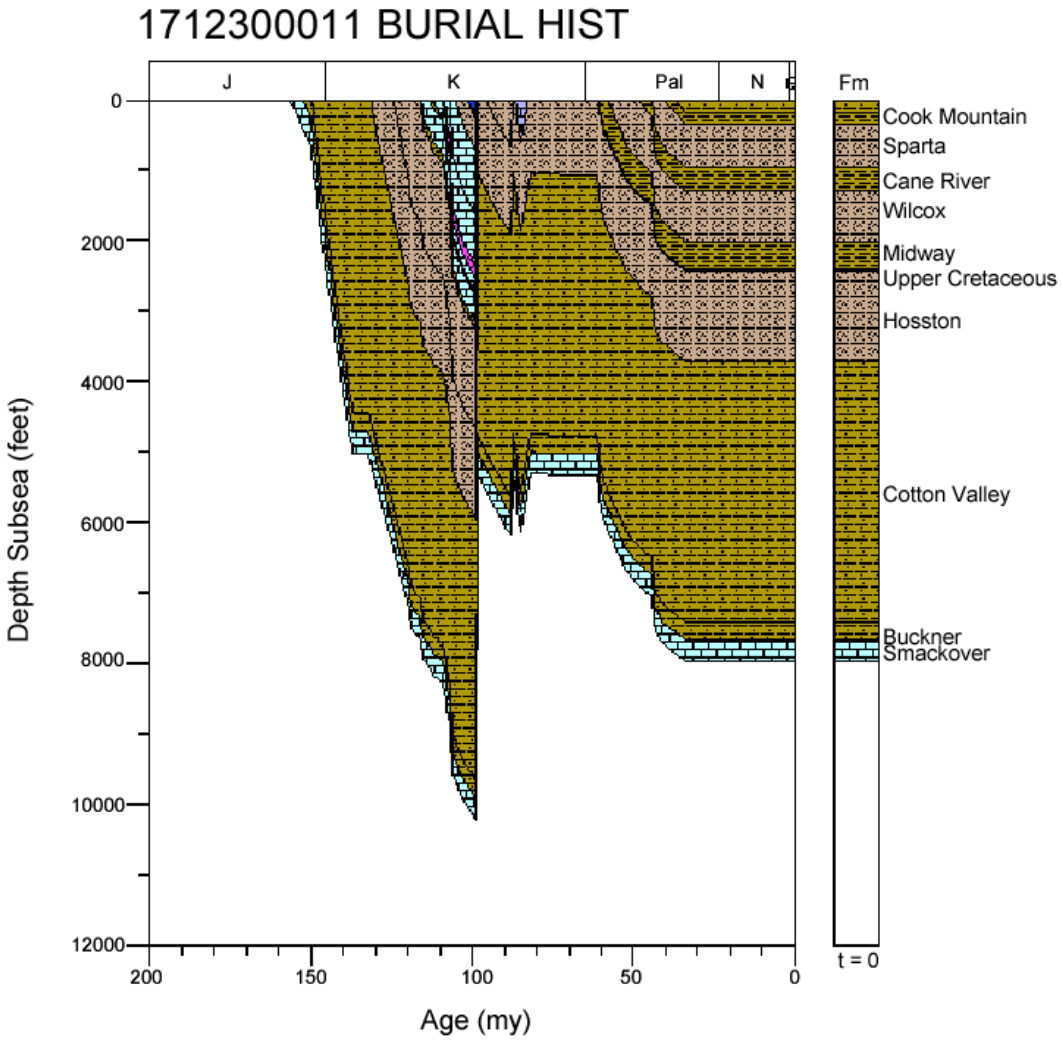


Figure 82. Burial history for well 1712300011, North Louisiana Salt Basin.

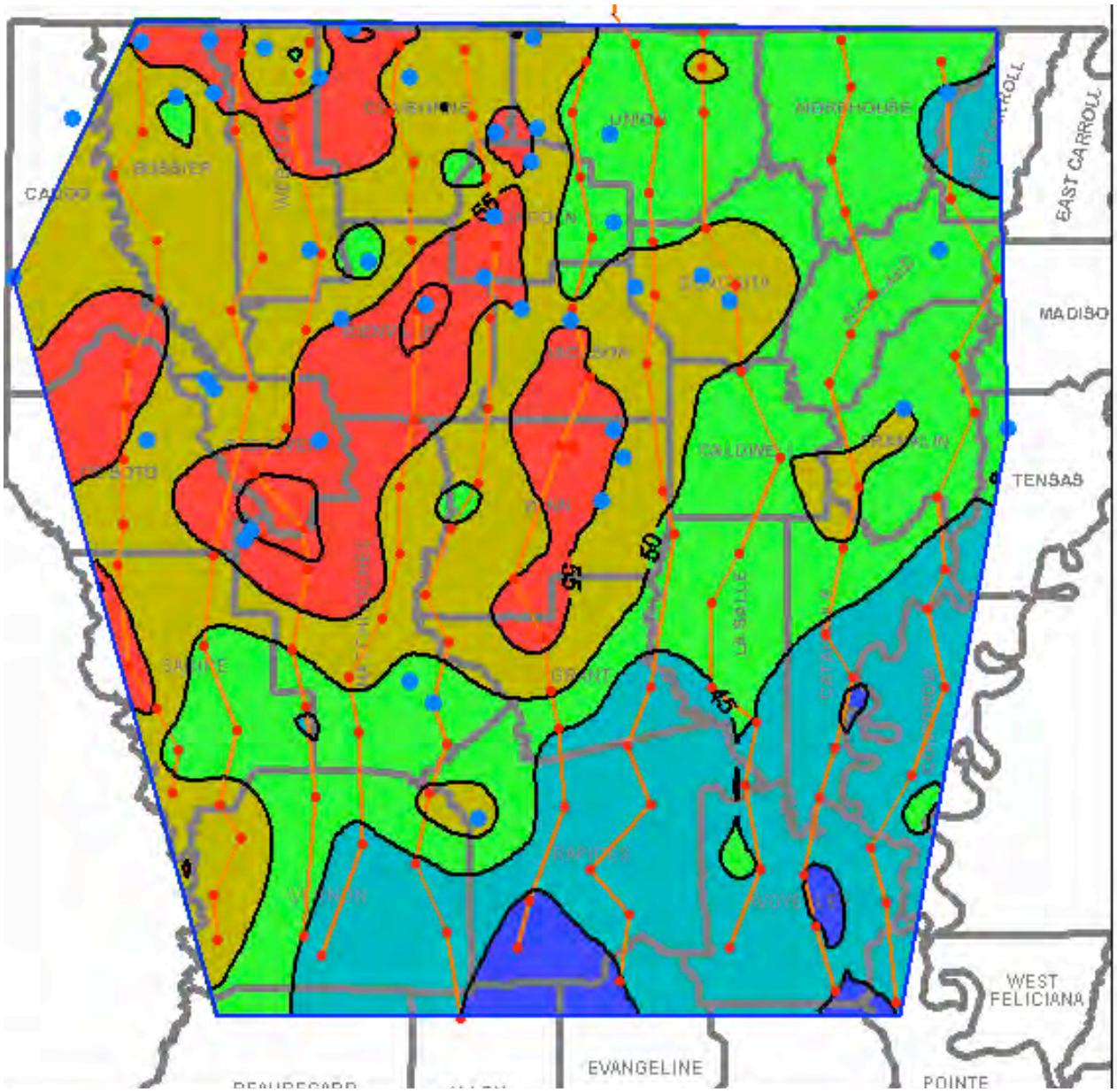


- wells w/ BHTs
- wells w/ BHTs & %Ro

55: heat flow value ($mW/m^2$)

Figure 83. Present-day heat flow values. Prepared by Roger Barnaby.

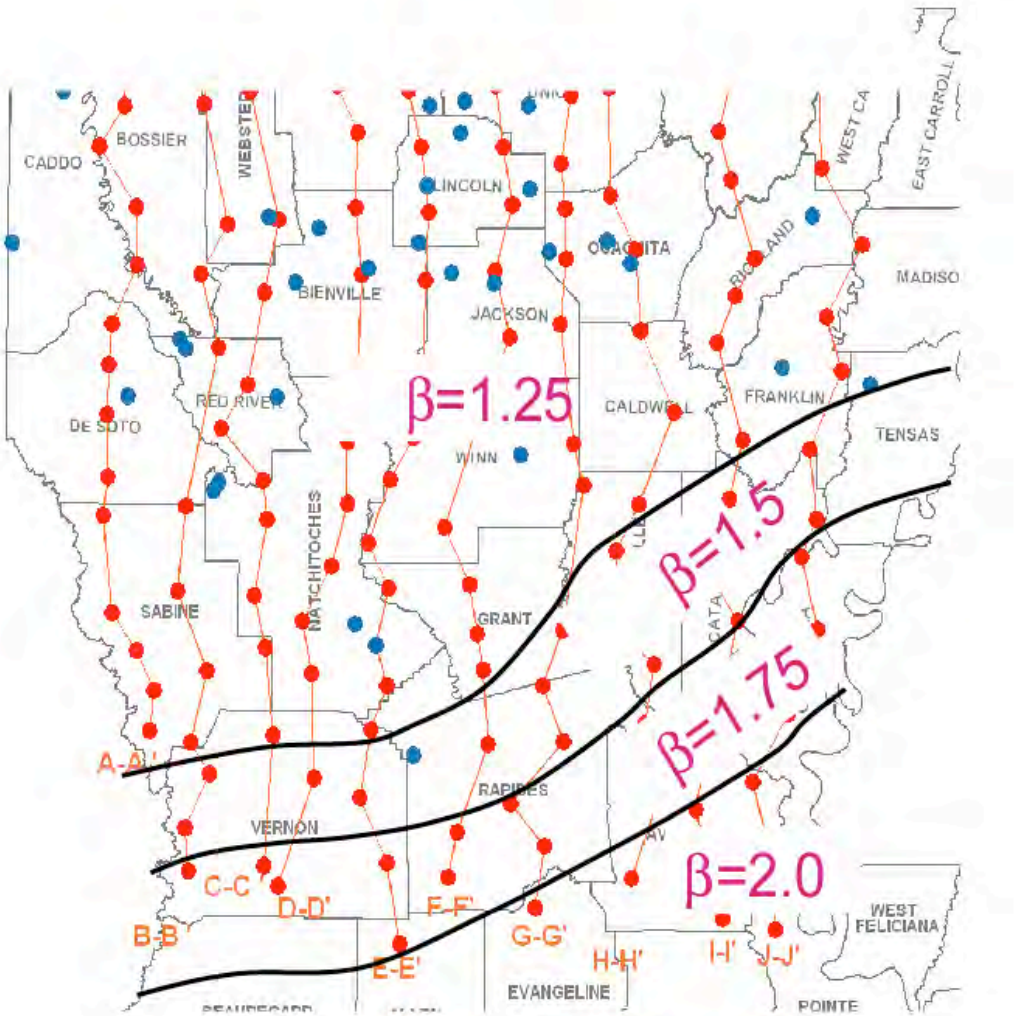


Figure 84. Lithospheric stretching beta factors. Prepared by Roger Barnaby.

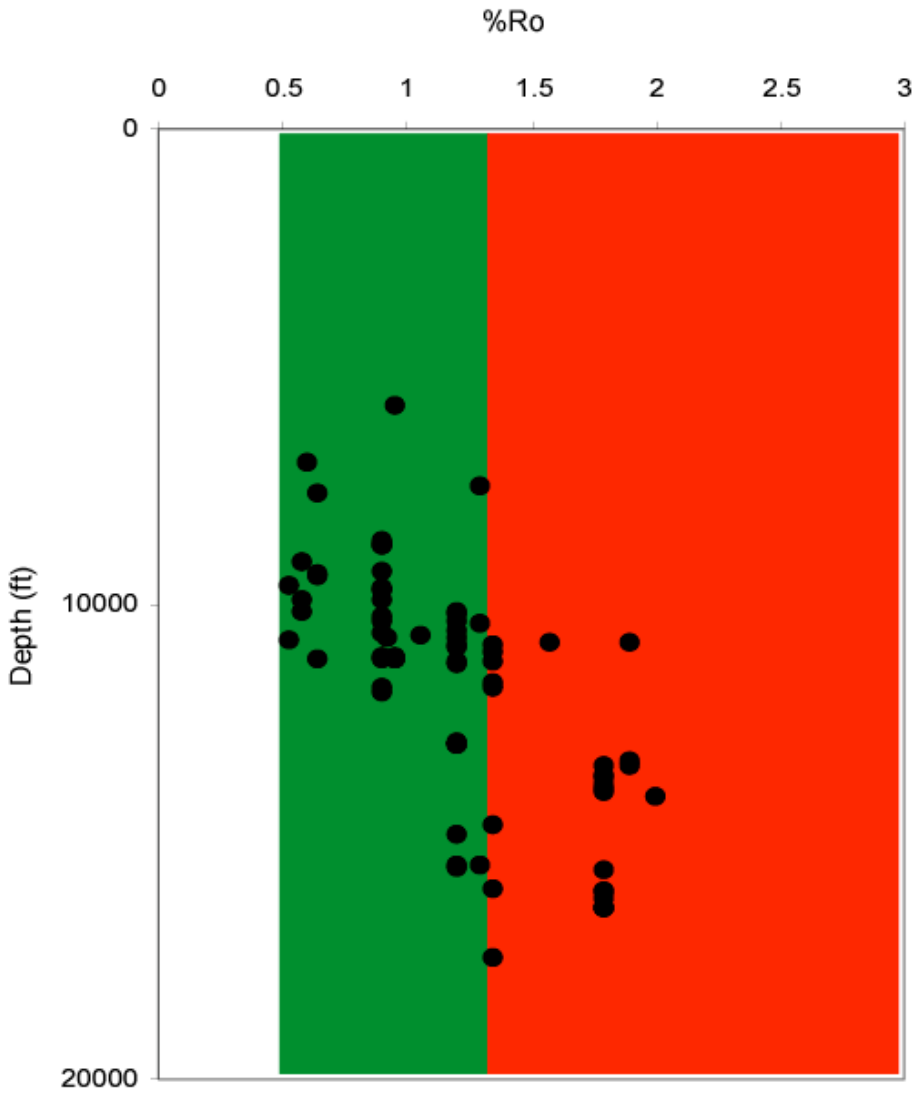


Figure 85. The relationship of vitrinite reflectance and depth. Prepared by Roger Barnaby.

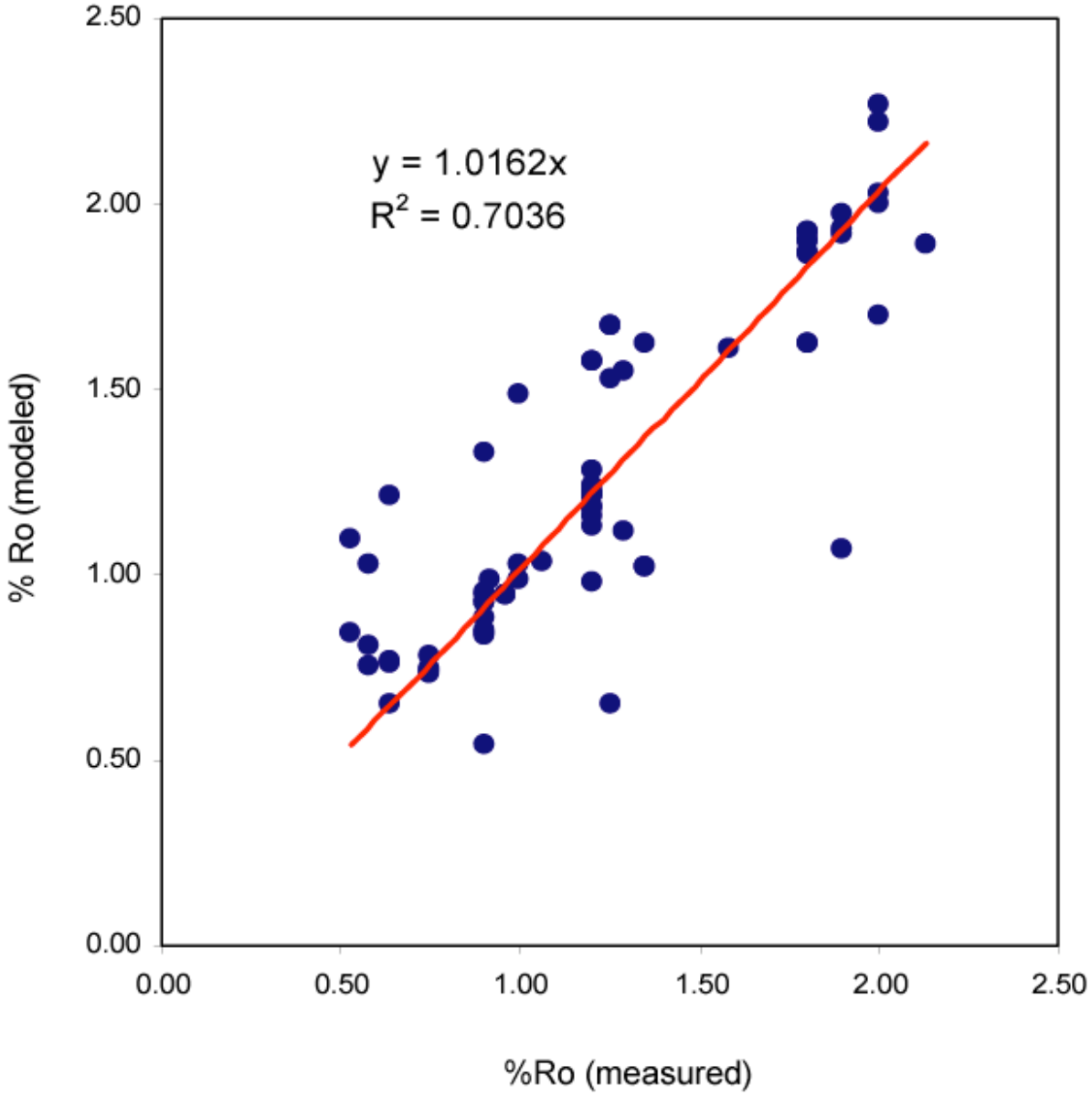


Figure 86. Comparison of the modeled %Ro with measured %Ro.
Prepared by Roger Barnaby.

profiles (Figs. 87-128) and hydrocarbon expulsion profiles (Figs. 129-170). Burial history (Figs. 171-219), thermal maturation history (Figs. 220-267), and hydrocarbon expulsion profiles (Figs. 268-312) were prepared for strata in the Mississippi Interior Salt Basin using the same methodologies as was used for strata in the North Louisiana Salt Basin, and burial history (Figs. 313-316), thermal maturation history (Figs. 317-320), and hydrocarbon expulsion profiles (Figs. 321-324) were prepared for the North Louisiana Salt Basin using a rift heat flow model for comparison purposes.

### *Tectonic History*

The origin of the North Louisiana Salt Basin is directly linked to the evolution of the Gulf of Mexico (Wood and Walper, 1974). The Gulf of Mexico is a divergent margin basin characterized by extensional rift tectonics and wrench faulting (Pilger, 1981; Miller, 1982; Klitgord, et al., 1984; Van Siclen, 1984; Pindell, 1985; Salvador, 1987; Winker and Buffler, 1988; Buffler, 1991). The history of the basin includes a phase of crustal extension and thinning, a phase of rifting and sea-floor spreading and a phase of thermal subsidence (Nunn, 1984). Rifting was in a northwest-southeast direction; however, early rifting may have been north-south (Pilger, 1981; MacRae and Watkins, 1996). The Gulf has been interpreted as opening by right lateral translation and with movement of the Yucatan block playing a major role in the opening (Van Siclen, 1984; Buffler and Sawyer, 1985). The structural and stratigraphic framework of the region was established during the Triassic and Jurassic (Salvador, 1987).

Two periods can be recognized in the evolution of the region: active rifting lasting from the Late Triassic to Middle Jurassic represented by the deposition of nonmarine

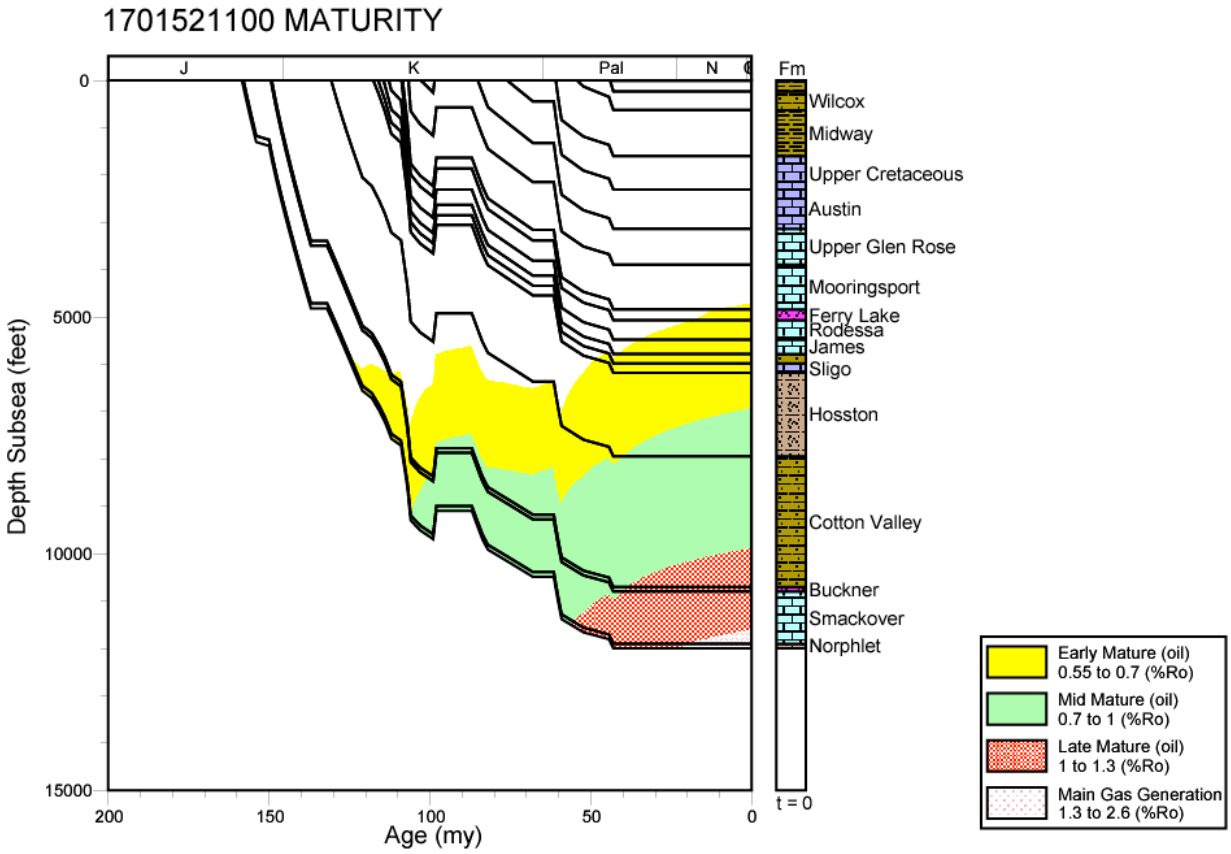


Figure 87. Thermal maturation profile for well 1701521100, North Louisiana Salt Basin.

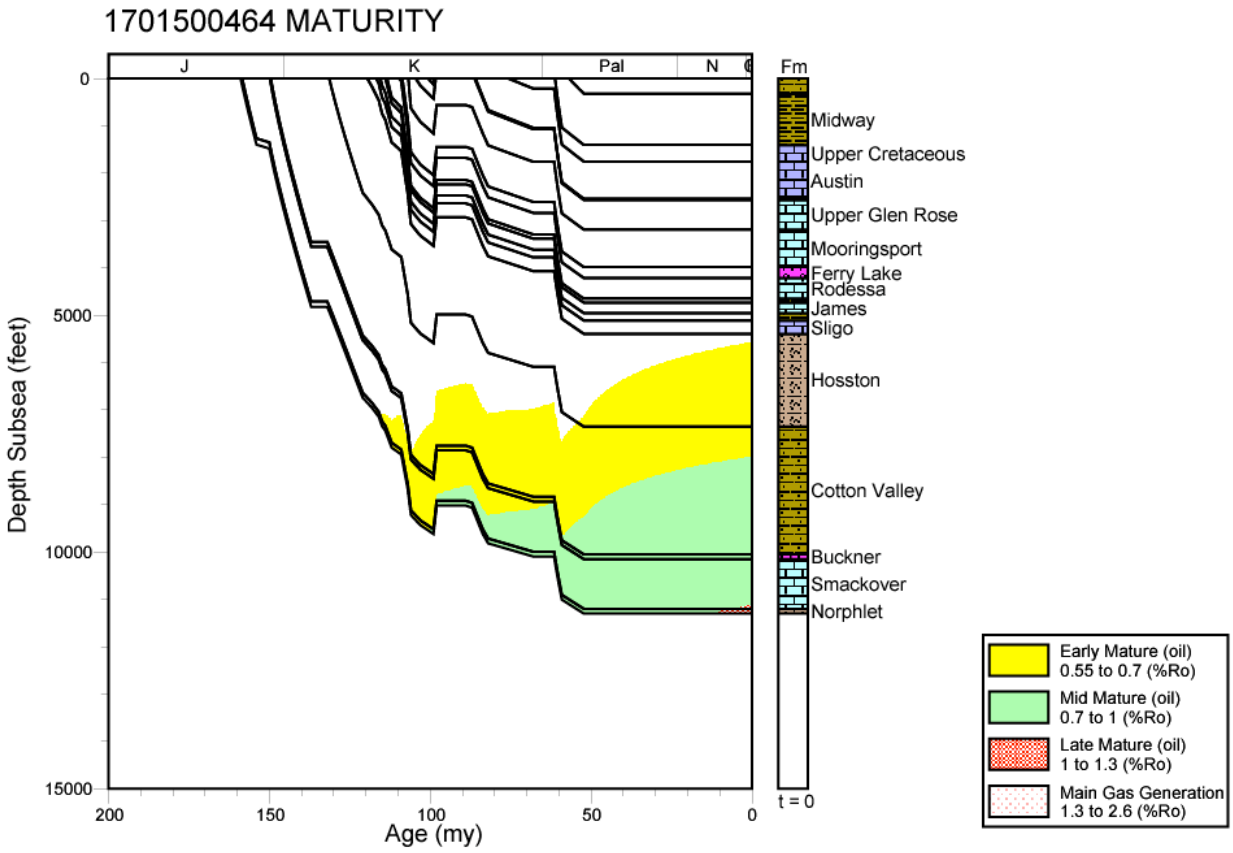


Figure 88. Thermal maturation profile for well 1701500464, North Louisiana Salt Basin.

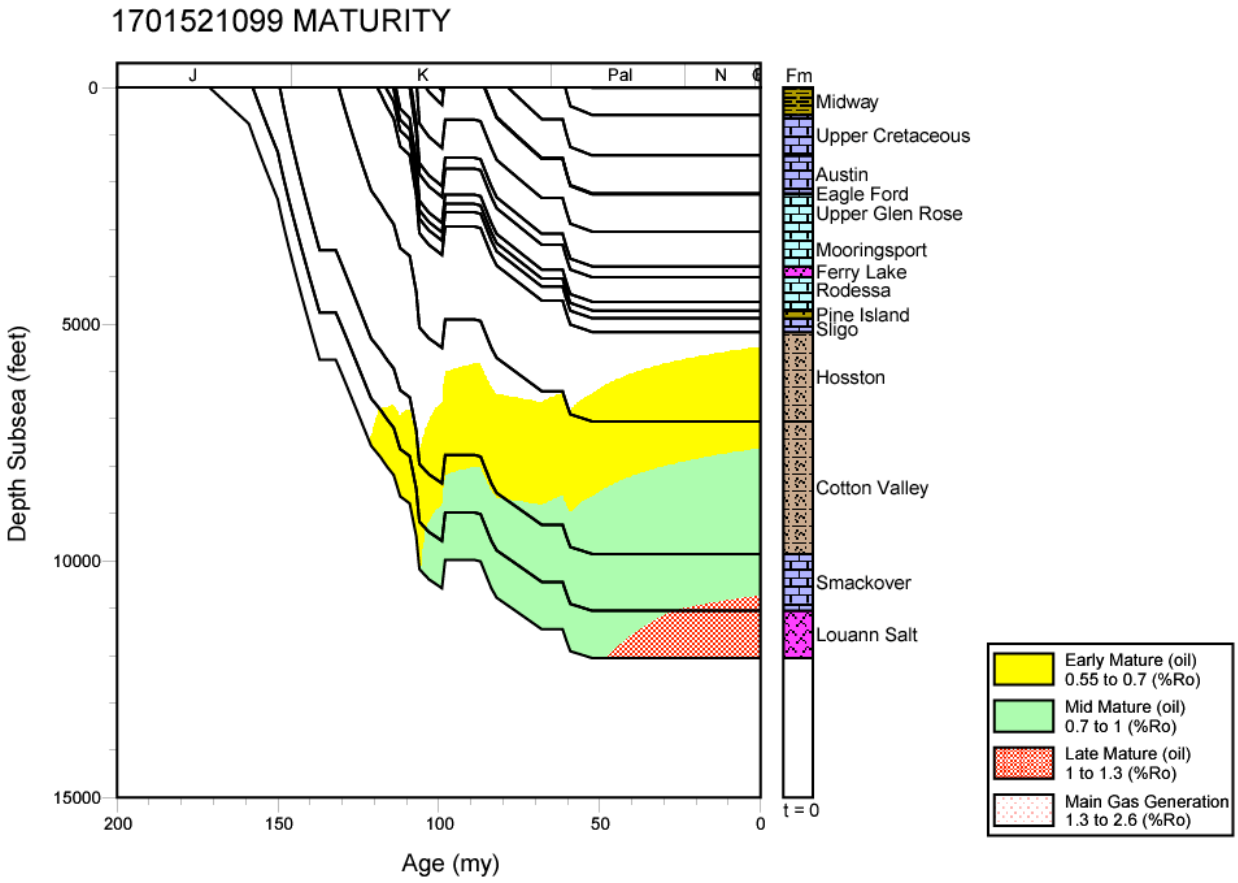


Figure 89. Thermal maturation profile for well 1701521099, North Louisiana Salt Basin.

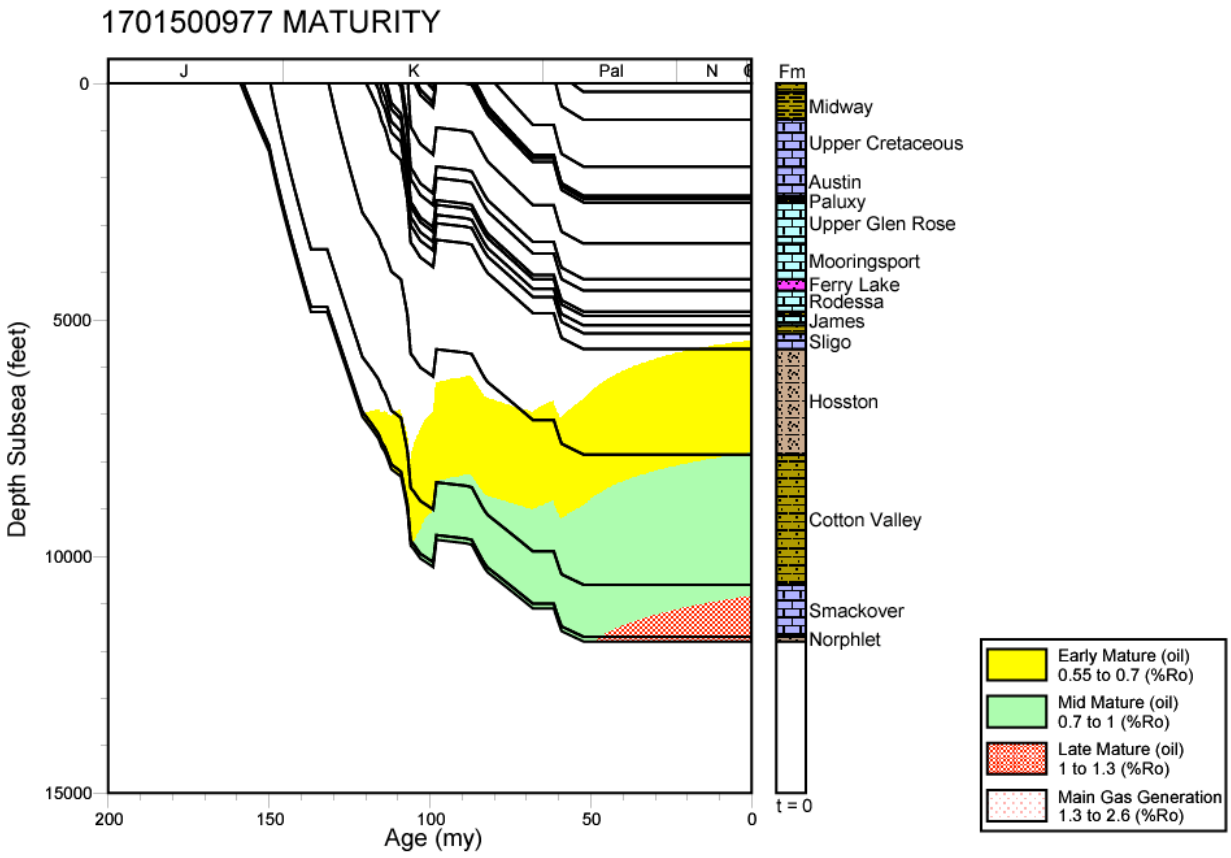


Figure 90. Thermal maturation profile for well 1701500977, North Louisiana Salt Basin.

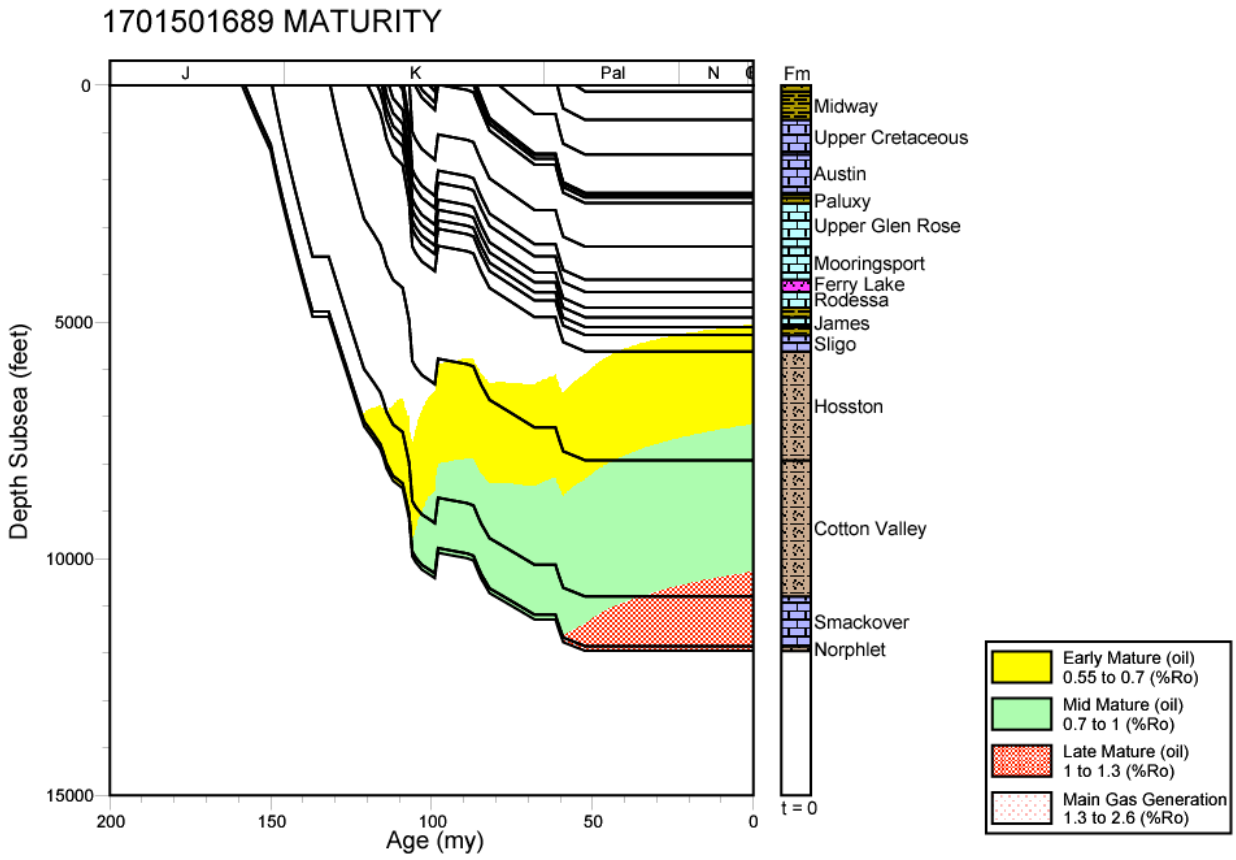


Figure 91. Thermal maturation profile for well 1701501689, North Louisiana Salt Basin.

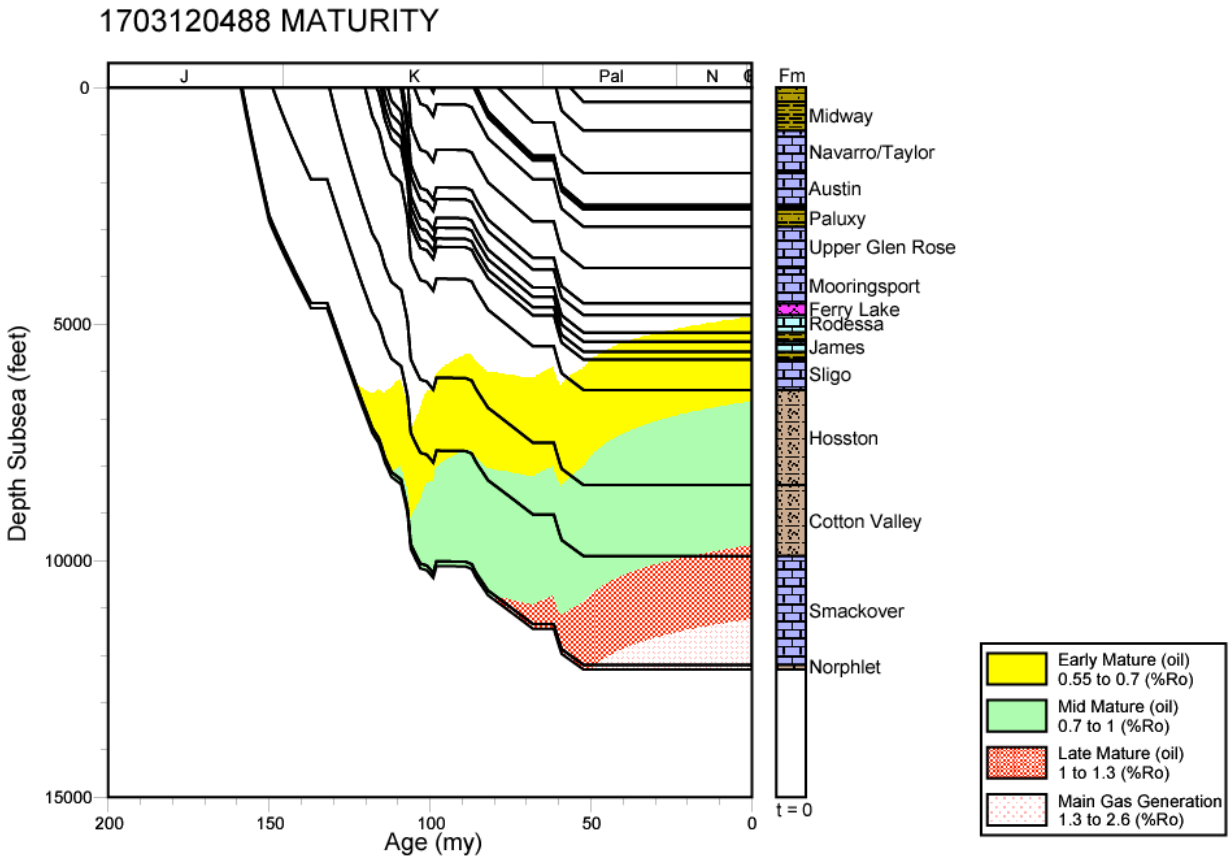


Figure 92. Thermal maturation profile for well 1703120488, North Louisiana Salt Basin.

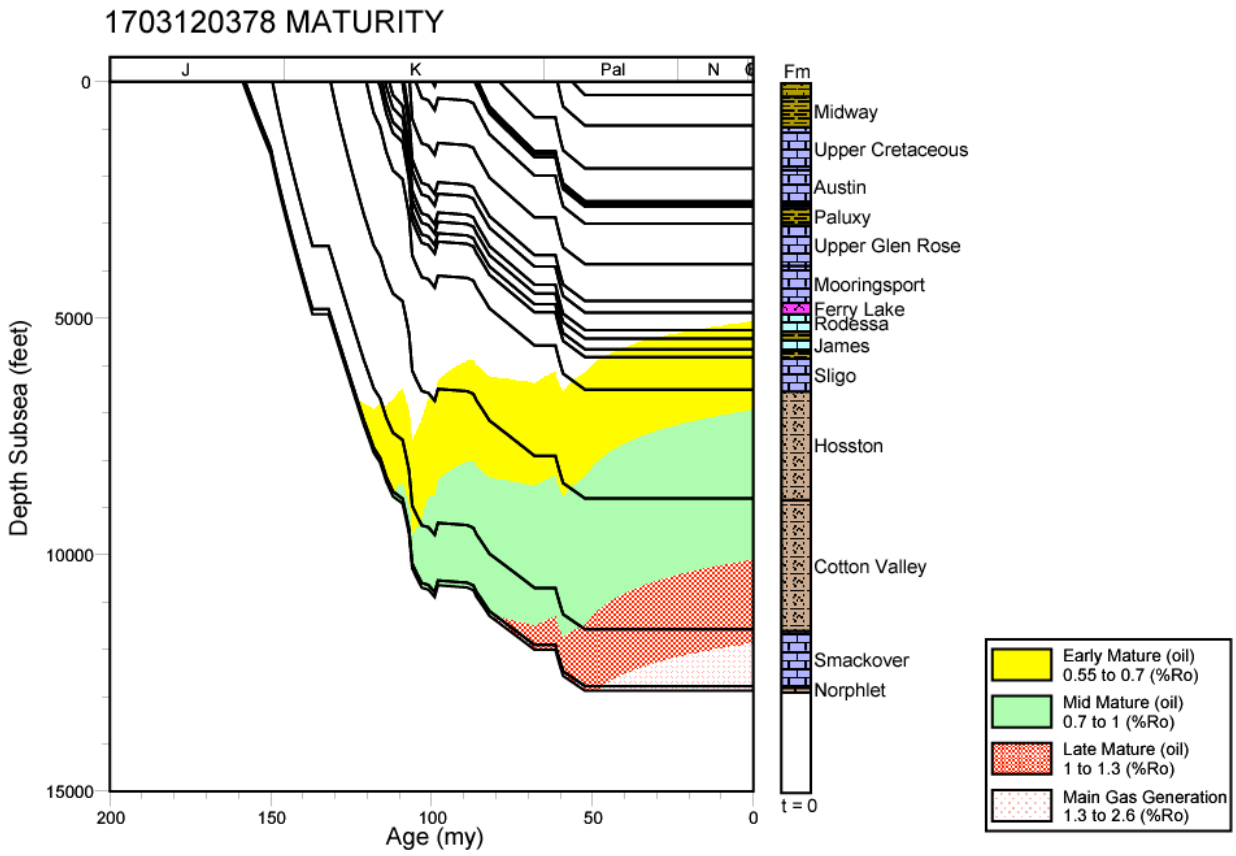


Figure 93. Thermal maturation profile for well 1703120378, North Louisiana Salt Basin.

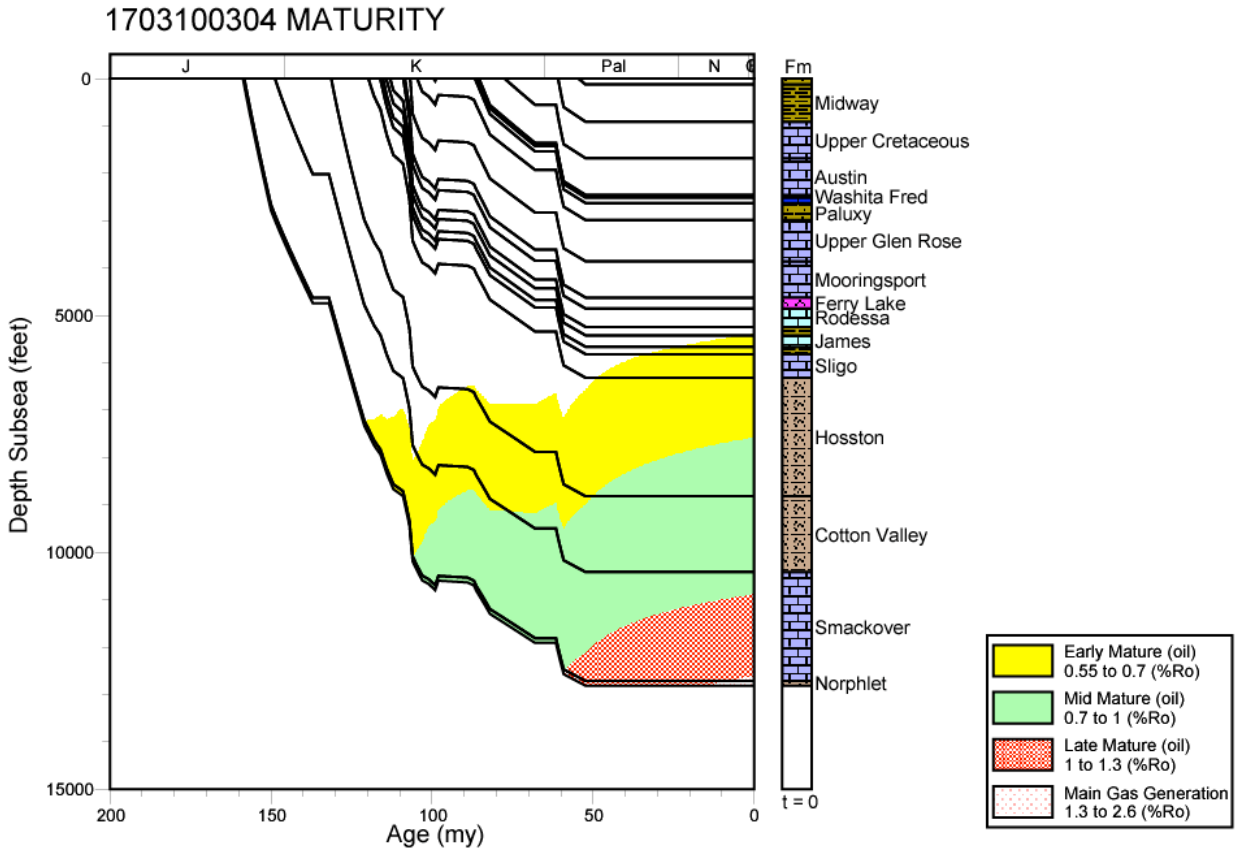


Figure 94. Thermal maturation profile for well 1703100304, North Louisiana Salt Basin.

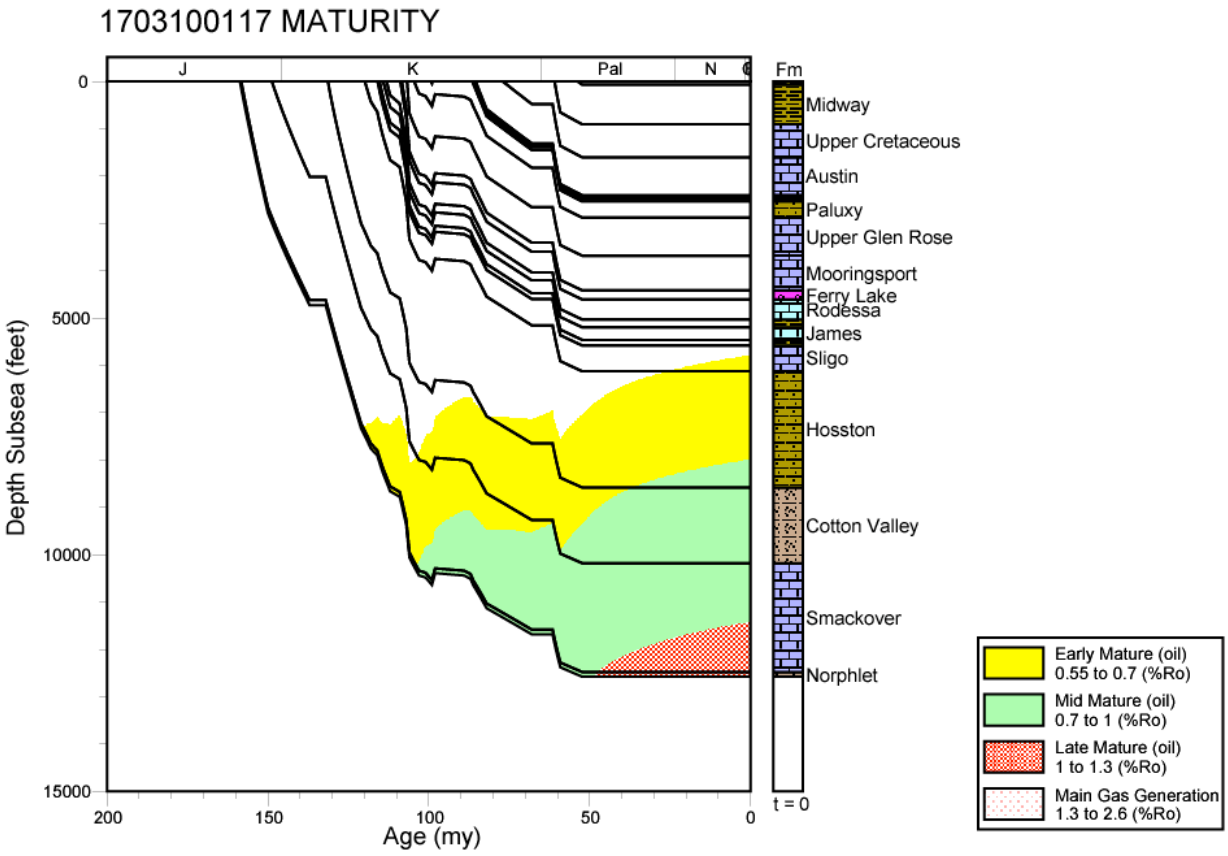


Figure 95. Thermal maturation profile for well 1703100117, North Louisiana Salt Basin.

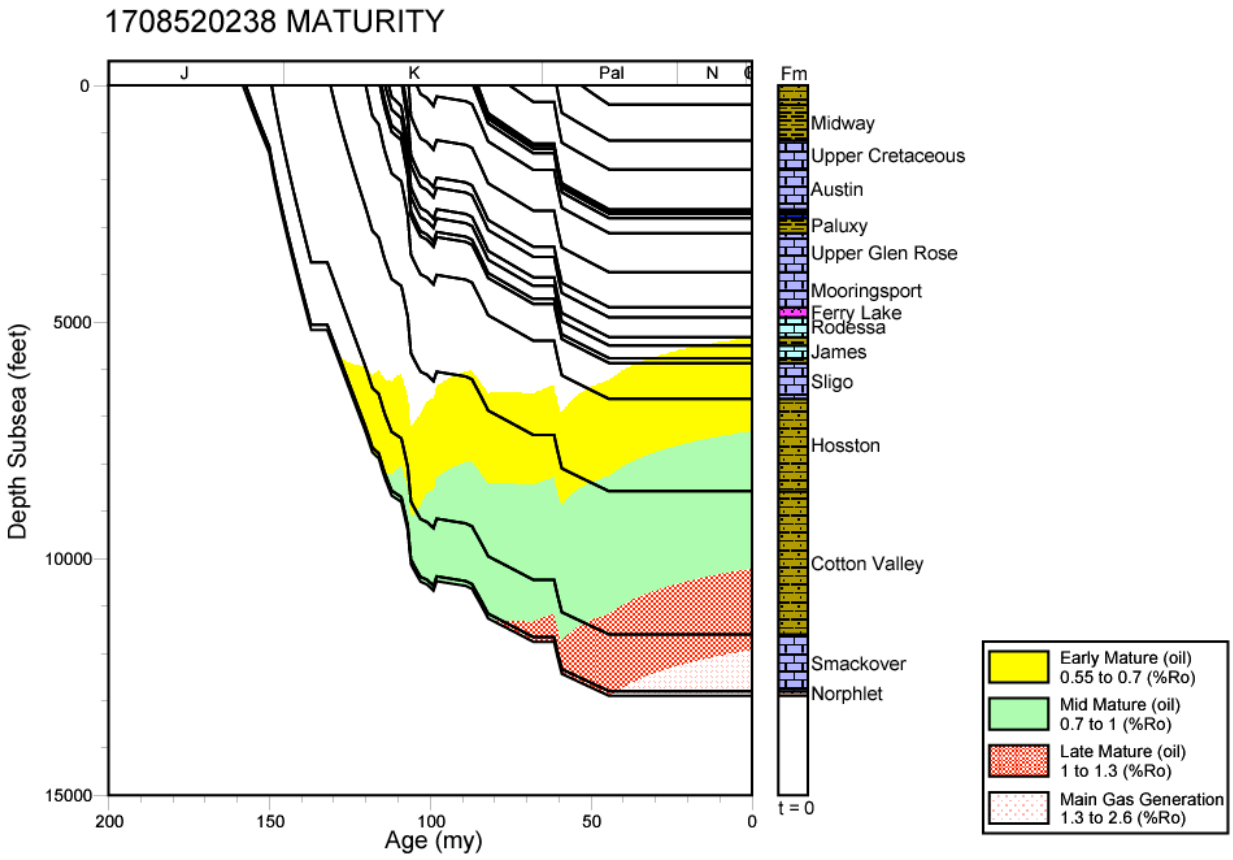


Figure 96. Thermal maturation profile for well 1708520238, North Louisiana Salt Basin.

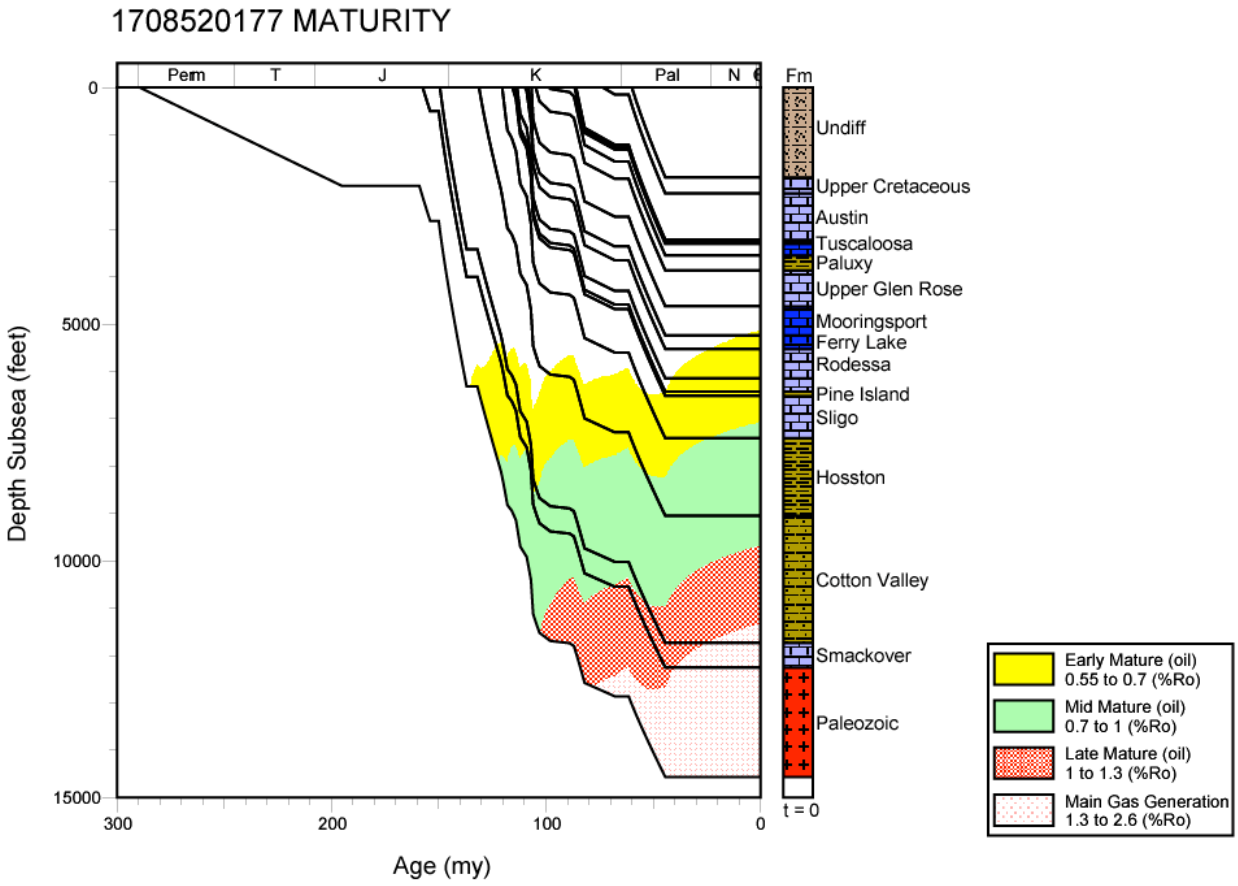


Figure 97. Thermal maturation profile for well 1708520177, North Louisiana Salt Basin.

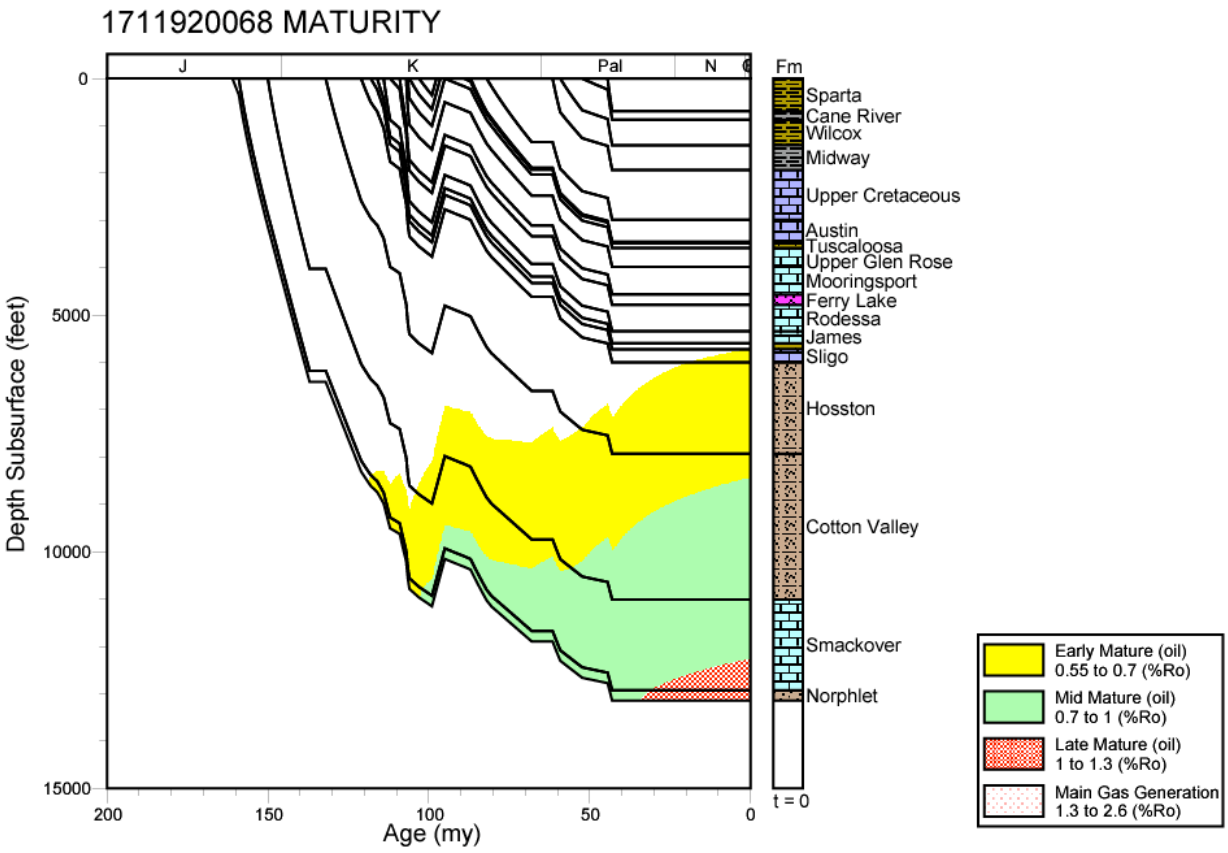


Figure 98. Thermal maturation profile for well 1711920068, North Louisiana Salt Basin.

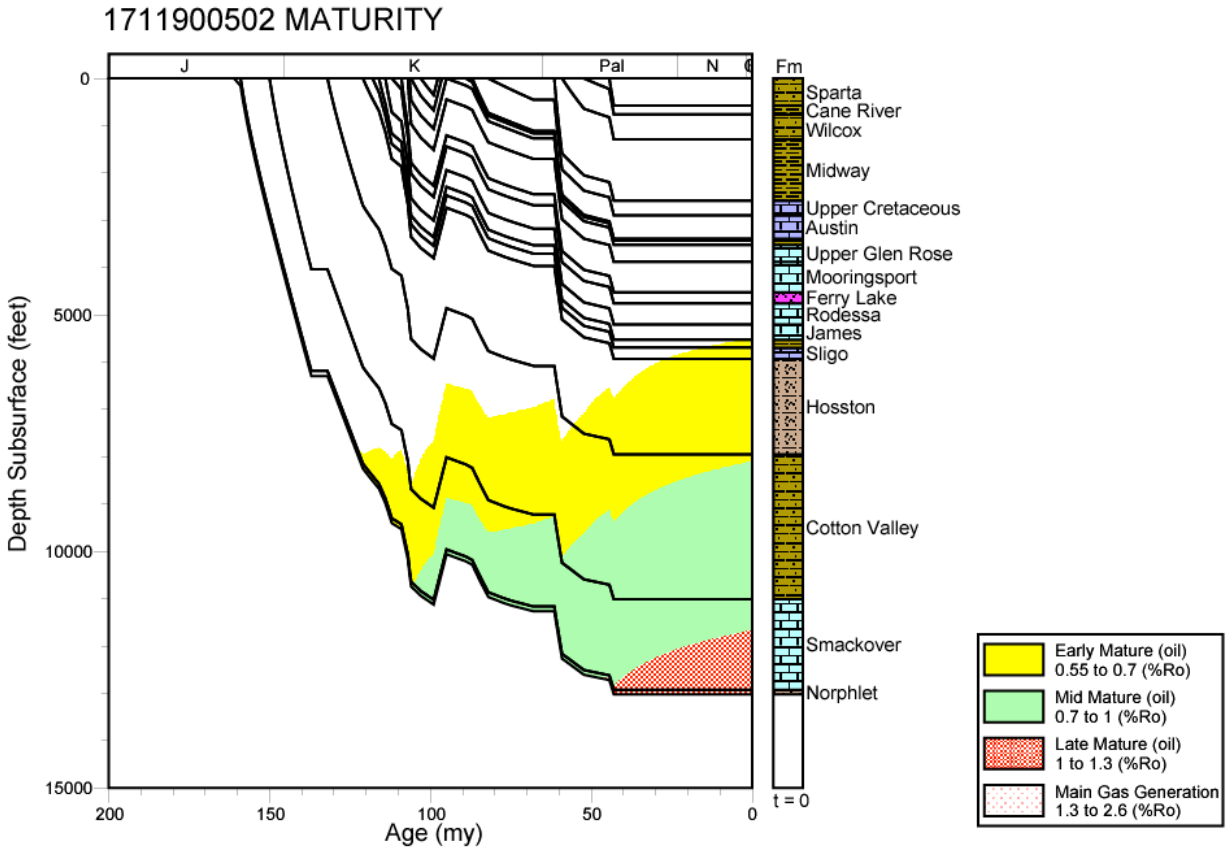


Figure 99. Thermal maturation profile for well 1711900502, North Louisiana Salt Basin.

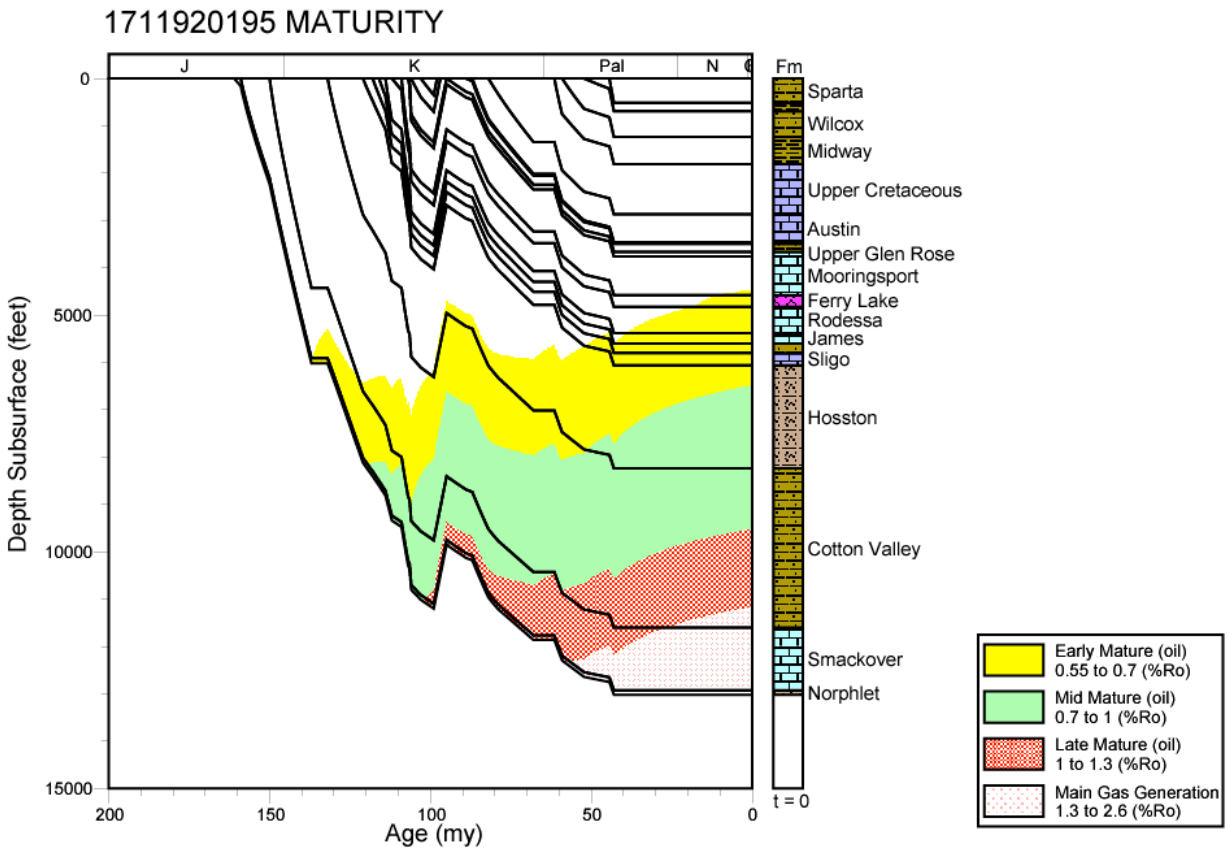


Figure 100. Thermal maturation profile for well 1711920195, North Louisiana Salt Basin.

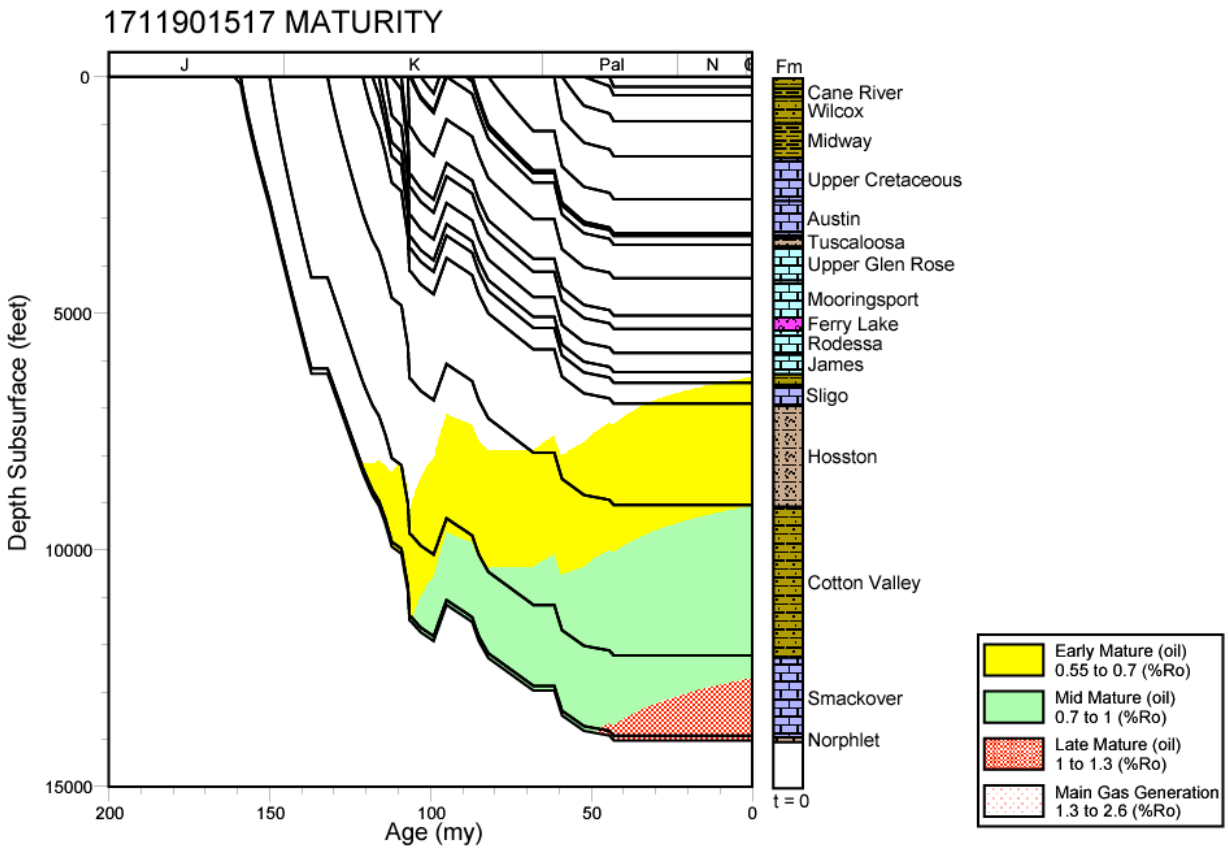


Figure 101. Thermal maturation profile for well 1711901517, North Louisiana Salt Basin.

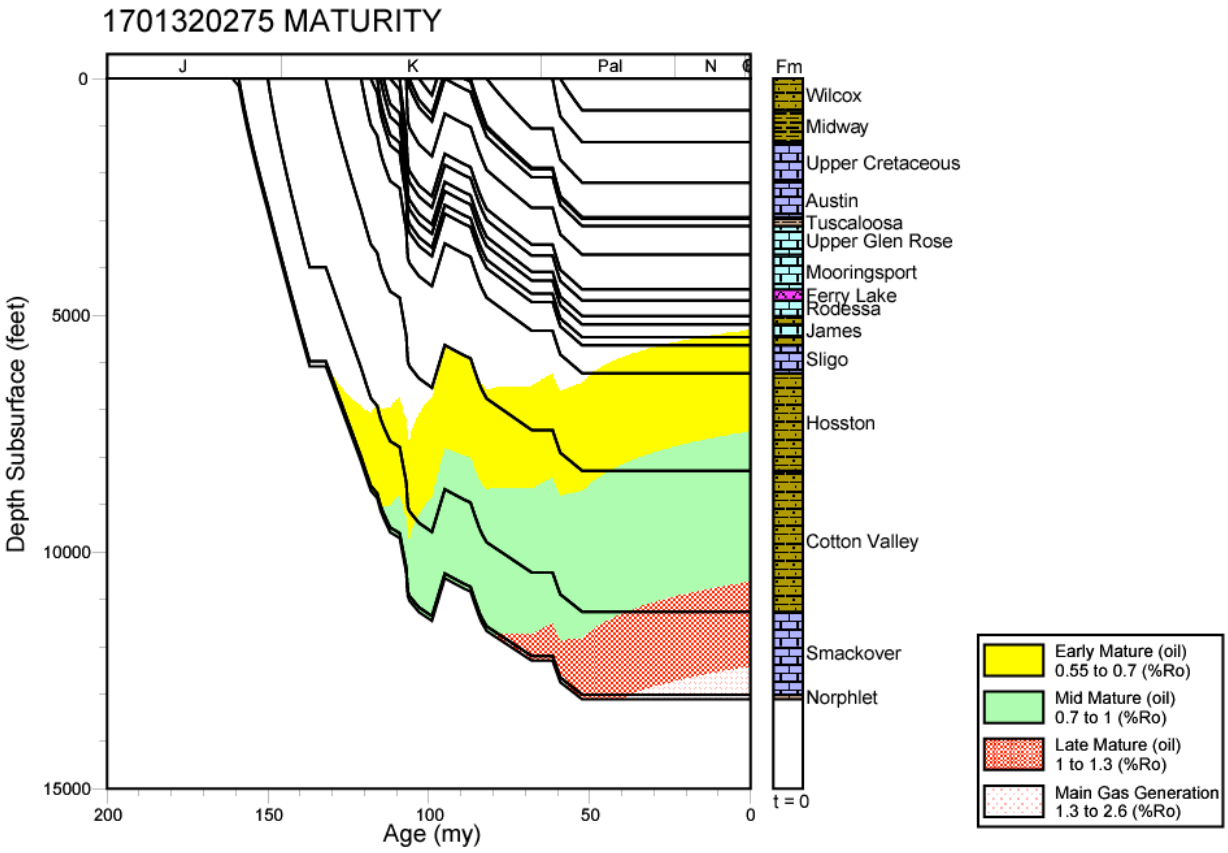


Figure 102. Thermal maturation profile for well 1701320275, North Louisiana Salt Basin.

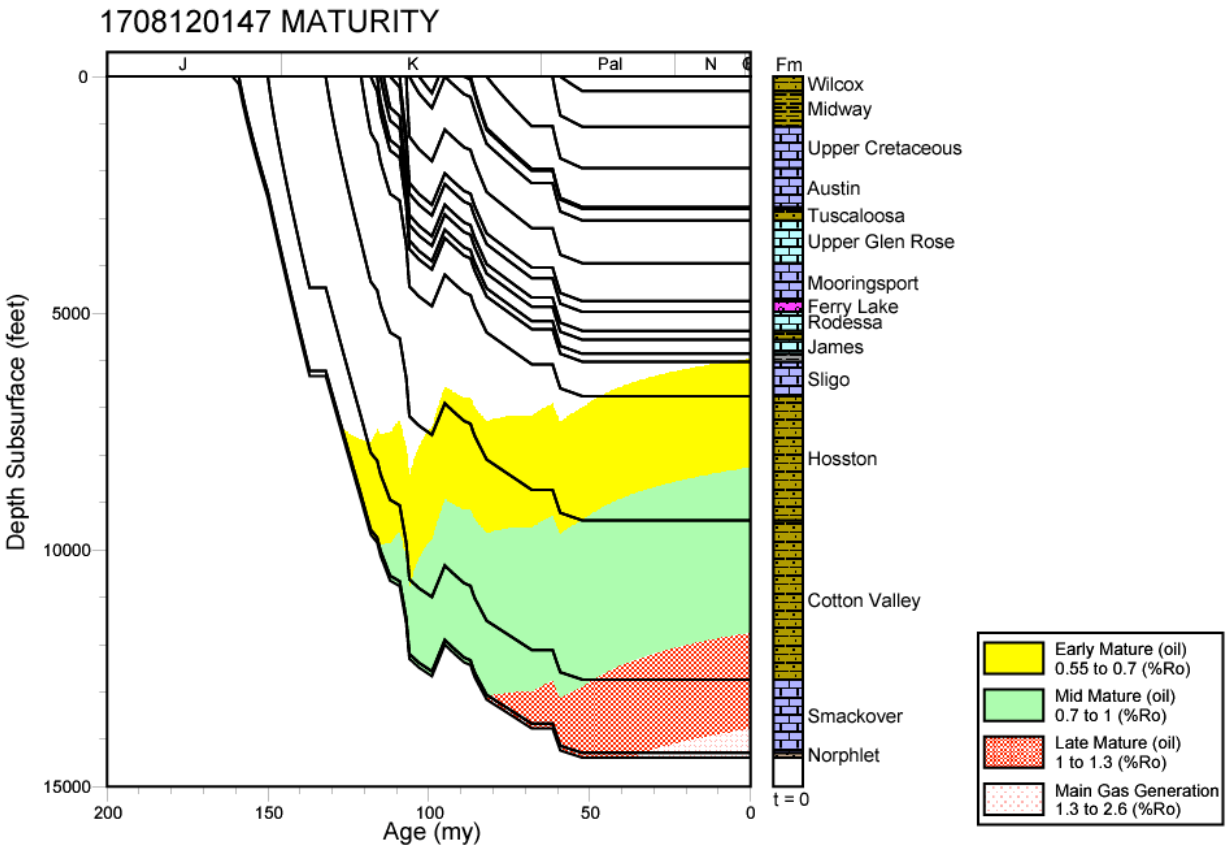


Figure 103. Thermal maturation profile for well 1708120147, North Louisiana Salt Basin.

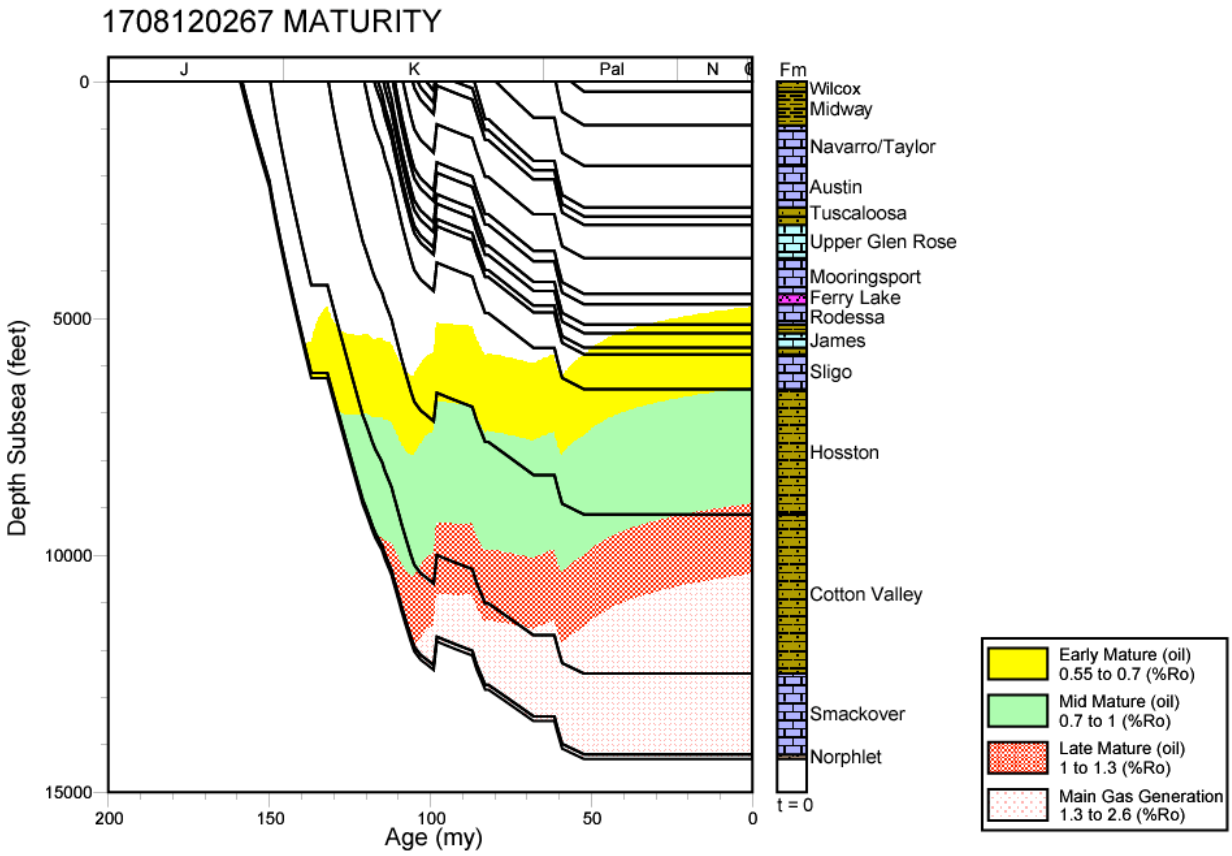


Figure 104. Thermal maturation profile for well 1708120267, North Louisiana Salt Basin.

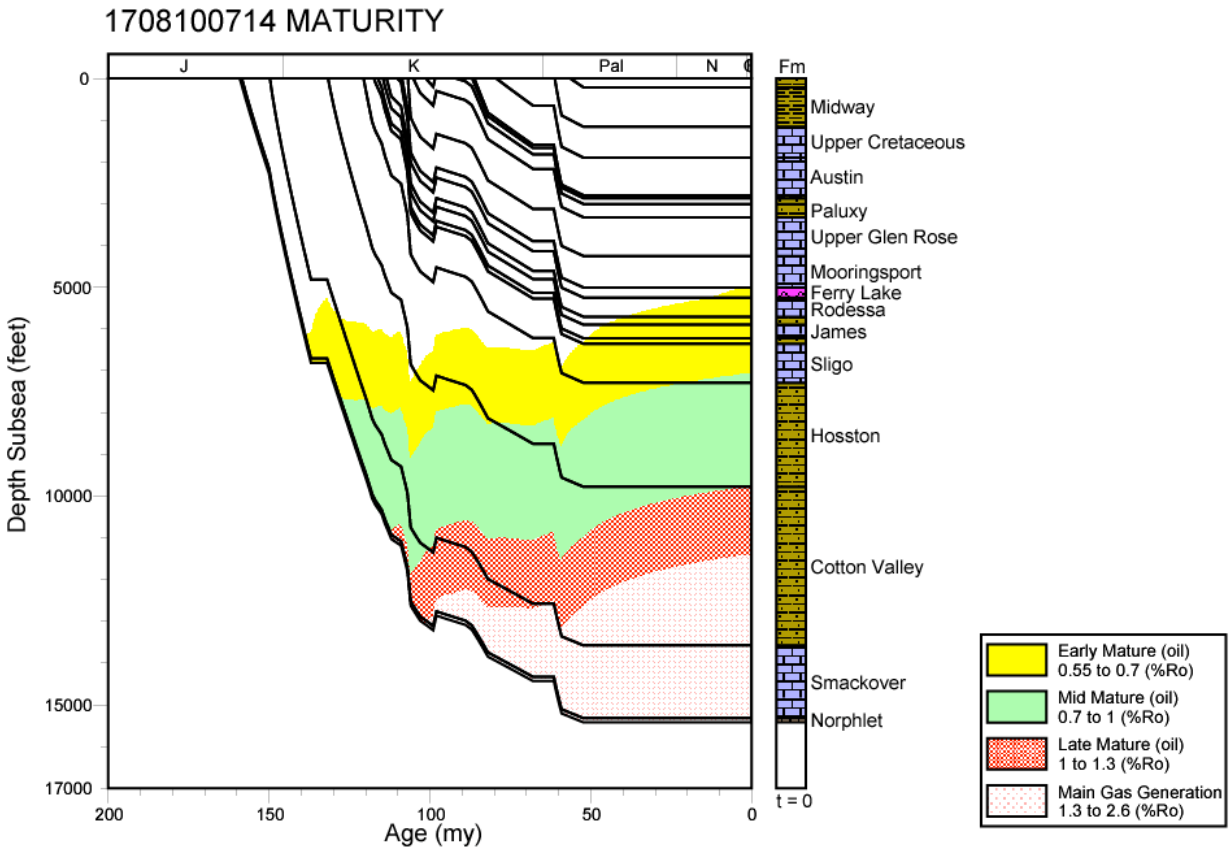


Figure 105. Thermal maturation profile for well 1708100714, North Louisiana Salt Basin.

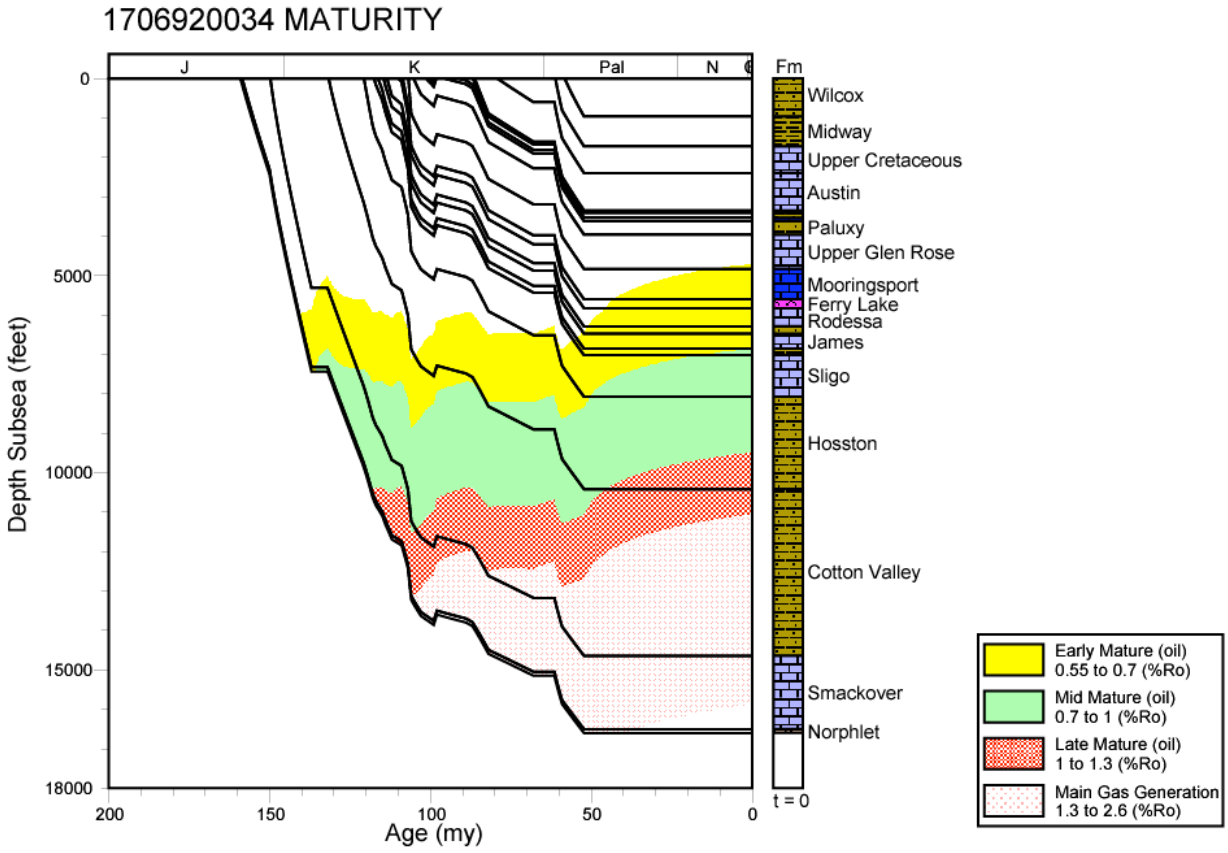


Figure 106. Thermal maturation profile for well 1706920034, North Louisiana Salt Basin.

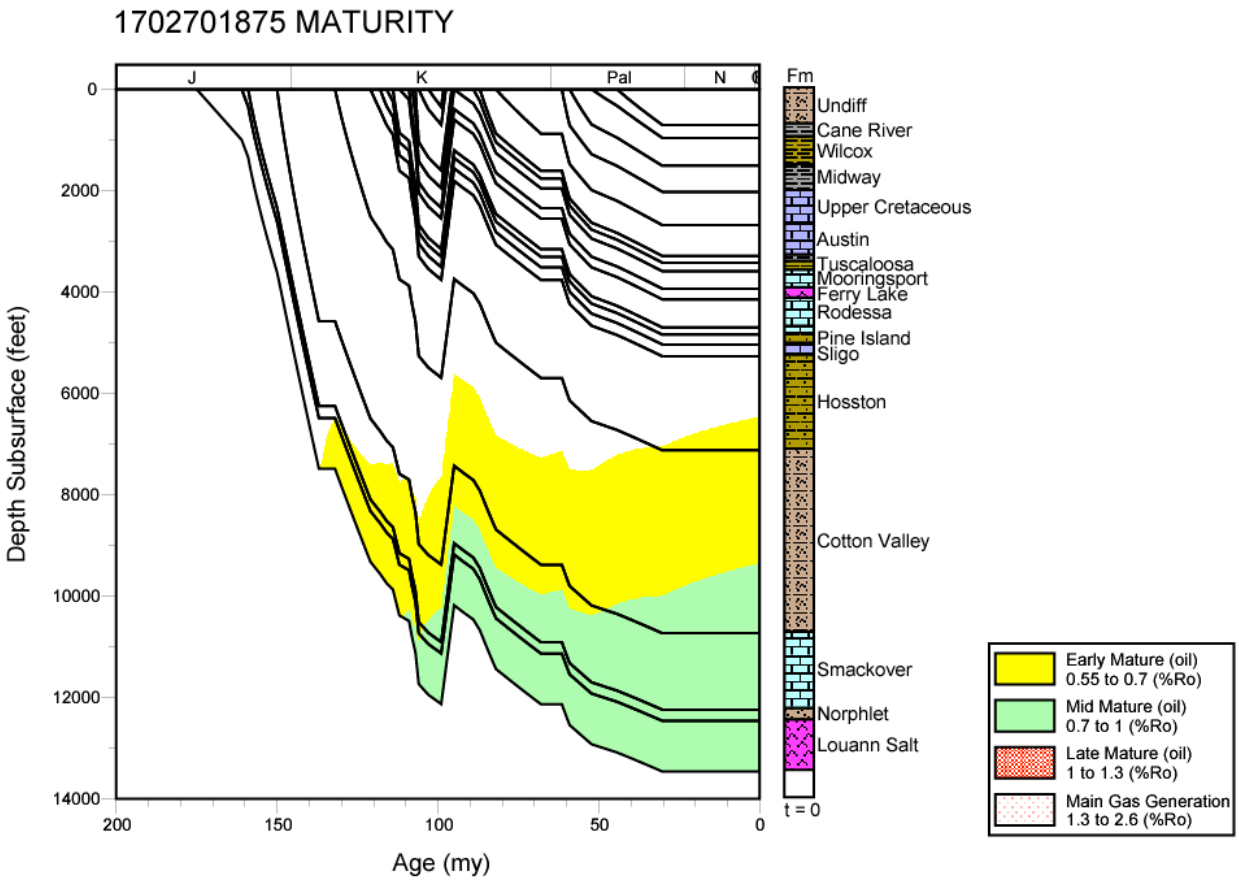


Figure 107. Thermal maturation profile for well 1702701875, North Louisiana Salt Basin.

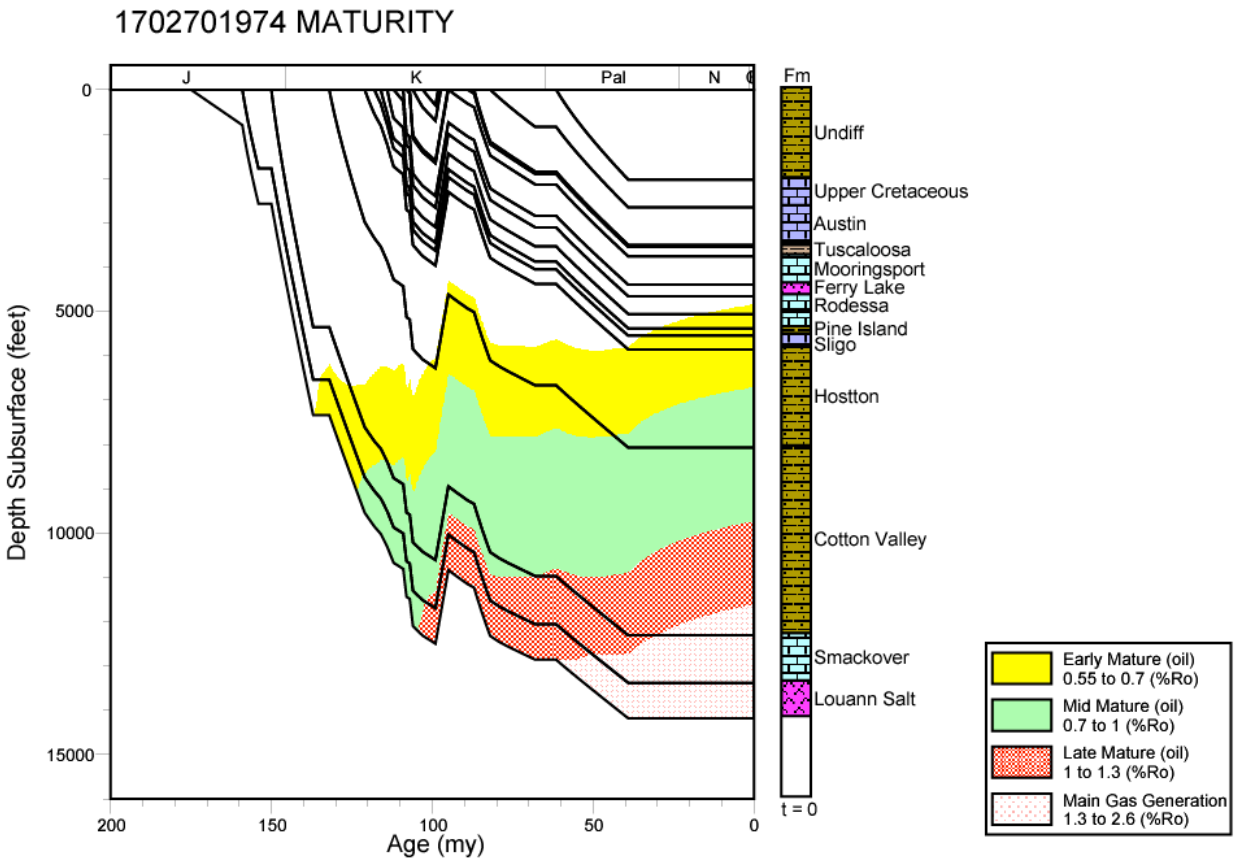


Figure 108. Thermal maturation profile for well 1702701974, North Louisiana Salt Basin.

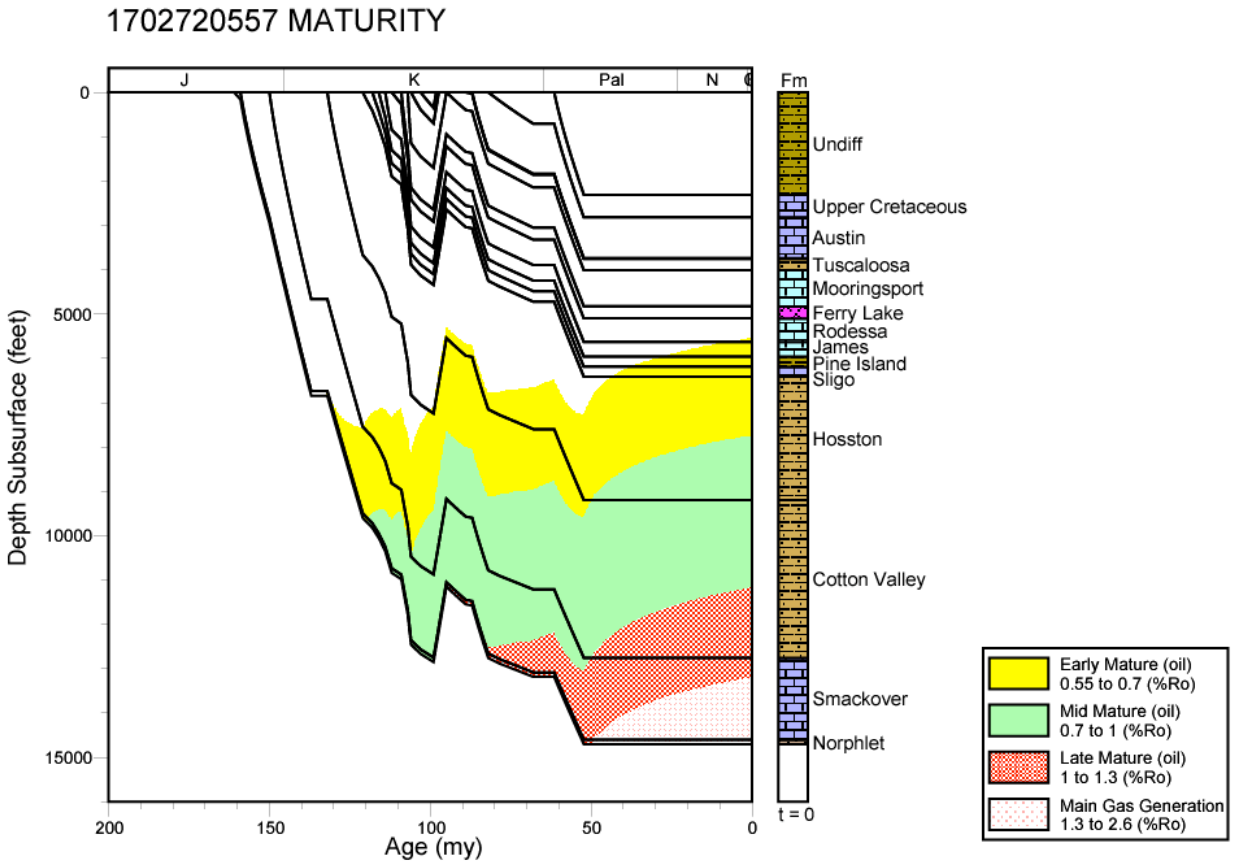


Figure 109. Thermal maturation profile for well 1702720557, North Louisiana Salt Basin.

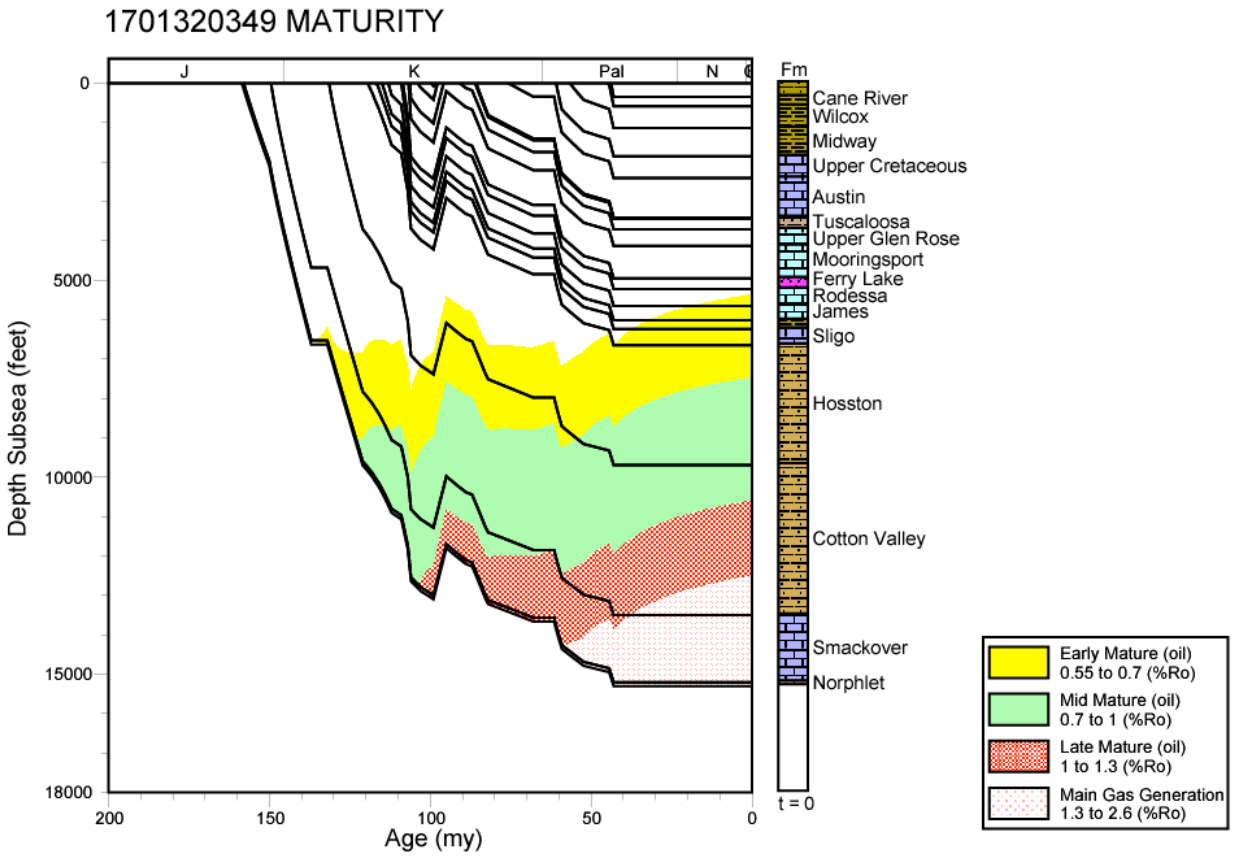


Figure 110. Thermal maturation profile for well 1701320349, North Louisiana Salt Basin.

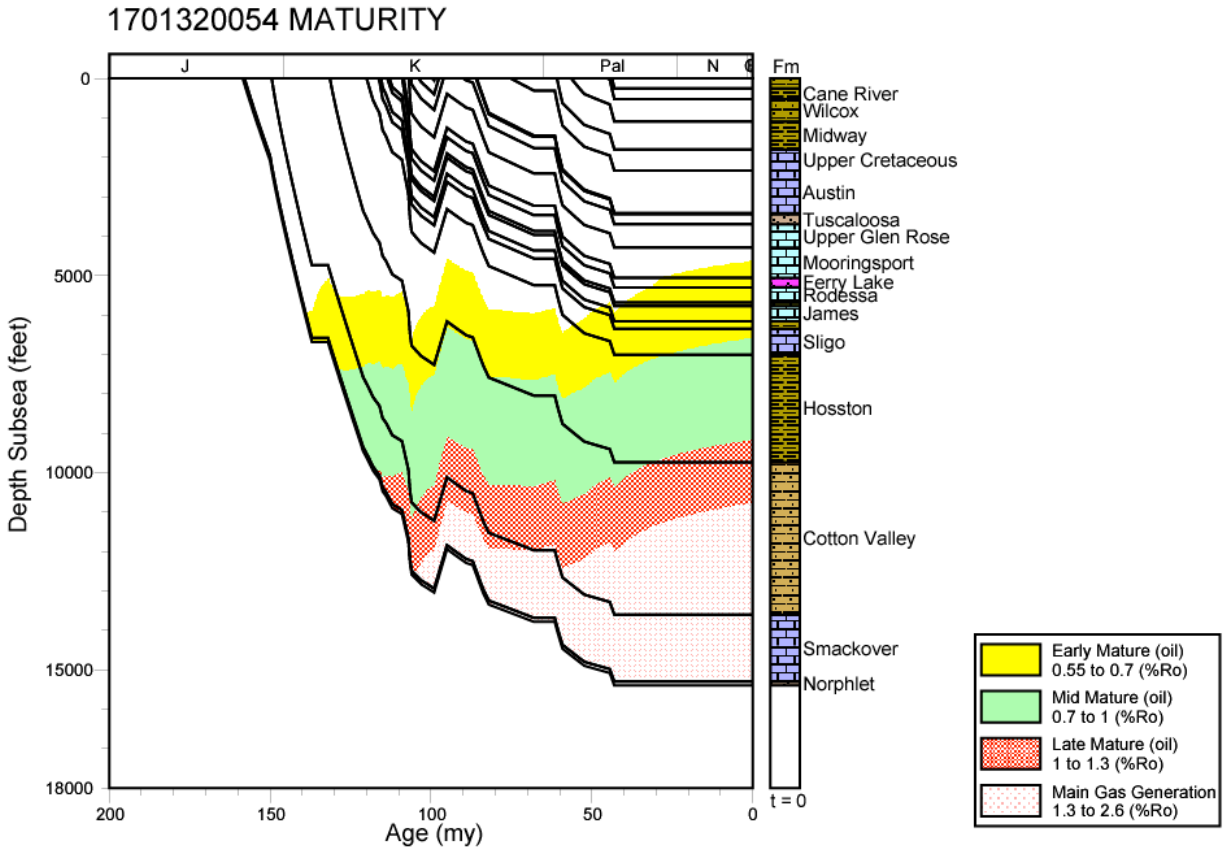


Figure 111. Thermal maturation profile for well 1701320054, North Louisiana Salt Basin.

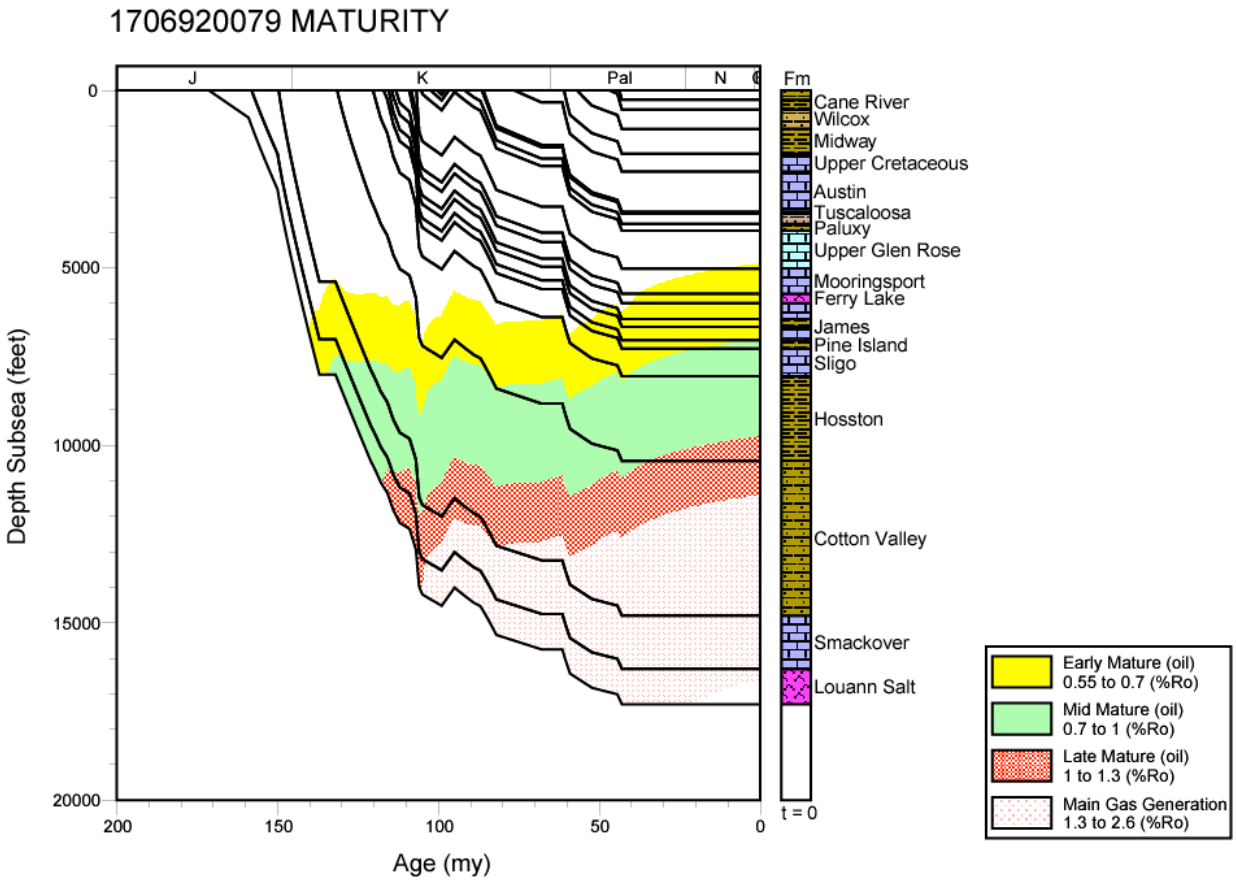


Figure 112. Thermal maturation profile for well 1706920079, North Louisiana Salt Basin.

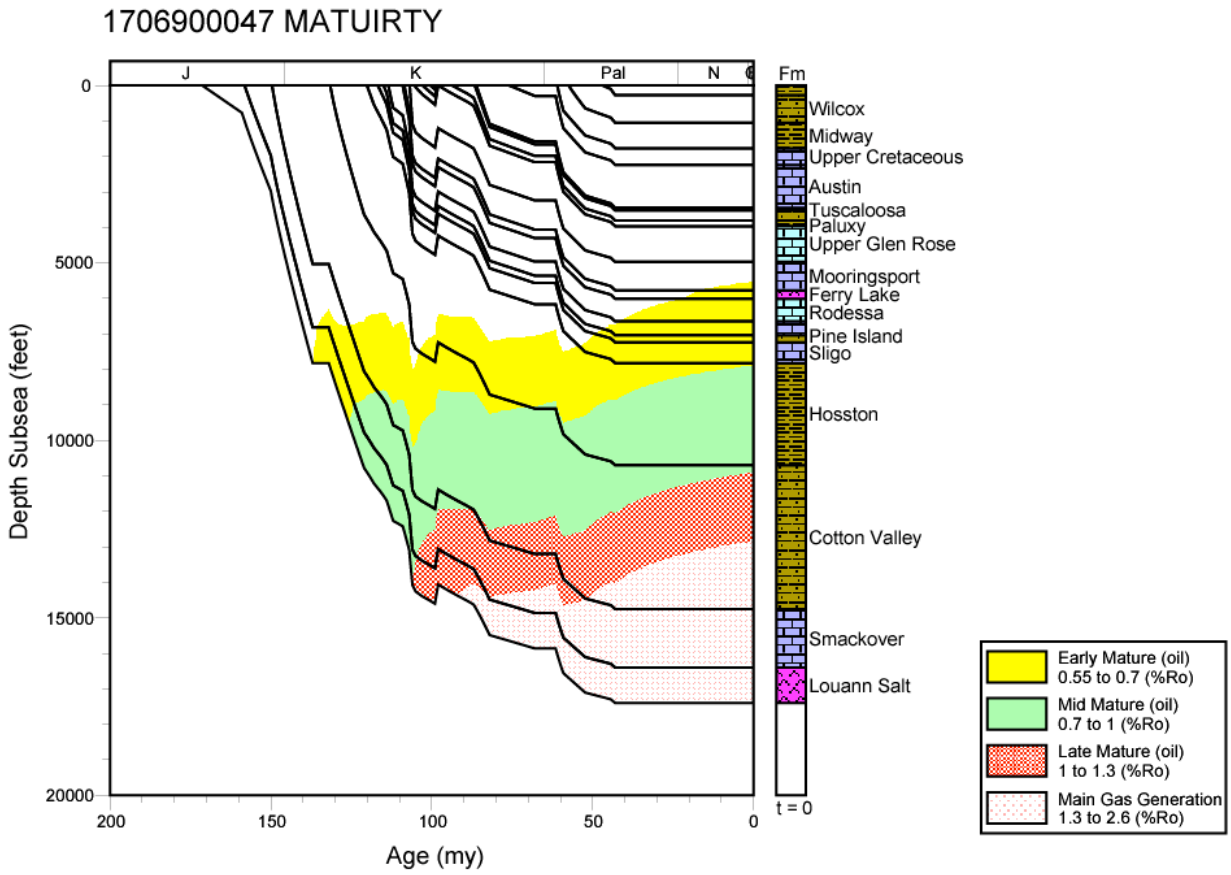


Figure 113. Thermal maturation profile for well 1706900047, North Louisiana Salt Basin.

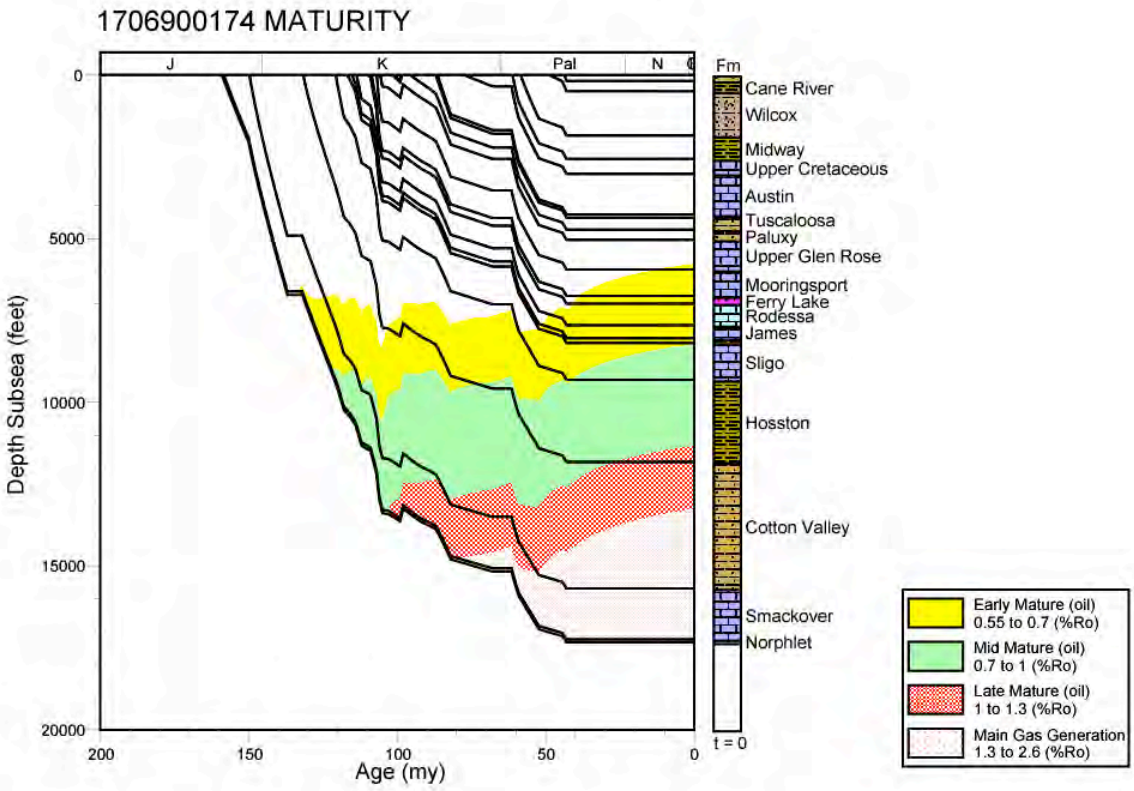


Figure 114. Thermal maturation profile for well 1706900174, North Louisiana Salt Basin.

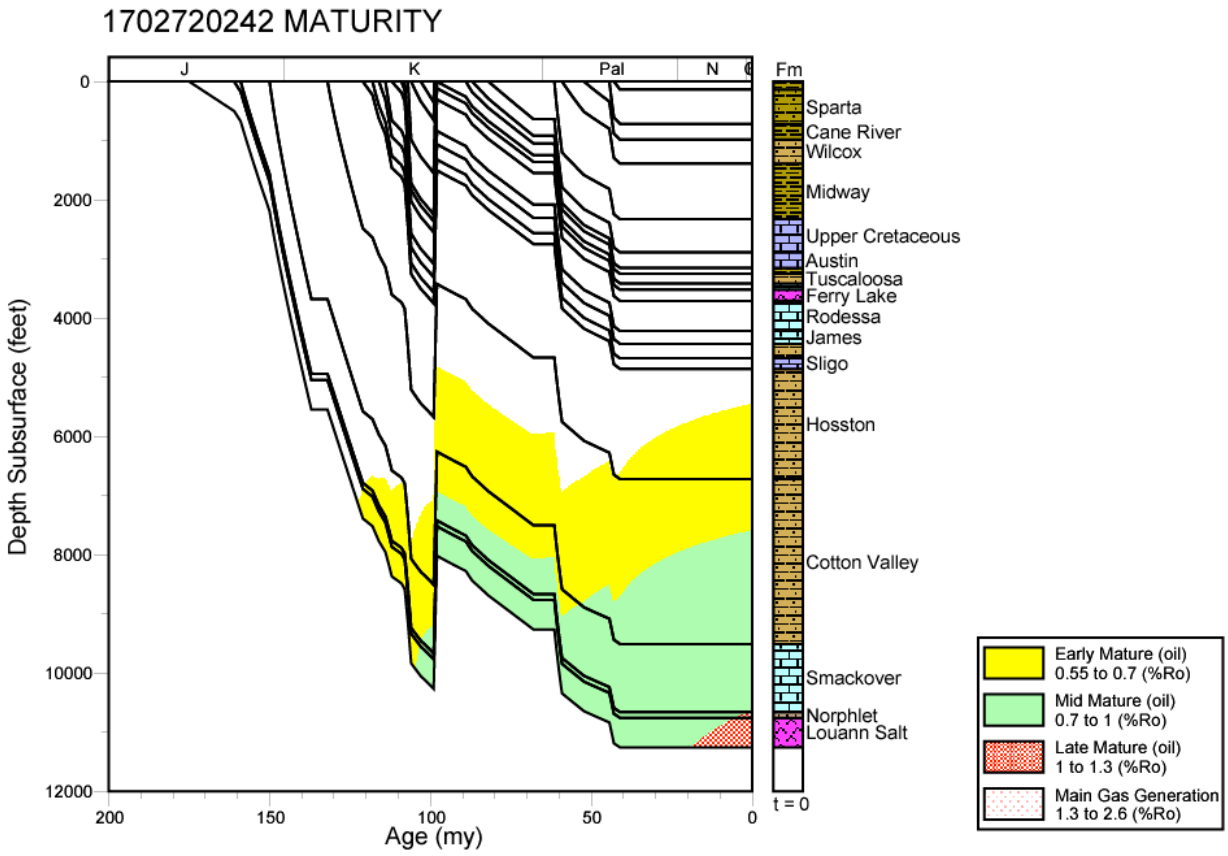


Figure 115. Thermal maturation profile for well 1702720242, North Louisiana Salt Basin.

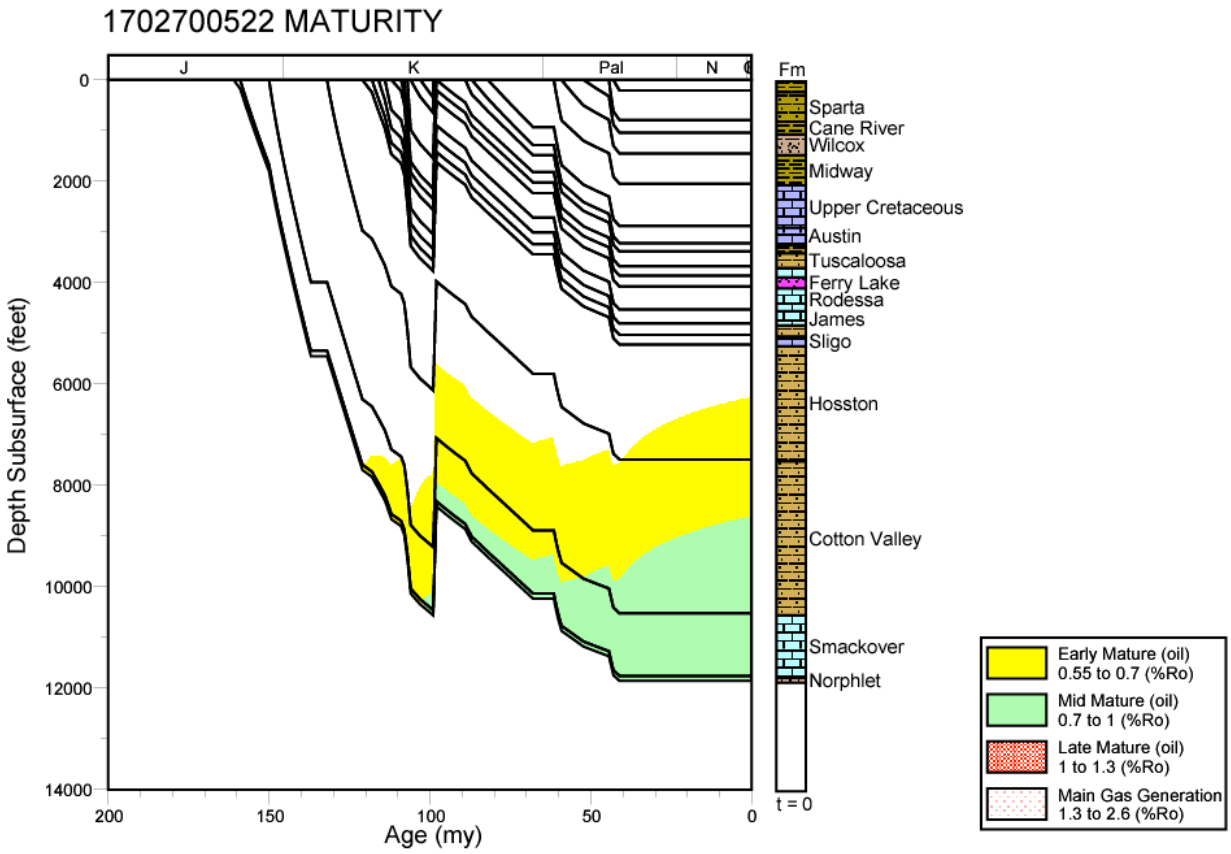


Figure 116. Thermal maturation profile for well 1702700522, North Louisiana Salt Basin.

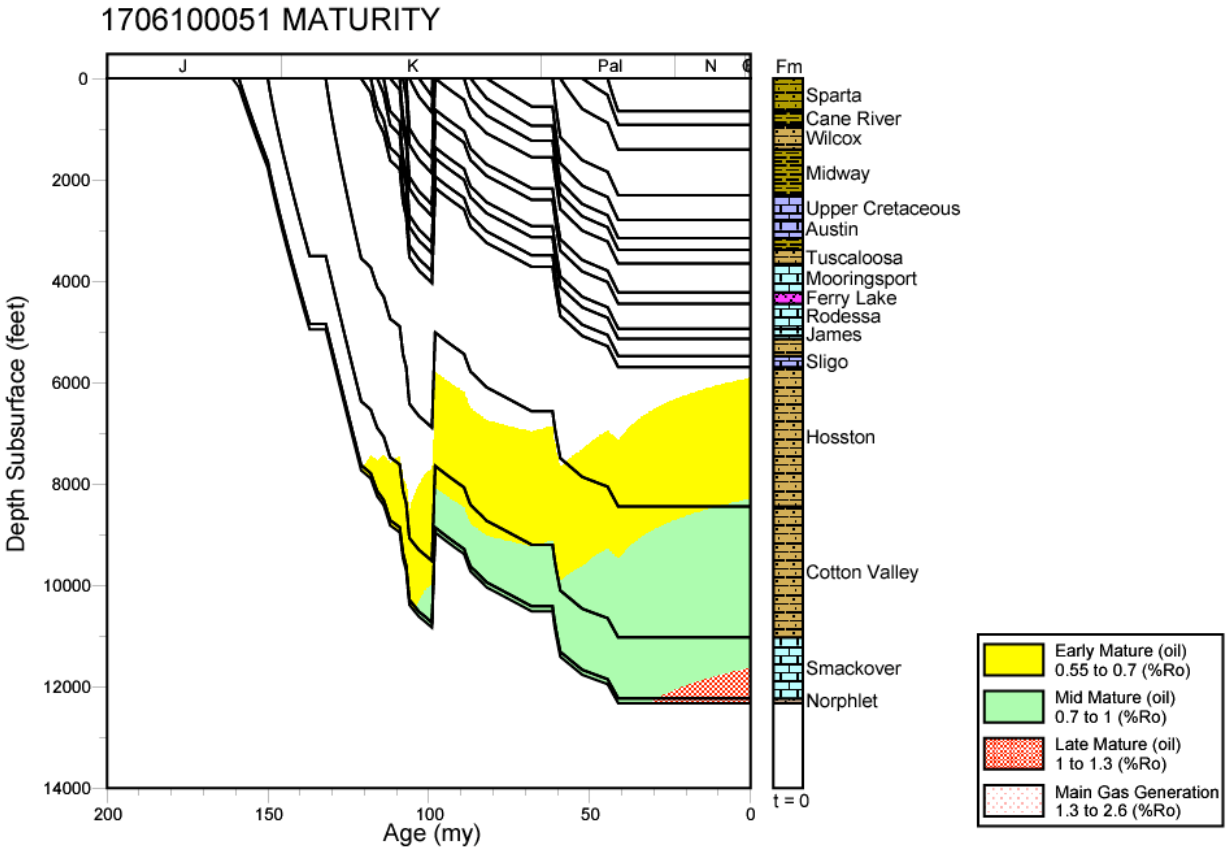


Figure 117. Thermal maturation profile for well 1706100051, North Louisiana Salt Basin.

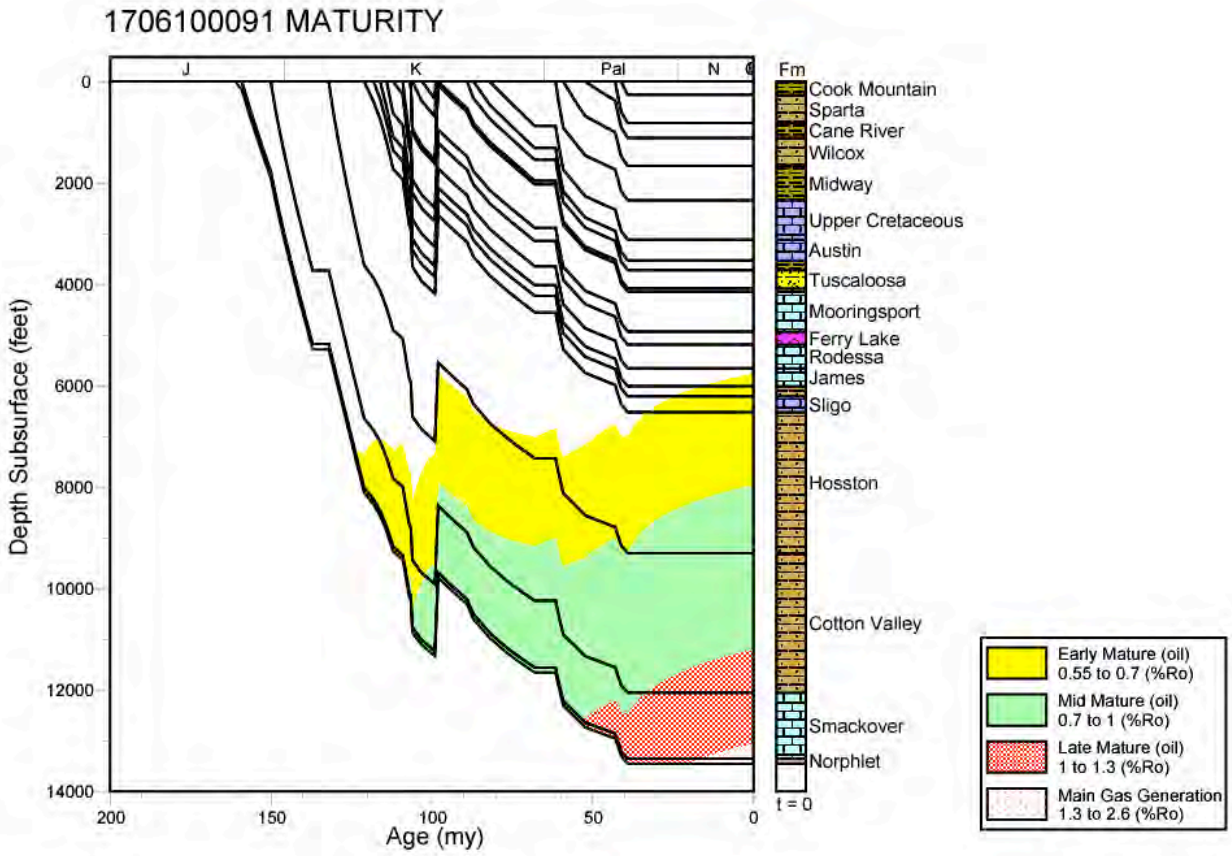


Figure 118. Thermal maturation profile for well 1706100091, North Louisiana Salt Basin.

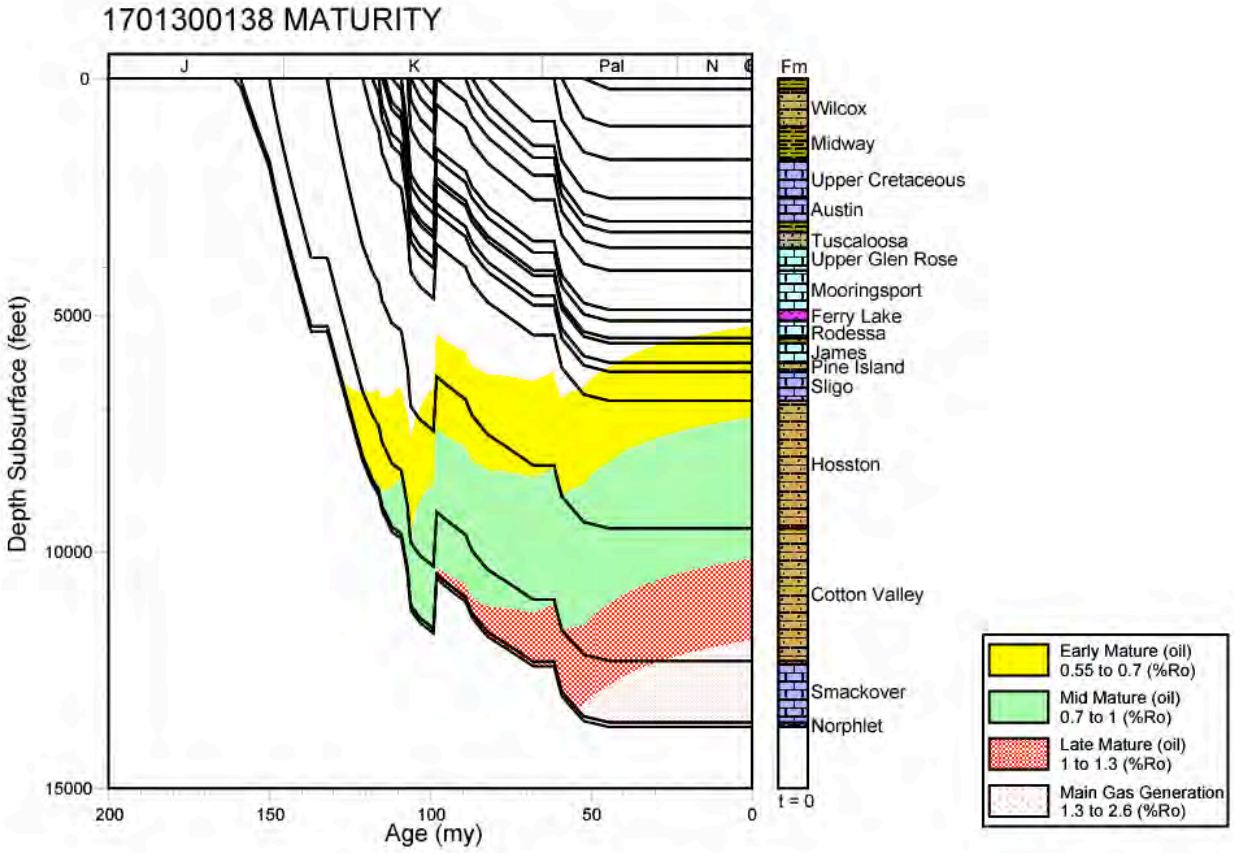


Figure 119. Thermal maturation profile for well 1701300138, North Louisiana Salt Basin.

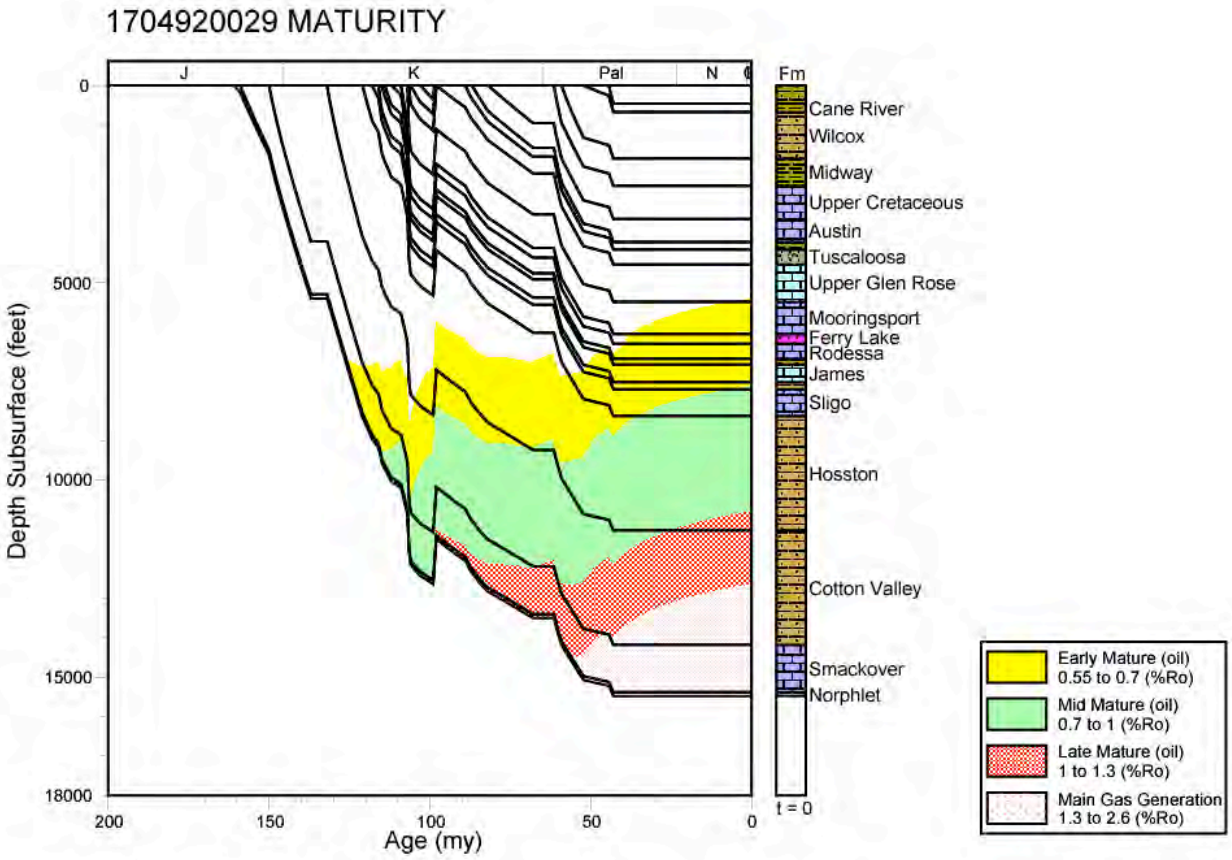


Figure 120. Thermal maturation profile for well 1704920029, North Louisiana Salt Basin.

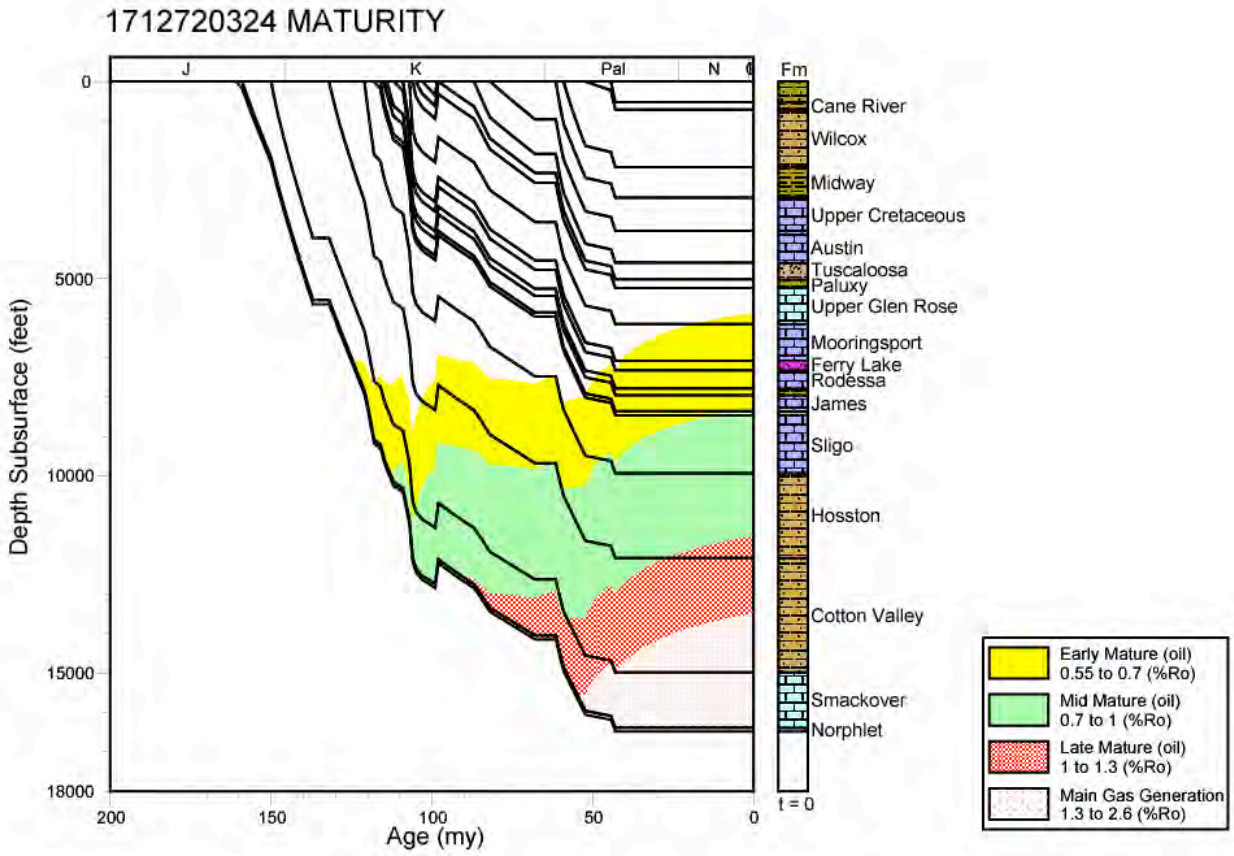


Figure 121. Thermal maturation profile for well 1712720324, North Louisiana Salt Basin.

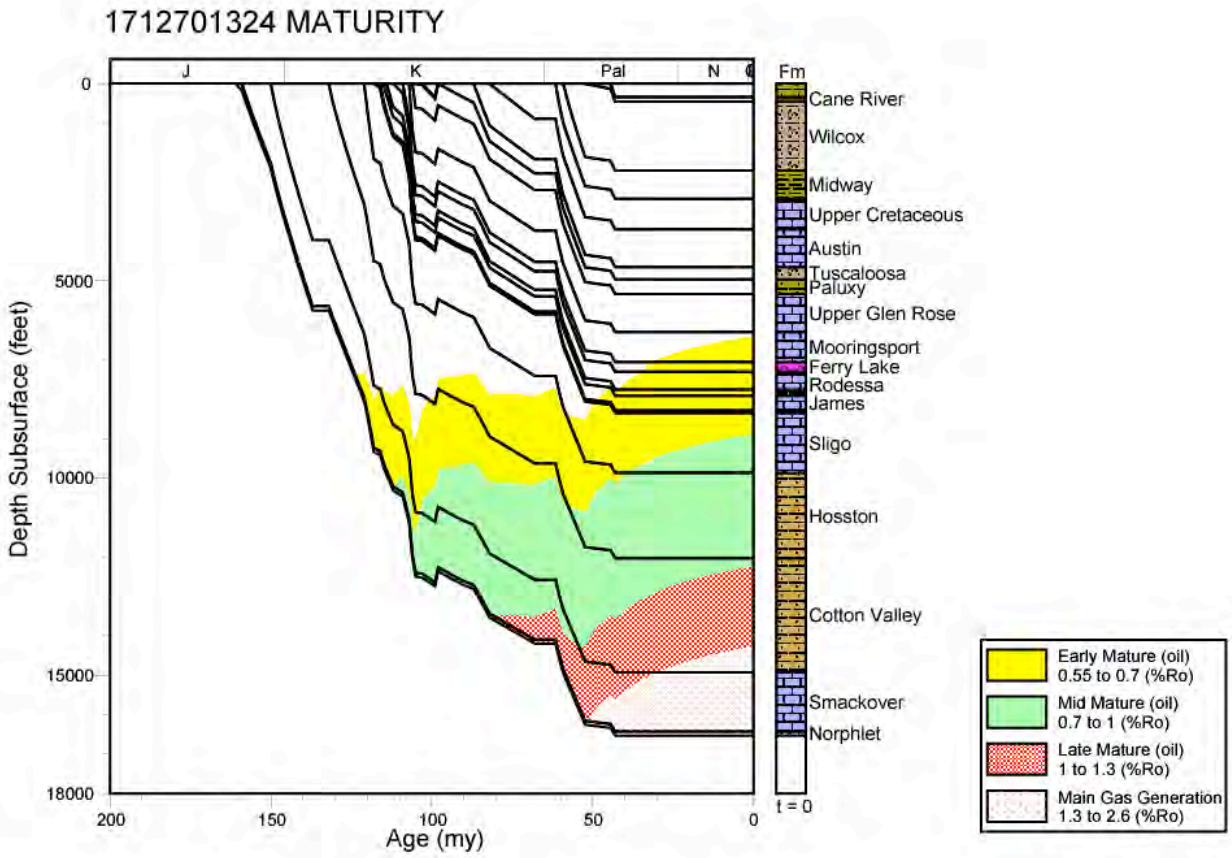


Figure 122. Thermal maturation profile for well 1712701324, North Louisiana Salt Basin.

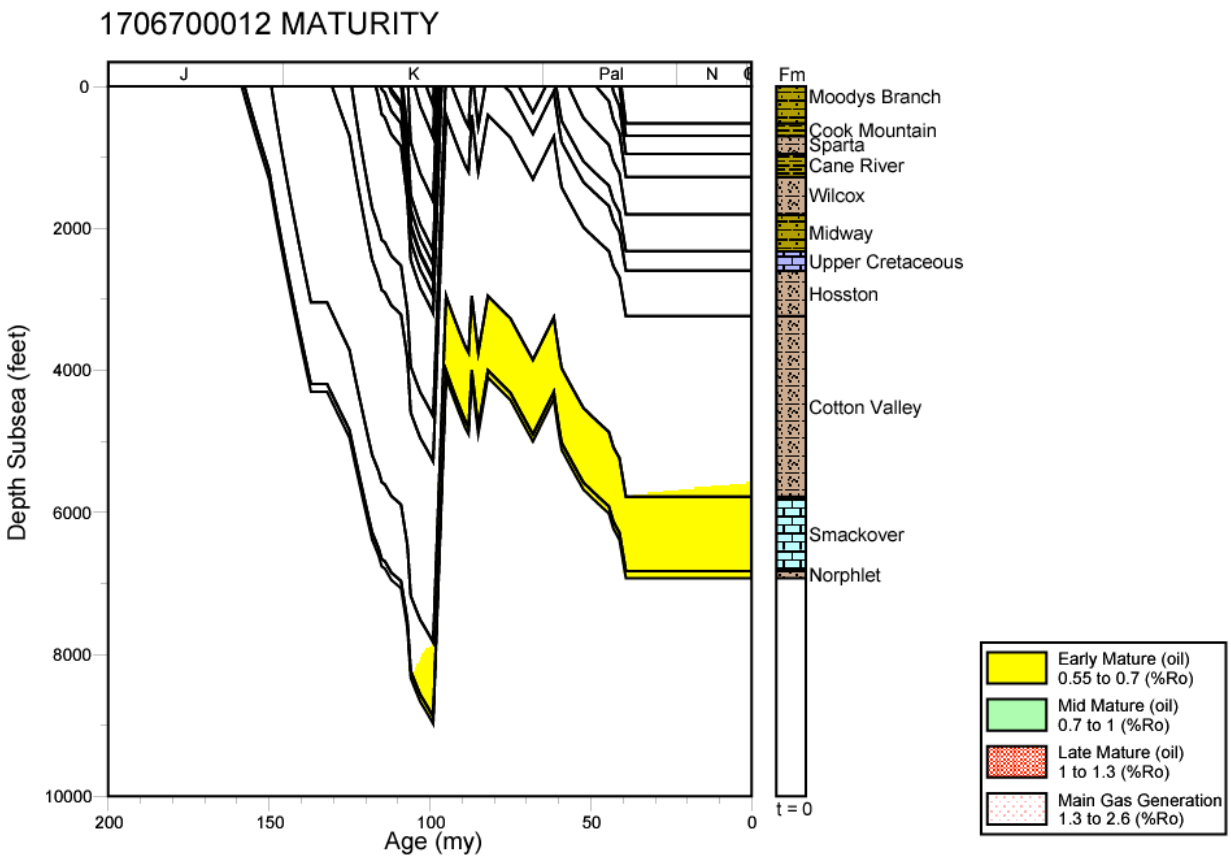


Figure 123. Thermal maturation profile for well 1706700012, North Louisiana Salt Basin.

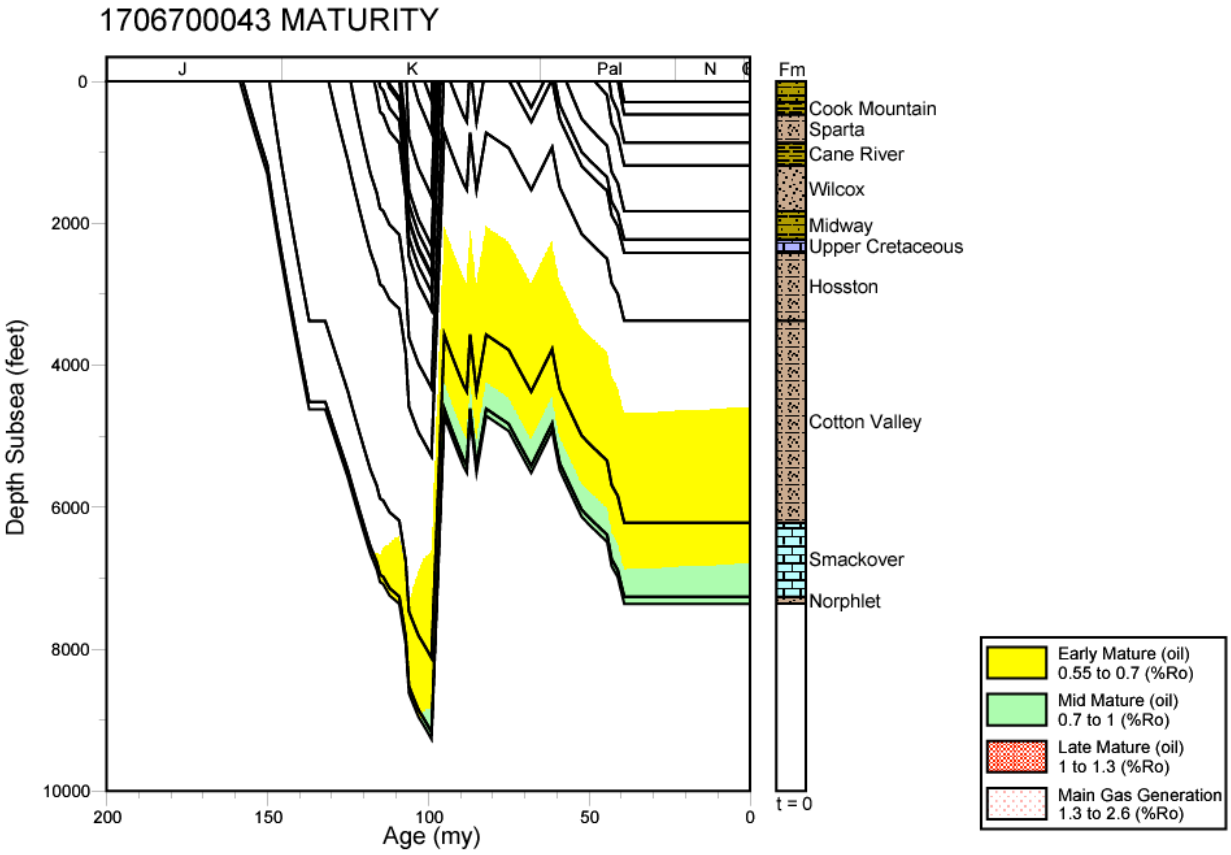


Figure 124. Thermal maturation profile for well 1706700043, North Louisiana Salt Basin.

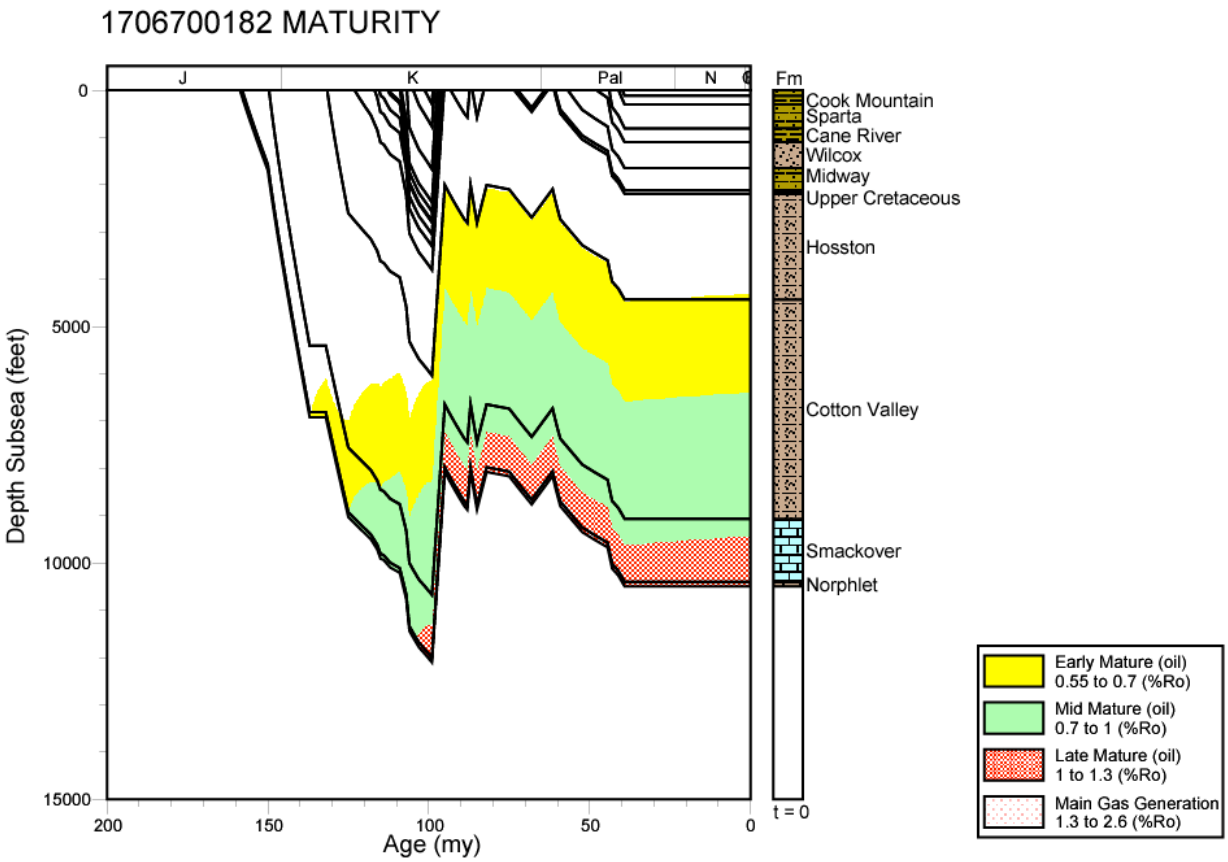


Figure 125. Thermal maturation profile for well 1706700182, North Louisiana Salt Basin.

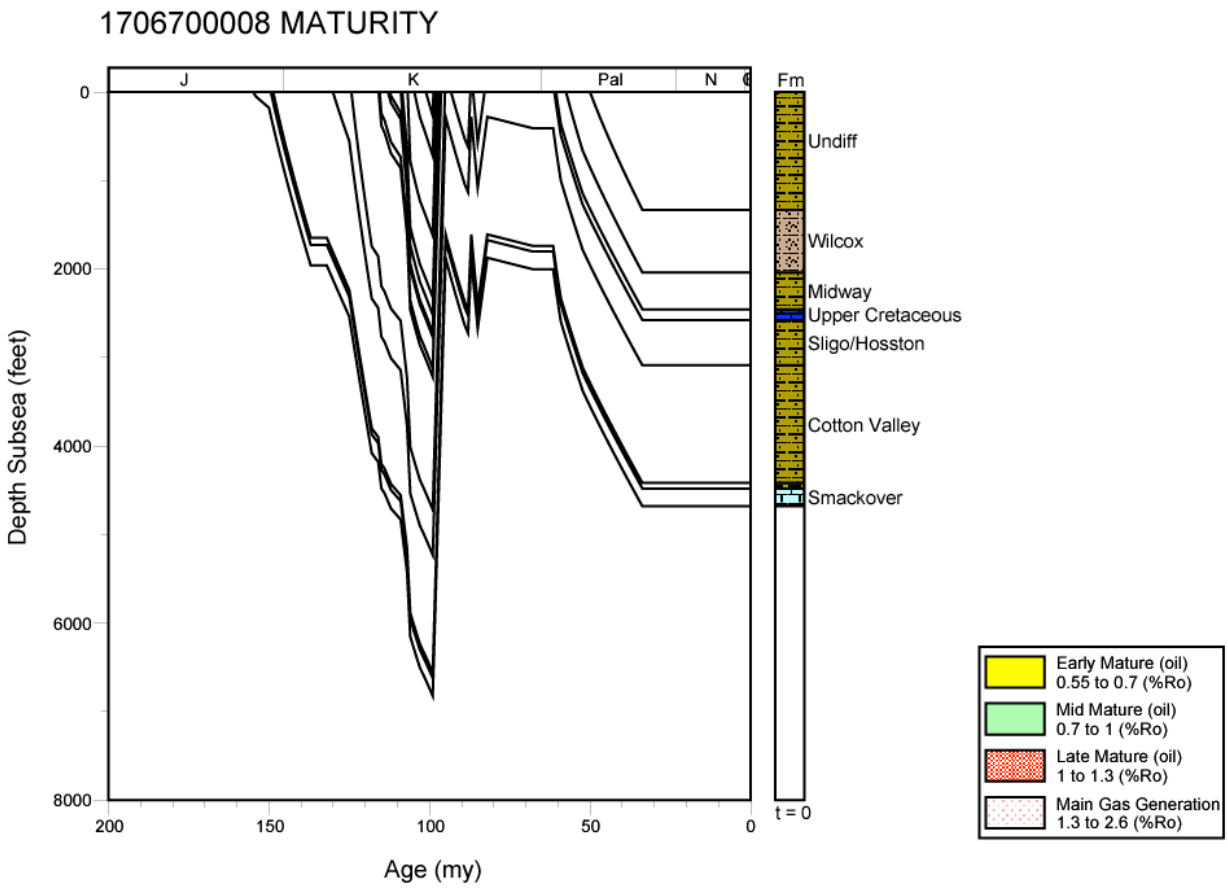


Figure 126. Thermal maturation profile for well 1706700008, North Louisiana Salt Basin.

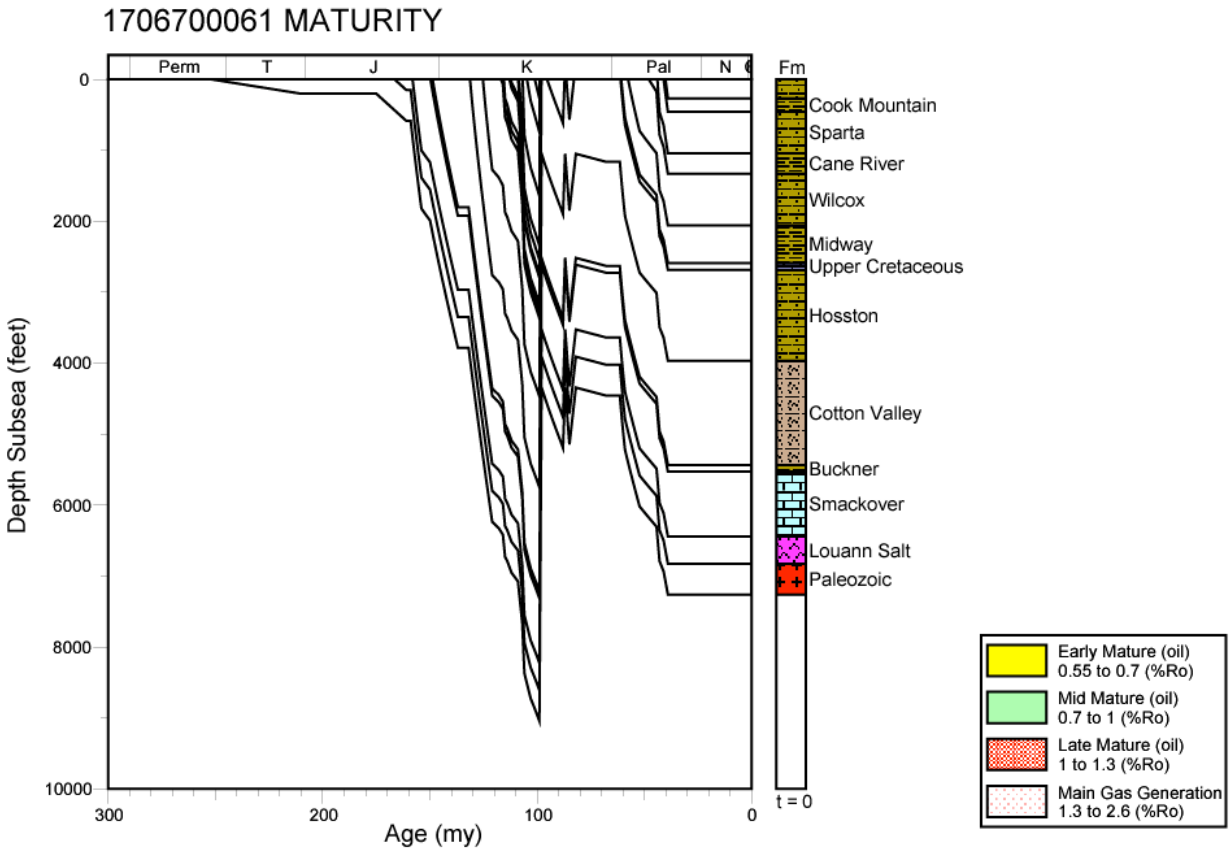


Figure 127. Thermal maturation profile for well 1706700061, North Louisiana Salt Basin.

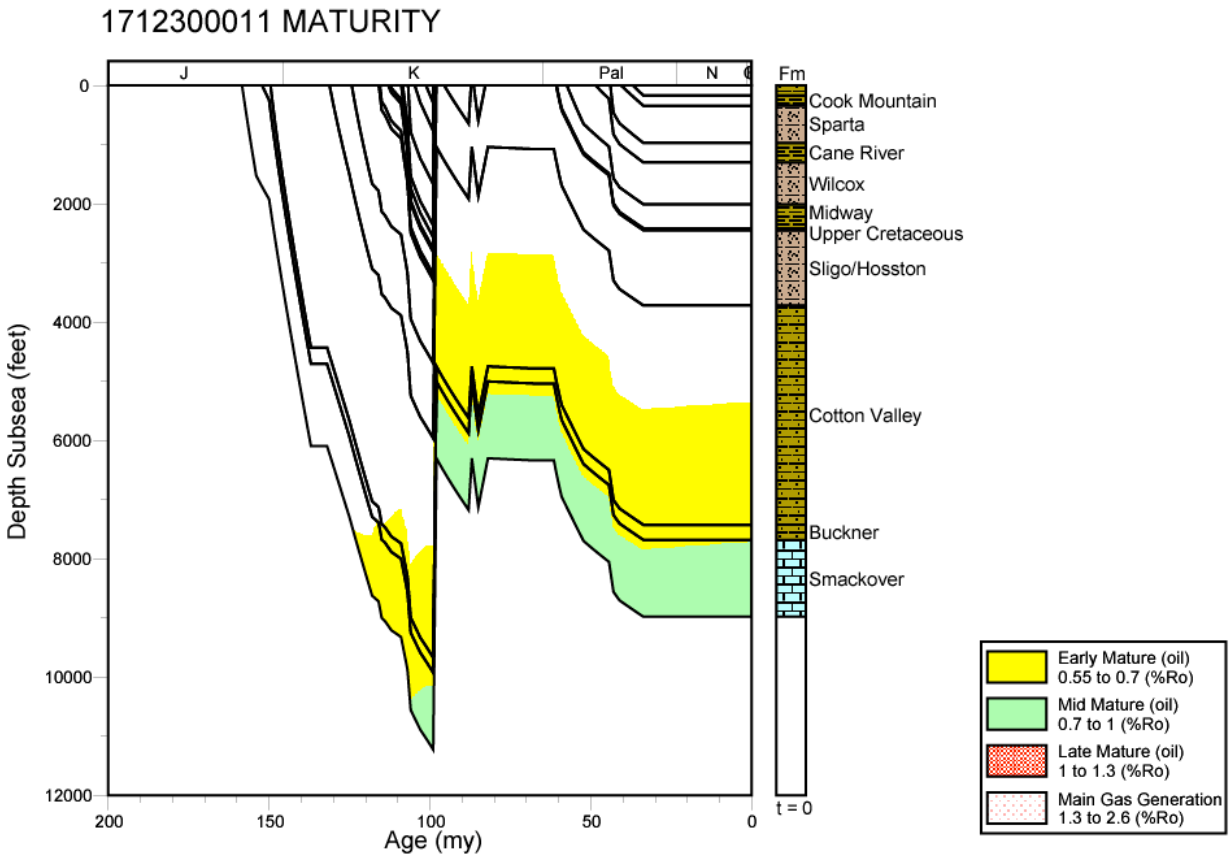


Figure 128. Thermal maturation profile for well 1712300011, North Louisiana Salt Basin.

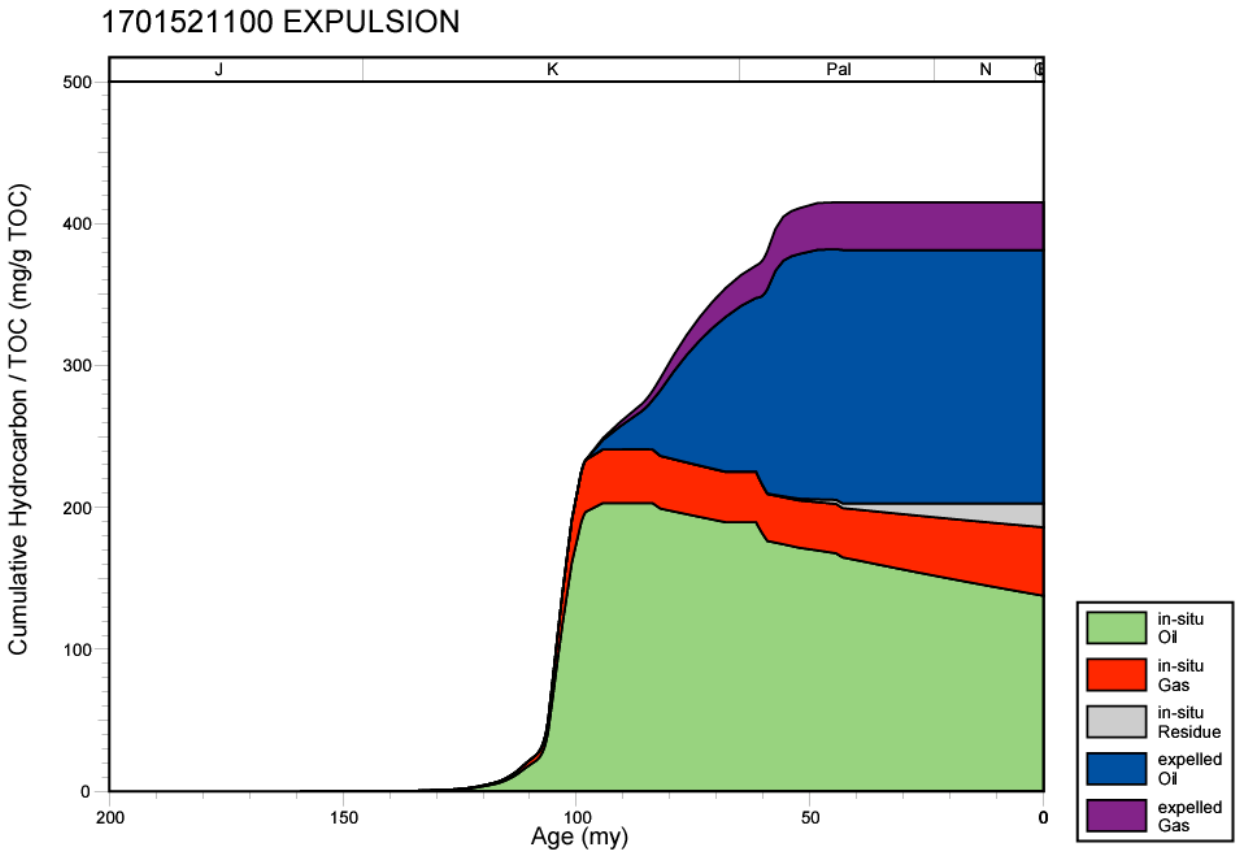


Figure 129. Hydrocarbon expulsion plot for well 1701521100, North Louisiana Salt Basin.

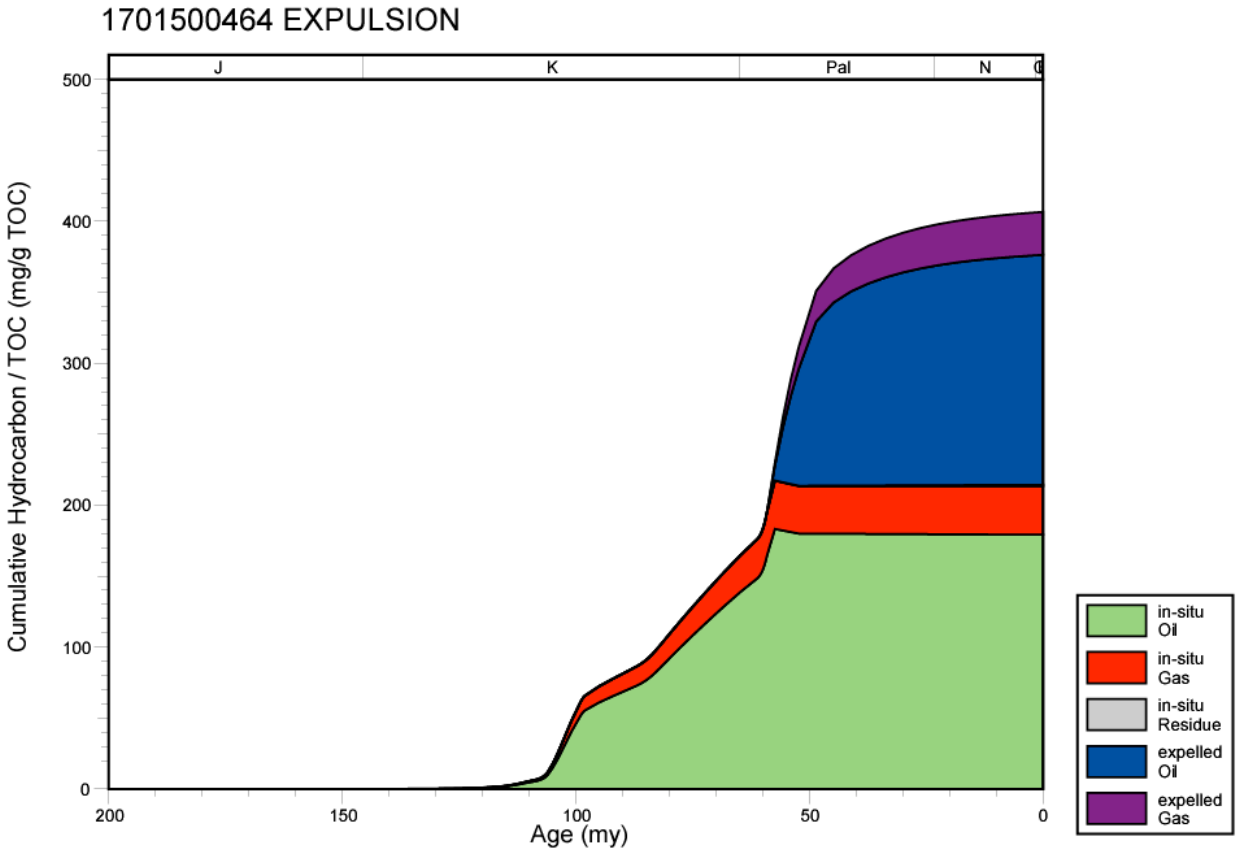


Figure 130. Hydrocarbon expulsion plot for well 1701500464, North Louisiana Salt Basin.

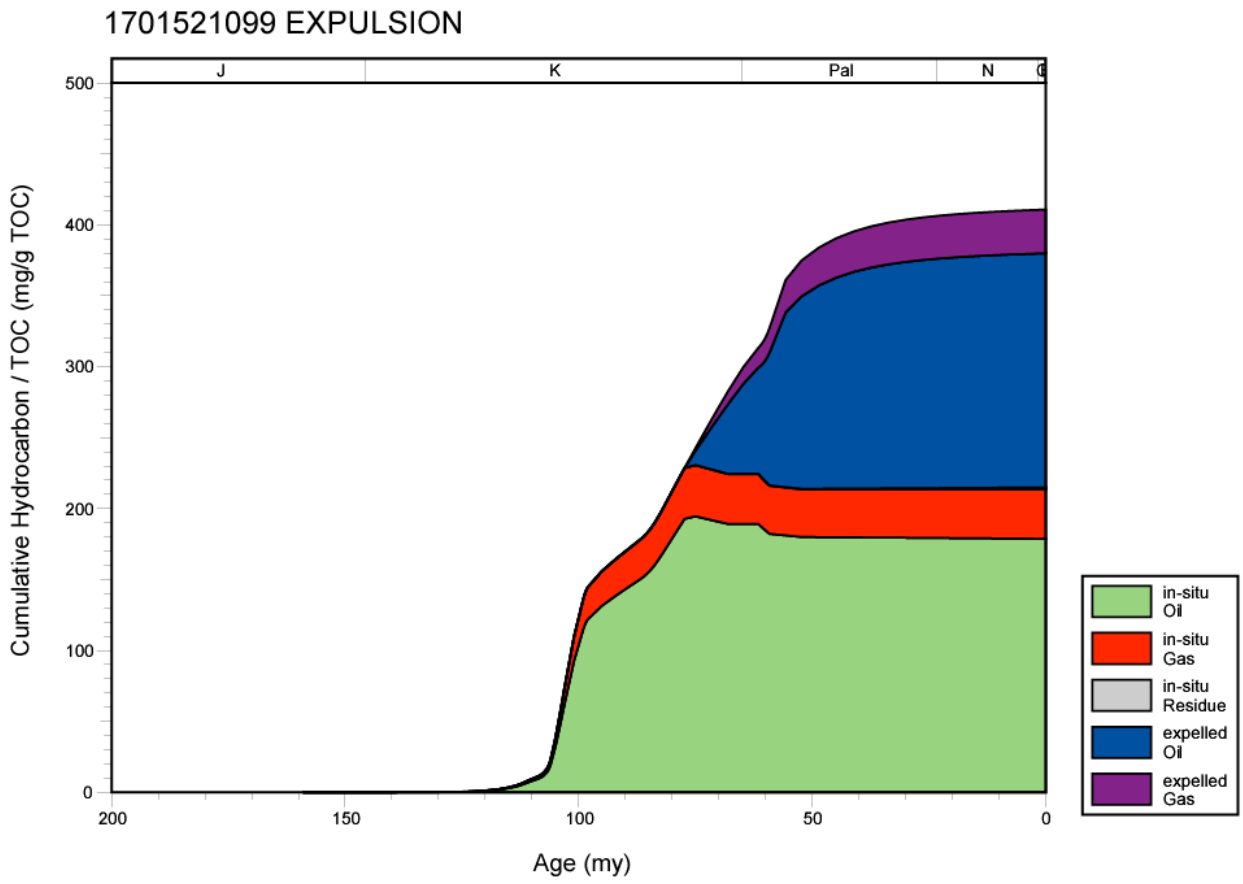


Figure 131. Hydrocarbon expulsion plot for well 1701521099, North Louisiana Salt Basin.

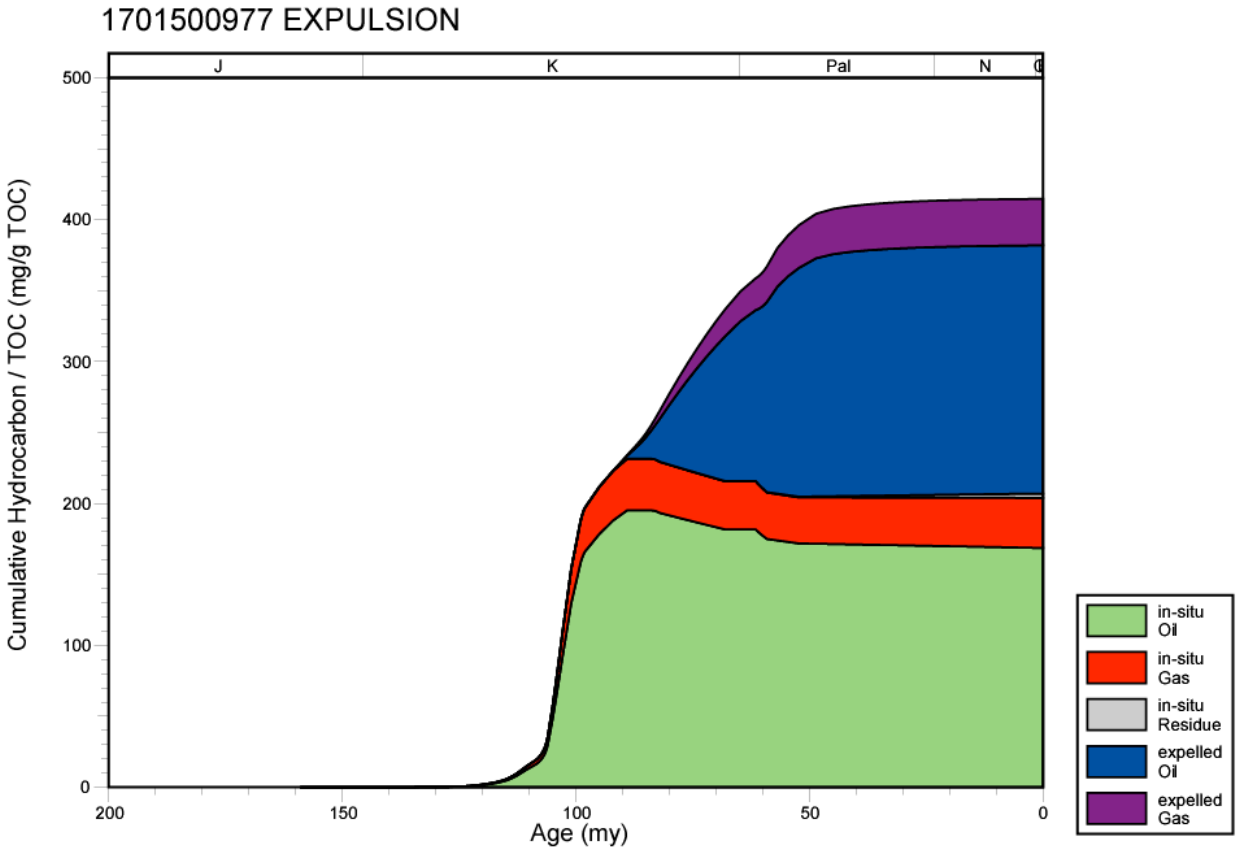


Figure 132. Hydrocarbon expulsion plot for well 1701500977, North Louisiana Salt Basin.

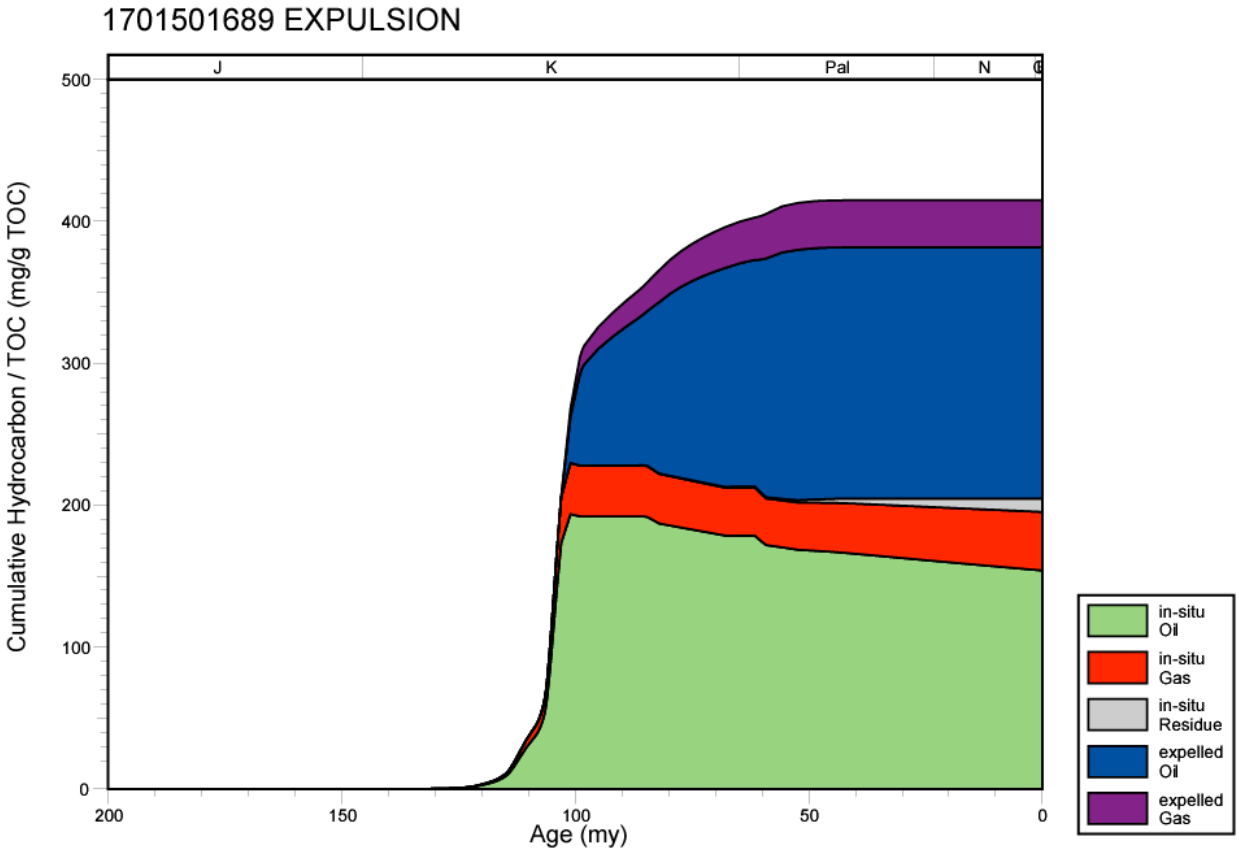


Figure 133. Hydrocarbon expulsion plot for well 1701501689, North Louisiana Salt Basin.

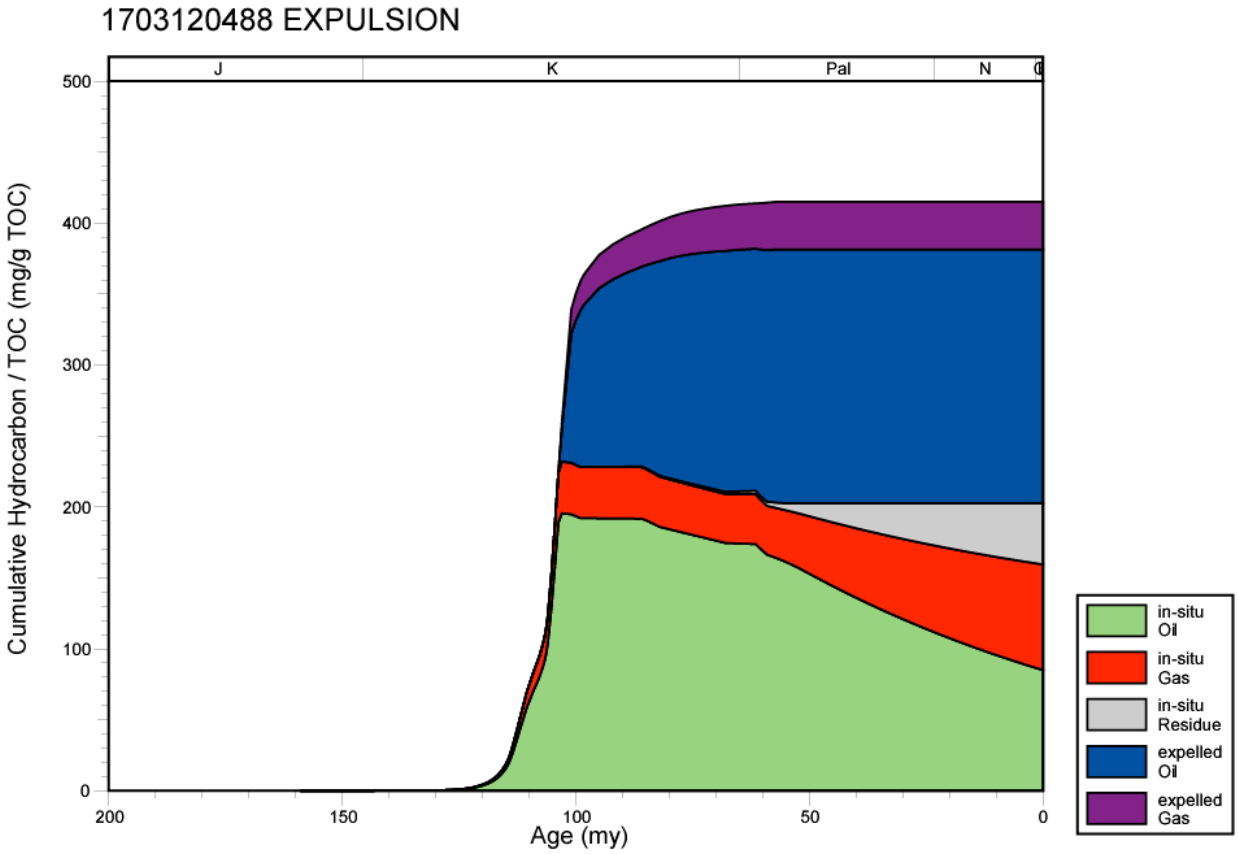


Figure 134. Hydrocarbon expulsion plot for well 1703120488, North Louisiana Salt Basin.

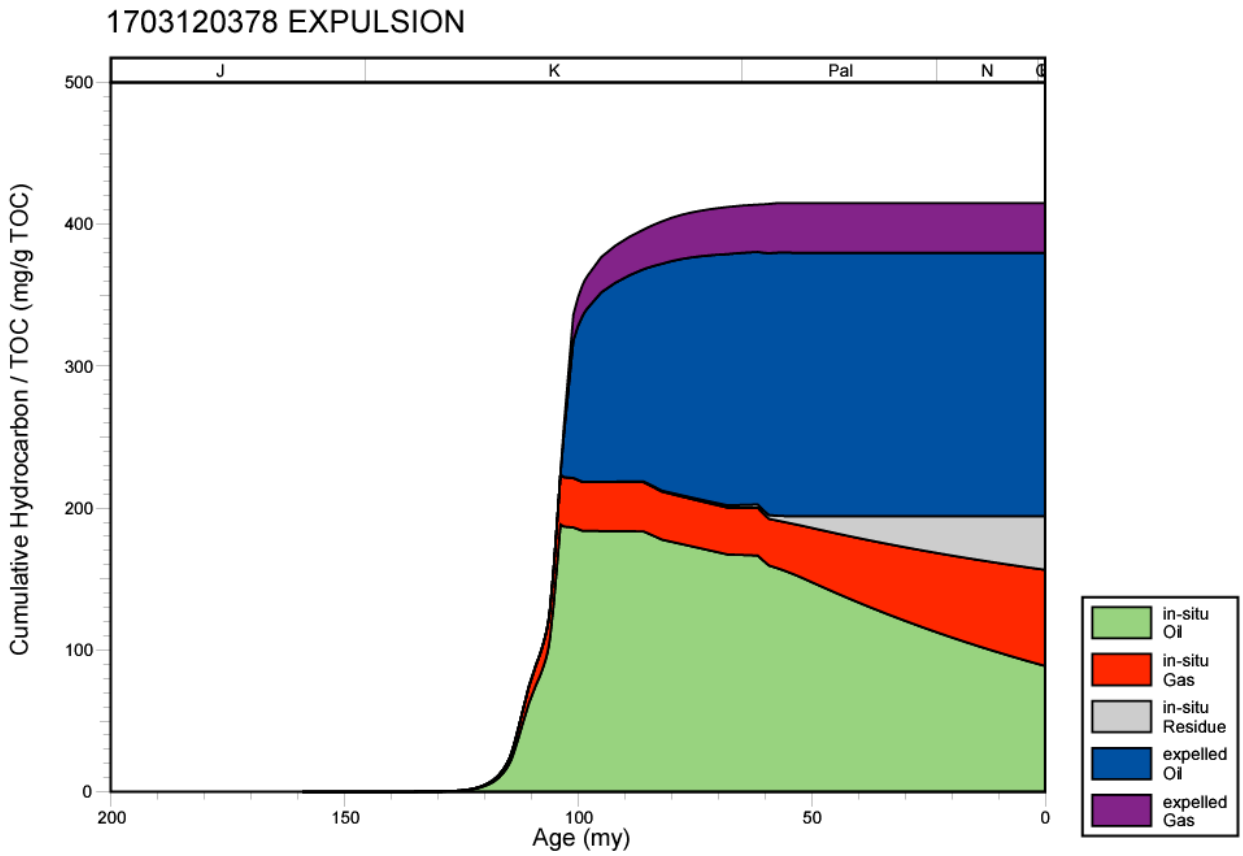


Figure 135. Hydrocarbon expulsion plot for well 1703120378, North Louisiana Salt Basin.

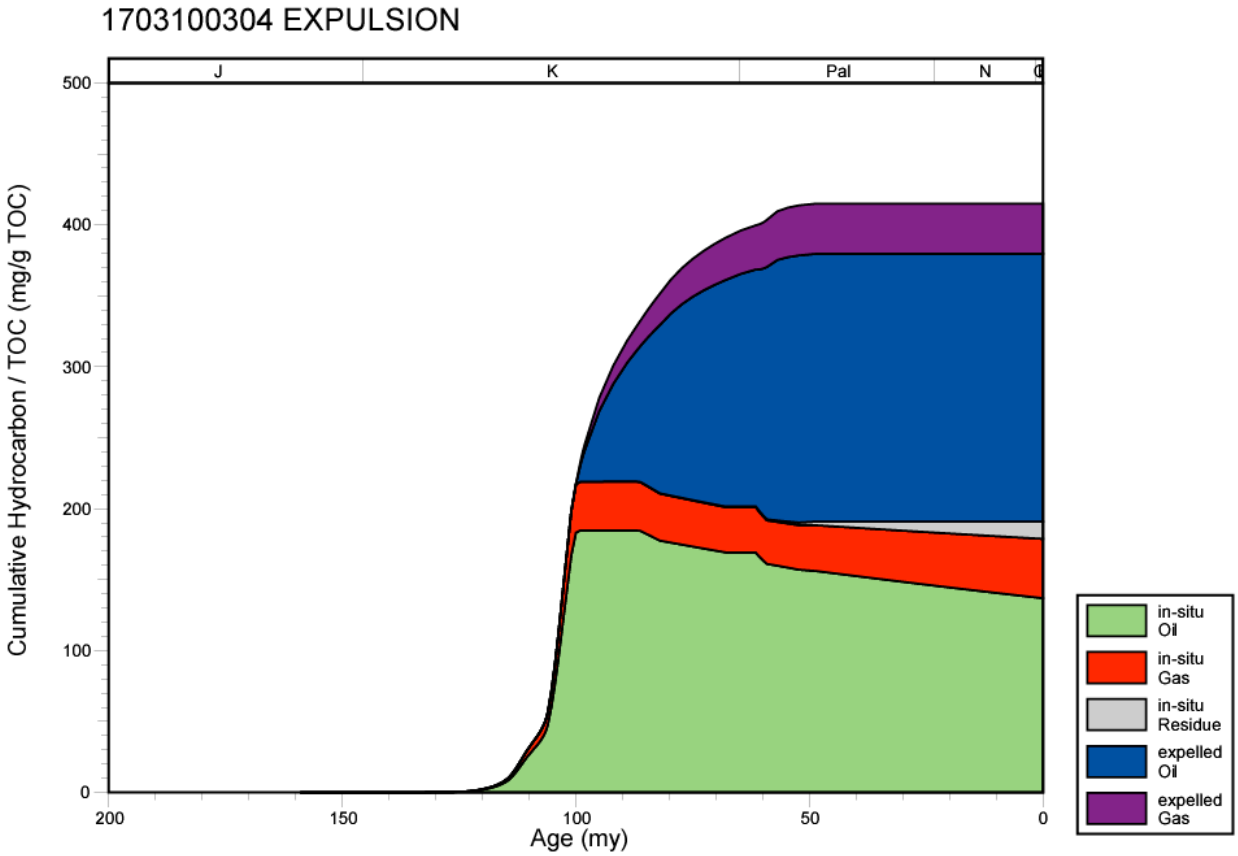


Figure 136. Hydrocarbon expulsion plot for well 1703100304, North Louisiana Salt Basin.

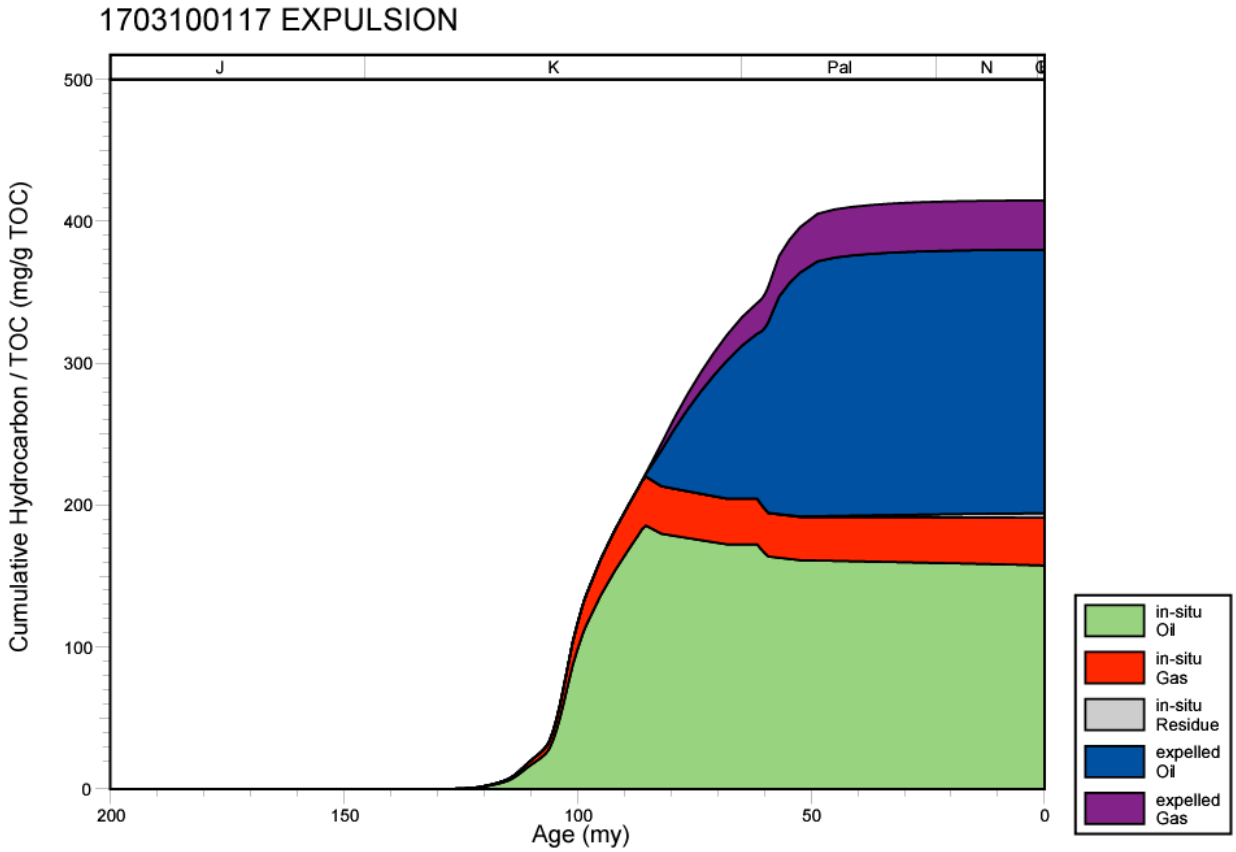


Figure 137. Hydrocarbon expulsion plot for well 1703100117, North Louisiana Salt Basin.

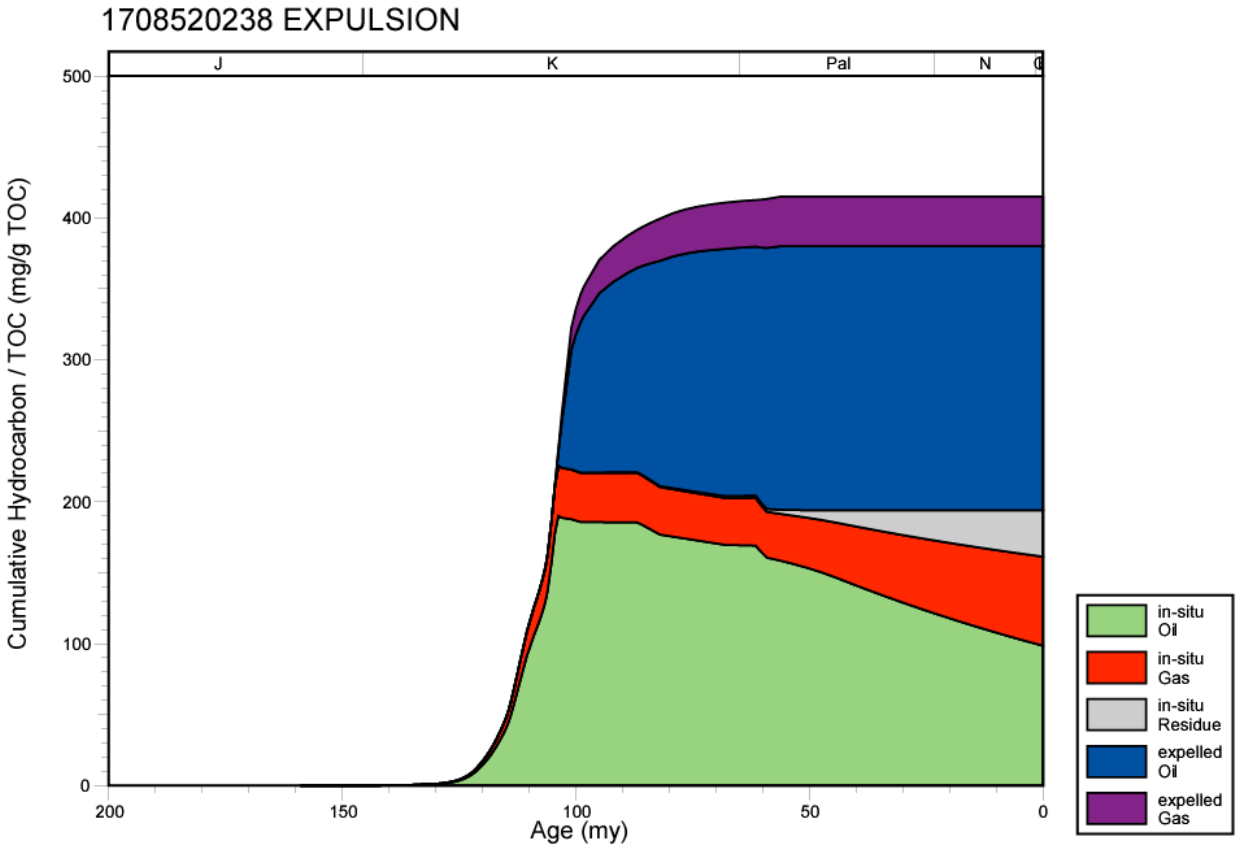


Figure 138. Hydrocarbon expulsion plot for well 1708520238, North Louisiana Salt Basin.

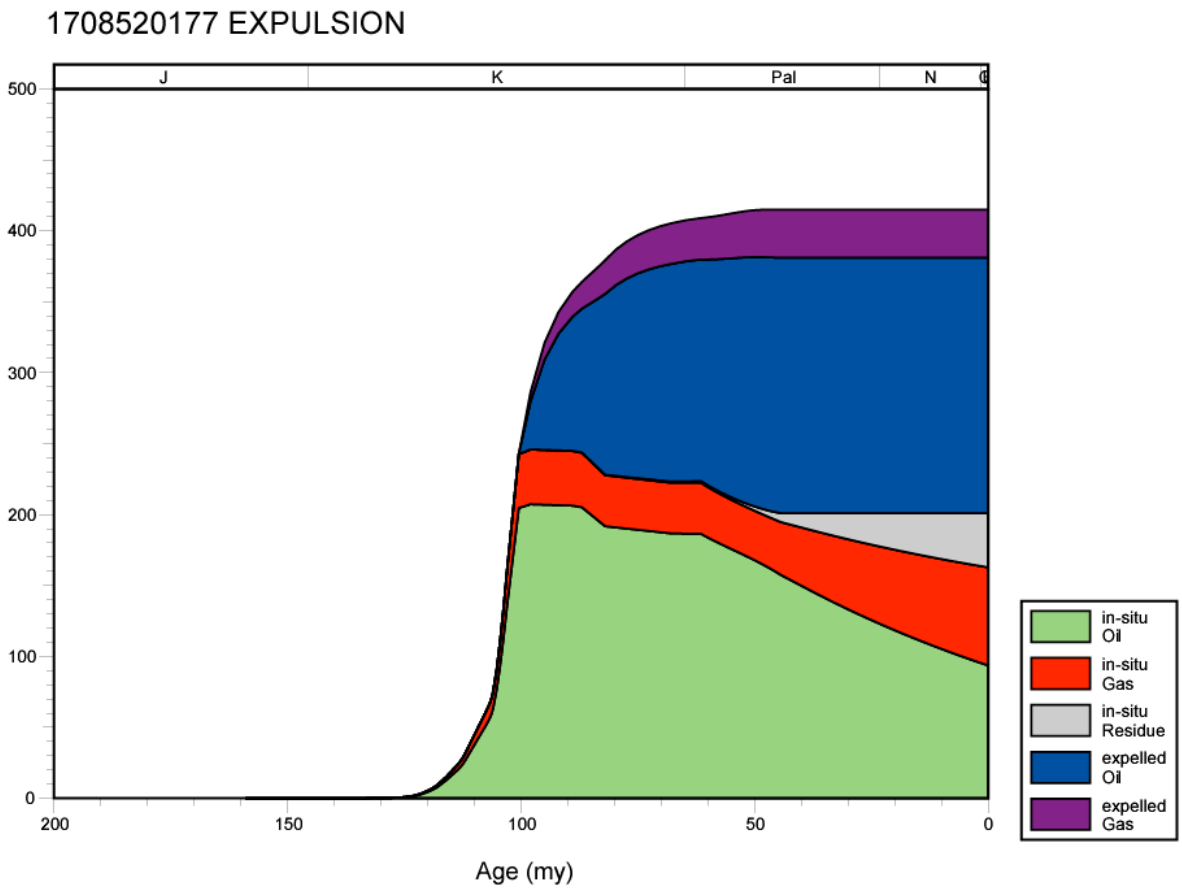


Figure 139. Hydrocarbon expulsion plot for well 1708520177, North Louisiana Salt Basin.

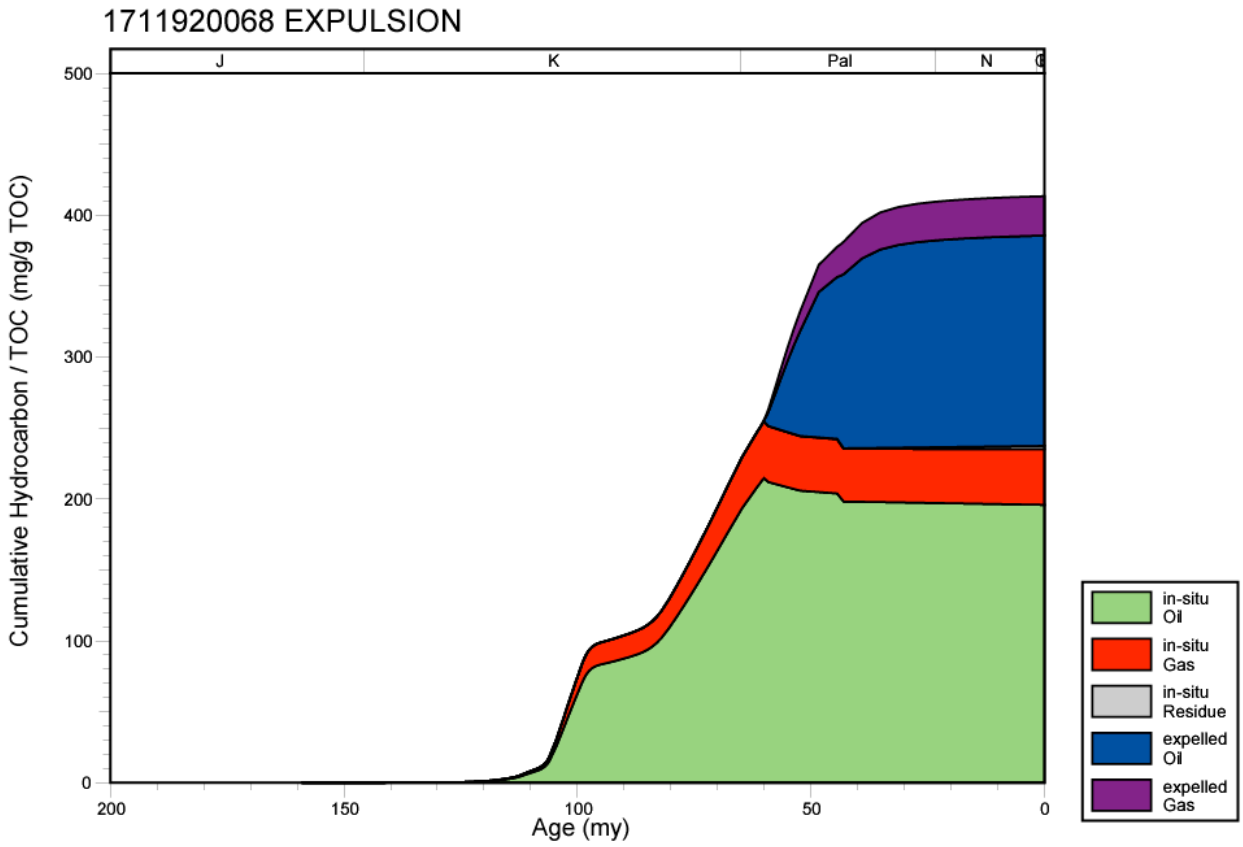


Figure 140. Hydrocarbon expulsion plot for well 1711920068, North Louisiana Salt Basin.

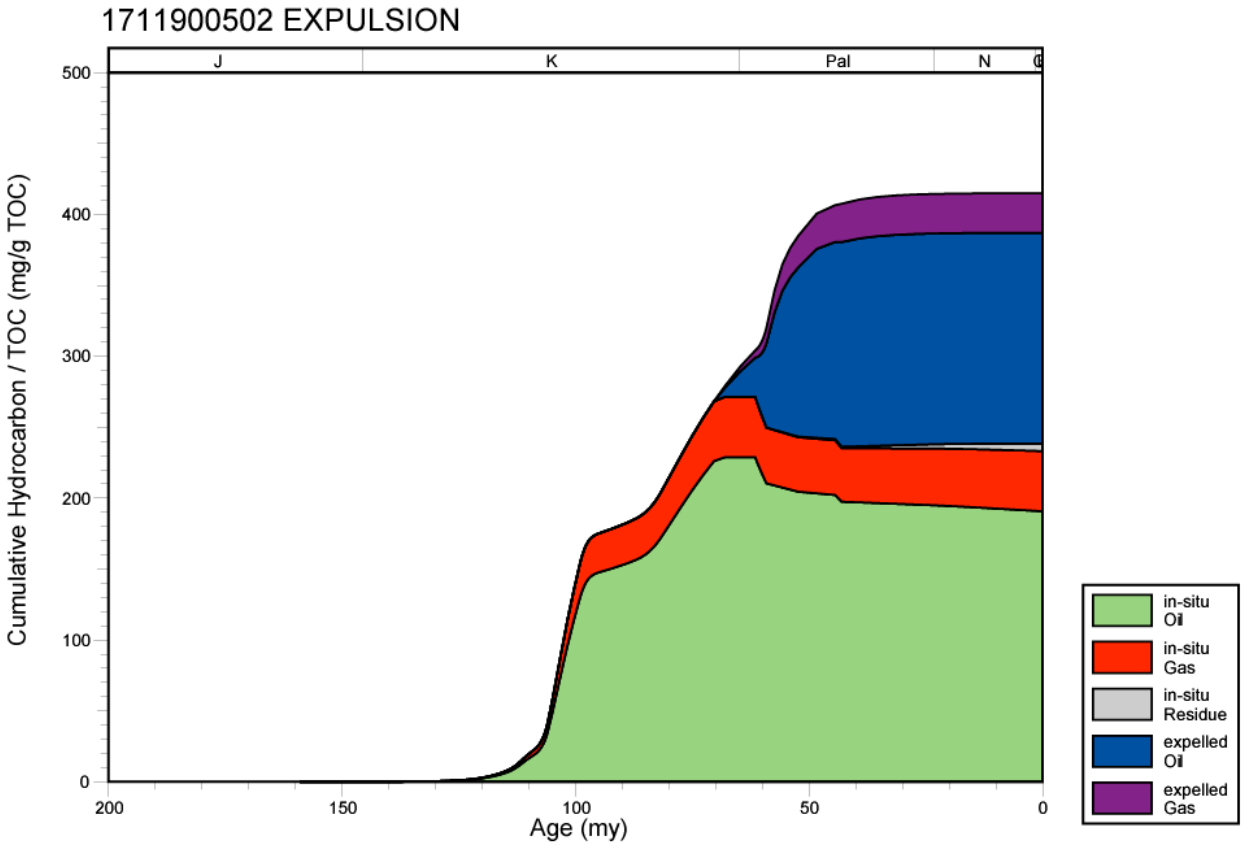


Figure 141. Hydrocarbon expulsion plot for well 1711900502, North Louisiana Salt Basin.

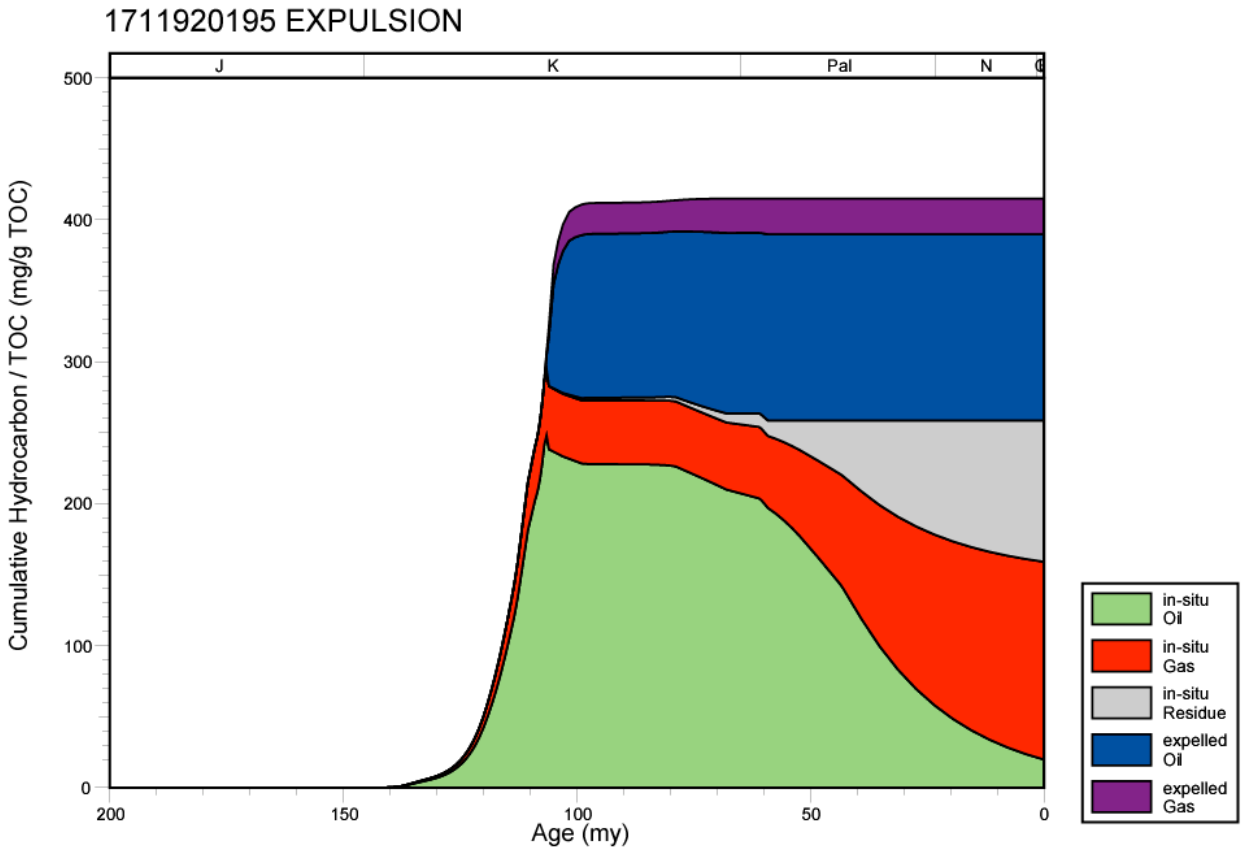


Figure 142. Hydrocarbon expulsion plot for well 1711920195, North Louisiana Salt Basin.

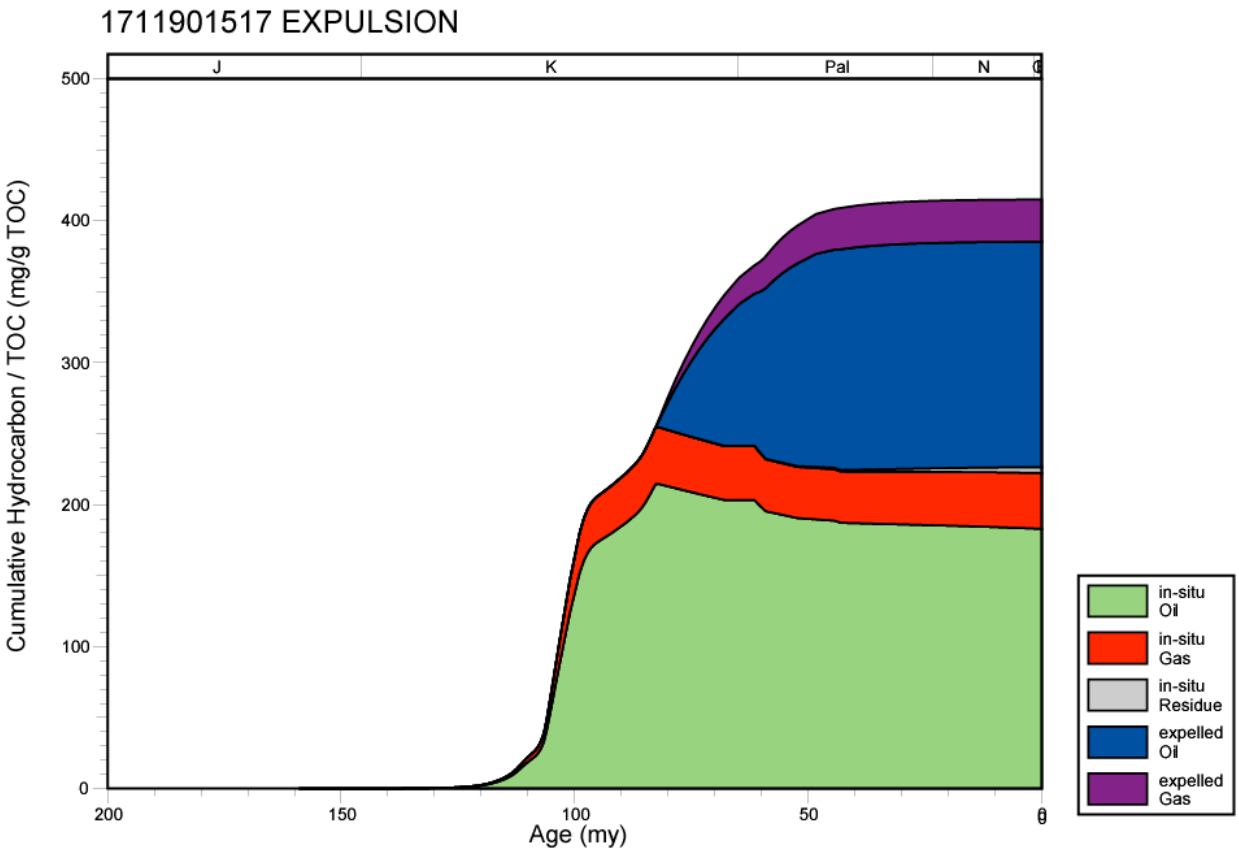


Figure 143. Hydrocarbon expulsion plot for well 1711901517, North Louisiana Salt Basin.

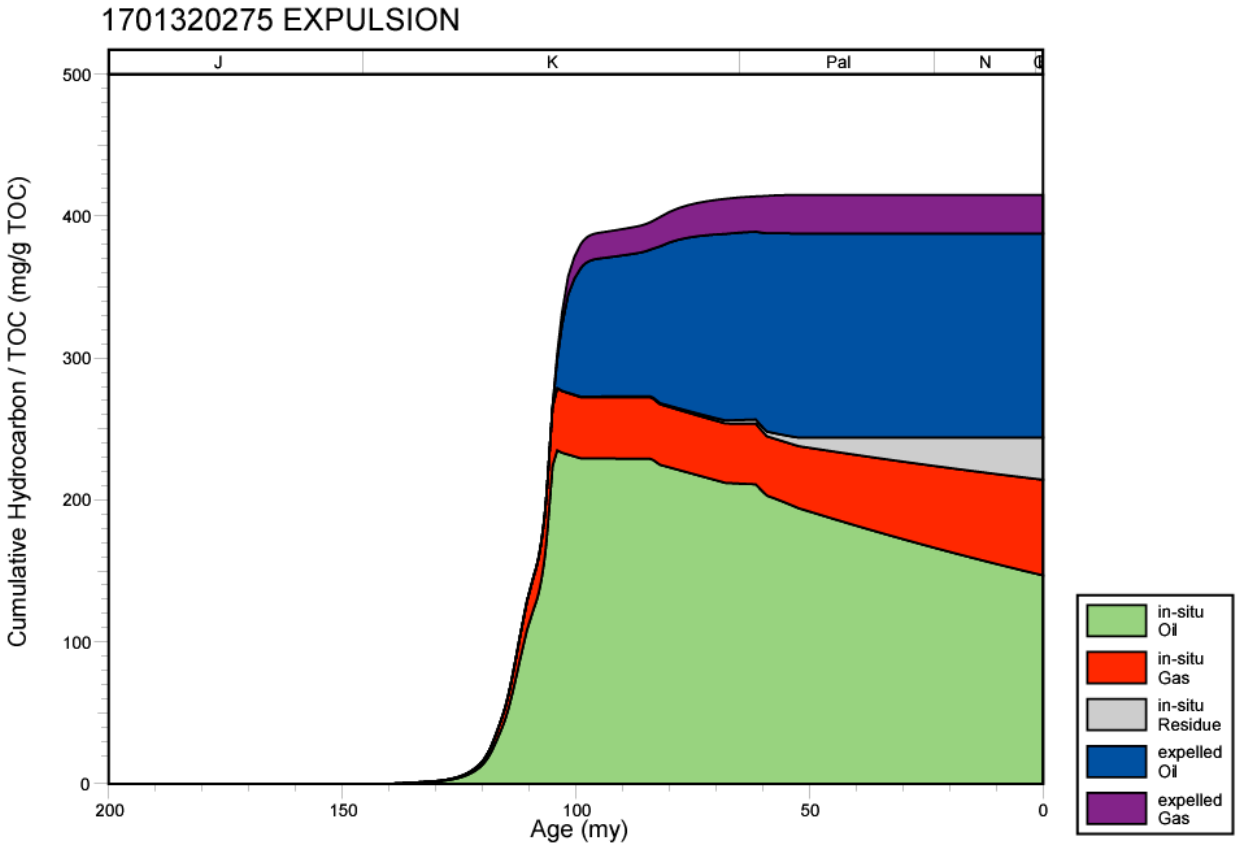


Figure 144. Hydrocarbon expulsion plot for well 1701320275, North Louisiana Salt Basin.

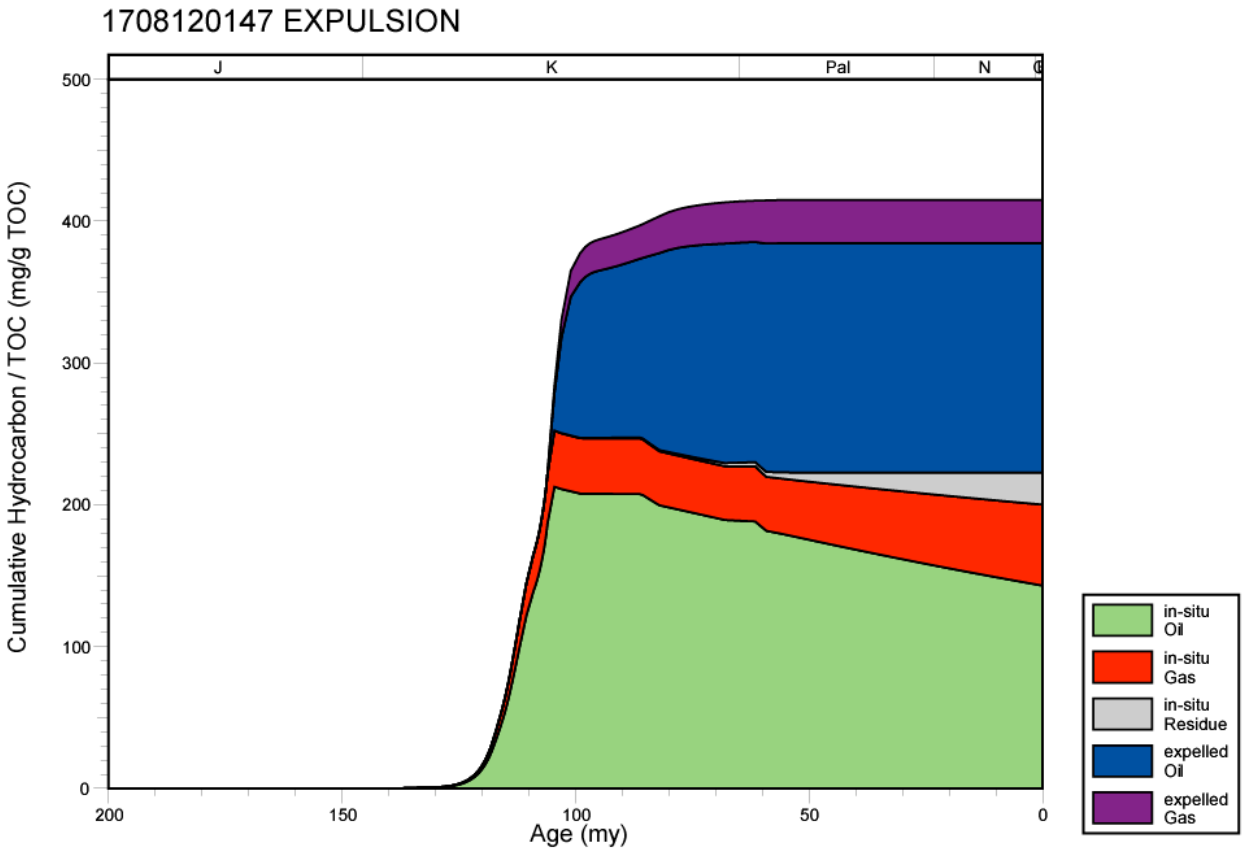


Figure 145. Hydrocarbon expulsion plot for well 1708120147, North Louisiana Salt Basin.

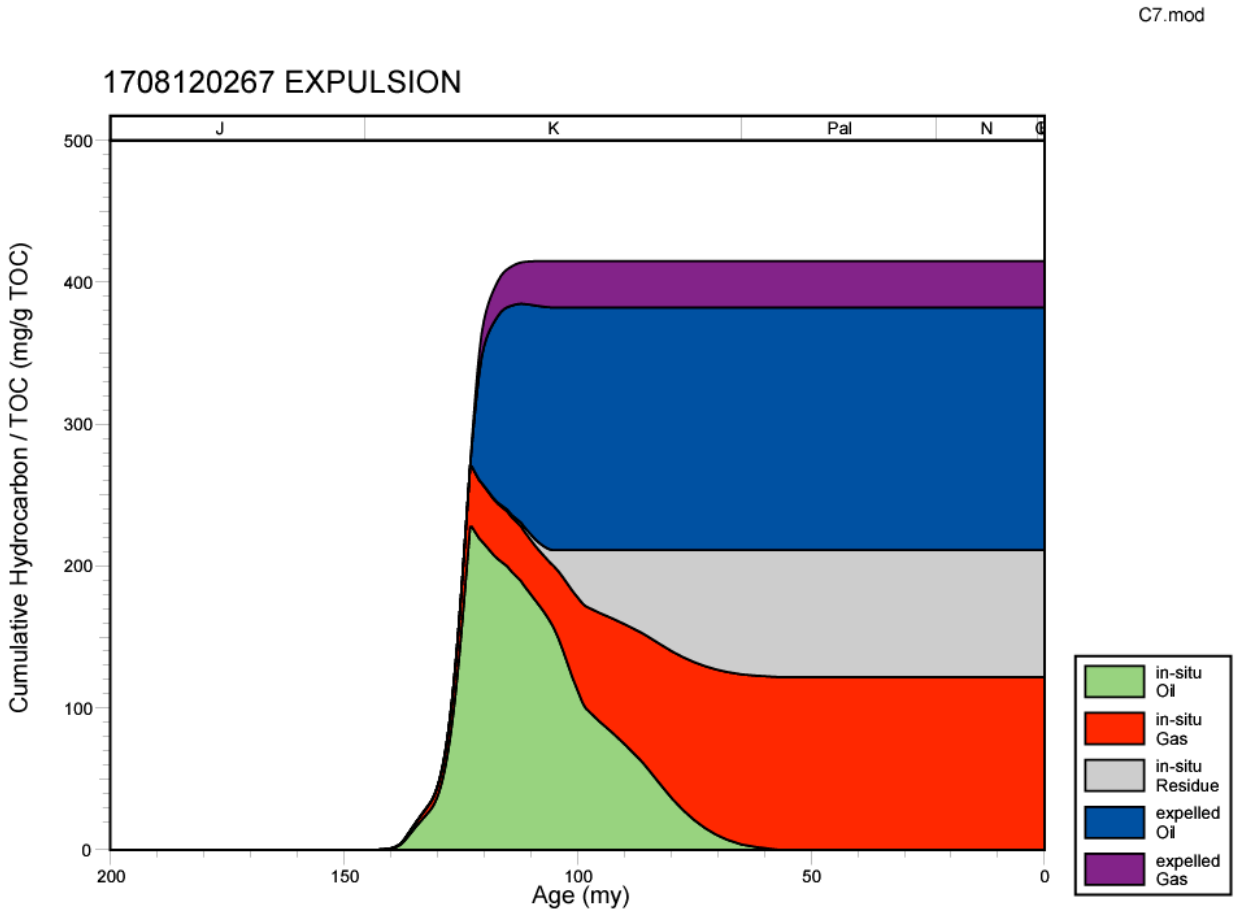


Figure 146. Hydrocarbon expulsion plot for well 1708120267, North Louisiana Salt Basin.

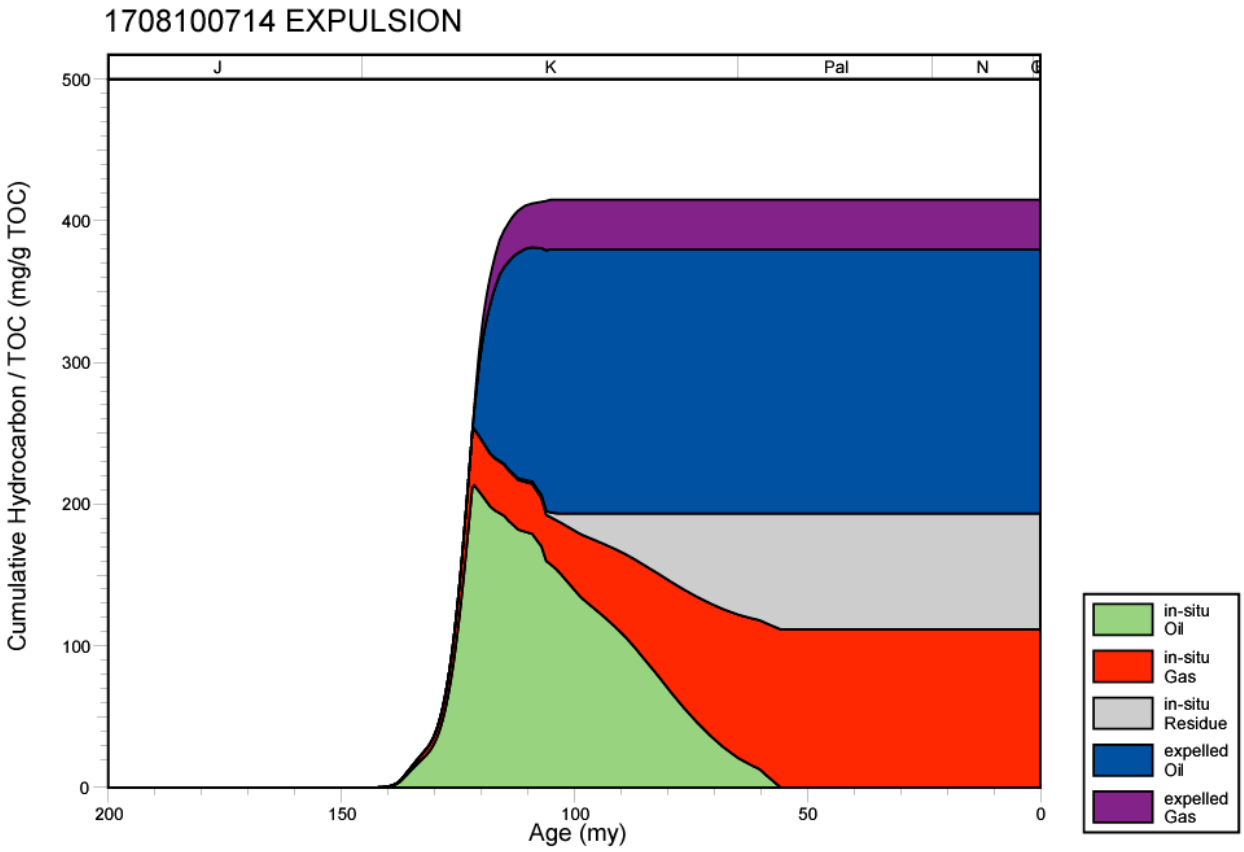


Figure 147. Hydrocarbon expulsion plot for well 1708100714, North Louisiana Salt Basin.

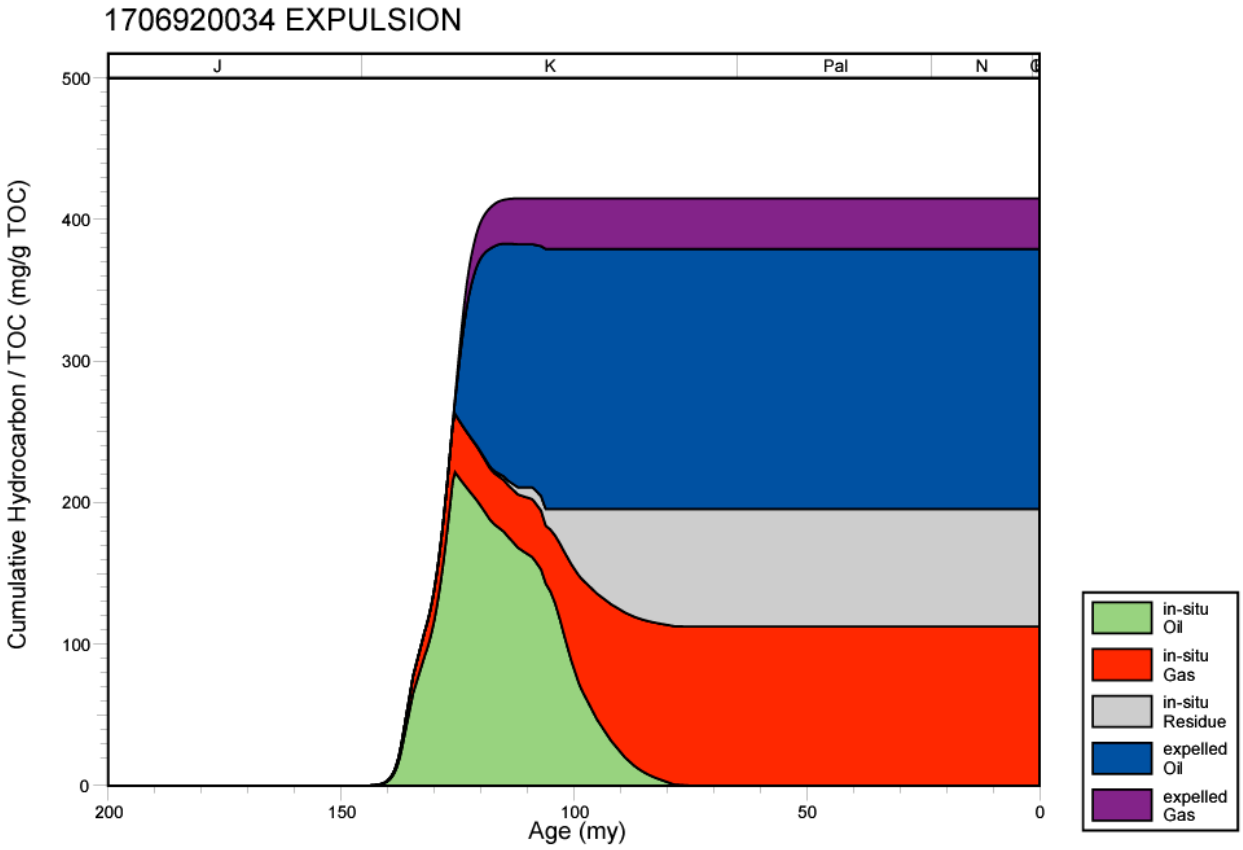


Figure 148. Hydrocarbon expulsion plot for well 1706920034, North Louisiana Salt Basin.

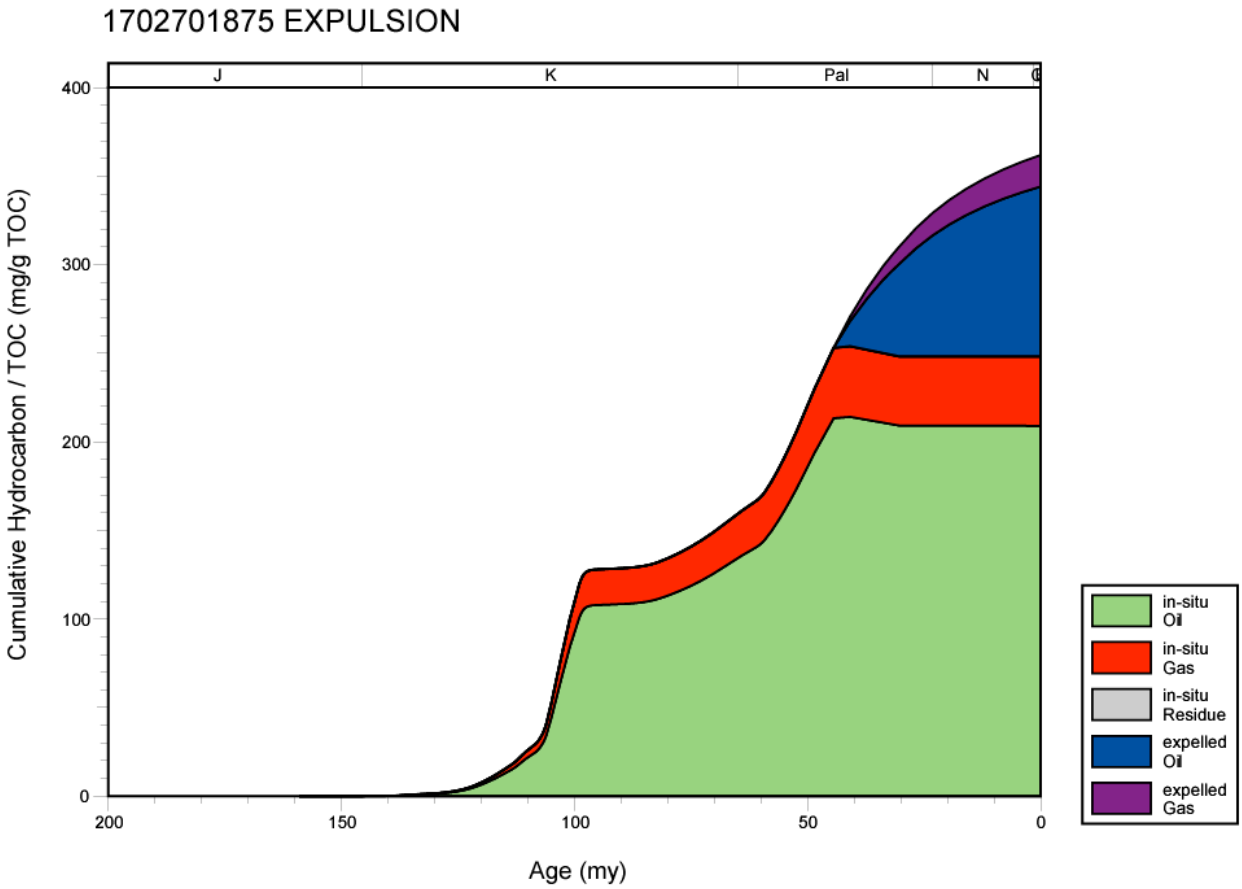


Figure 149. Hydrocarbon expulsion plot for well 1702701875, North Louisiana Salt Basin.

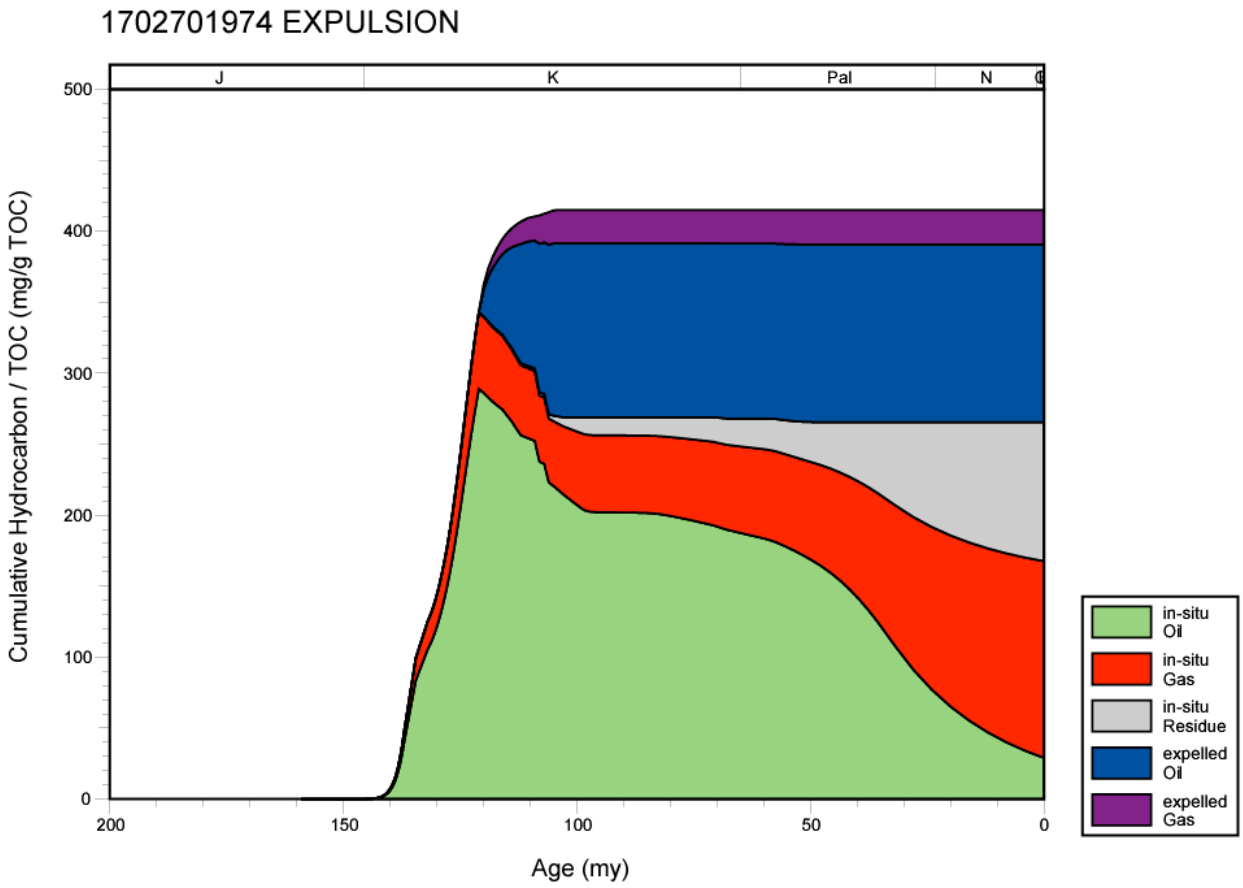


Figure 150. Hydrocarbon expulsion plot for well 1702701974, North Louisiana Salt Basin.

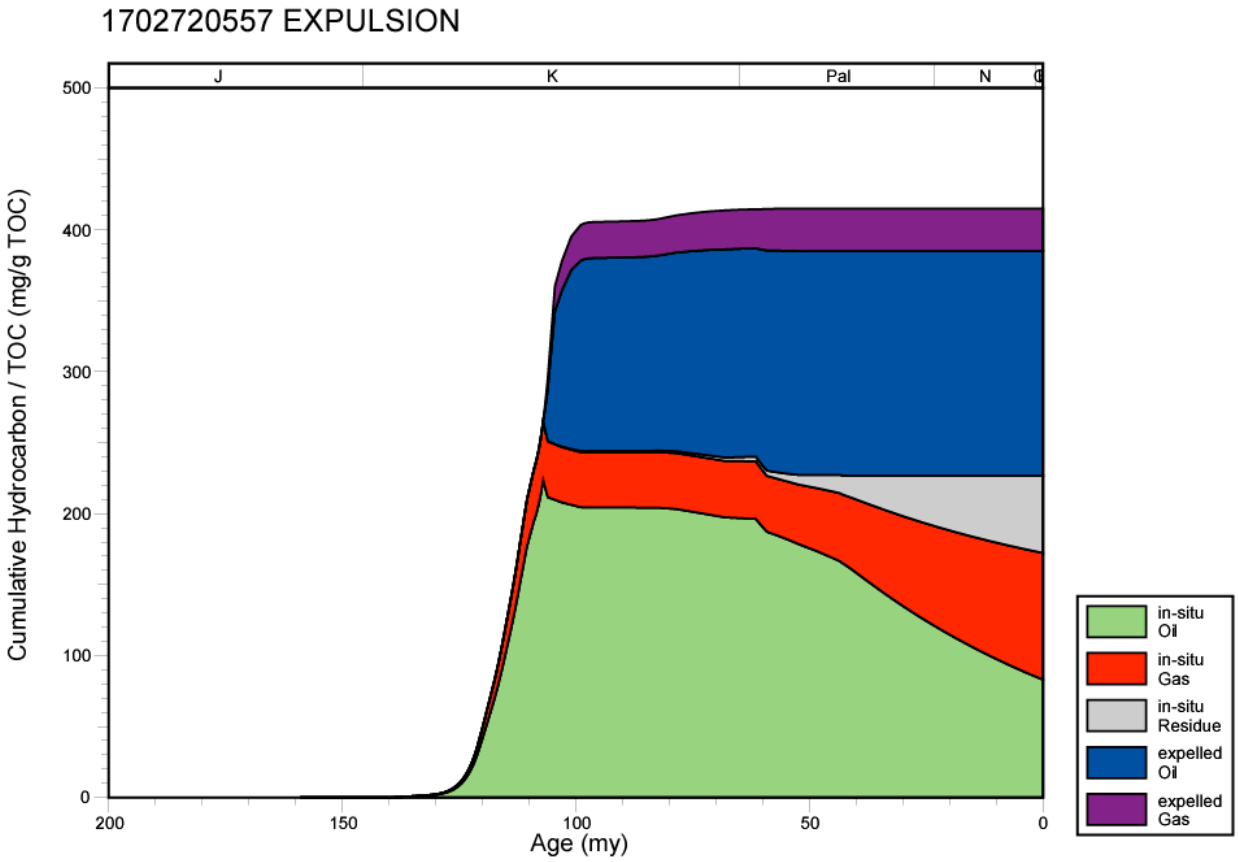


Figure 151. Hydrocarbon expulsion plot for well 1702720557, North Louisiana Salt Basin.

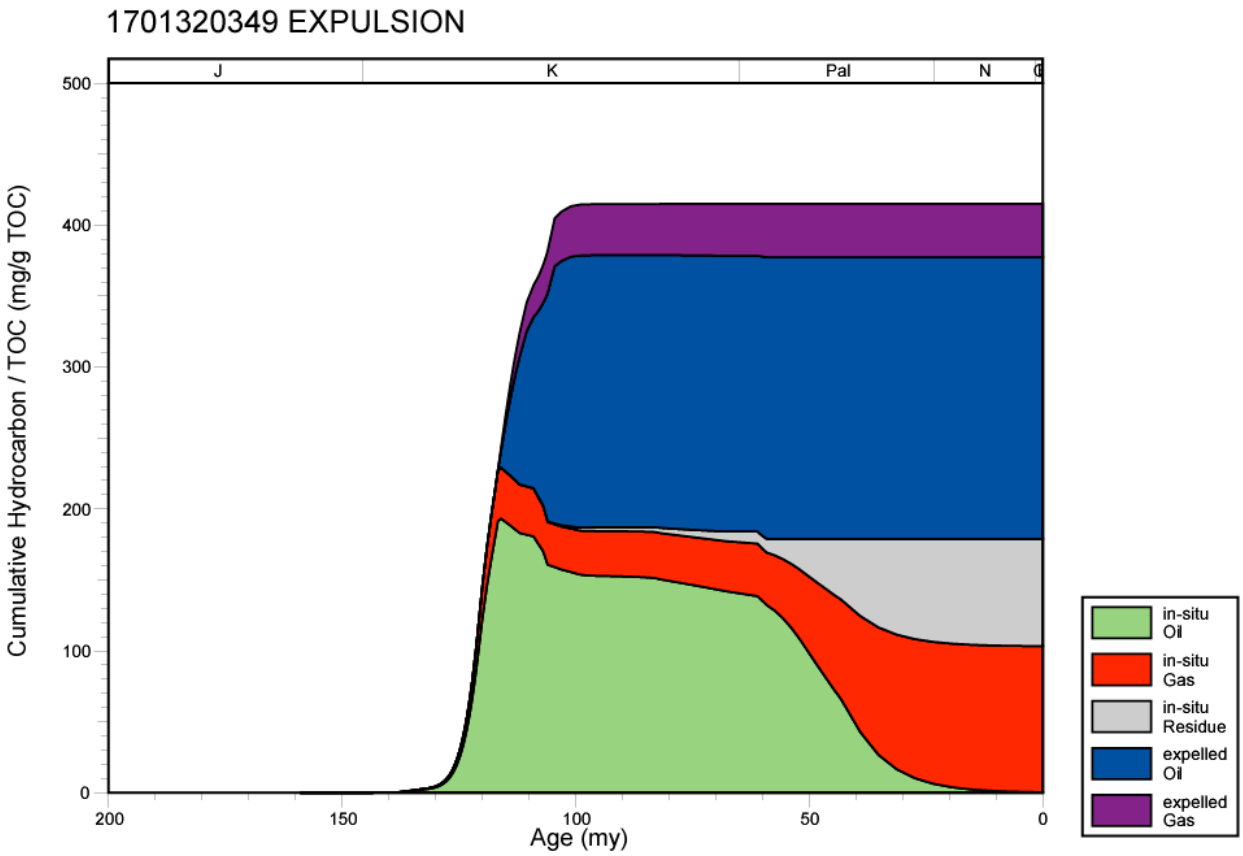


Figure 152. Hydrocarbon expulsion plot for well 1701320349, North Louisiana Salt Basin.

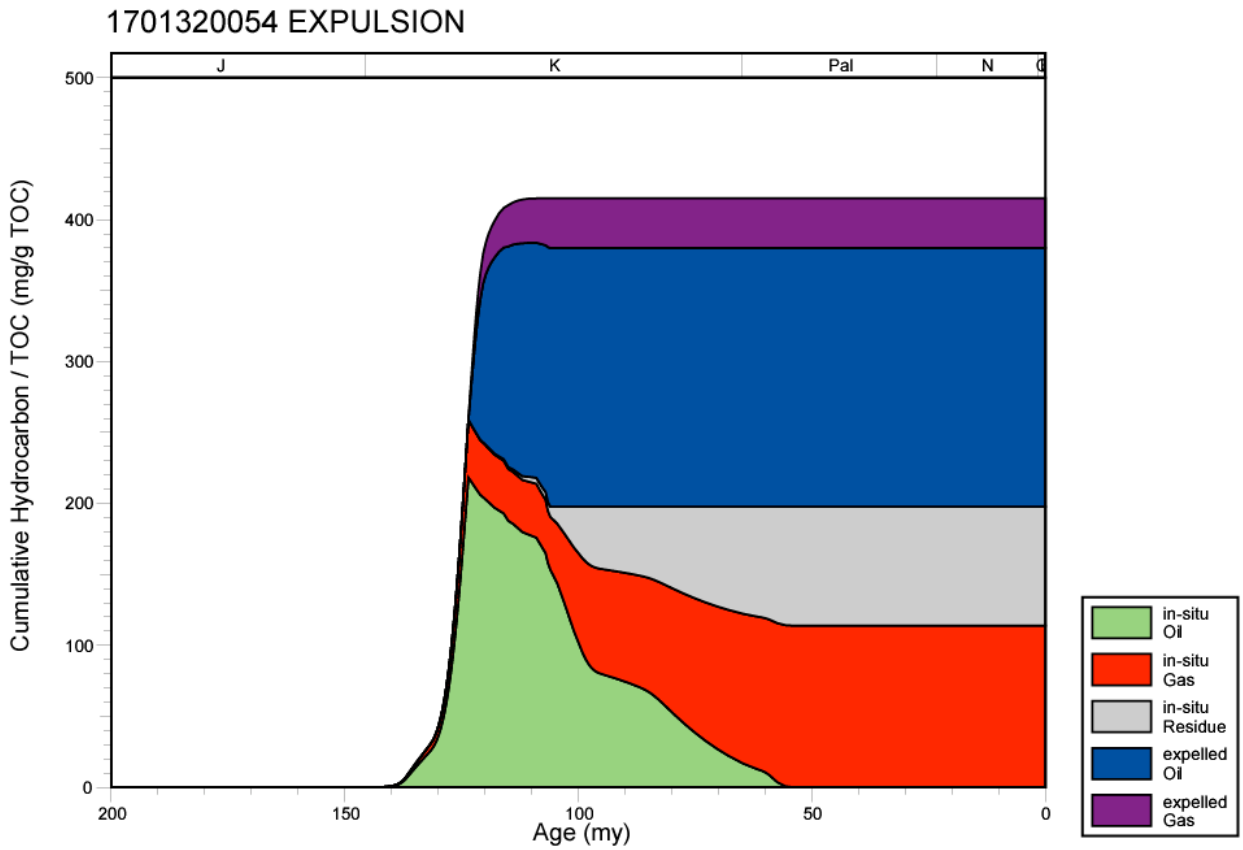


Figure 153. Hydrocarbon expulsion plot for well 1701320054, North Louisiana Salt Basin.

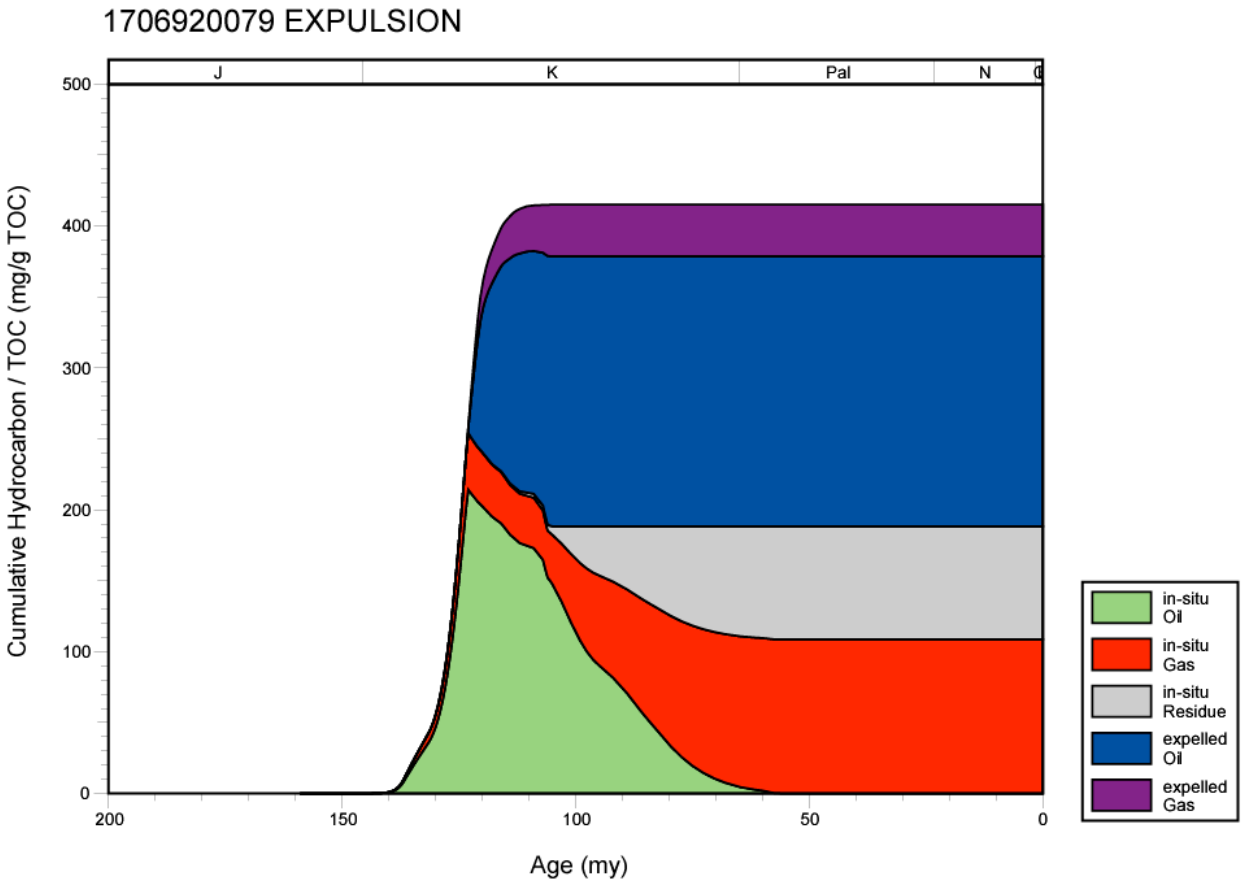


Figure 154. Hydrocarbon expulsion plot for well 1706920079, North Louisiana Salt Basin.

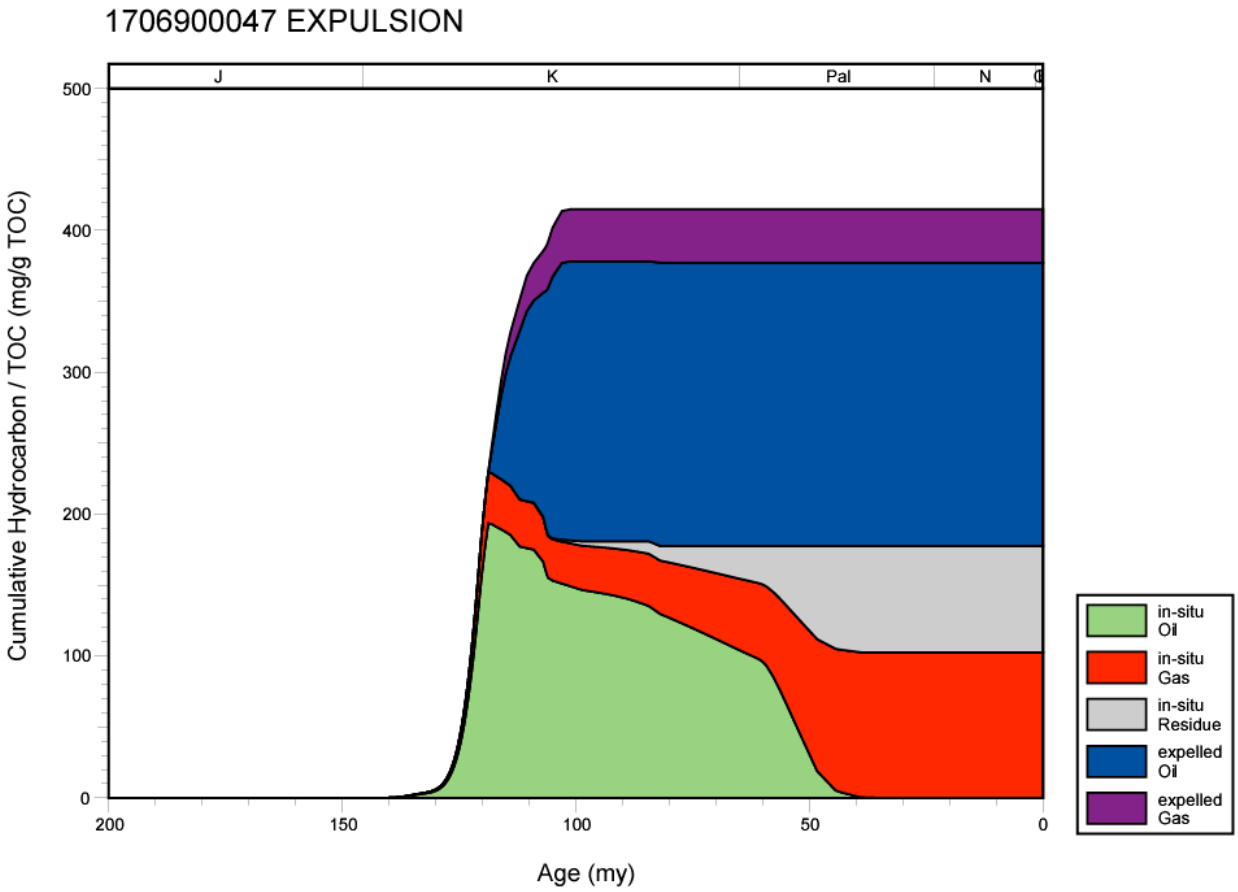


Figure 155. Hydrocarbon expulsion plot for well 1706900047, North Louisiana Salt Basin.

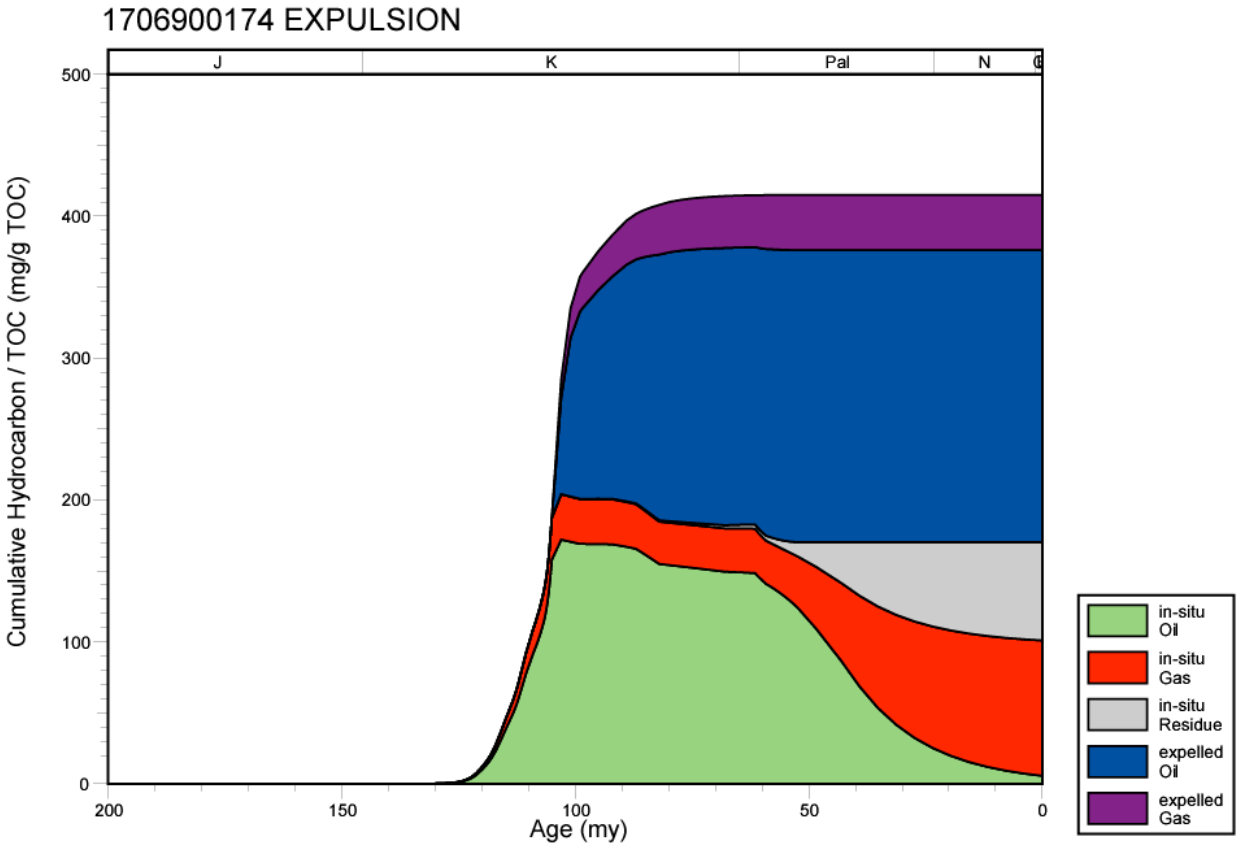


Figure 156. Hydrocarbon expulsion plot for well 1706900174, North Louisiana Salt Basin.

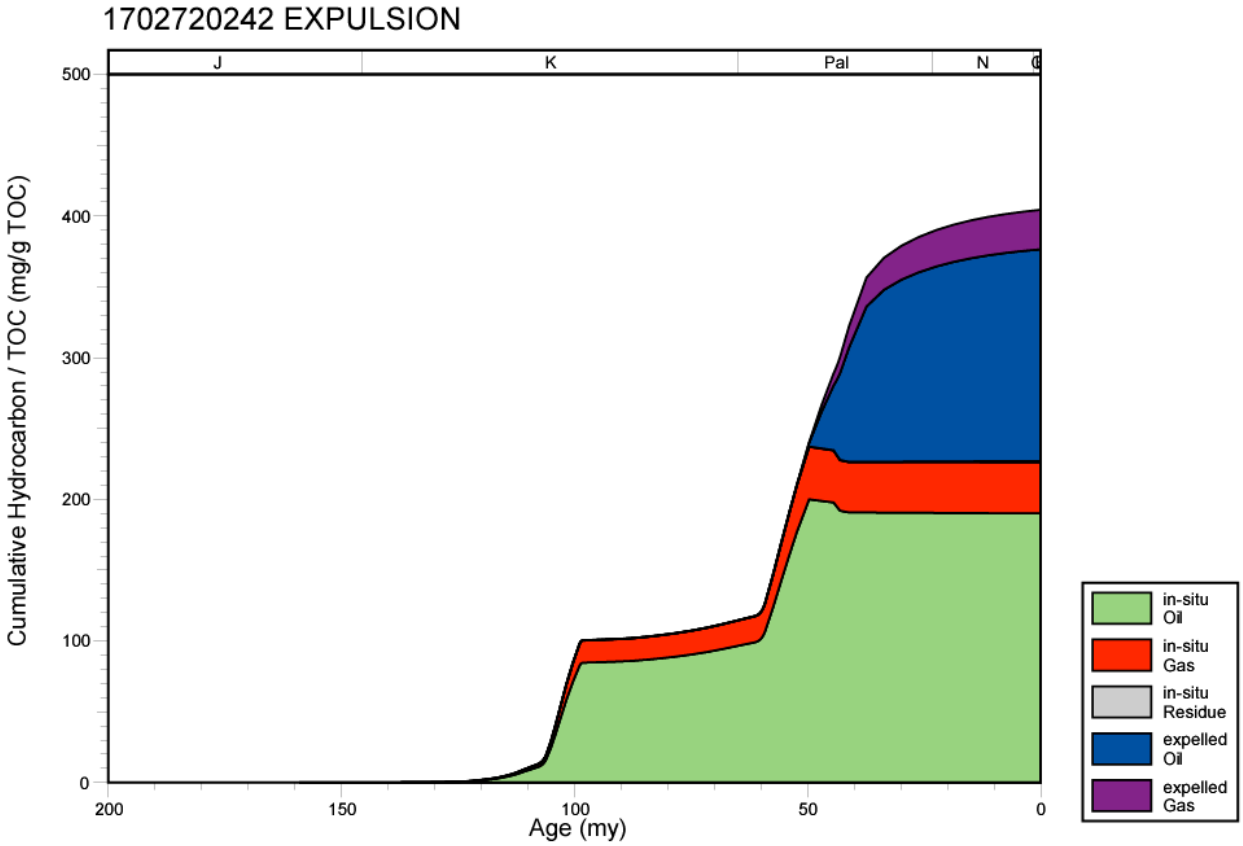


Figure 157. Hydrocarbon expulsion plot for well 1702720242, North Louisiana Salt Basin.

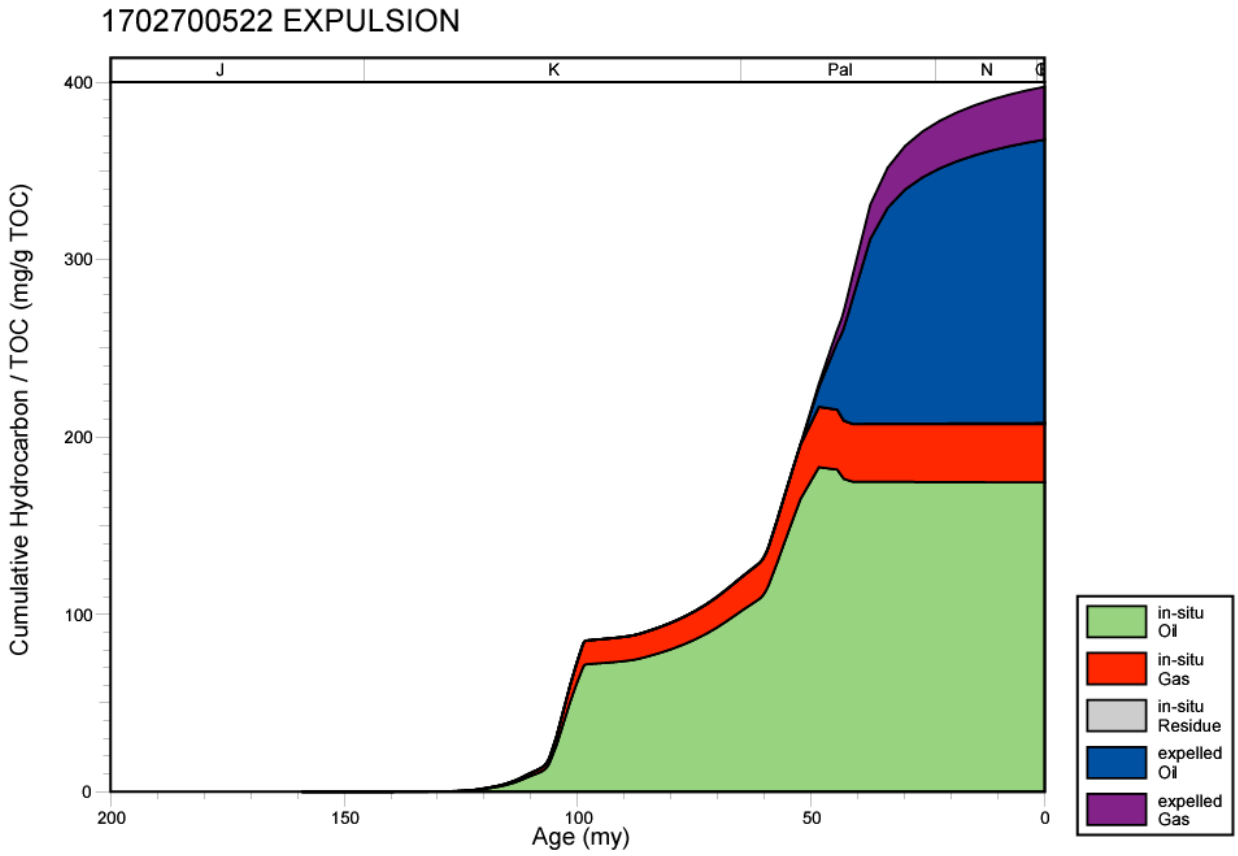


Figure 158. Hydrocarbon expulsion plot for well 1702700522, North Louisiana Salt Basin.

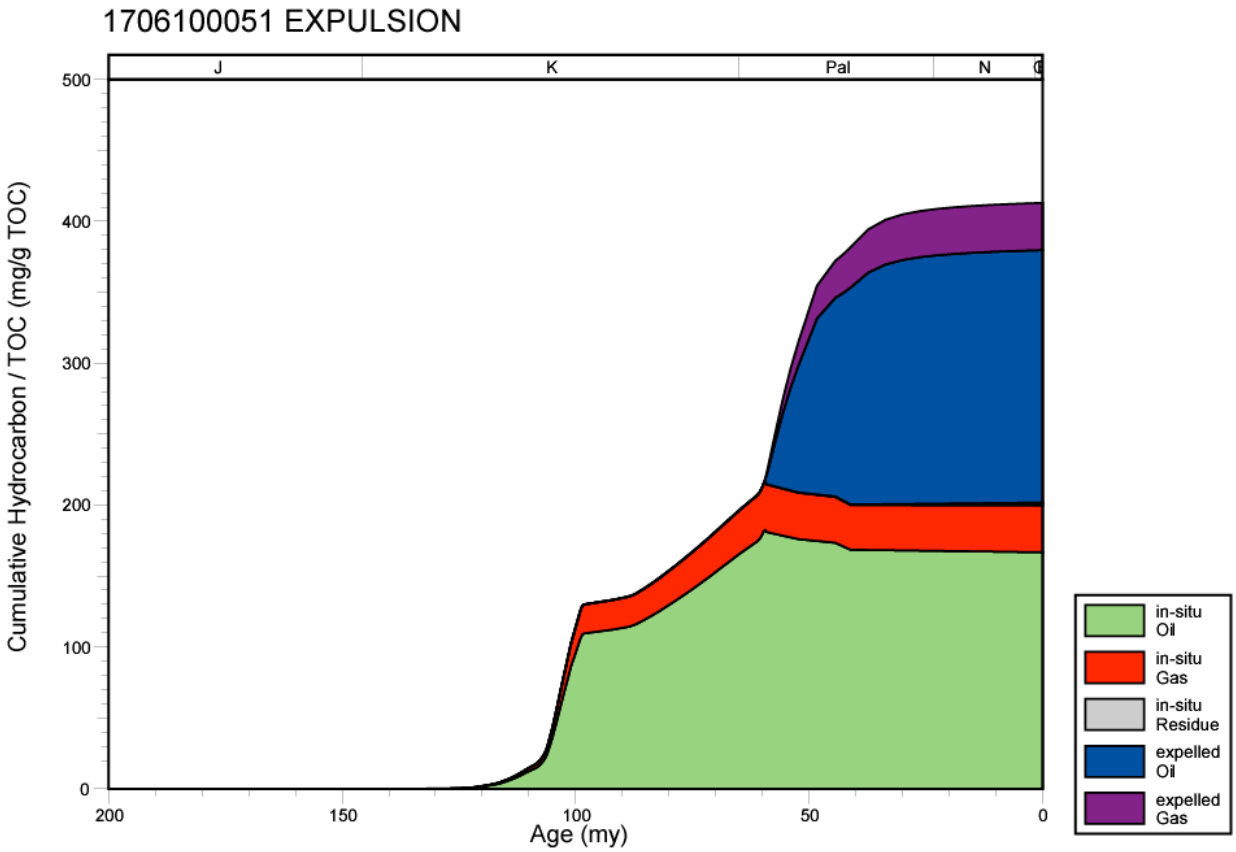


Figure 159. Hydrocarbon expulsion plot for well 1706100051, North Louisiana Salt Basin.

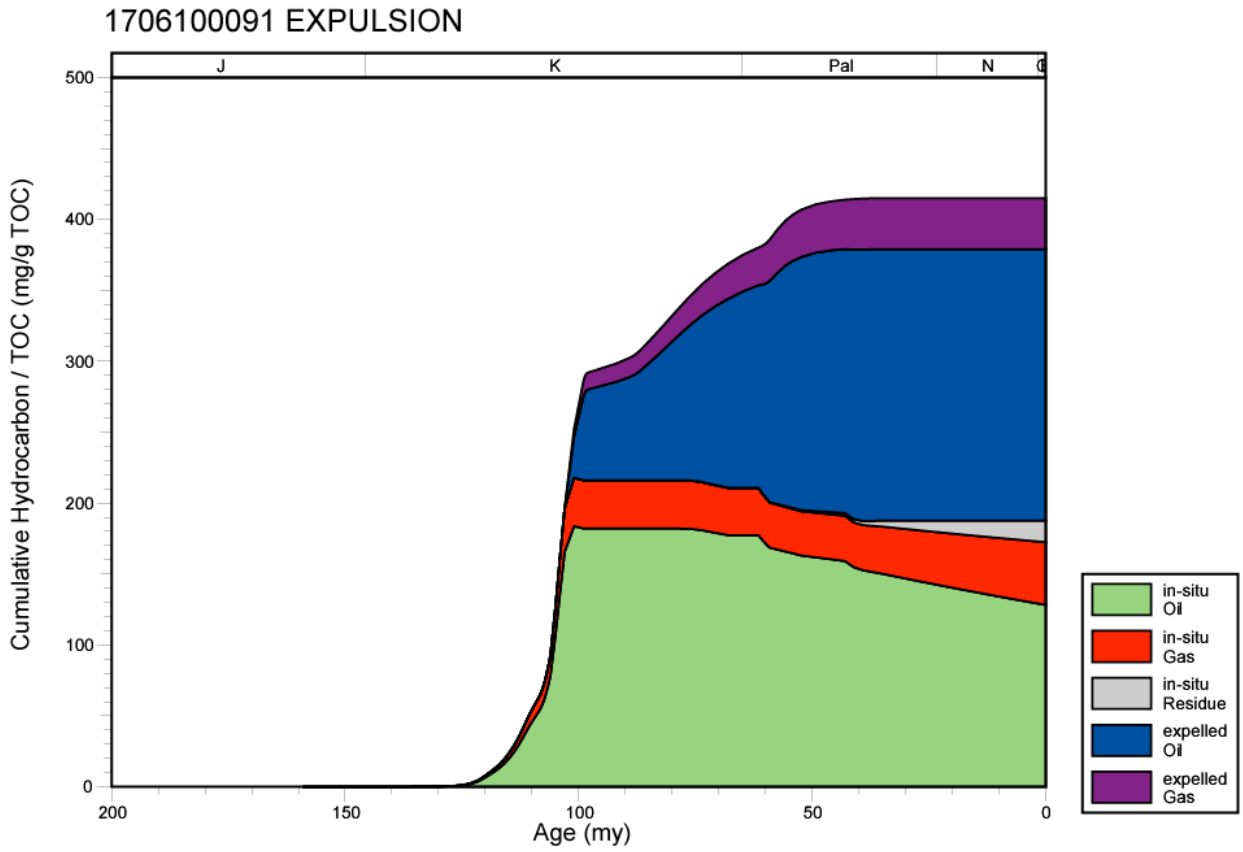


Figure 160. Hydrocarbon expulsion plot for well 1706100091, North Louisiana Salt Basin.

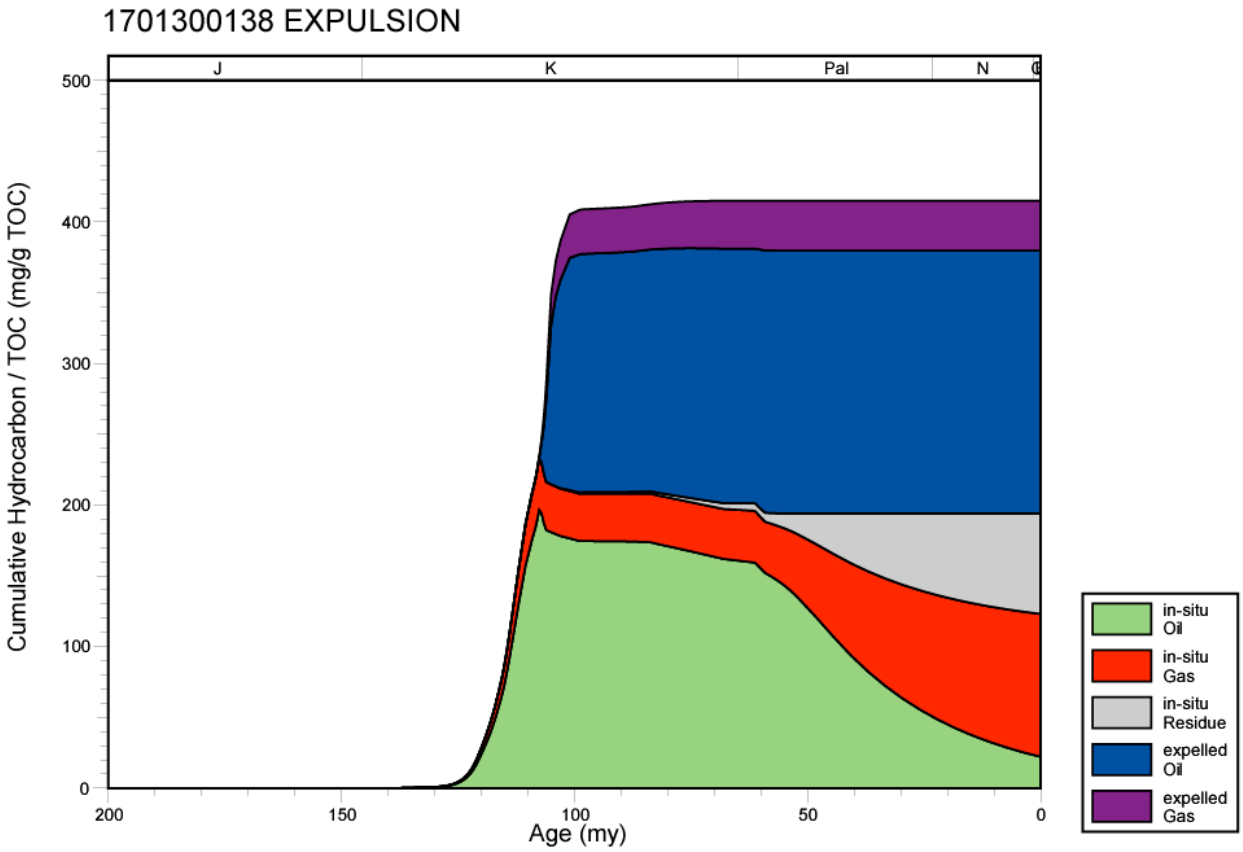


Figure 161. Hydrocarbon expulsion plot for well 1701300138, North Louisiana Salt Basin.

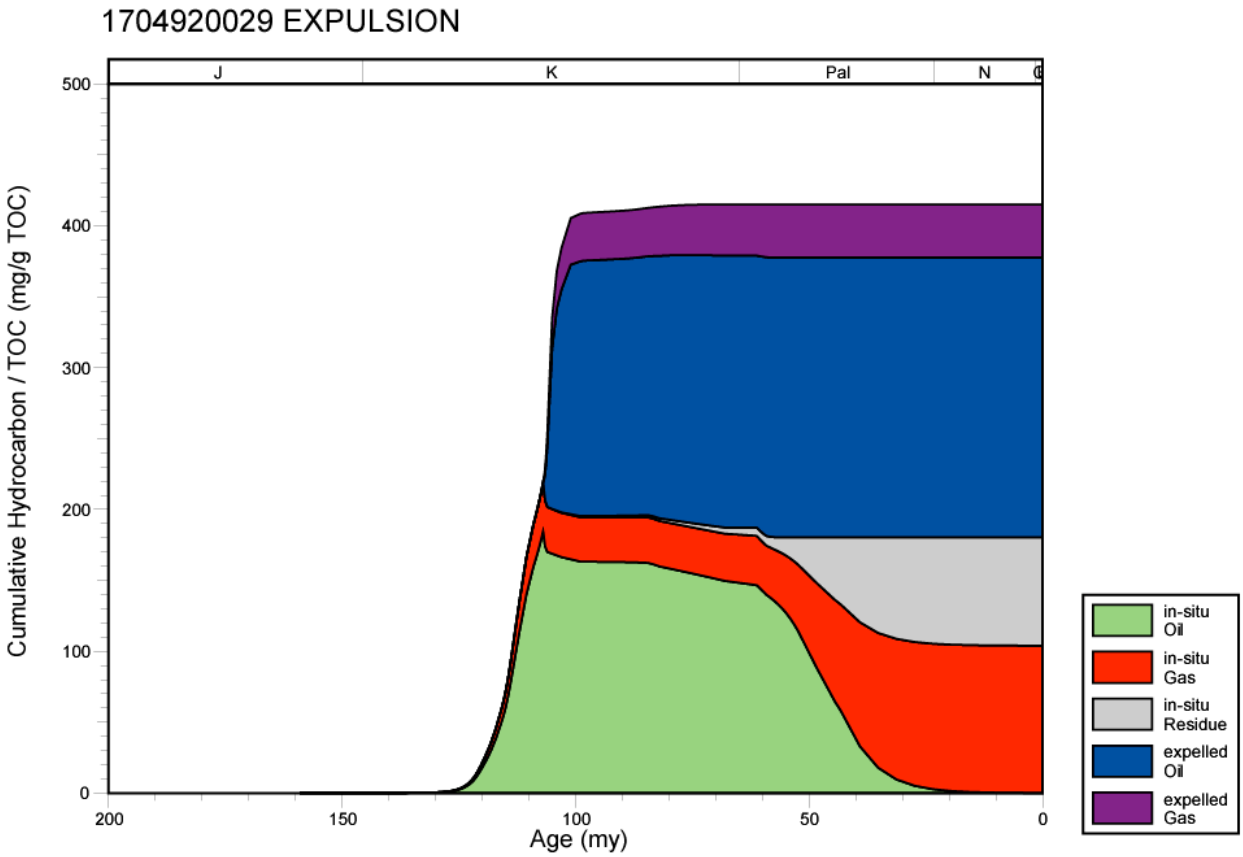


Figure 162. Hydrocarbon expulsion plot for well 1704920029, North Louisiana Salt Basin.

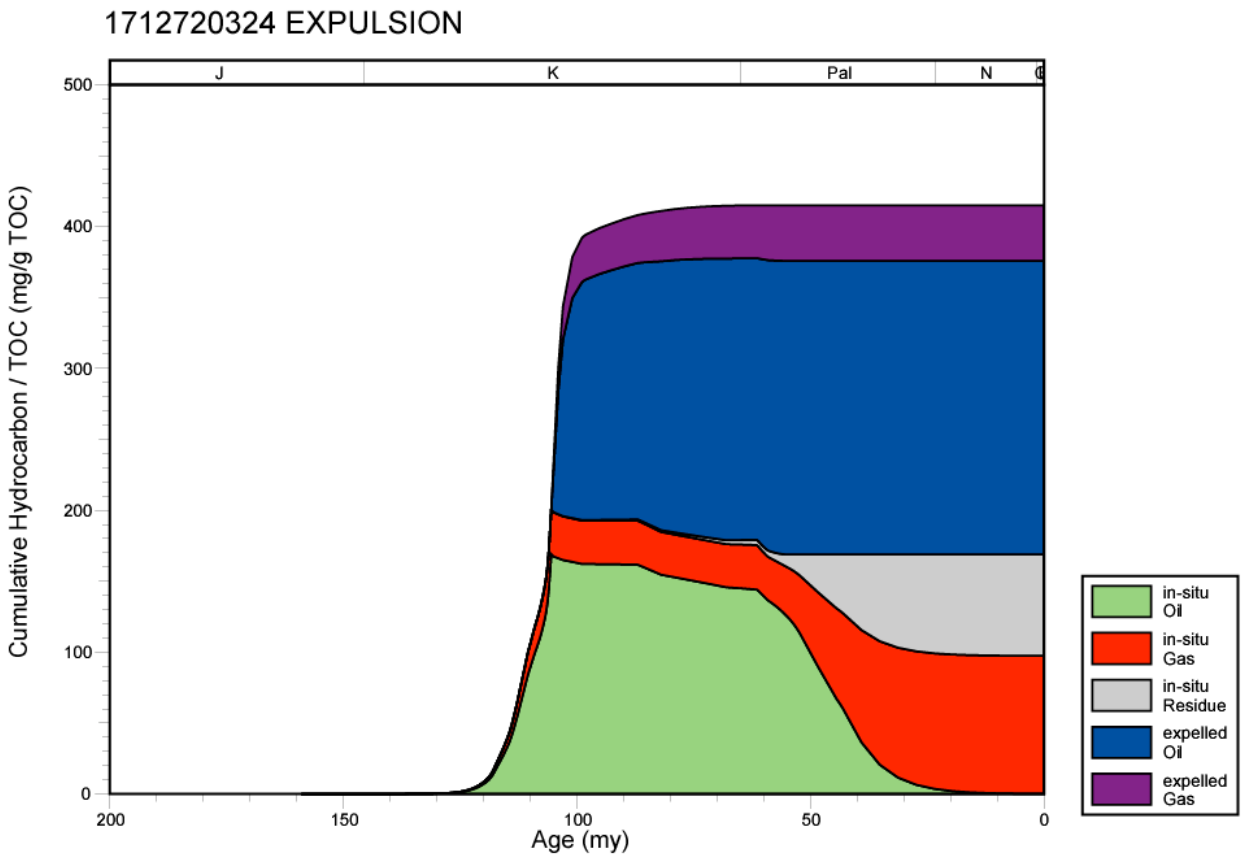


Figure 163. Hydrocarbon expulsion plot for well 1712720324, North Louisiana Salt Basin.

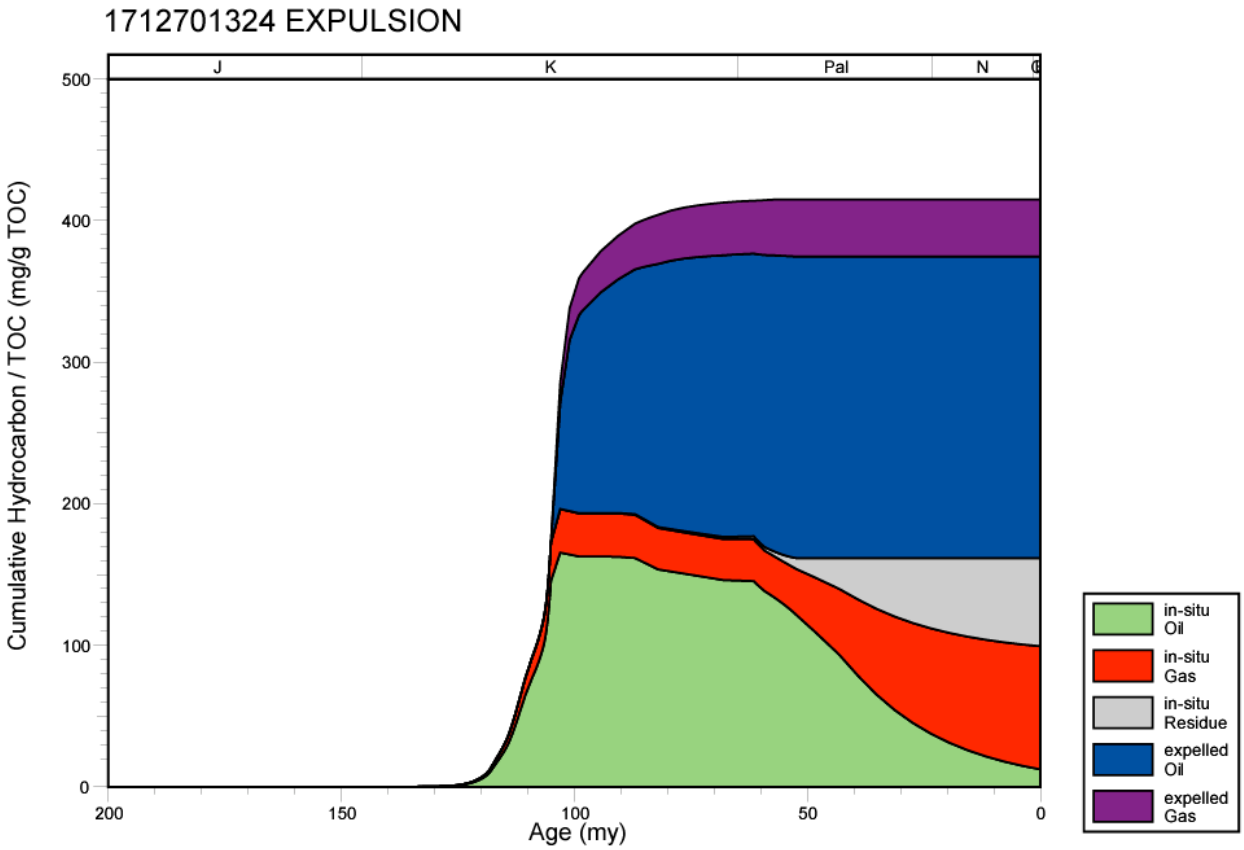


Figure 164. Hydrocarbon expulsion plot for well 1712701324, North Louisiana Salt Basin.

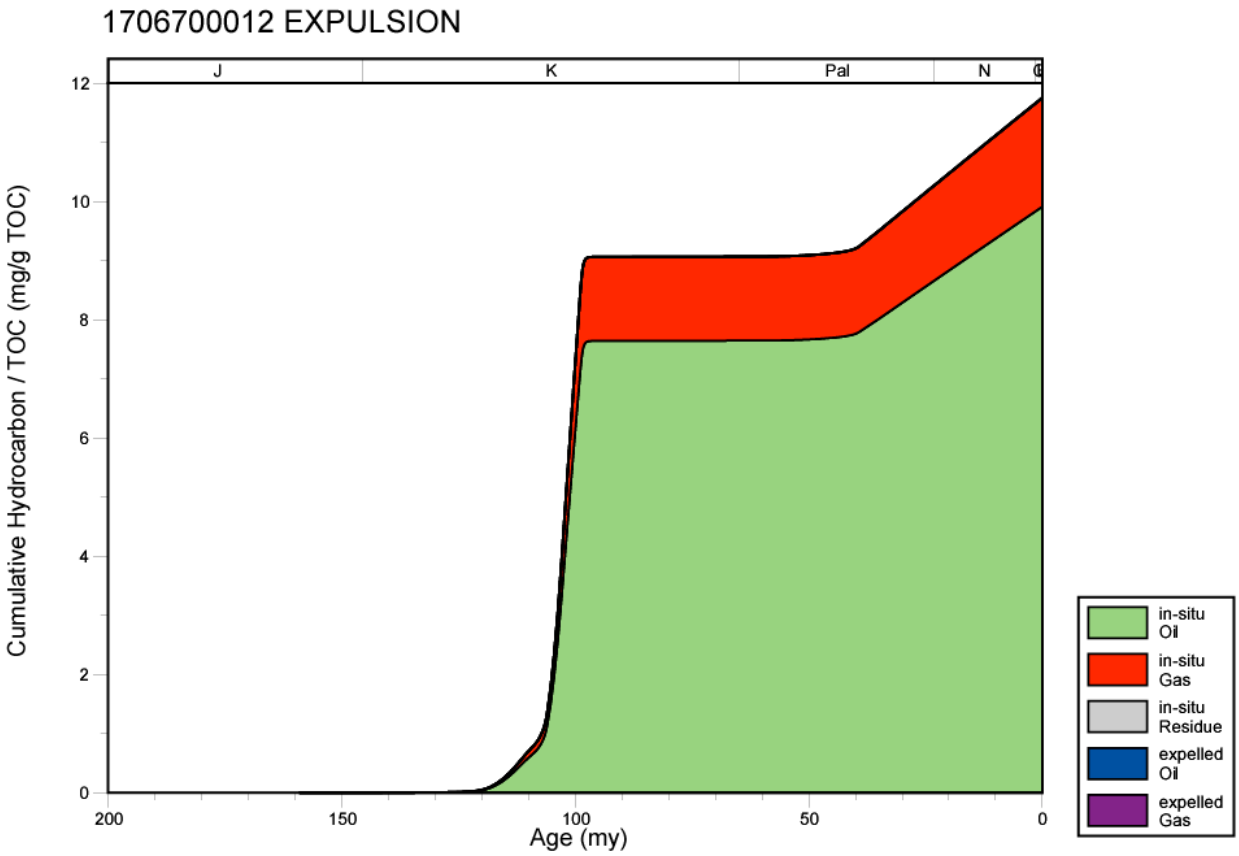


Figure 165. Hydrocarbon expulsion plot for well 1706700012, North Louisiana Salt Basin.

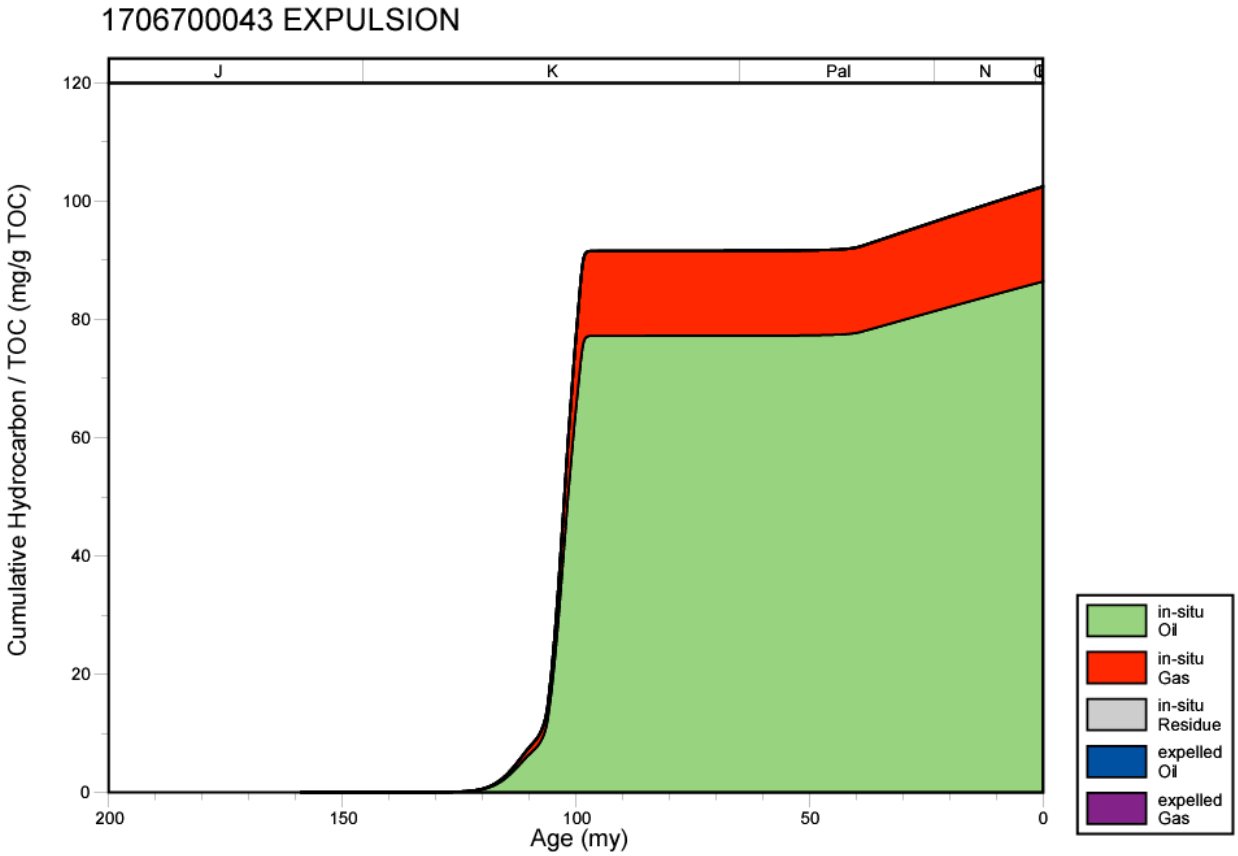


Figure 166. Hydrocarbon expulsion plot for well 1706700043, North Louisiana Salt Basin.

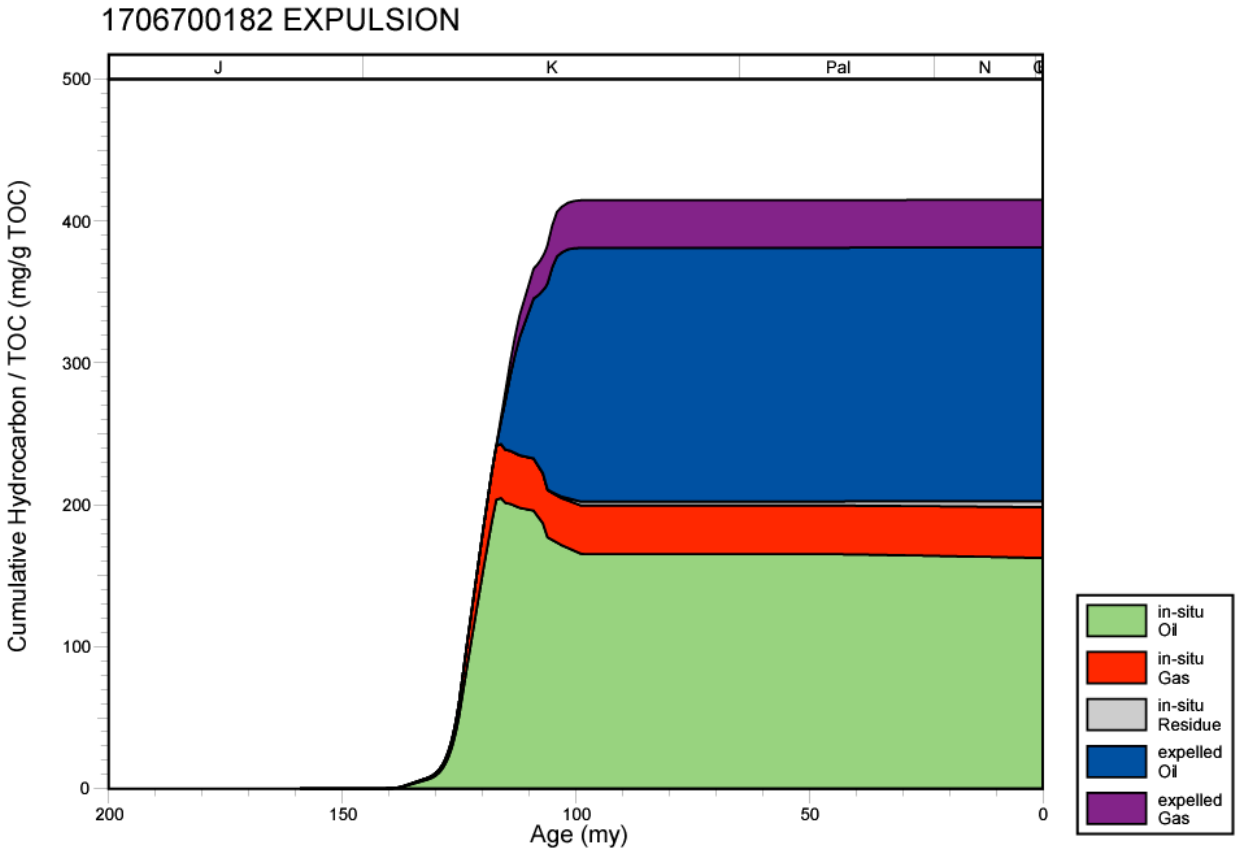


Figure 167. Hydrocarbon expulsion plot for well 1706700182, North Louisiana Salt Basin.

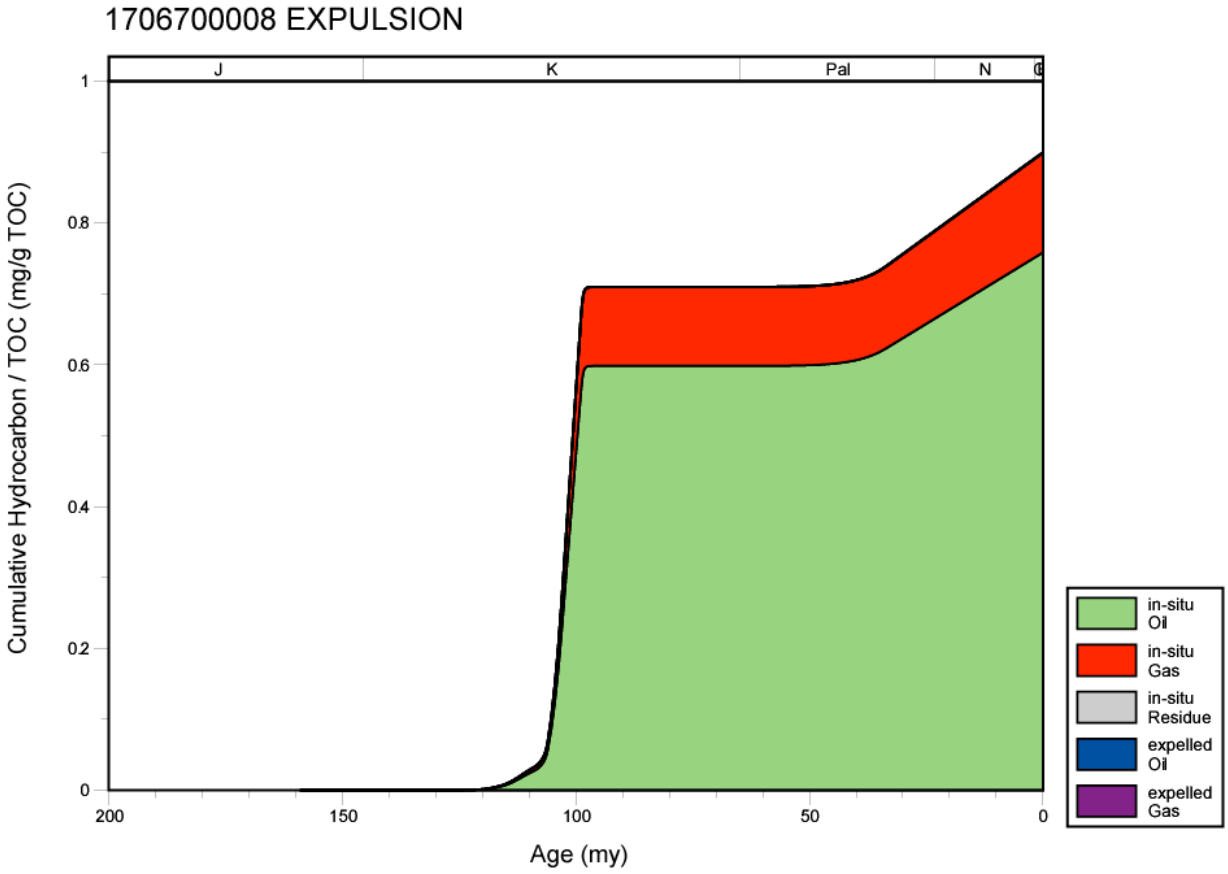


Figure 168. Hydrocarbon expulsion plot for well 1706700008, North Louisiana Salt Basin.

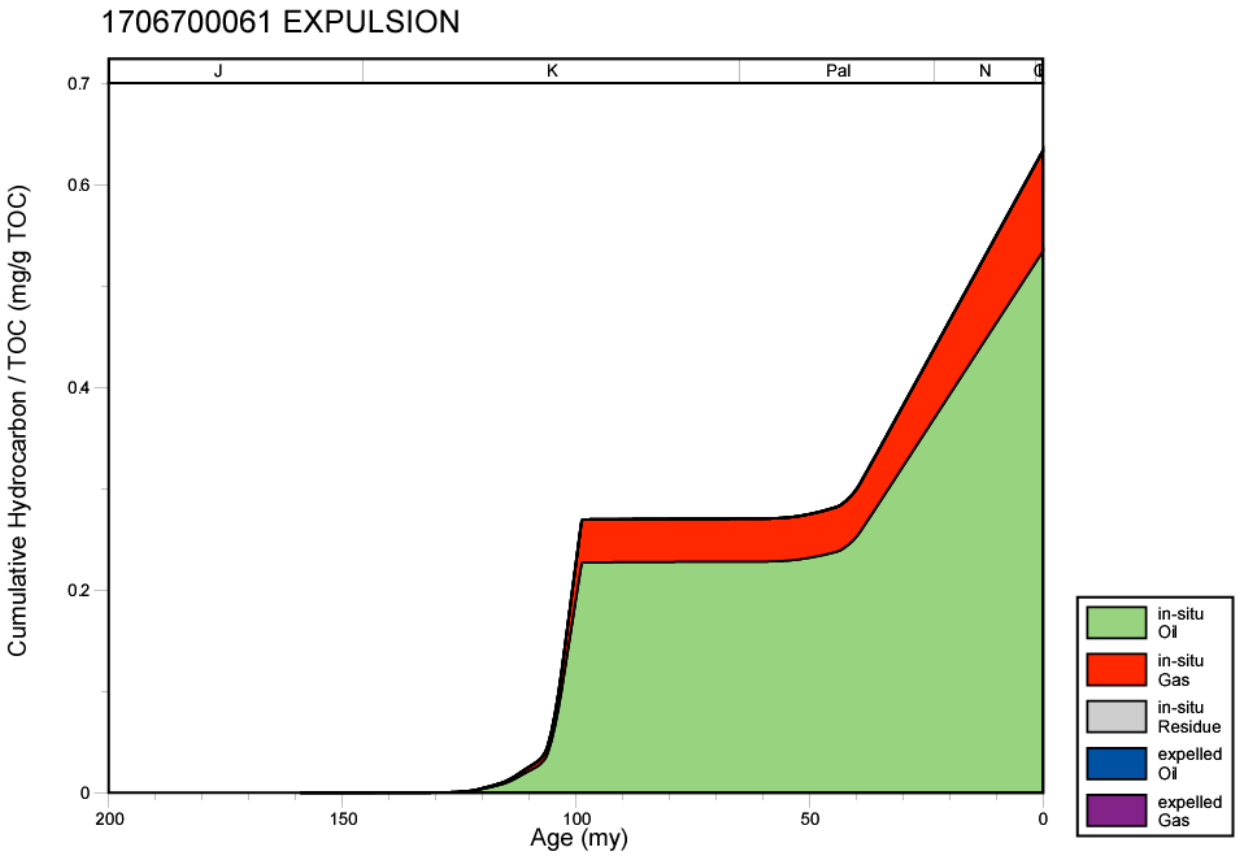


Figure 169. Hydrocarbon expulsion plot for well 1706700061, North Louisiana Salt Basin.

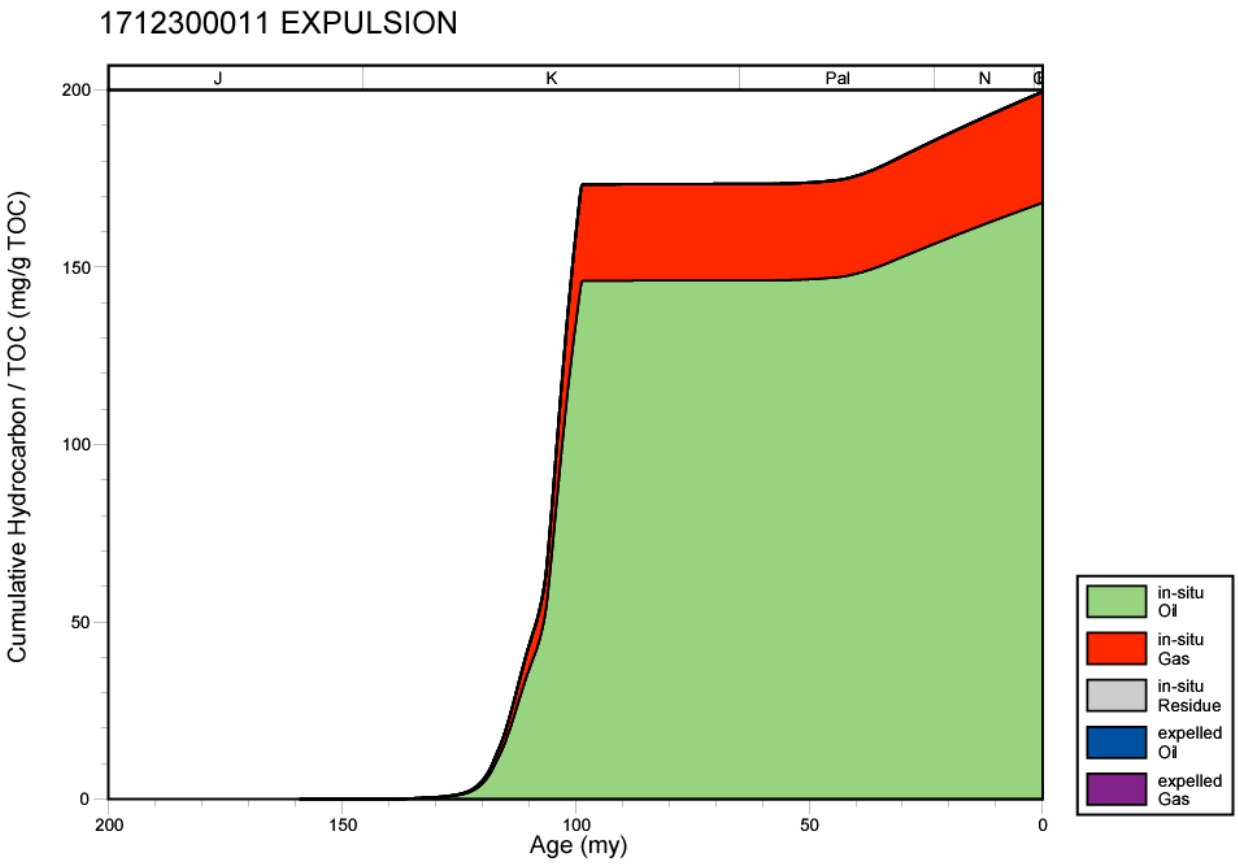


Figure 170. Hydrocarbon expulsion plot for well 1712300011, North Louisiana Salt Basin.

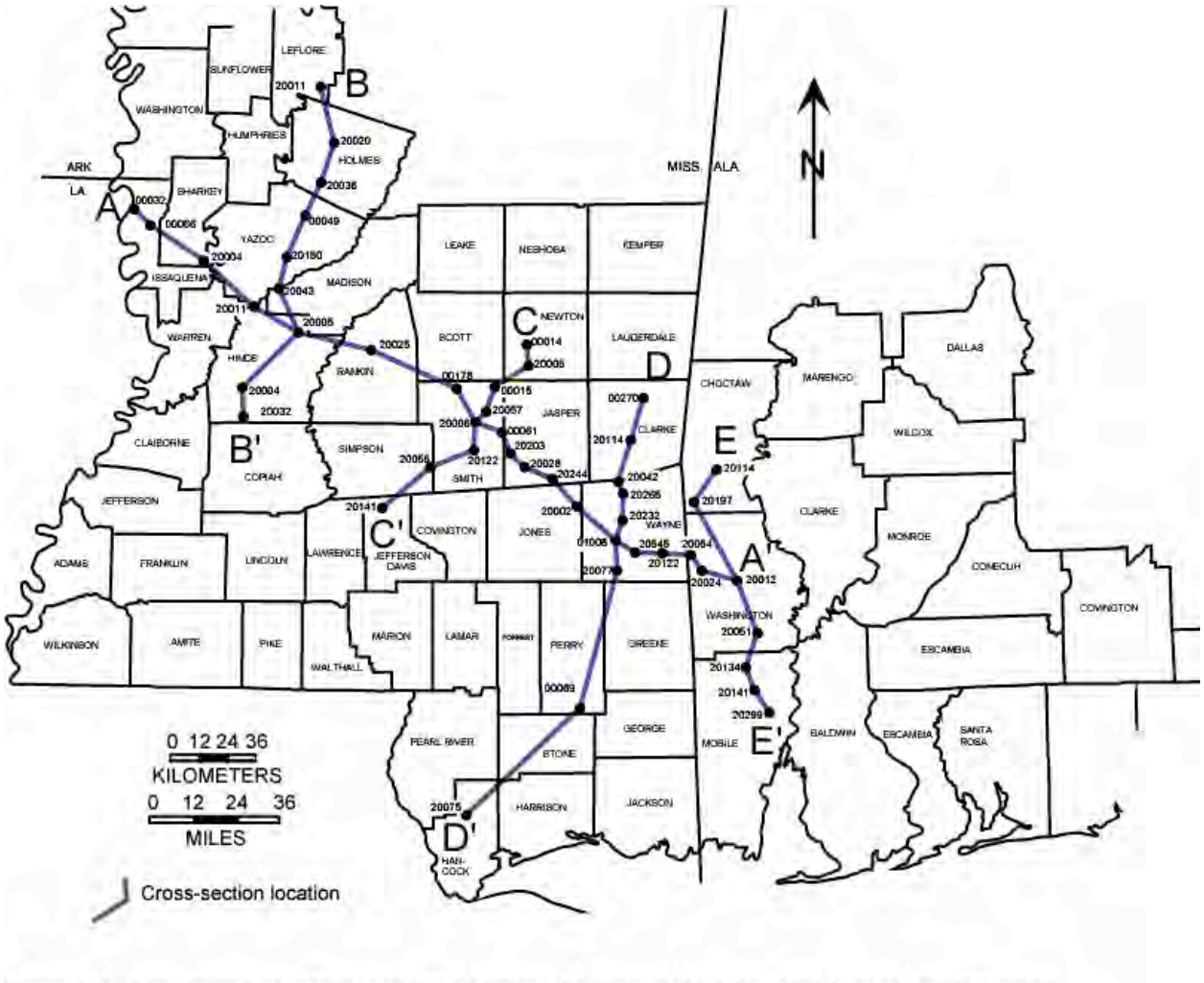


Figure 171. Map illustrating locations of cross sections for study in the Mississippi Interior Salt Basin area.

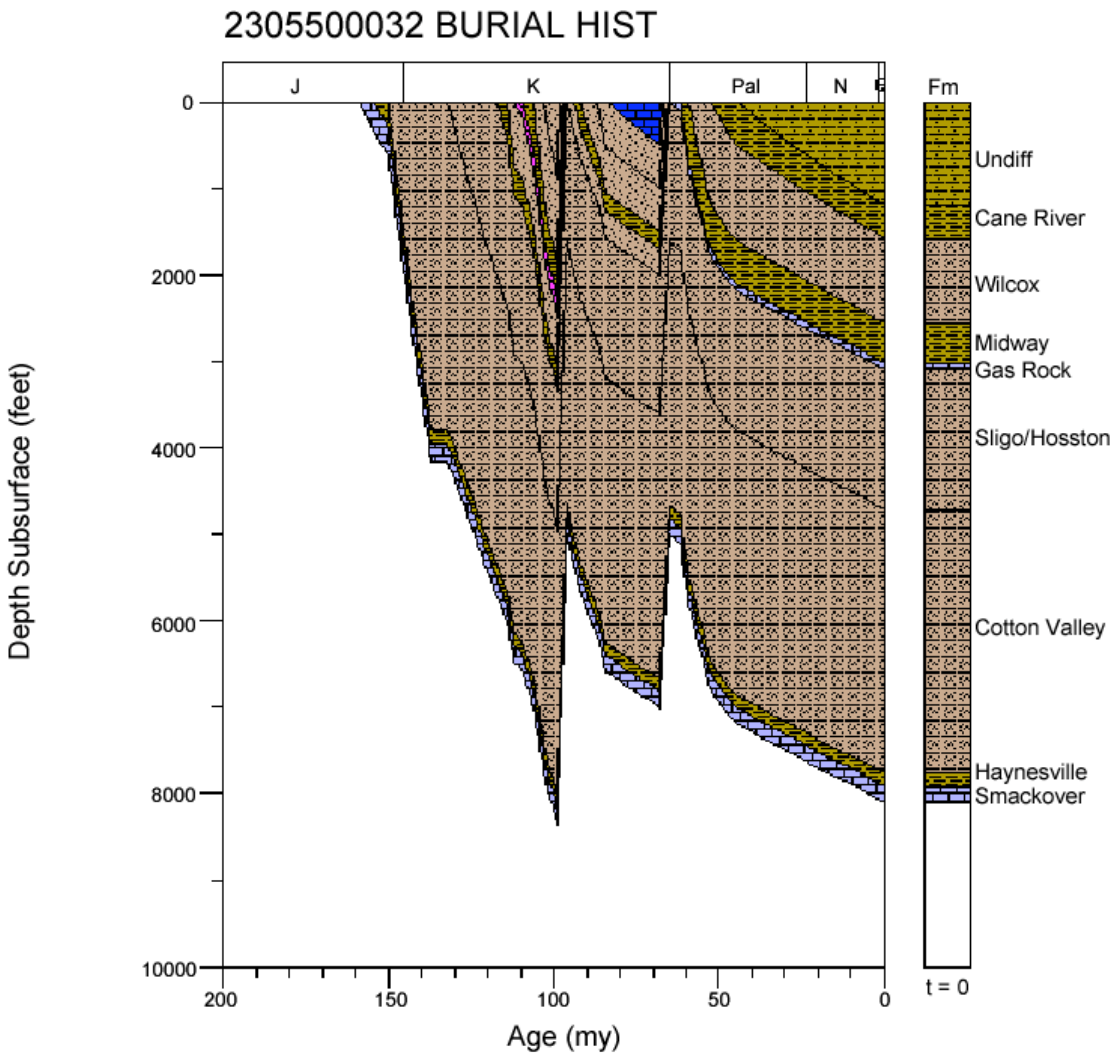


Figure 172. Burial history for well 2305500032, Mississippi Interior Salt Basin.

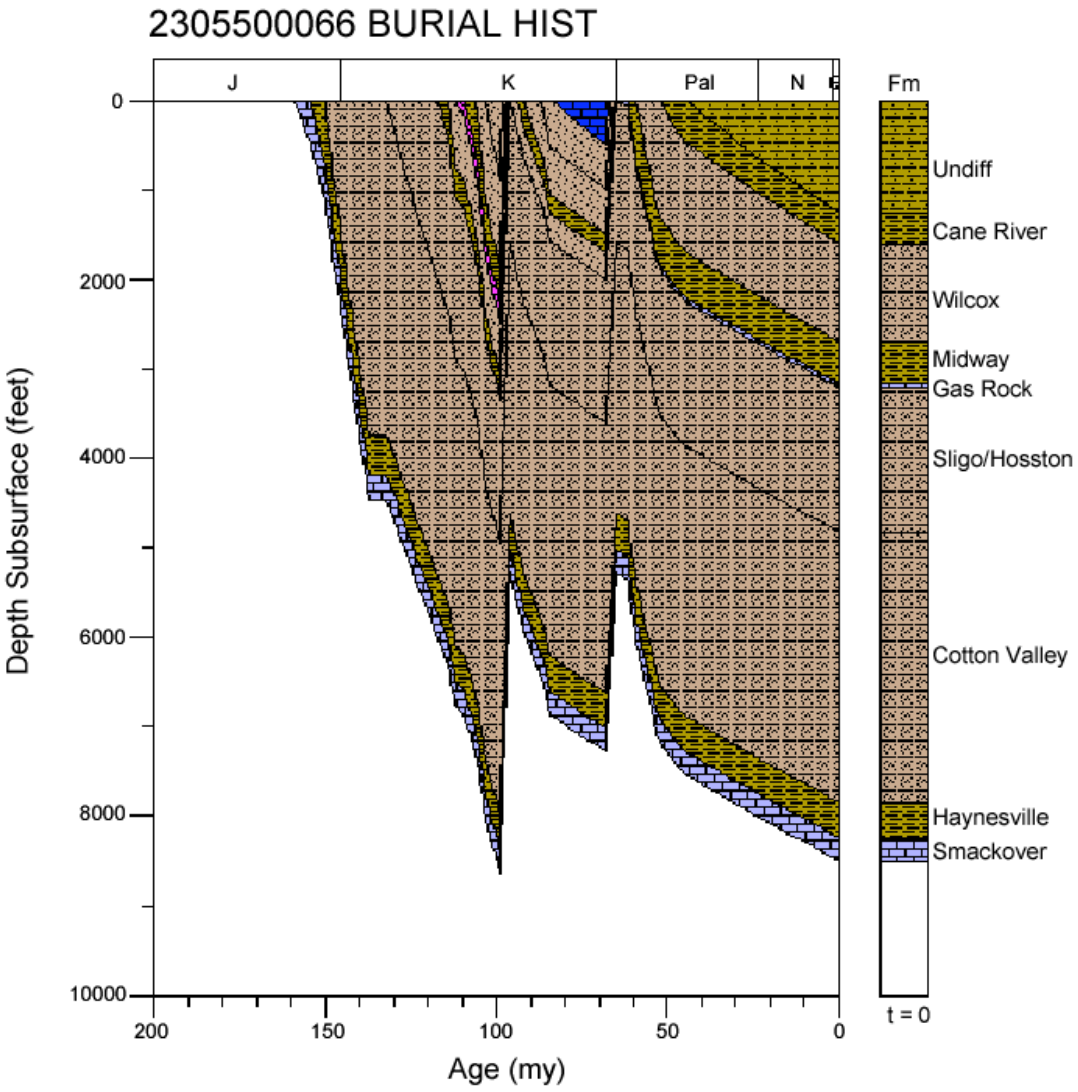


Figure 173. Burial history for well 2305500066, Mississippi Interior Salt Basin.

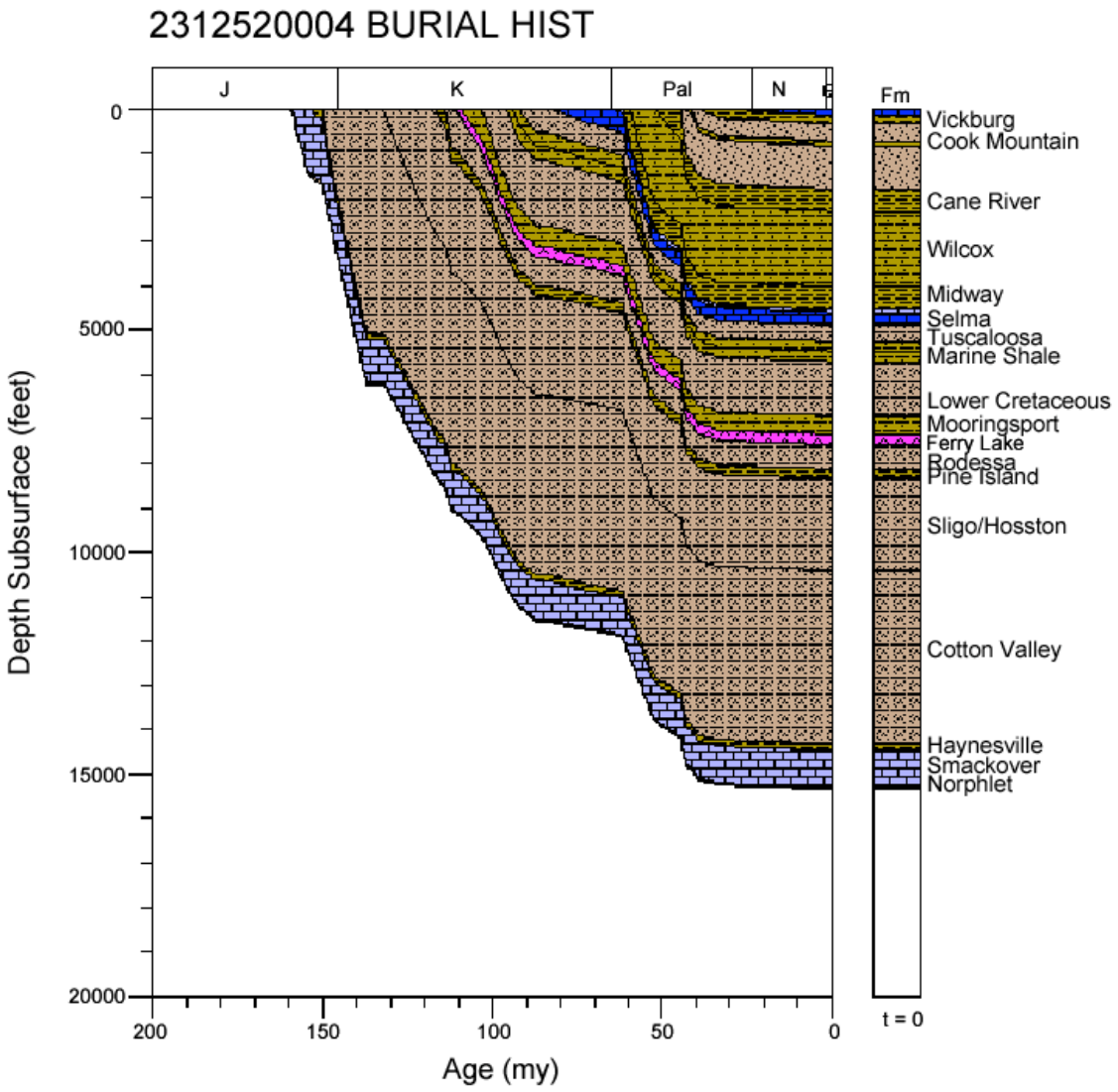


Figure 174. Burial history for well 2312520004, Mississippi Interior Salt Basin.

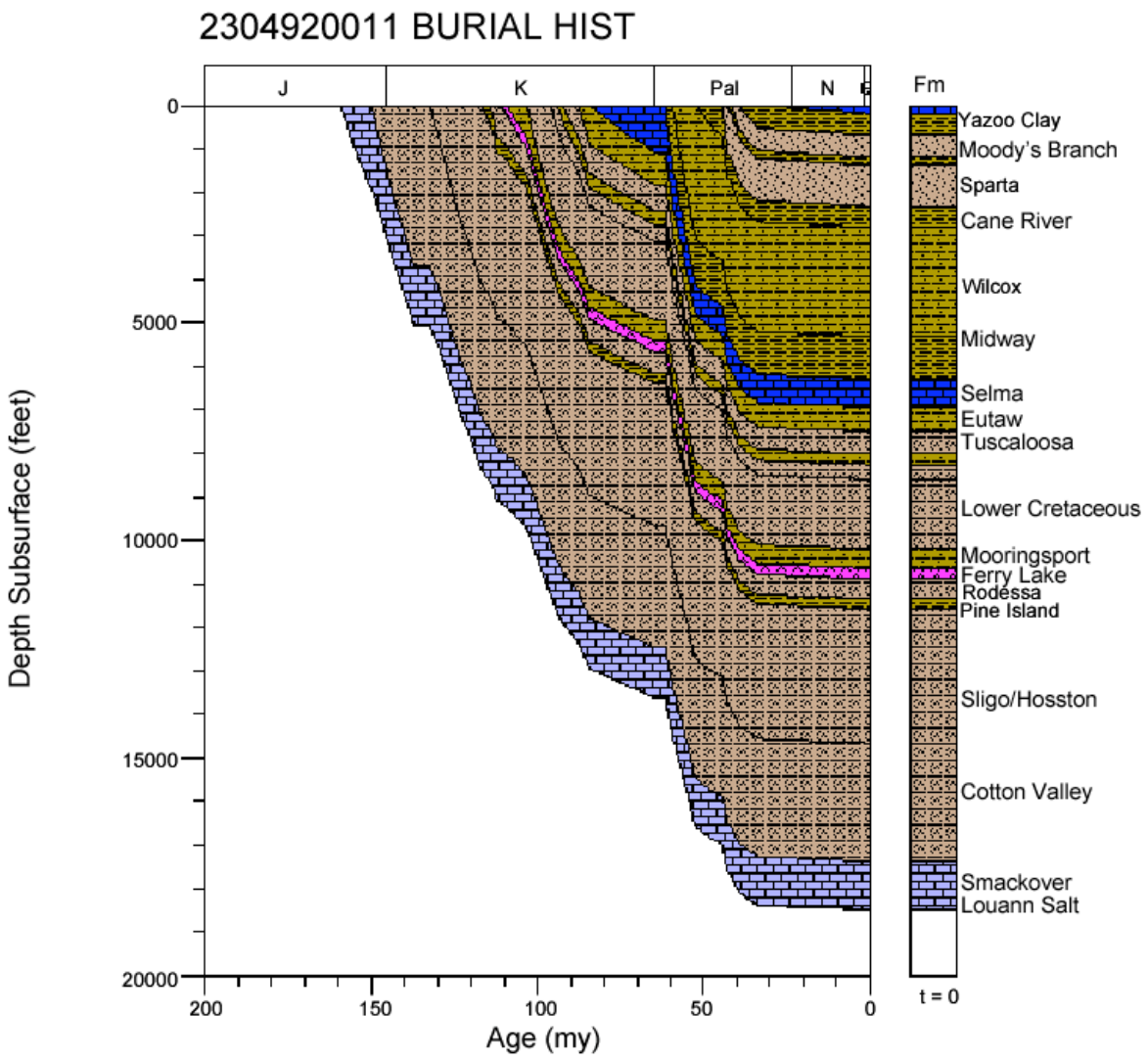


Figure 175. Burial history for well 2304920011, Mississippi Interior Salt Basin.

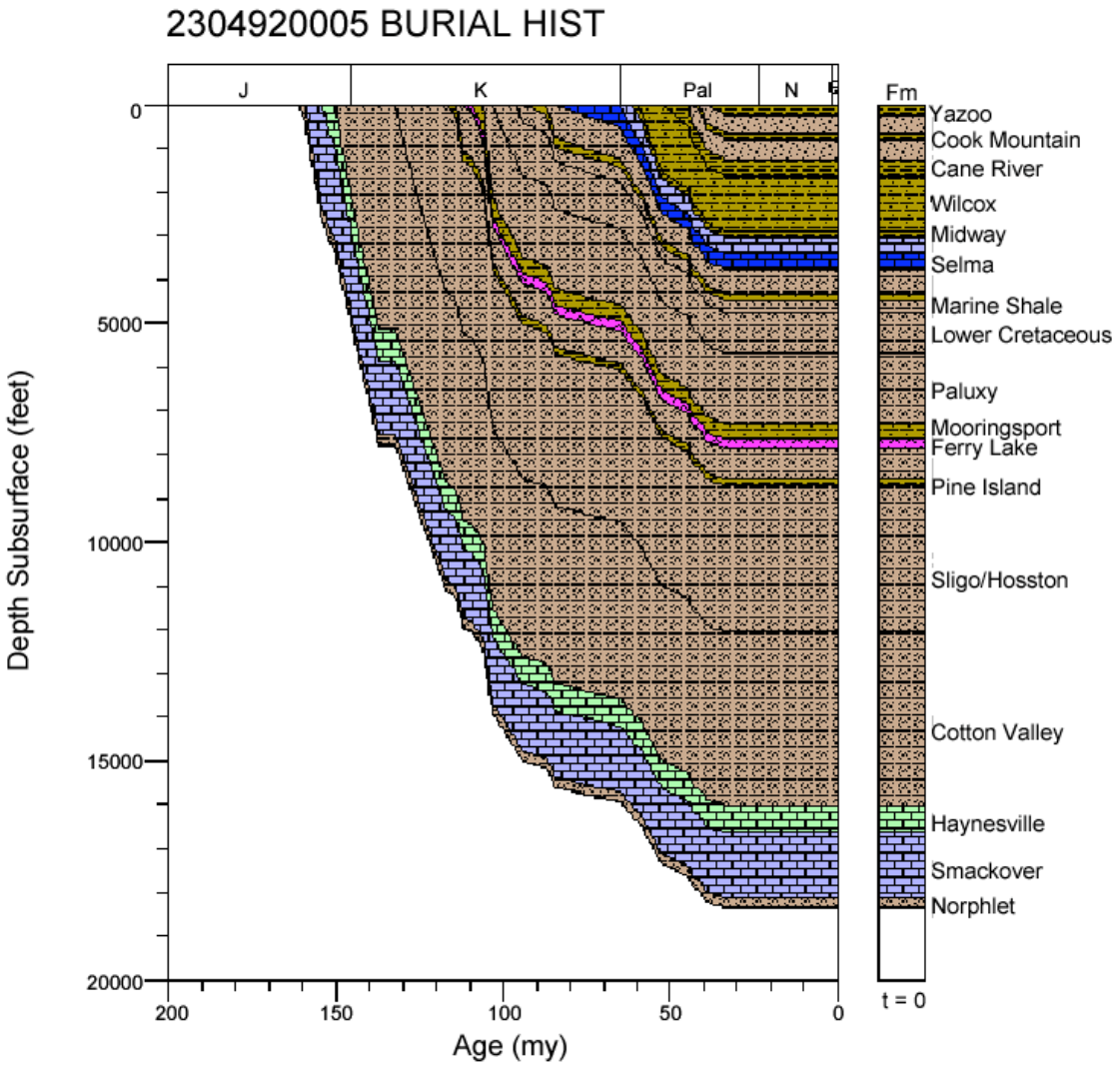


Figure 176. Burial history for well 2304920005, Mississippi Interior Salt Basin.

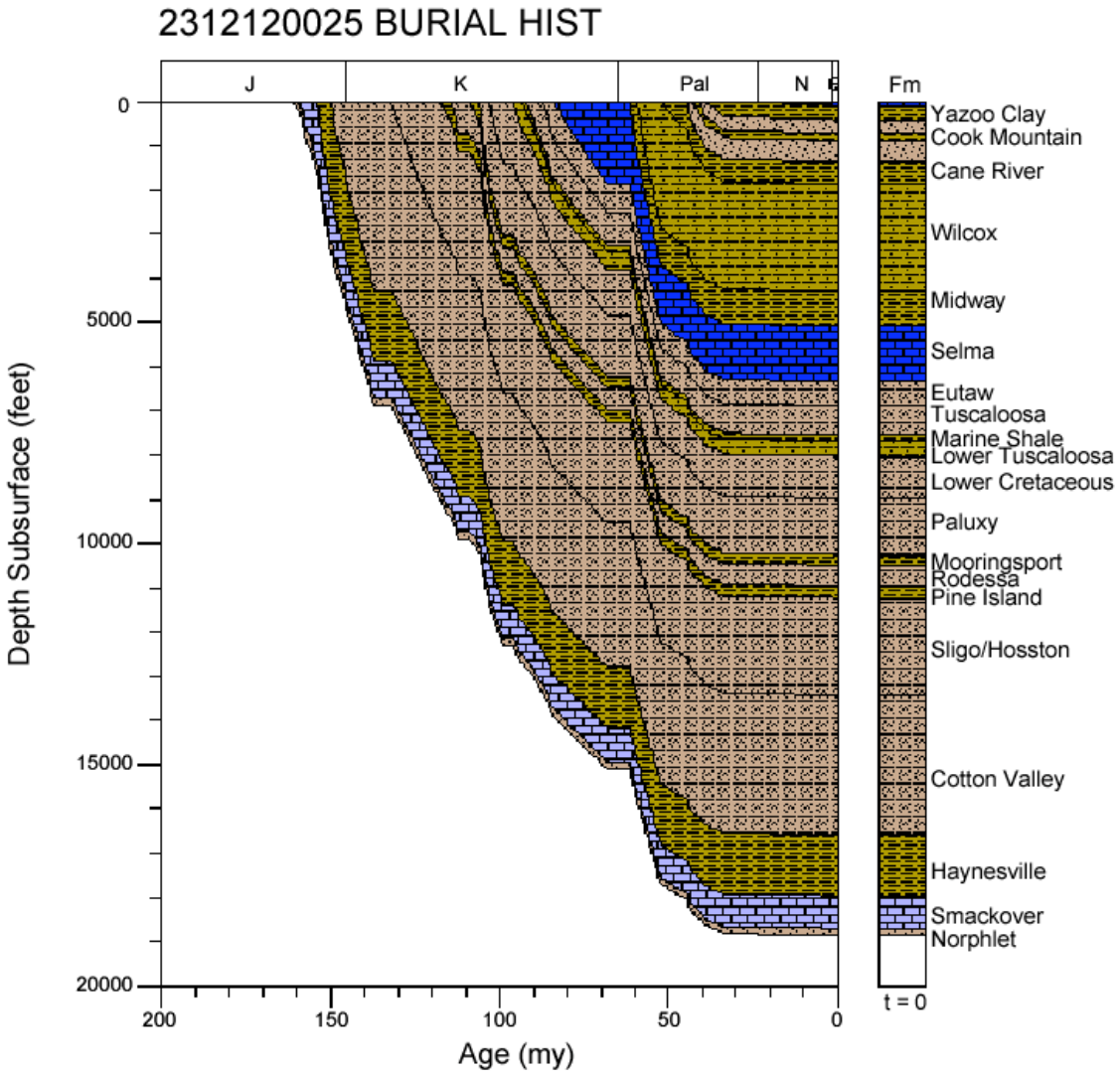


Figure 177. Burial history for well 2312120025, Mississippi Interior Salt Basin.

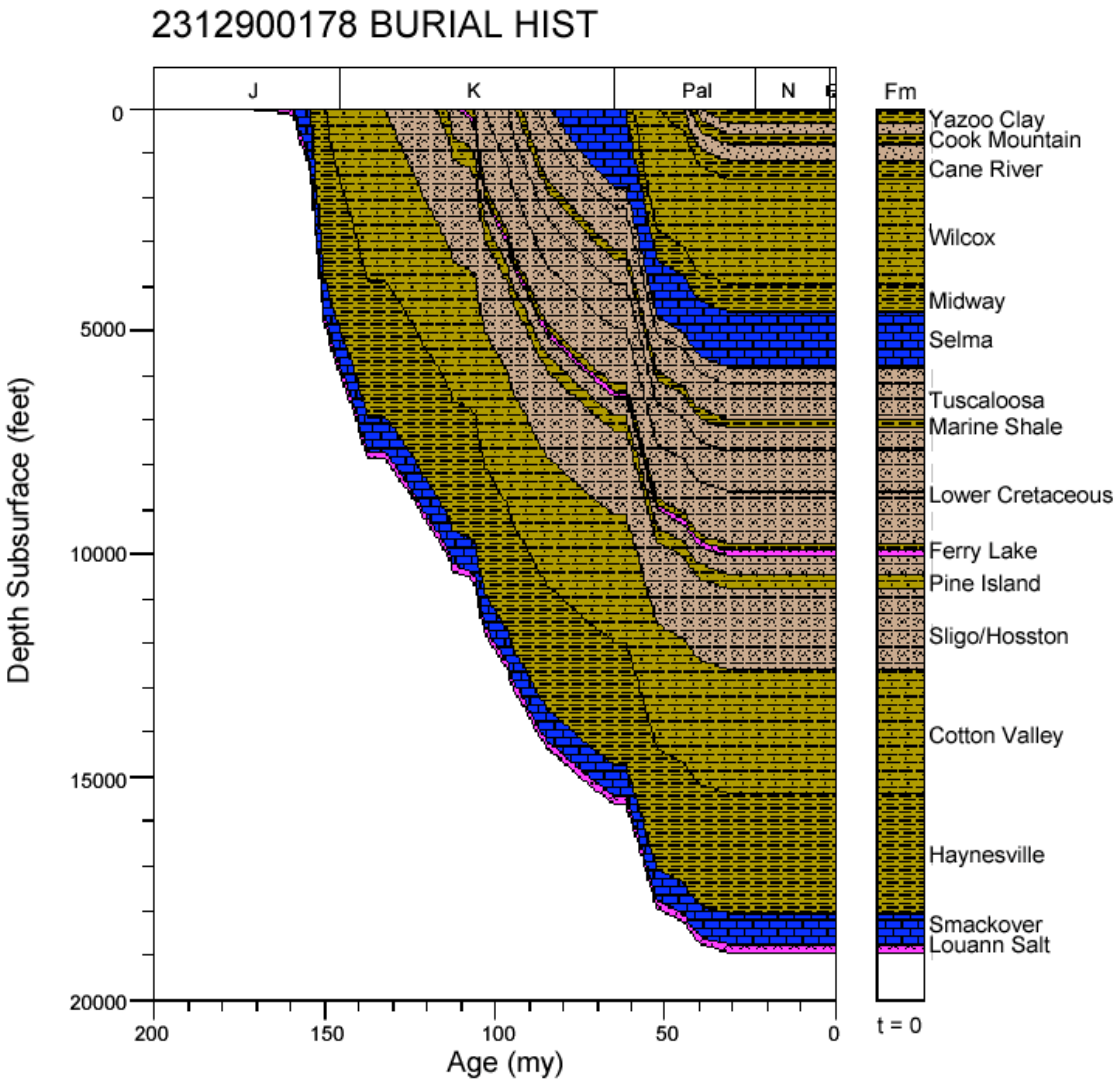


Figure 178. Burial history for well 2312900178, Mississippi Interior Salt Basin.

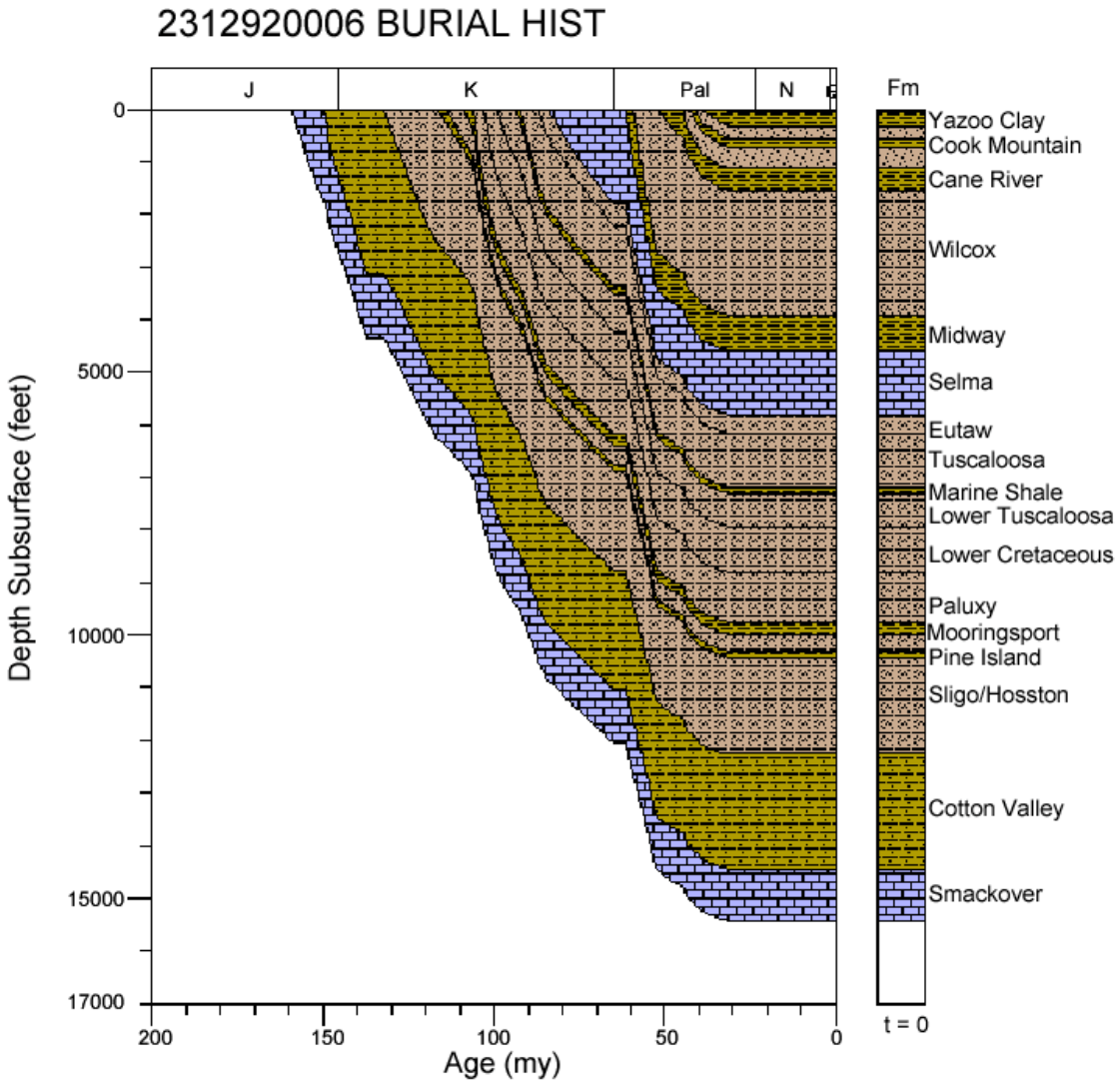


Figure 179. Burial history for well 2312920006, Mississippi Interior Salt Basin.

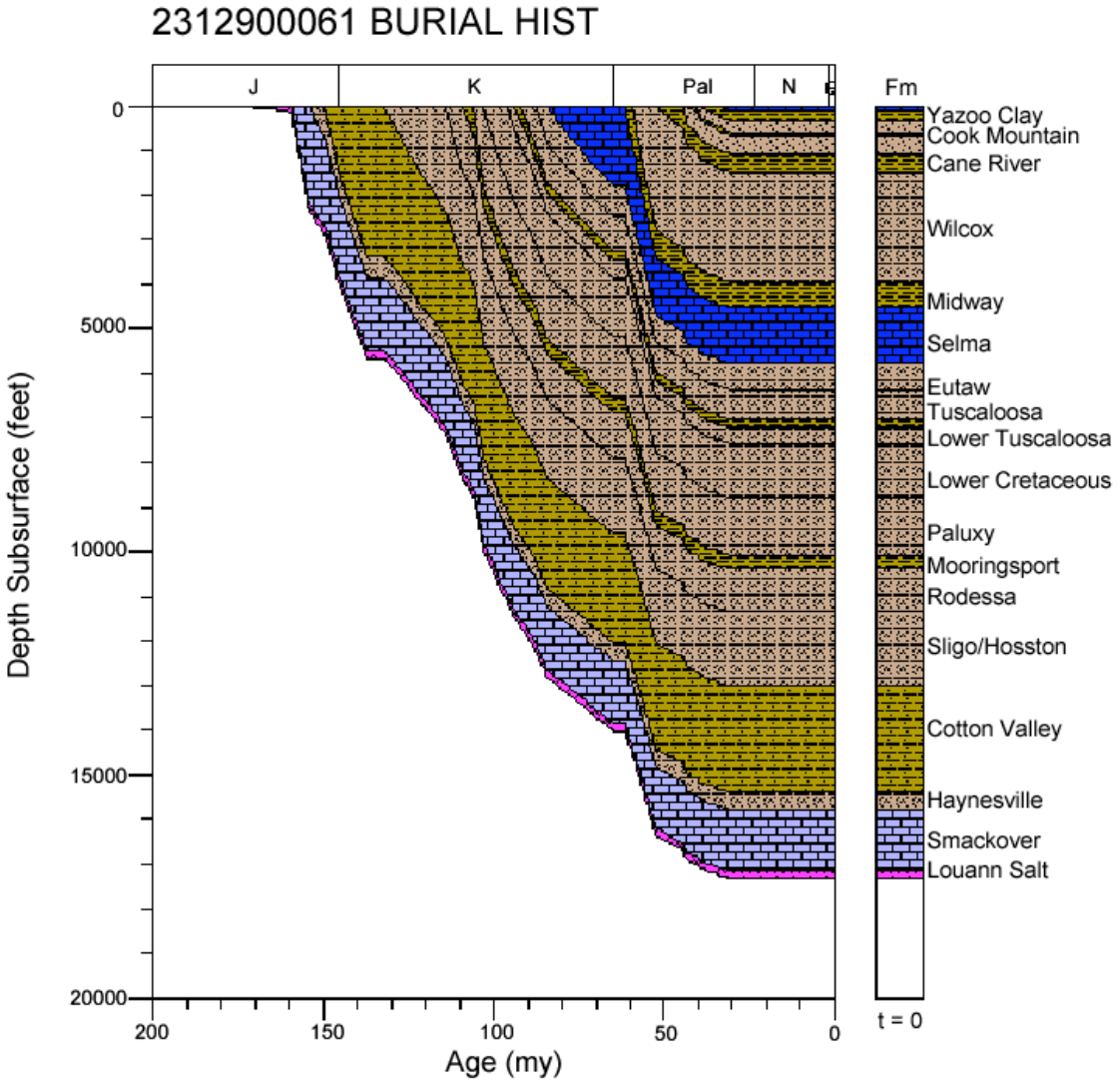


Figure 180. Burial history for well 2312900061, Mississippi Interior Salt Basin.

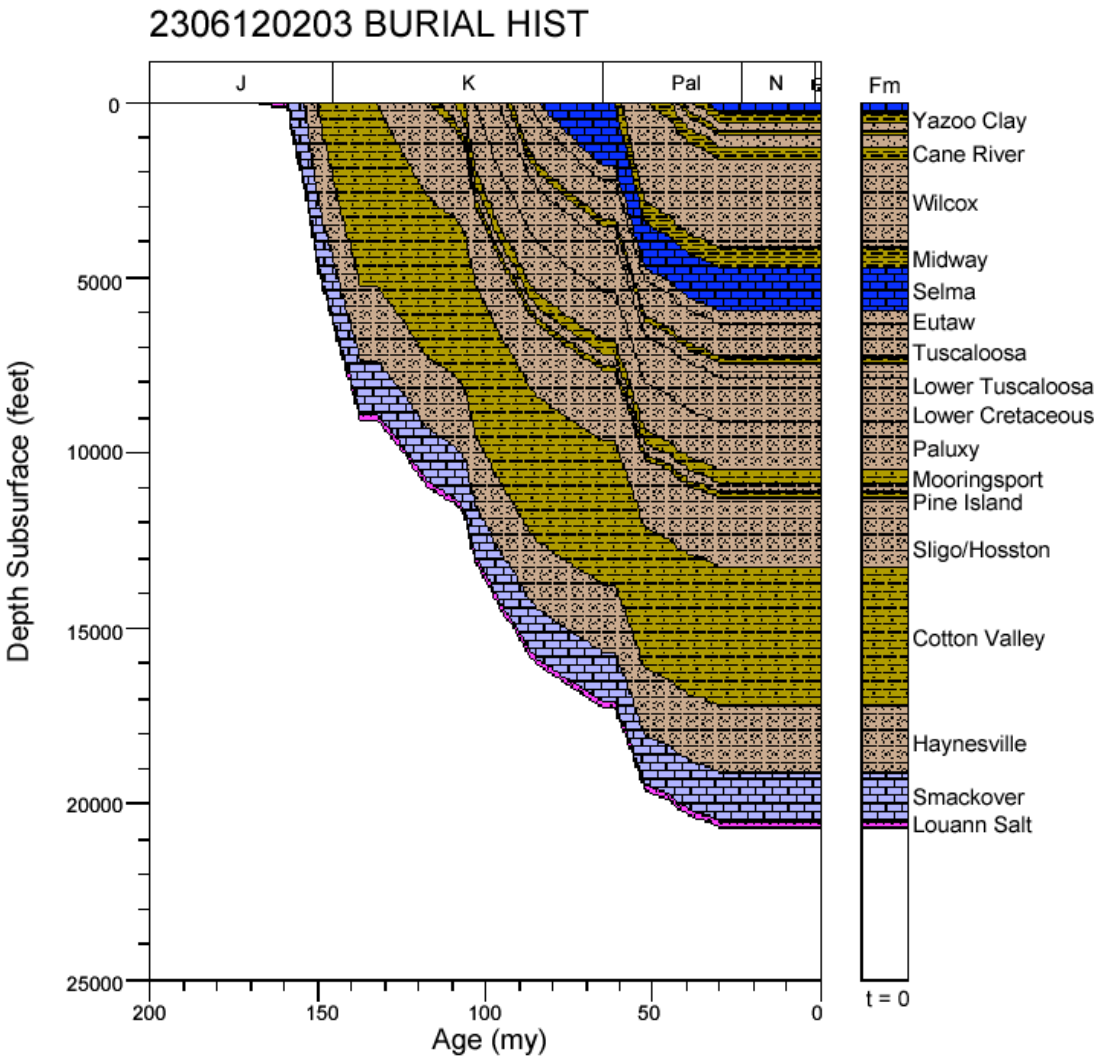


Figure 181. Burial history for well 2306120203, Mississippi Interior Salt Basin.

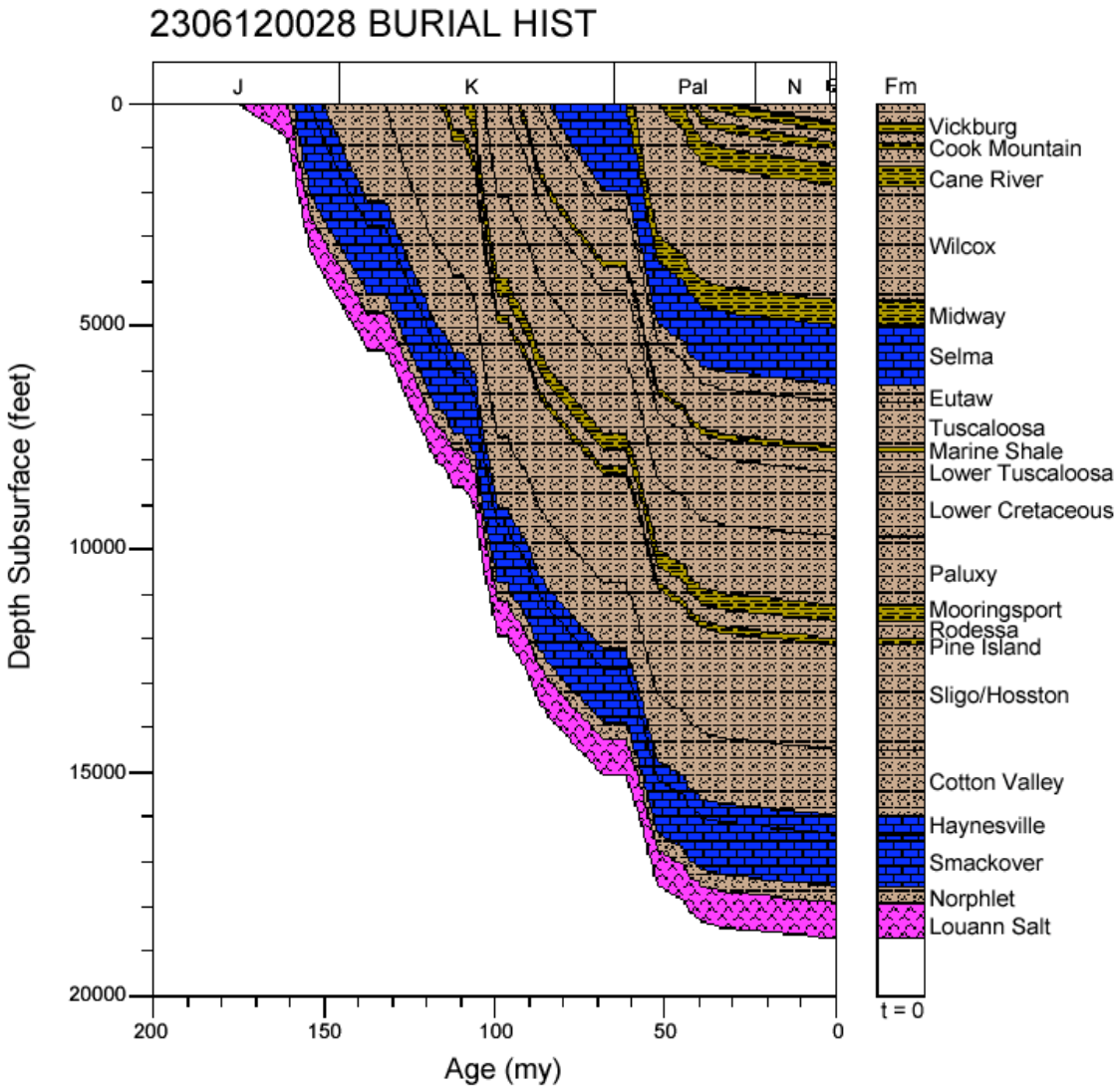


Figure 182. Burial history for well 2306120028, Mississippi Interior Salt Basin.

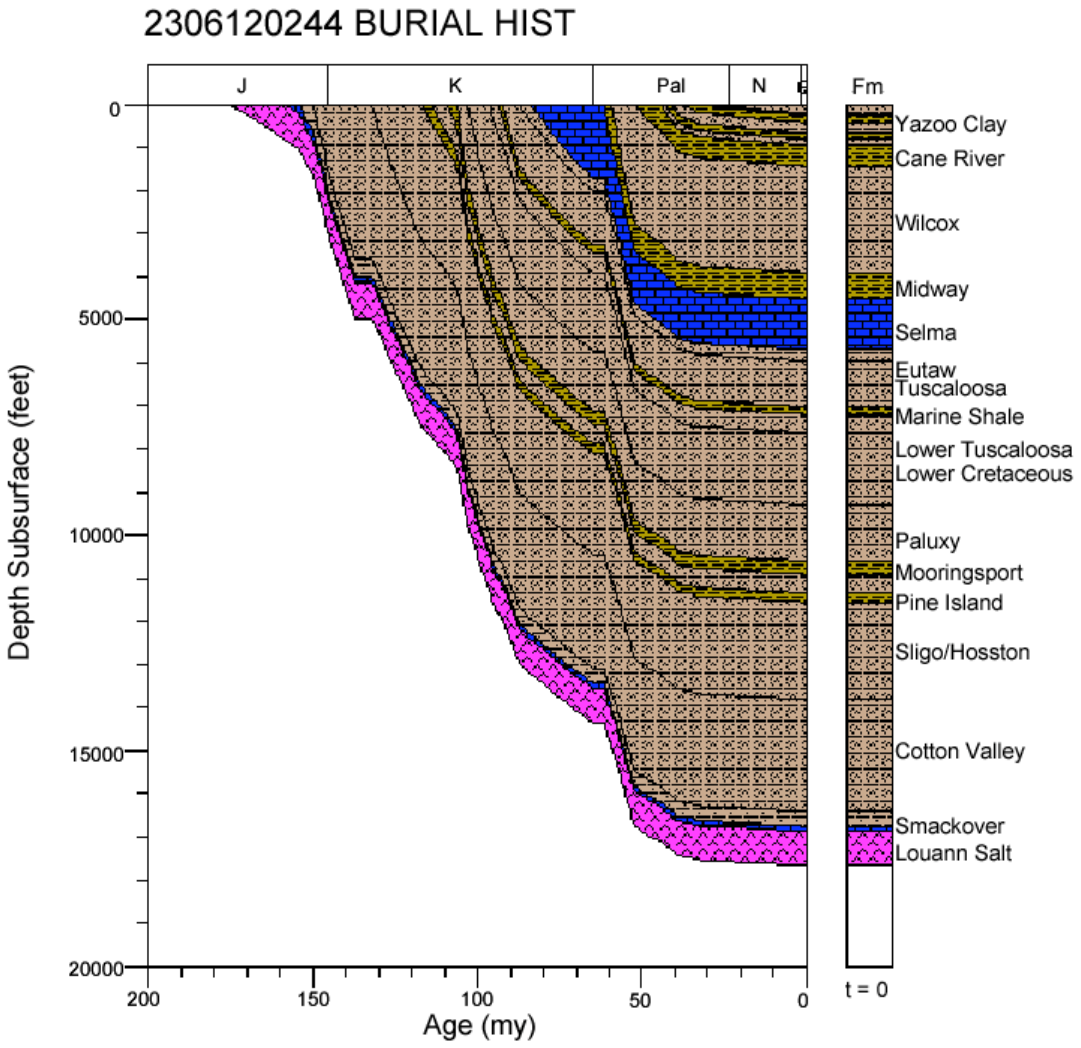


Figure 183. Burial history for well 2306120244, Mississippi Interior Salt Basin.

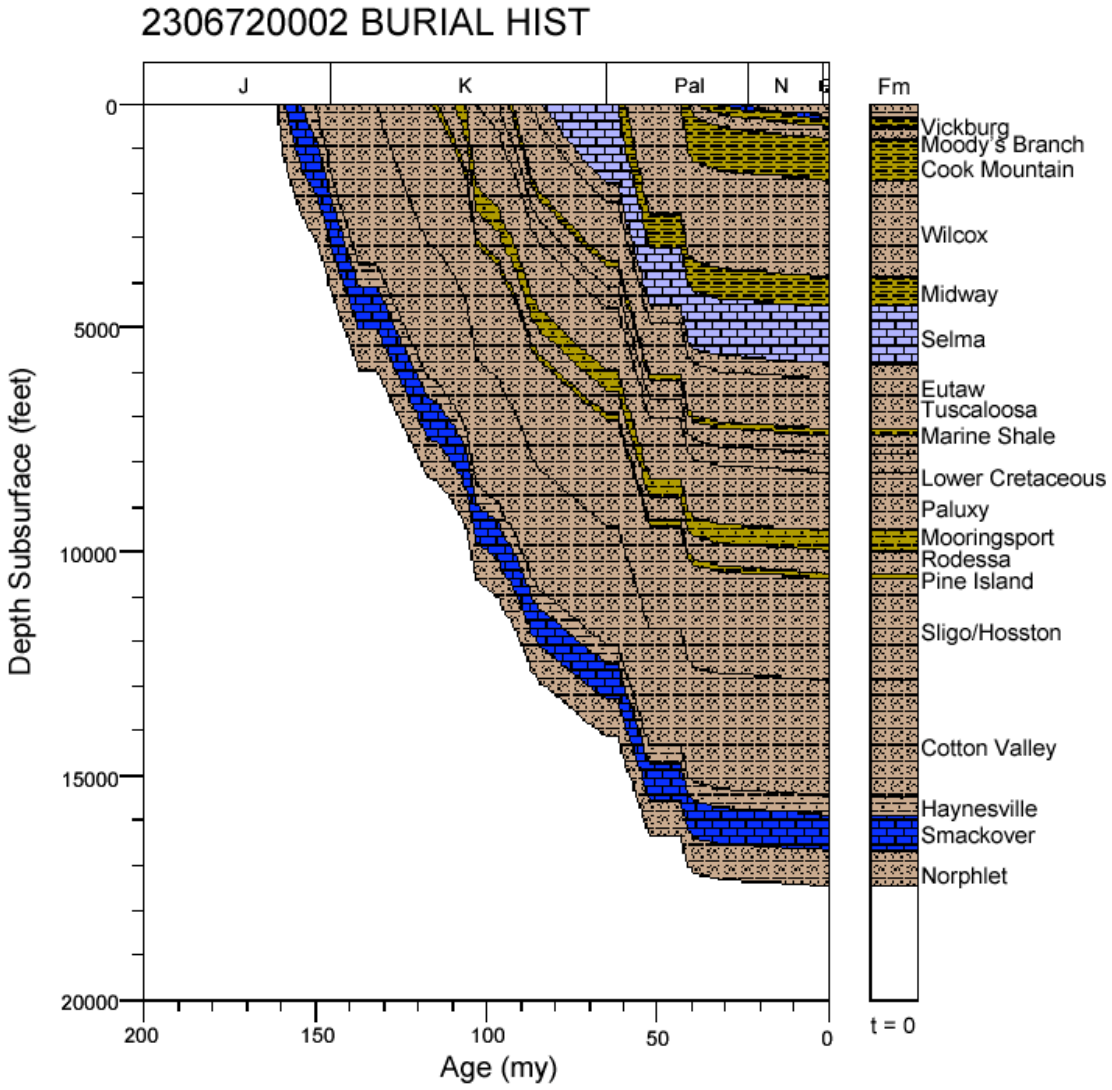


Figure 184. Burial history for well 2306720002, Mississippi Interior Salt Basin.

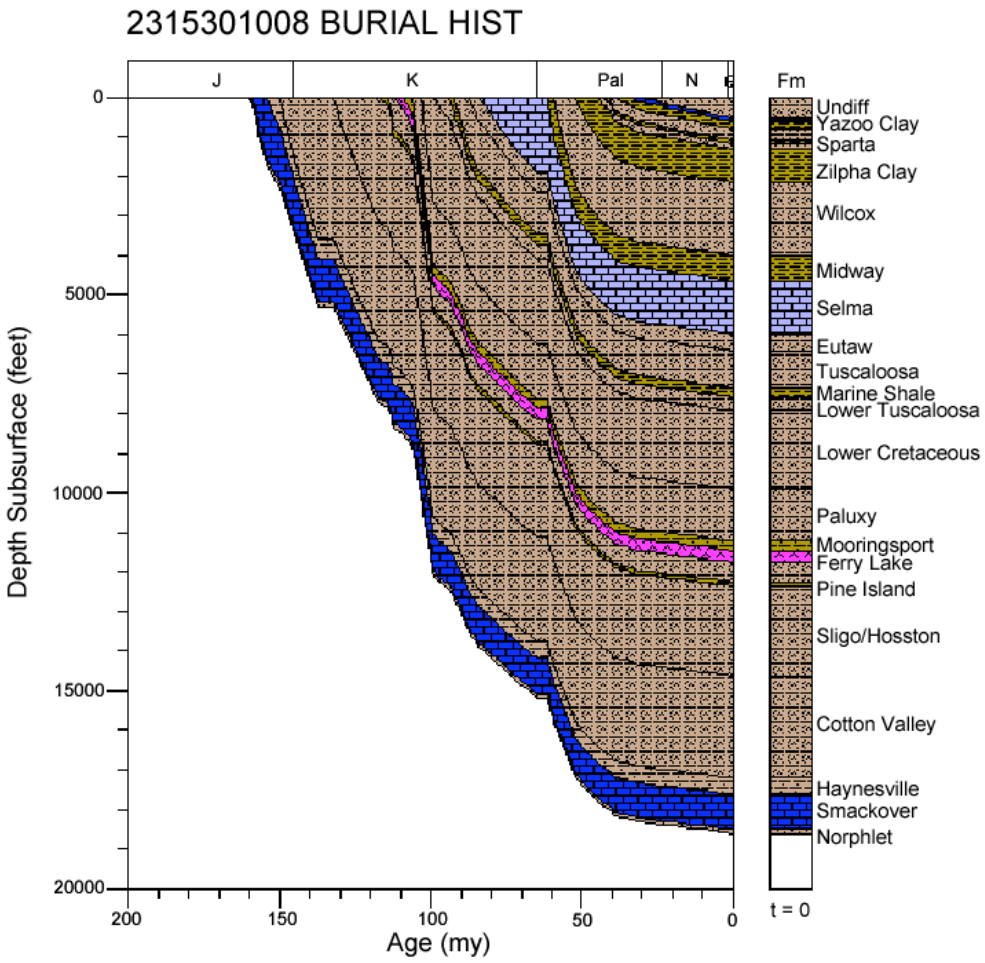


Figure 185. Burial history for well 2315301008, Mississippi Interior Salt Basin.

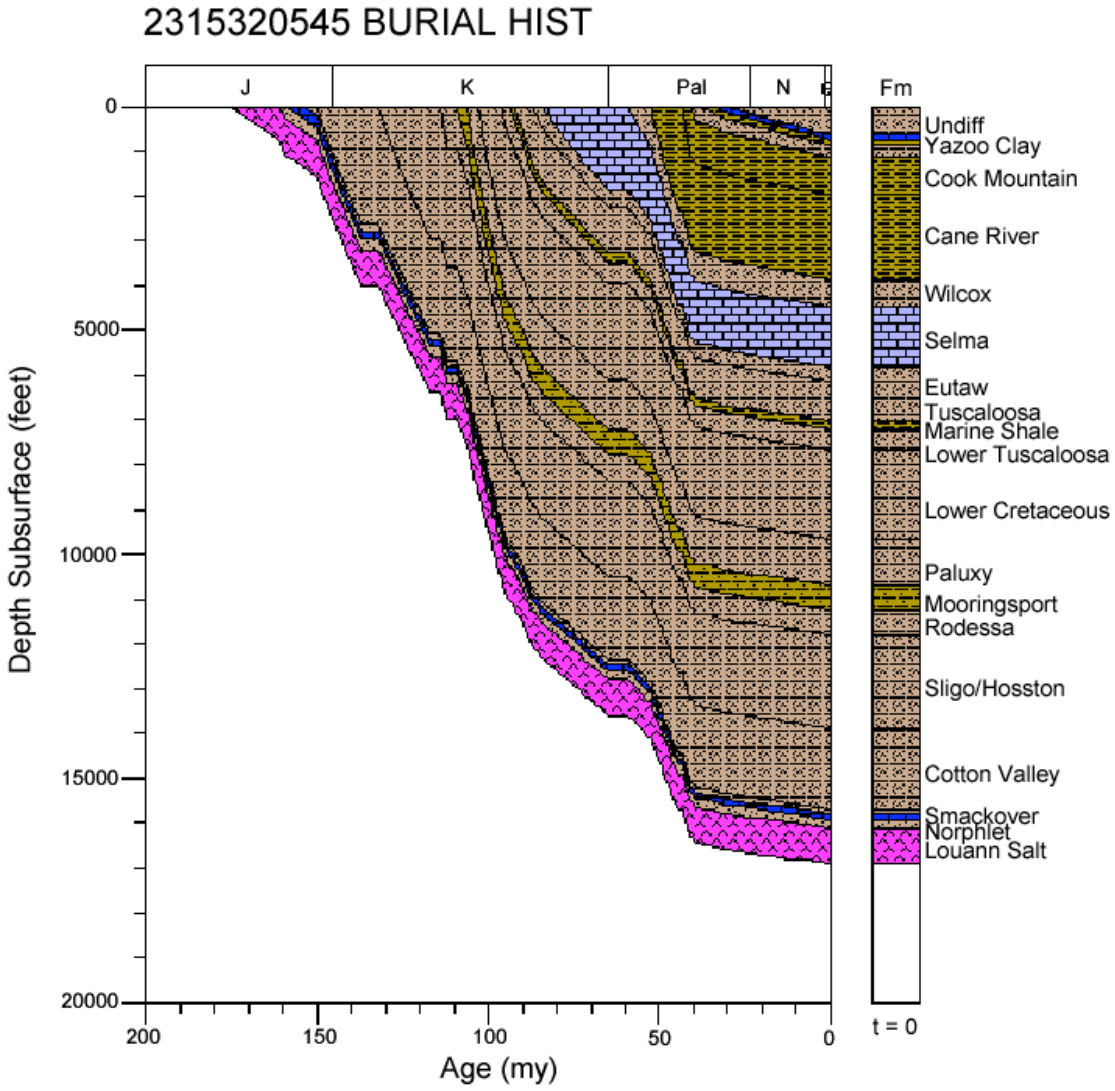


Figure 186. Burial history for well 2315320545, Mississippi Interior Salt Basin.

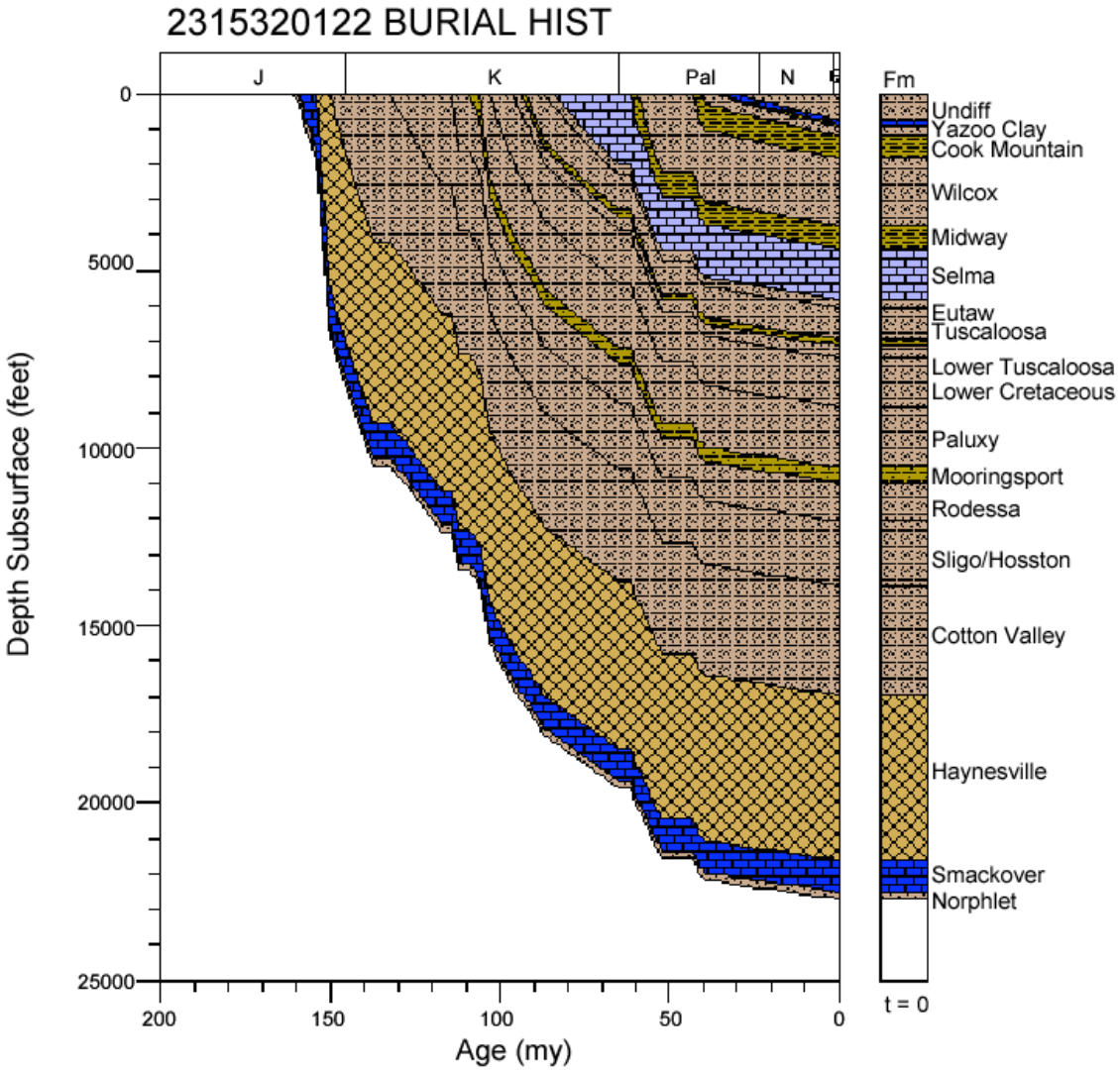


Figure 187. Burial history for well 2315320122, Mississippi Interior Salt Basin.

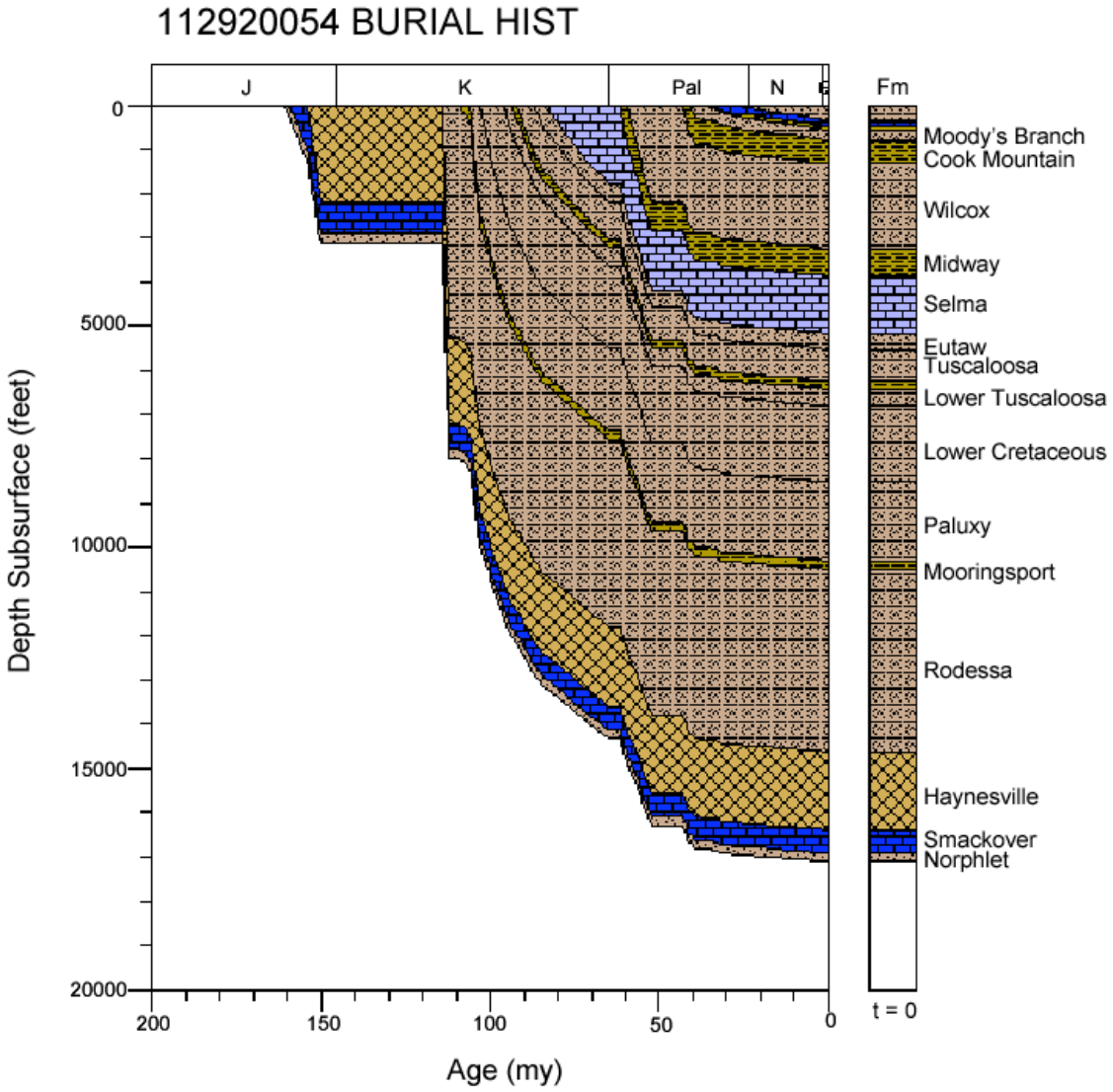


Figure 188. Burial history for well 112920054, Mississippi Interior Salt Basin.

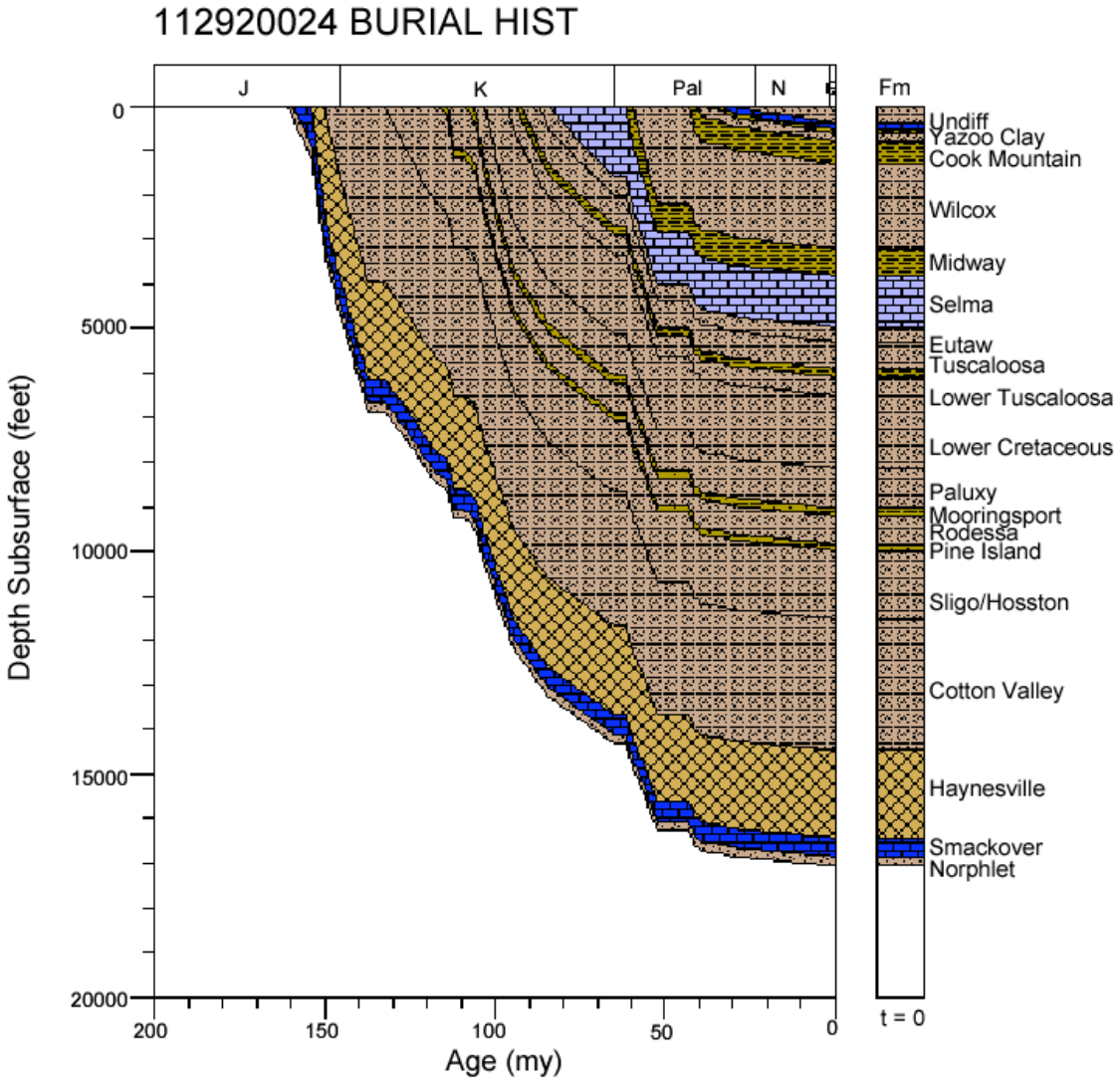


Figure 189. Burial history for well 112920024, Mississippi Interior Salt Basin.

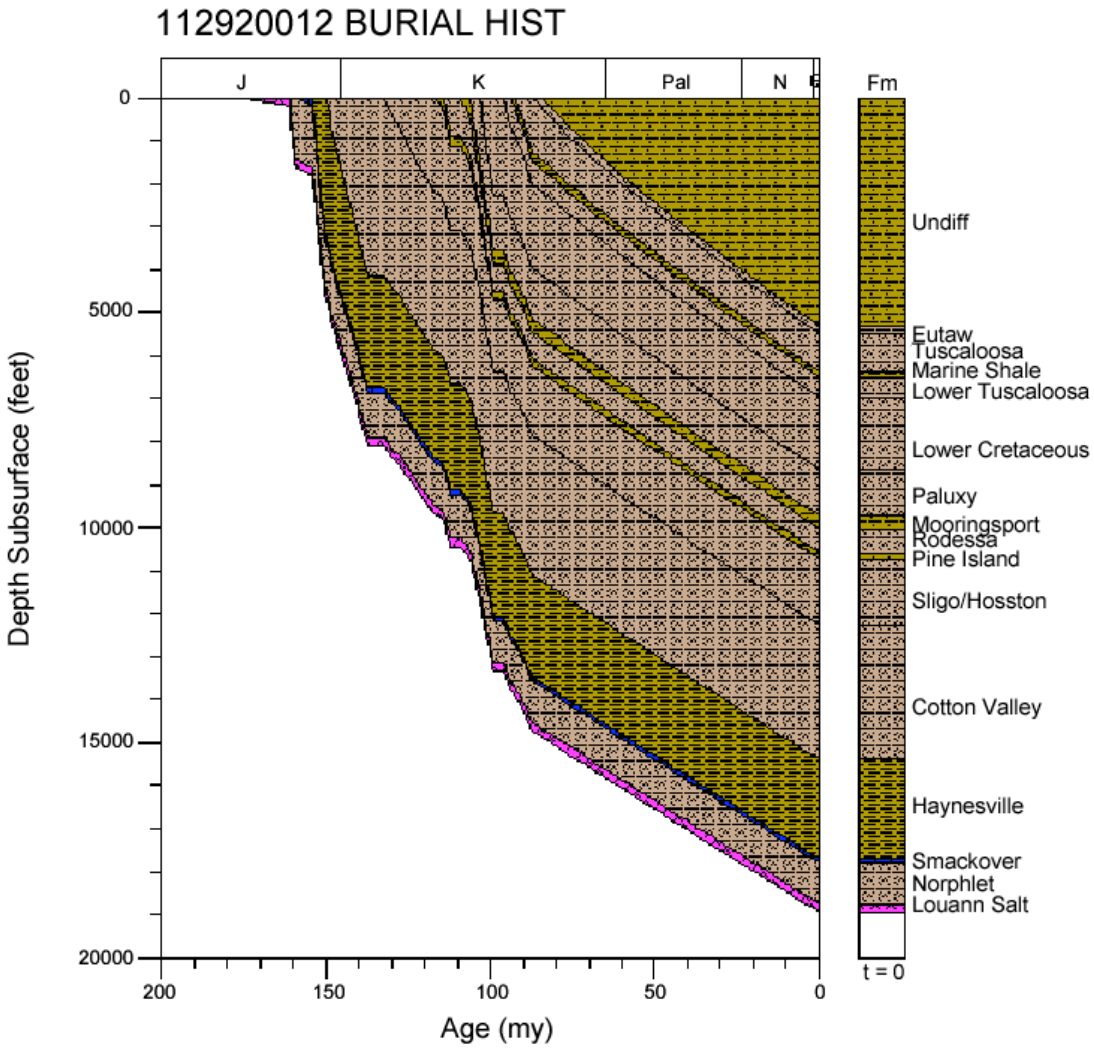


Figure 190. Burial history for well 112920012, Mississippi Interior Salt Basin.

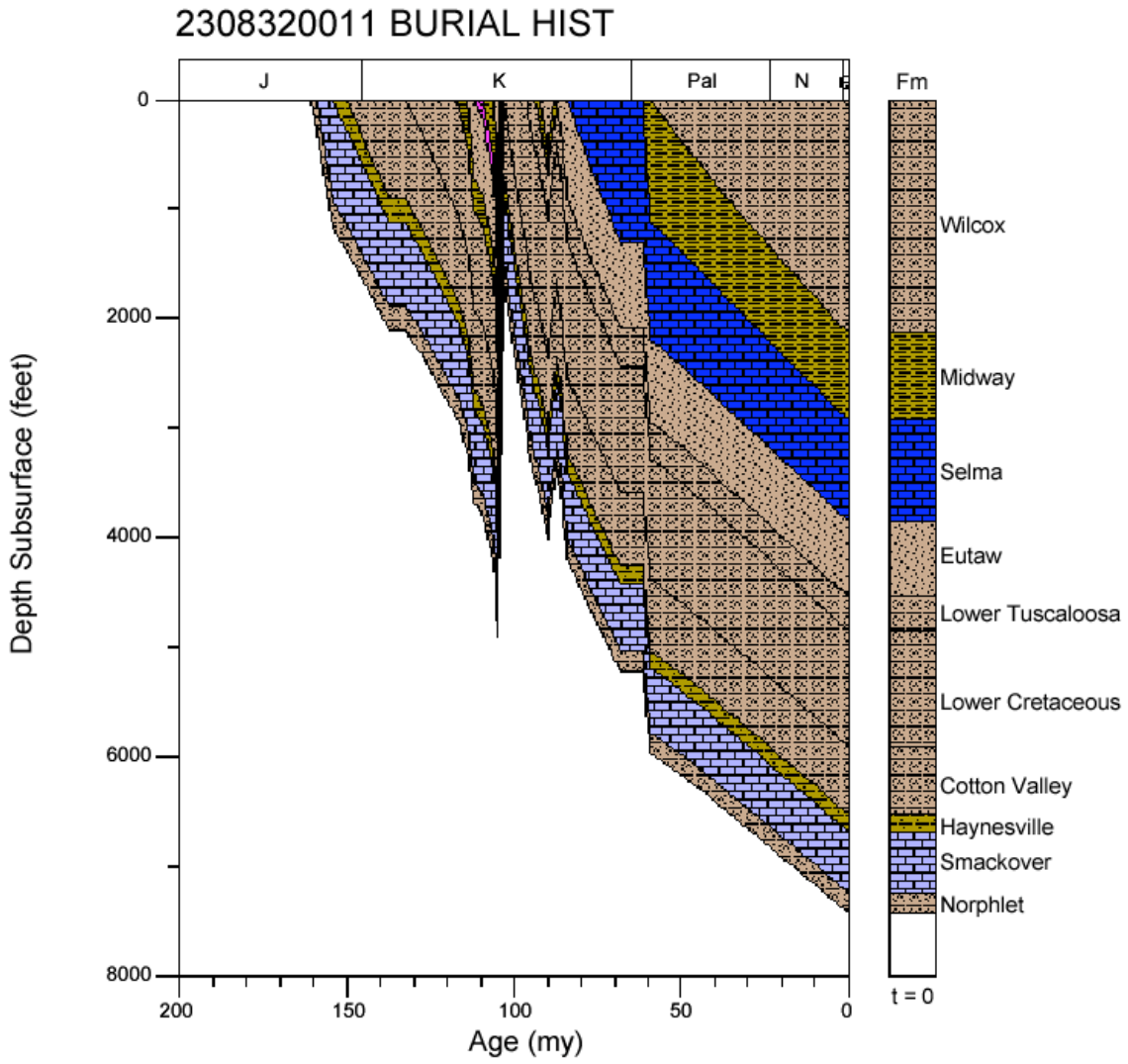


Figure 191. Burial history for well 2308320011, Mississippi Interior Salt Basin.

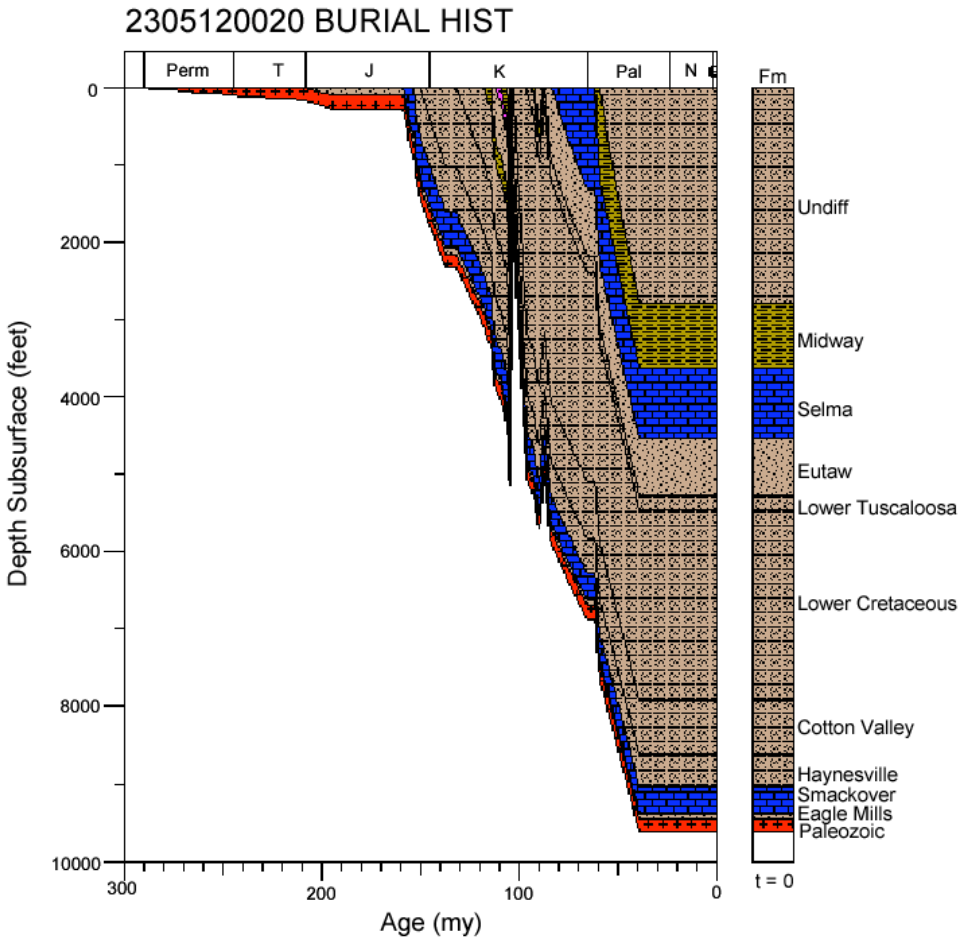


Figure 192. Burial history for well 2305120020, Mississippi Interior Salt Basin.

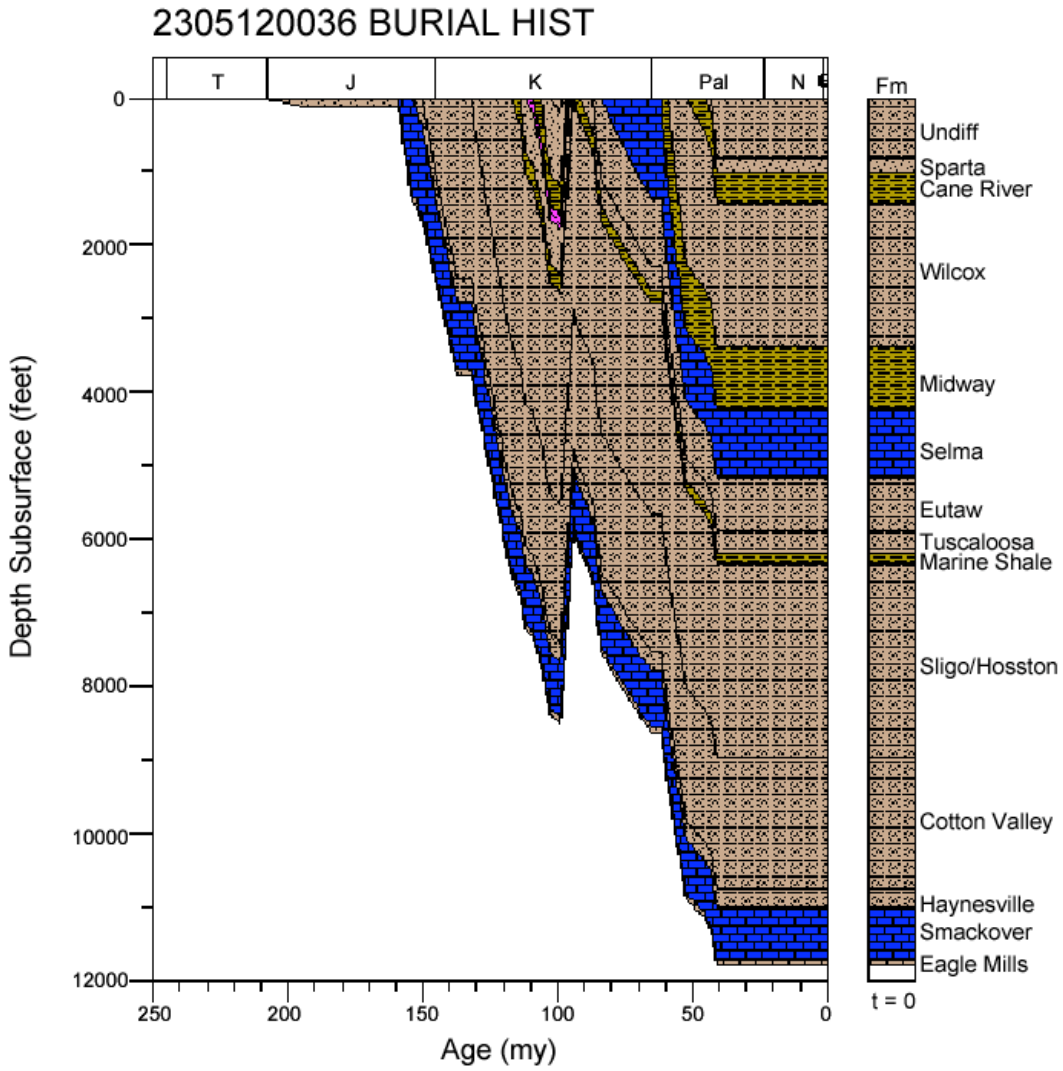


Figure 193. Burial history for well 2305120036, Mississippi Interior Salt Basin.

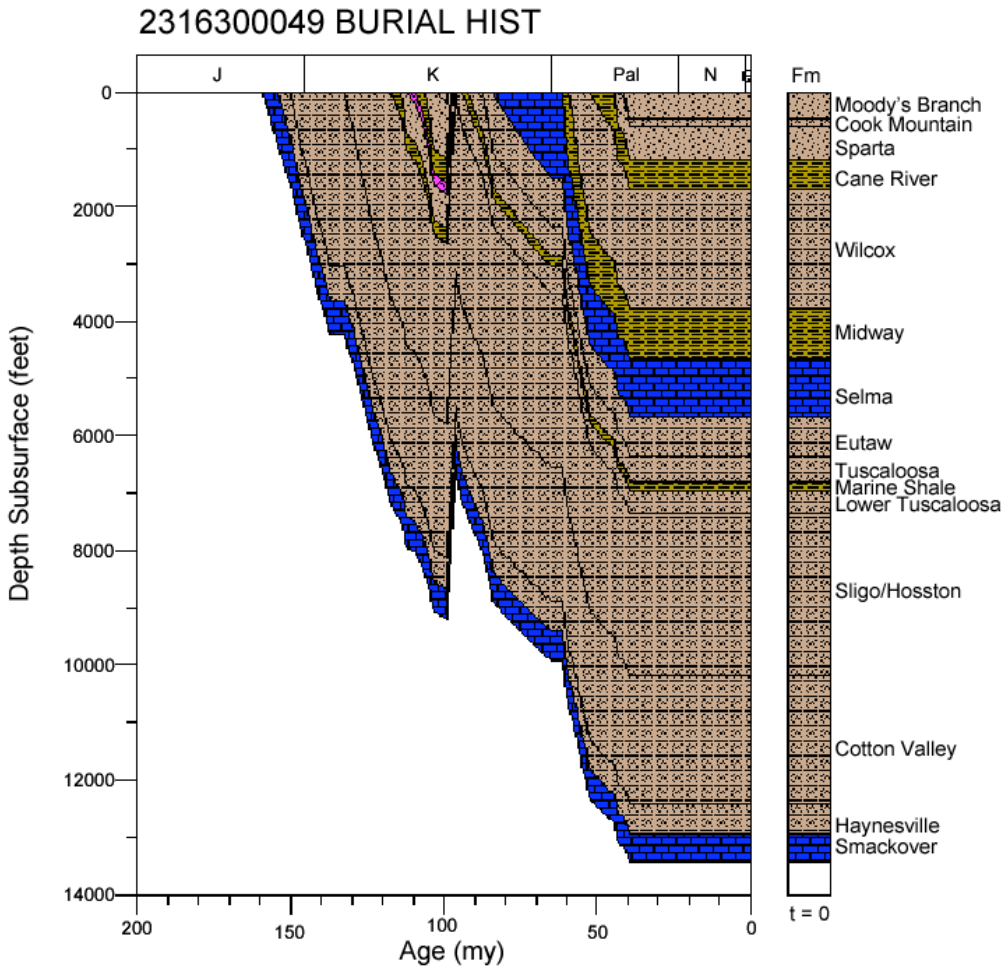


Figure 194. Burial history for well 2316300049, Mississippi Interior Salt Basin.

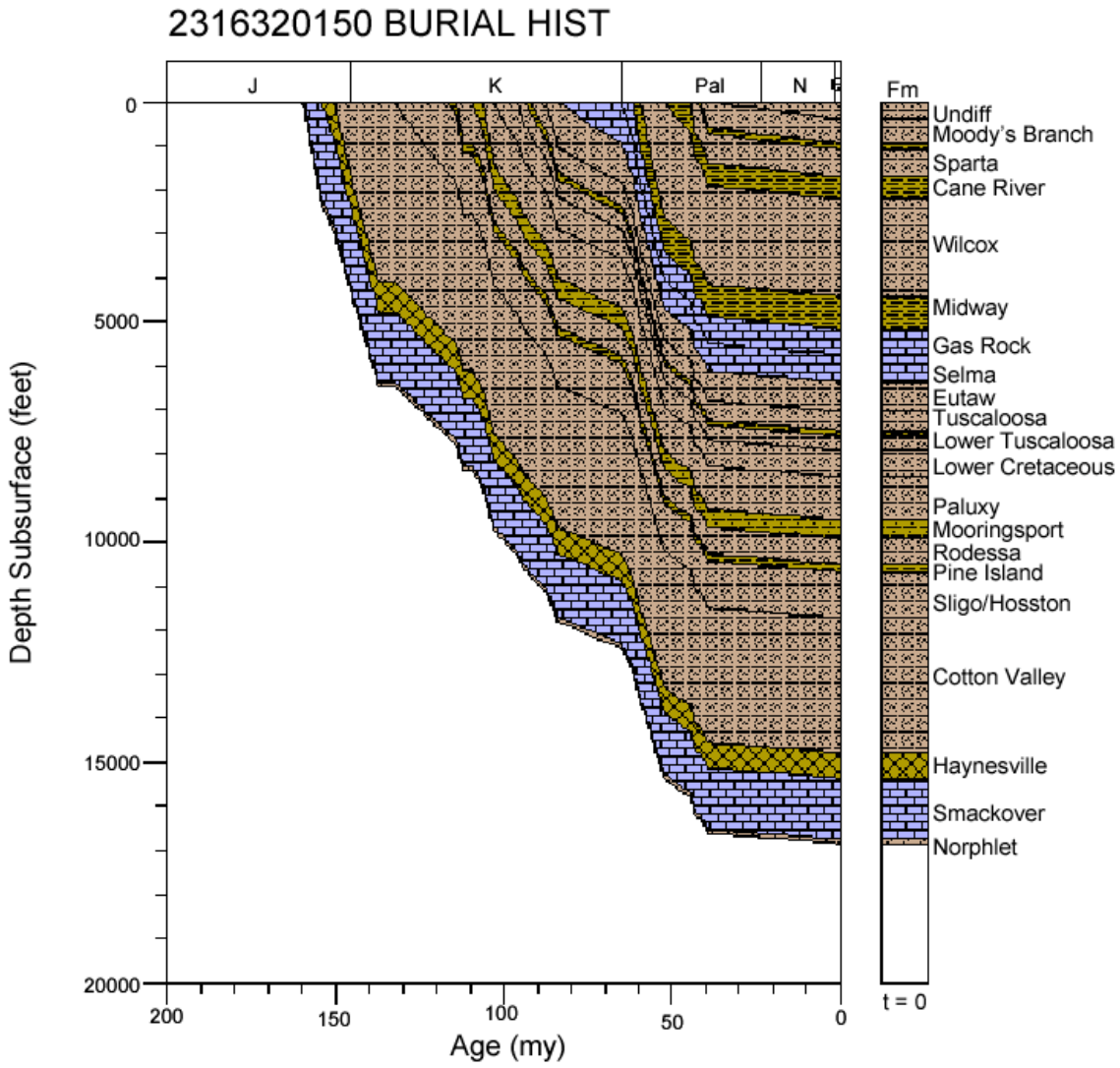


Figure 195. Burial history for well 2316320150, Mississippi Interior Salt Basin.

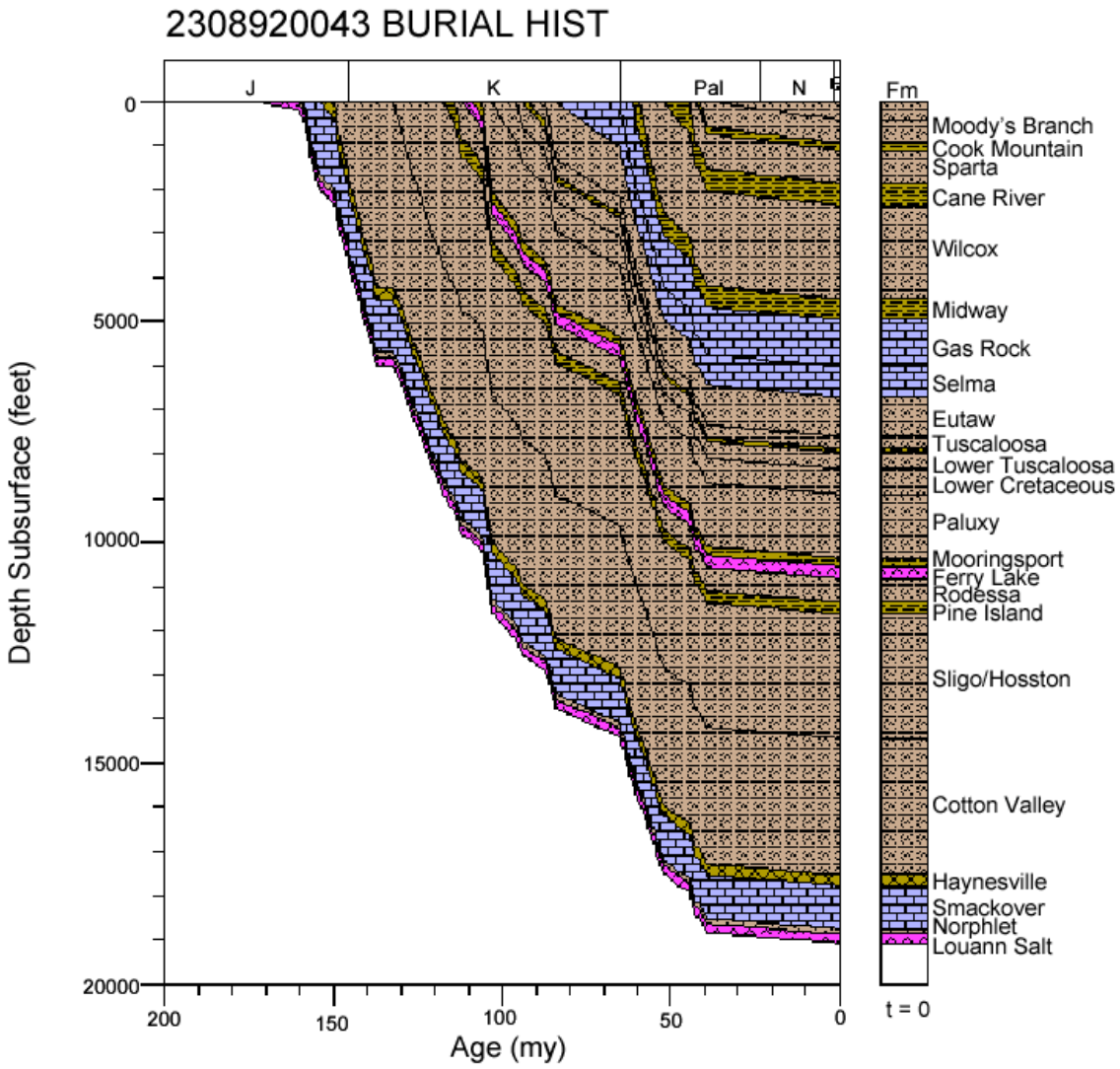


Figure 196. Burial history for well 2308920043, Mississippi Interior Salt Basin.

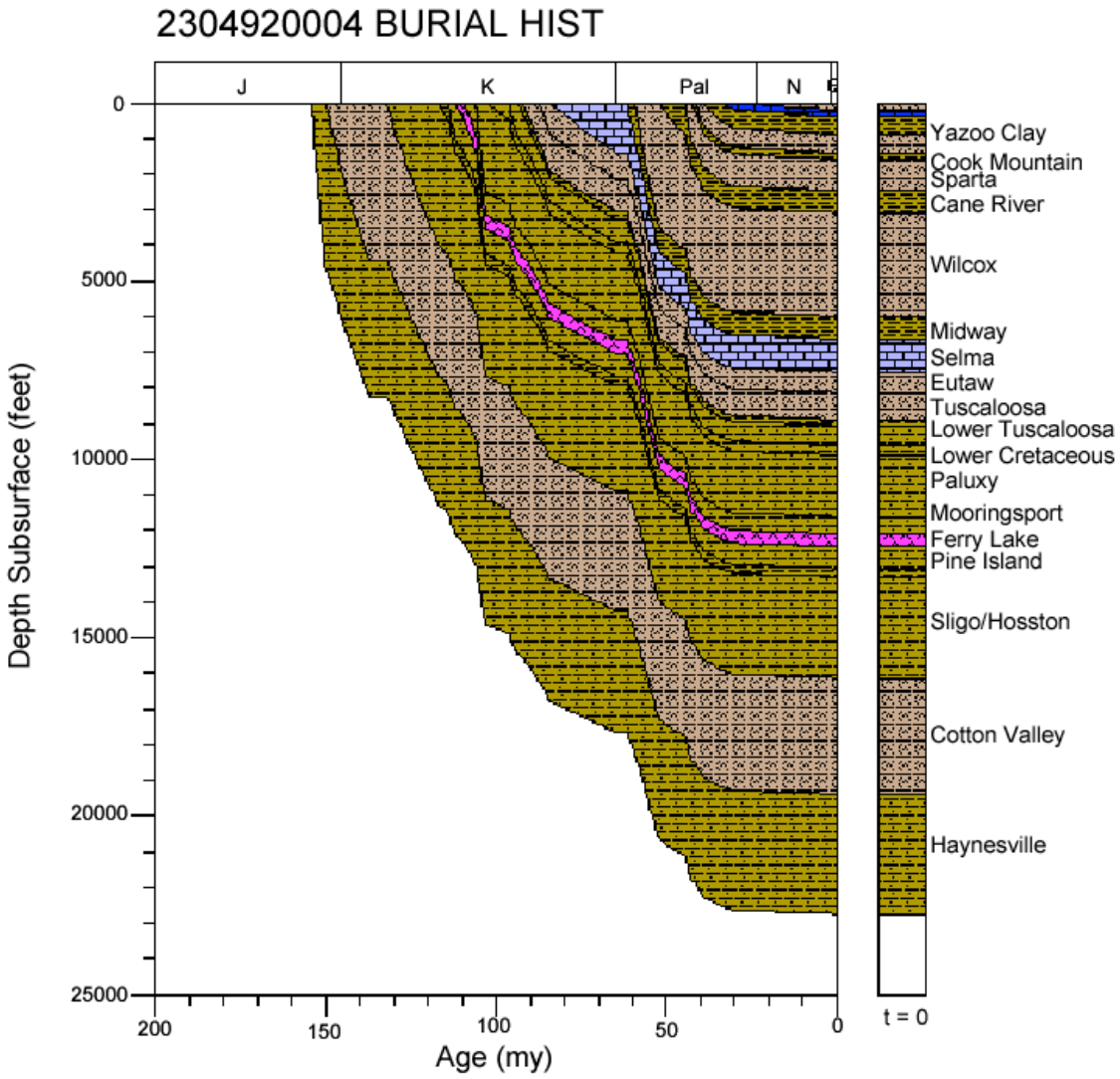


Figure 197. Burial history for well 2304920004, Mississippi Interior Salt Basin.

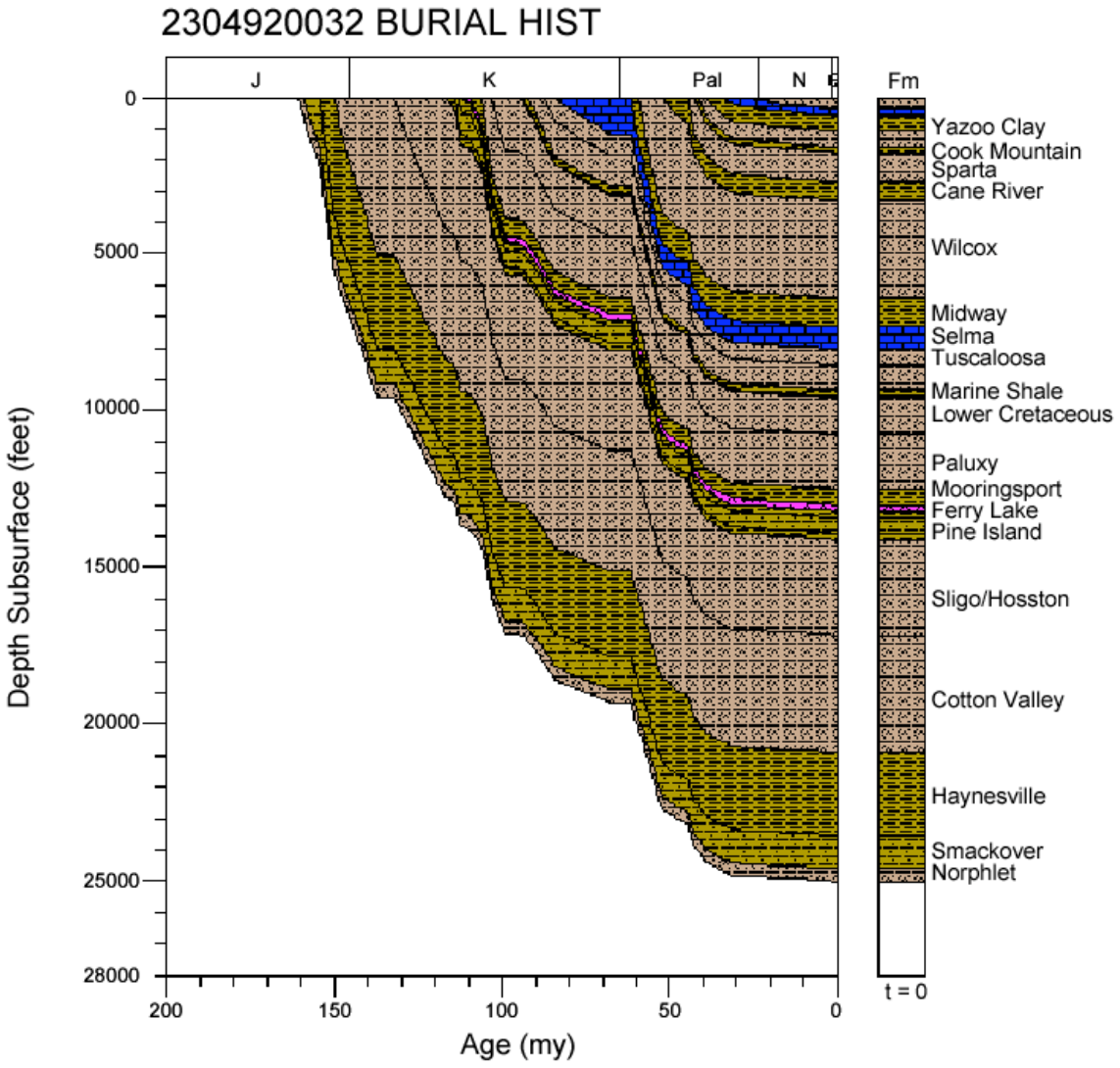


Figure 198. Burial history for well 2304920032, Mississippi Interior Salt Basin.

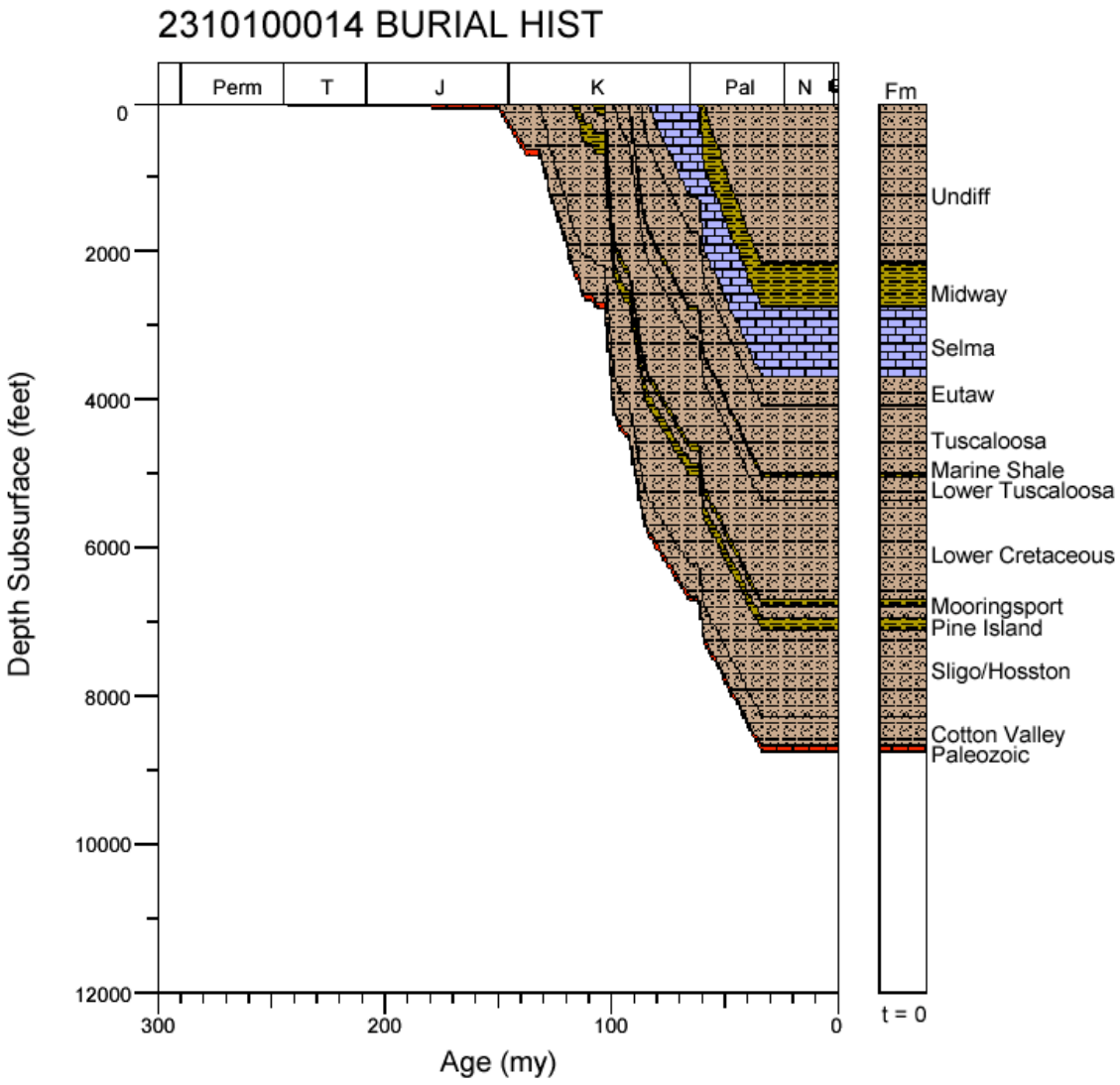


Figure 199. Burial history for well 2310100014, Mississippi Interior Salt Basin.

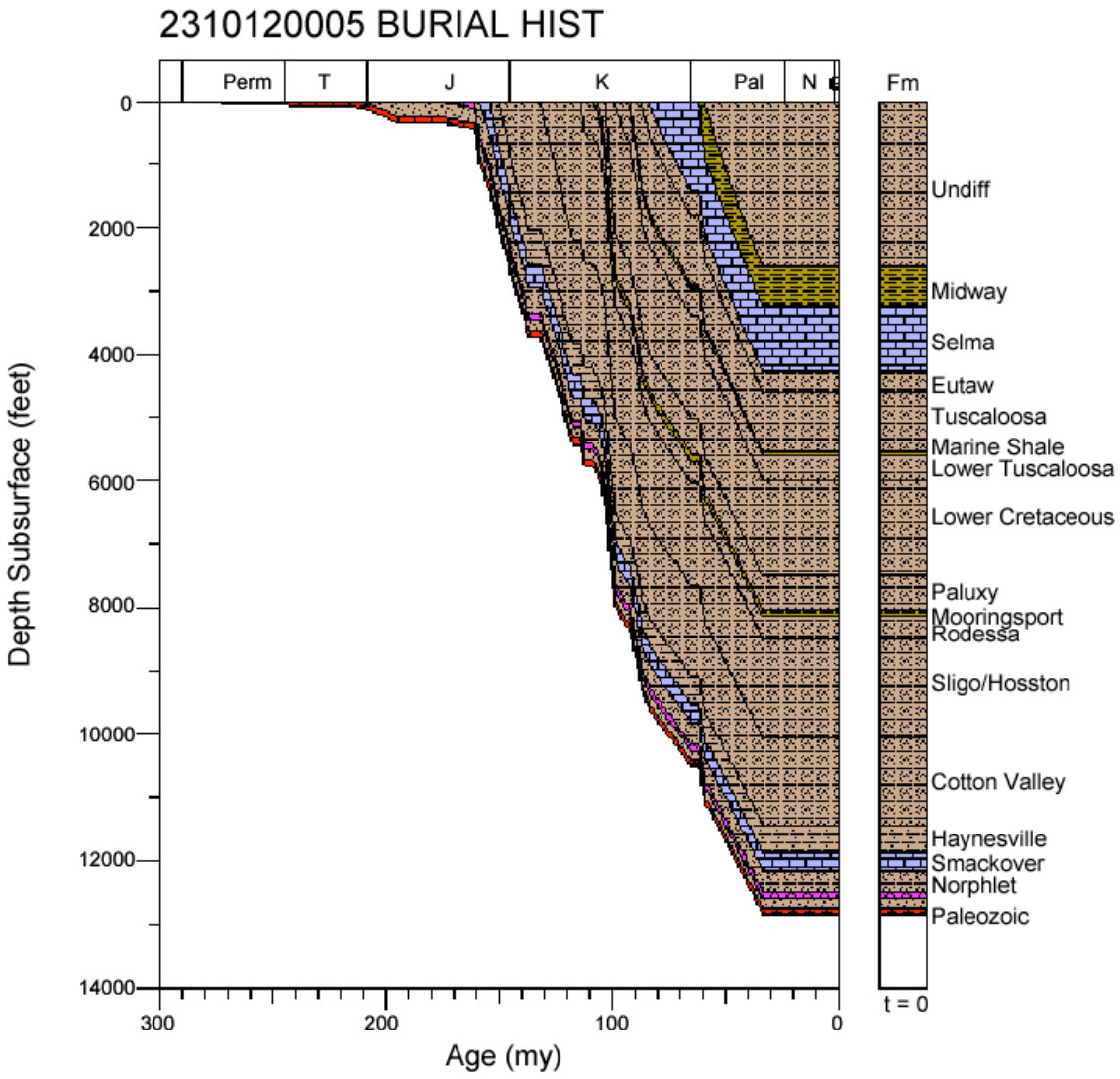


Figure 200. Burial history for well 2310120005, Mississippi Interior Salt Basin.

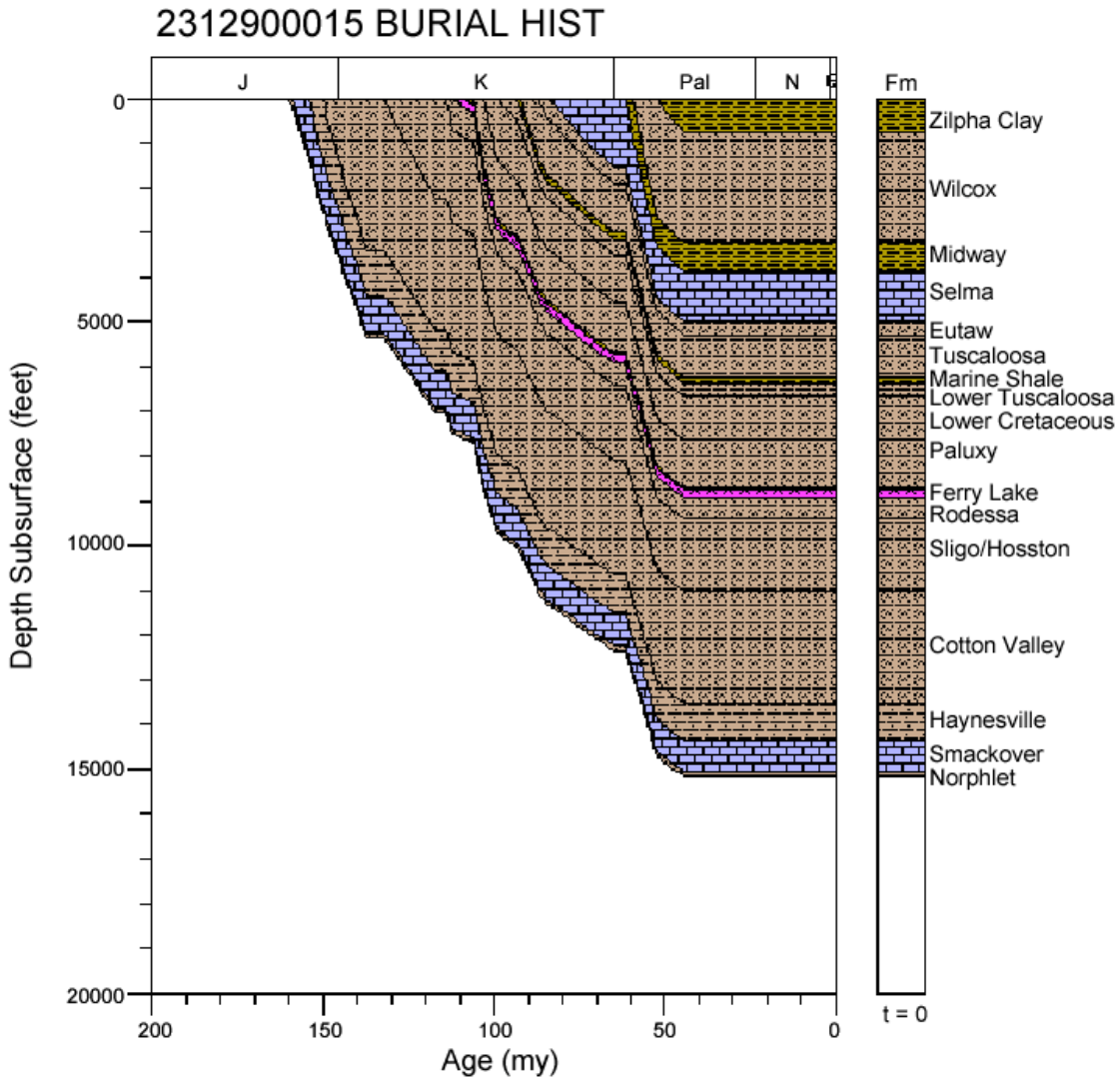


Figure 201. Burial history for well 2312900015, Mississippi Interior Salt Basin.

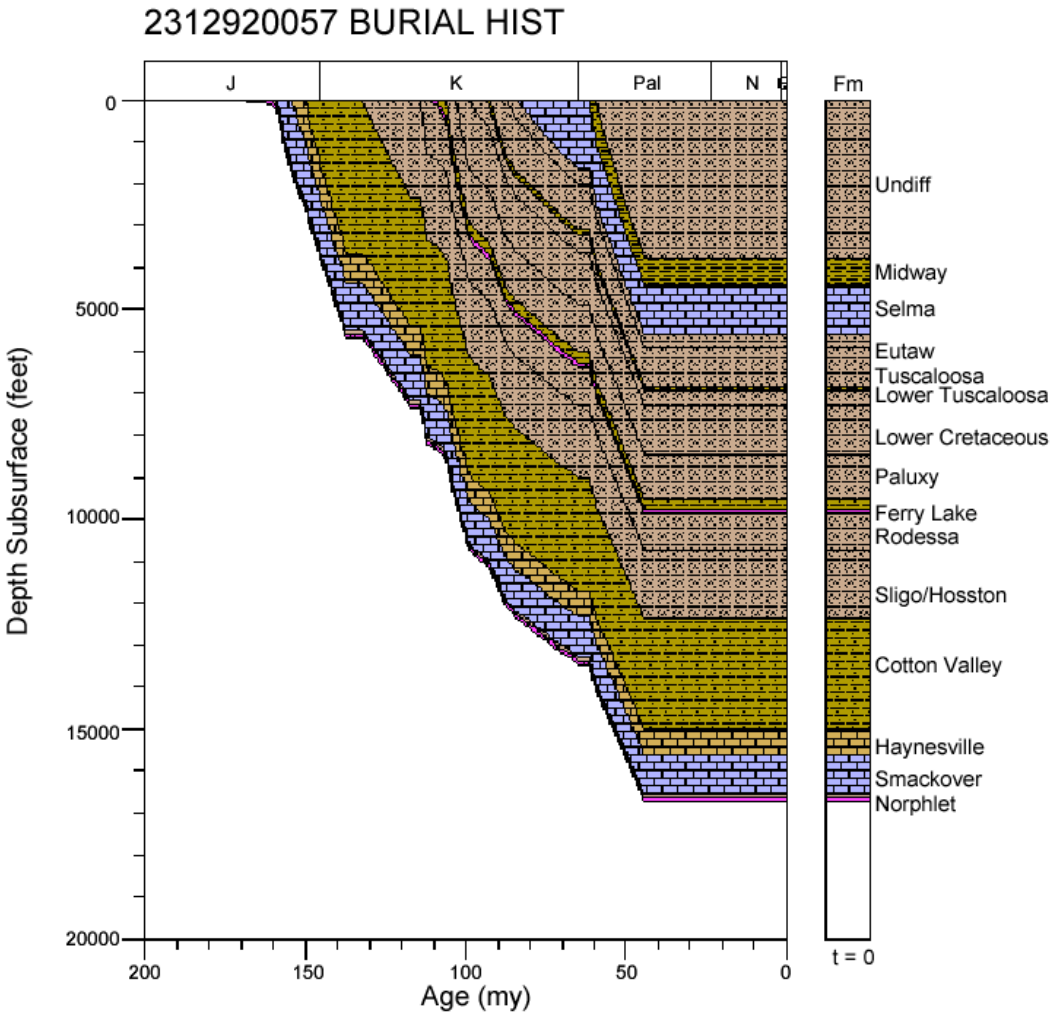


Figure 202. Burial history for well 2312920057, Mississippi Interior Salt Basin.

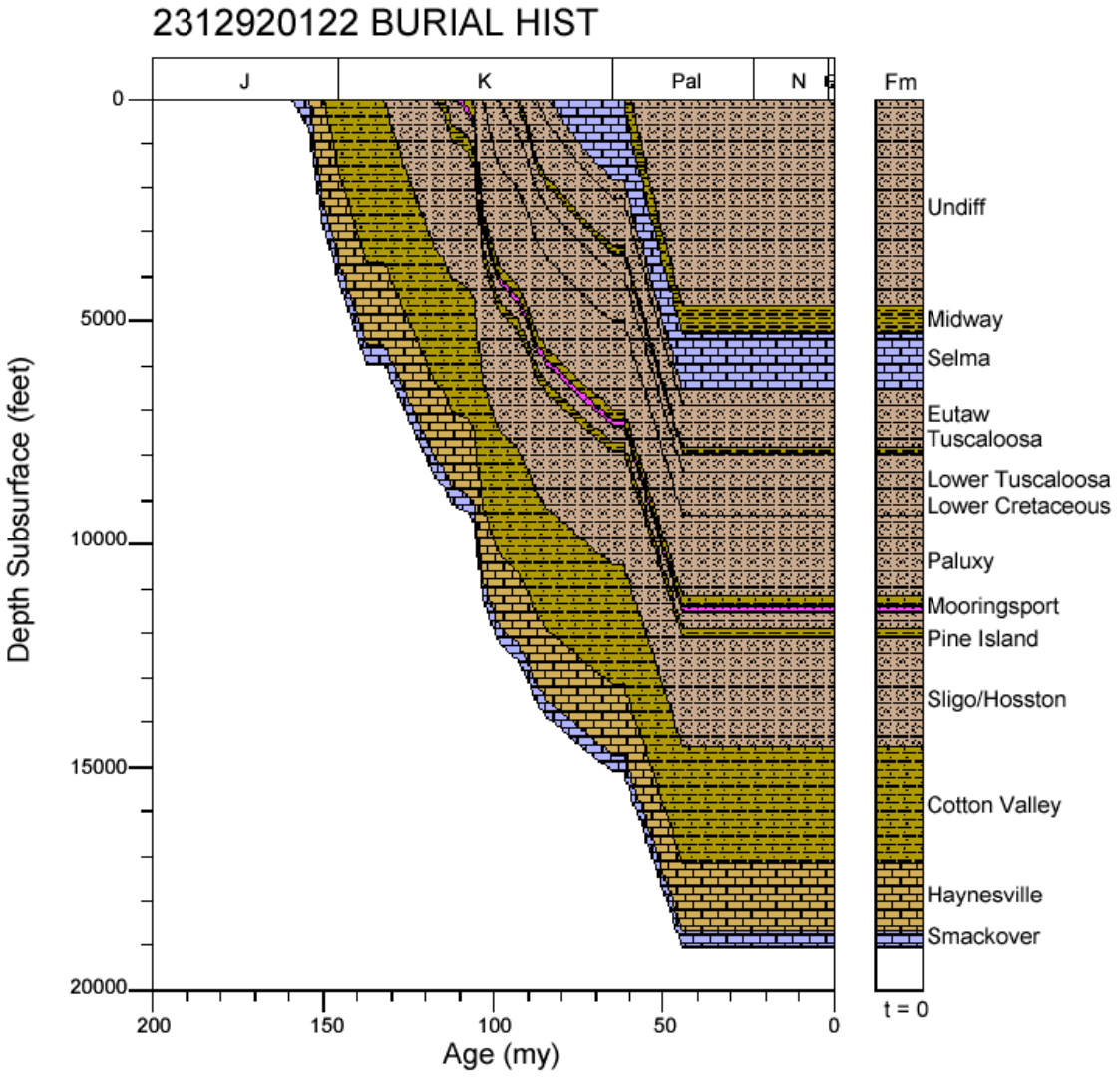


Figure 203. Burial history for well 2312920122, Mississippi Interior Salt Basin.

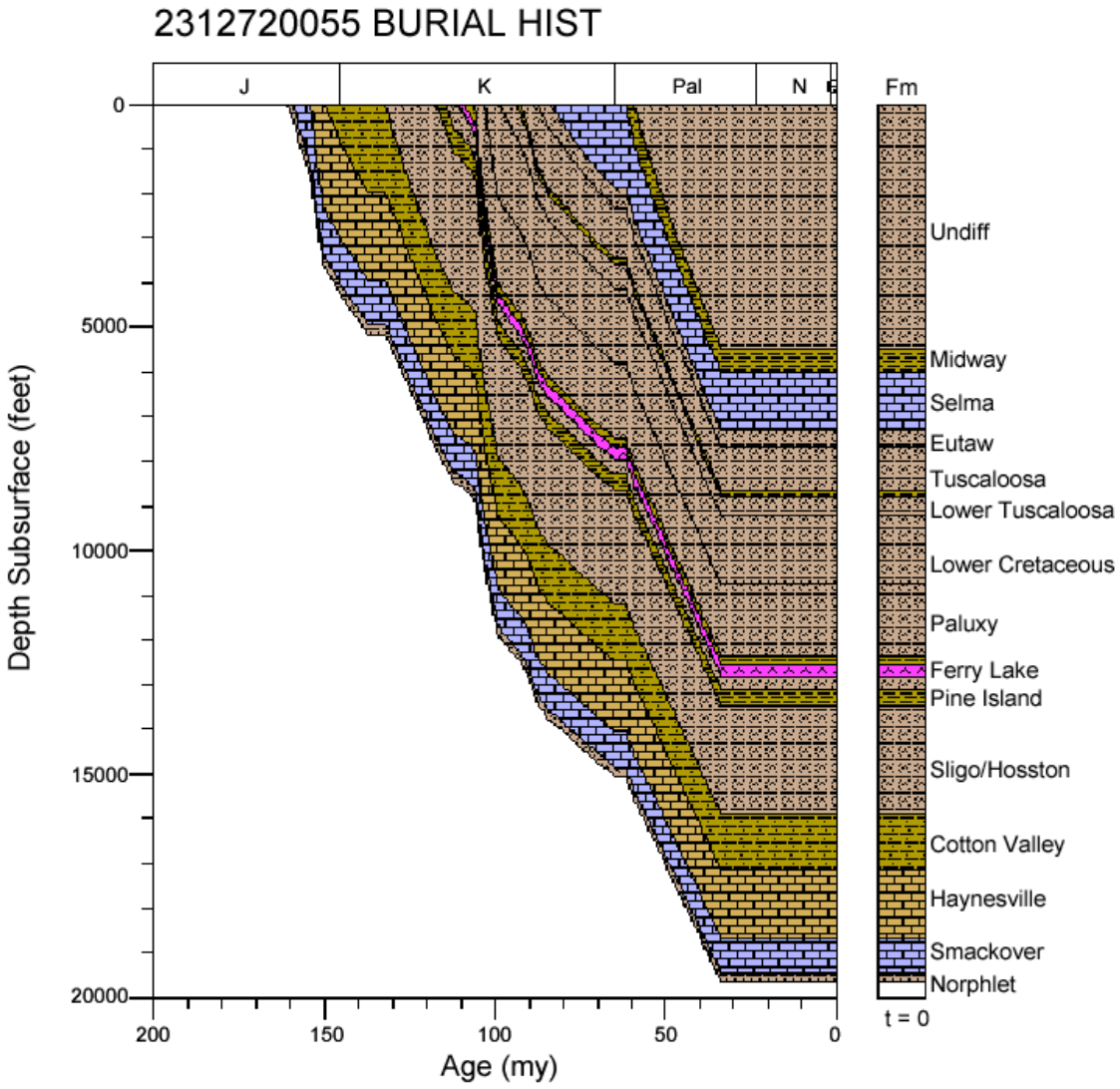


Figure 204. Burial history for well 2312720055, Mississippi Interior Salt Basin.

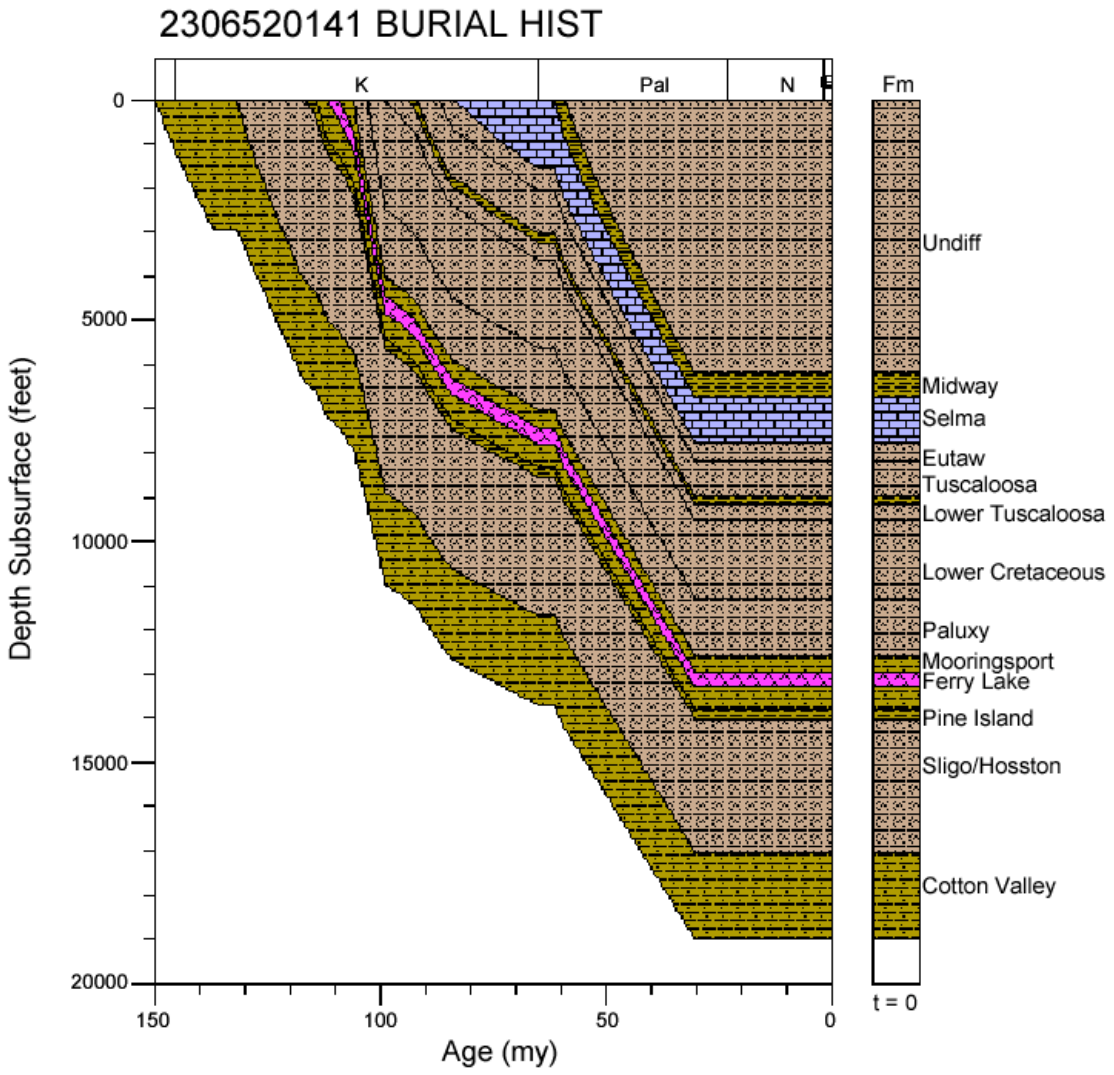


Figure 205. Burial history for well 2306520141, Mississippi Interior Salt Basin.

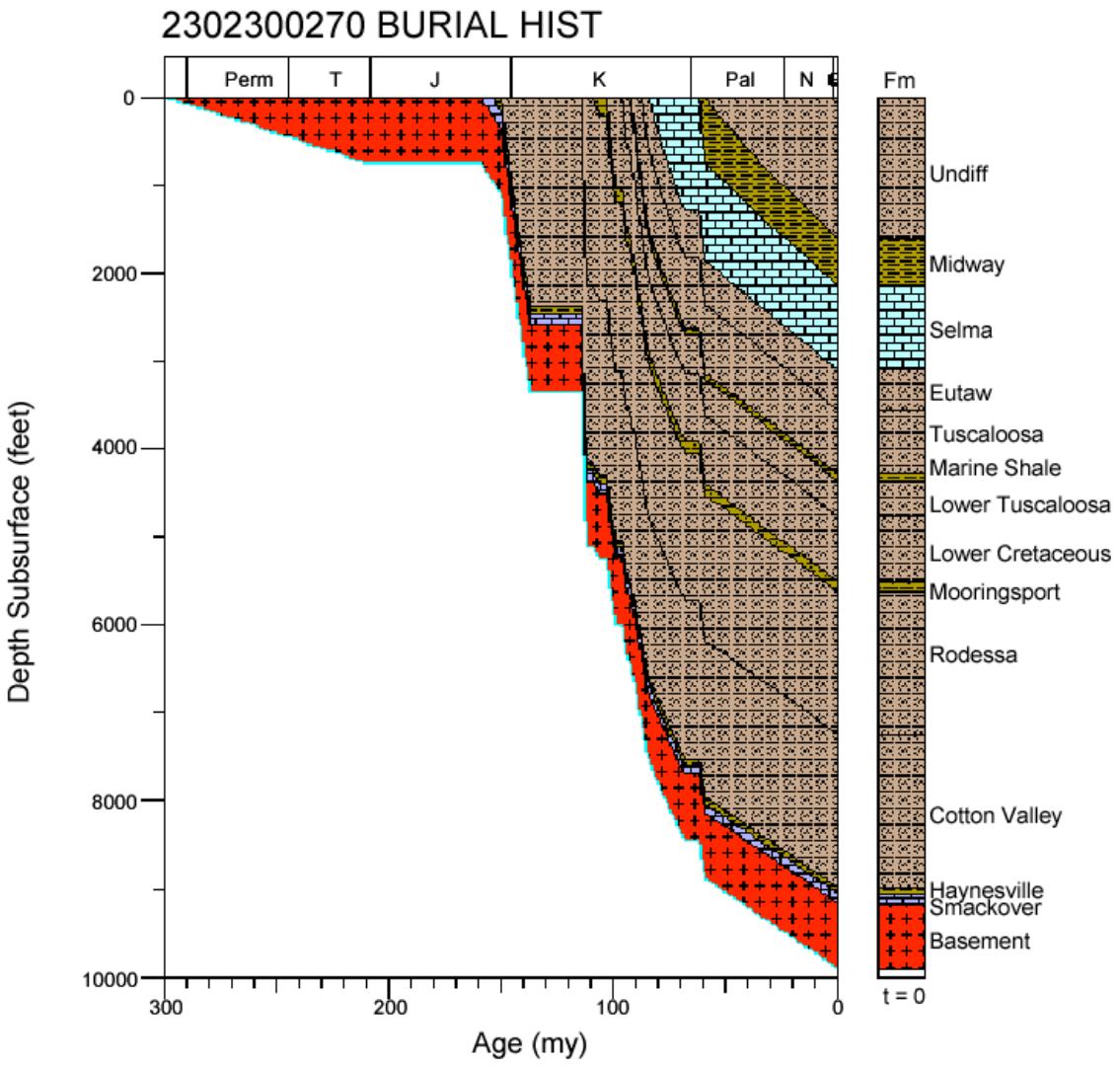


Figure 206. Burial history for well 2302300270, Mississippi Interior Salt Basin.

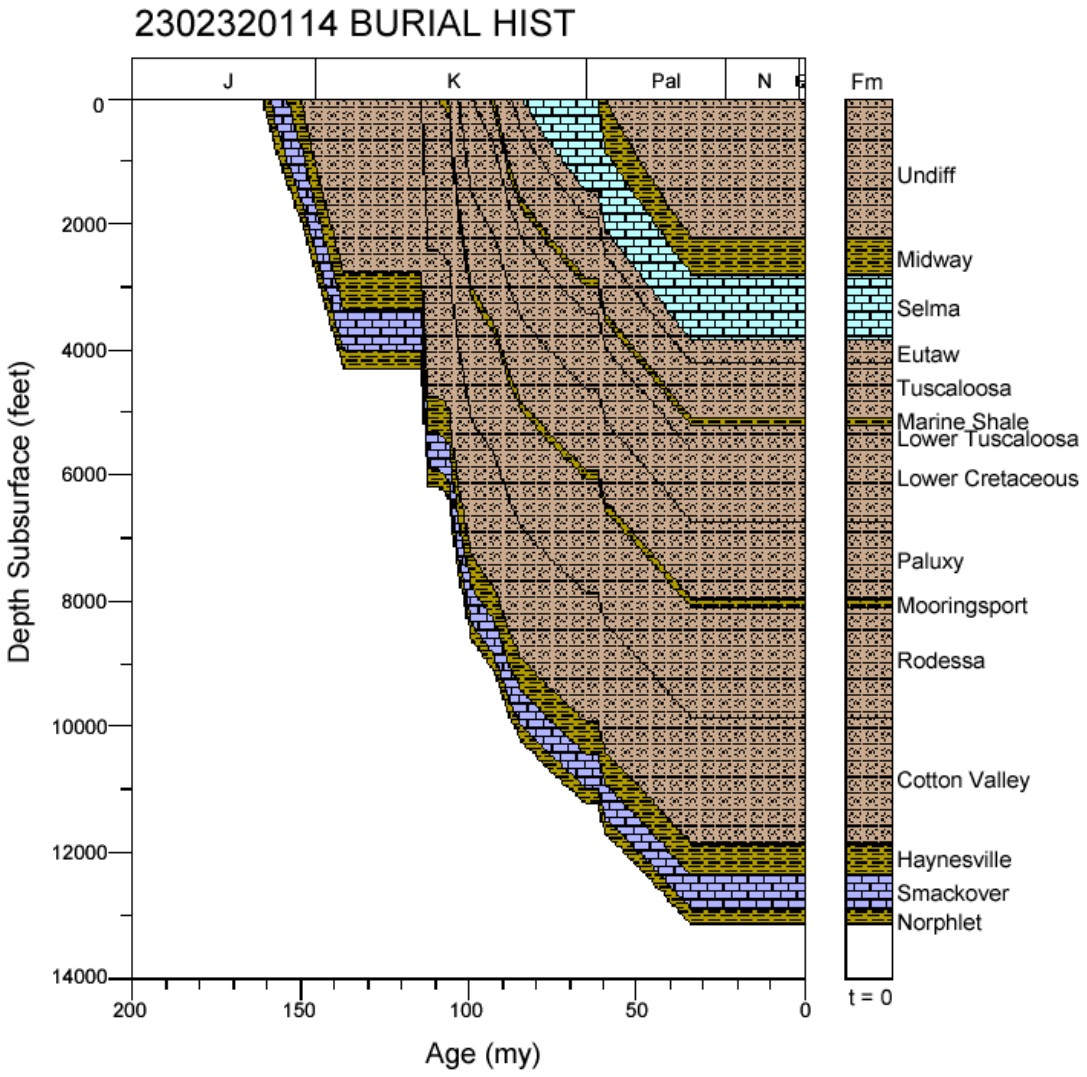


Figure 207. Burial history for well 2302320114, Mississippi Interior Salt Basin.

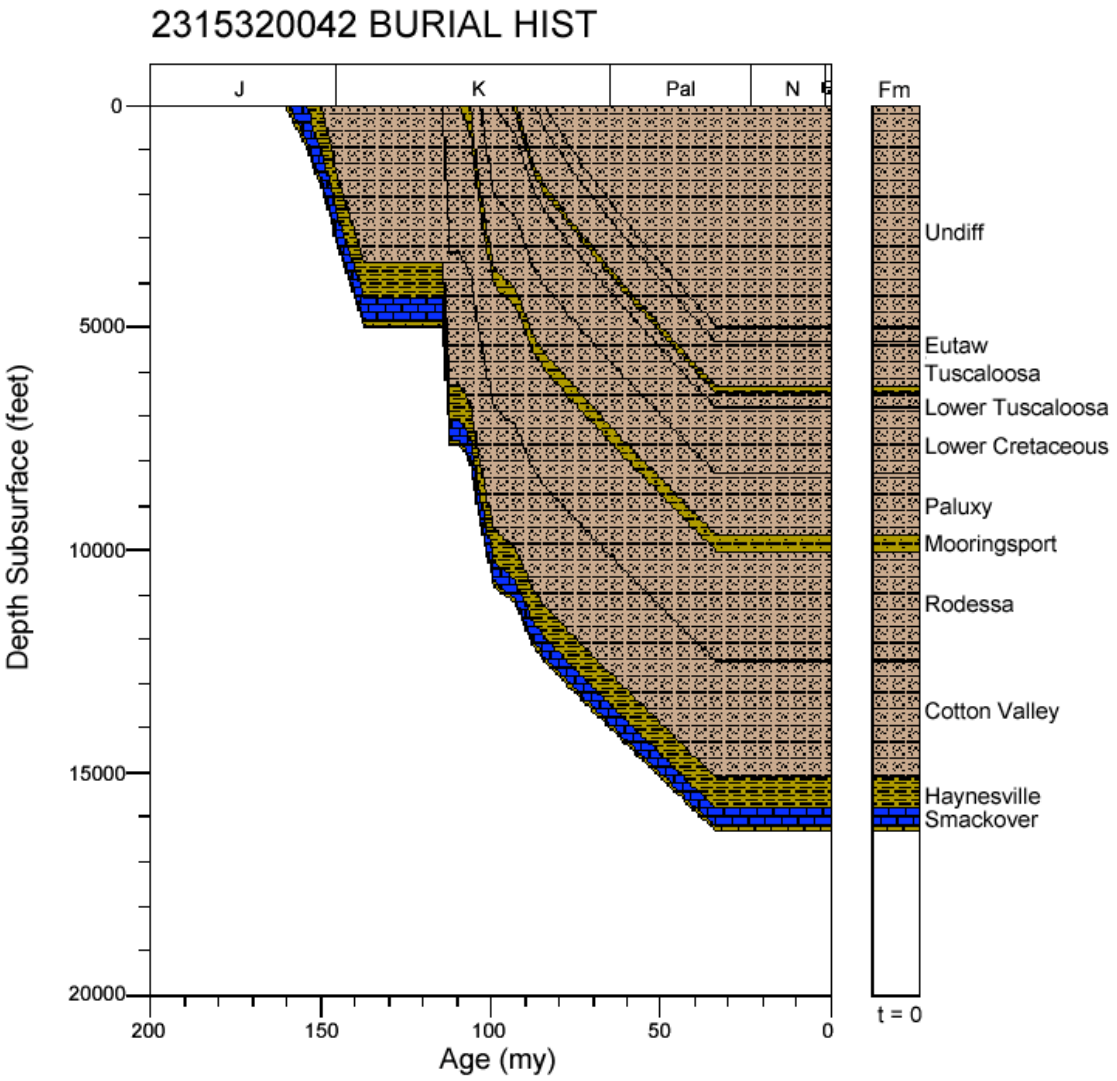


Figure 208. Burial history for well 2315320042, Mississippi Interior Salt Basin.

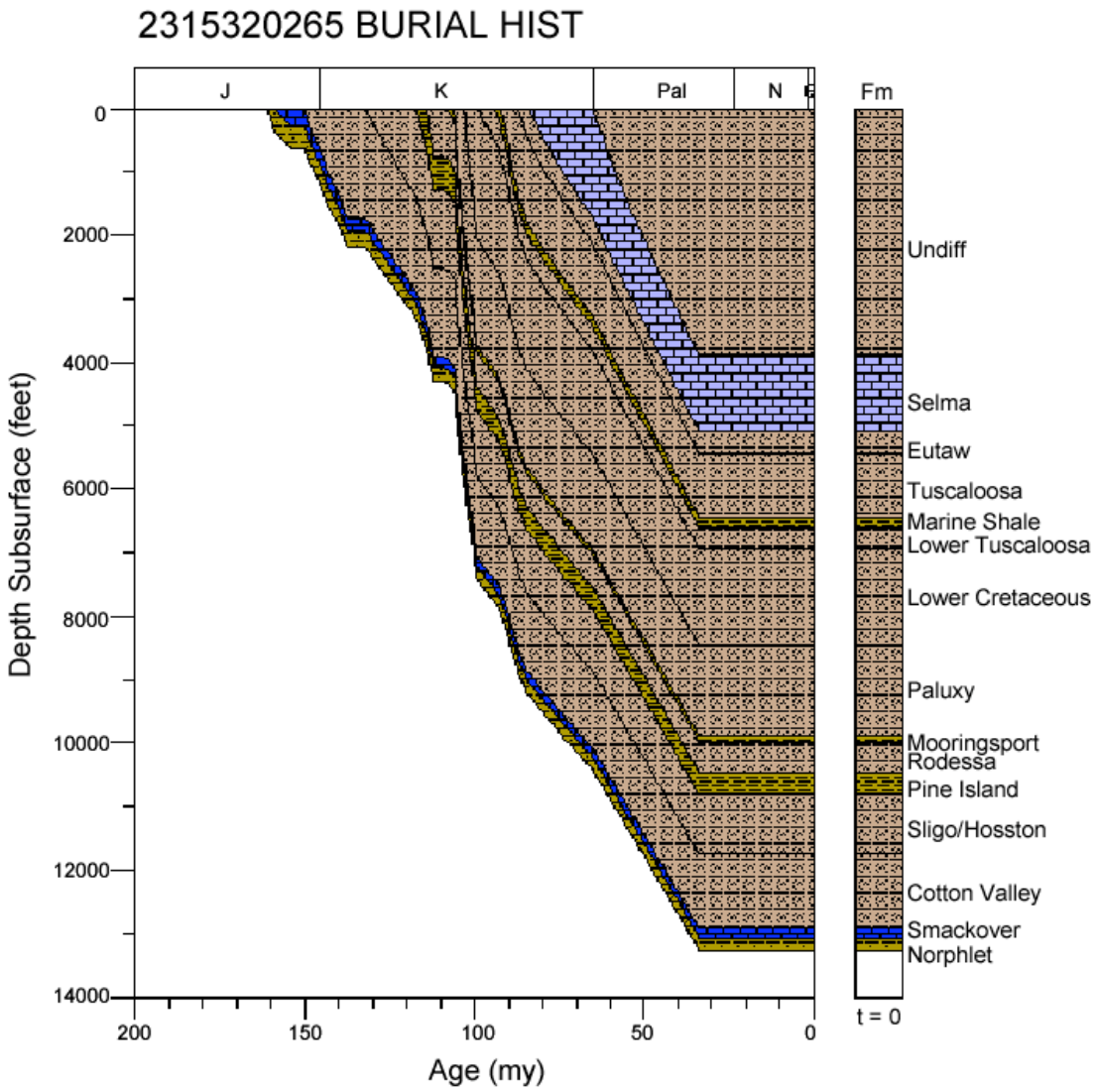


Figure 209. Burial history for well 2315320265, Mississippi Interior Salt Basin.

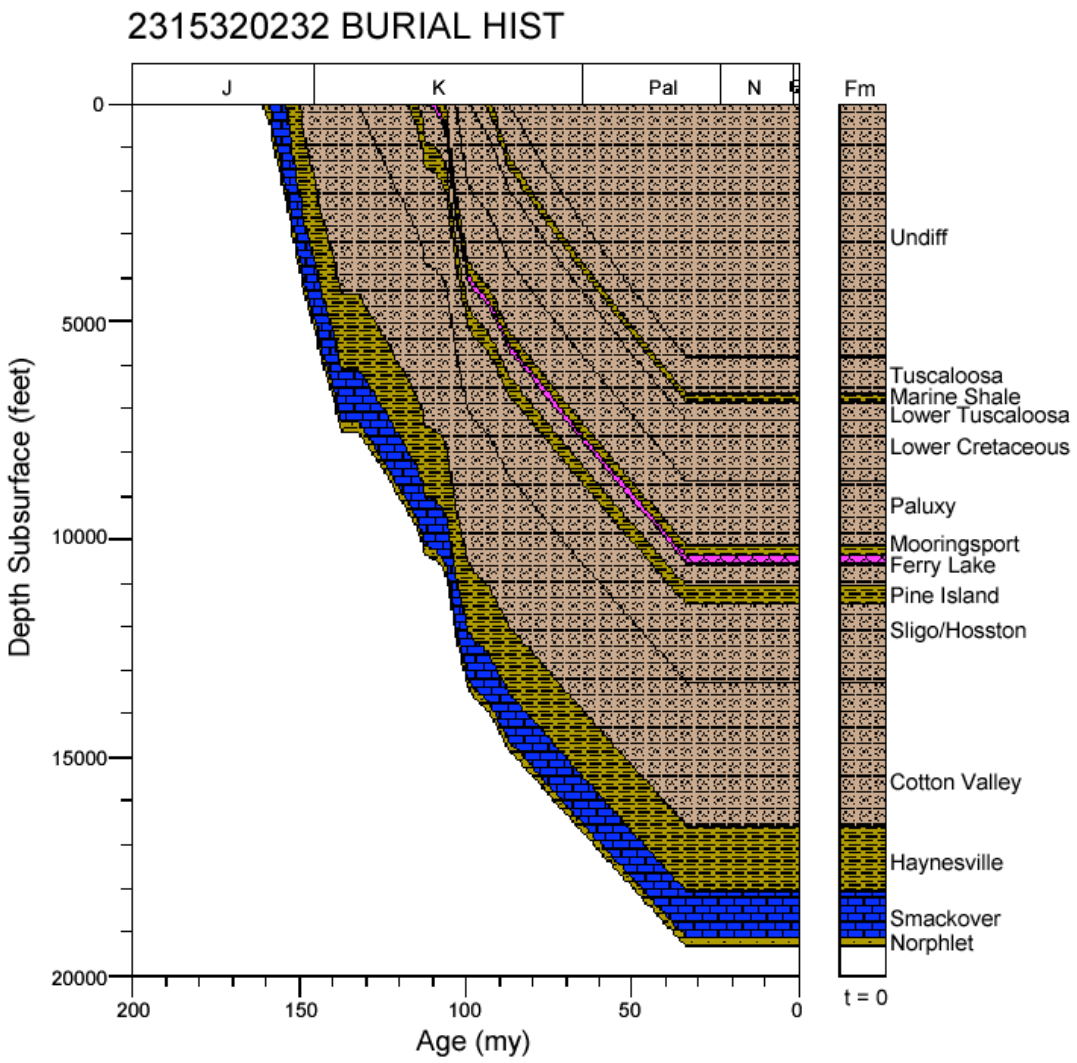


Figure 210. Burial history for well 2315320232, Mississippi Interior Salt Basin.

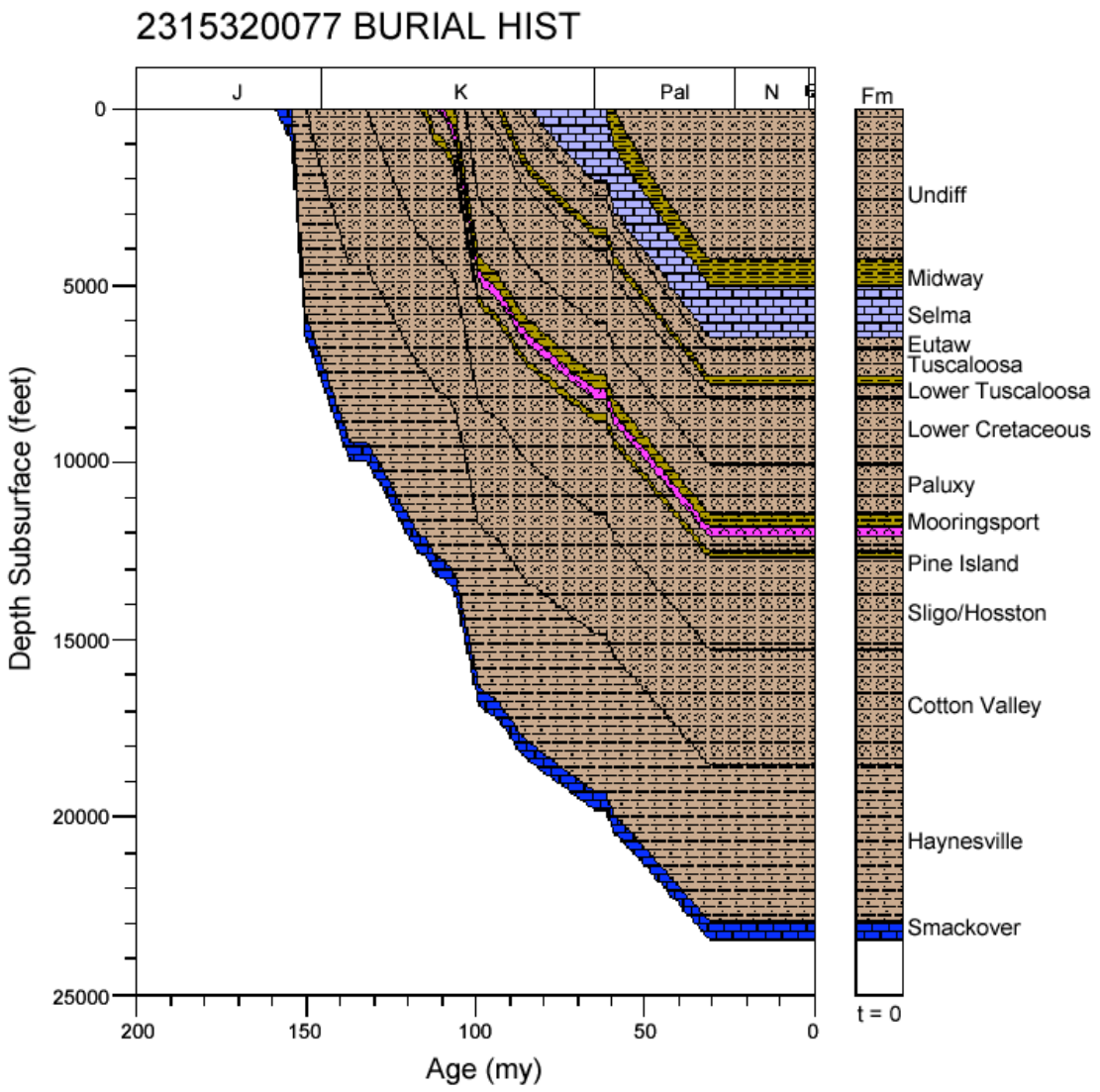


Figure 211. Burial history for well 2315320077, Mississippi Interior Salt Basin.

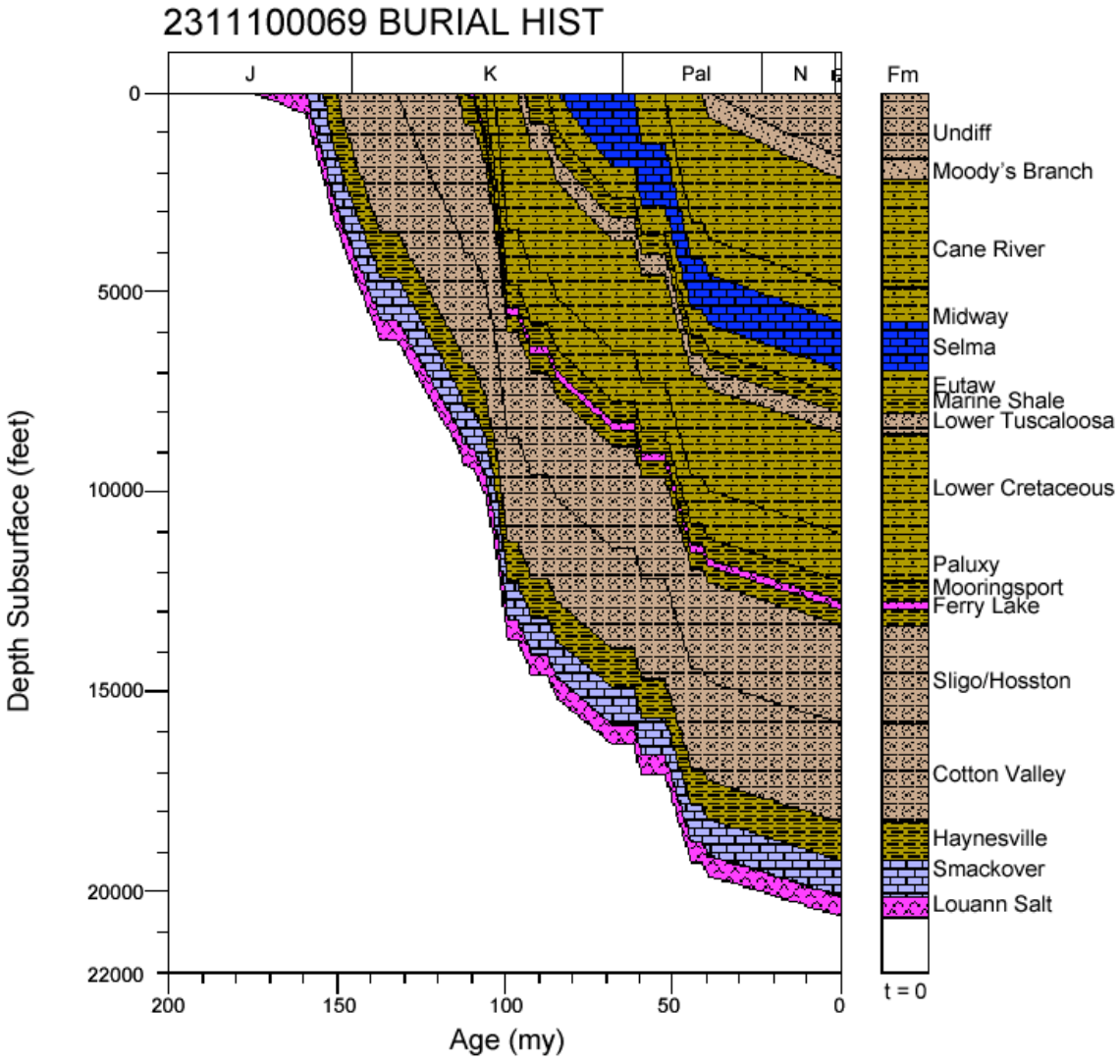


Figure 212. Burial history for well 2311100069, Mississippi Interior Salt Basin.

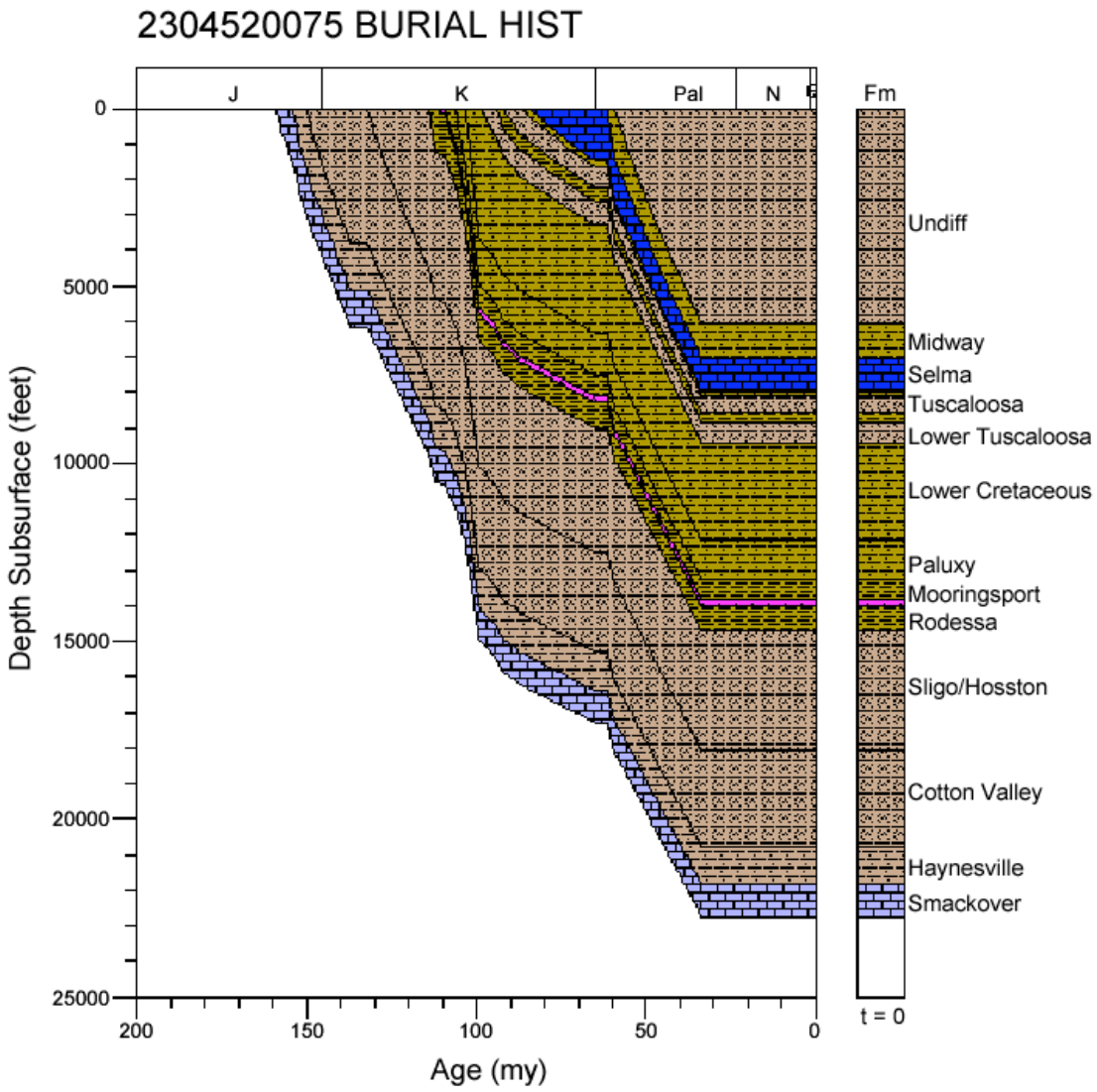


Figure 213. Burial history for well 2304520075, Mississippi Interior Salt Basin.

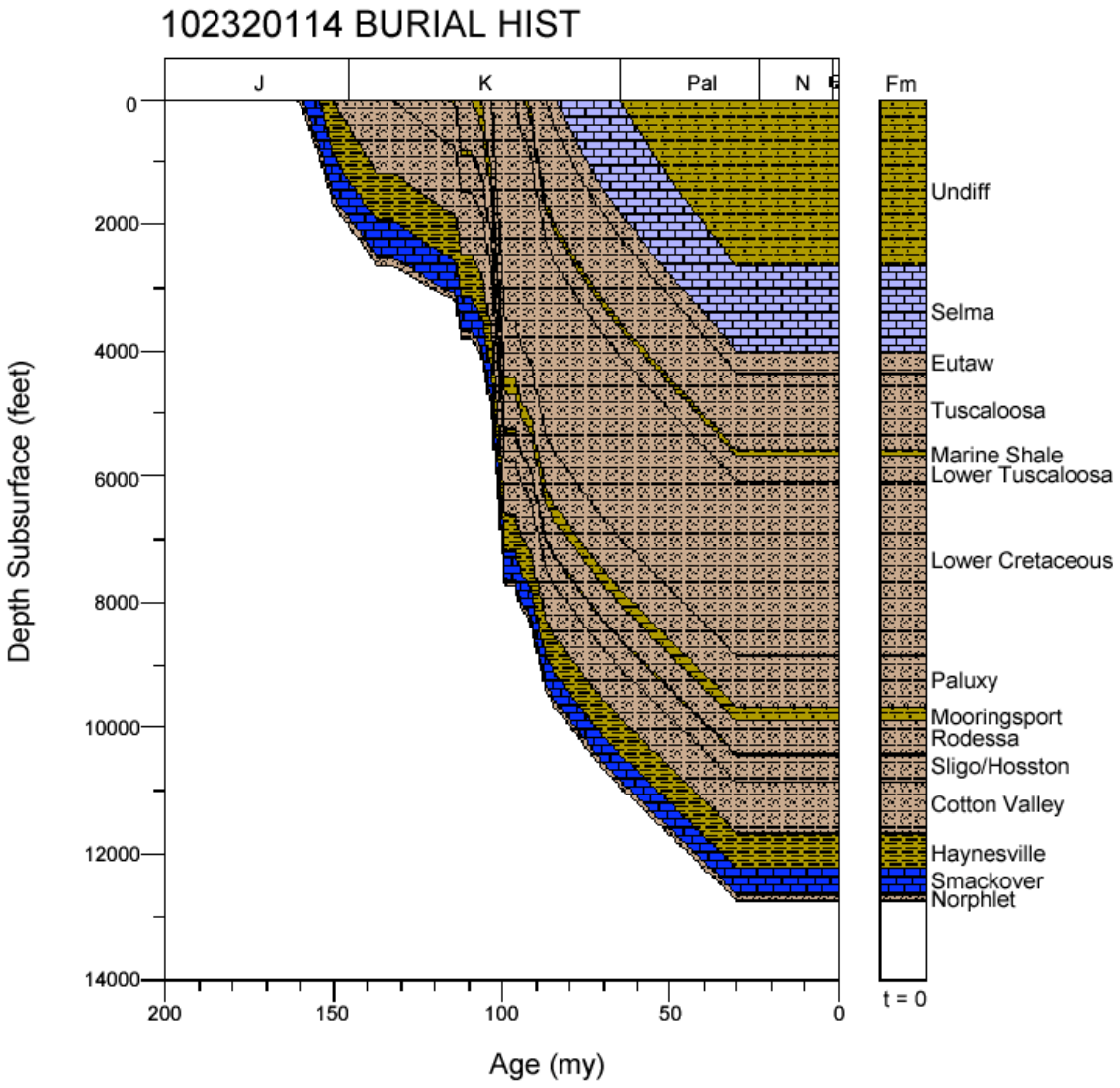


Figure 214. Burial history for well 102320114, Mississippi Interior Salt Basin.

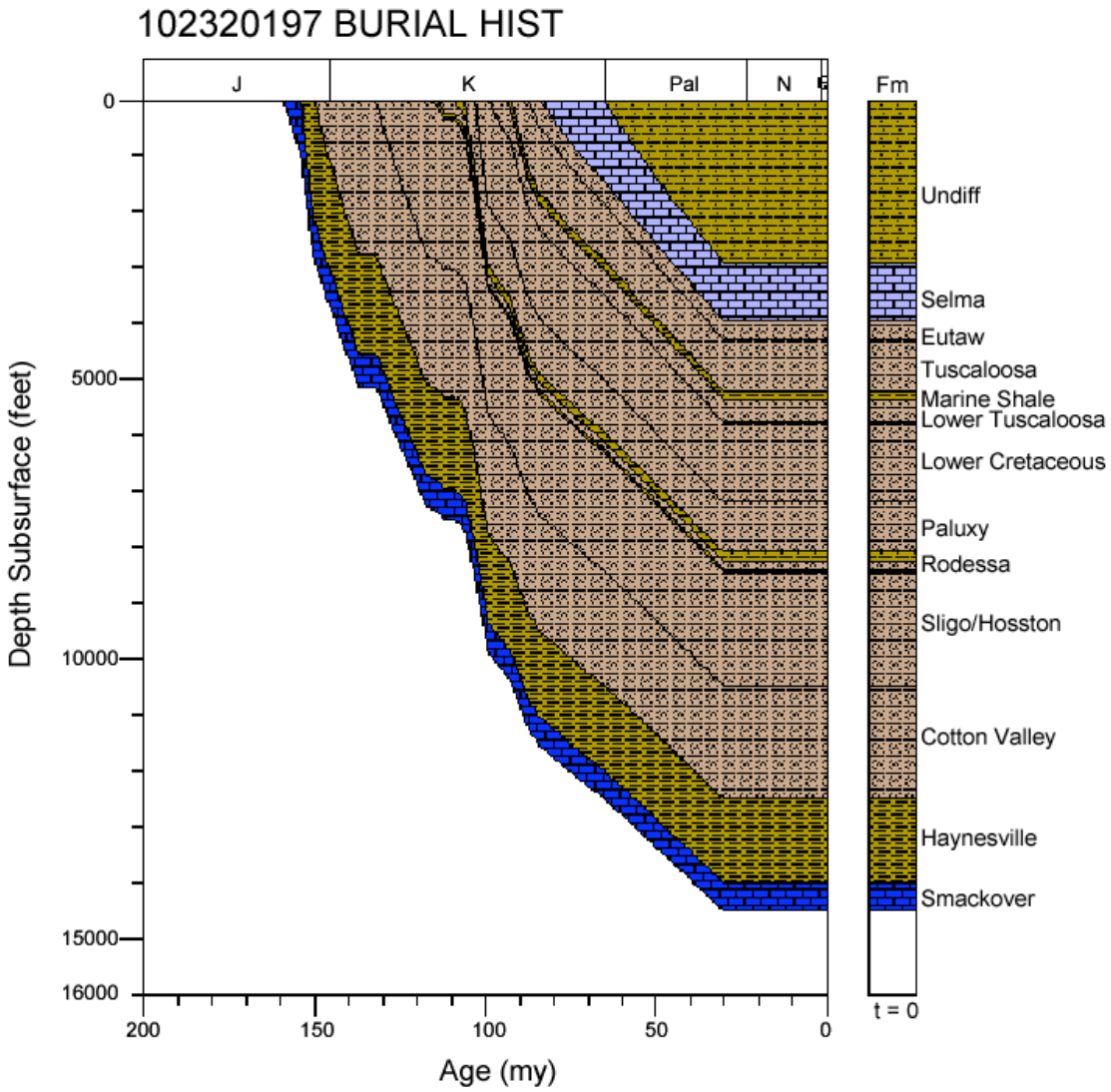


Figure 215. Burial history for well 102320197, Mississippi Interior Salt Basin.

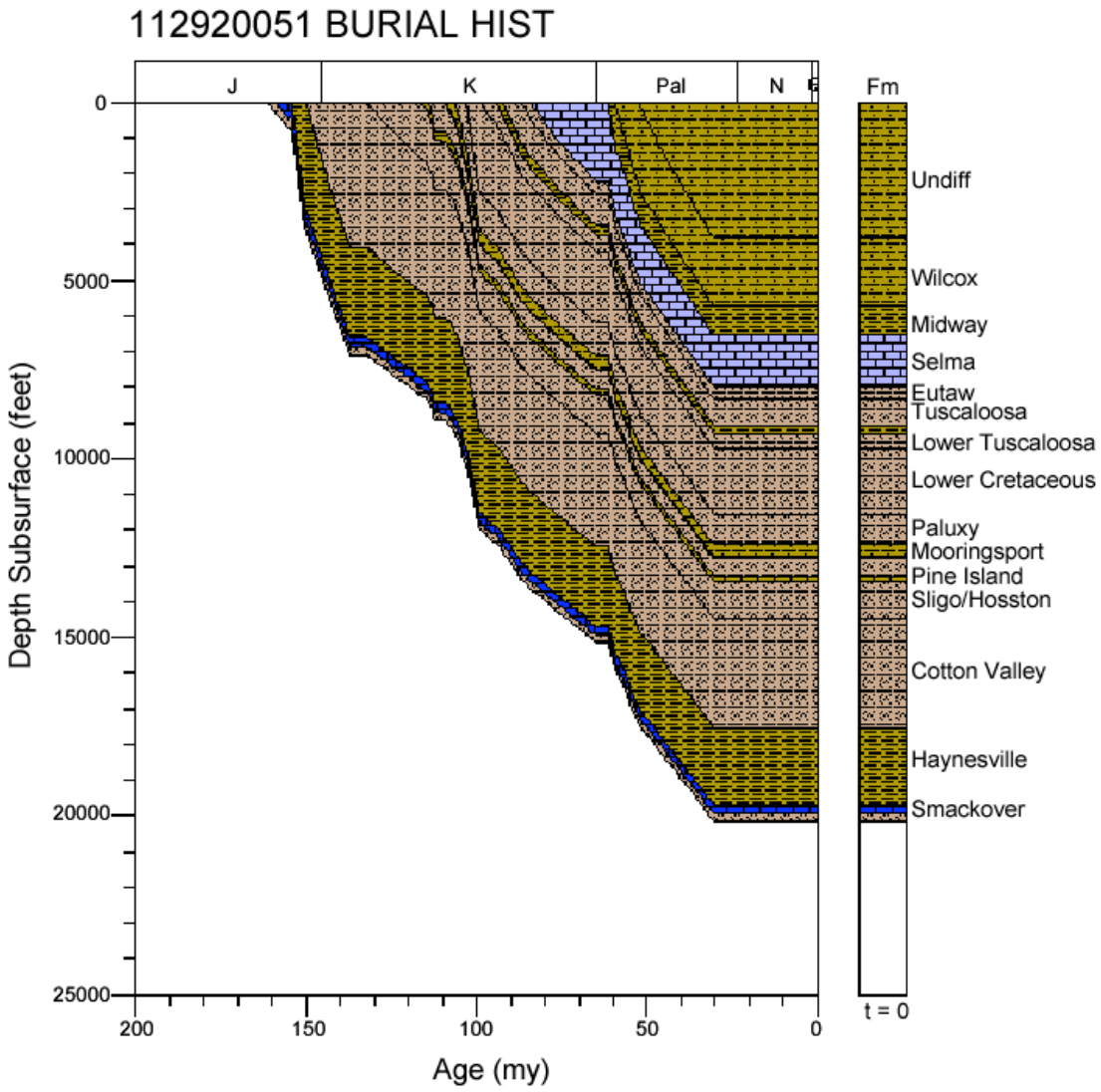


Figure 216. Burial history for well 112920051, Mississippi Interior Salt Basin.

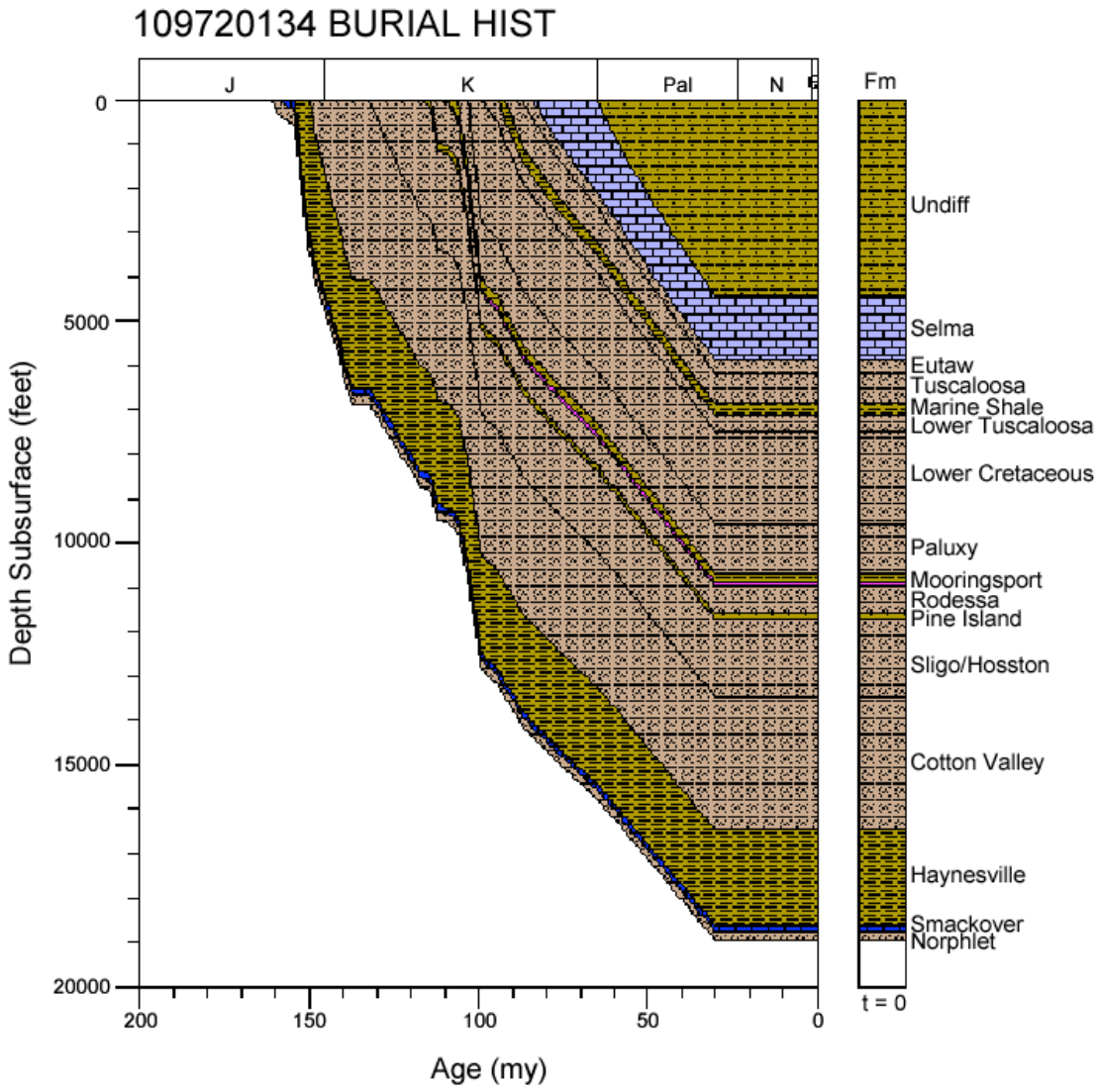


Figure 217. Burial history for well 109720134, Mississippi Interior Salt Basin.

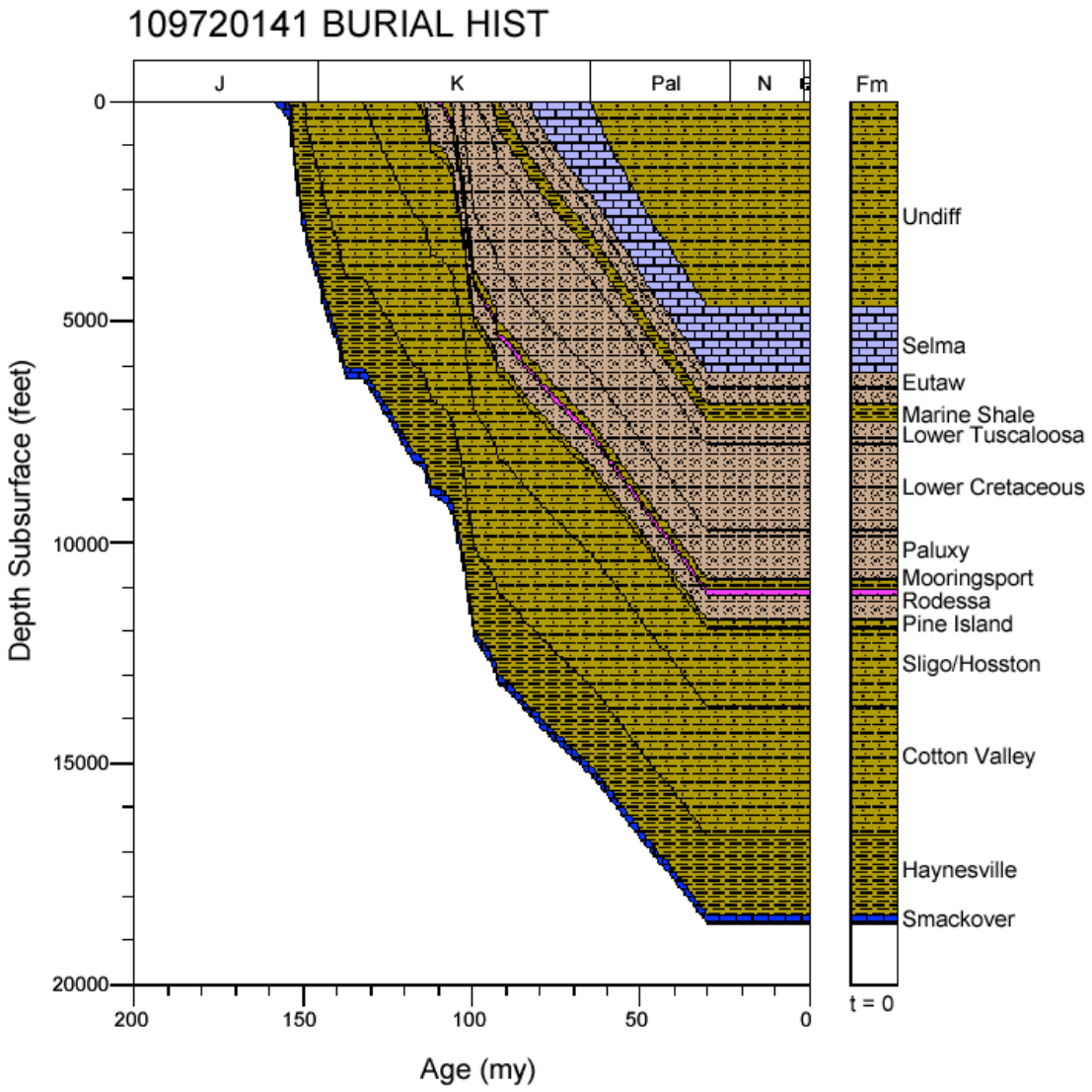


Figure 218. Burial history for well 109720141, Mississippi Interior Salt Basin.

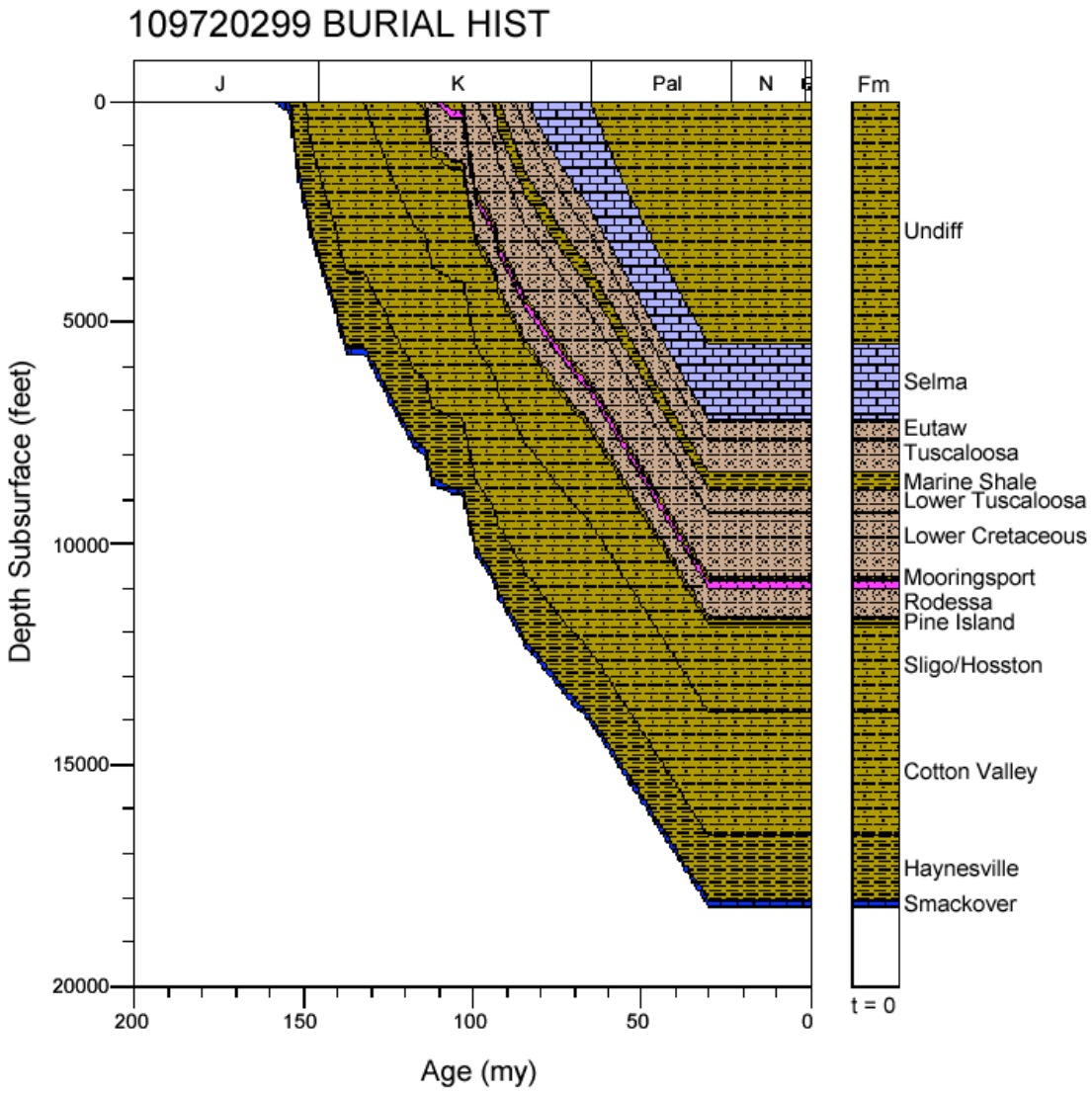


Figure 219. Burial history for well 109720299, Mississippi Interior Salt Basin.

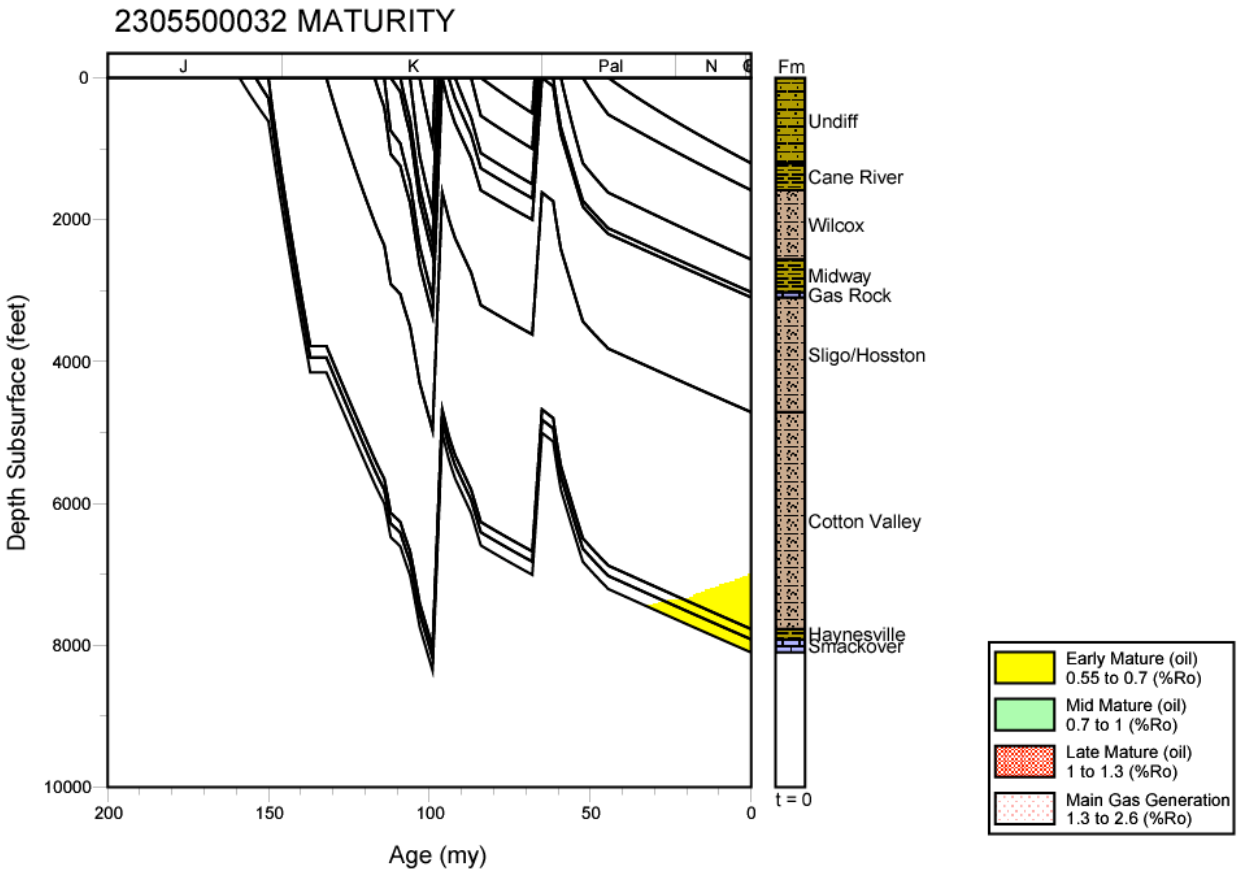


Figure 220. Thermal maturation profile for well 2305500032, Mississippi Interior Salt Basin.

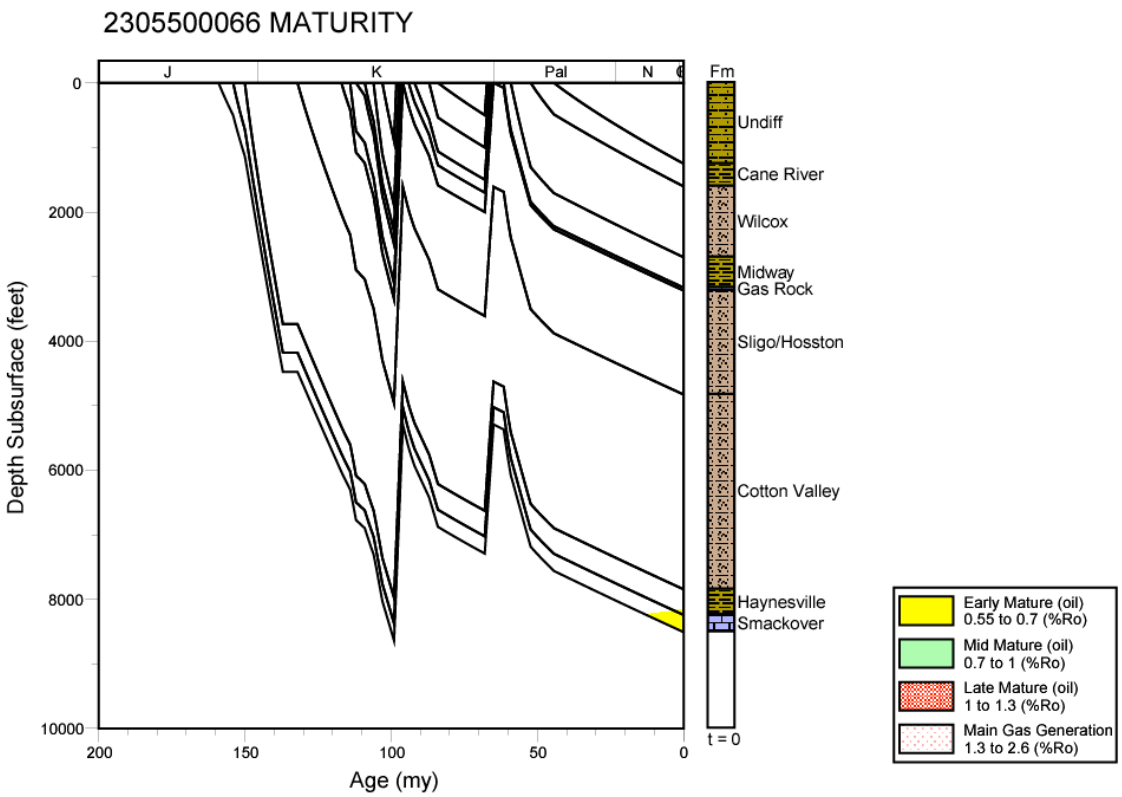


Figure 221. Thermal maturation profile for well 2305500066, Mississippi Interior Salt Basin.

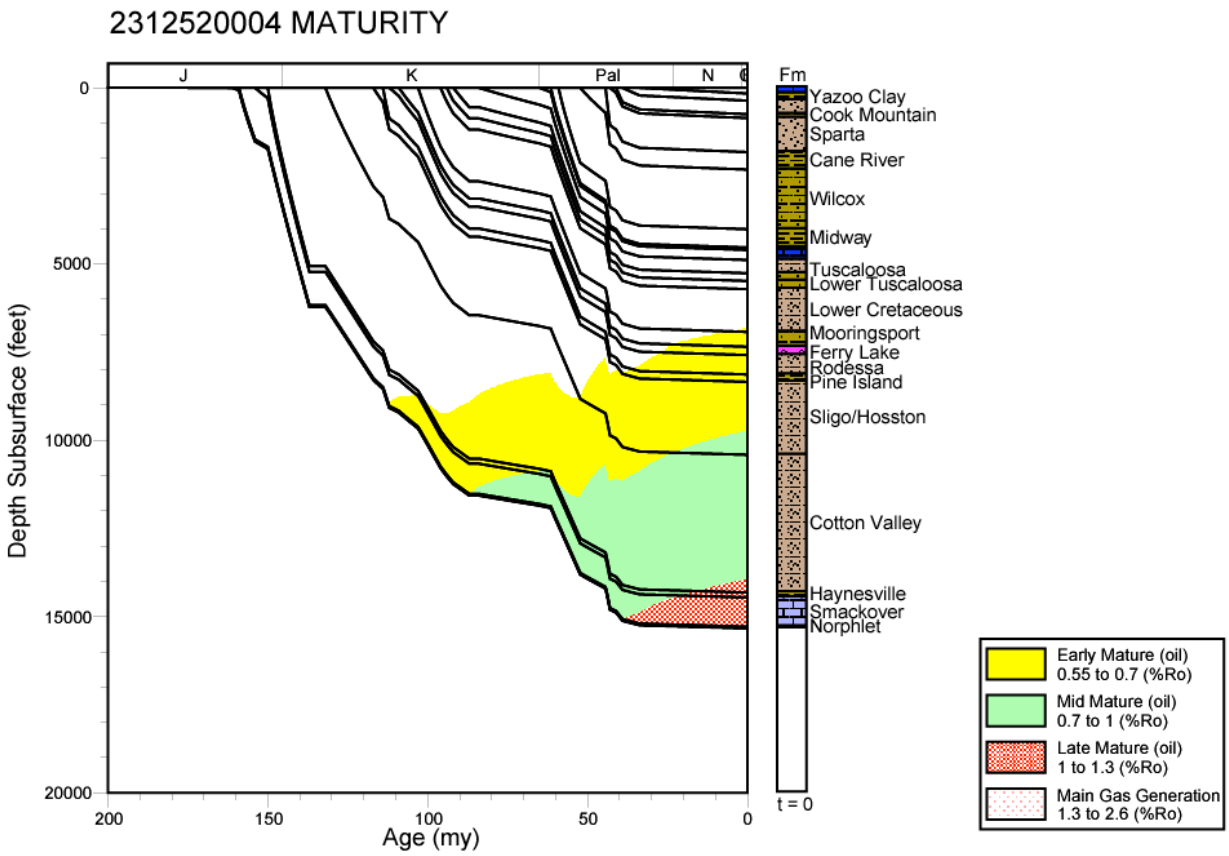


Figure 222. Thermal maturation profile for well 2312520004, Mississippi Interior Salt Basin.

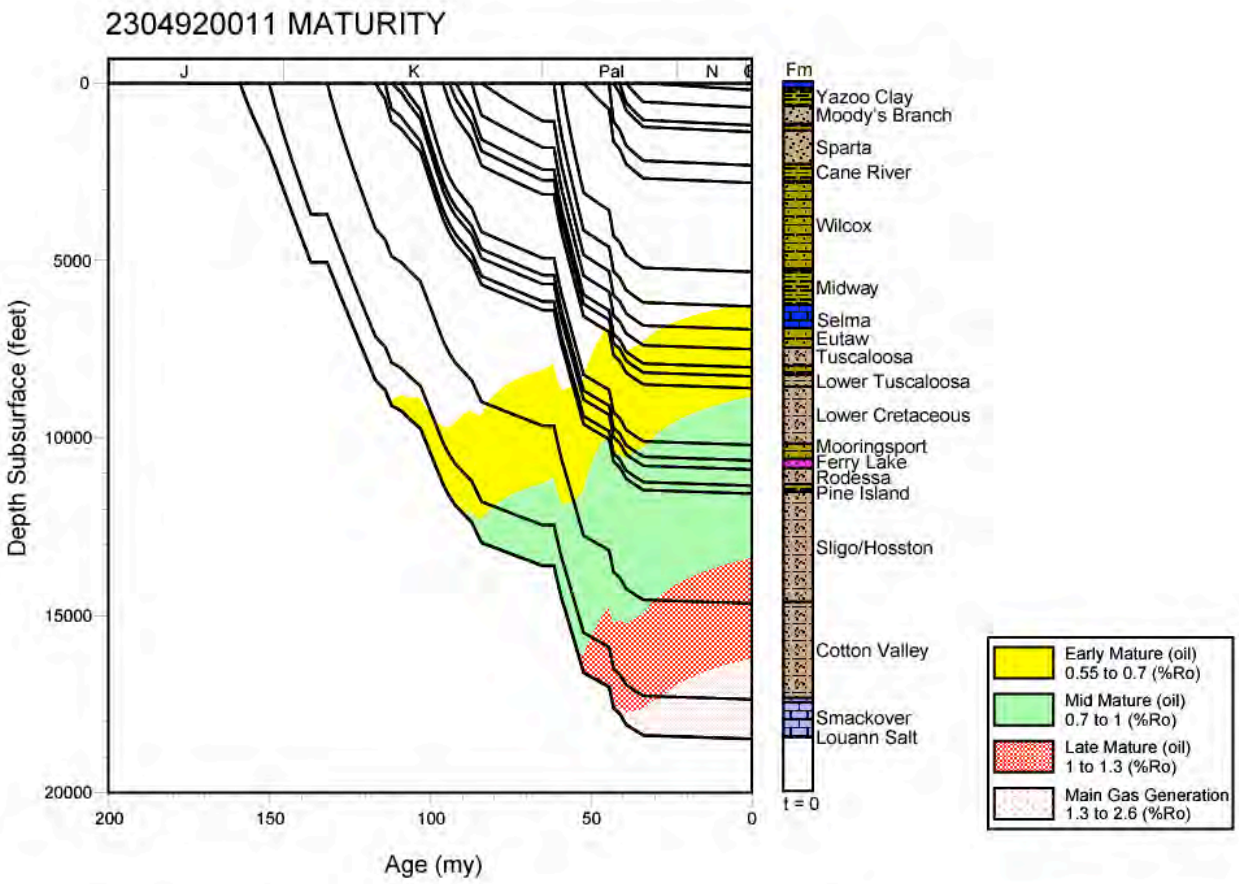


Figure 223. Thermal maturation profile for well 2304920011, Mississippi Interior Salt Basin.

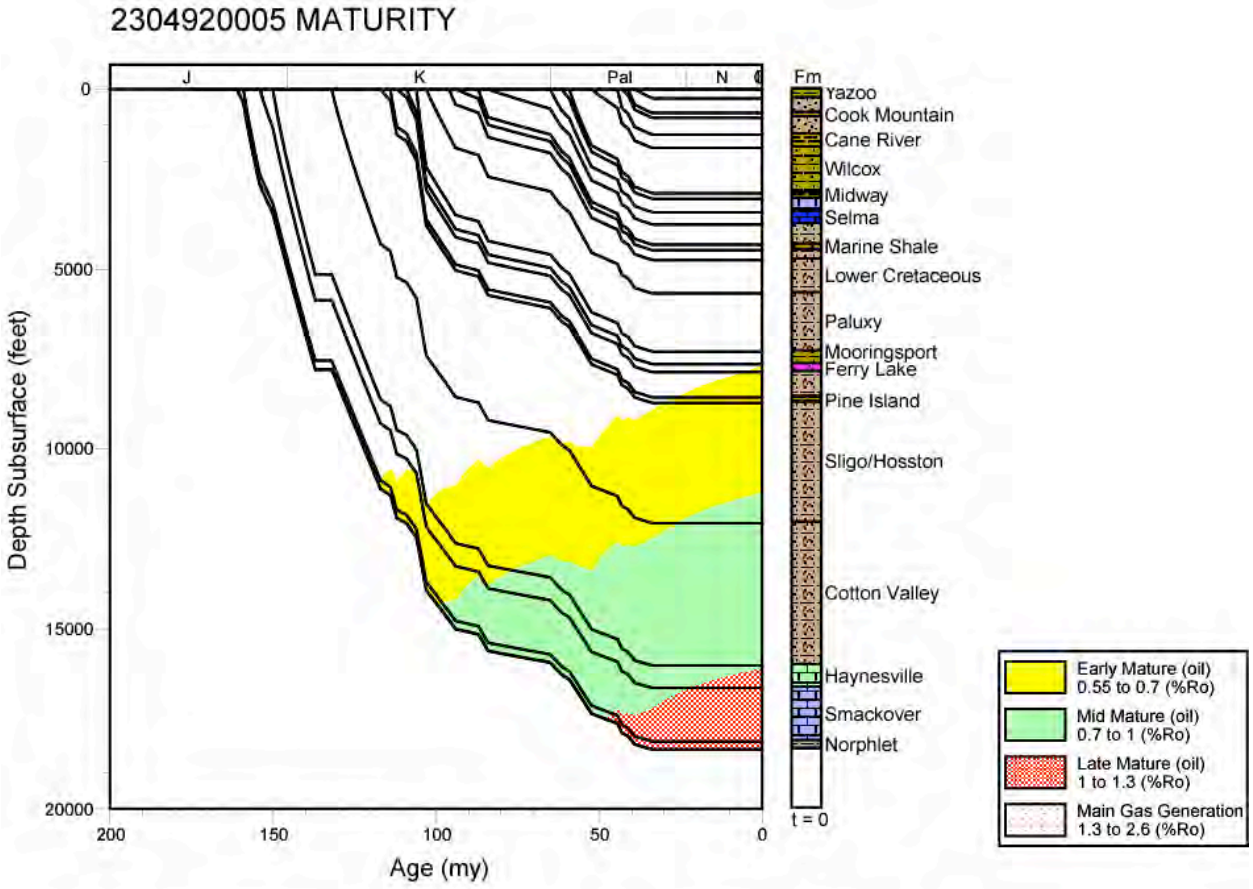


Figure 224. Thermal maturation profile for well 2304920005, Mississippi Interior Salt Basin.

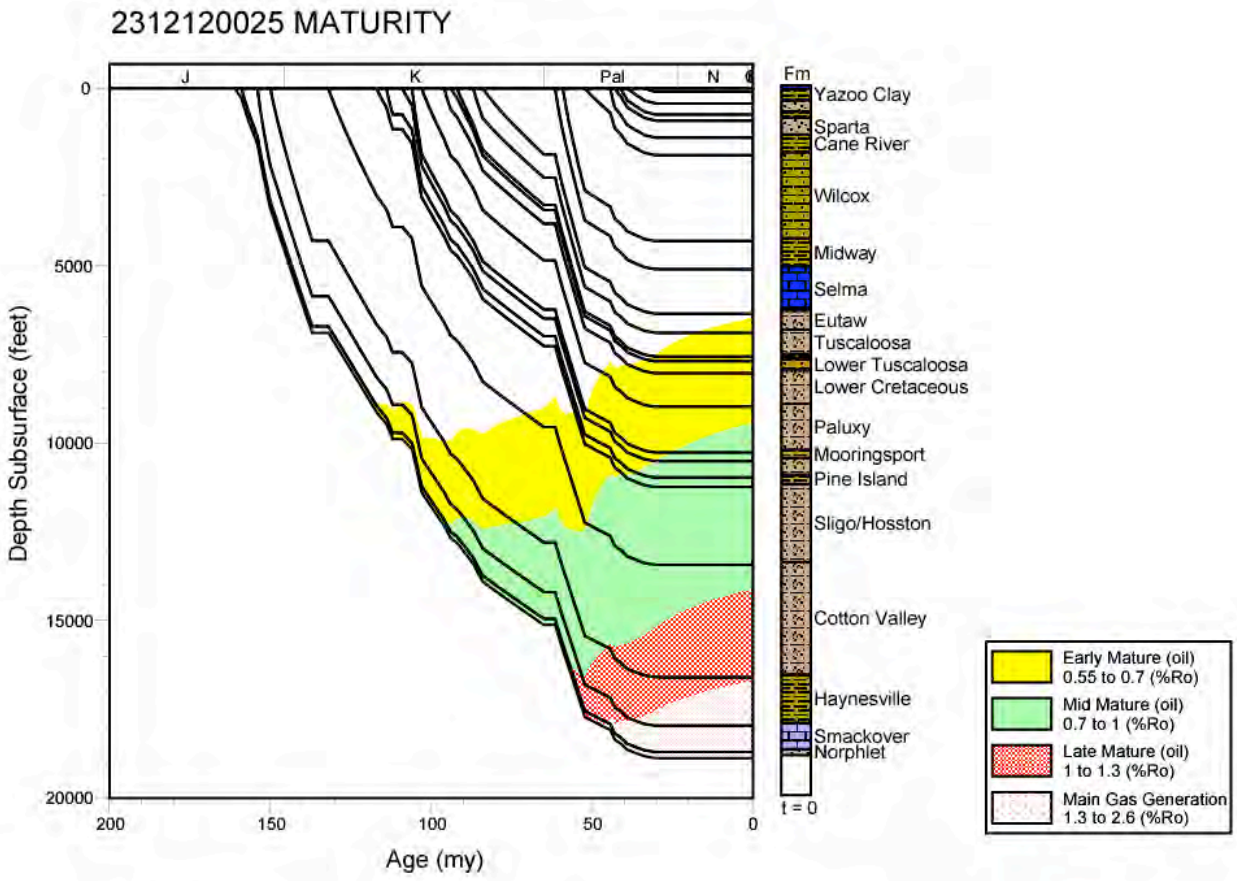


Figure 225. Thermal maturation profile for well 2312120025, Mississippi Interior Salt Basin.

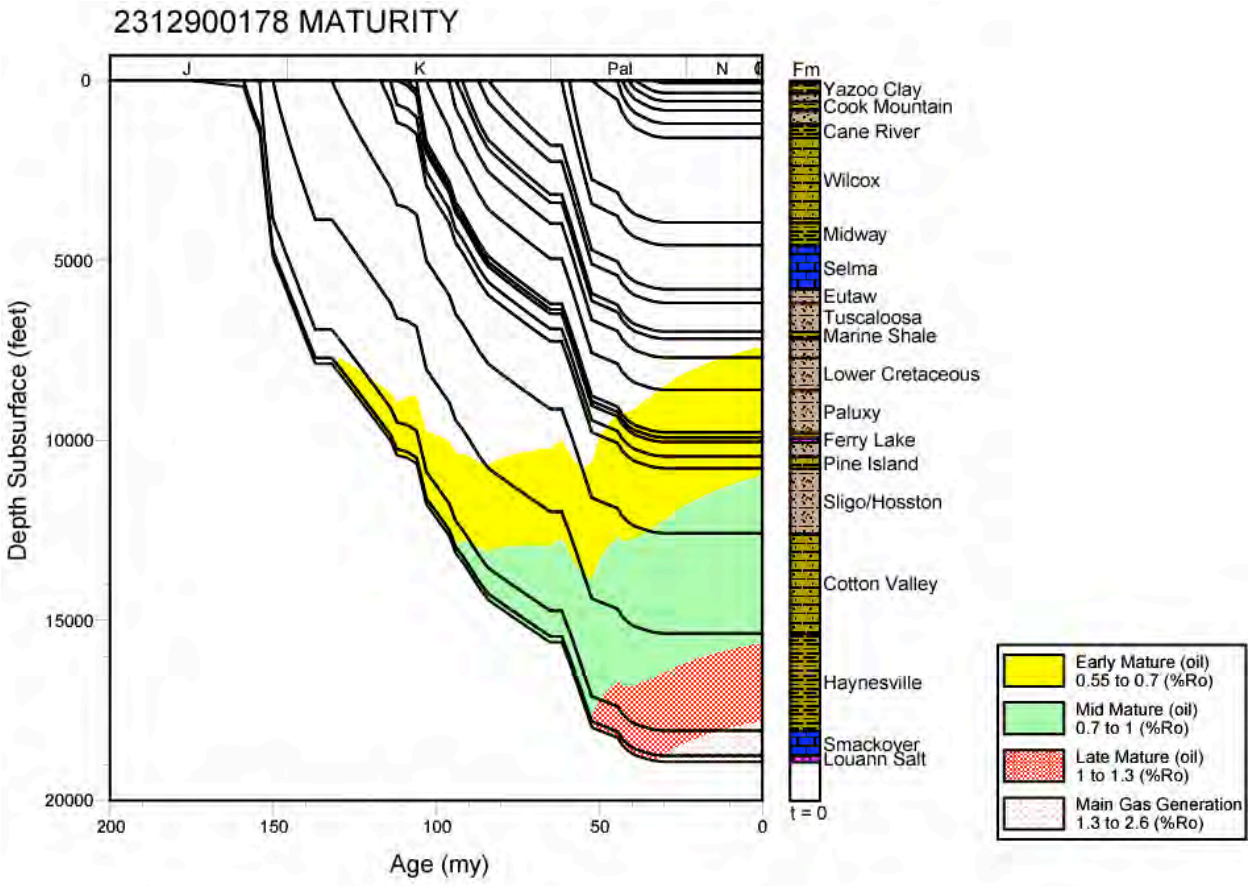


Figure 226. Thermal maturation profile for well 2312900178, Mississippi Interior Salt Basin.

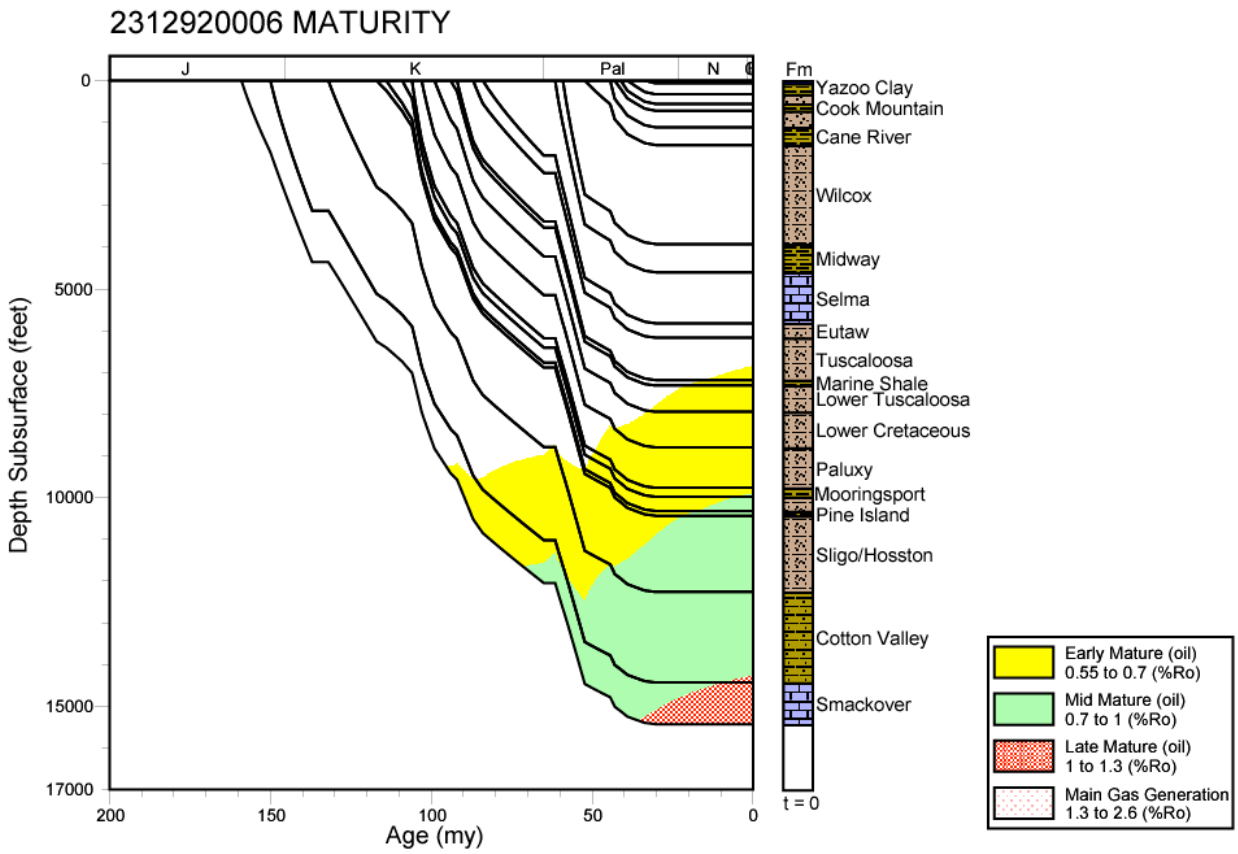


Figure 227. Thermal maturation profile for well 2312920006, Mississippi Interior Salt Basin.

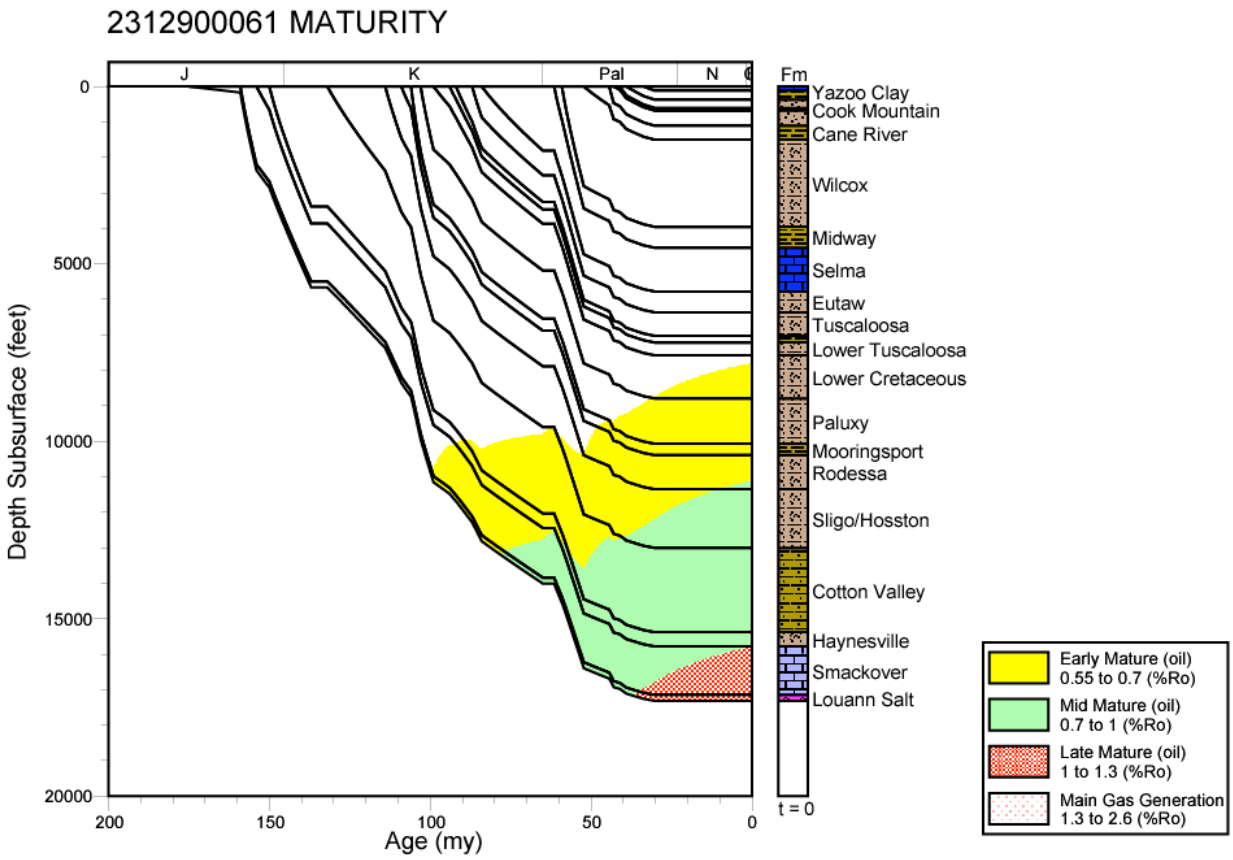


Figure 228. Thermal maturation profile for well 2312900061, Mississippi Interior Salt Basin.

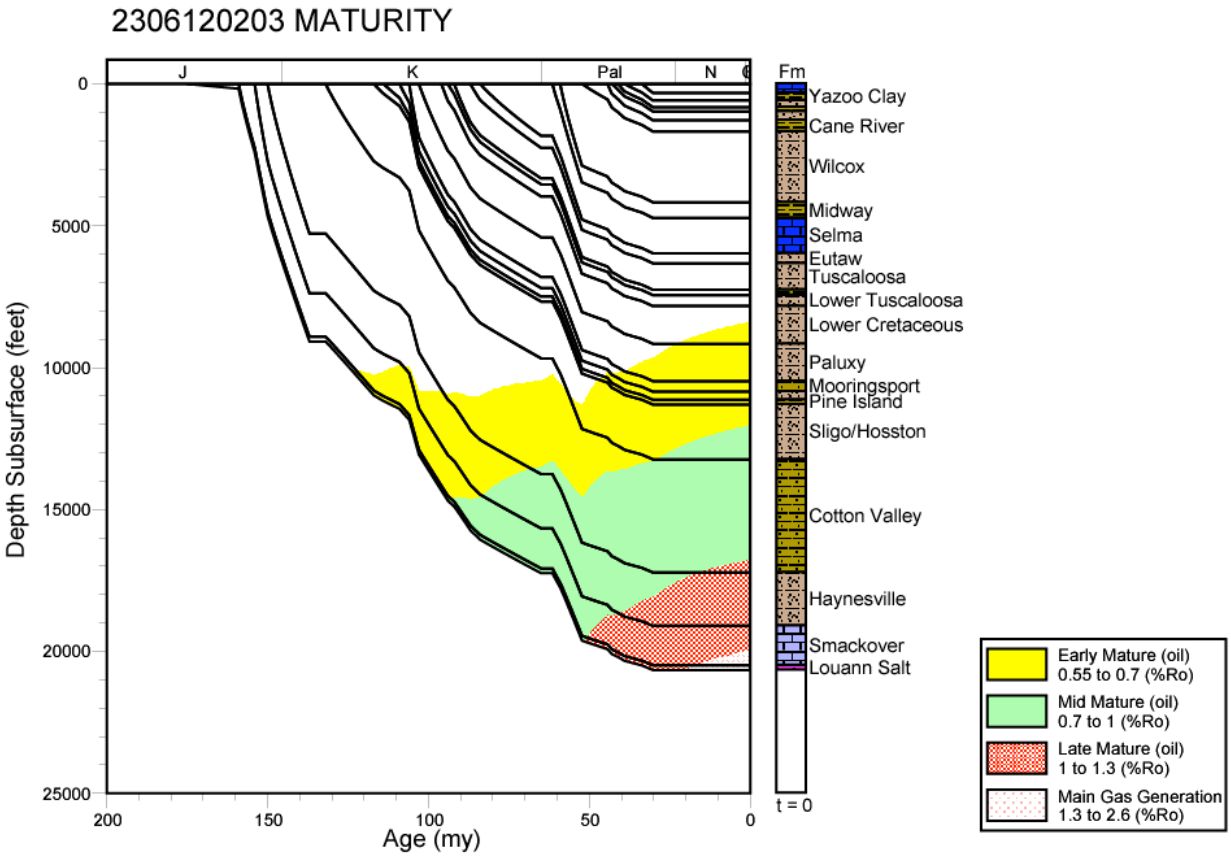


Figure 229. Thermal maturation profile for well 2306120203, Mississippi Interior Salt Basin.

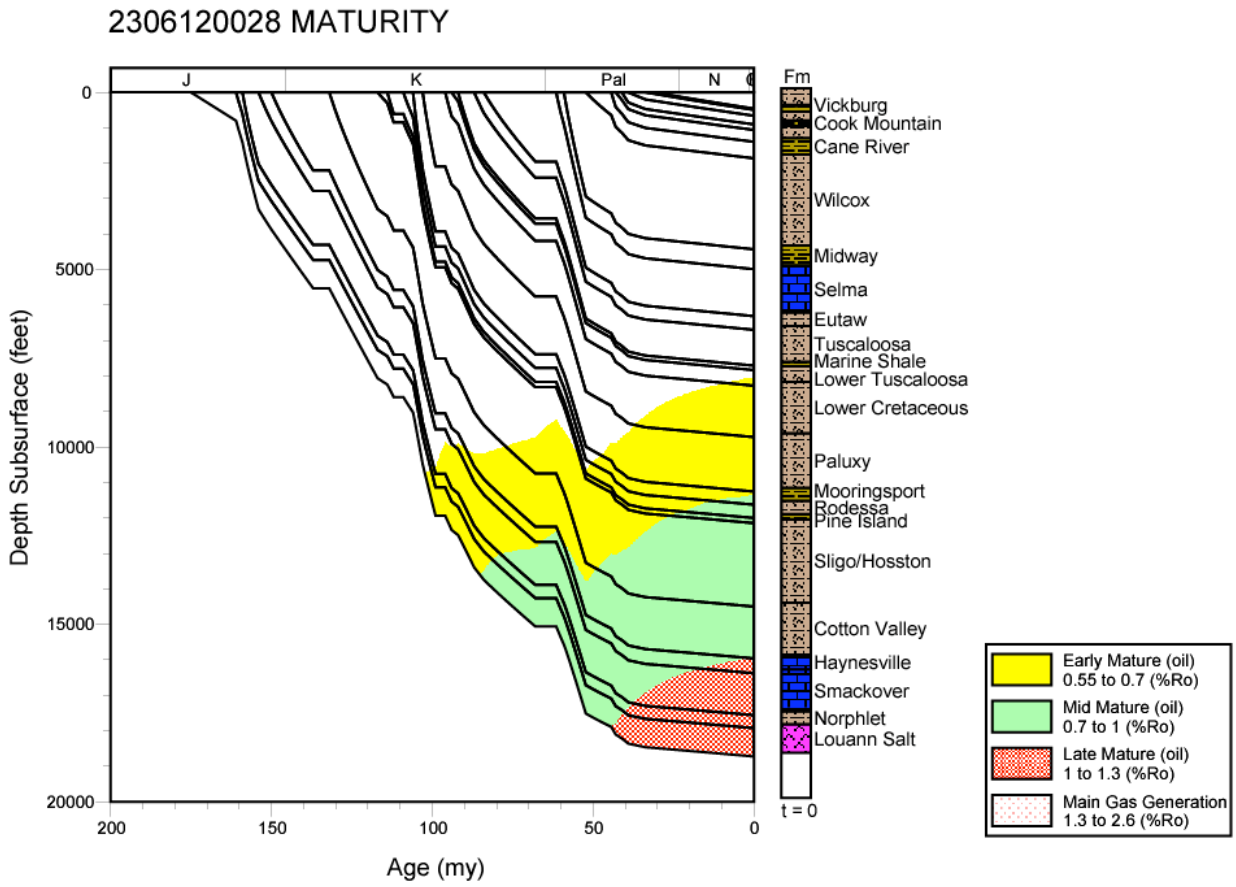


Figure 230. Thermal maturation profile for well 2306120028, Mississippi Interior Salt Basin.

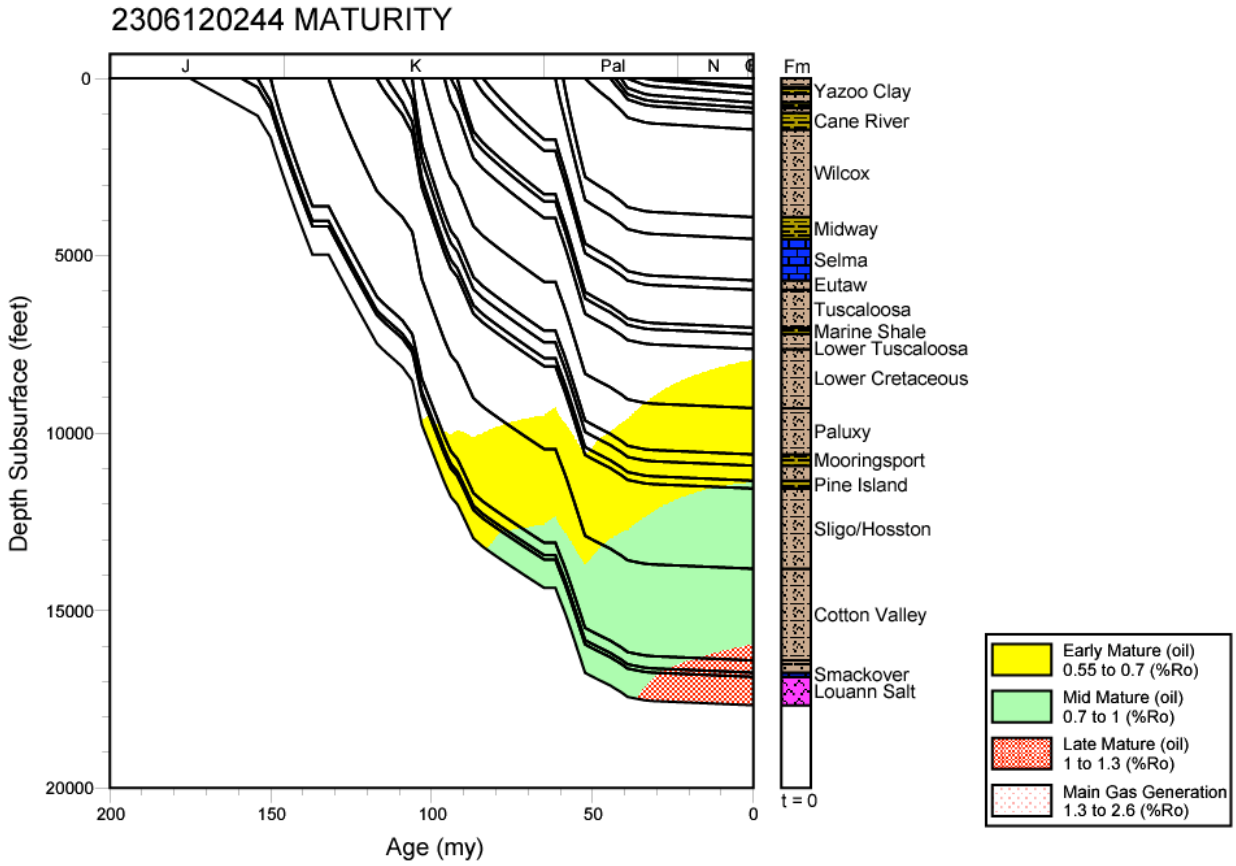


Figure 231. Thermal maturation profile for well 2306120244, Mississippi Interior Salt Basin.

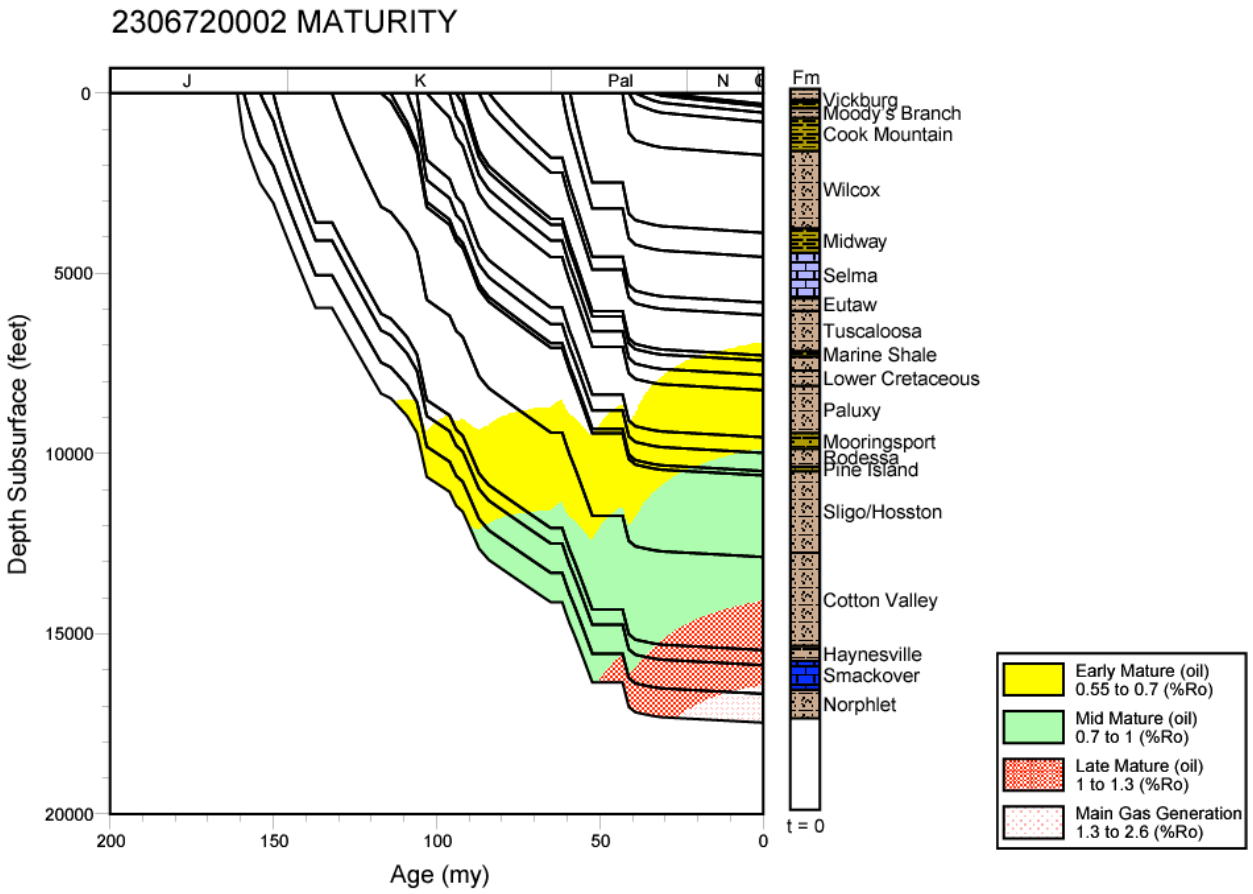


Figure 232. Thermal maturation profile for well 2306720002, Mississippi Interior Salt Basin.

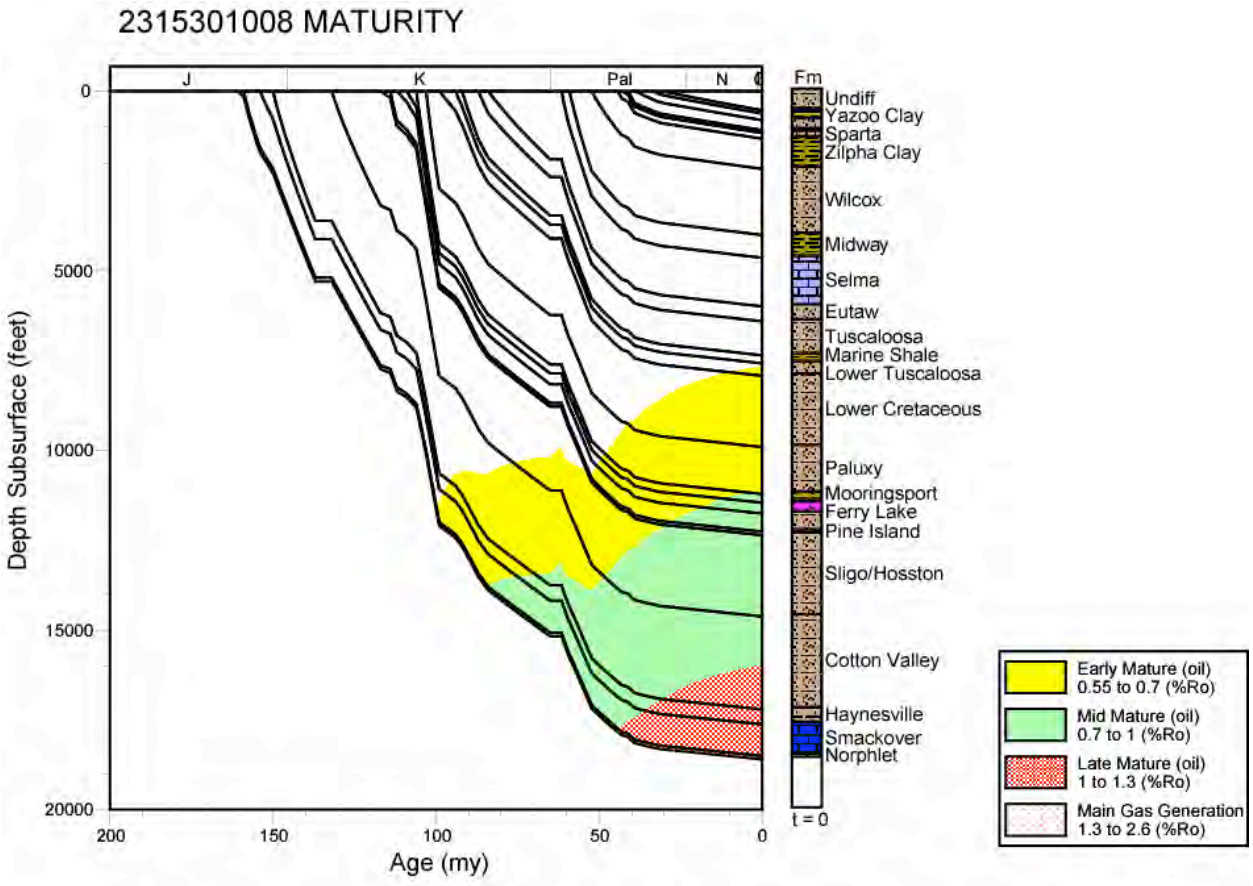


Figure 233. Thermal maturation profile for well 2315301008, Mississippi Interior Salt Basin.

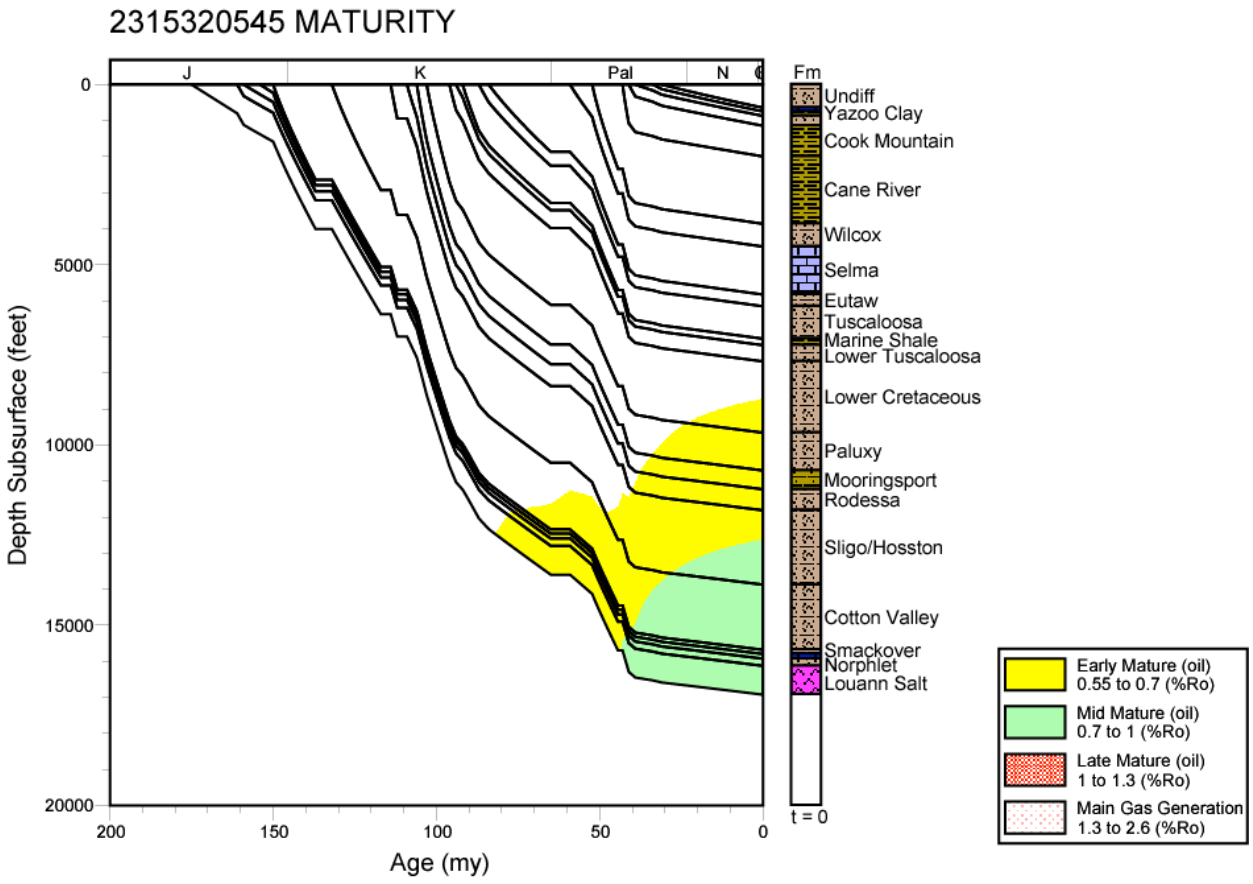


Figure 234. Thermal maturation profile for well 2315320545, Mississippi Interior Salt Basin.

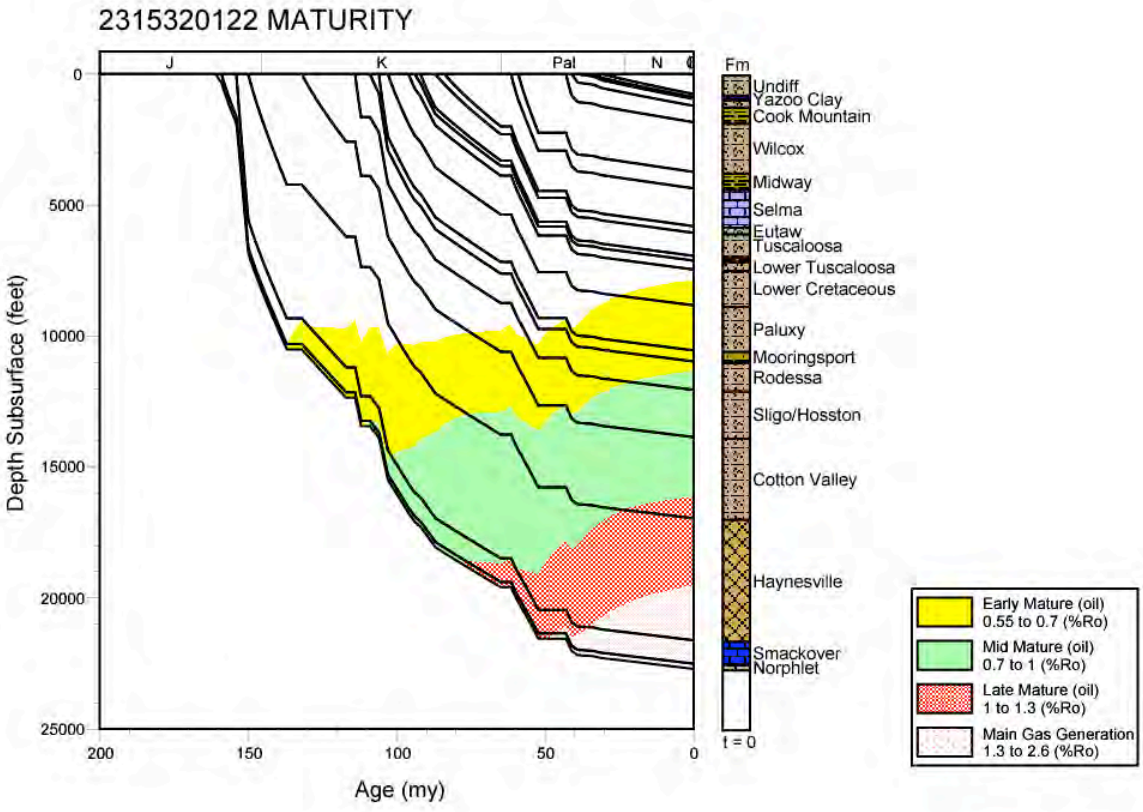


Figure 235. Thermal maturation profile for well 2315320122, Mississippi Interior Salt Basin.

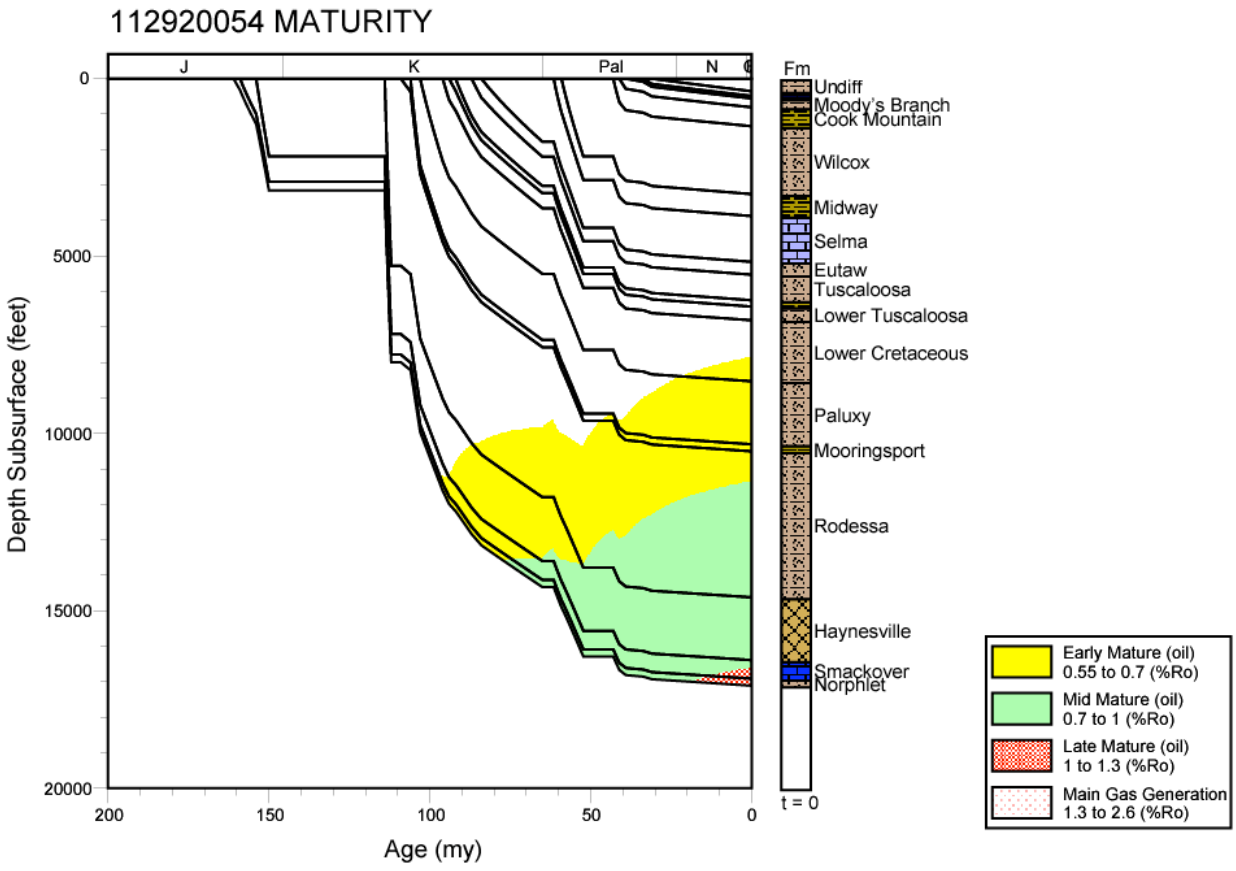


Figure 236. Thermal maturation profile for well 112920054, Mississippi Interior Salt Basin.

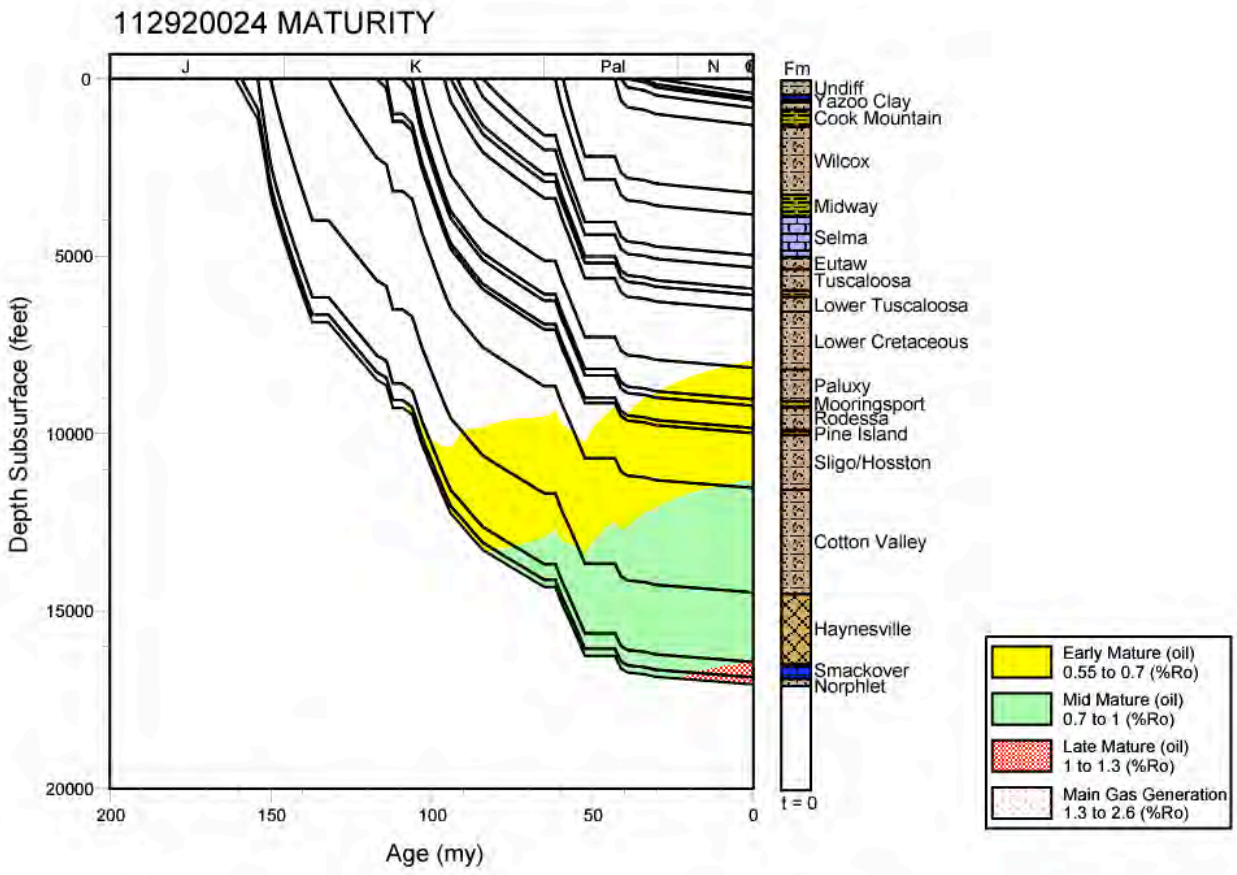


Figure 237. Thermal maturation profile for well 112920024, Mississippi Interior Salt Basin.

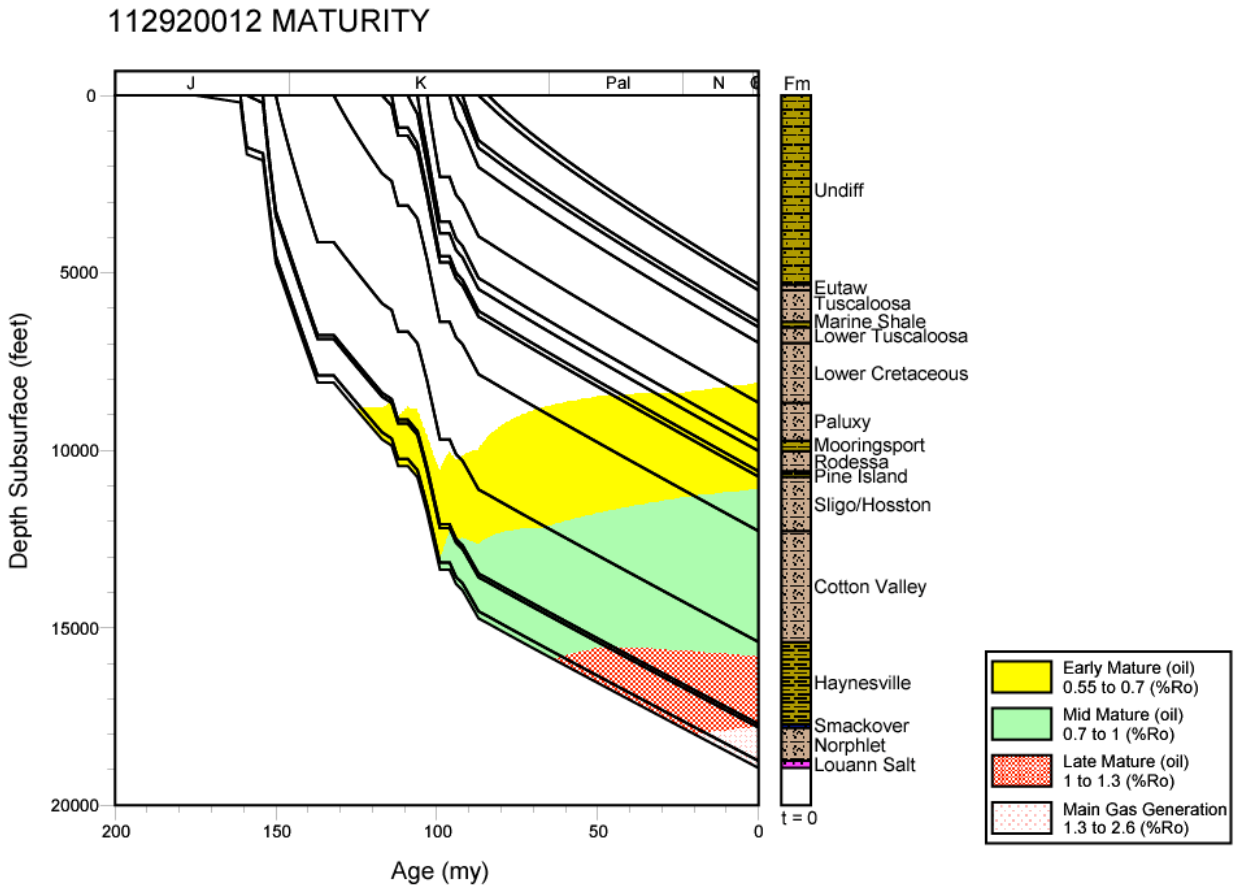


Figure 238. Thermal maturation profile for well 112920012, Mississippi Interior Salt Basin.

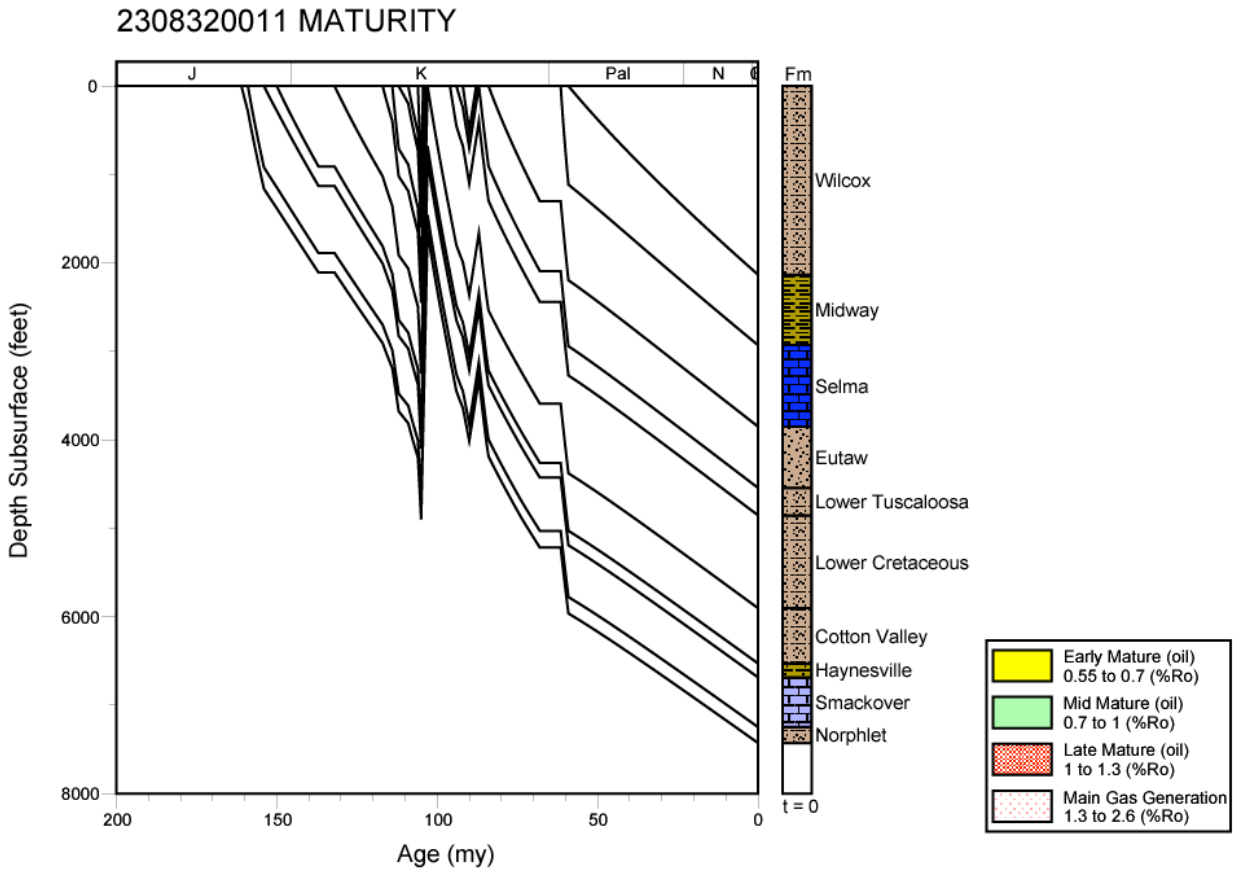


Figure 239. Thermal maturation profile for well 2308320011, Mississippi Interior Salt Basin.

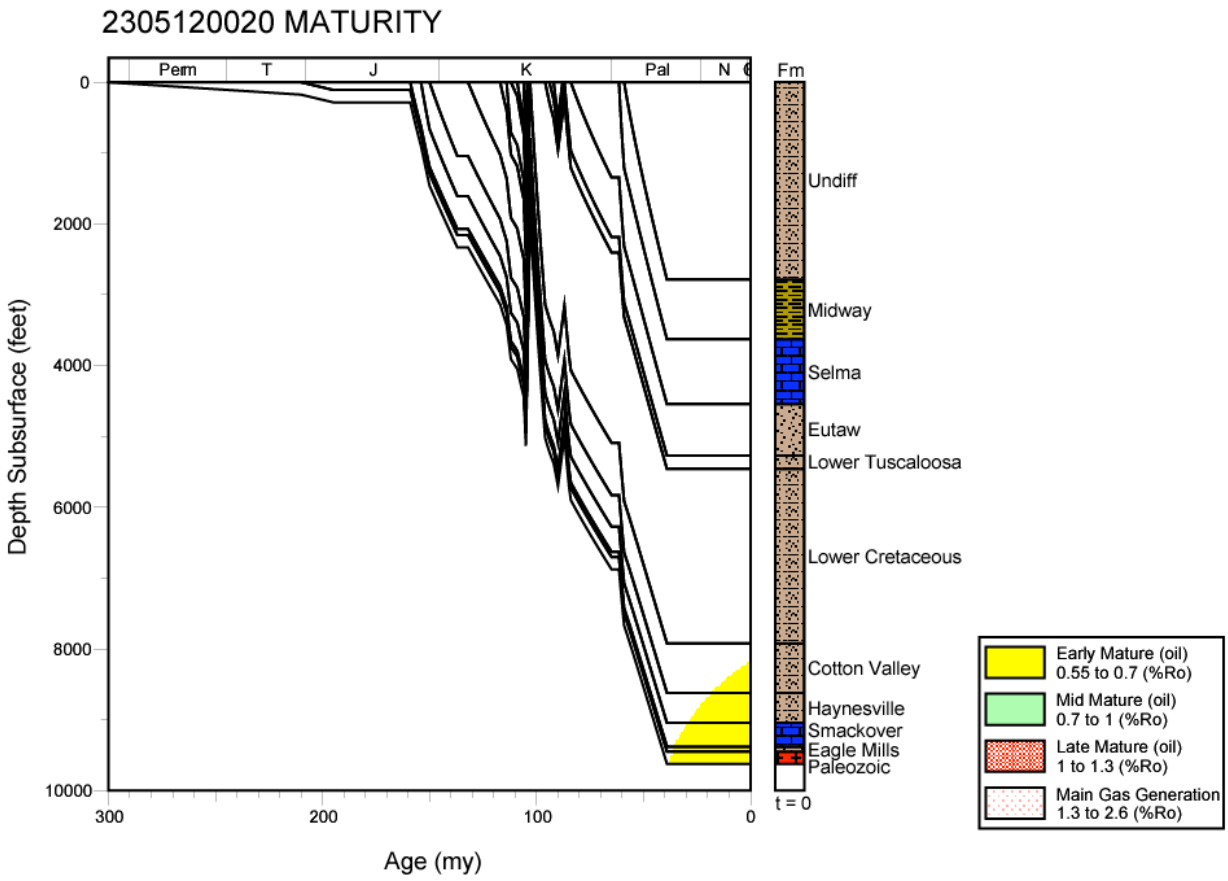


Figure 240. Thermal maturation profile for well 2305120020, Mississippi Interior Salt Basin.

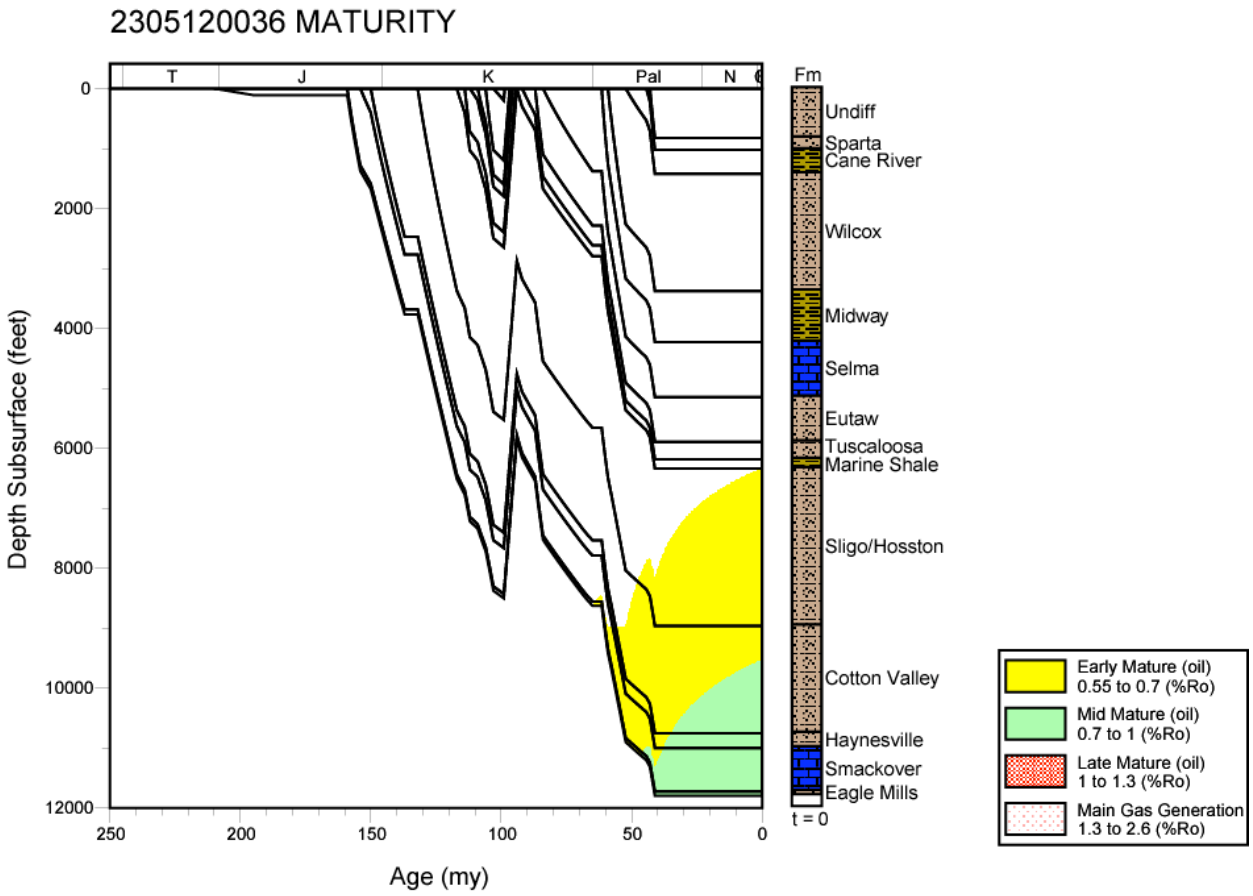


Figure 241. Thermal maturation profile for well 2305120036, Mississippi Interior Salt Basin.

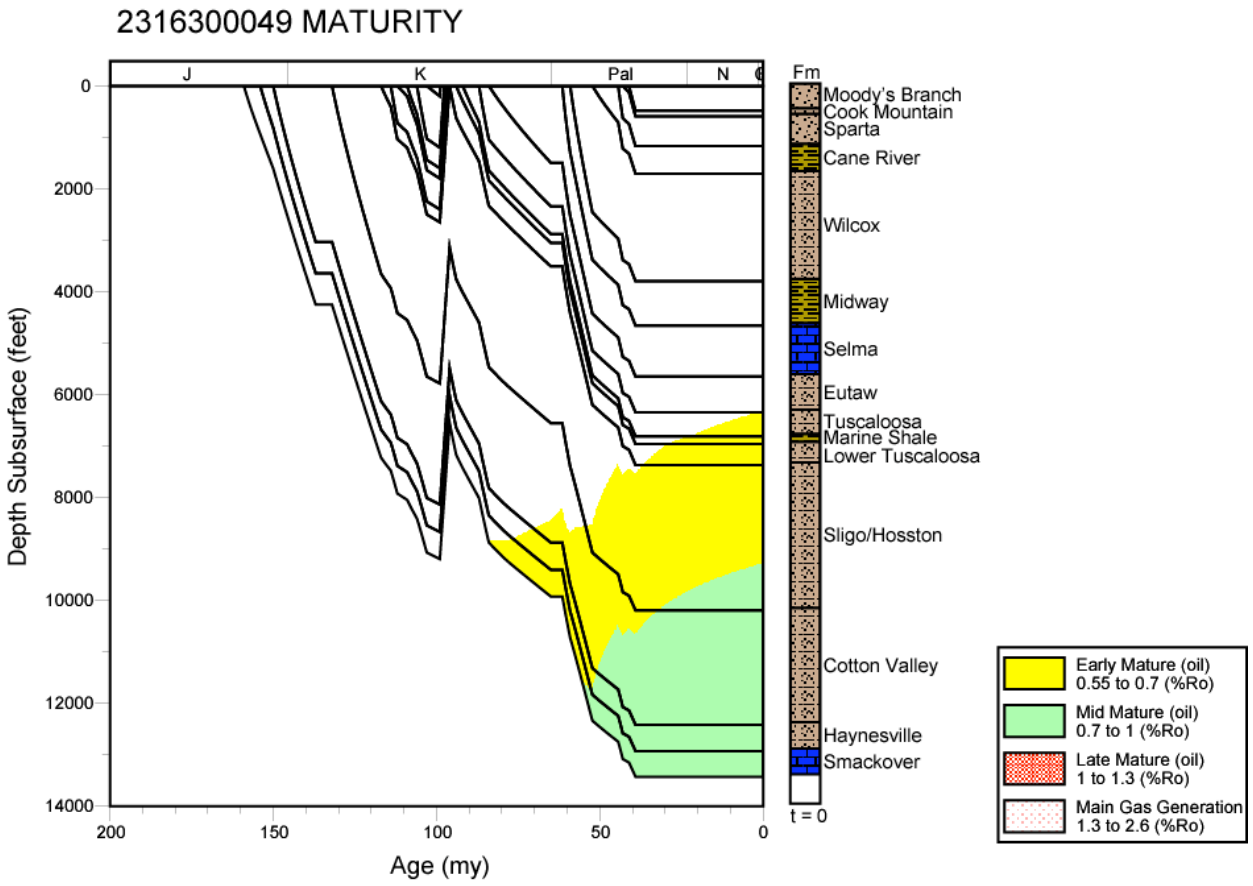


Figure 242. Thermal maturation profile for well 2316300049, Mississippi Interior Salt Basin.

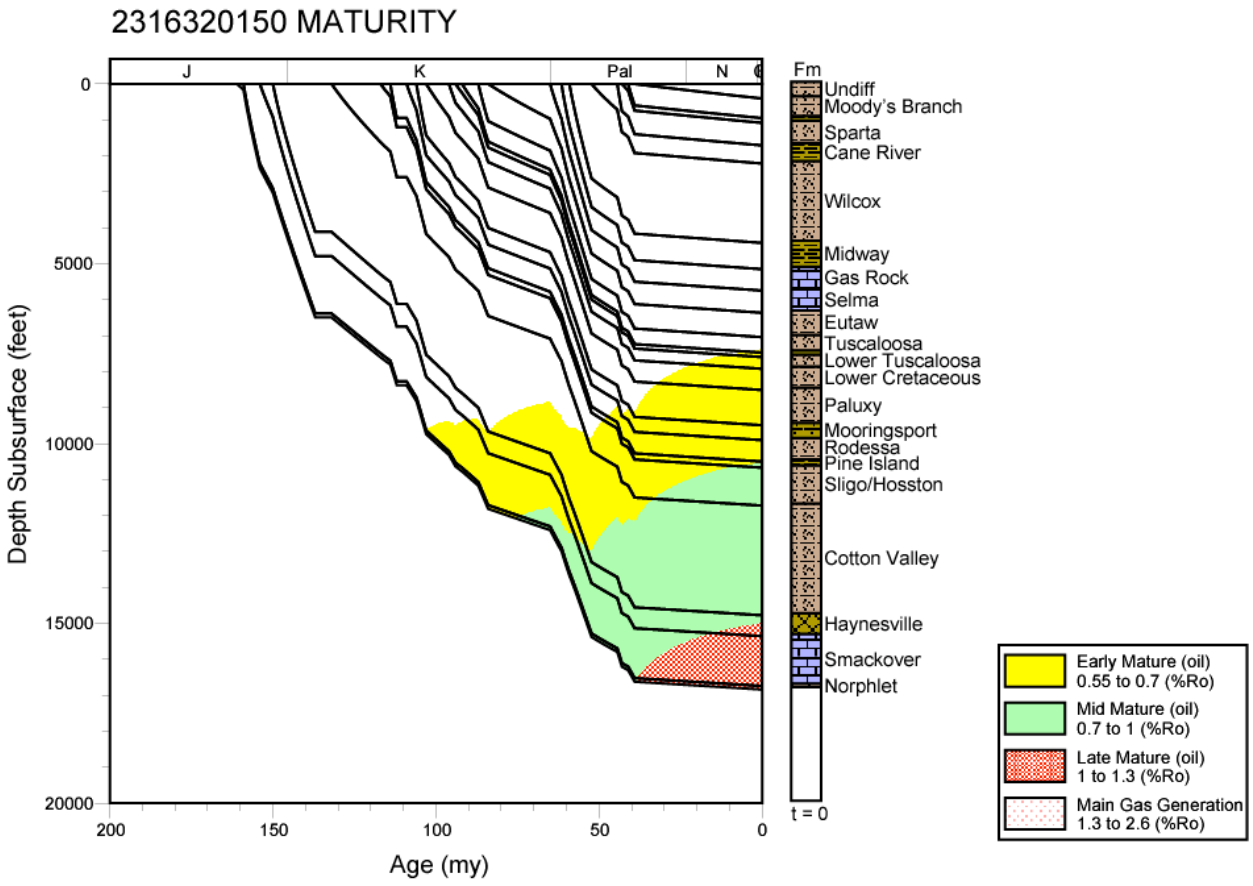


Figure 243. Thermal maturation profile for well 2316320150, Mississippi Interior Salt Basin.

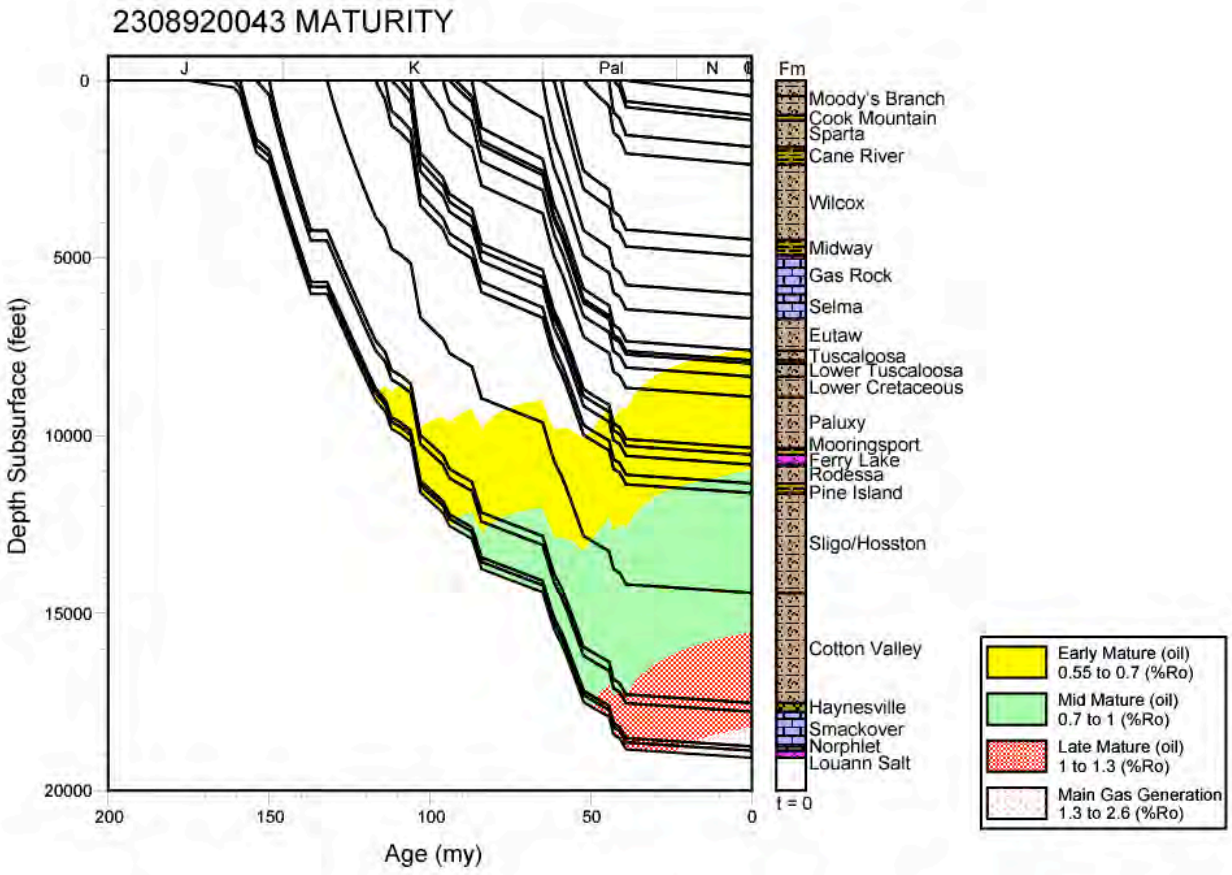


Figure 244. Thermal maturation profile for well 2308920043. Mississippi Interior Salt Basin.

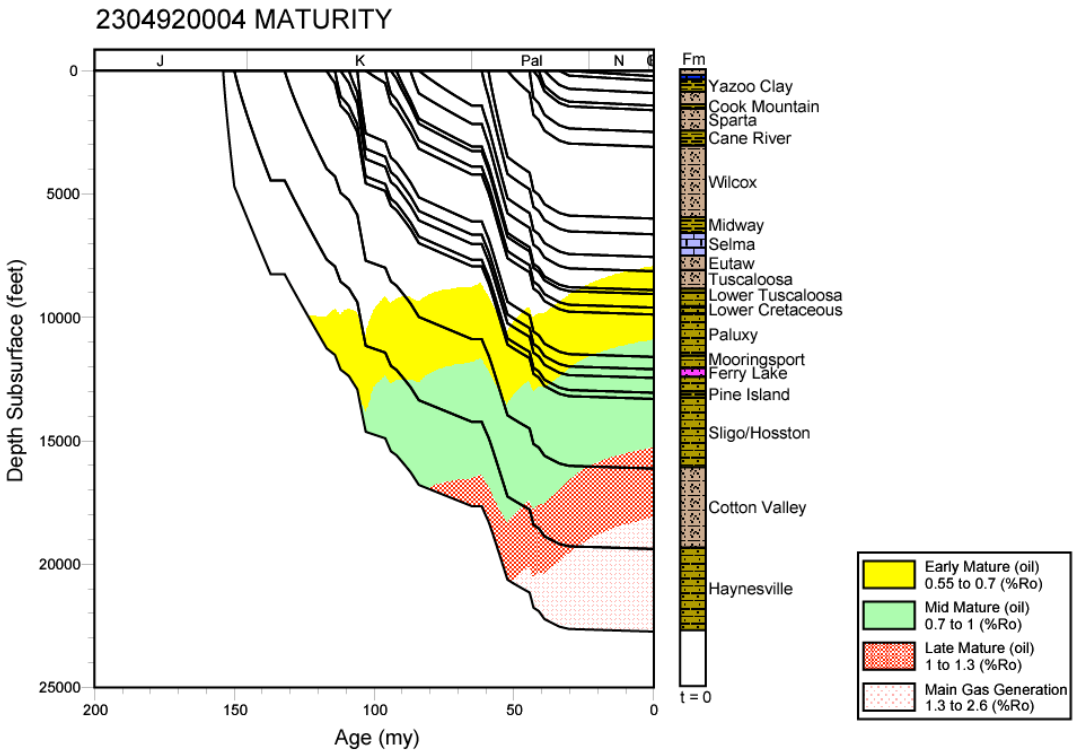


Figure 245. Thermal maturation profile for well 2304920004, Mississippi Interior Salt Basin.

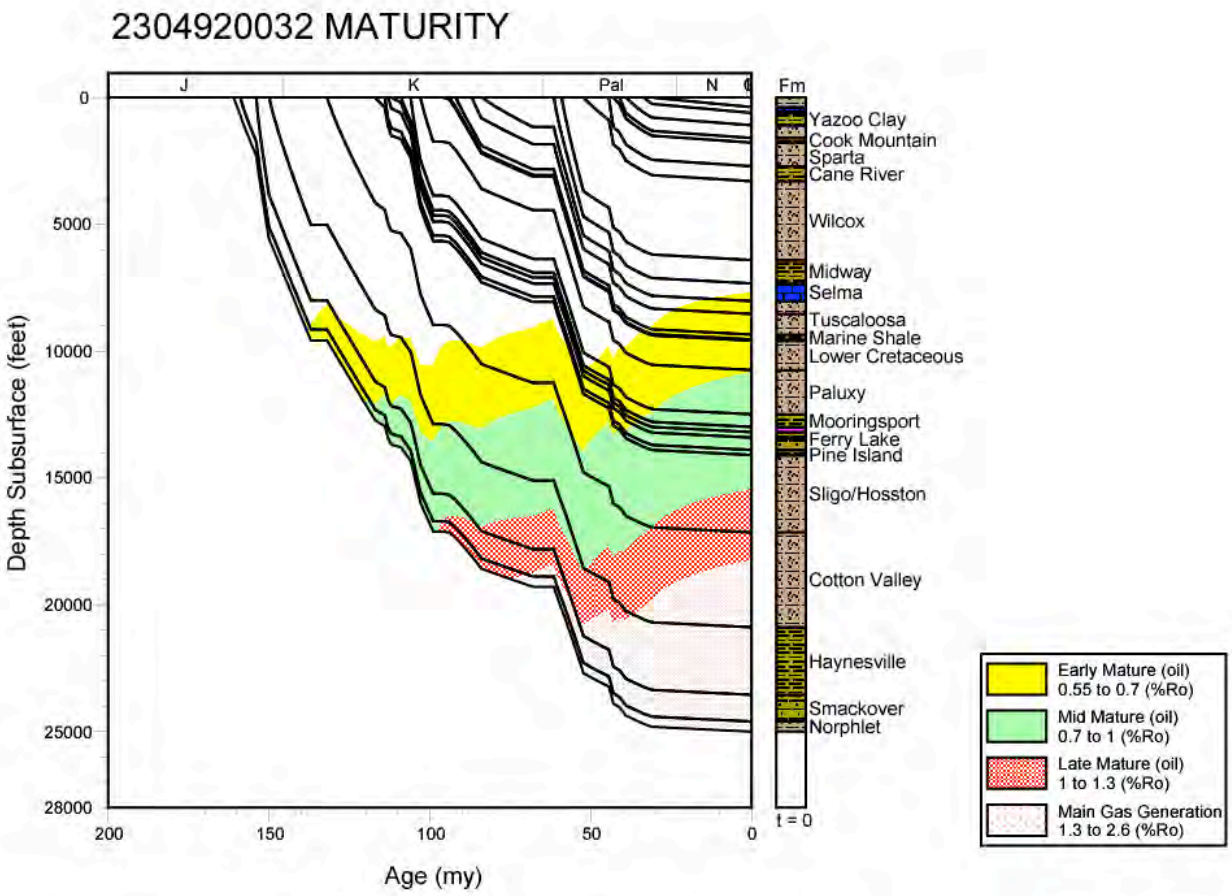


Figure 246. Thermal maturation profile for well 2304920032, Mississippi Interior Salt Basin.

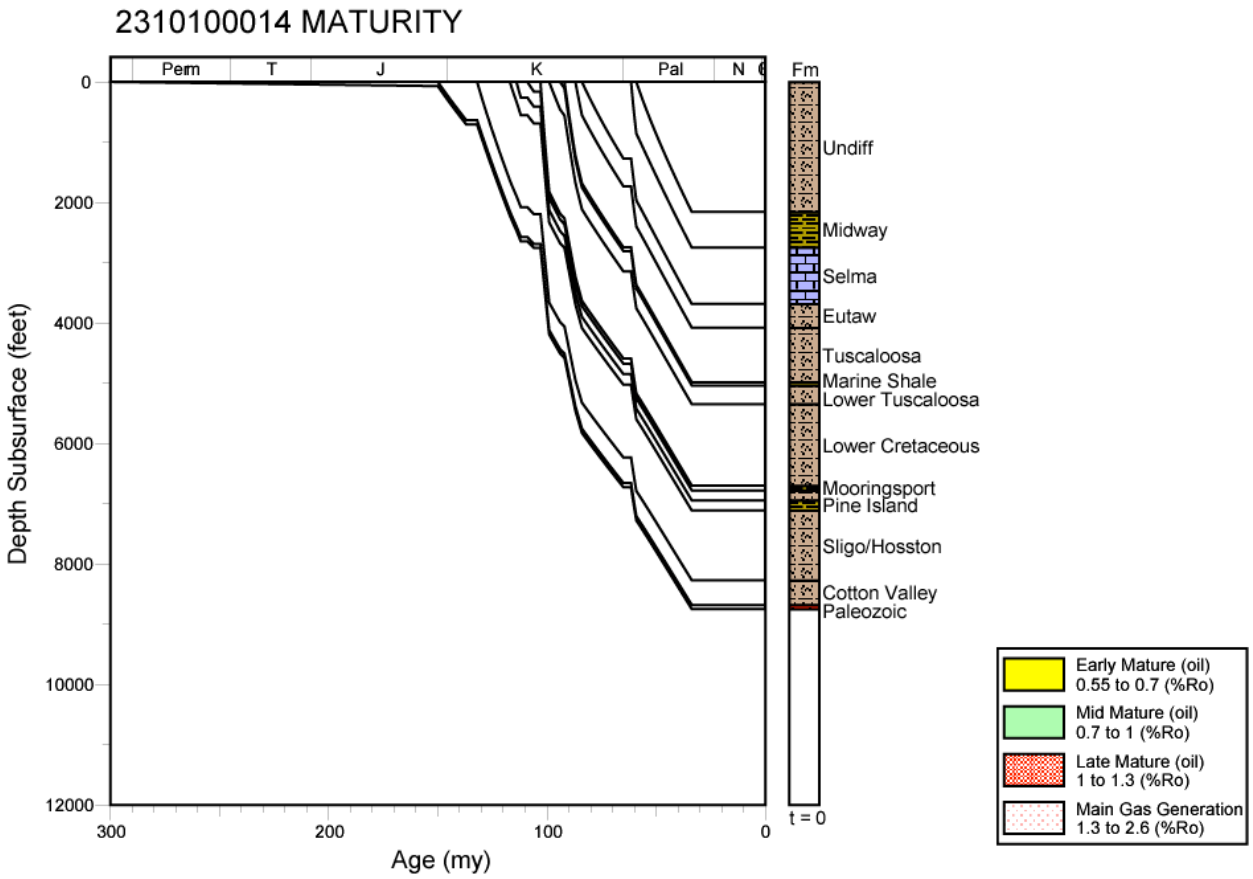


Figure 247. Thermal maturation profile for well 2310100014, Mississippi Interior Salt Basin.

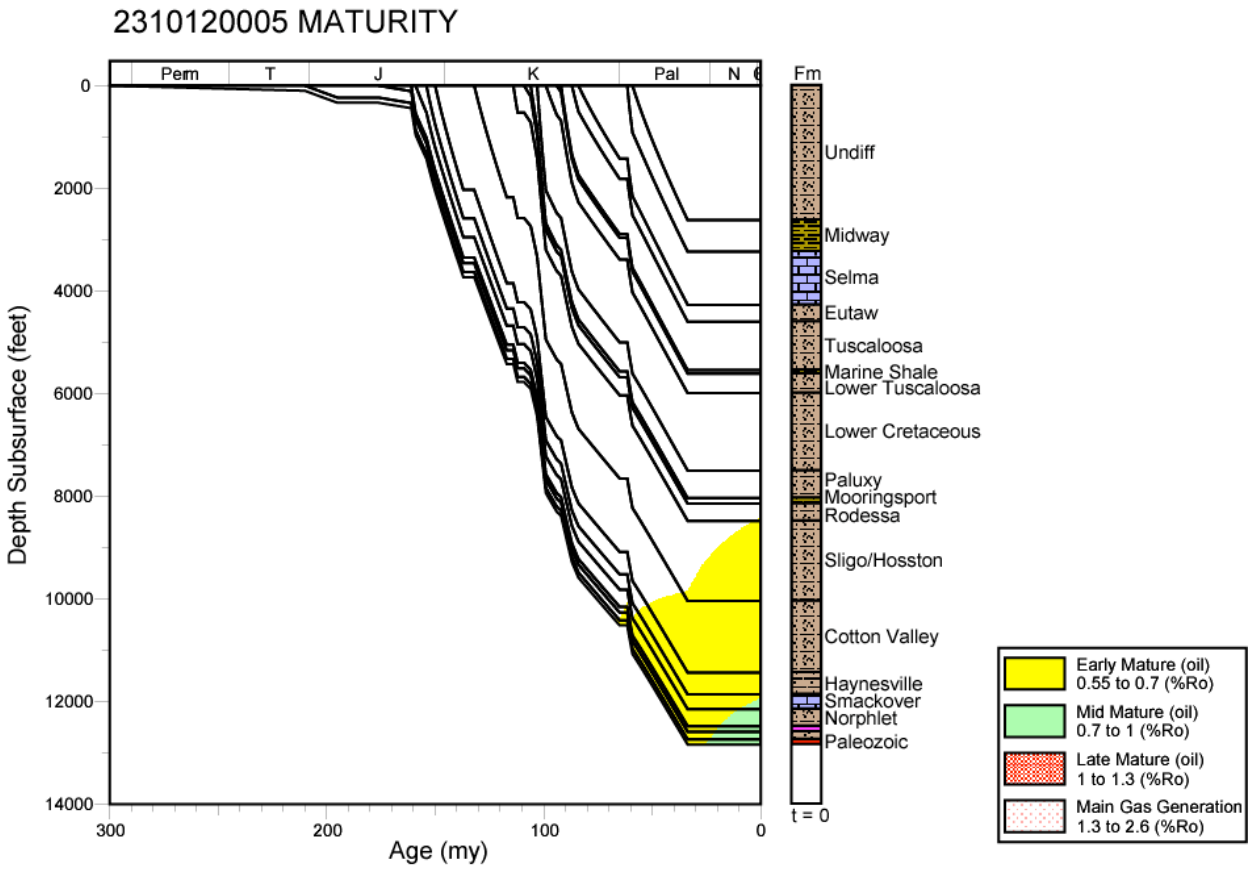


Figure 248. Thermal maturation profile for well 2310120005, Mississippi Interior Salt Basin.

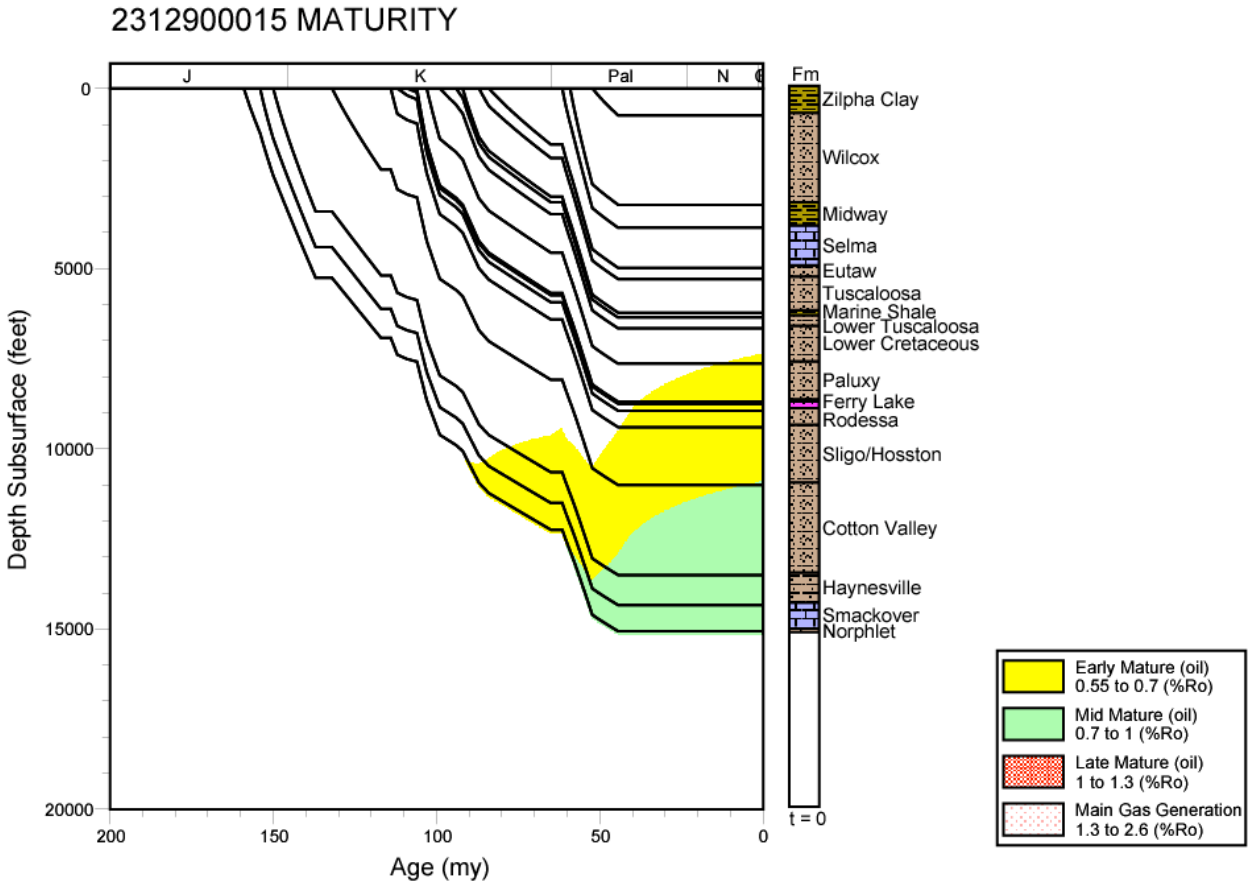


Figure 249. Thermal maturation profile for well 2312900015, Mississippi Interior Salt Basin.

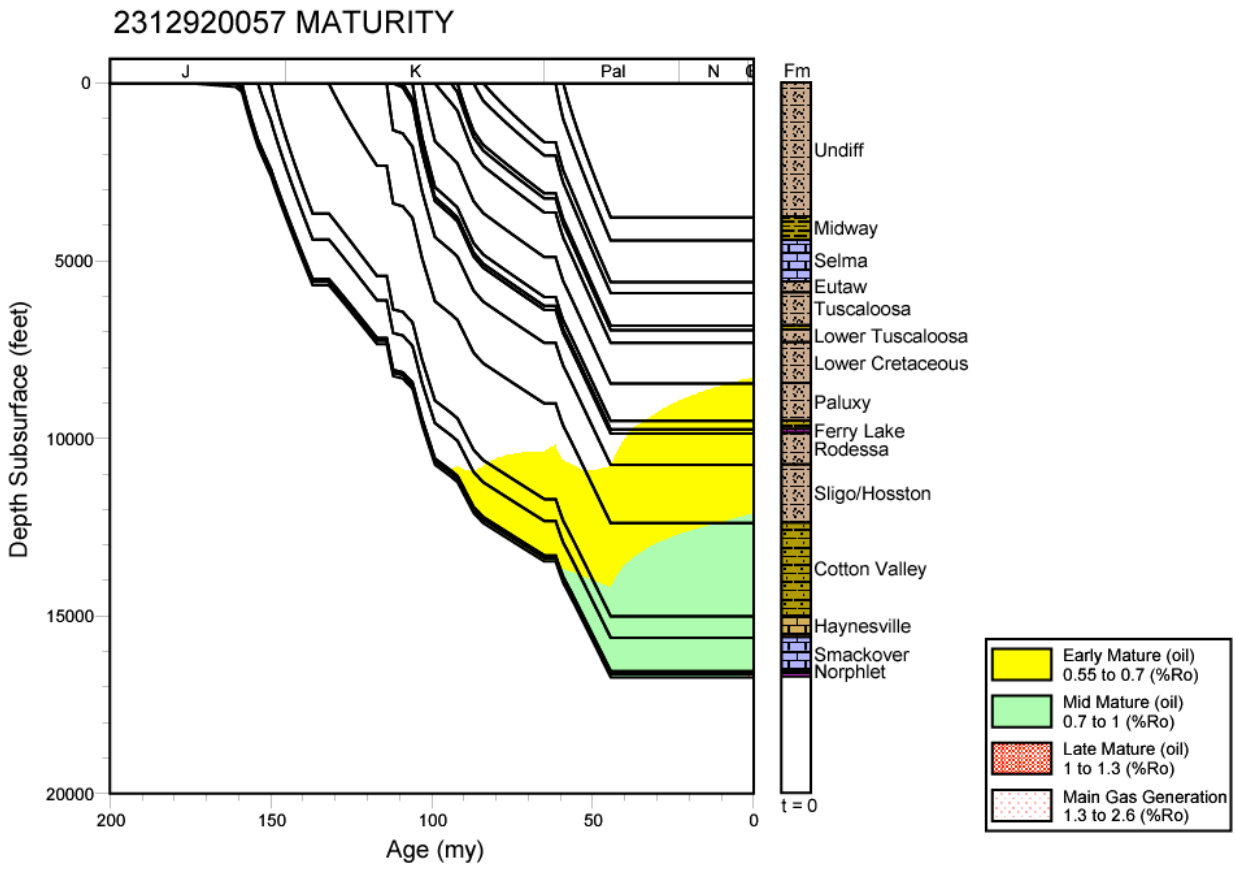


Figure 250. Thermal maturation profile for well 2312920057, Mississippi Interior Salt Basin.

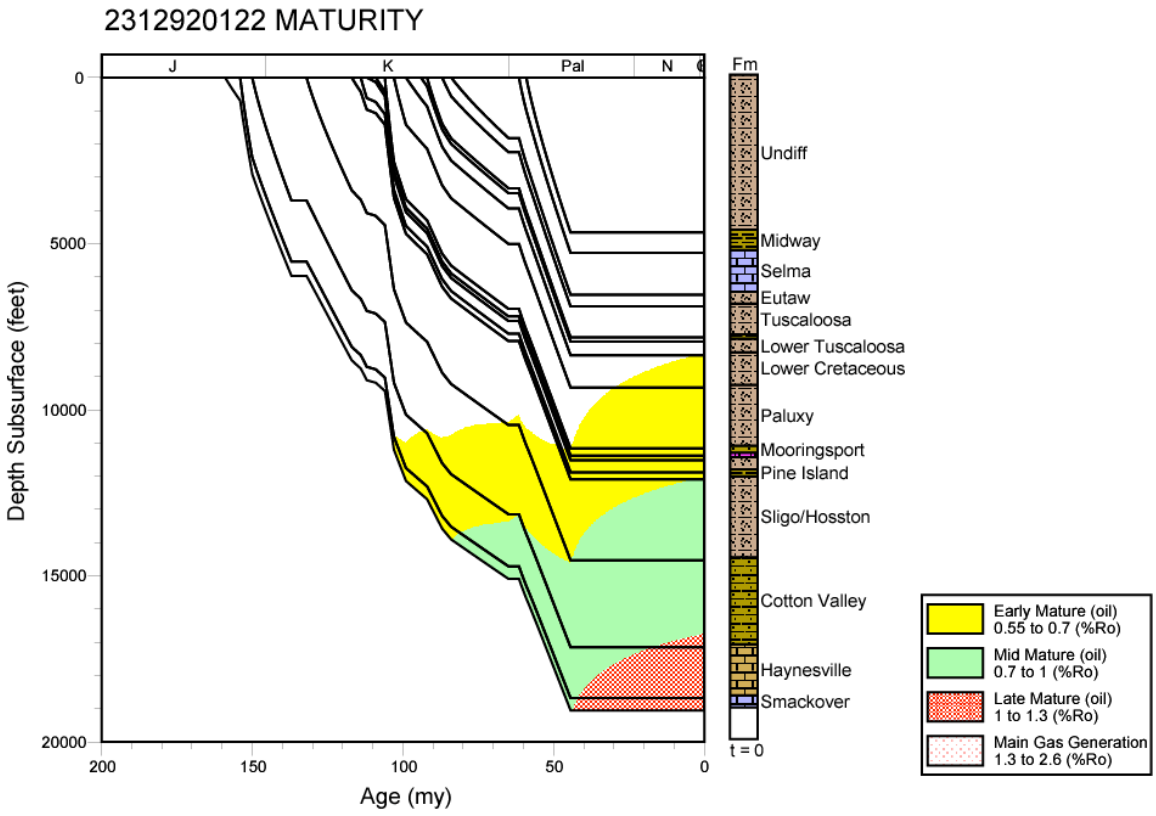


Figure 251. Thermal maturation profile for well 2312920122, Mississippi Interior Salt Basin.

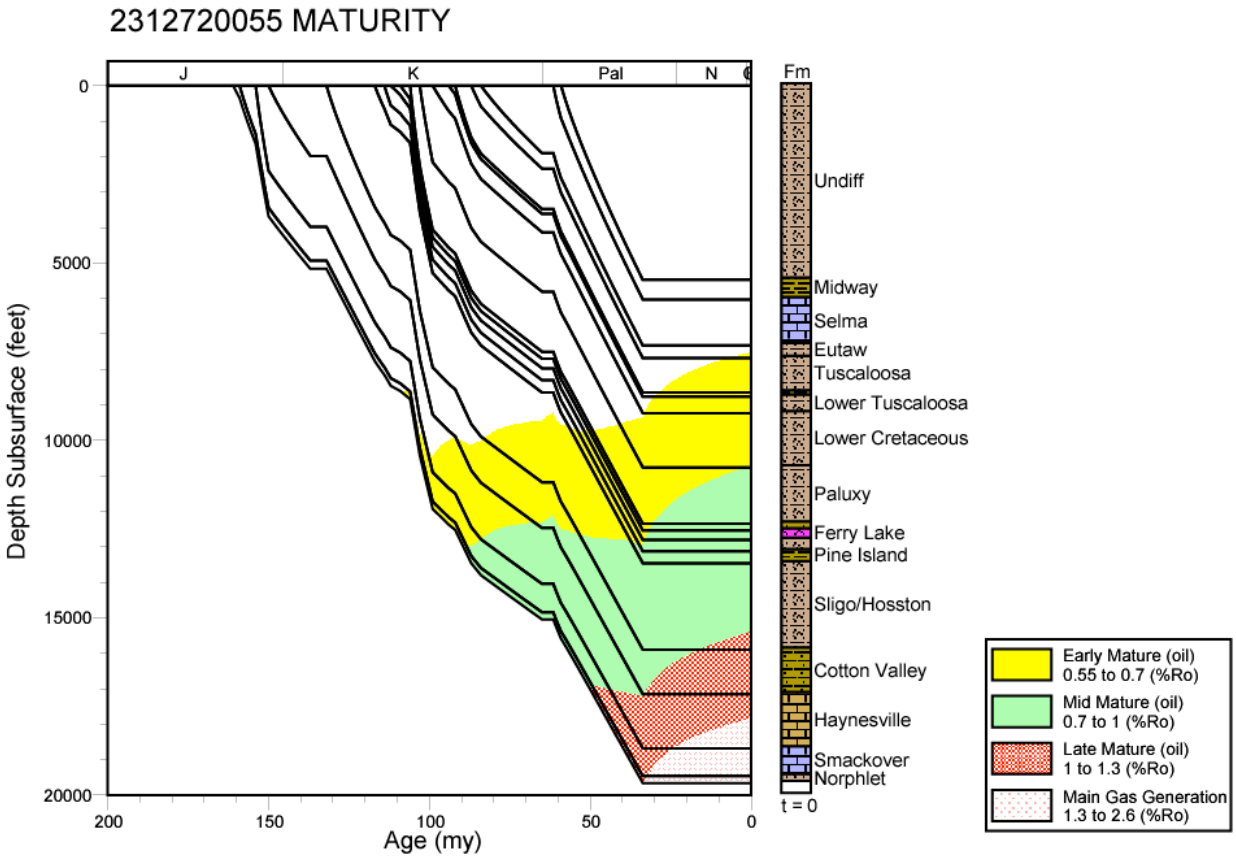


Figure 252. Thermal maturation profile for well 2312720055, Mississippi Interior Salt Basin.

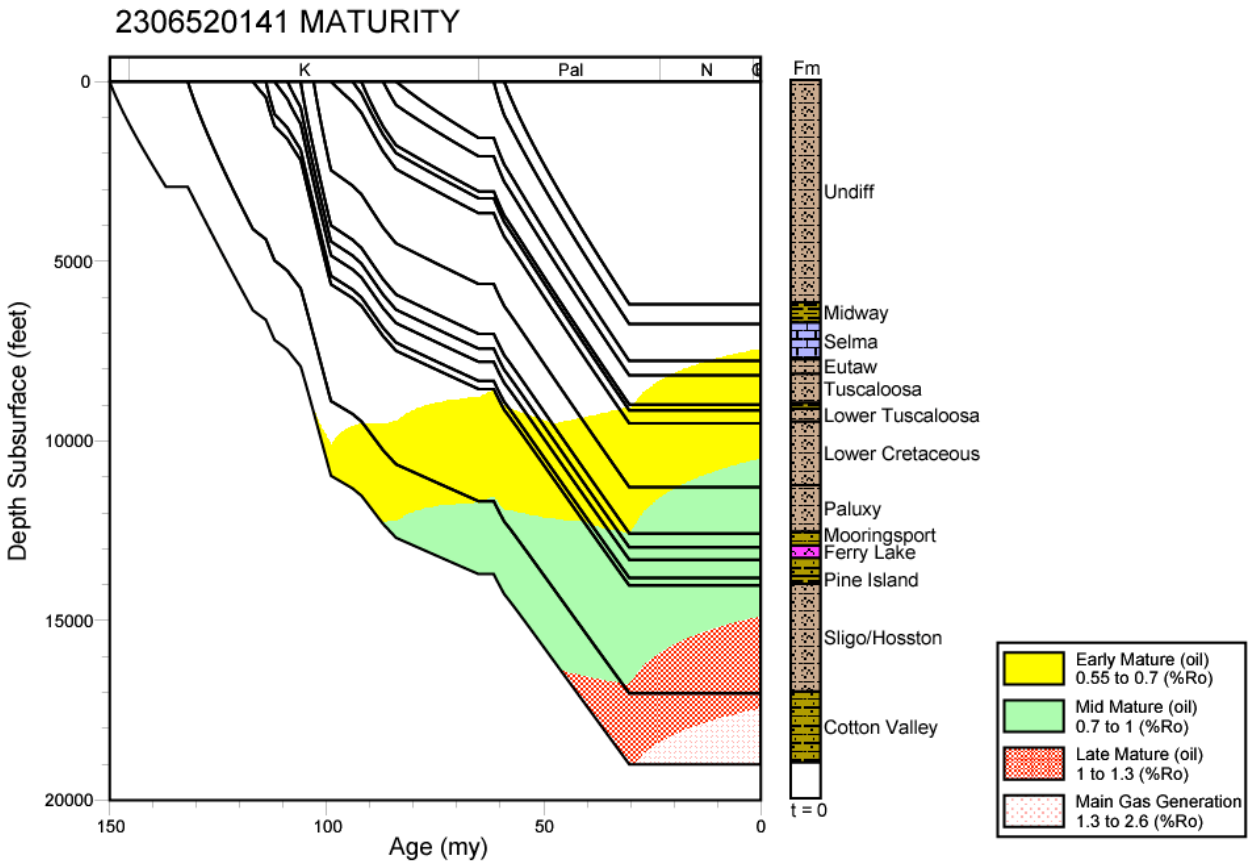


Figure 253. Thermal maturation profile for well 2306520141, Mississippi Interior Salt Basin.

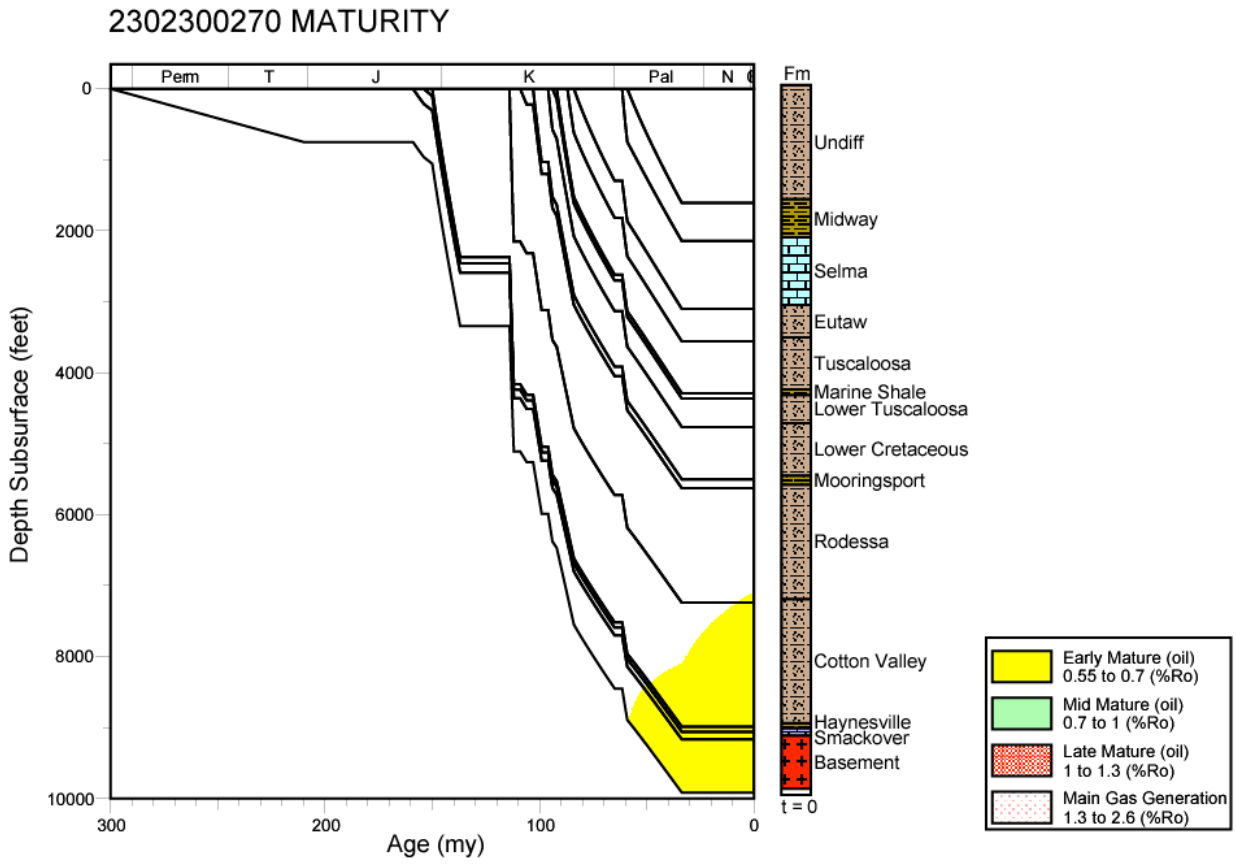


Figure 254. Thermal maturation profile for well 2302300270, Mississippi Interior Salt Basin.

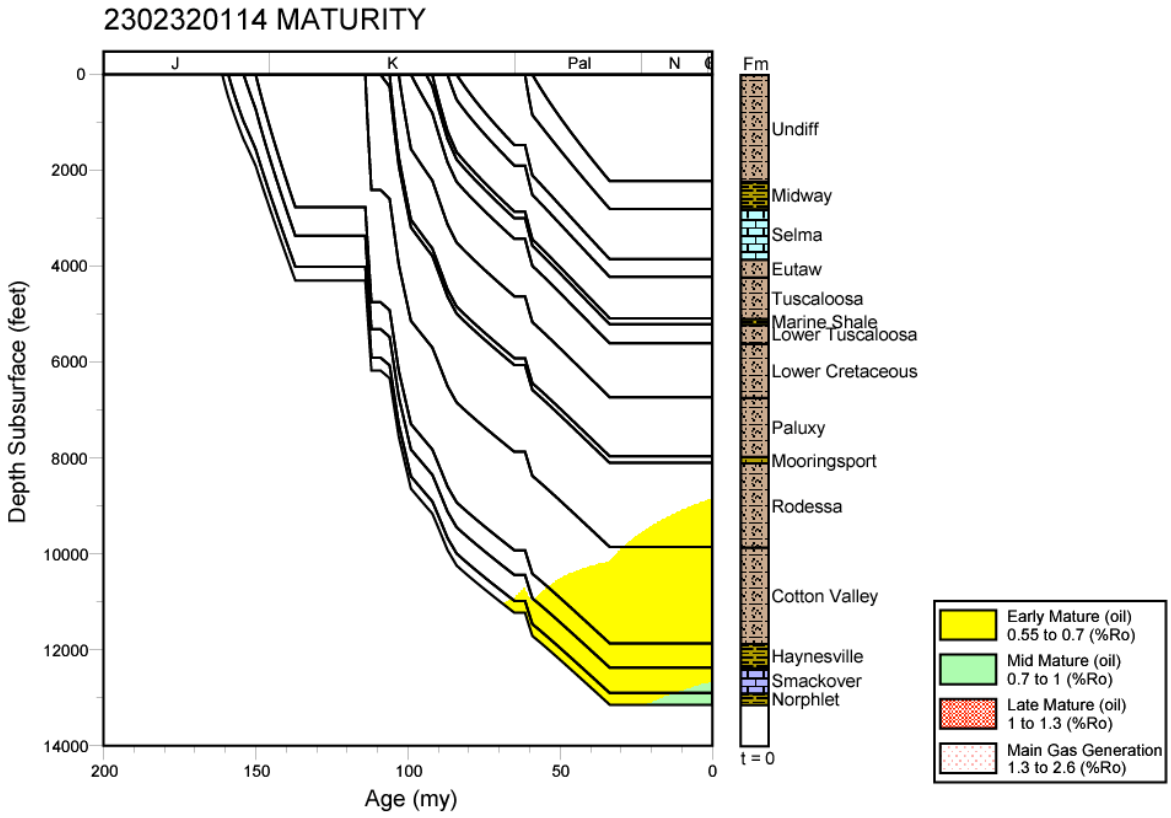


Figure 255. Thermal maturation profile for well 2302320114, Mississippi Interior Salt Basin.

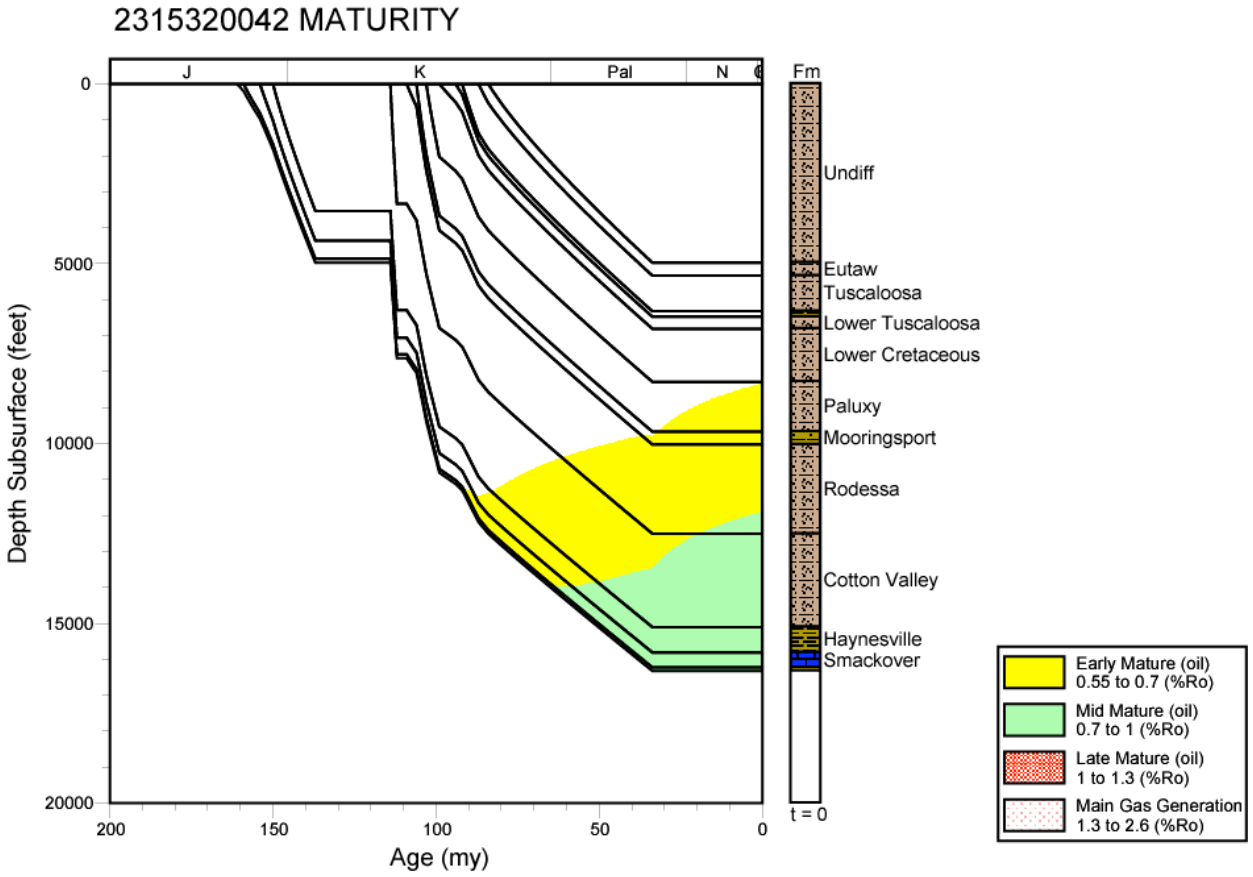


Figure 256. Thermal maturation profile for well 2315320042, Mississippi Interior Salt Basin.

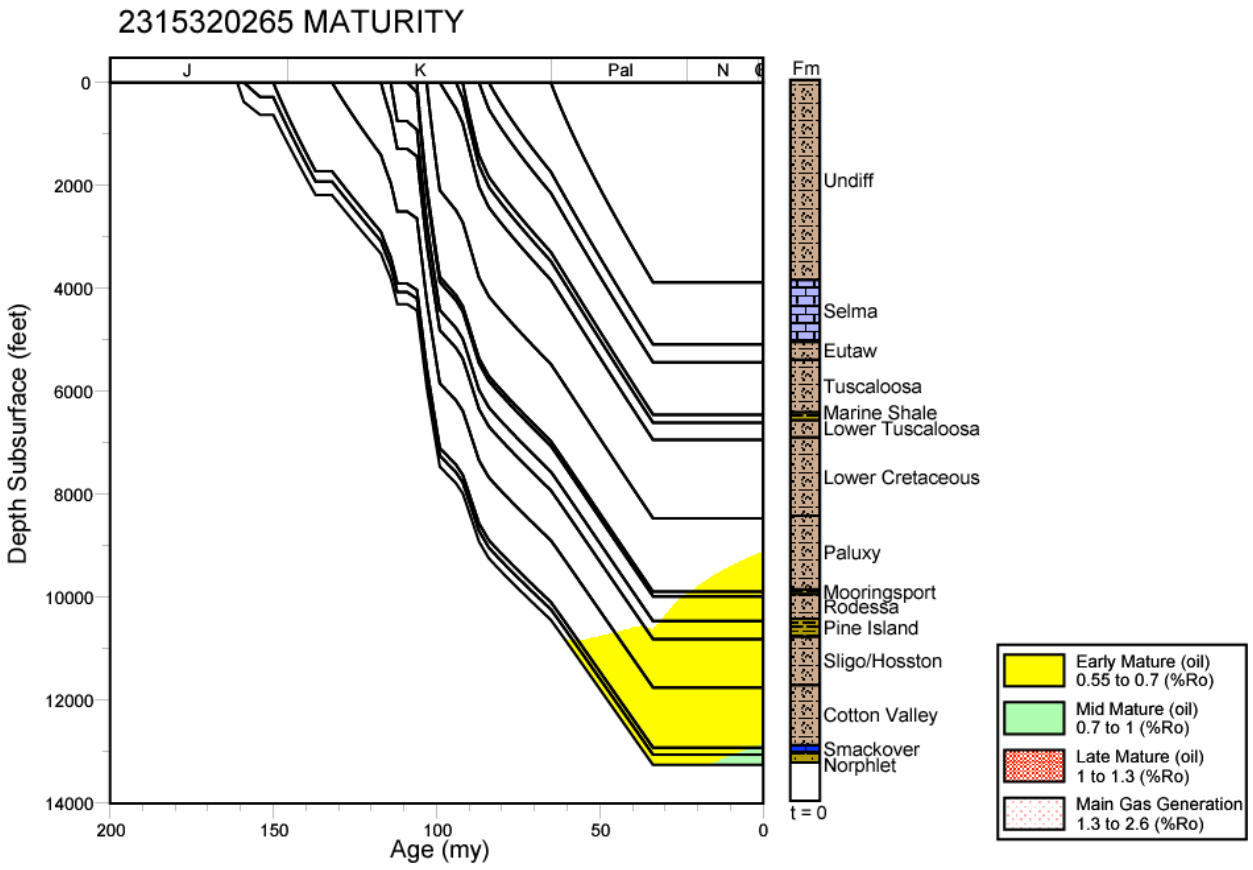


Figure 257. Thermal maturation profile for well 2315320265, Mississippi Interior Salt Basin.

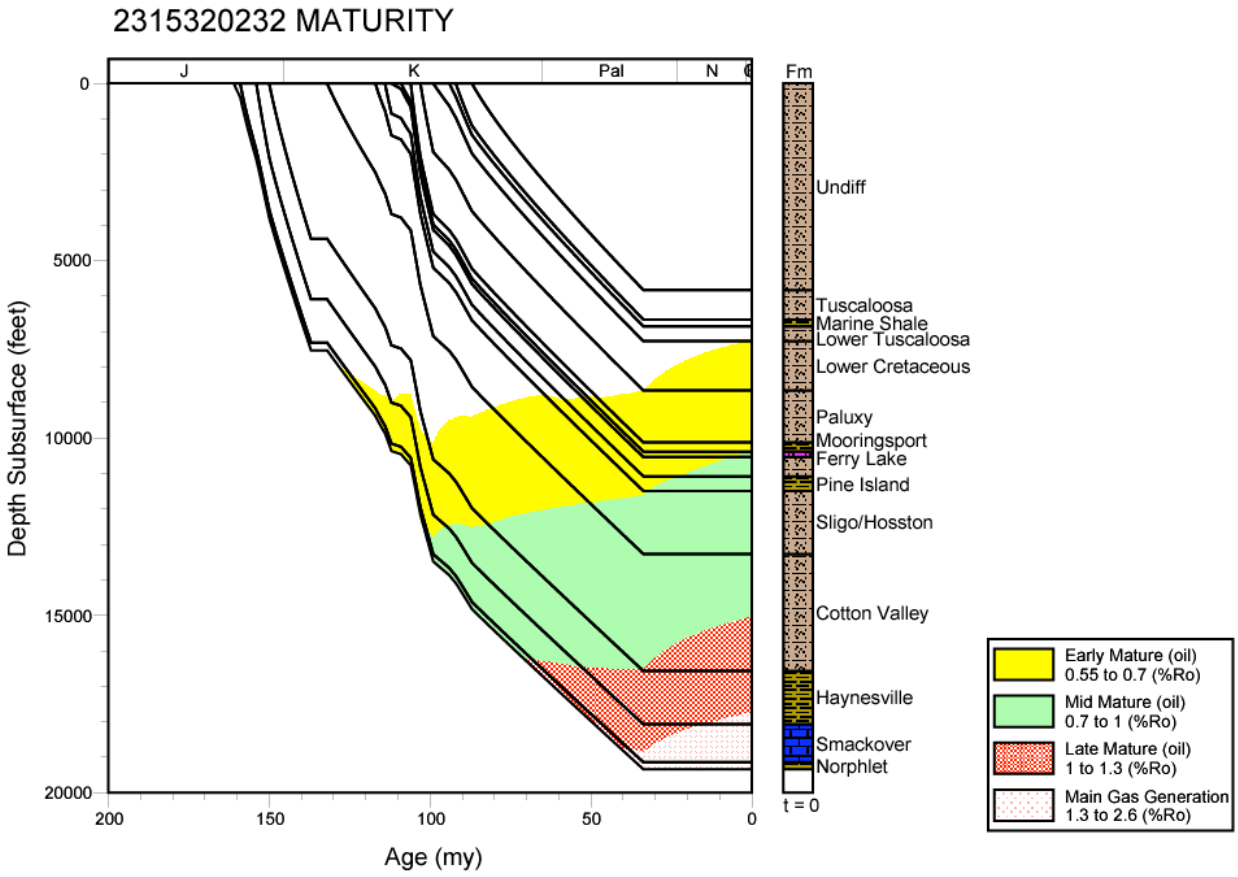


Figure 258. Thermal maturation profile for well 2315320232, Mississippi Interior Salt Basin.

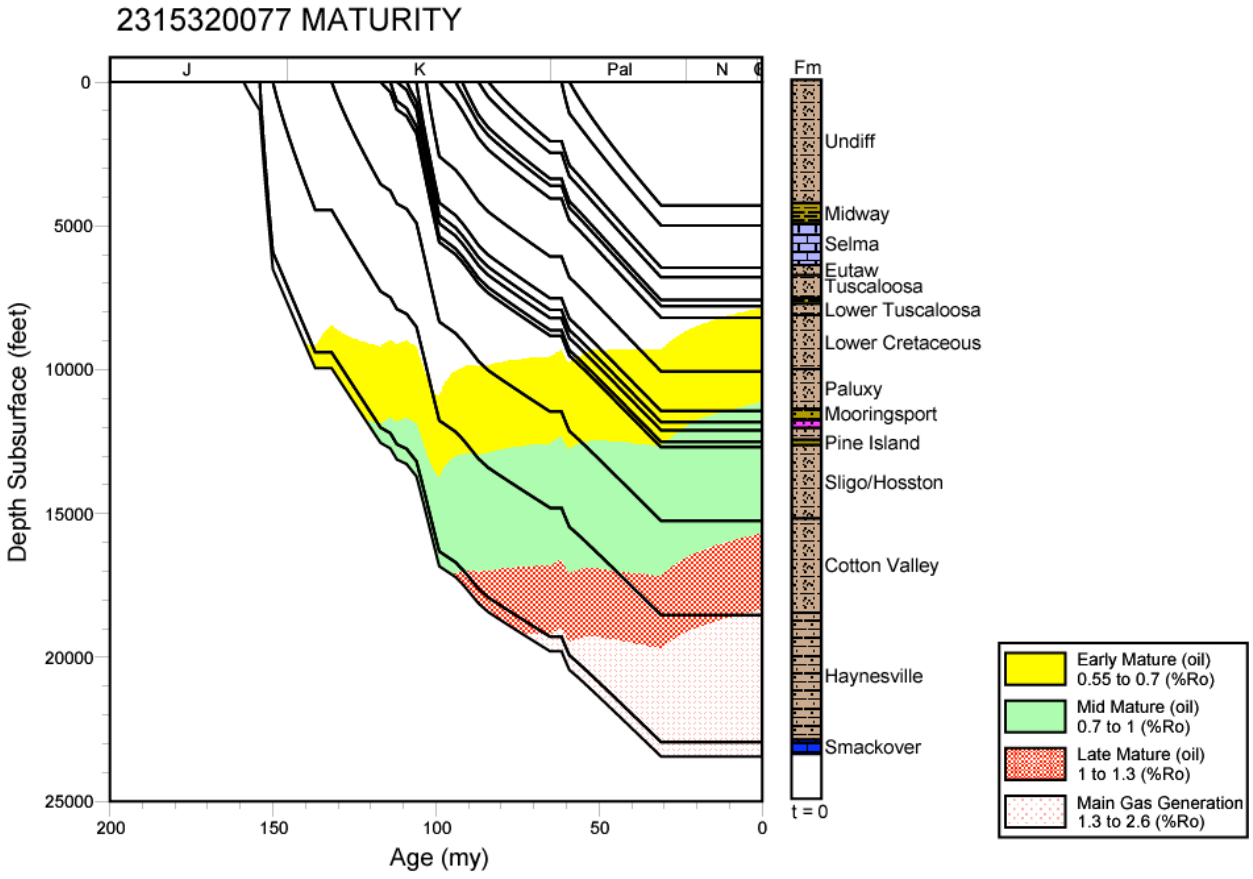


Figure 259. Thermal maturation profile for well 2315320077, Mississippi Interior Salt Basin.

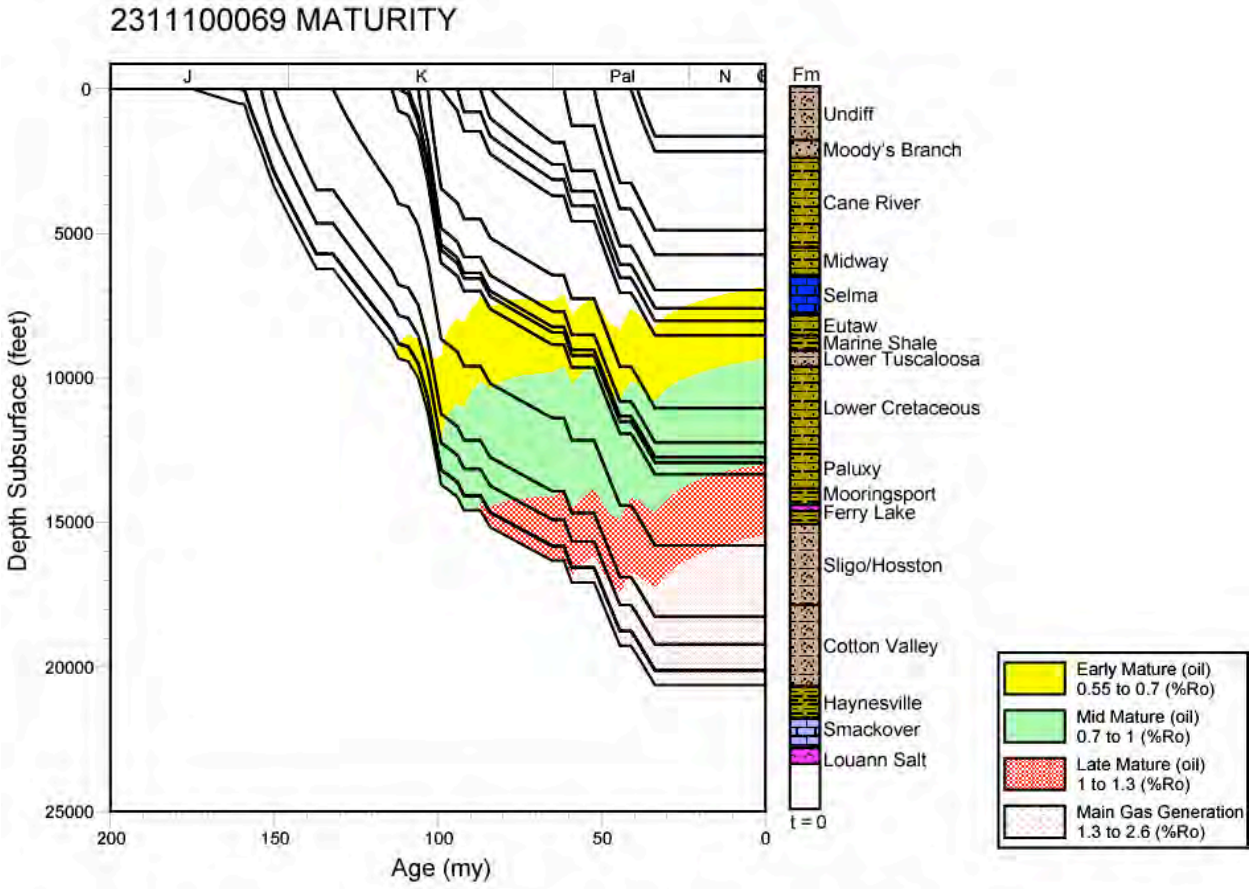


Figure 260. Thermal maturation profile for well 2311100069, Mississippi Interior Salt Basin.

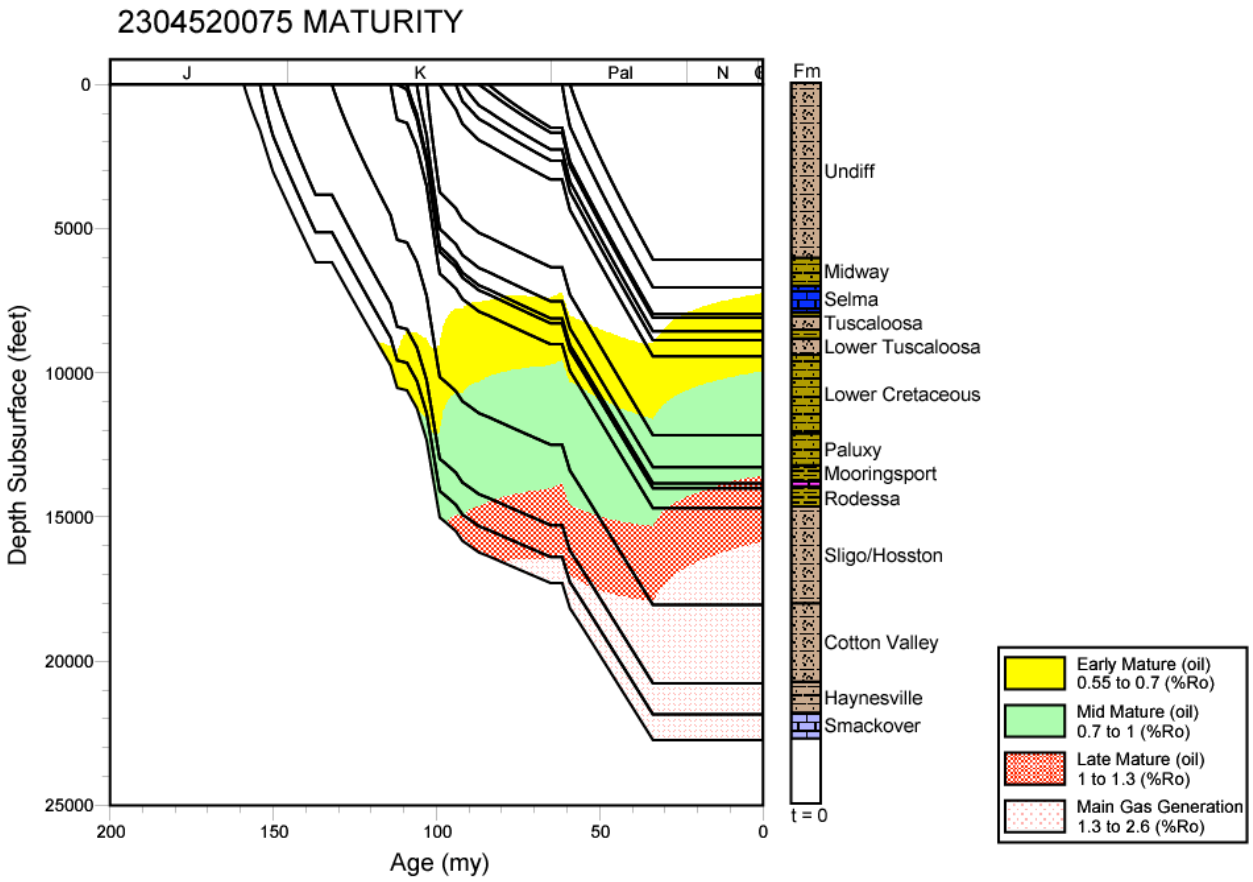


Figure 261. Thermal maturation profile for well 2304520075, Mississippi Interior Salt Basin.

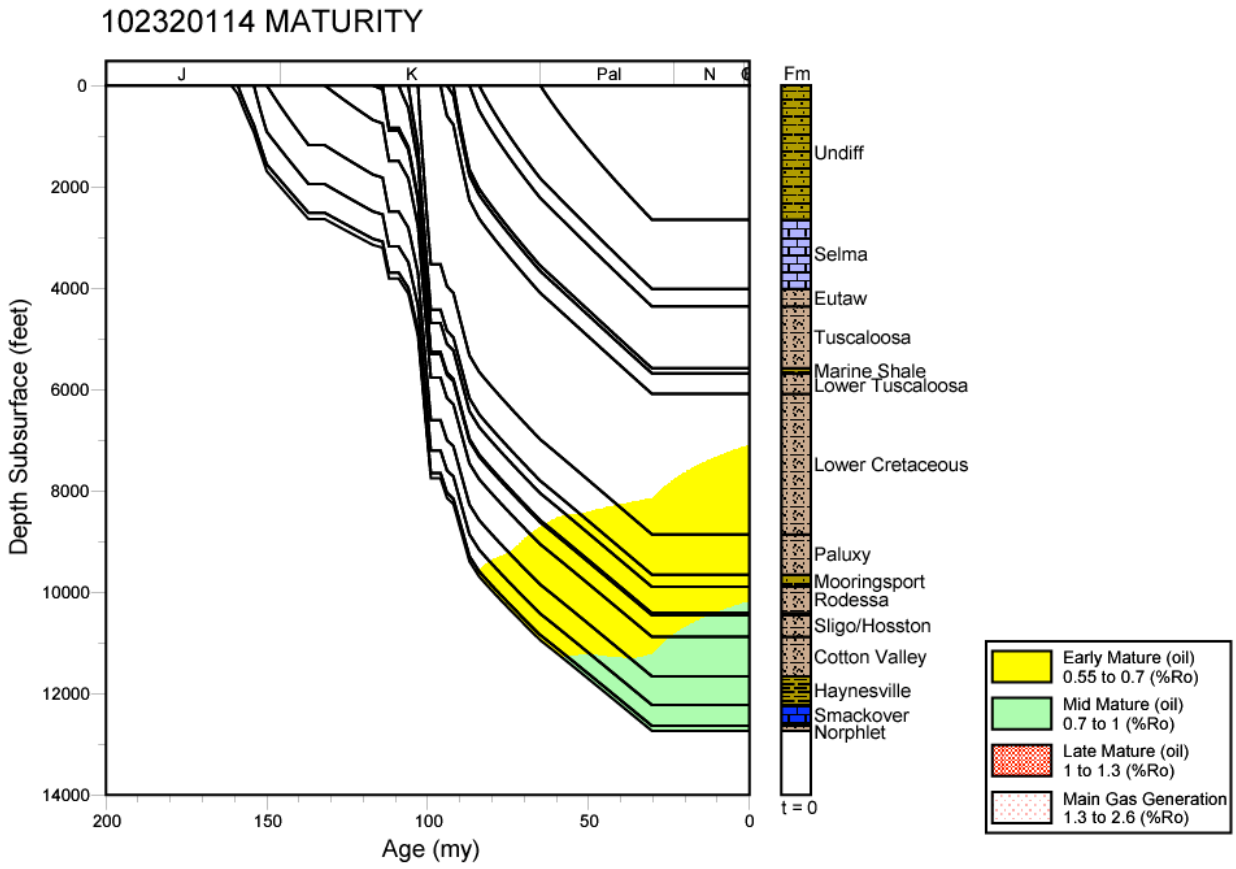


Figure 262. Thermal maturation profile for well 102320114, Mississippi Interior Salt Basin.

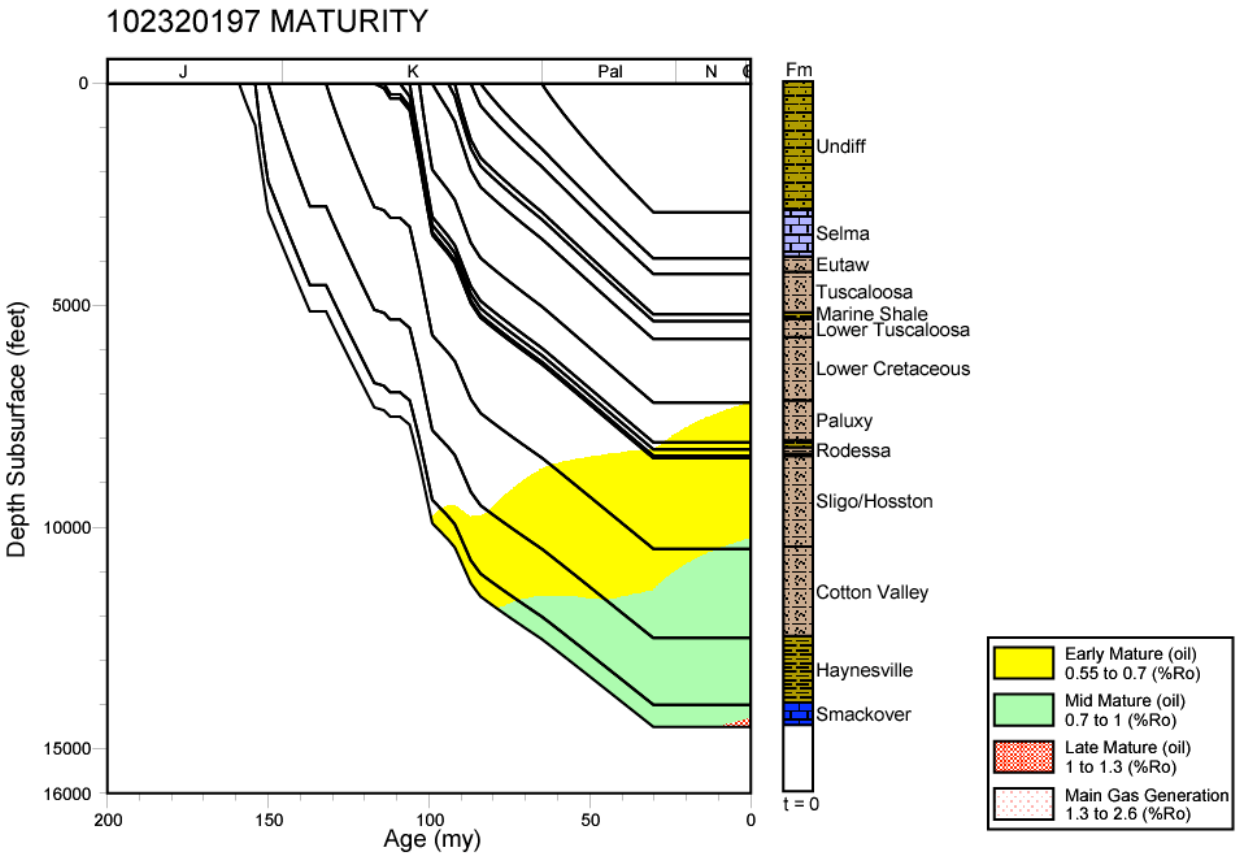


Figure 263. Thermal maturation profile for well 102320197, Mississippi Interior Salt Basin.

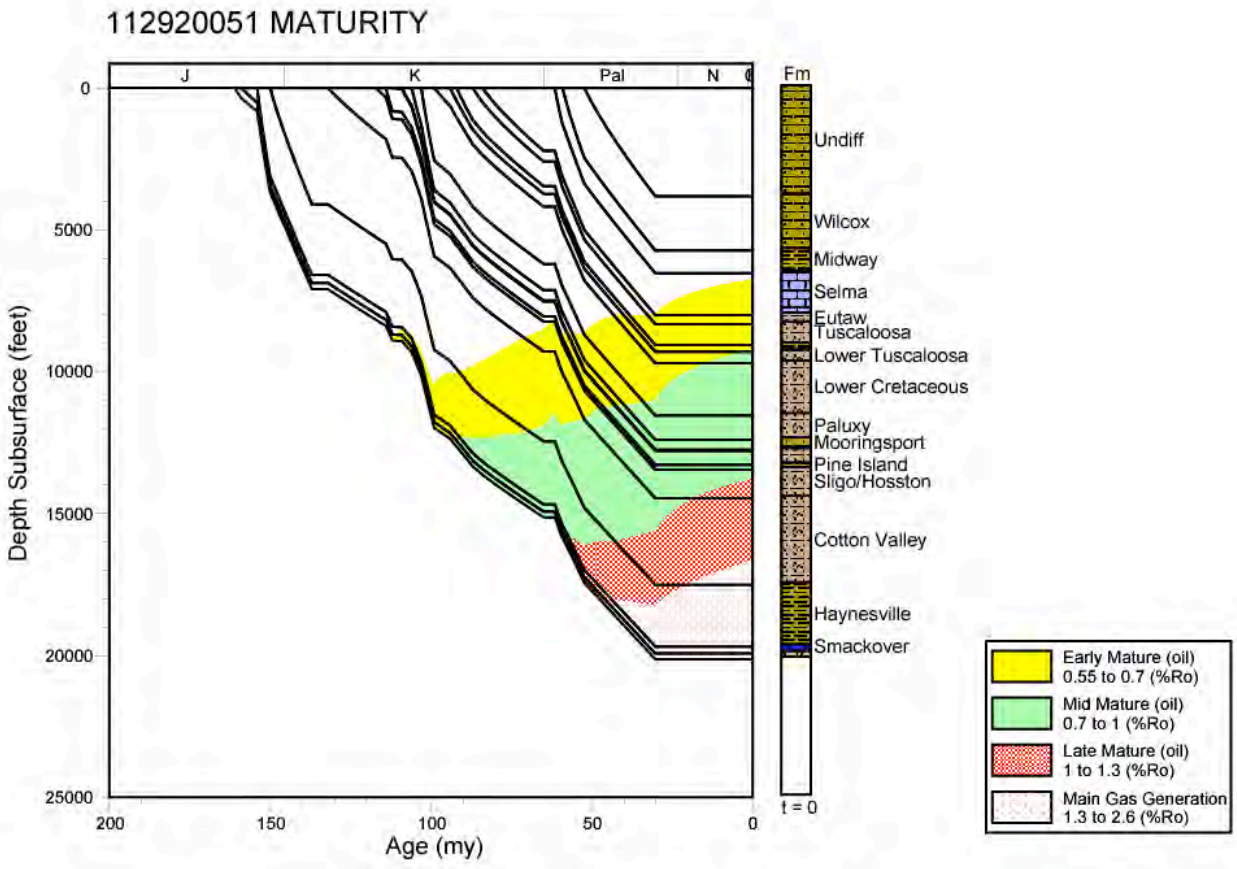


Figure 264. Thermal maturation profile for well 112920051, Mississippi Interior Salt Basin.

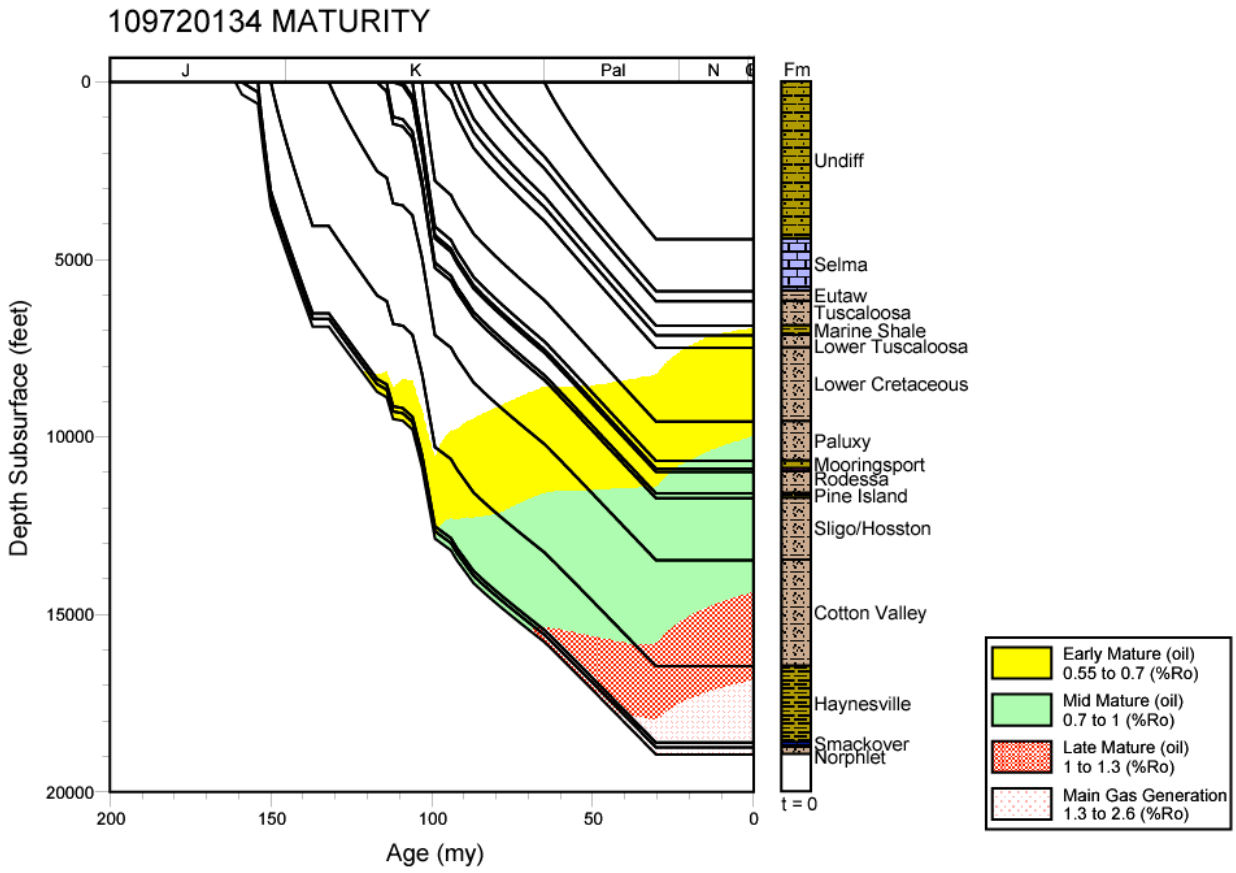


Figure 265. Thermal maturation profile for well 109720134, Mississippi Interior Salt Basin.

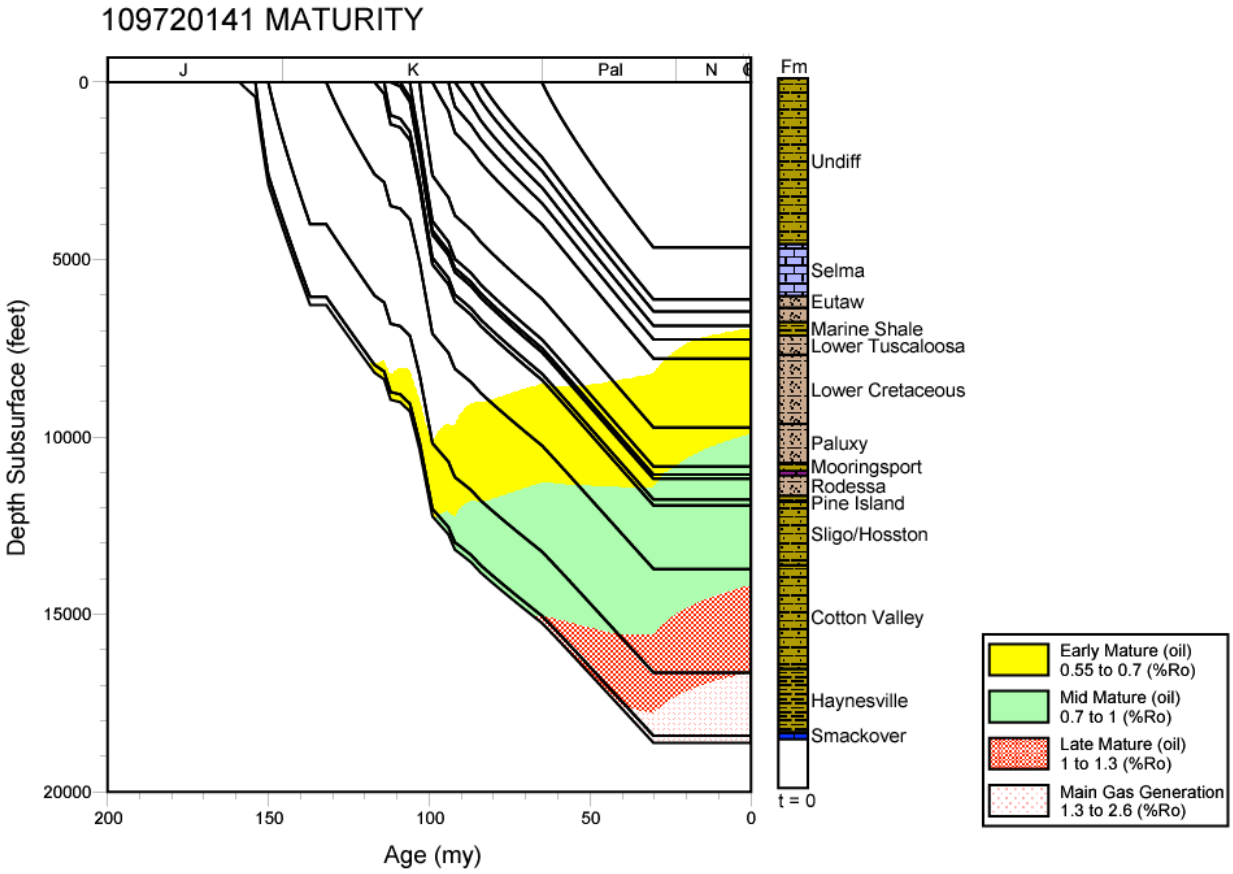


Figure 266. Thermal maturation profile for well 109720141, Mississippi Interior Salt Basin.

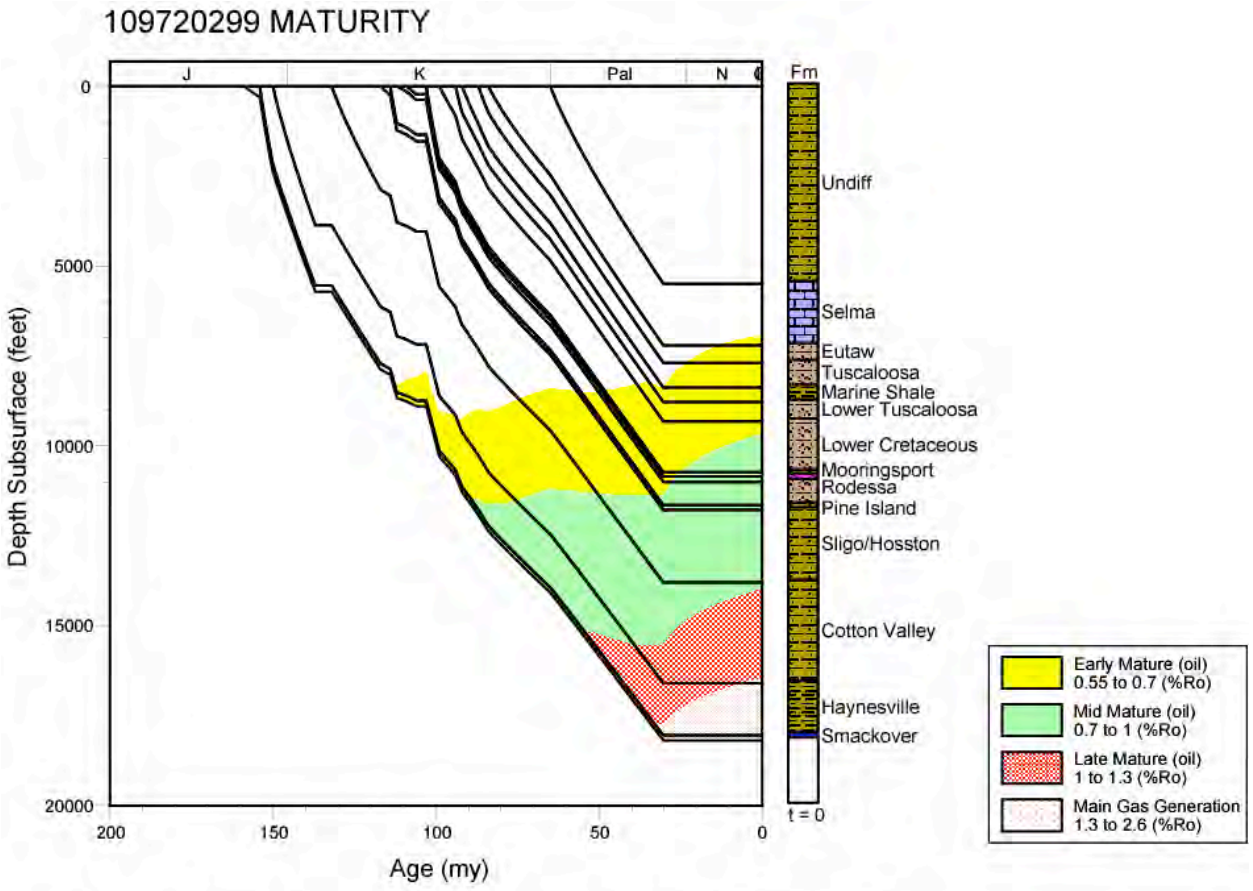


Figure 267. Thermal maturation profile for well 109720299, Mississippi Interior Salt Basin.

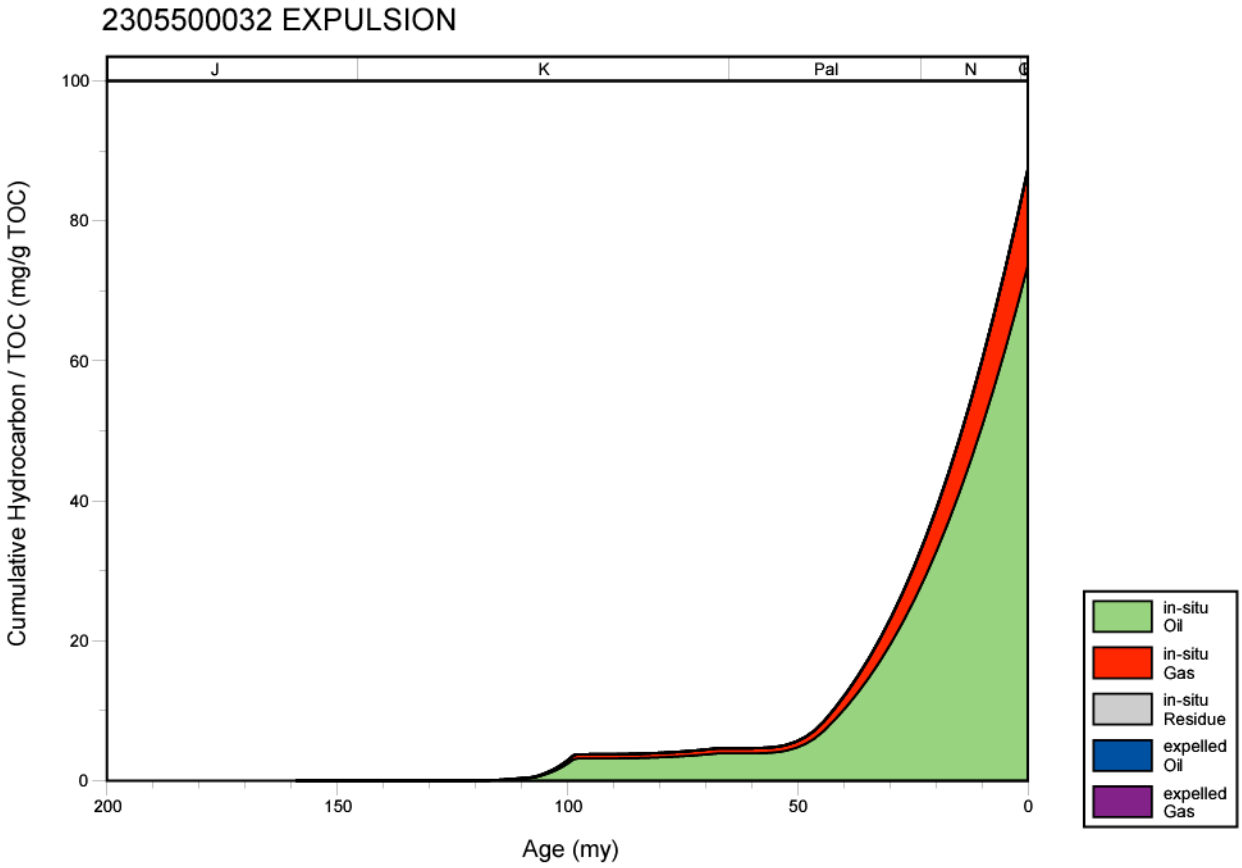


Figure 268. Hydrocarbon expulsion plot for well 2305500032, Mississippi Interior Salt Basin.

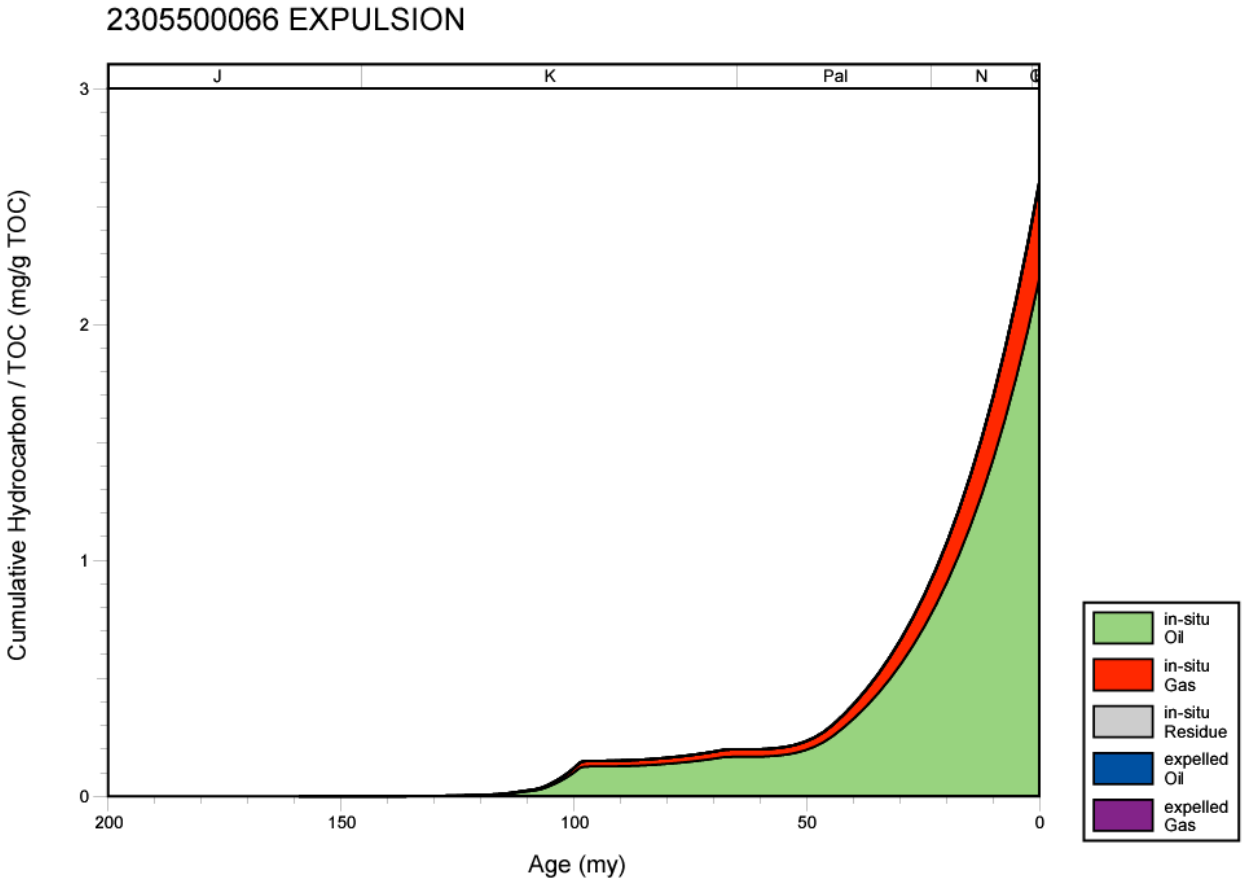


Figure 269. Hydrocarbon expulsion plot for well 2305500066, Mississippi Interior Salt Basin.

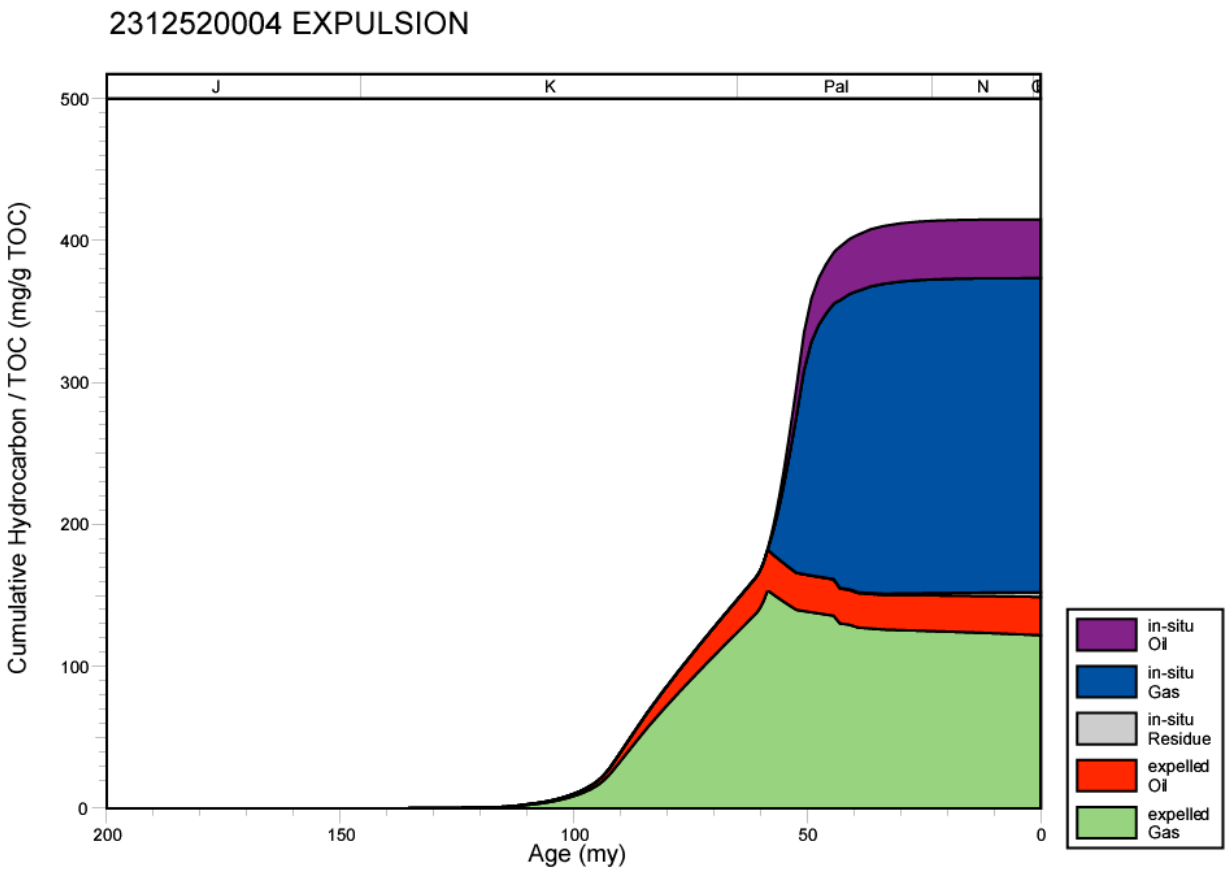


Figure 270. Hydrocarbon expulsion plot for well 2312520004, Mississippi Interior Salt Basin.

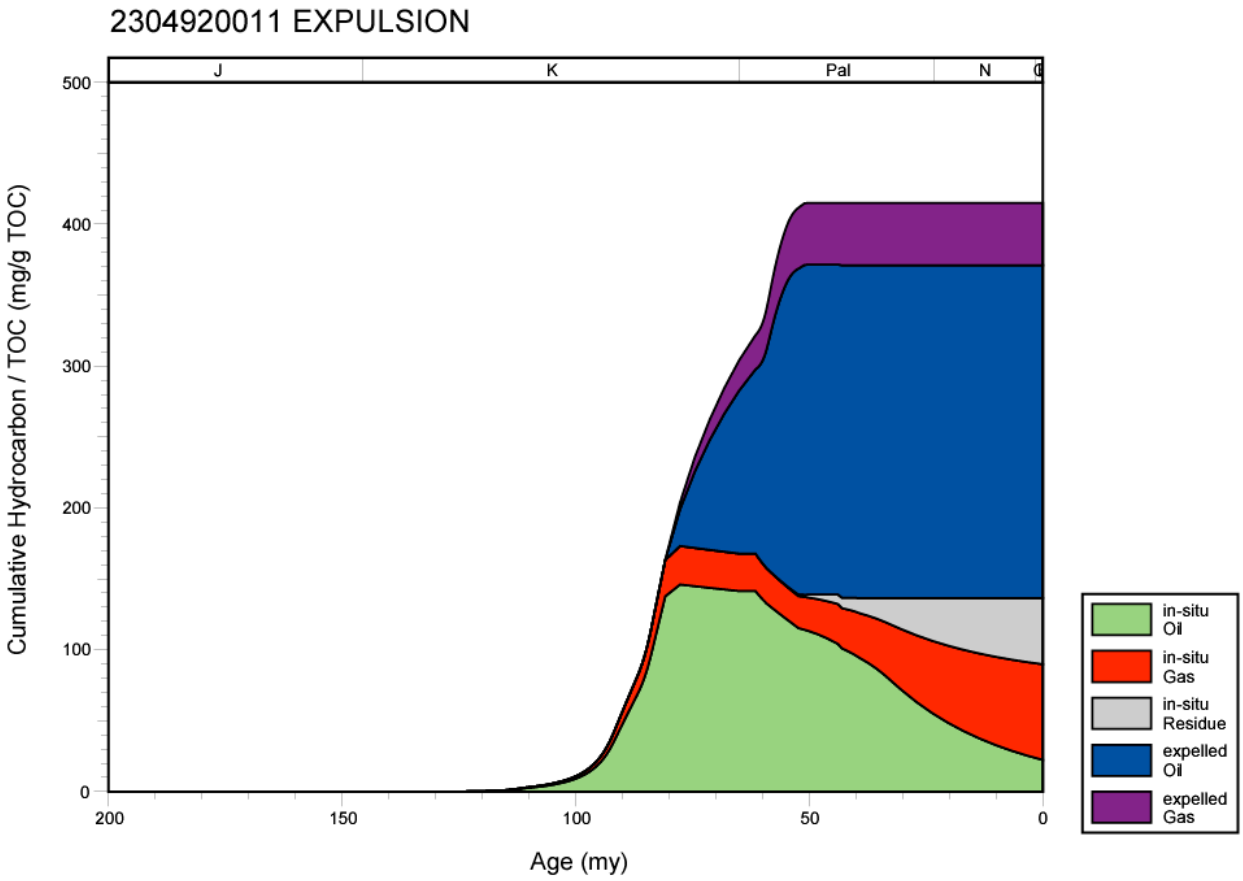


Figure 271. Hydrocarbon expulsion plot for well 2304920011, Mississippi Interior Salt Basin.

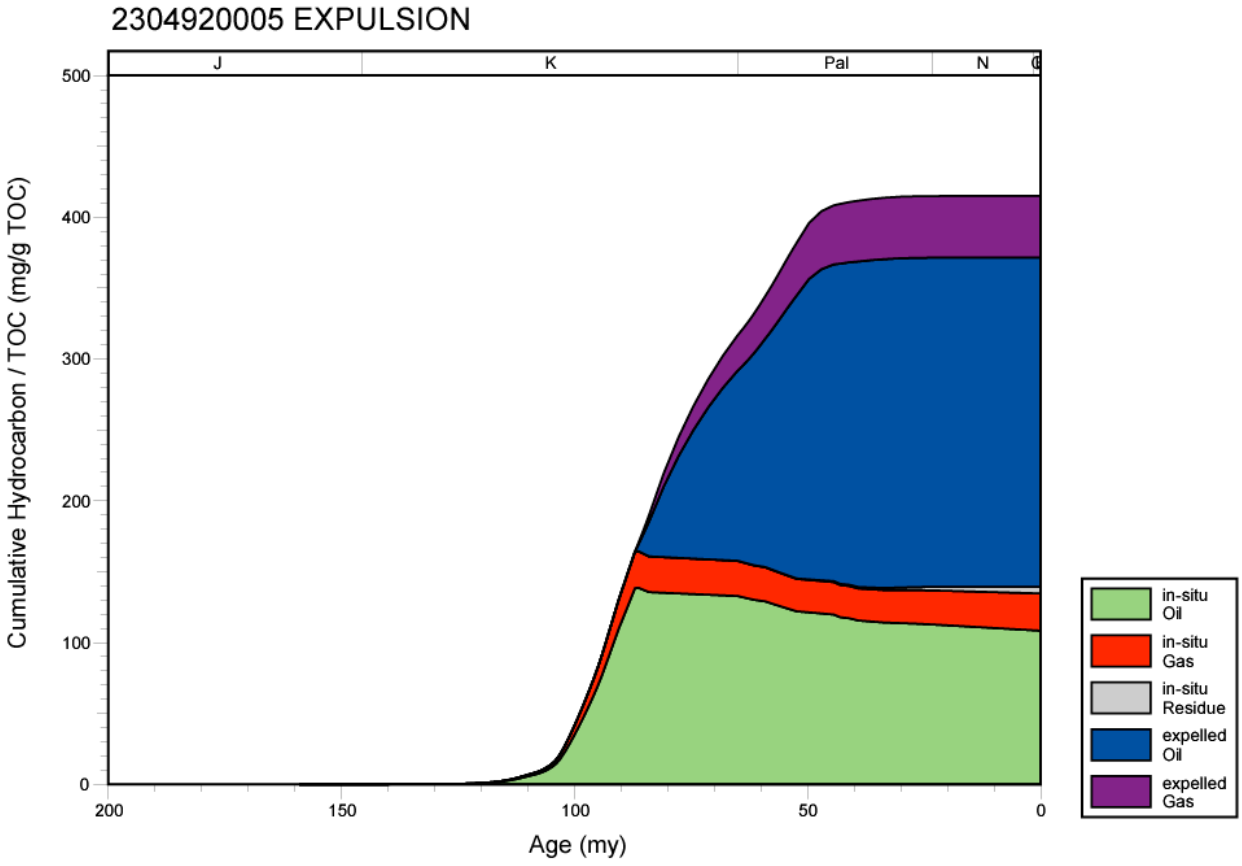


Figure 272. Hydrocarbon expulsion plot for well 2304920005, Mississippi Interior Salt Basin.

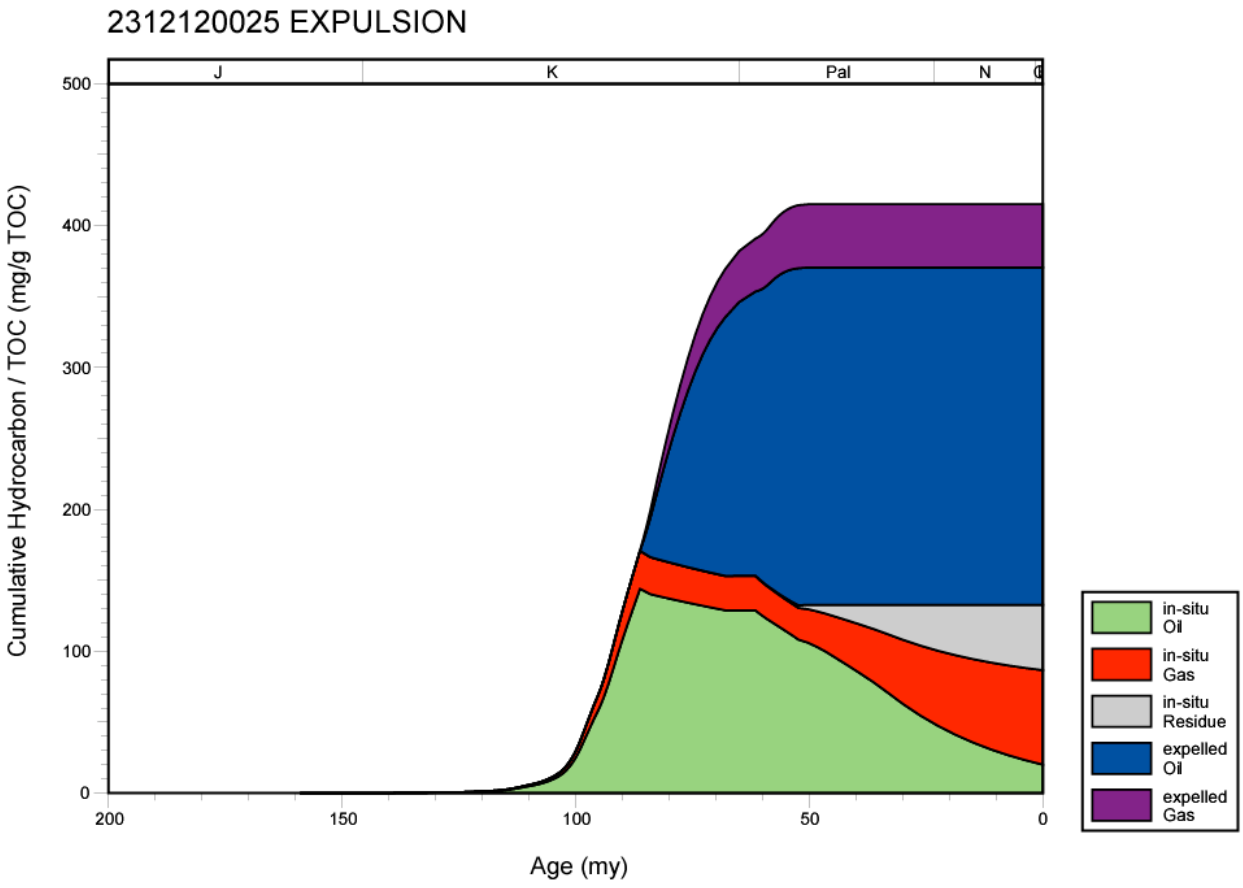


Figure 273. Hydrocarbon expulsion plot for well 2312120025, Mississippi Interior Salt Basin.

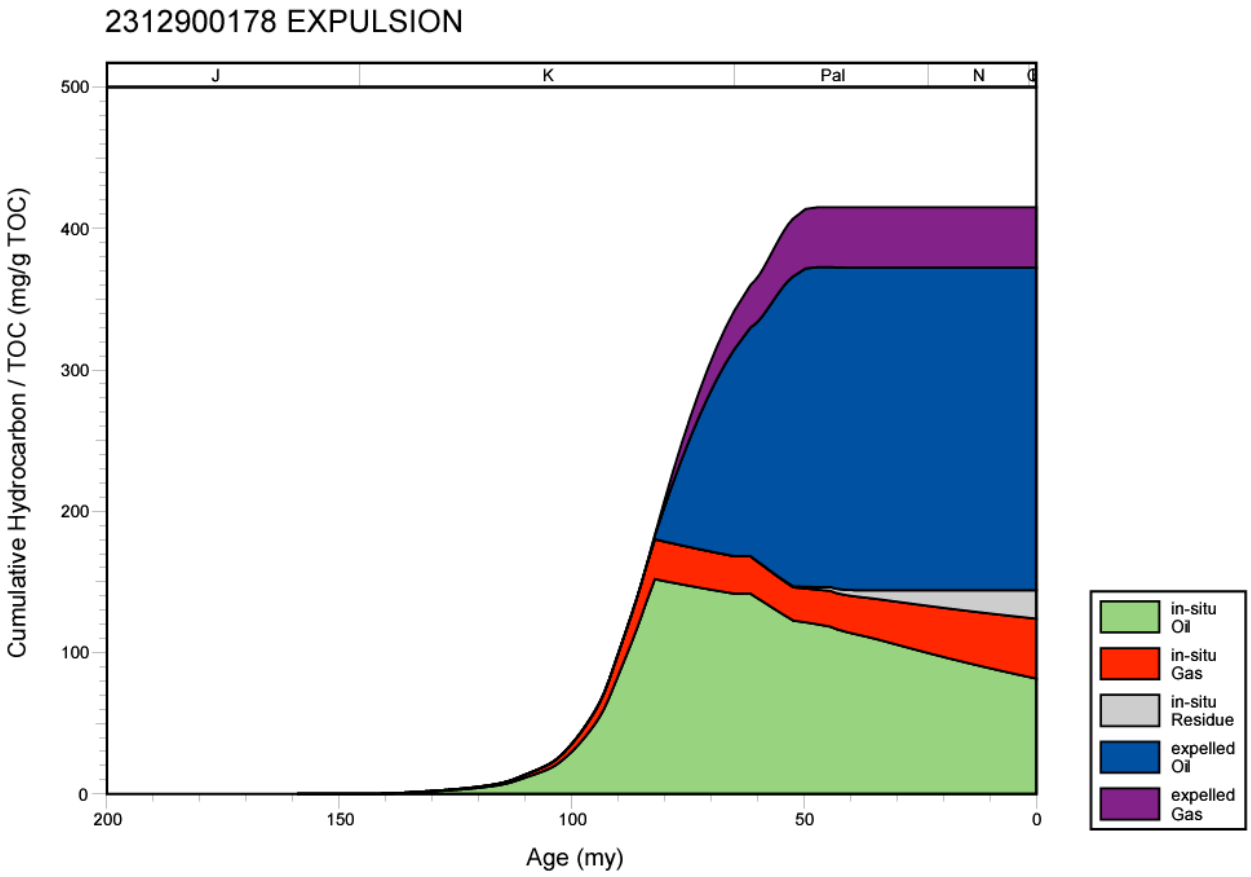


Figure 274. Hydrocarbon expulsion plot for well 2312900178, Mississippi Interior Salt Basin.

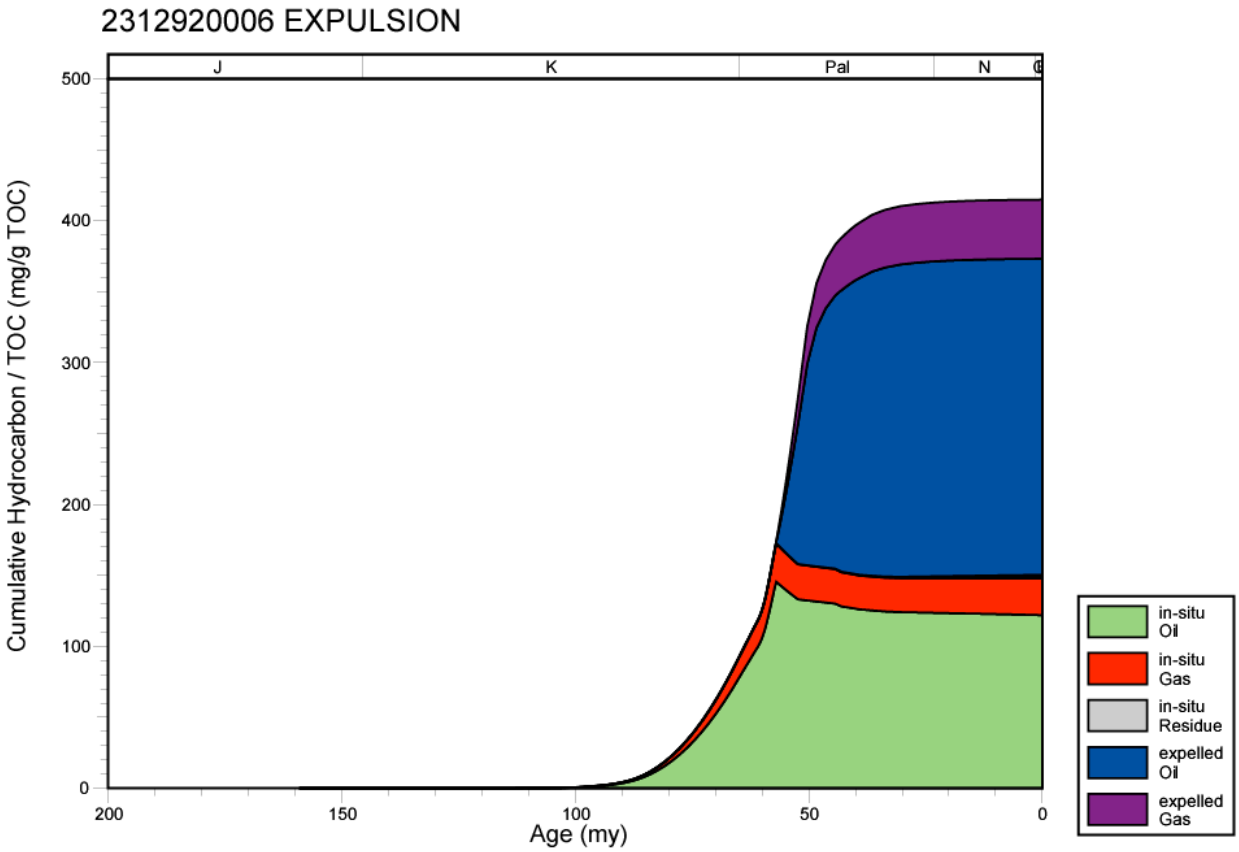


Figure 275. Hydrocarbon expulsion plot for well 2312920006, North Louisiana Salt Basin.

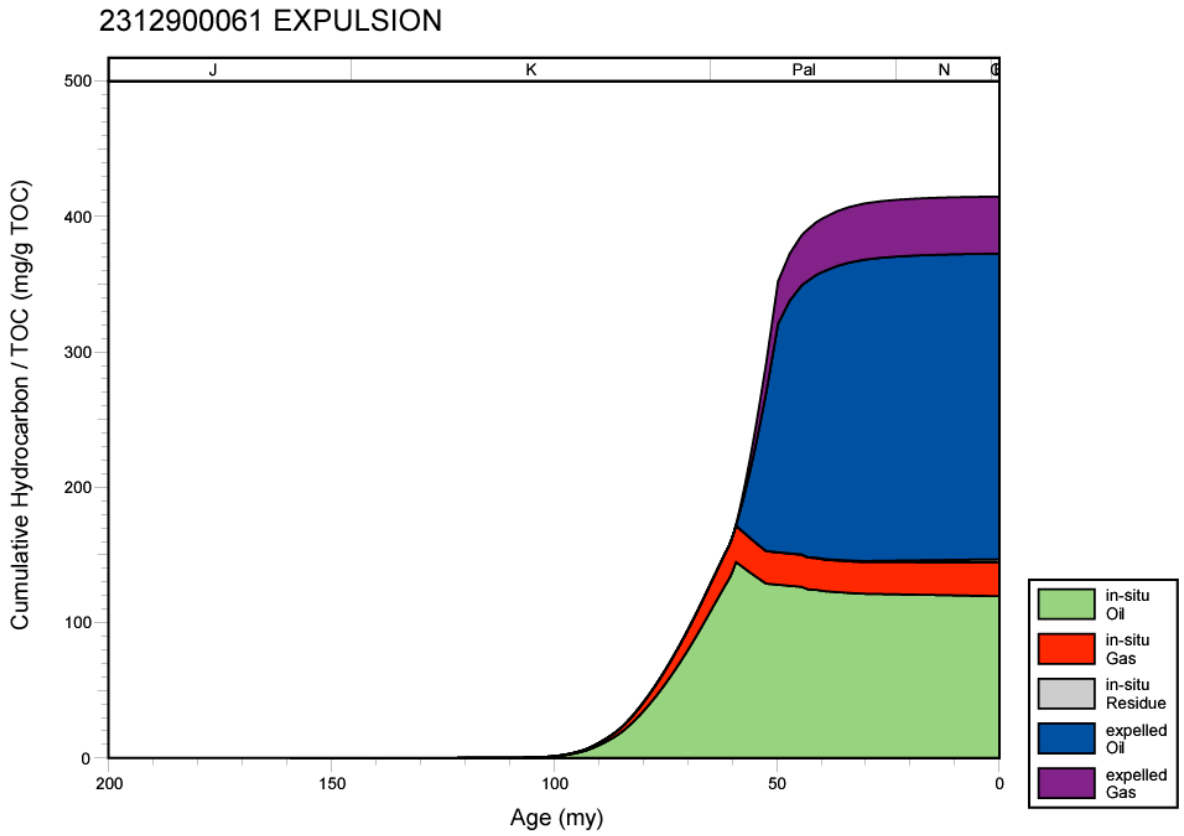


Figure 276. Hydrocarbon expulsion plot for well 2312900061, Mississippi Interior Salt Basin.

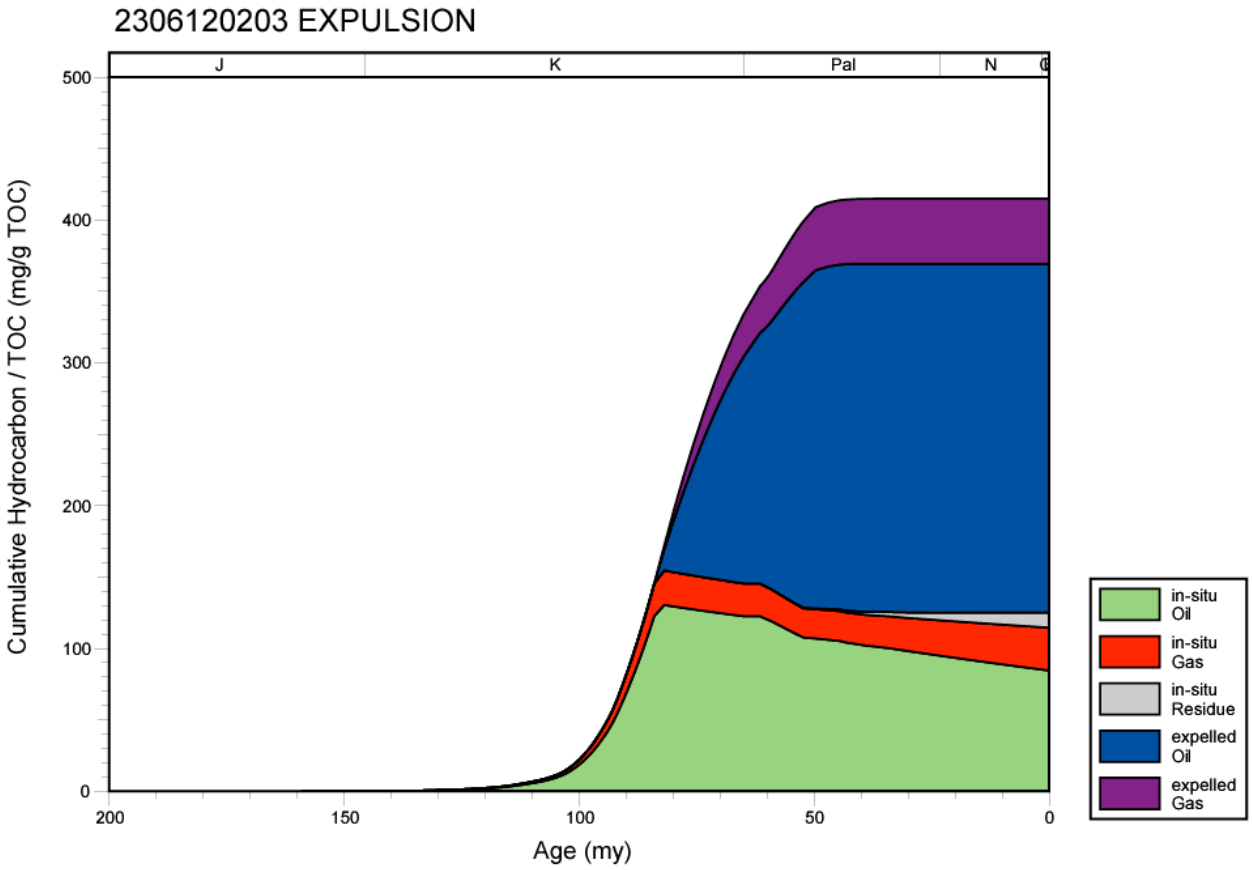


Figure 277. Hydrocarbon expulsion plot for well 2306120203, Mississippi Interior Salt Basin.

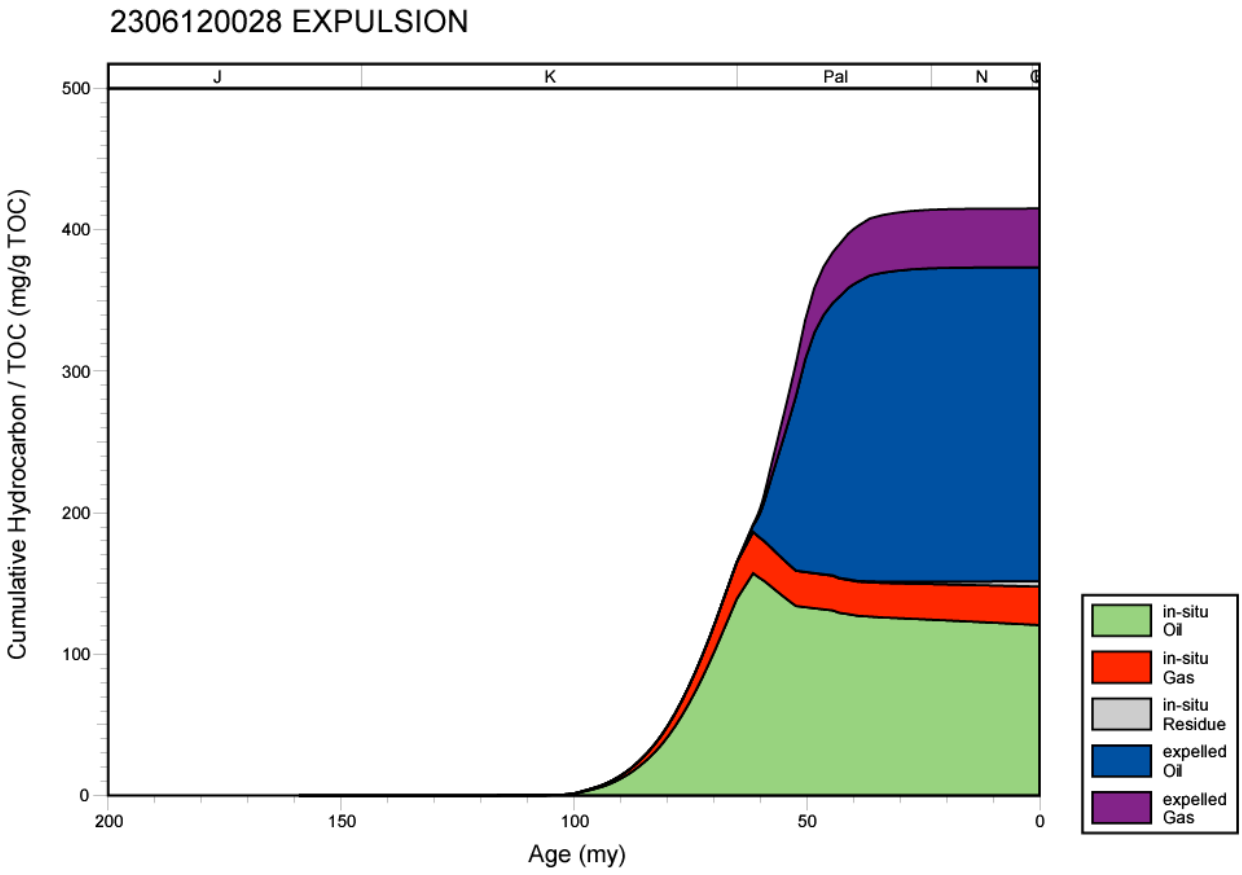


Figure 278. Hydrocarbon expulsion plot for well 2306120028, Mississippi Interior Salt Basin.

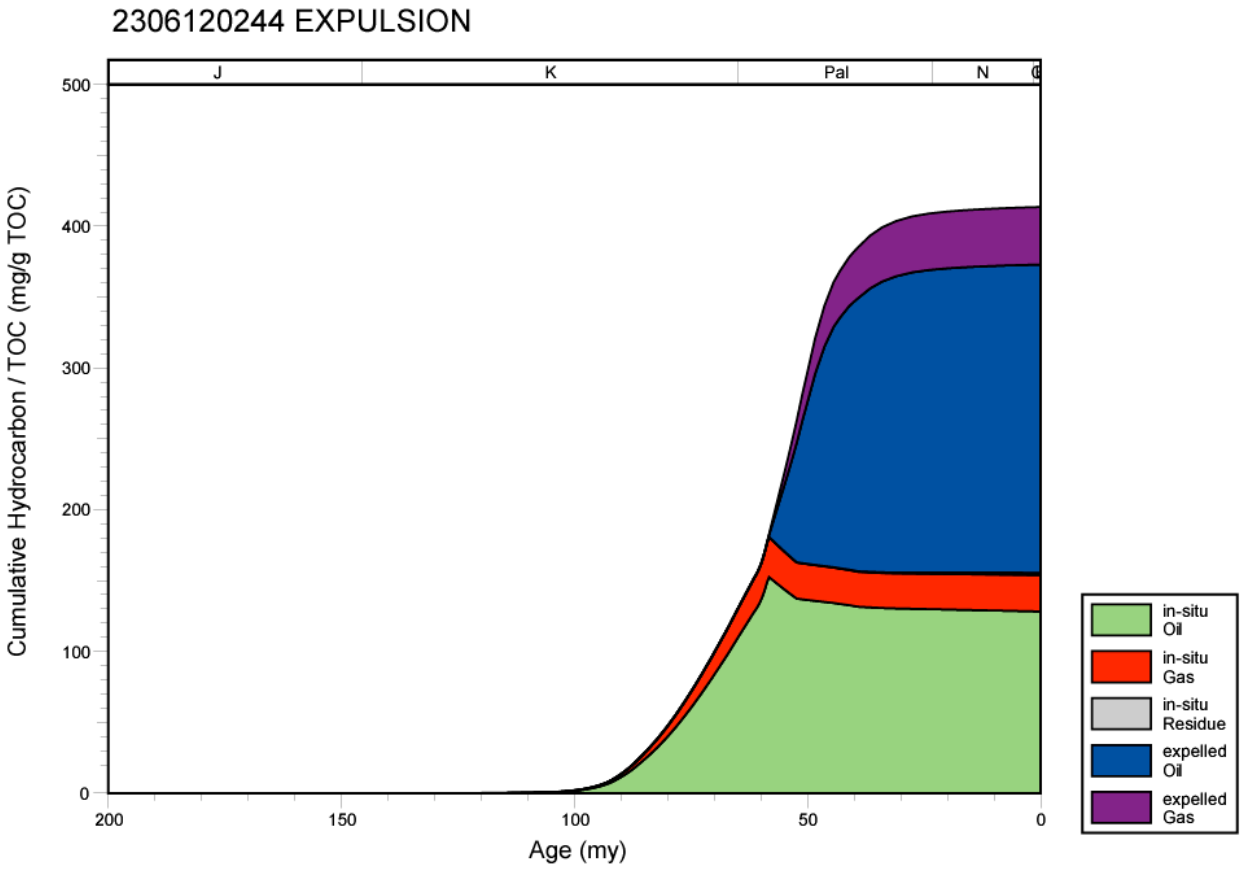


Figure 279. Hydrocarbon expulsion plot for well 2306120244, Mississippi Interior Salt Basin.

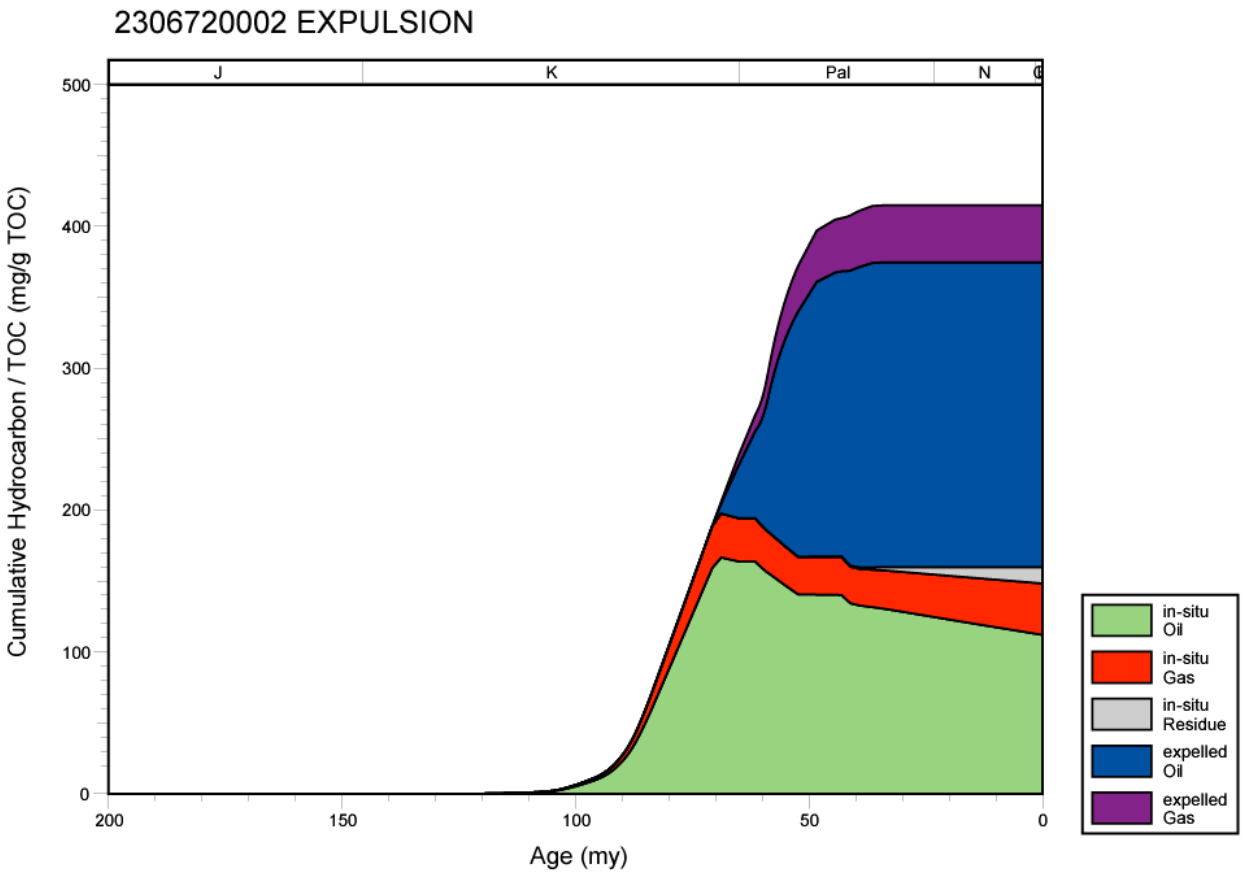


Figure 280. Hydrocarbon expulsion plot for well 2306720002, Mississippi Interior Salt Basin.

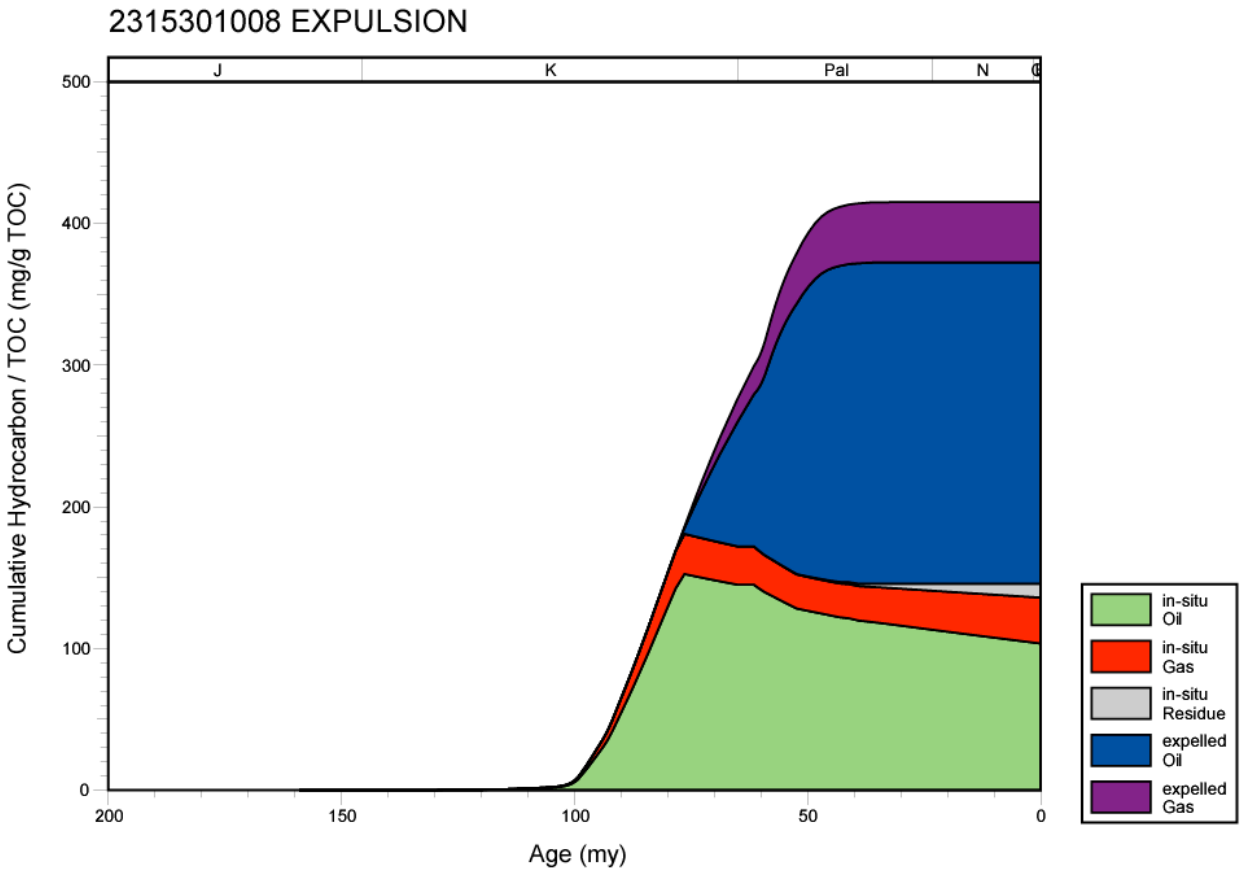


Figure 281. Hydrocarbon expulsion plot for well 2315301008, Mississippi Interior Salt Basin.

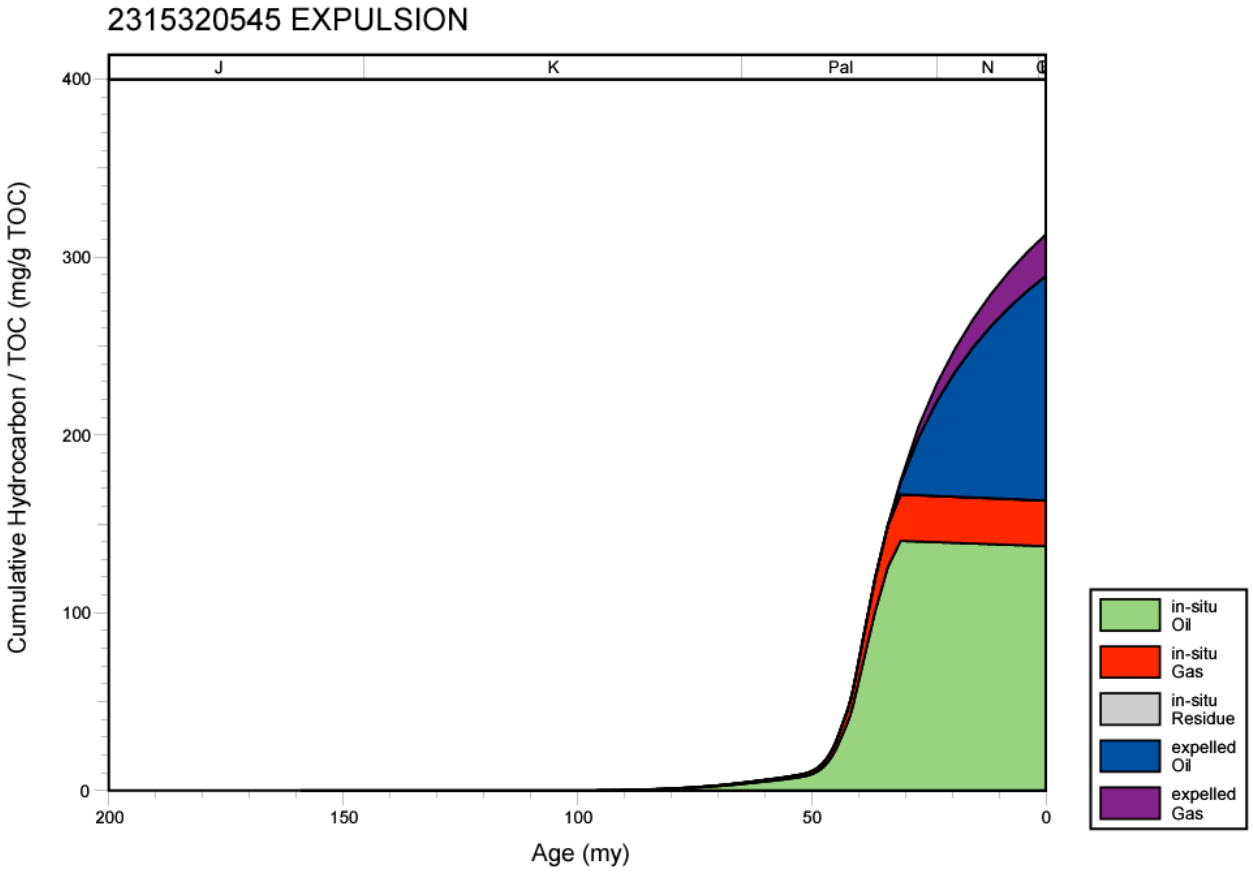


Figure 282. Hydrocarbon expulsion plot for well 2315320545, Mississippi Interior Salt Basin.

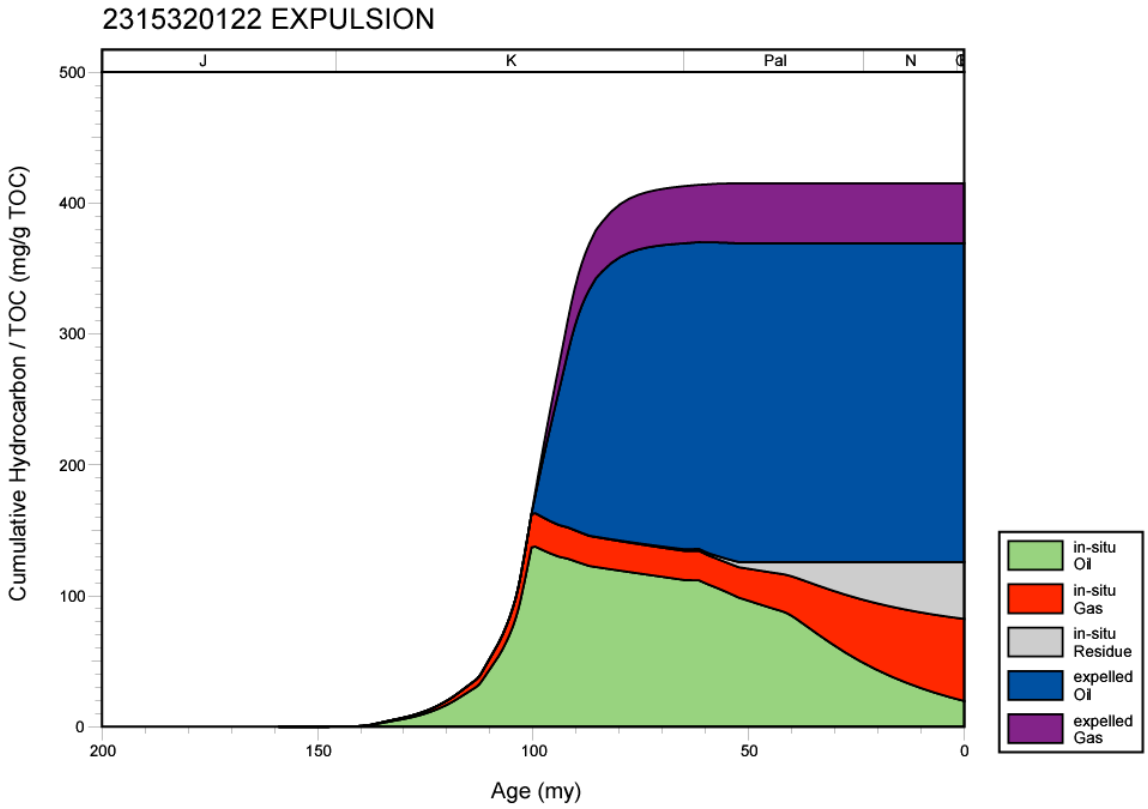


Figure 283. Hydrocarbon expulsion plot for well 2315320122, Mississippi Interior Salt Basin.

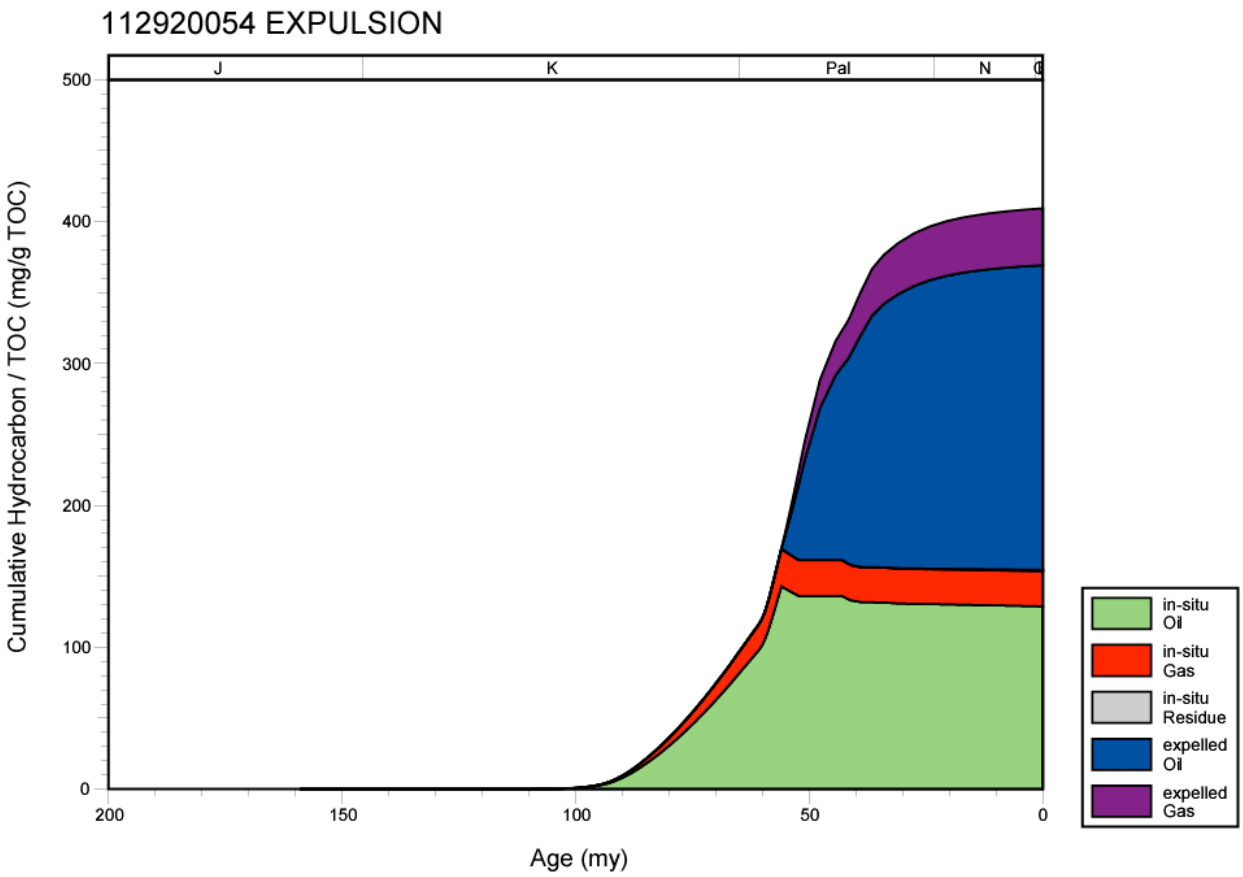


Figure 284. Hydrocarbon expulsion plot for well 112920054, Mississippi Interior Salt Basin.

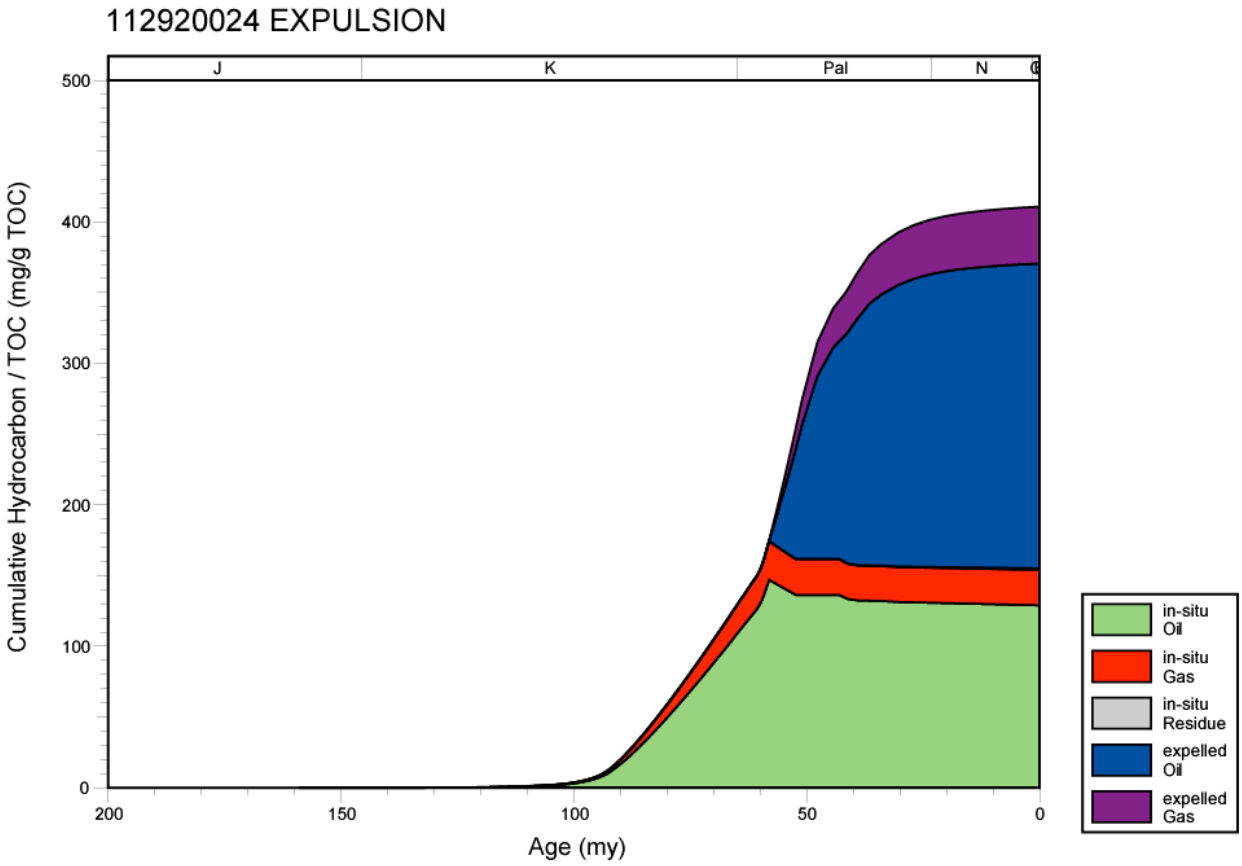


Figure 285. Hydrocarbon expulsion plot for well 112920024, Mississippi Interior Salt Basin.

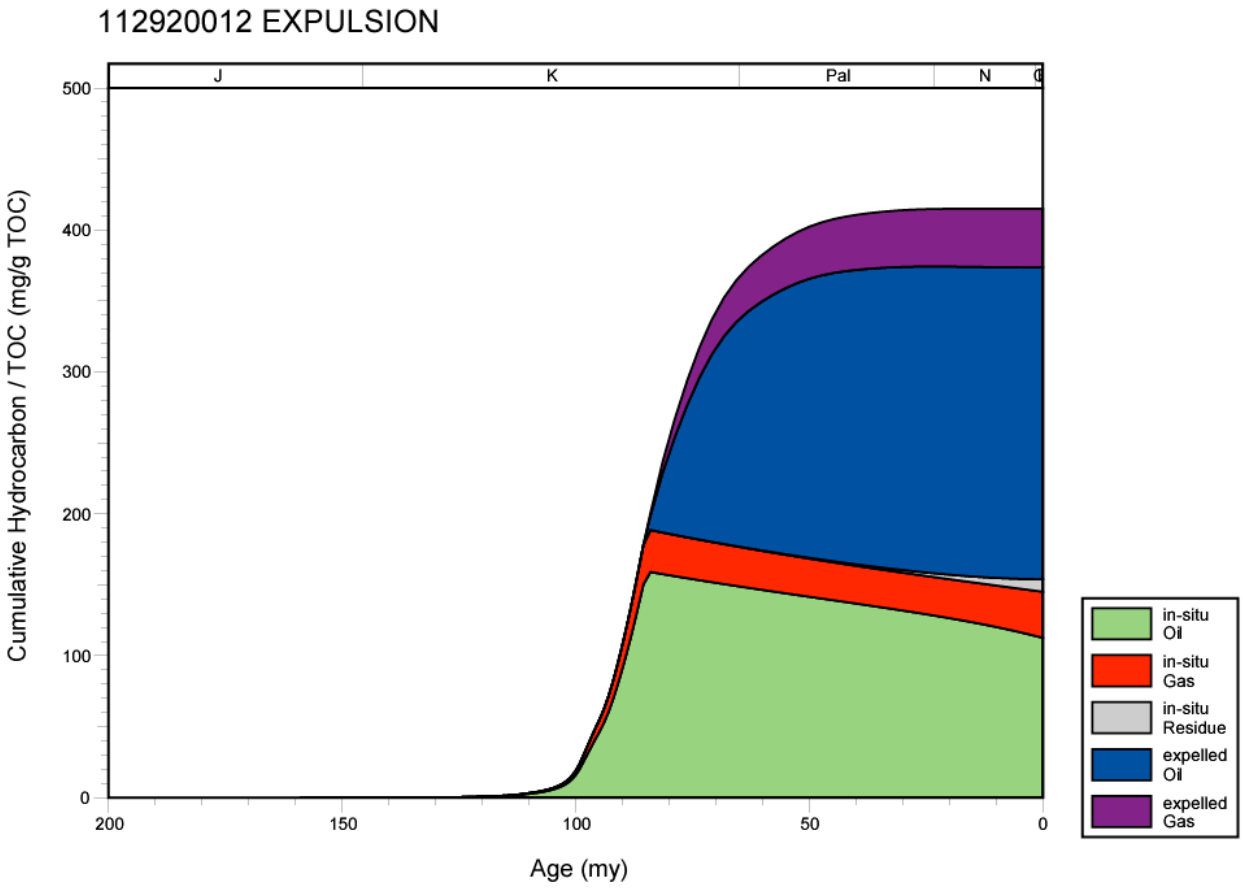


Figure 286. Hydrocarbon expulsion plot for well 112920012, Mississippi Interior Salt Basin.

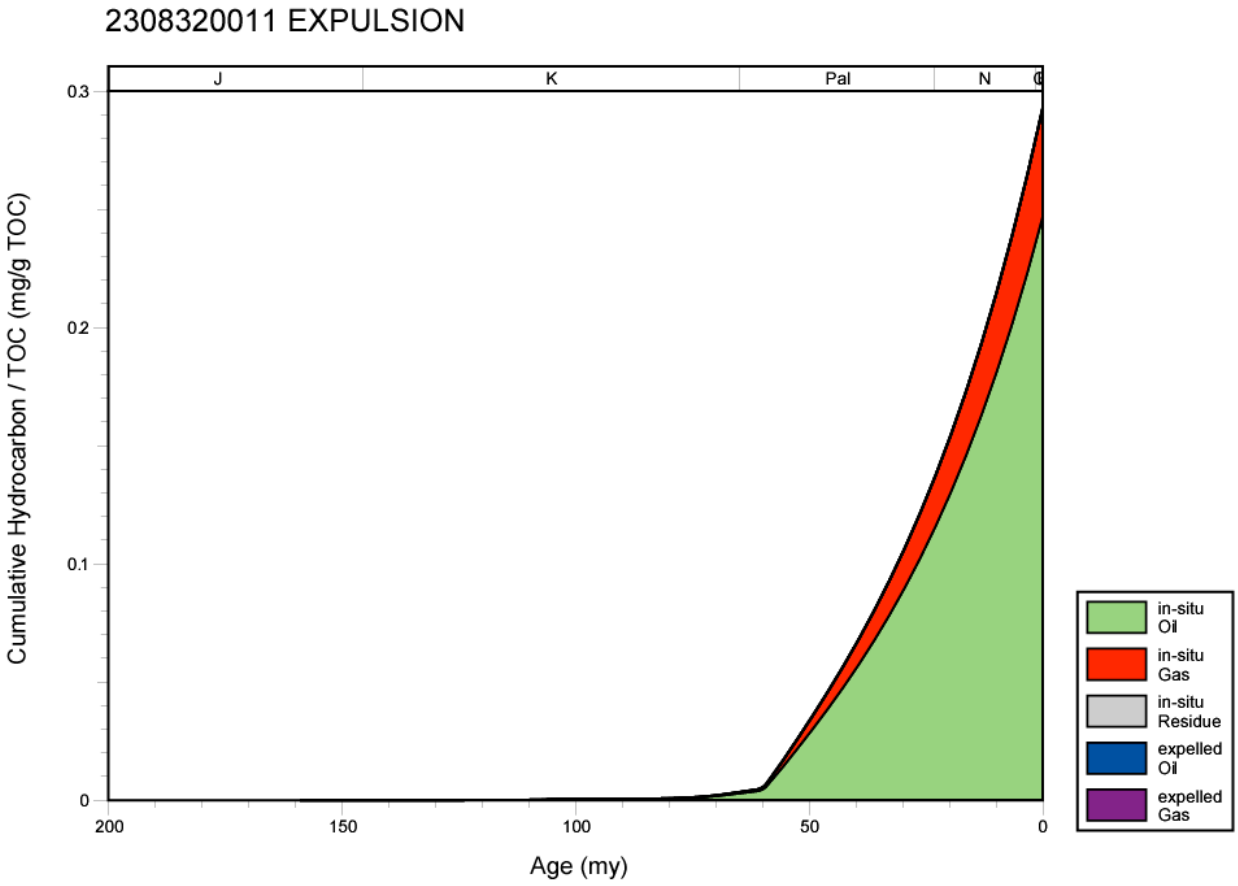


Figure 287. Hydrocarbon expulsion plot for well 2308320011, Mississippi Interior Salt Basin.

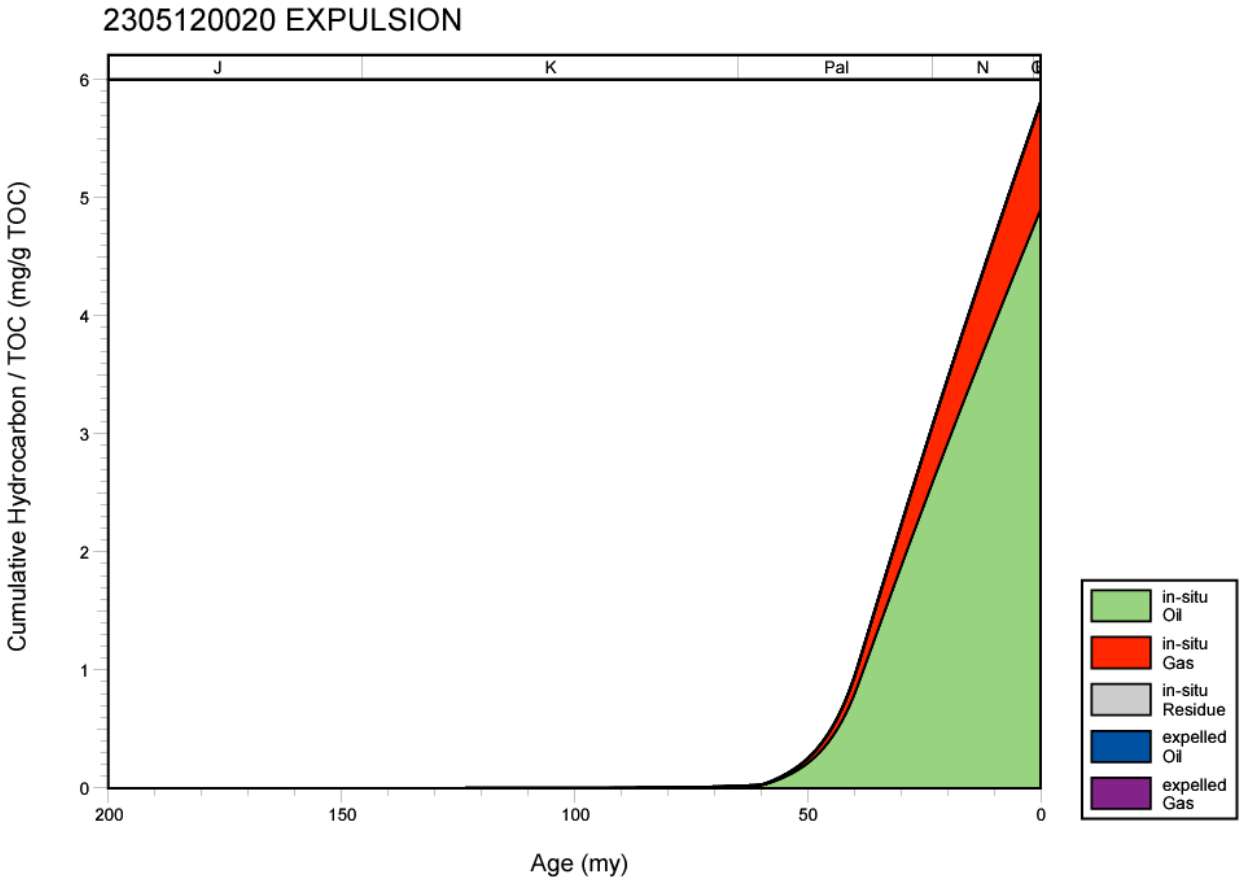


Figure 288. Hydrocarbon expulsion plot for well 2305120020, Mississippi Interior Salt Basin.

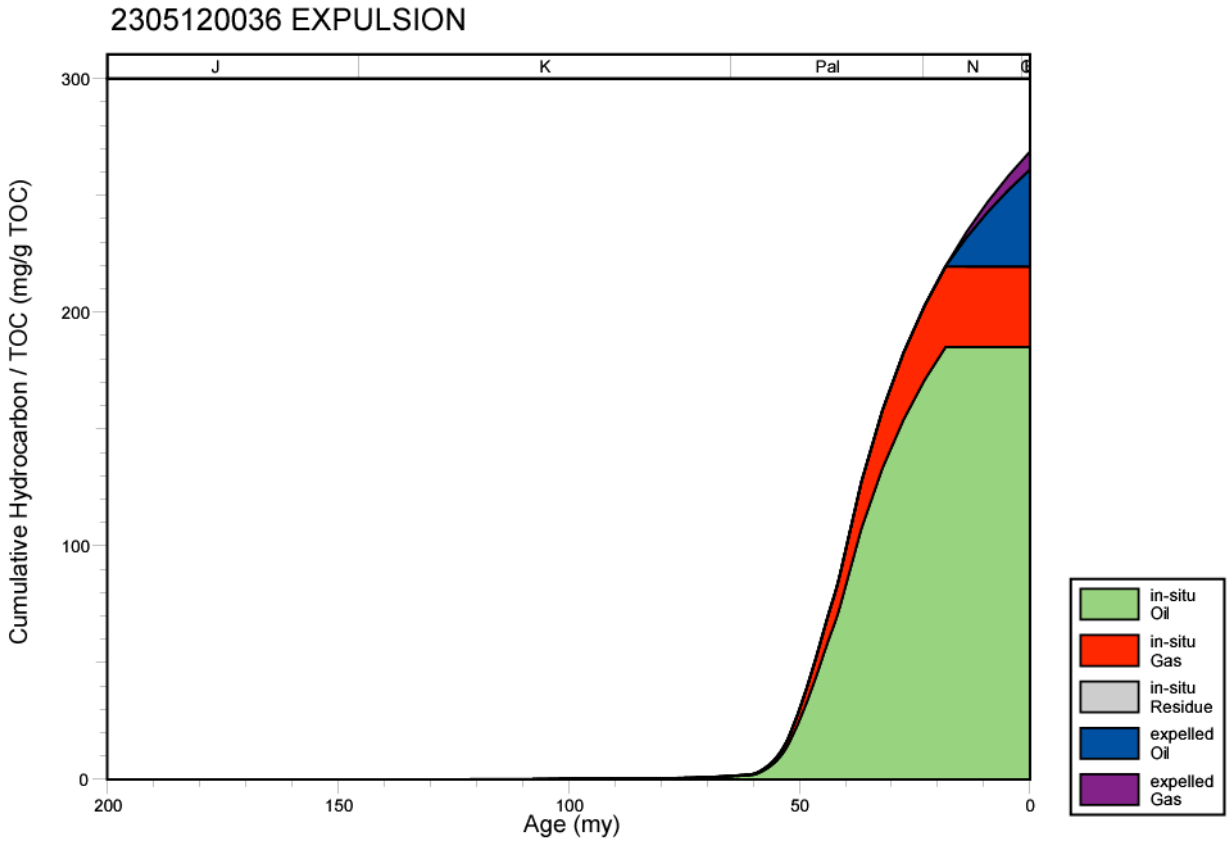


Figure 289. Hydrocarbon expulsion plot for well 2305120036, Mississippi Interior Salt Basin.

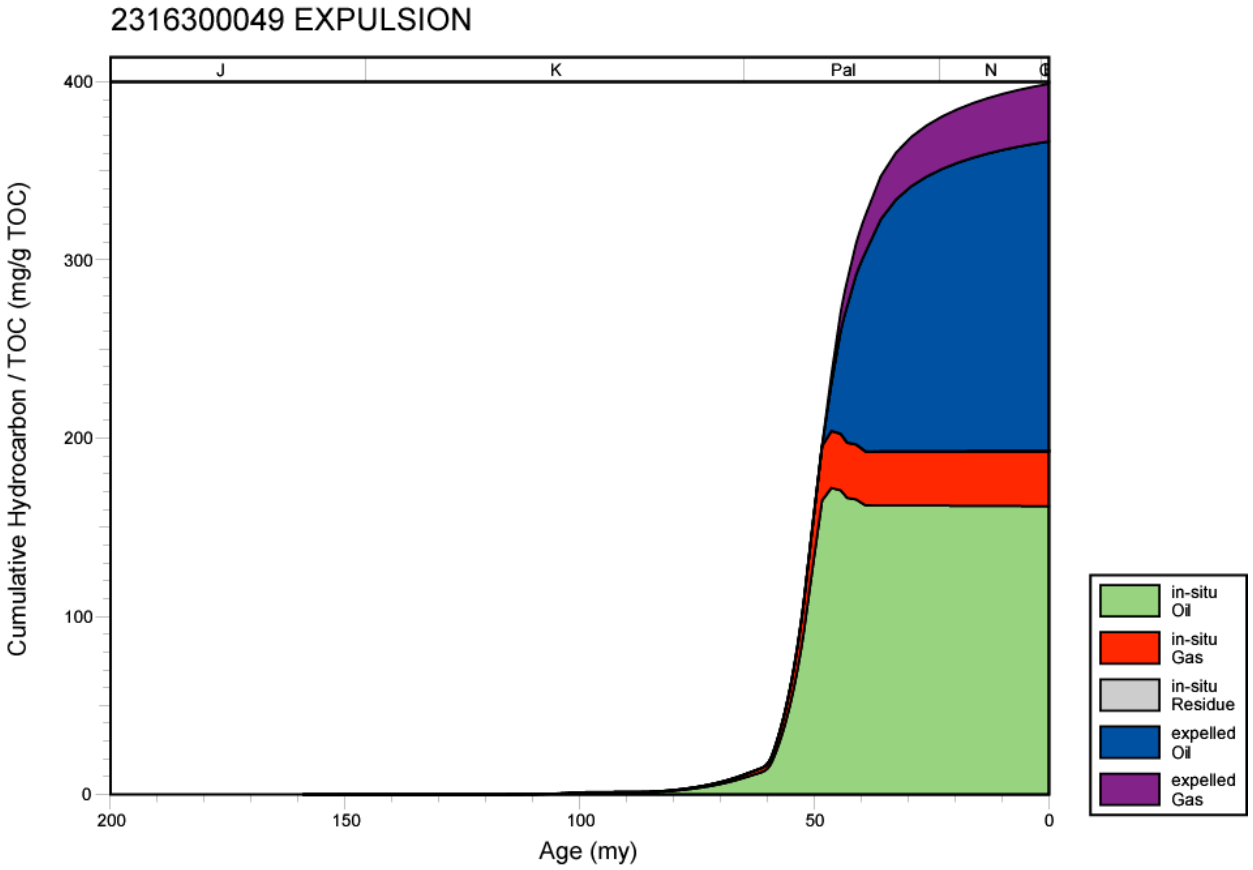


Figure 290. Hydrocarbon expulsion plot for well 2316300049, Mississippi Interior Salt Basin.

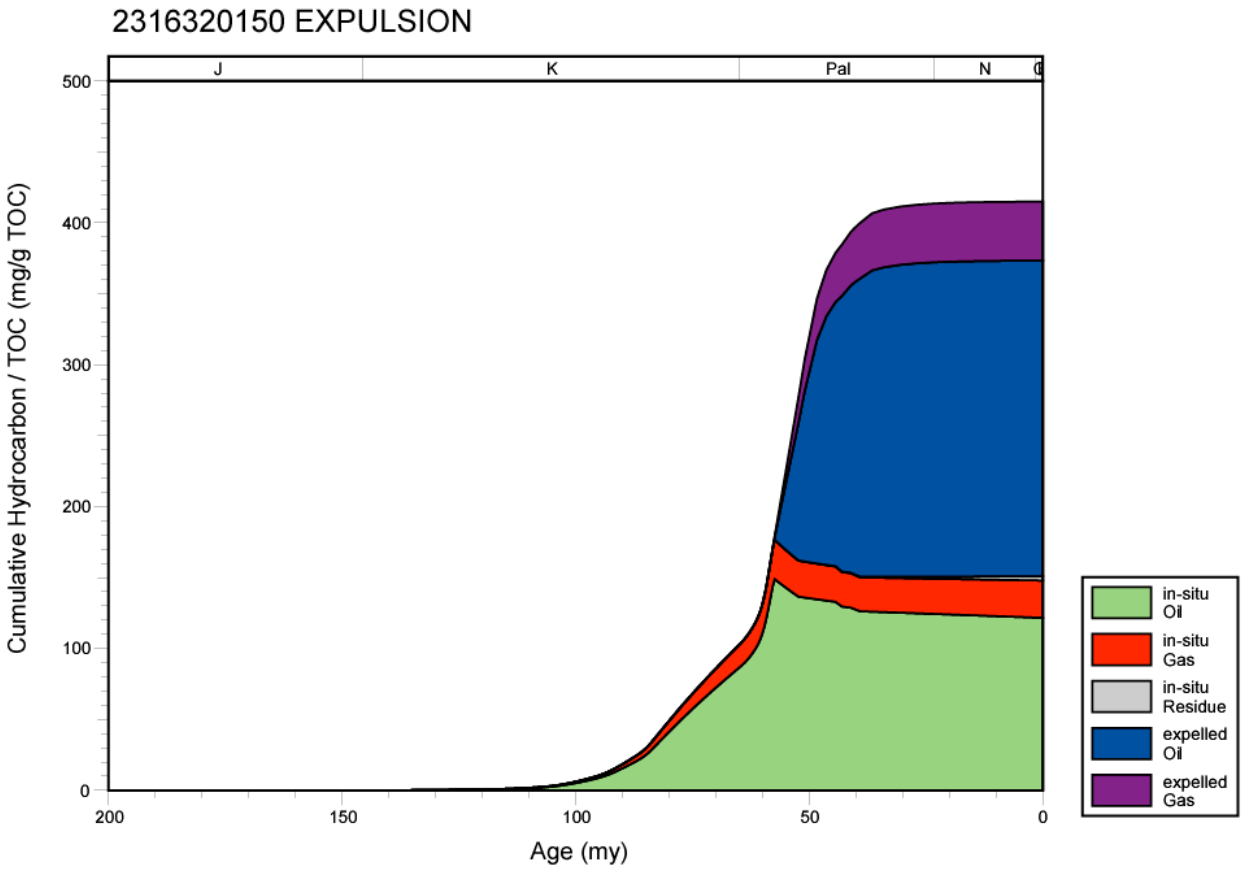


Figure 291. Hydrocarbon expulsion plot for well 2316320150, Mississippi Interior Salt Basin.

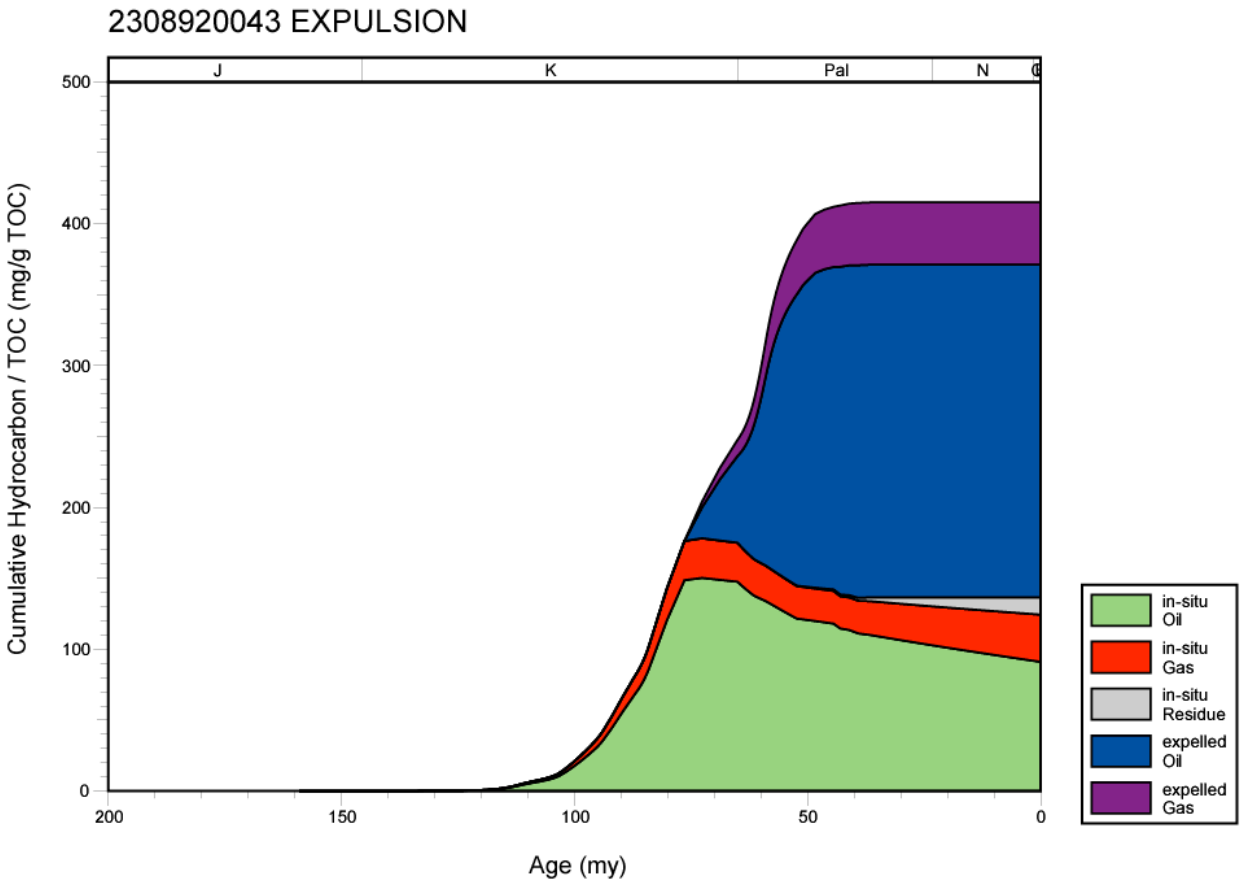


Figure 292. Hydrocarbon expulsion plot for well 2308920043, Mississippi Interior Salt Basin.

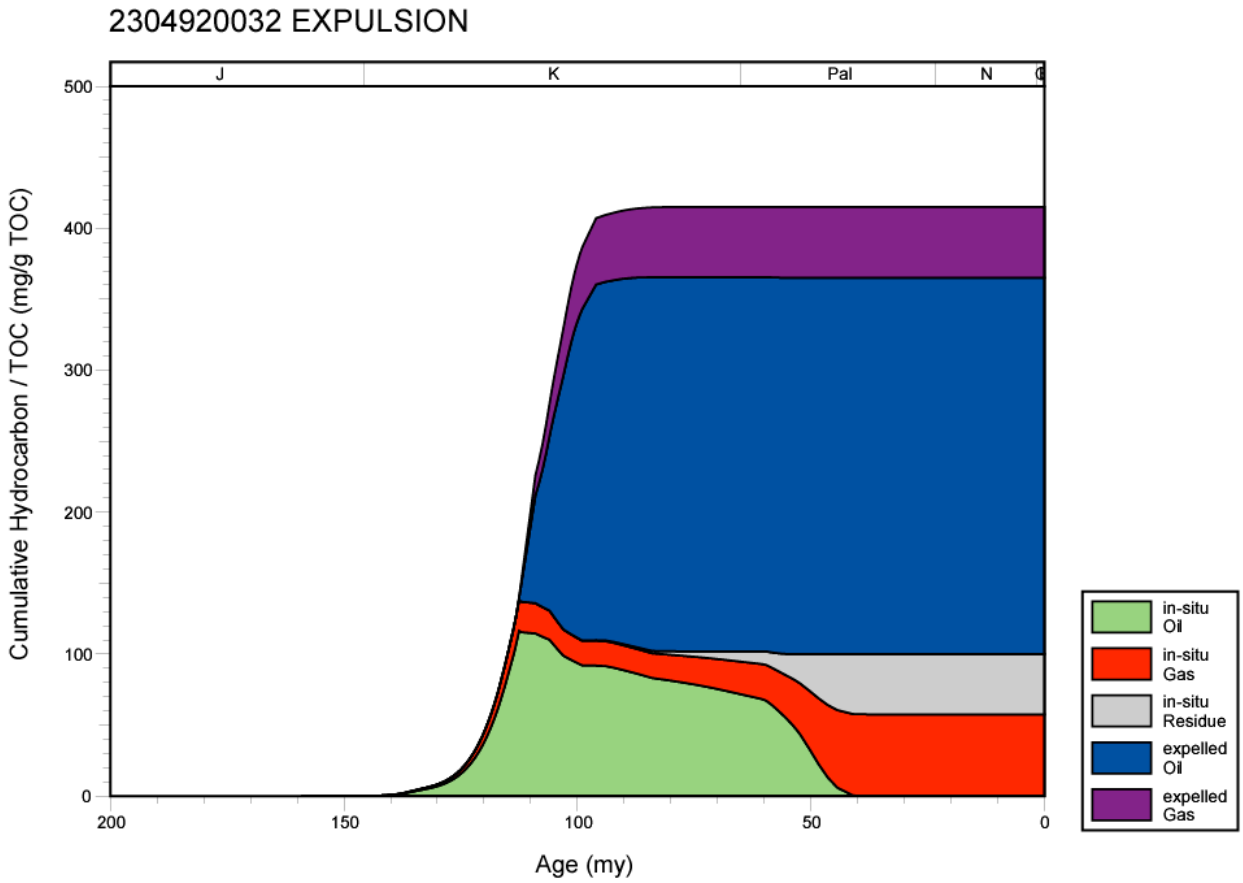


Figure 293. Hydrocarbon expulsion plot for well 2304920032, Mississippi Interior Salt Basin.

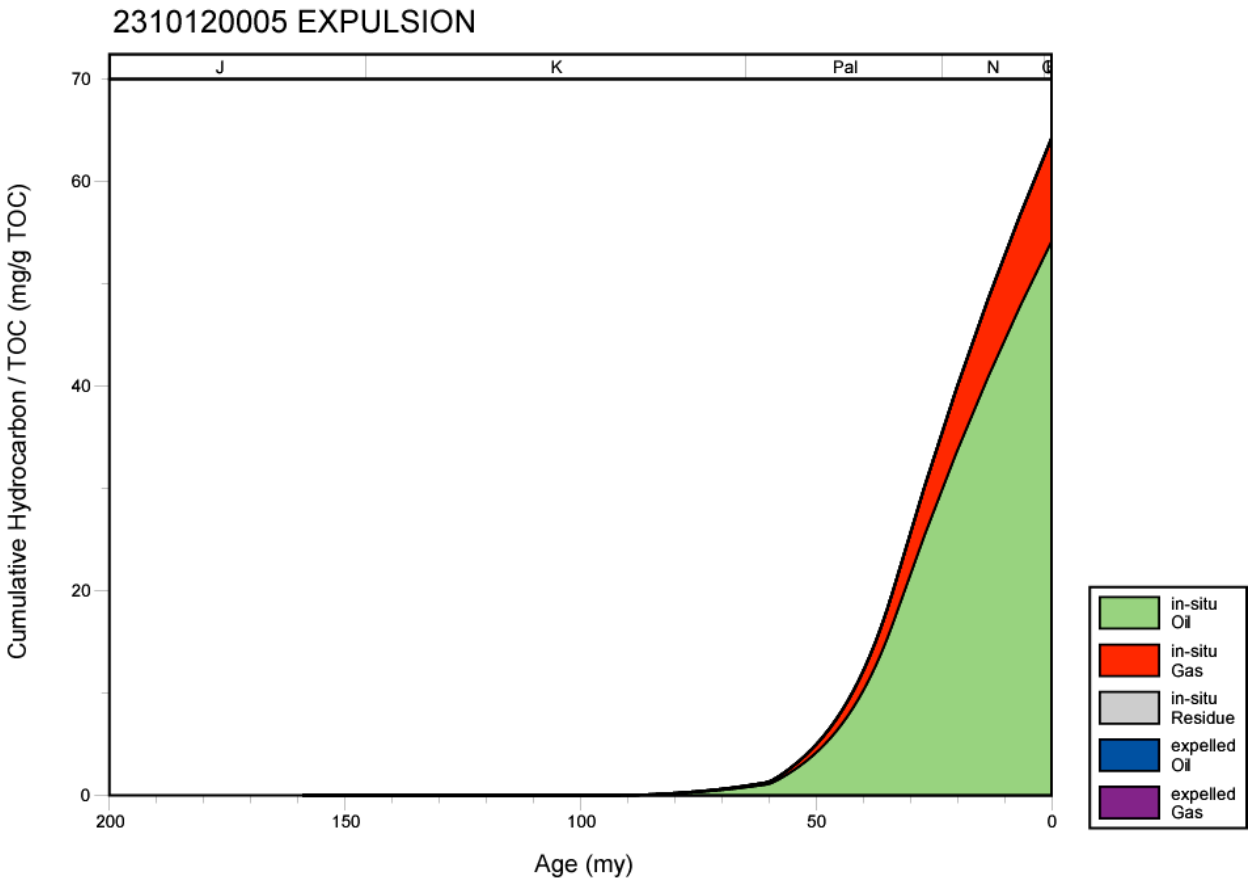


Figure 294. Hydrocarbon expulsion plot for well 2310120005, Mississippi Interior Salt Basin.

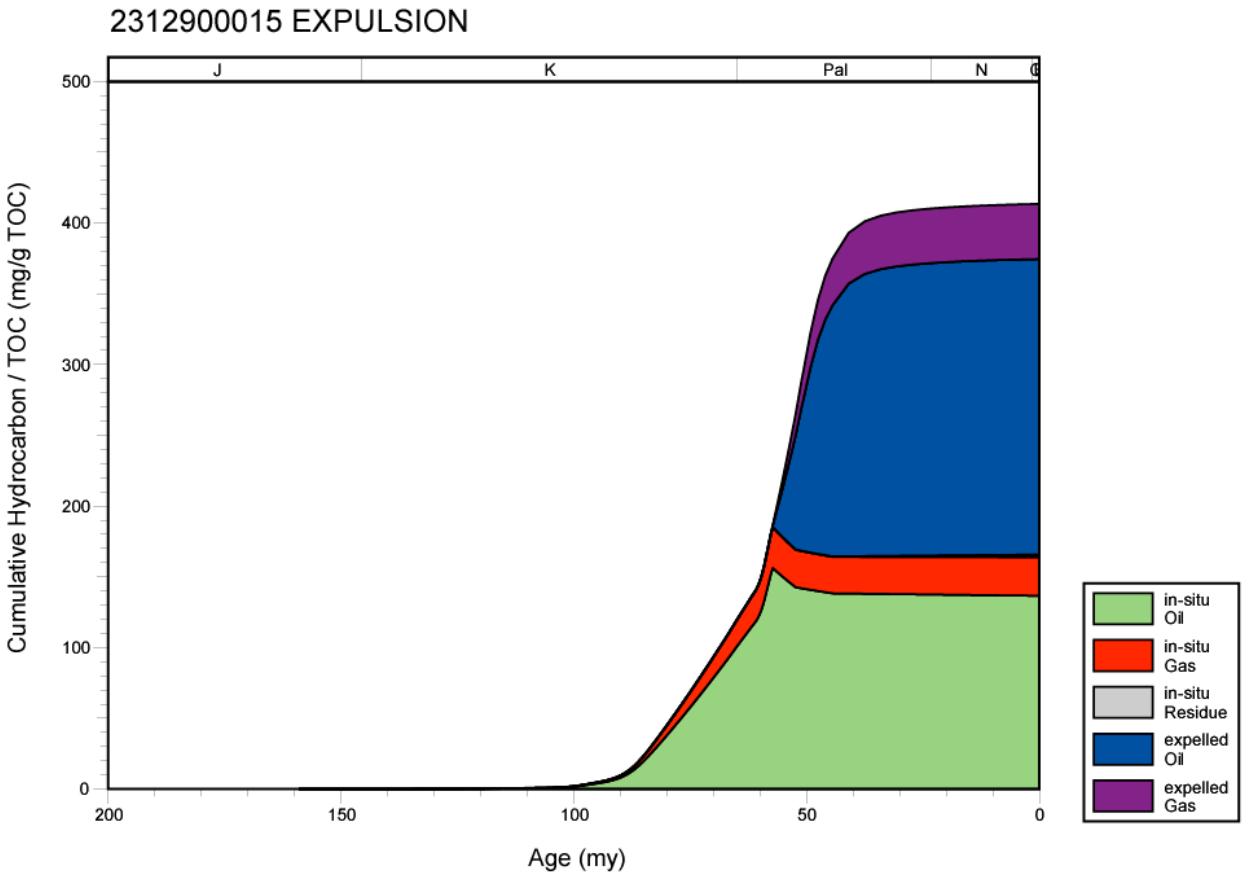


Figure 295. Hydrocarbon expulsion plot for well 2312900015, Mississippi Interior Salt Basin.

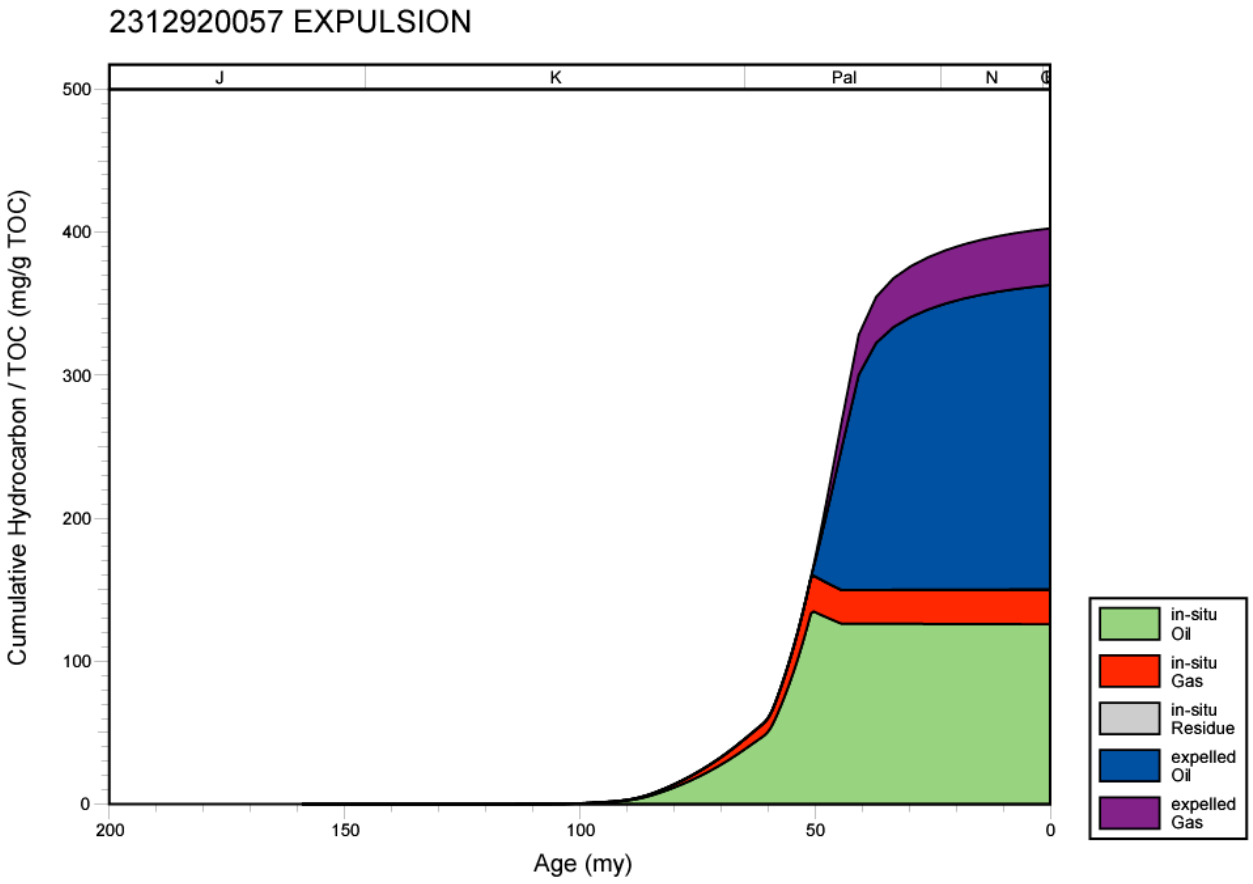


Figure 296. Hydrocarbon expulsion plot for well 2312920057, Mississippi Interior Salt Basin.

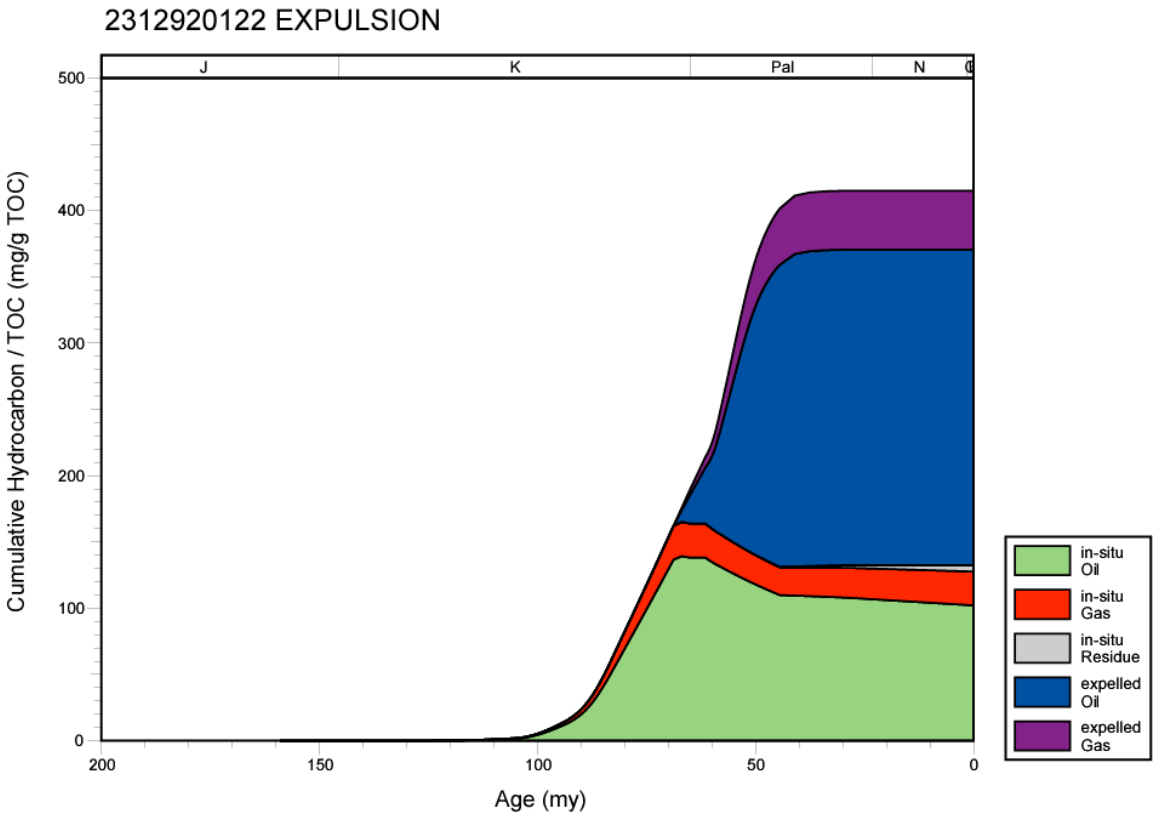


Figure 297. Hydrocarbon expulsion plot for well 2312920122, Mississippi Interior Salt Basin.

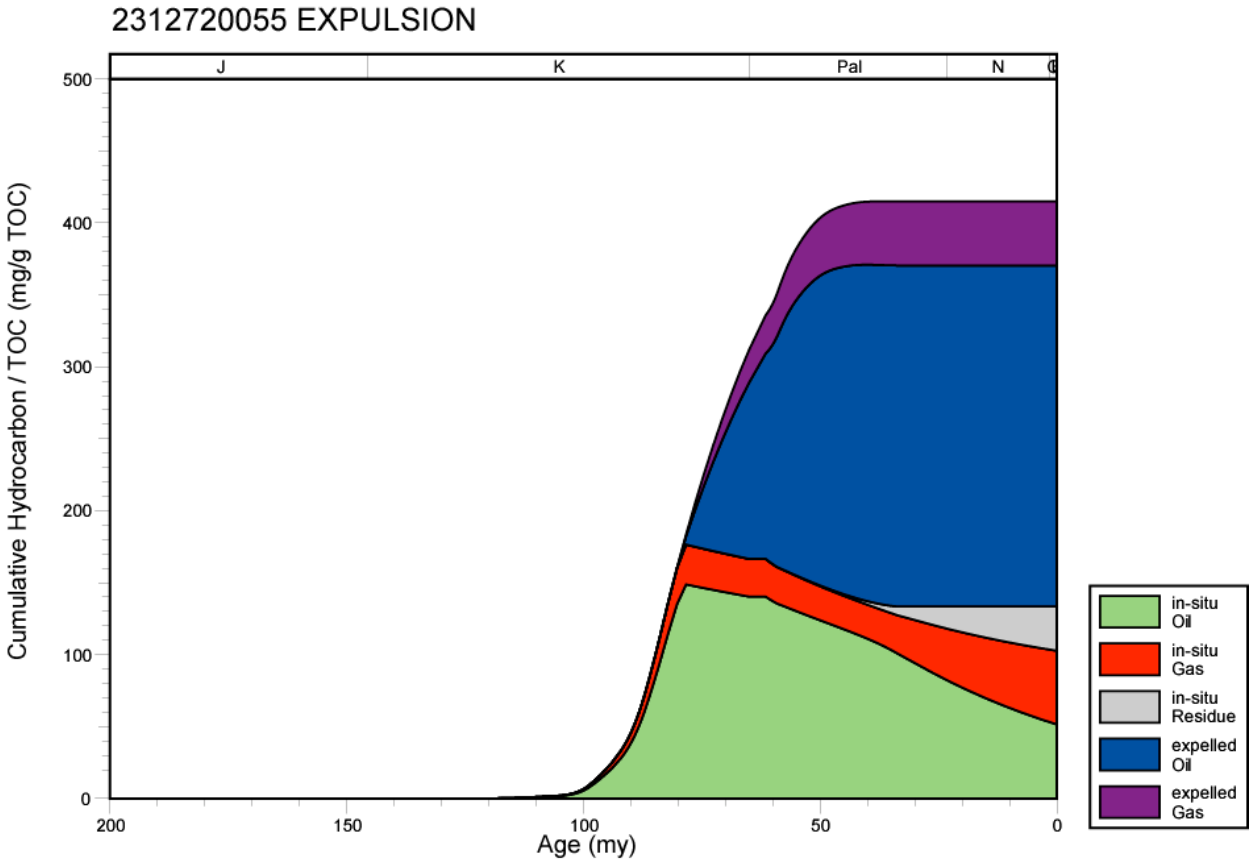


Figure 298. Hydrocarbon expulsion plot for well 2312720055, Mississippi Interior Salt Basin.

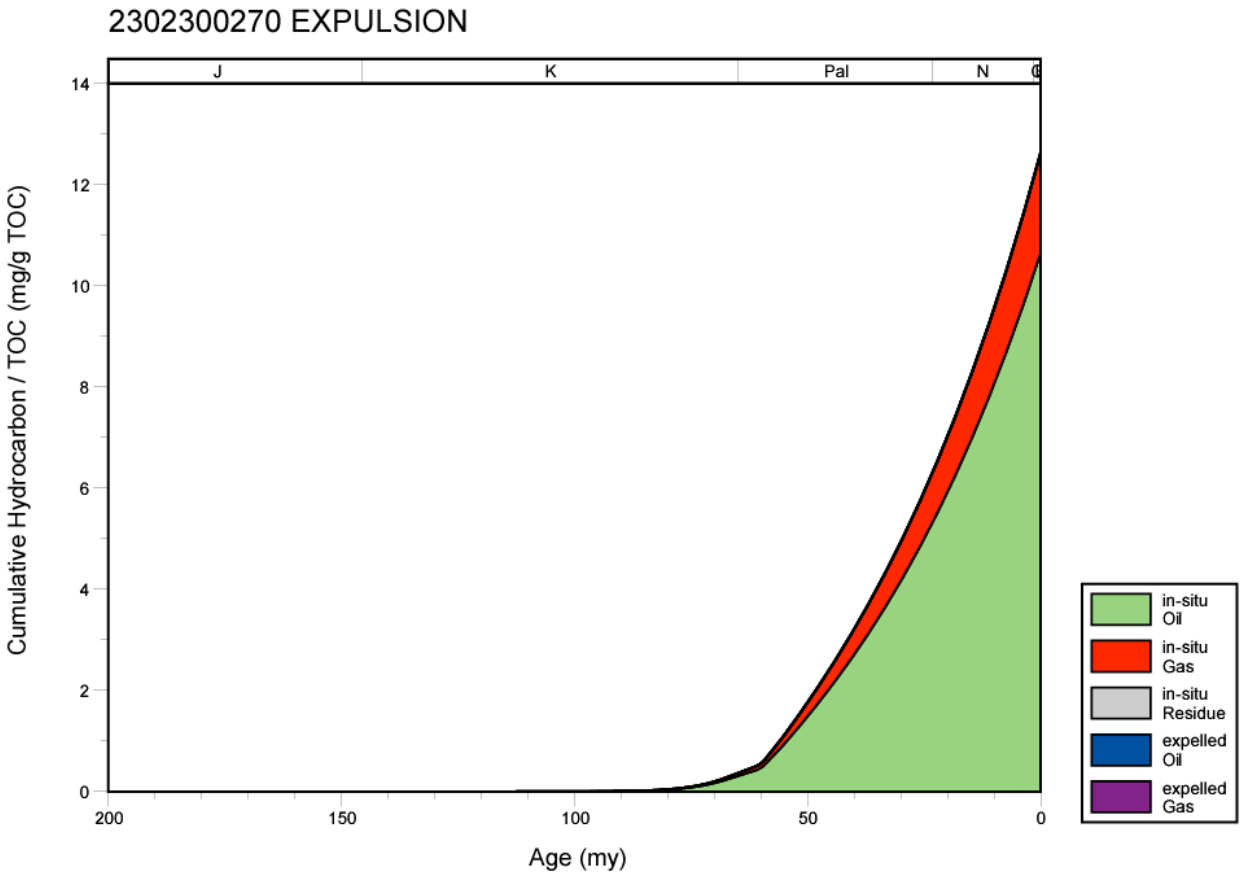


Figure 299. Hydrocarbon expulsion plot for well 2302300270, Mississippi Interior Salt Basin.

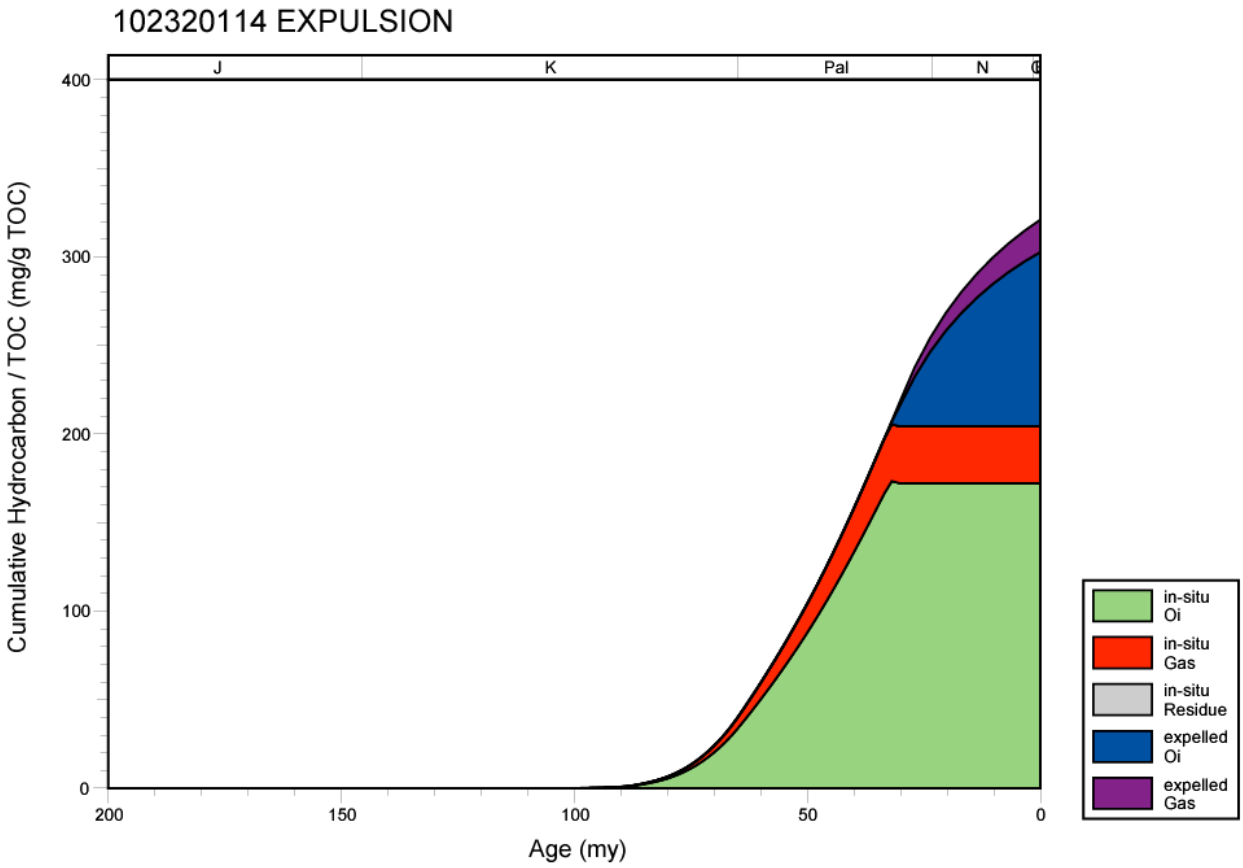


Figure 300. Hydrocarbon expulsion plot for well 102320114, Mississippi Interior Salt Basin.

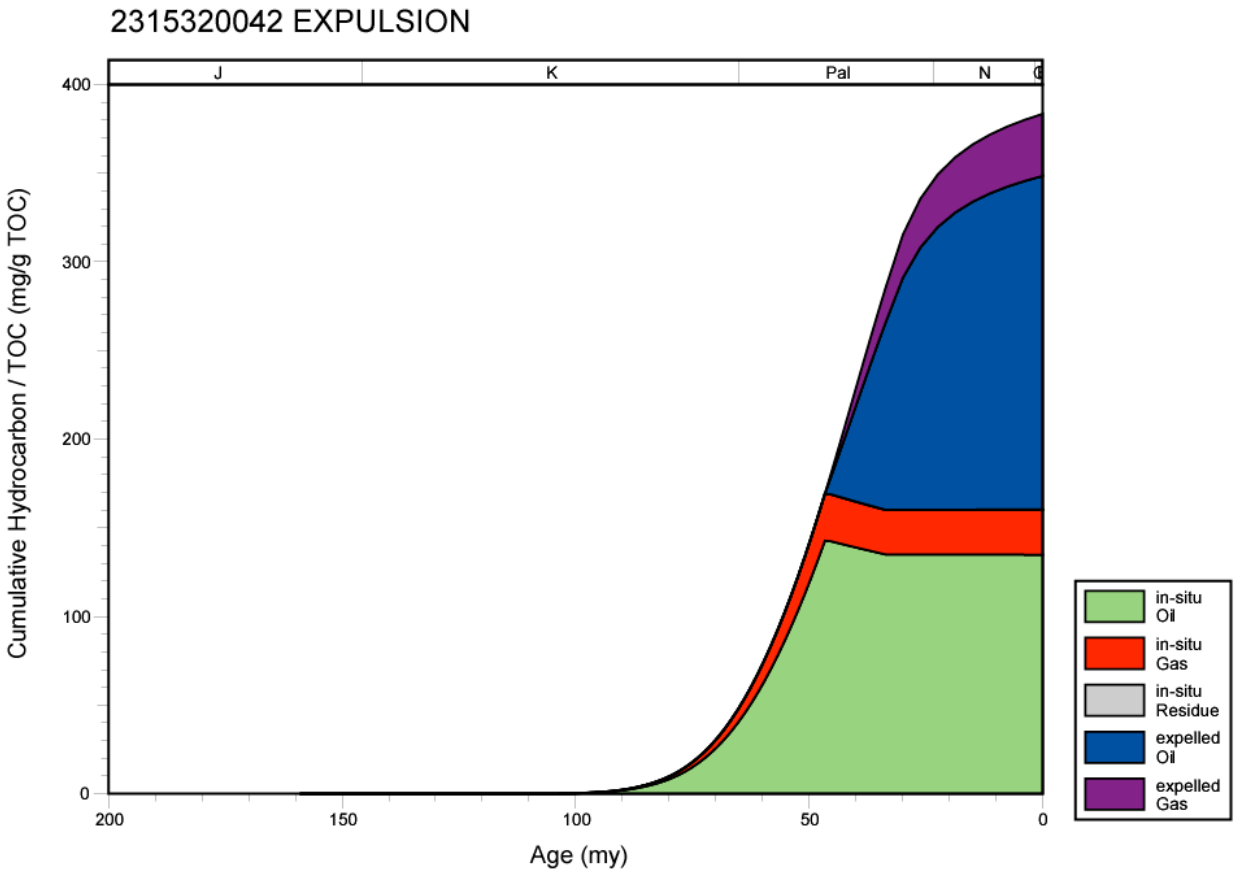


Figure 301. Hydrocarbon expulsion plot for well 2315320042, Mississippi Interior Salt Basin.

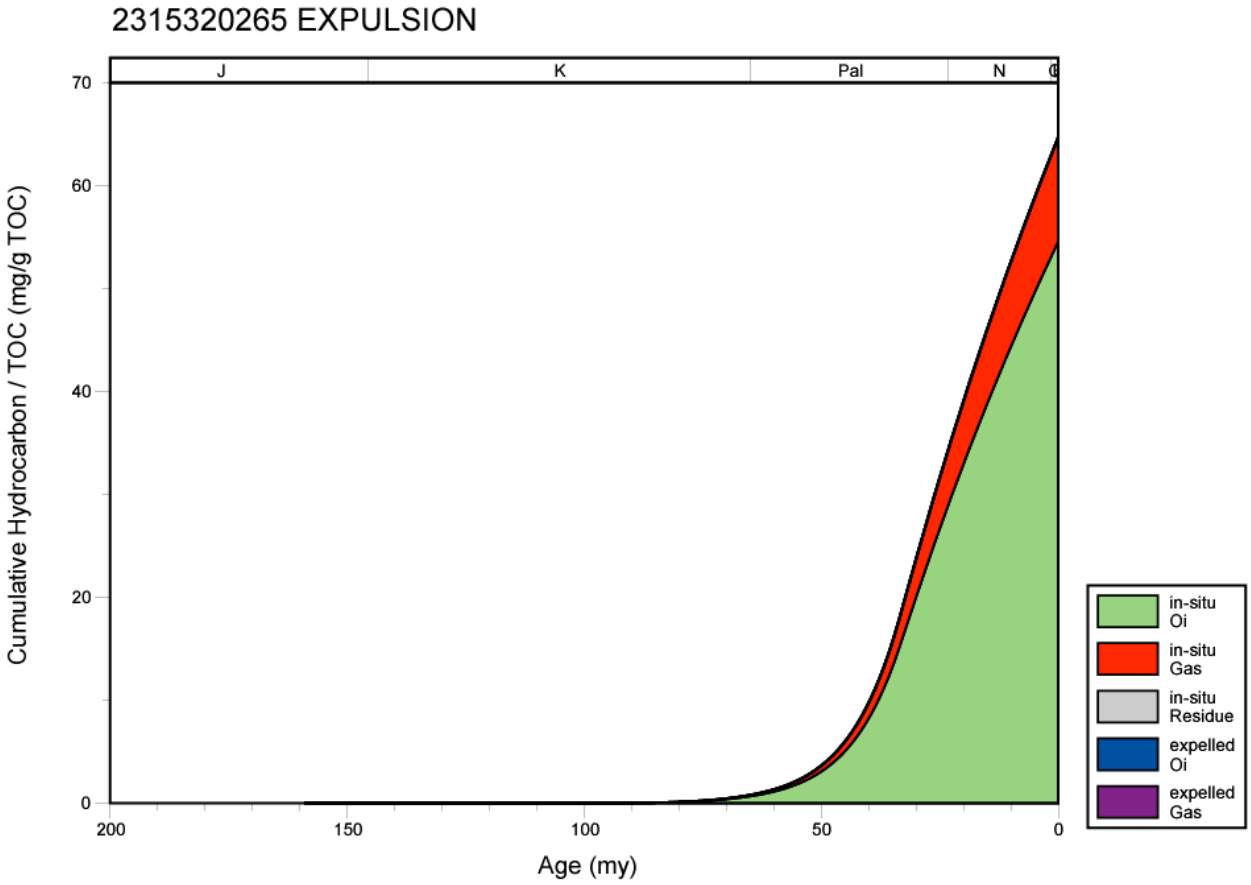


Figure 302. Hydrocarbon expulsion plot for well 2315320265, Mississippi Interior Salt Basin.

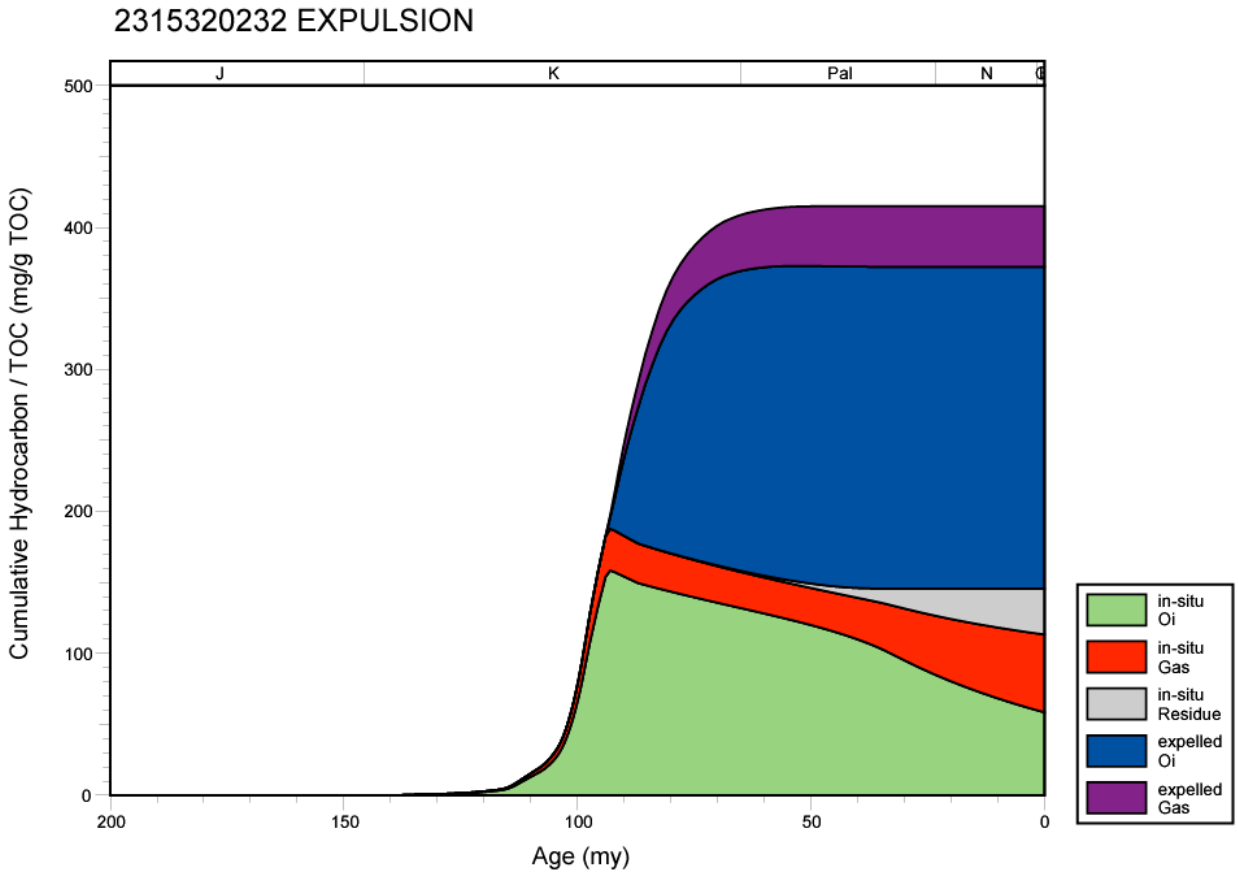


Figure 303. Hydrocarbon expulsion plot for well 2315320232, Mississippi Interior Salt Basin.

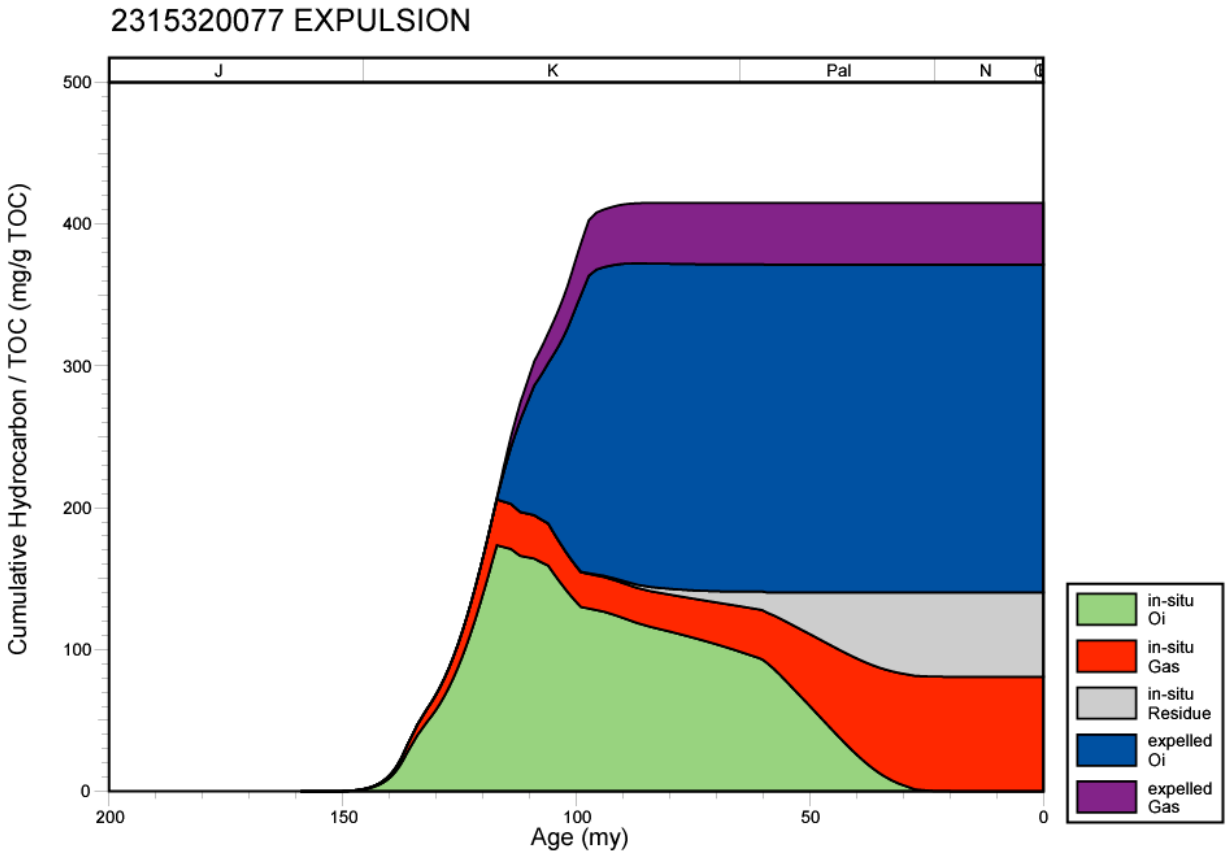


Figure 304. Hydrocarbon expulsion plot for well 2315320077, Mississippi Interior Salt Basin.

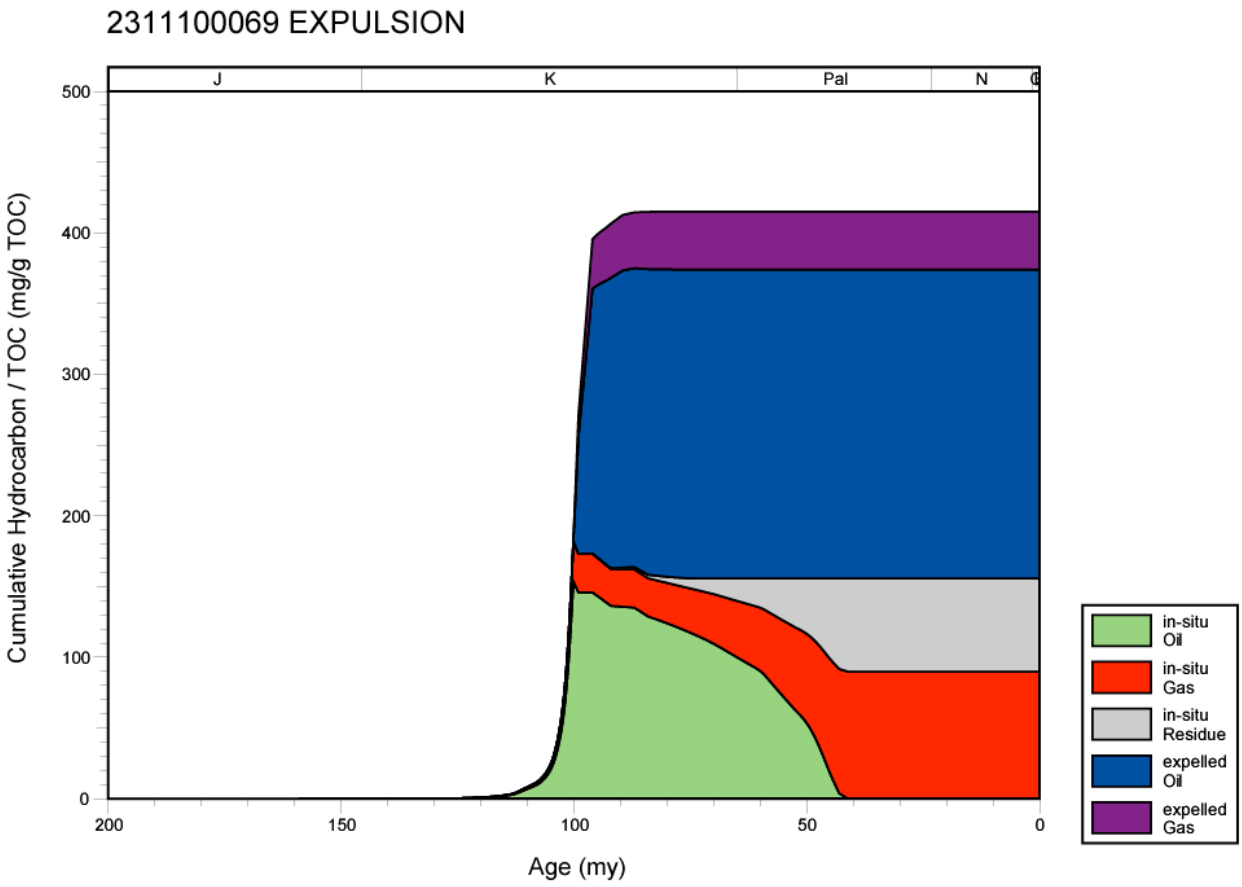


Figure 305. Hydrocarbon expulsion plot for well 2311100069, Mississippi Interior Salt Basin.

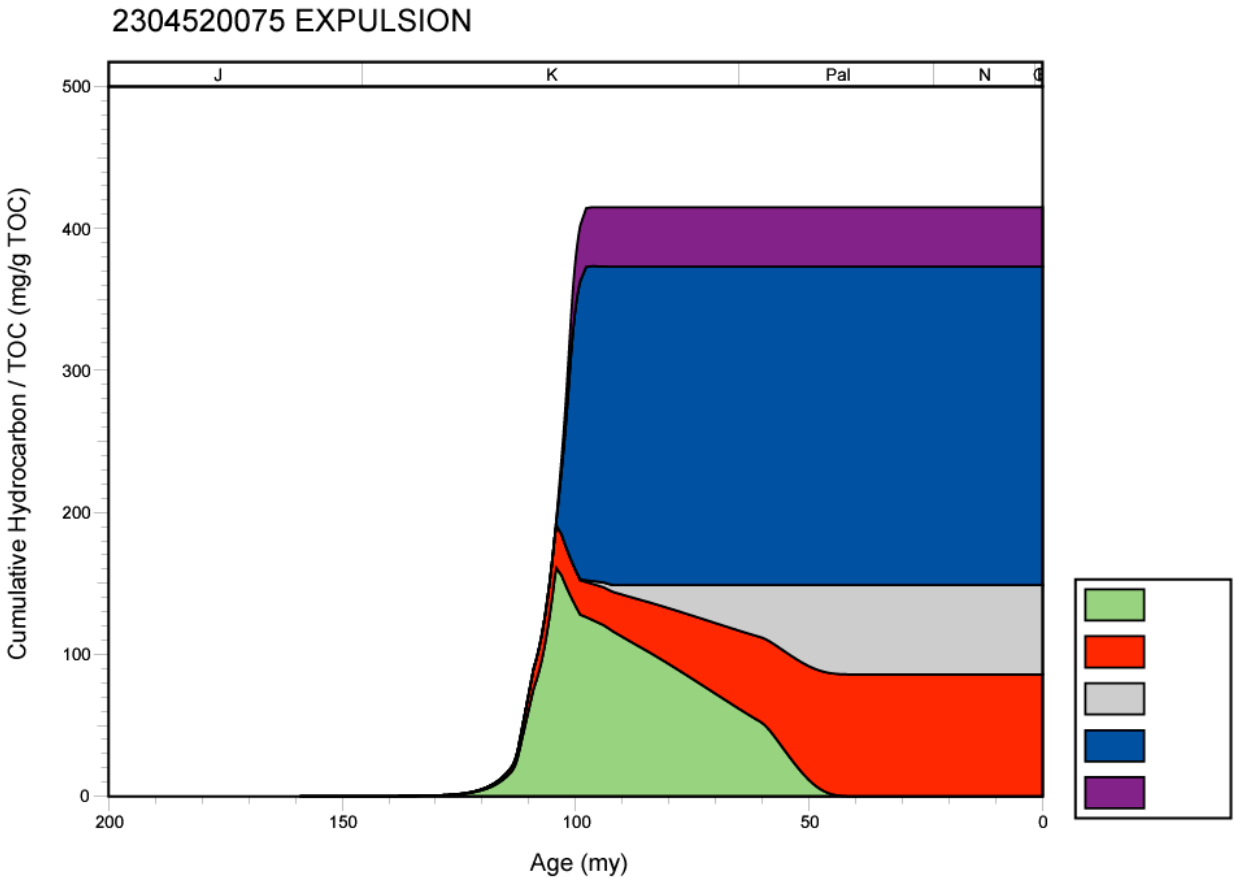


Figure 306. Hydrocarbon expulsion plot for well 2304520075, Mississippi Interior Salt Basin.

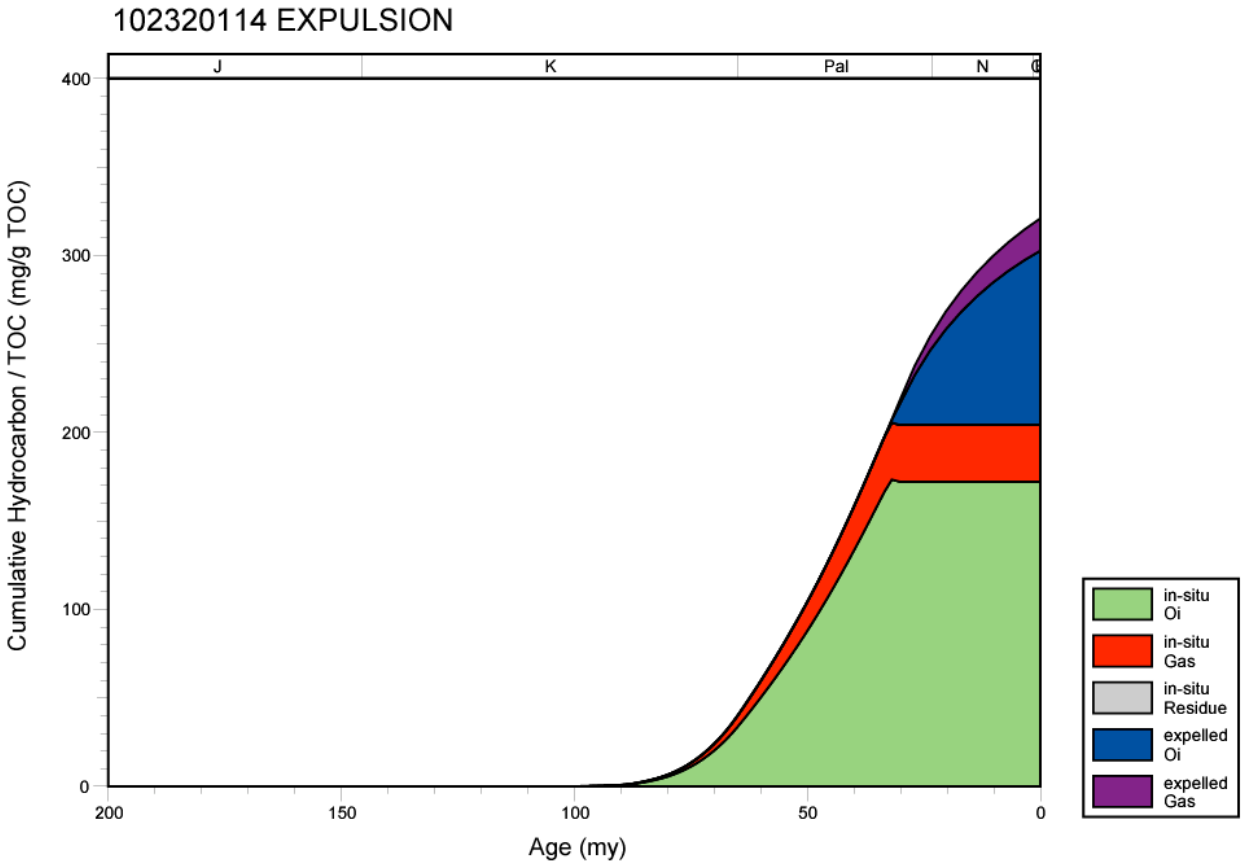


Figure 307. Hydrocarbon expulsion plot for well 102320114, Mississippi Interior Salt Basin.

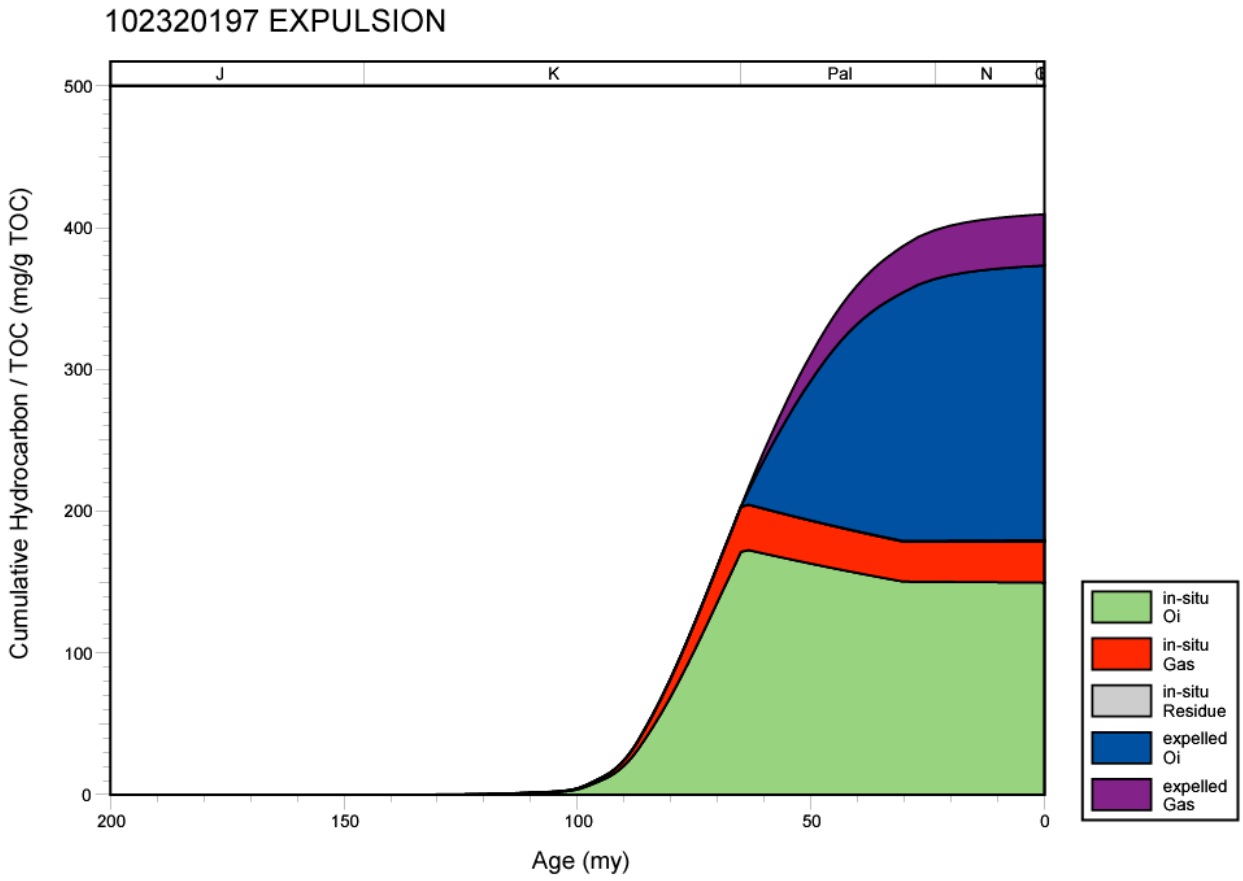


Figure 308. Hydrocarbon expulsion plot for well 102320197, Mississippi Interior Salt Basin.

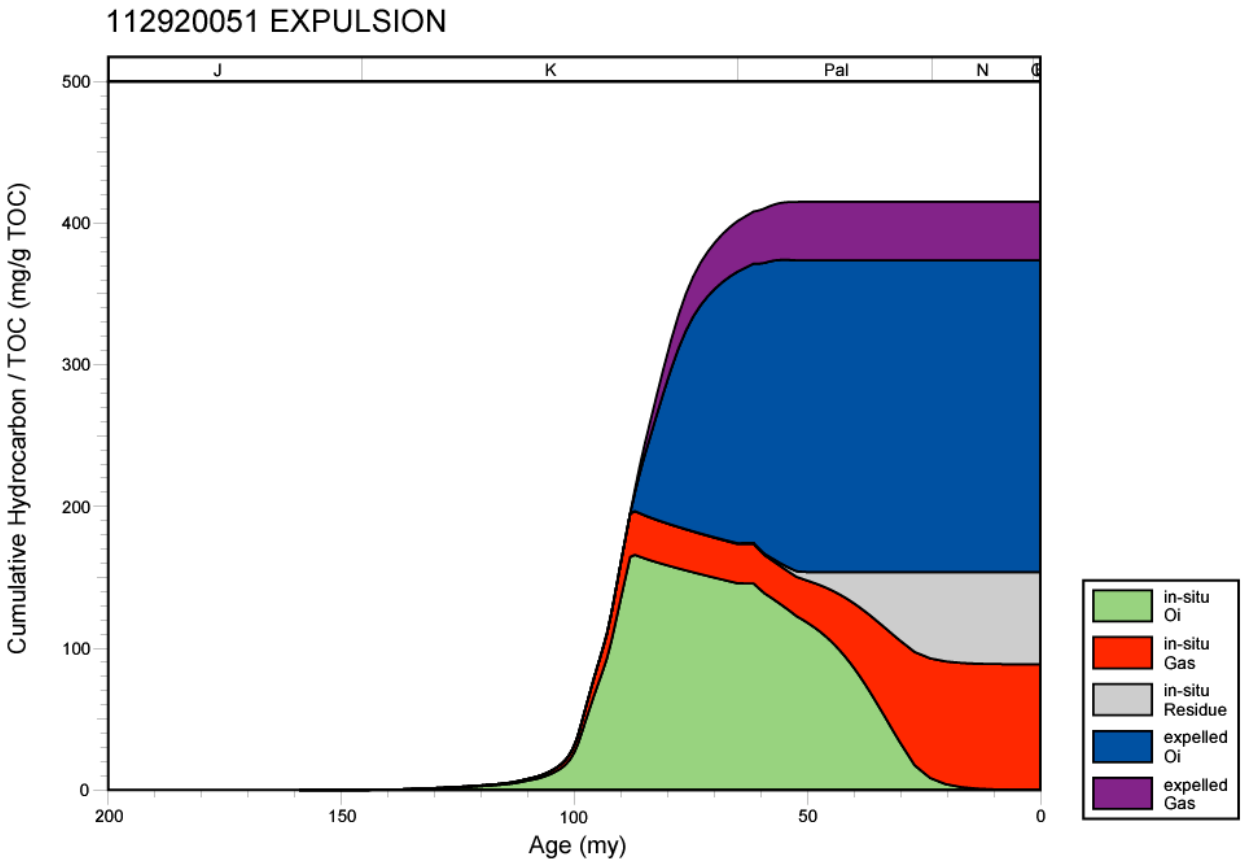


Figure 309. Hydrocarbon expulsion plot for well 112920051, Mississippi Interior Salt Basin.

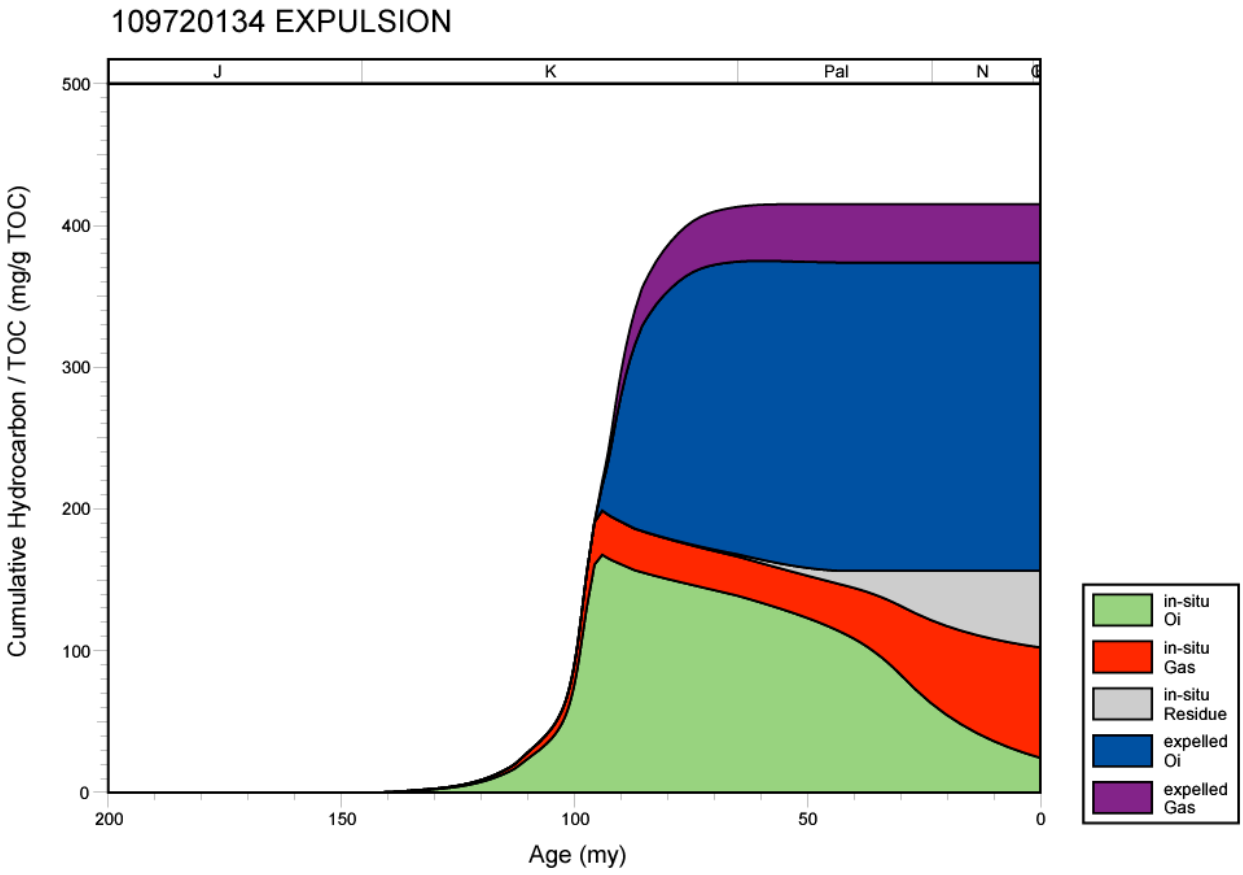


Figure 310. Hydrocarbon expulsion plot for well 109720134, Mississippi Interior Salt Basin.

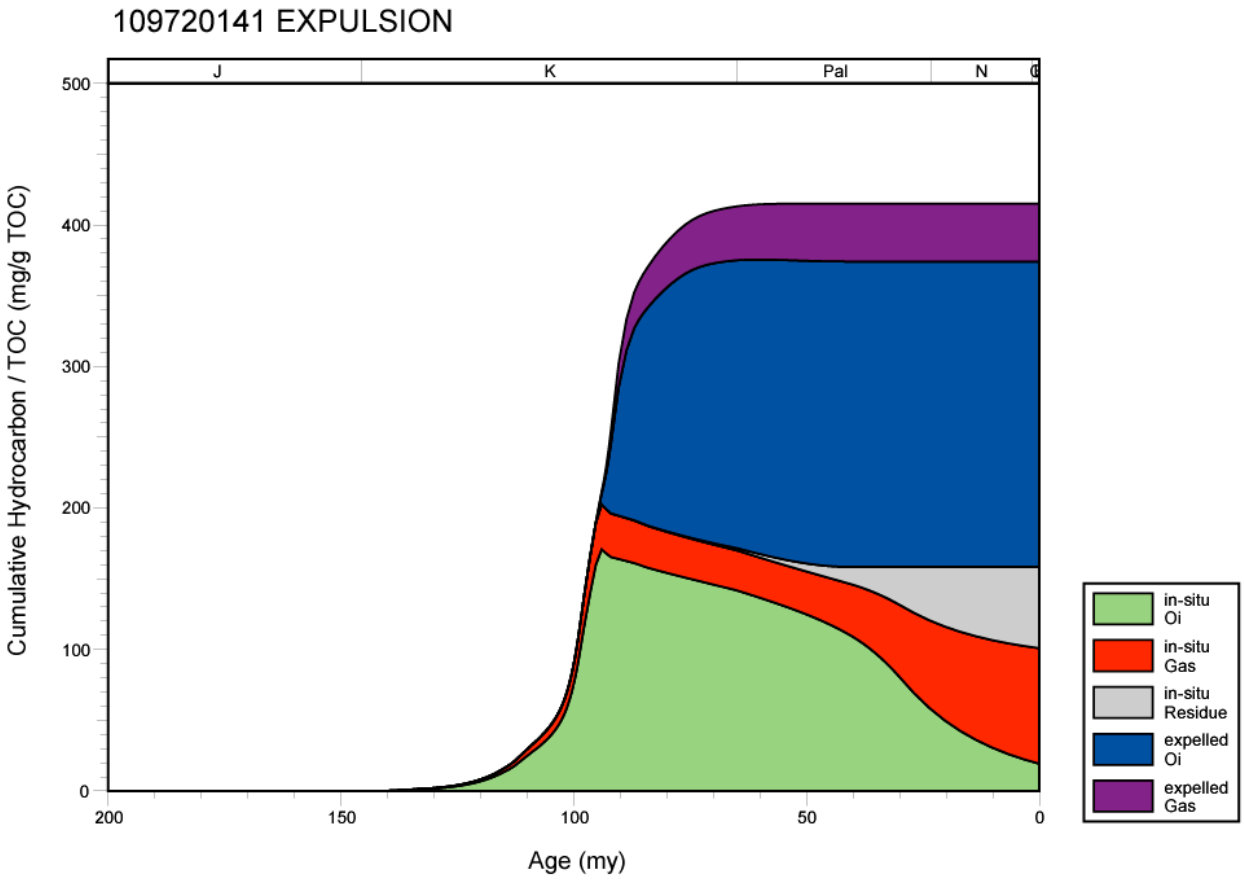


Figure 311. Hydrocarbon expulsion plot for well 109720141, Mississippi Interior Salt Basin.

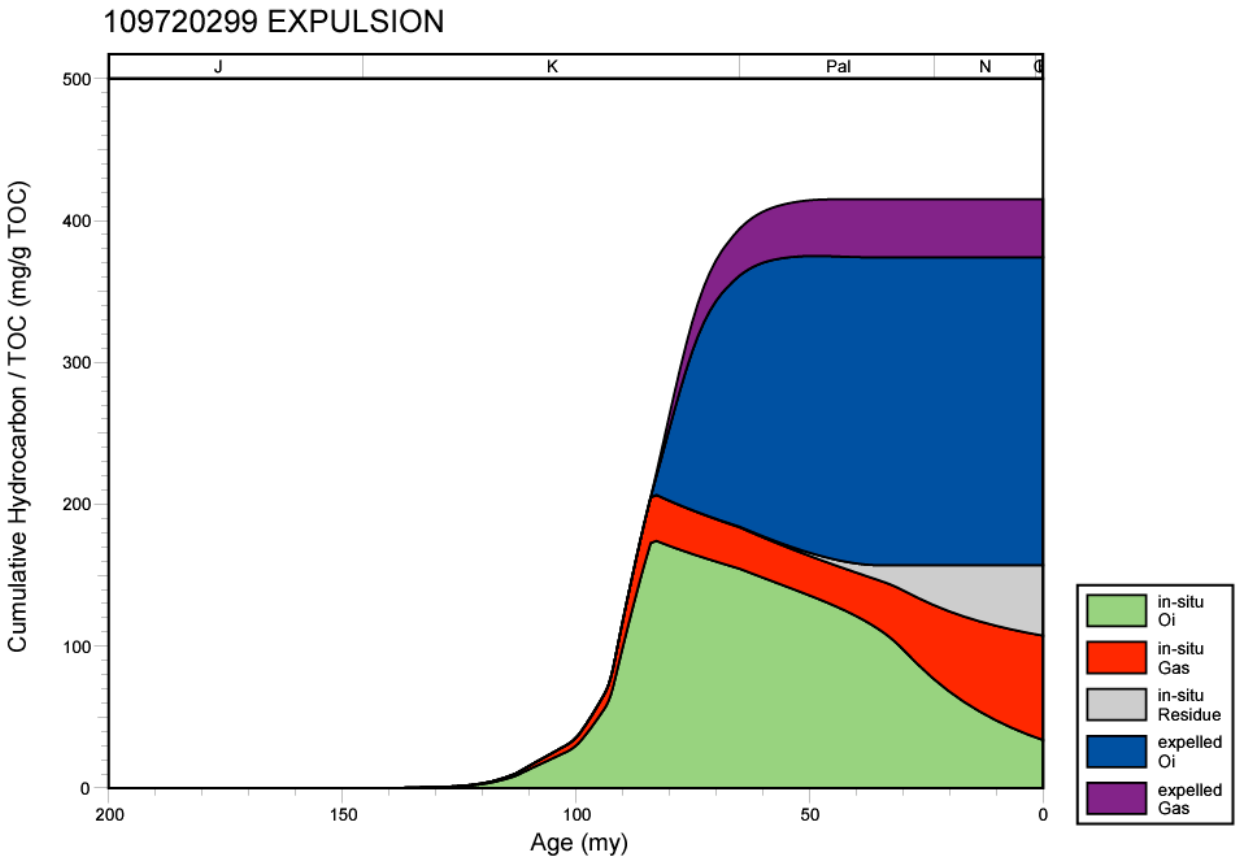


Figure 312. Hydrocarbon expulsion plot for well 109720299, Mississippi Interior Salt Basin.

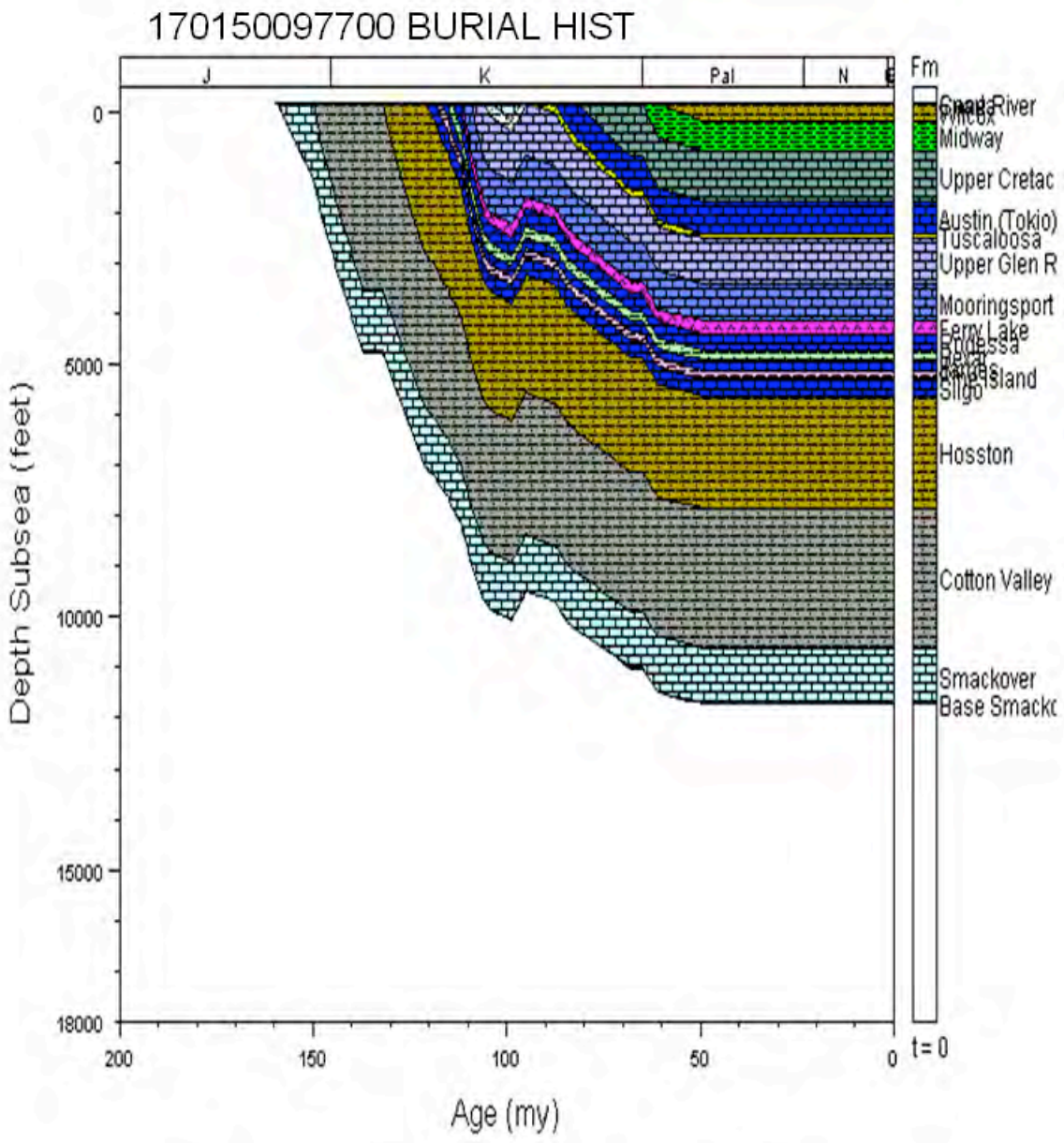


Figure 313. Burial history for well 170150097700. Sabine Uplift.
Prepared by Roger Barnaby.

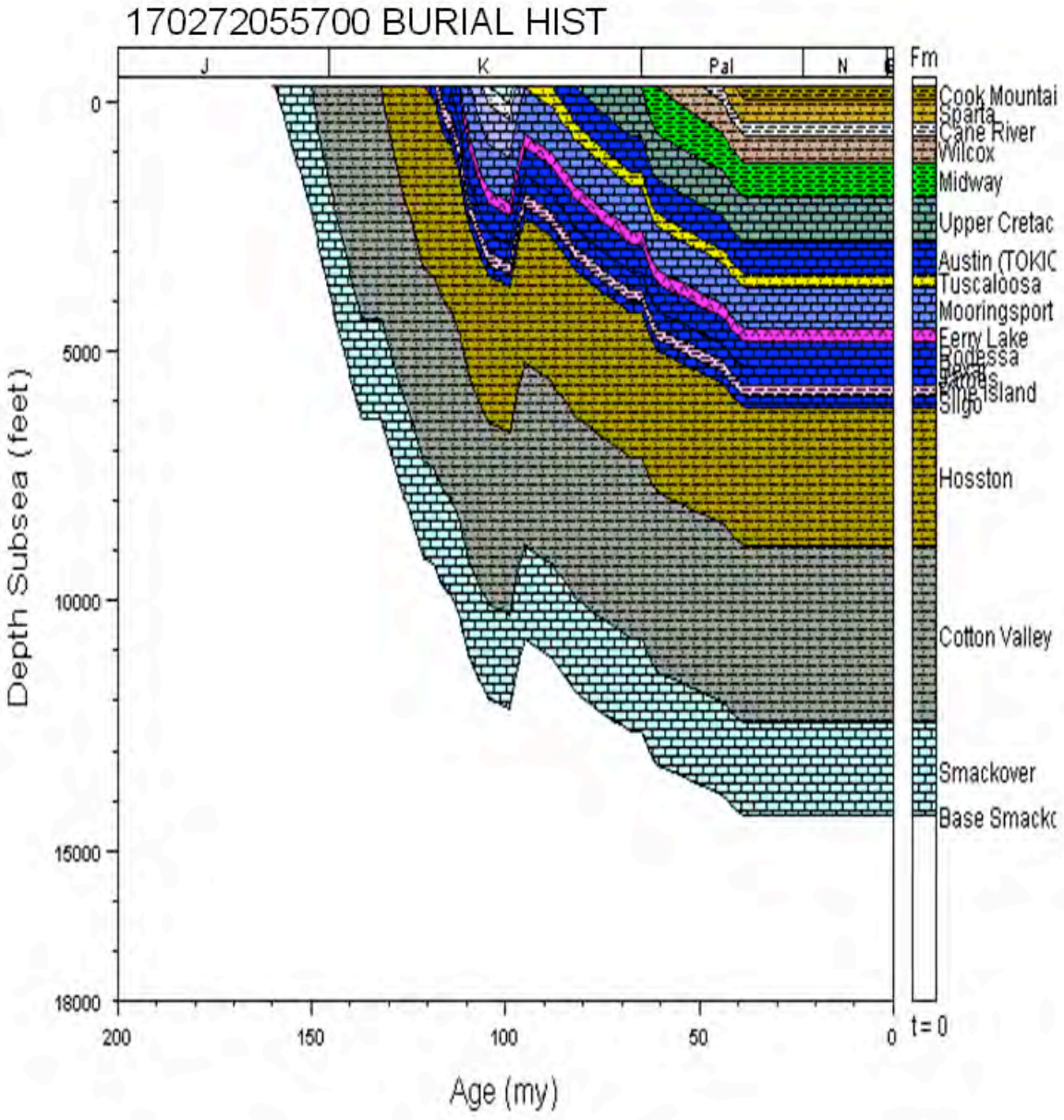


Figure 314. Burial history for well 170272055700. Updip/Margin. Prepared by Roger Barnaby.

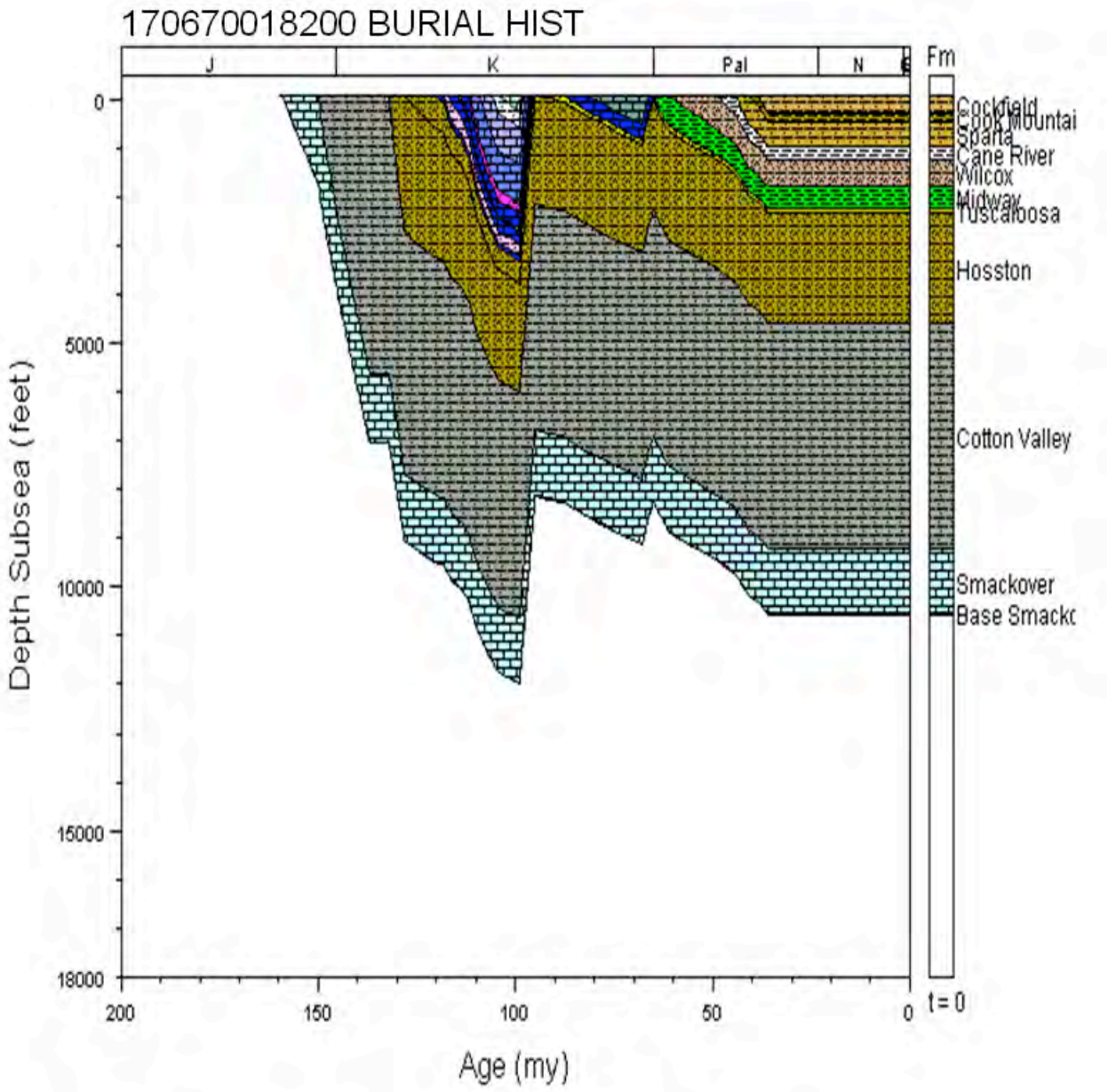


Figure 315. Burial history for well 170670018200. Monroe Uplift.
Prepared by Roger Barnaby.

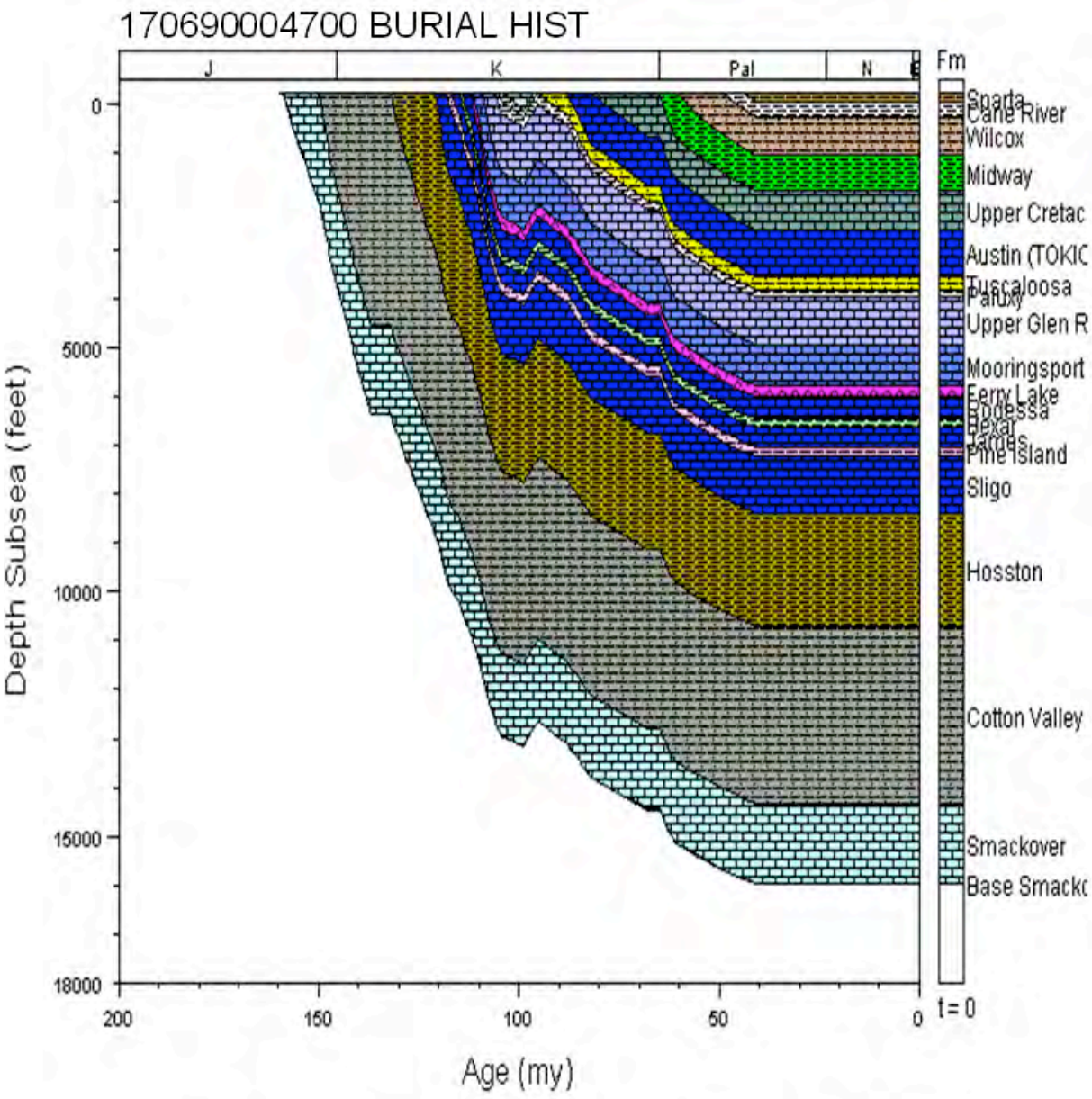


Figure 316. Burial history for well 170690004700. Downdip/Basin Center. Prepared by Roger Barnaby.

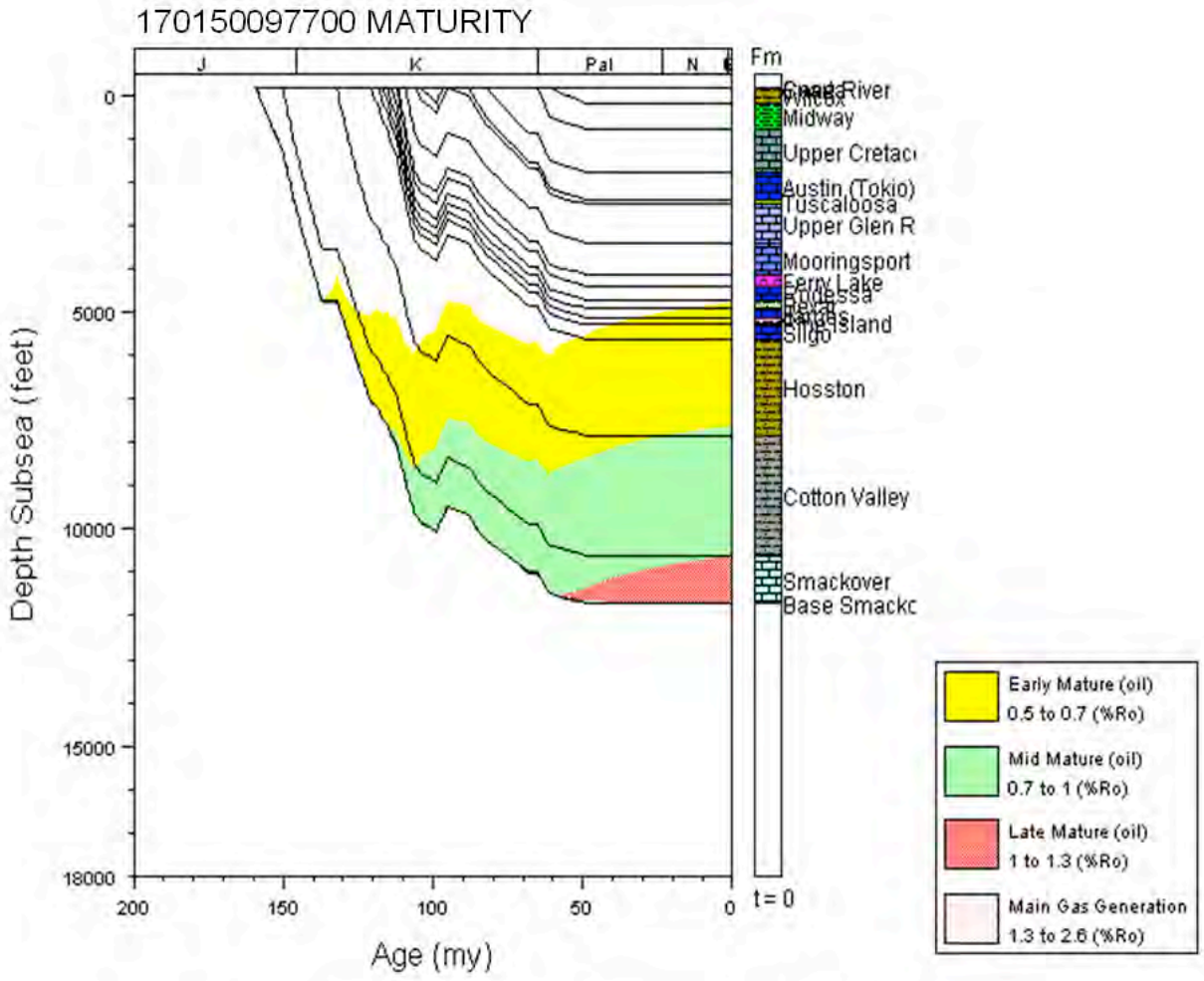


Figure 317. Thermal maturation profile for well 170150097700. Sabine Uplift. Prepared by Roger Barnaby.

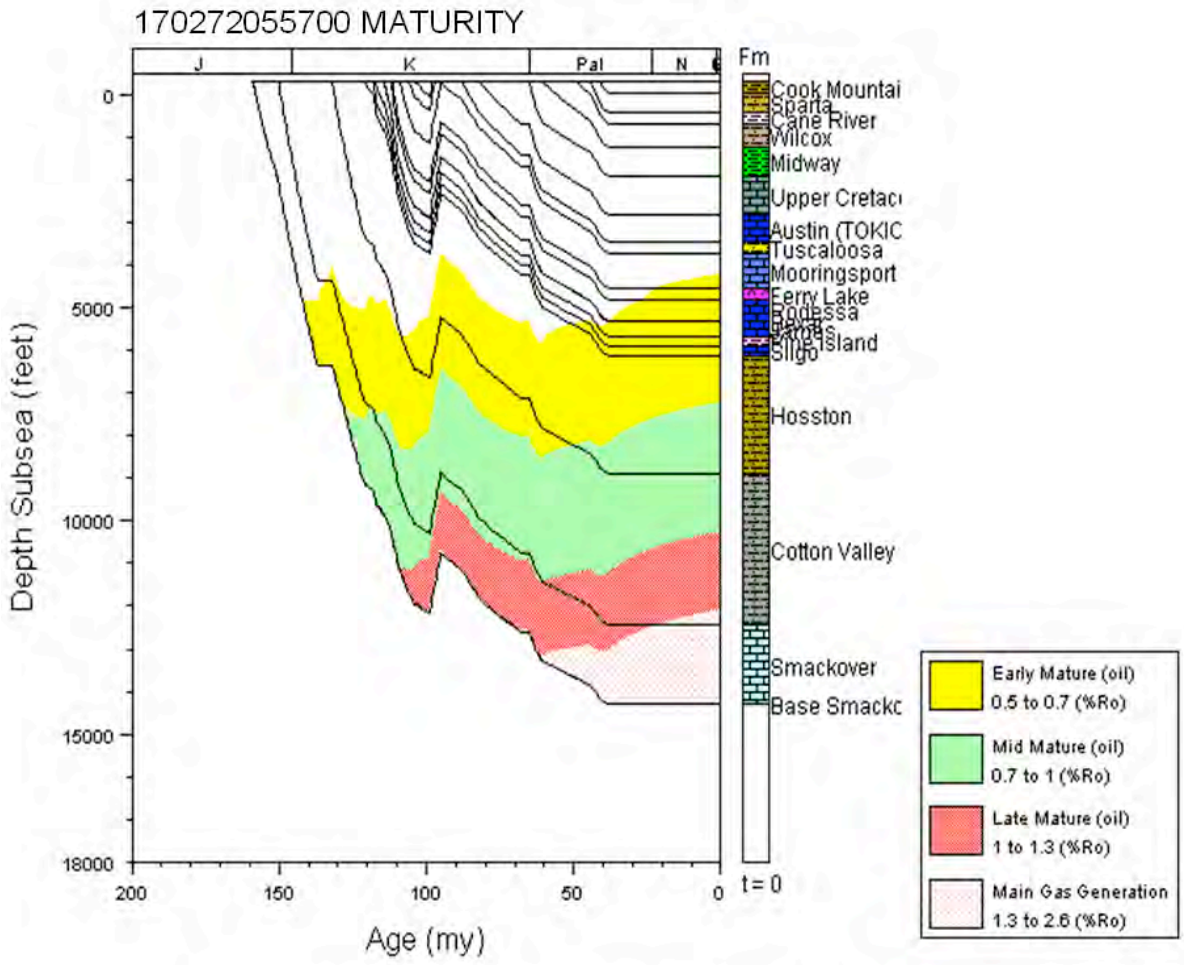


Figure 318. Thermal maturation profile for well 170272055700. Updip/Margin. Prepared by Roger Barnaby.

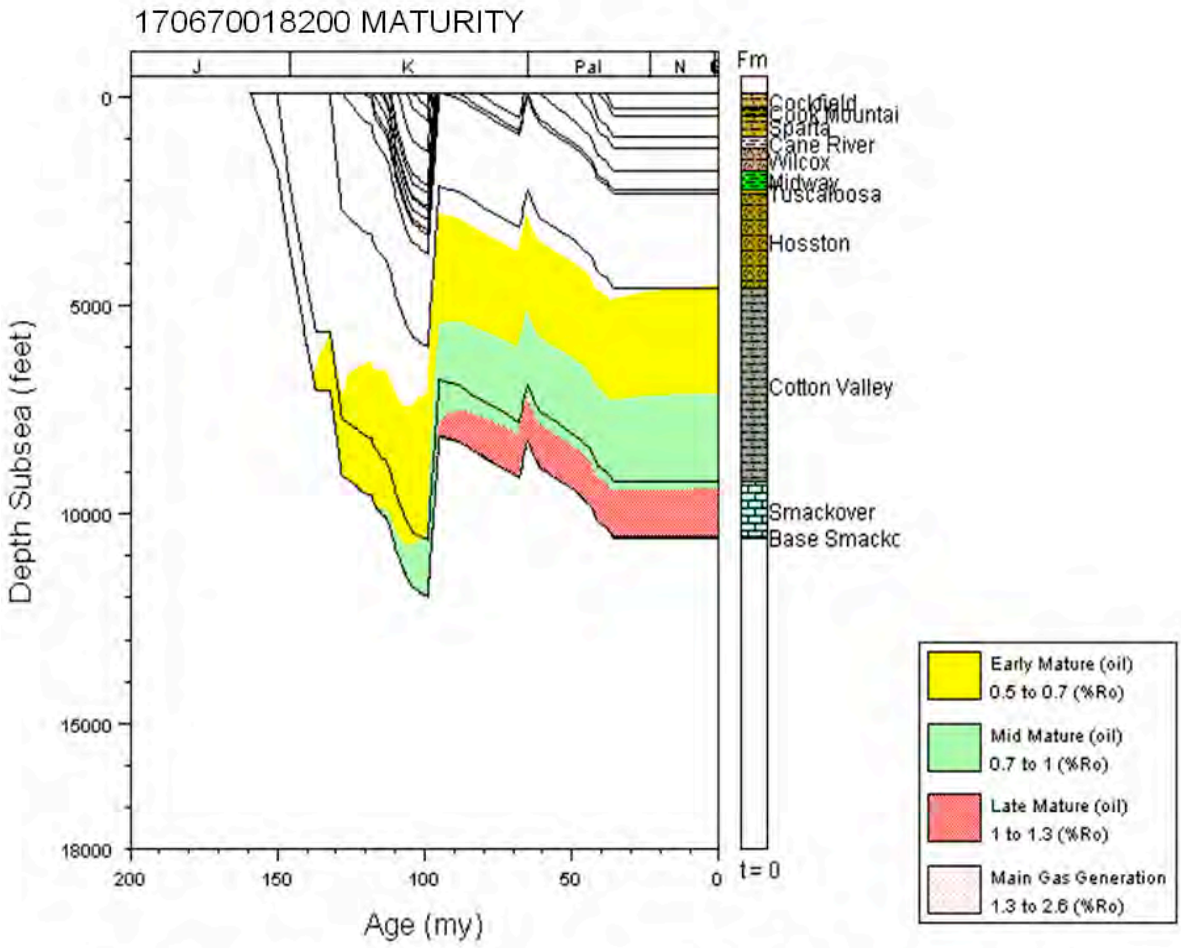


Figure 319. Thermal maturation profile for well 170670018200. Monroe Uplift. Prepared by Roger Barnaby.

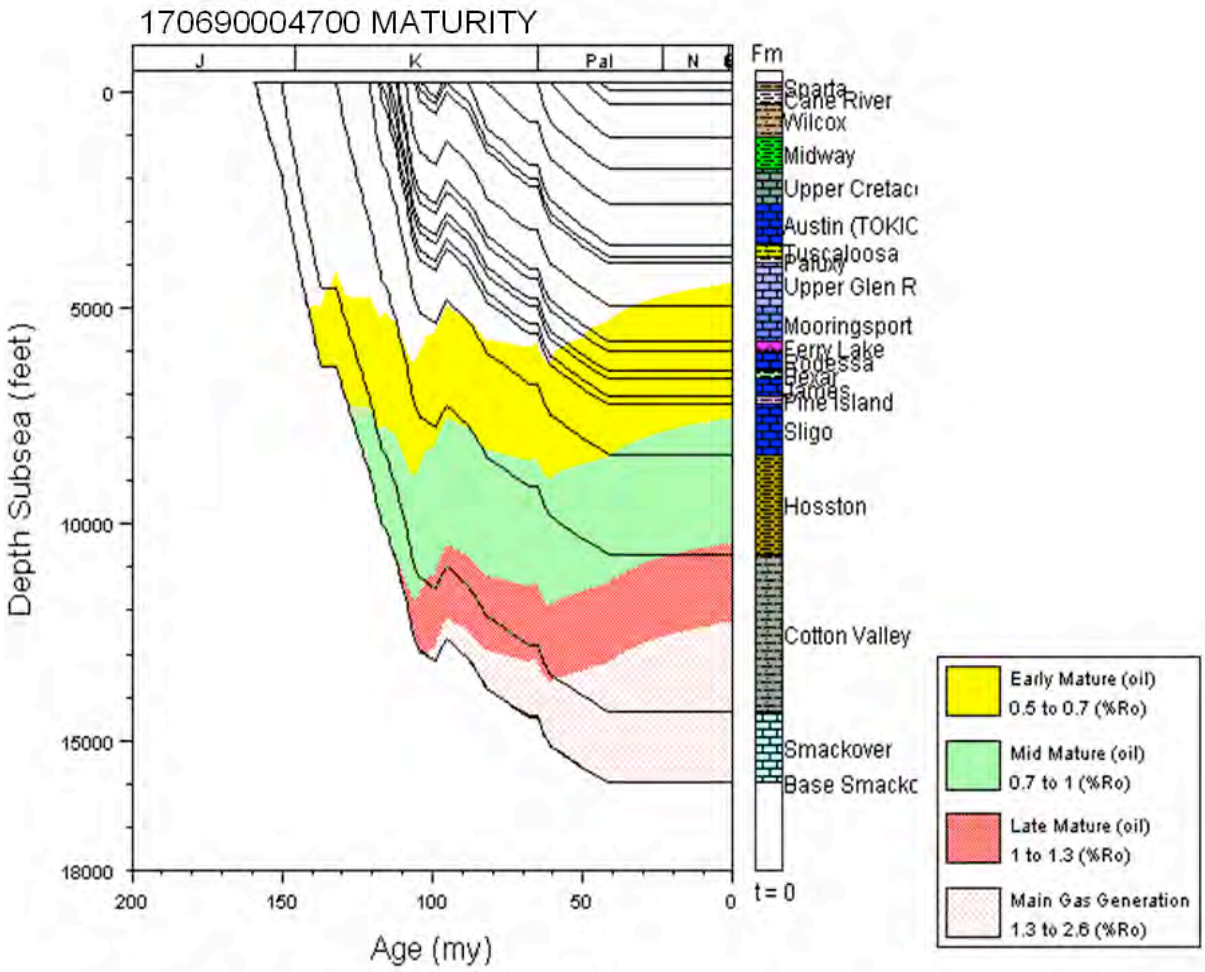


Figure 320. Thermal maturation profile for well 170690047700. Downdip/Basin Center. Prepared by Roger Barnaby.

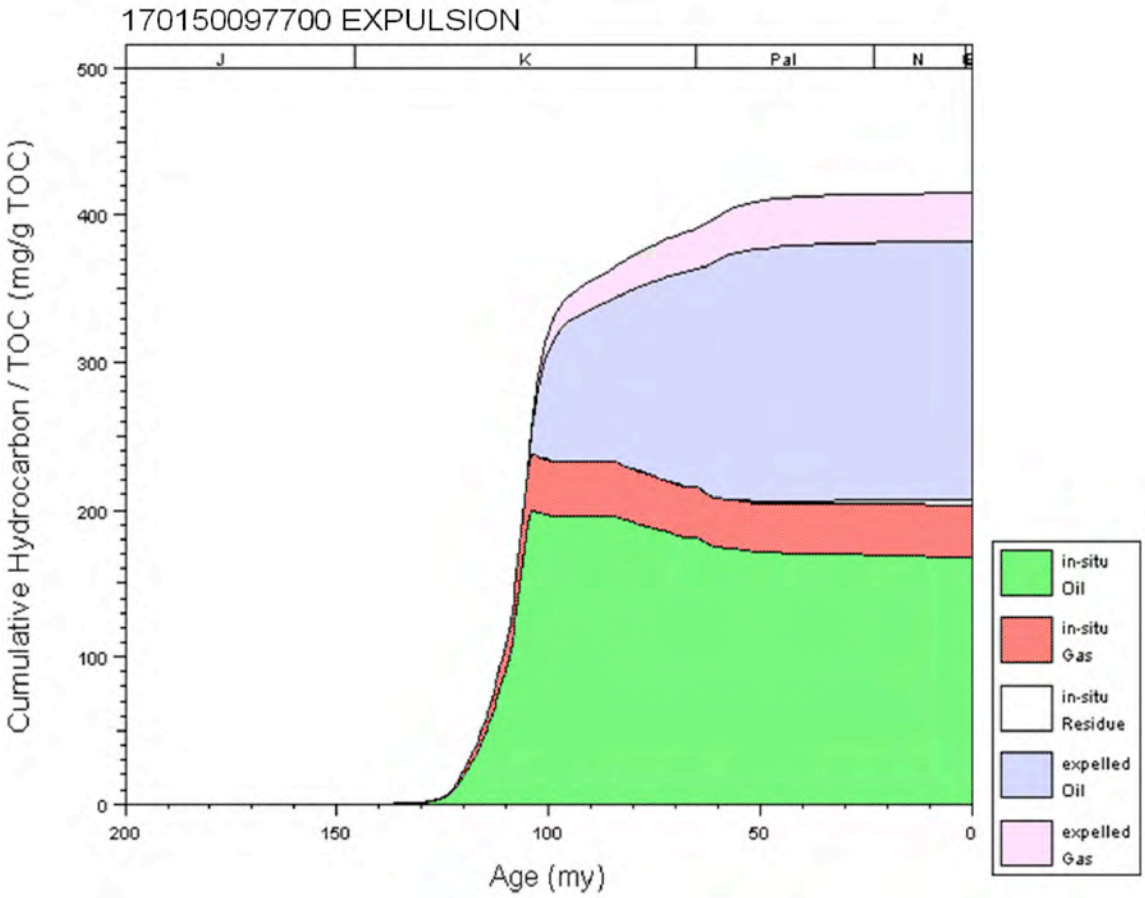


**Figure 321. Hydrocarbon expulsion plot for well 170150097700. Sabine Uplift. Prepared by Roger Barnaby.**

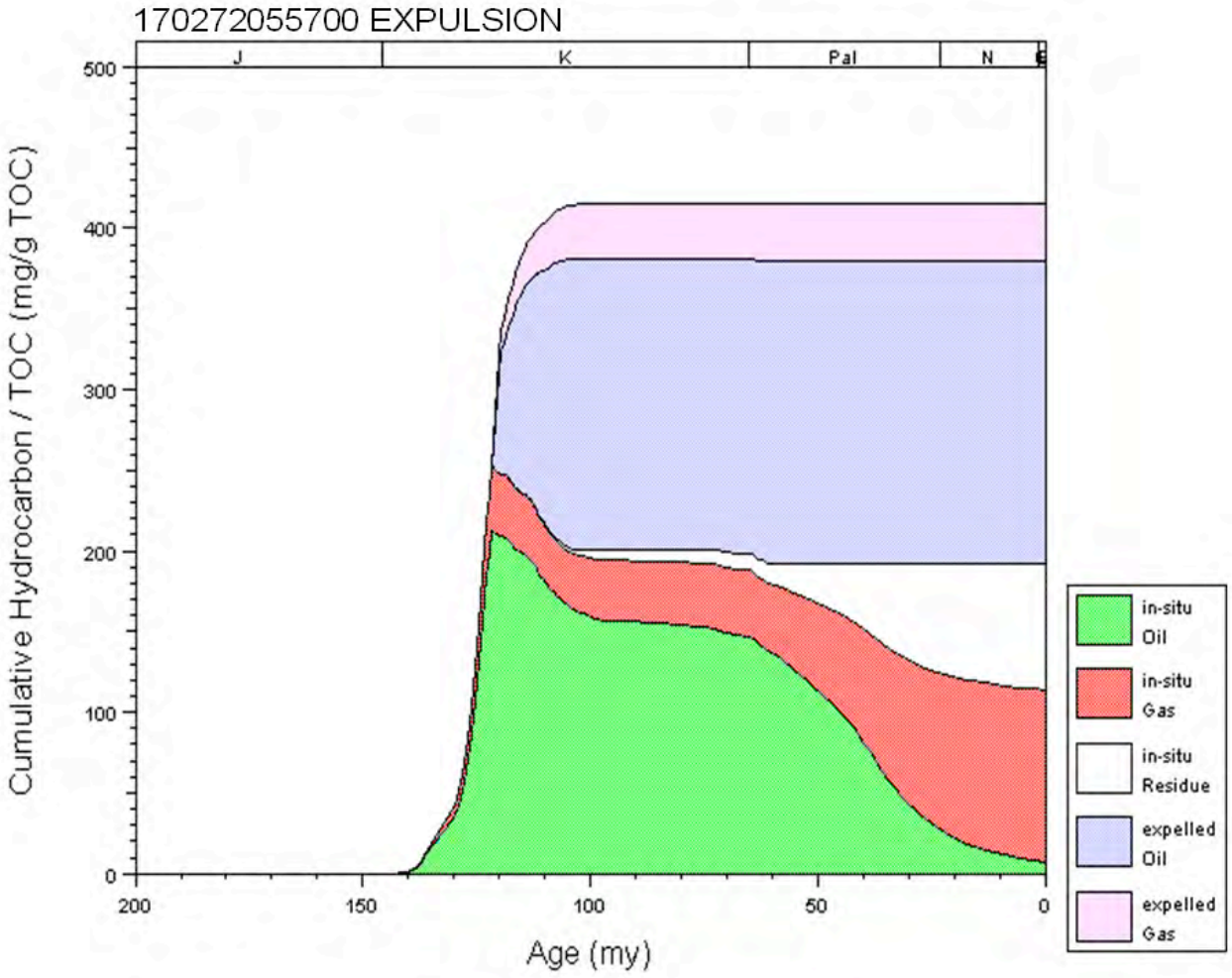


Figure 322. Hydrocarbon expulsion plot for well 170272055700. Updip/Margin. Prepared by Roger Barnaby.

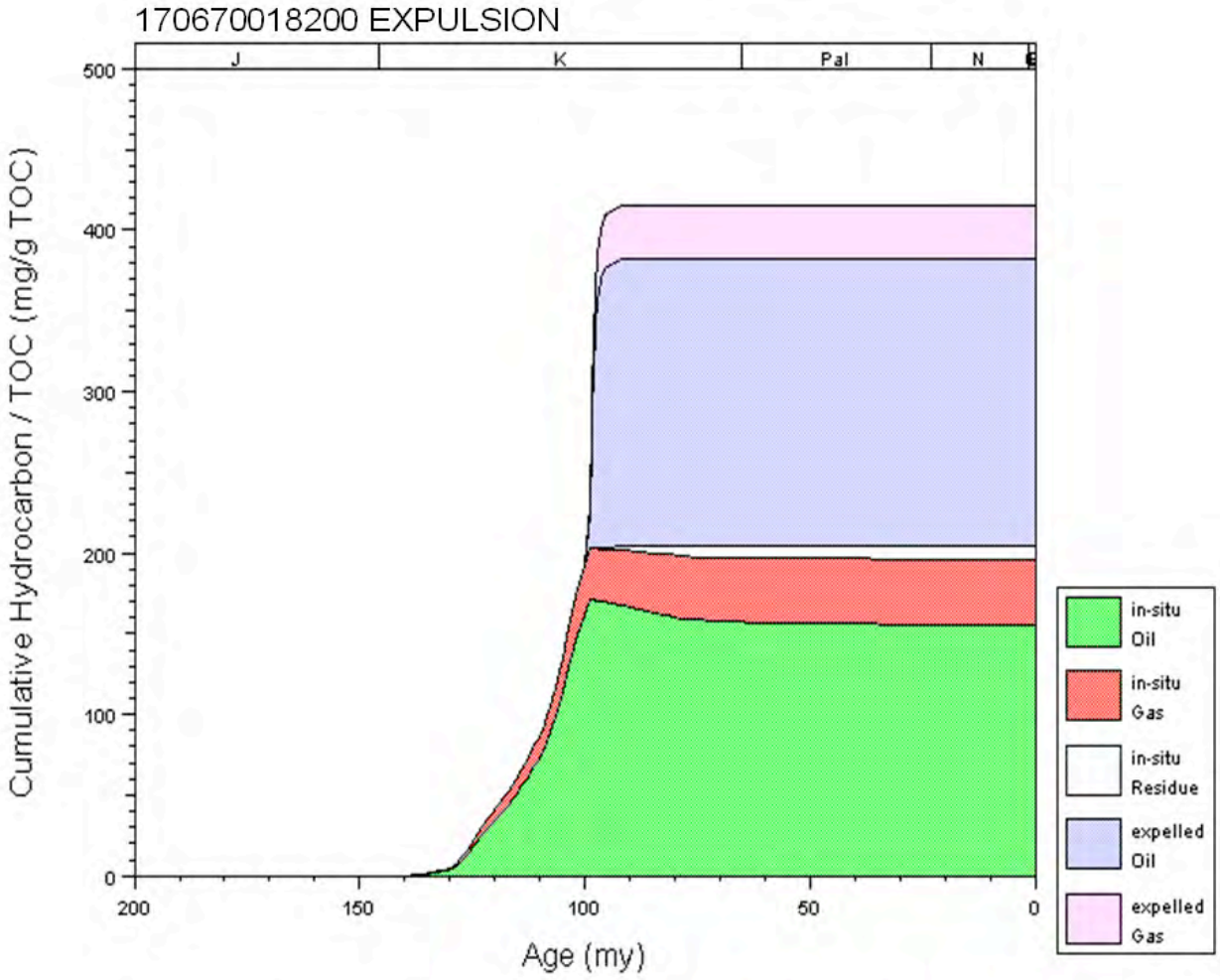


Figure 323. Hydrocarbon expulsion plot for well 170670018200. Monroe Uplift. Prepared by Roger Barnaby.

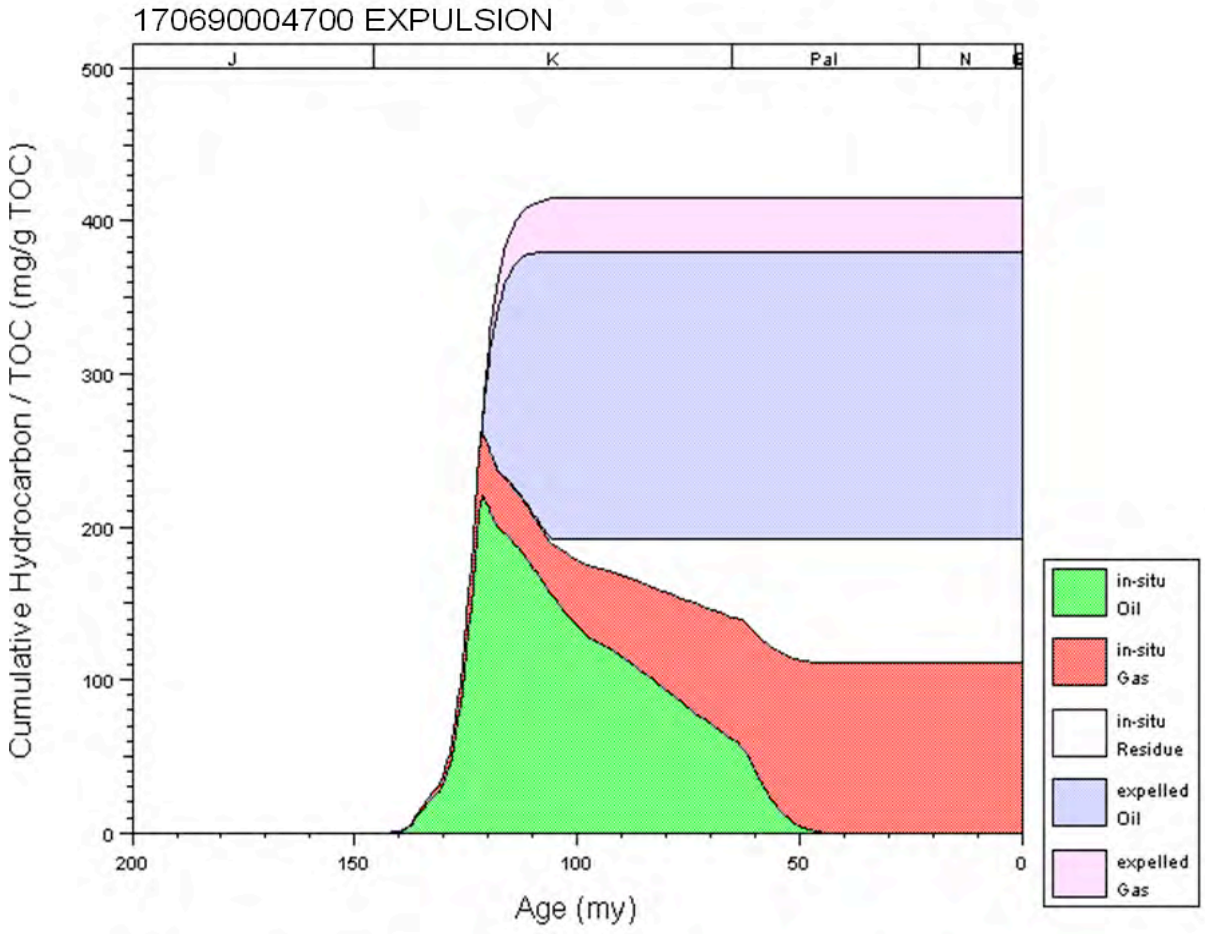


Figure 324. Hydrocarbon expulsion plot for well 170690004700. Downdip/Basin Center. Prepared by Roger Barnaby.

siliciclastic sediments (red beds) and associated volcanics in rapidly subsiding grabens and the accumulation of thick salt deposits and prolonged crustal cooling and subsidence from the Late Jurassic into the Cretaceous (Salvador, 1991a). In the Gulf, oceanic crust is surrounded by attenuated continental crust (Winker and Buffler, 1988) (Fig. 325). The transition from continental crust (predated the formation of the Gulf of Mexico and has not been significantly modified) to thick transitional crust (extended, thinned and/or intruded as a result of rifting) corresponds to a regional hinge zone or flexure in the basement and approximates the updip limit of Louann Salt deposition (Sawyer et al., 1991). The boundary is defined as a series of faults, including the Bahamas Fracture Zone offshore and regional peripheral fault trend onshore (Winker and Buffler, 1988; Sawyer et al., 1991). Alignment of these fault systems indicates a large-scale, left-slip series of transform and wrench faults that were active during the Late Triassic to Early Jurassic rift phase and the middle Jurassic to Late Jurassic opening of the Gulf of Mexico (Sawyer et al., 1991). The transition from thick transitional crust to thin transitional crust corresponds to a major tectonic hinge zone in the basement and approximates the Lower Cretaceous shelf margin (Sawyer et al., 1991) (Fig. 325). The boundary is defined by the Cuba Fracture Zone and Pearl River Transfer Fault (Dobson and Buffler, 1991; MacRae and Watkins, 1996). Within the zone of thick transitional crust, a pattern of alternating relict basement highs and lows occurs which represents areas of greater or lesser attenuation (Winker and Buffler, 1988). The paleotopographic highs are interpreted to be continental blocks that are relicts of rifting that have rotated counterclockwise and have not experienced much extension or internal deformation (Sawyer et al., 1991). The lows

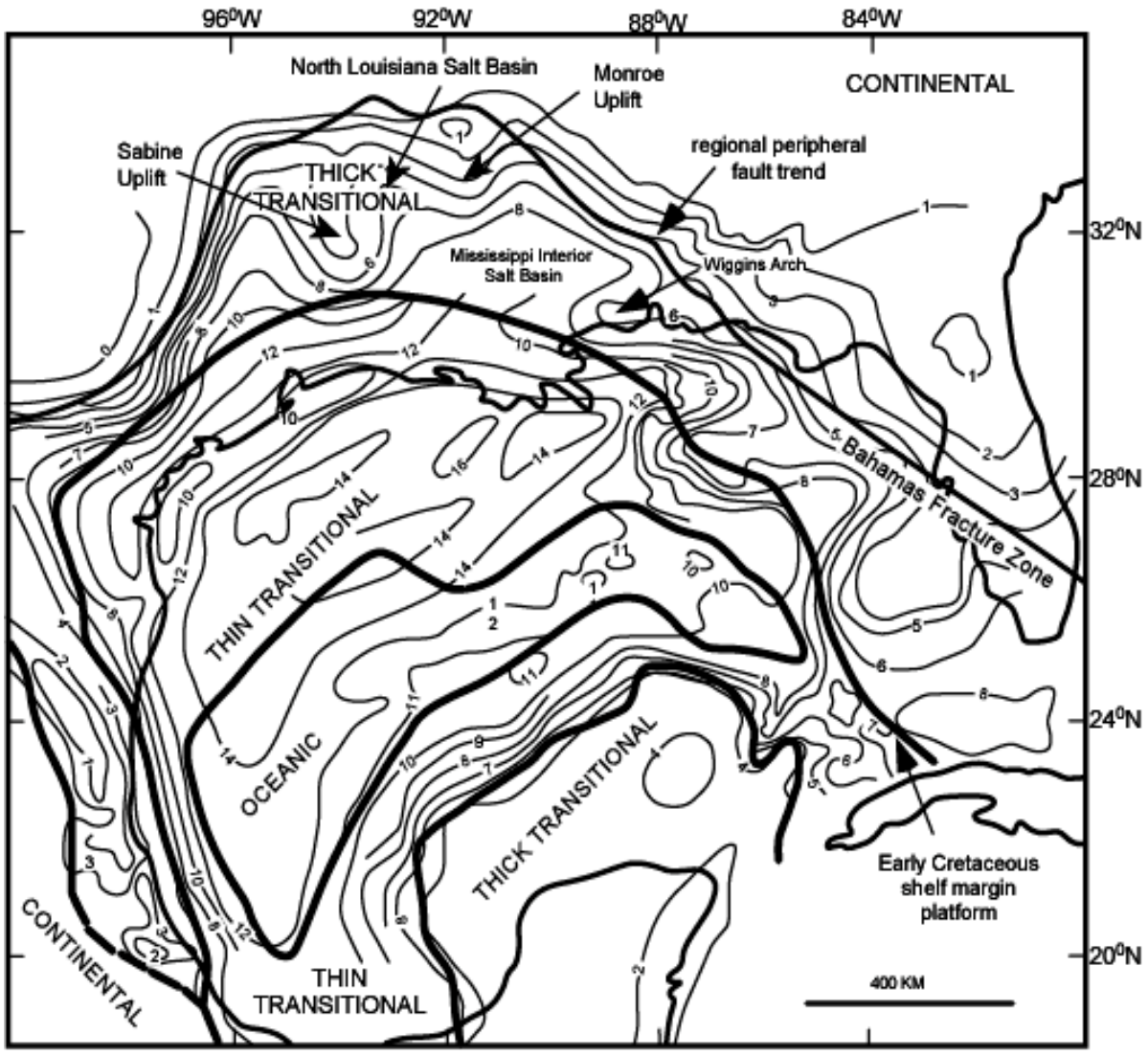


Figure 325. Distribution of crustal types and depth to basement in the Gulf of Mexico basin. Depth to basement is in kilometers (modified from Buffler, 1991).

would be depressions in the basement that formed due to greater crustal extension between these continental blocks (Sawyer et al., 1991). An example of a relict high is the Wiggins Arch and examples of basement lows that acted as depocenters are the Mississippi Interior Salt Basin and North Louisiana Salt Basin.

Based on the distribution of crust type, Sawyer et al. (1991) proposed the following as a model for the evolution of the Gulf of Mexico and related Mississippi Interior Salt Basin and North Louisiana Salt Basin. A Late Triassic-Early Jurassic early rifting phase is characterized by large and small half-grabens bounded by listric normal faults and filled with nonmarine siliciclastic sediments (red beds) and volcanics. A Middle Jurassic phase of rifting, crustal attenuation and the formation of transitional crust is characterized by the evolution of a pattern of alternating basement highs and lows and the accumulation of thick salt deposits (Fig. 326). A Late Jurassic phase of sea-floor spreading and oceanic crust formation in the deep central Gulf of Mexico is characterized by a regional marine transgression as a result of crustal cooling and subsidence. Subsidence continued into the Early Cretaceous and a carbonate shelf margin developed along the tectonic hinge zone of differential subsidence between thick and thin transitional crust. This pattern of deposition was broken by a period of igneous activity and global sea-level fall during the Late Cretaceous (mid-Cenomanian) that produced a major lowering of sea level in the region and resulted in the exposure of the shallow Cretaceous platform margin that rimmed the Gulf (Salvador, 1991b). This mid-Cenomanian unconformity is most pronounced in the northern Gulf of Mexico area.

The Mesozoic and Cenozoic strata of the northeastern Gulf of Mexico were deposited as part of a seaward - dipping wedge of sediment that accumulated in

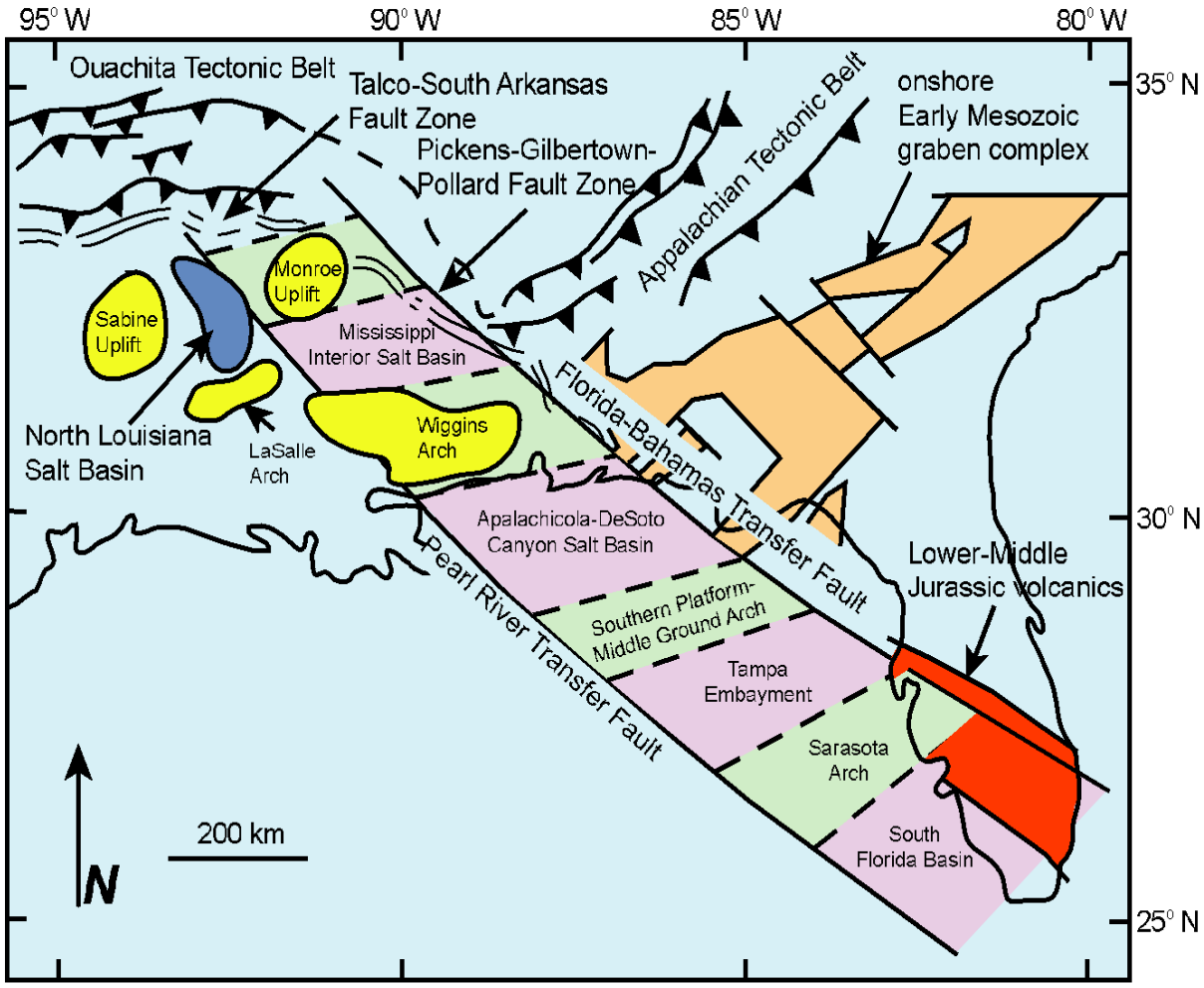


Figure 326. Tectonic framework of part of the northern Gulf of Mexico region (modified from MacRae and Watkins, 1996).

differentially subsiding basins on the passive margin of the North American continent. Basement cooling and subsidence resulted in a progressive infilling of the accommodation space throughout the Jurassic. Structural elements that affected the general orientation of these strata include basement features associated with plate movement and features formed due to halokinesis of Jurassic salt. The basement surface is dissected by the regional basement rift system that consists of a rift-related trend of divergent wrench-type basement faults and associated grabens and half grabens (Mink et al., 1990; Tew et al., 1991). The major basement faults are the northwest-southeast trending Florida-Bahamas and Pearl River transfer faults. The graben system is a result of rifting and its geometry is a reflection of the direction of plate separation (MacRae and Watkins, 1996). The Lower Cretaceous shelf margin that corresponds to a major basement hinge dominated carbonate deposition throughout the Early Cretaceous.

The major positive basement features that influenced the distribution and nature of Mesozoic deposits in the northern Gulf of Mexico are the Sabine Uplift, Monroe Uplift, Wiggins Arch, Middle Ground Arch-Southern Platform, Choctaw Ridge, the Conecuh Ridge, the Pensacola Arch, and the Decatur Ridge. These structural elements, such as the Choctaw, Conecuh, Pensacola, and Decatur Ridge complexes, are associated with the Appalachian fold and thrust structural trend that was formed in the late Paleozoic by tectonic events resulting from convergence of the North American and African-South American continental plates. The Sabine Uplift, Monroe Uplift, Wiggins Arch and Middle Ground Arch-Southern Platform are associated with crustal extensional and rifting (Miller, 1982; Sawyer et al., 1991). These basement features may be remnants of the rifted continental margin of North America. The Wiggins Arch consists of pre-rift

Paleozoic metamorphic and granitic rocks (Cagle and Khan, 1983) and the Middle Ground Arch includes pre-rift Paleozoic and Triassic rocks (Dobson, 1990). The Middle Ground Arch is a broad structural nose that plunges southwest toward the Southern Platform (Dobson, 1990). Paleotopography had a significant impact on the distribution of sediment, and positive areas within basins and along basin margins provided sources for Mesozoic terrigenous sediments (Mancini et al., 1985b). The East Texas Salt Basin, North Louisiana Salt Basin, Mississippi Interior Salt Basin and the Apalachicola-De Soto Canyon Salt Basin, which are major negative structural features in the northern Gulf of Mexico, are classified as the interior fracture portion of a margin sag basin using the classification of Kingston et al. (1983). These extensional basins were associated with early rifting linked with wrench faulting and were actively subsiding depocenters throughout the Mesozoic and into the Cenozoic. The North Louisiana Salt Basin is bounded on the west by the Sabine Uplift, on the east by the Monroe Uplift and LaSalle Arch, and on the south by the Angelina Flexure. The North Louisiana Salt Basin has a maximum sediment filled depth of 27,000 ft (Scardina, 1982).

Most, but not all, of the distinctively salt movement related structural features recognized in the North Louisiana Salt Basin today developed between the Mesozoic and the end of the Cretaceous. However, rejuvenated movements of the Louann Salt occurred in some parts of the basin in the early part of the Tertiary. In general, following the deposition of the Louann Salt, the basin underwent a prolonged gradual subsidence and loading that was only interrupted occasionally by episodes of sub-regional uplift and erosion. Lowrie et al. (1993) proposed a model for the chronostratigraphy and tectonic

history of the northern margin of the Gulf of Mexico. Their analysis is listed herein and summarized as follows:

- End of Proterozoic-early Paleozoic, possibly through the Ordovician (some 450 mya), passive margin;
- Late Paleozoic (365-310 mya), Ouachita Orogeny, plate collision, emplacement of Sabine Terrane;
- Late Pennsylvanian-Permian (310-250 mya), deposition of carbonates over Sabine Terrane;
- Early and/or Middle Triassic (260-230 mya), regional extension of northern Mississippi Embayment area due to mantle plume/continental rifting episode;
- Late Triassic (230-200 mya), localized rifting south of Ouachita Orogeny, generally along an east-west trending basin, deposition of Eagle Mills Formation;
- Early Jurassic (200-180 mya), continental crust attenuation;
- Middle Jurassic (180-160 mya), rifting in north central Louisiana, beginning of North Louisiana Salt Basin proper and the area northward to edge of the Mississippi Embayment, origination of spreading in central North Atlantic and in central Gulf of Mexico, deposition of Louann Salt, incursion of seawater from Pacific Basin, relative uplift of Sabine uplift region;
- Late Jurassic (Kimmeridgian through Oxfordian, 155-130 mya), seafloor spreading in central Gulf of Mexico, as per Klitgord and Schoutan (1980), deposition of prograding Smackover, Buckner, and Cotton Valley formations in a deepening basin, depositional environments ranging from coastal plain and shelf

to slope, regional subsidence from the edge of Mississippi Embayment through North Louisiana Salt Basin, including proto-Sabine uplift;

- Early Cretaceous (130-110 mya), deposition of Hosston-Sligo formations in inner shelf environments, conditions occasionally suitable for deposition of carbonates, cessation of central Gulf of Mexico spreading and initiation of tectonic subsidence in North Louisiana-South Arkansas Basin and beginning of subsidence in the South Louisiana Salt Basin, continued regional subsidence from edge of Mississippi Embayment through proto-Sabine uplift region;
- Mid-Cretaceous formation of widespread unconformity in central Gulf of Mexico Basin, probable re-uplifting of the Sabine Uplift, subsidence of North Louisiana Salt Basin slows dramatically and is reduced by about 50%.

The sedimentary “basement” or starting point for the North Louisiana Salt Basin begins with Late Triassic terrestrial deposition in a structural crustal extensional setting. Evolving grabens were filled with red bed sequences of fluvial and freshwater lake sediments and deposition remained active during the early part of the Early Jurassic. This initial cycle of deposition culminated with the Upper Triassic-Lower Jurassic Eagle Mills Formation (Fig. 327) (Salvador, 1987). Early references to these deposits have been provided by Shearer (1938) and Weeks (1938). Subsurface penetrations of the formation have yielded red, reddish-brown, purplish, greenish-gray, or mottled shales, mudstones, and siltstones with lesser amounts of sandstone and conglomerate. As also reported by Scott et al. (1961), the Eagle Mills red bed deposits, where they have been penetrated in wells in south Arkansas, contain conglomeratic sandstones and red shales with diabase pebbles. These Eagle Mills terrestrial strata are positioned as the pre-syngenetic deposits

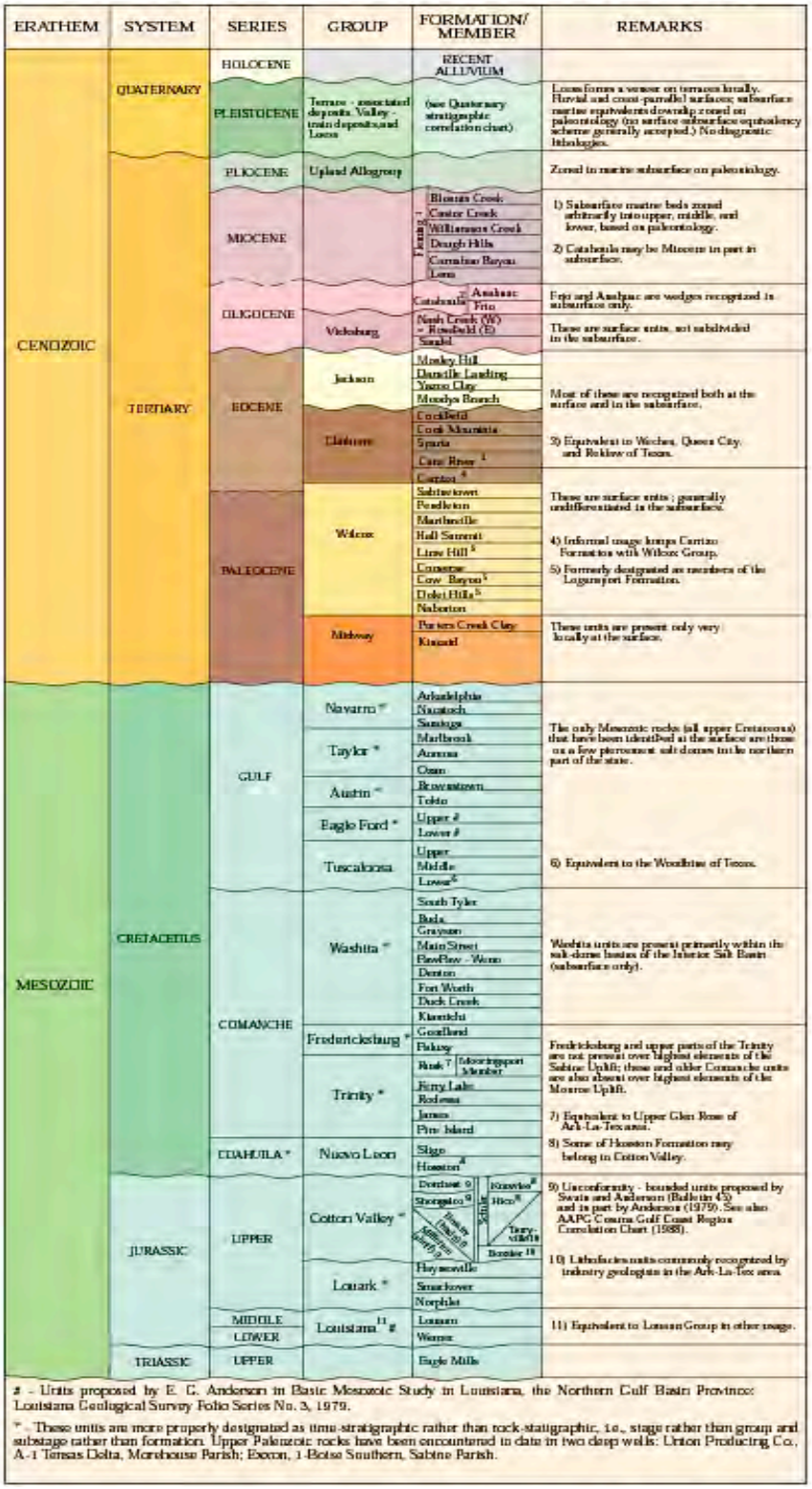


Figure 327. Stratigraphic section (By Louisiana Geological Survey).

of the overlying Middle Jurassic Werner and Louann evaporites that were laid down on the rifted, trailing plate margin of North America (Zimmerman, 1992). Following the deposition of the Eagle Mills in the early Jurassic, the North Louisiana Salt Basin underwent continental crust attenuation (200-180 mya). Subsequently (180-160 mya), middle Jurassic rifting occurred in central north Louisiana. The rifting provided a 40 million year period in which a hiatus in the depositional record developed as a result of non-deposition and/or erosion across the area.

In southern Arkansas, northern Louisiana, and adjacent parts of Texas and Mississippi, a unit predominantly composed of anhydrite, commonly associated with conglomerates and red siliciclastics at the base, underlies the Louann Salt. The formation was named the Werner Anhydrite by Hazzard et al. (1947). This underlying Werner-Louann sequence unconformably overlies the Eagle Mills Formation or older "basement" rocks, and it is in turn, overlain by the basal siltstone and sandstone unit (Norphlet Formation) of the Upper Jurassic.

The Louann Salt forms an extremely incompetent and ductile layer, particularly where it has accumulated to mid-basin thicknesses in excess of several thousands of feet. This layer, after it had been overlain by several thousand feet of younger sediments, was generally deformed into extensive massifs, walls, ridges, domal features, and spines, or into pillows and swells in the core of salt-supported anticlines. The thick salt layer has only been penetrated by wells along the northern rim of the basin, where it lies within economically drillable depths. However, most data concerning the distribution, type of occurrence, and thickness of the salt have been derived from oil and gas exploration

seismic reflection profiles. The “top of the salt” has also been reached by many wells drilled on or around diapiric salt features.

Probably, as the North Louisiana Salt Basin and the Mississippi Interior Salt Basin were developing, the Werner, and more particularly, thick Louann Salt deposits were separated physically by a stranded transform-faulted relic segment of an attenuated high crustal block (LaSalle Arch of Zimmerman, 1995). Only thin (probably less than 500 ft thick) Louann Salt was deposited across the feature’s crestal area. The physical separation between the East Texas Salt Basin and the North Louisiana Salt Basin was provided by the Sabine Uplift. Exploration wells on crestal areas of the uplift have encountered Paleozoic rocks beneath Oxfordian sediments with Louann, Werner, and Eagle Mills deposits missing because of non-deposition or erosion.

Seawater first invaded the North Louisiana Salt Basin during the late Bathonian or the Callovian (Salvador, 1987). This encroachment was then followed in the Oxfordian by a widespread and prolonged marine invasion. The initial Oxfordian influx created an increasingly larger and deeper body of water with unrestricted circulation and normal salinity—the ancestral Gulf of Mexico. Within the basin, Upper Jurassic Norphlet and Smackover sediments were deposited downdip directly on the Louann Salt, and updip on Werner Anhydrite or Eagle Mills siliciclastic red beds.

The Norphlet Formation, although deposited over most of the area, varies in thickness and lithology between a thin (0-50 ft thick) dolomitic or sandy siltstone and shale to a sandstone or conglomerate eolian-alluvial deposit (up to 50 ft thick). Eustatic rise in sea level occurred toward the end of the Callovian at about 160 mya. Such a sea-

level rise would have inundated Norphlet deposits and set the stage for carbonate deposition throughout the basin.

The northern edge of the Smackover Formation is at the updip subcrop or truncated edge of the Jurassic marine section. The formation varies in thickness between the truncated edges to probably several thousands of feet in the downdip areas of the central basin area (Zimmerman, 1992). In general, the formation can be divided into 3 stratigraphic units: 1) an upper grayish to brown dolomitic grainstone with interbedded lime mudstone, dolomitic-quartzose siltstone, and sandstone; 2) a middle brown dense, laminated siliceous, dolomitic-lime mudstone with occasional thin sandstone interbeds; and 3) a lower dark gray to black fine-grained argillaceous limestone (Zimmerman, 1992). The maximum thickness of the basinal facies developed during the Oxfordian in the lower Smackover. Although there is no pronounced abrupt basinal thickening indicated from seismic profiles, the deepest penetrations through the Smackover are in a downdip prograded ramp setting. These are illustrated in Gamble (1986). The updip upper Smackover petroleum productive facies is illustrated in Bishop (1968). Backstripping of the Smackover and the overlying Kimmeridgian and Tithonian sequences (Haynesville and Cotton Valley) indicates there was gradual basinwide tectonic subsidence accompanied by compaction at this time (Zimmerman, 1999b).

The Lower Kimmeridgian (Haynesville/Buckner) strata indicate a general shallowing in depositional environment following the Oxfordian. Buckner evaporitic deposits and their associated red beds apparently resulted from deposition in hypersaline coastal lagoons or sabkhas. The Upper Kimmeridgian (Haynesville/Bossier) strata indicate that more marine conditions existed during the late Kimmeridgian in the

southern (deeper) part of the basin. In the central and toward the northern (landward) part of the basin, the section grades from a marine dark calcareous shale to a coarser grained, locally nonmarine siliciclastic sequence. Salt tectonics became an early integral part of the basin during Buckner/Haynesville time with both lateral and vertical salt movement occurring. The evolution of salt structures originating from bedded salt (Louann) into vertical salt stocks involved pillow and diaper structures with their associated concomitant concentric structural lows being filled with sediments (Kupfer et al., 1976; Lobao and Pilger, 1985). Kupfer et al. (1976) and Lobao and Pilger (1985) concluded that the major time of salt dome growth occurred during the late Jurassic and continued into the early Cretaceous with lesser movement in the late Cretaceous and early Cenozoic. Further, Lobao and Pilger (1985) indicate that there was a greater intensity and more rapid growth in diapers located in the southern and central parts of the basin when compared to the intensity and growth of diapers located in the north during their major development in the early Cretaceous. Along with the initiation of vertical (and lateral) salt movement, major faults formed on the northern rim of the basin. The State Line fault complex occurs near the updip limit of thick salt and generally defines the northern boundary of the basin. Fault zones also are developed along the northern periphery of thick salt basins in the eastern Gulf (Mancini et al., 1999).

Cotton Valley units reflect a variation in depositional environments that extended southward in a deepening basin (Forgotson, 1954). These environments of deposition range from coastal plain and shelf to slope. Regional subsidence from the edge of the Mississippi River Embayment area and throughout the basin accommodated a broad progradation of thick Cotton Valley sediments. By the end of the Berriasian (end of

Cotton Valley time, i.e., in the early Cretaceous), the progradation had essentially filled the salt basin with Werner/Louann, Norphlet, Smackover, Buckner/Haynesville and some Cotton Valley sediments, and formed the first greater Gulf Basin continental shelf edge across the southern area of central Louisiana (Zimmerman, 1999a and Zimmerman, 2000). An estimated 4,000 to 6,000 ft of combined Haynesville and Cotton Valley sediments filled the basin in the area of the shelf edge. These sediments were deposited on some 1,400 to 2,000 ft of Norphlet and Smackover deposits, which for the most part, rested on thin Werner/Louann Salt and/or probable Eagle Mills or transitional crust.

A hiatus in the sedimentary record occurred between approximately 128 to 121 mya, reflecting non-deposition and/or erosion across the area. The hiatus essentially includes all of the Valanginian Stage of the Lower Cretaceous.

Sedimentary units of the Lower Cretaceous that were deposited in the basin are, from bottom to top, Hosston, Sligo, Trinity (Pine Island, James, Rodessa, Ferry Lake, Mooringsport, Upper Glen Rose), Fredericksburg (Paluxy, Walnut, Goodland), and Washita. It is noted that because of the Comanchean/Sub-Gulfian erosional unconformity, upper parts of the Trinity Group, parts of the Fredericksburg Group, and parts of the Washita Group have been removed in the northern part of the basin. It is also noted that some of the upper units of the Washita Group may be late Cretaceous in age and preserved in the central part of the basin. The formation of the unconformity is probably a result of reactivation of upward movement of the Sabine and Monroe Uplifts as well as uplifting on the north flank of the basin. Tectonic subsidence within the basin apparently slowed to a point of being halved after peaking in the early Cretaceous (Lowrie et al., 1993).

The geologic time span for the deposition of the early Cretaceous formations was between 121 and ~96 to 94 mya. In that period of time, there was continued subsidence in the basin as indicated by shelf/slope deposition during Hosston time (Zimmerman and Goddard, 2001). These authors predicted a deep downdip slope environment with turbidite sandstone deposition in southern north Louisiana.

A shelfal environment of deposition persisted from Sligo to Washita time with the shelf edge migrating further south. Shelfal deposition culminated during the Washita (Lower Cretaceous barrier reef trend) across southernmost north Louisiana (Adams, 1985). In general, it is concluded that there were two cycles of progradation during the early Cretaceous—Coahuilan (Hosston/Sligo) and Comanchean (Pine Island-Washita).

There are four groups of lithologic units within the Upper Cretaceous in the basin. From bottom to top, these are: Tuscaloosa, Austin, Taylor and Navarro. The geologic time span for late Cretaceous deposition was ~96 to ~66.5 mya. The entire Upper Cretaceous section resulted from deposition in what undoubtedly was a slowly subsiding shallow shelf environment that, from time to time, changed to a deeper water shelf environment because of rises in sea level.

At the end of the Cretaceous, there was a reactivation of upward movement in the Monroe Uplift (Johnson, 1961) that was accompanied by igneous activity (Kidwell, 1951) that probably elevated the basin's geothermal gradient considerably (Zimmerman and Sassen, 1993).

The Tertiary strata consist of eight stratigraphic units ranging in age from Paleocene (Midway and lower Wilcox), Eocene (upper Wilcox, Claiborne, and Jackson), Oligocene (Vicksburg and Catahoula), Miocene (Fleming), and Pliocene. Deposition occurred in a

time frame spanning from approximately 66.5 to 1.6 mya (Andersen, 1993). For the most part, deposition occurred in a slowly subsiding shallow shelf environment that, from time to time, changed to a deeper water shelf environment because of rises in sea level. The range in depositional environments includes deep-shelf through shallow-shelf to paralic/deltaic and fluvial. From time to time, erosional conditions occurred, especially at the end of the Claiborne, Jackson, Vicksburg, late Miocene (end of Blounts Creek time or ~ 5.2 mya), and the end of the Pliocene. A drop in sea level was the cause of each of the erosional episodes.

Quaternary deposition and erosional cycles were controlled by sea-level fluctuations. Development of coastal terraces related to Pleistocene sea level changes dominated. Terrace, valley train, and loess deposition occurred in a setting having little or no tectonic subsidence. Stream terrace and valley train deposits dominated the northern part of the basin, whereas in the southern part of the basin coastal terraces also comprised a greater part of the deposition. The Holocene is marked by recent alluvium and alluvial-fluvial deposition associated with streams draining and/or traversing the basin.

This section was prepared by Ronald Zimmerman with contributions by Ernest Mancini.

### *Depositional History*

Sedimentation in the northern Gulf of Mexico was associated with rifted continental margin tectonics resulting from the breakup of Pangea and the opening of the Gulf of Mexico. Triassic graben-fill red beds were deposited locally as the oldest Mesozoic strata above pre-rift Paleozoic basement during the early stages of extension and rifting (Tolson et al., 1983; Dobson, 1990).

**Paleozoic (Pennsylvanian-Permian)**

The oldest sediments drilled in the subsurface of north Louisiana are in the late Pennsylvanian-Permian (310-250 mya) carbonate section over a Sabine Terrane (Lowrie et al., 1993). An example is found in a crestal area located in Sabine Parish, Louisiana (Zimmerman, 2000). In southern Arkansas and extending southward to the north side of the North Louisiana Salt Basin, folded Pennsylvanian-Mississippian sandstone and shale of the Ouachita are present. Imlay (1942) considered the Morehouse Formation as representing this unit of rocks in the deeper parts of the basin.

***Morehouse Formation***

One of the older sedimentary rocks drilled to date in the subsurface of north Louisiana is the gray shale with rare siltstone and limestone of the Morehouse Formation. It is found from 9,285 to 10,475 ft in depth in the Union Producing well (No. A-1 Tensas Delta), drilled in Morehouse Parish (Sec. 8, T. 22 N., R. 4 E) (Imlay, 1942; Bishop, 1967). Because this well was still in the Morehouse Formation at total depth and no other wells have penetrated it, the exact thickness of the formation is unknown. This well also indicated that the Morehouse is overlain directly by Werner red beds (Hazzard et al., 1947; Scott et al., 1961). According to these authors the Morehouse was deposited prior to the Eagle Mills, and later removed in south Arkansas by pre-Werner erosion. Other geologists define the Morehouse either as a marine wedge overlying the Eagle Mills or as a downdip marine facies of that formation.

According to Imlay (1942), a distinctive gastropod and assemblage of other pelecypods found in cores from the No. A-1 Tensas Delta well suggest a late Paleozoic age, probably not older than Pennsylvanian, for the Morehouse Formation. In a core from

the same well, Pennsylvanian plant spores were recovered, which allowed Imlay (1942) to assign a middle to late Pennsylvanian age to the formation.

**Late Triassic-Early Jurassic (Eagle Mills)**

***Eagle Mills Formation***

The Eagle Mills Formation (Fig. 315) extends in the subsurface from east Texas through south Arkansas into Alabama. However, it has not been penetrated by the drill in north Louisiana, and is absent in the Union No. A-1 Tensas Delta well (Bishop, 1967). Some early papers report the Eagle Mills to be Permian in age similar to the Morehouse and that the two formations were deposited on opposite sides of a buried ridge along the Arkansas-Louisiana line (Chapman, 1963). According to Scott et al. (1961), the Eagle Mills unconformably overlies beds of Paleozoic age and is overlapped unconformably on the north by the Jurassic Werner. These authors were unable to establish the northern depositional limit in south Arkansas, and reported that the eroded edge has been fairly well defined in the subsurface where, the Eagle Mills was found to be approximately 7,000 ft thick in the Humble No. 1 Royston well in Hempstead County, Arkansas. Based on cores from this well, Scott et al. (1961) suggested a late Triassic age for the Eagle Mills. These authors observed plant fossils, including *Macrotaeniopteris magnifolia*, and reported that the fossils are closely comparable with those of known late Triassic rocks, particularly the Newark Group of the eastern seaboard and the Chinle Formation of Arizona.

More recent work by Dawson and Callendar (1991) and based on information from several deep wells (12,000-18,000 ft) in northeast Texas and southwest Arkansas, the Eagle Mills is considered to be of Triassic-Jurassic age. The lithology given is the

following: green, red, and pink conglomeratic lithic arenites and fine- to coarse-grained, feldspathic arenites, interbedded with red and greenish gray shales and siltstones. Lithic arenites contain basalt, chert, quartzite, and dolomite rock fragments; plagioclase is the predominant feldspar. The sandstones have low textural and mineralogic maturities. Eagle Mills red beds and associated intrusive igneous rocks (diabase and basalt dikes and sills) represent the fillings of grabens or rift basins that actively subsided during deposition in alluvial, fluvial-deltaic, and lacustrine paleoenvironments.

**Middle Jurassic (Werner, Louann)**

***Werner Formation***

The Werner Formation unconformably overlies both the Eagle Mills and Morehouse Formations and grades into the overlying Louann Salt; north of the limit of the salt, the Werner is overlain unconformably by the Norphlet (Bishop, 1967). Hazzard et al. (1947) mentioned the Werner contains a lower red bed member consisting of red shale and sandstone, commonly conglomeratic at the base, and an upper anhydrite member of relatively pure, dense, granular anhydrite. They reported that the members are conformable, and that the Werner-Louann sequence represents a continuous cycle of deposition.

The Werner anhydrite underlies the greater part of south Arkansas and is present in north Louisiana. About 50 ft of red beds and sandstone between the Werner anhydrite and the dark shale of the Morehouse in the A-1 Tensas Delta well is probably the equivalent Werner red bed member. Several workers in the region have reported apparent excessive thickness of Louann Salt as compared to the average 50 to 100 ft of underlying Werner anhydrite (Andrews, 1960).

***Louann Salt***

The Louann Salt conformably overlies the Werner anhydrite, and is unconformably overlain by the Upper Jurassic Norphlet **(**Bishop, 1967). This unconformity of unknown magnitude and the undetermined age of the Eagle Mills make it difficult to determine the exact age of the salt. However, most authors (Murray, 1961; Bishop, 1967) favored an early to middle Jurassic age for the Werner-Louann and gave the following reasons: (1) the evaporite sequence of the Sabinas basin of Mexico, which could be the sulfate concentrate of the Louann Salt, appears to be continuous with beds of the coastal province; (2) the formations underlie strata of known late Jurassic age, and there is no positive evidence for a pre-Mesozoic age; (3) they are stratigraphically equivalent to evaporites and red shale in the Mexican portion of the coastal province which have been determined to be approximately of middle Jurassic age and to overlie, at least in part, Lower Jurassic rocks (Murray, 1961); (4) thick (more than 2,000 ft) salt appears to occur only basinward from the Mexia-Talco, South Arkansas, and Pickens-Gilbertown fault system which also appears to be the approximate updip limit of thick Upper Jurassic sediments; and (5) spores of Mesozoic age have been identified from salt domes of northern Cuba which may be the same age as domes of the United States.

Andrews (1960) described undisturbed bedded Louann Salt as being coarsely crystalline, free of terrigenous siliciclastic material, and containing anhydrite streaks. A core taken in the Ohio No. H-1 Waller well (Sec. 3, T. 23 N., R. 8 W) in Claiborne Parish, Louisiana, showed the salt to be white to gray in color. Other salt cores are pale pinkish orange, a color attributed to meteoric water percolating through the Norphlet during deposition. The salt core from this well shows an absence of spores and pollen and

the high iron content seems to support the existence of the pre-Norphlet unconformity. From subsurface control, it appears as though the salt is laterally continuous and underlies parts of Texas, Arkansas, Alabama, and Mississippi, and nearly all of Louisiana (Andrews, 1960). A maximum thickness of 1,300 ft was recorded in the Placid No. 3 Freeman-Smith (Sec. 14, T. 16 S., R. 13 W.), Calhoun County, Arkansas, and more than 3,300 ft (still in salt at total depth of 14,890 ft) in the C.V.O.C. No. 2 Banks well (Sec. 34, T. 21 N., R. 10 W.), Webster Parish, Louisiana. The thickness is believed to be associated with salt flowage, and may have been the result of basinward thickening of the salt. An original deposition of about 5,000 ft of bedded salt has been postulated but because of the topographically irregular floor of the basin, the thickness was not uniform (Parker and McDowell, 1955; Andrews, 1960). Bishop (1967) reported that precipitation of as much as 5,000 ft of Louann Salt was the result of concentrated marine waters flowing periodically into the basin, more or less isolated from the open sea by barrier bars. The $CaCO_3$ and $CaSO_4$ were precipitated, and the produced concentrated brines of NaCl were deposited in the basin.

**Upper Jurassic Louark (Norphlet, Smackover, Haynesville-Buckner)**

***Norphlet Formation***

The Norphlet unconformably overlies the Louann Salt and older units near the margins of the basin where the Louann was not deposited or has been removed by erosion. Based on the relation of the Norphlet to the overlying Smackover, it has been assigned to the Upper Jurassic (Hazzard et al., 1947; Bishop, 1967). The Norphlet of Arkansas, Louisiana, and Texas attains a maximum thickness of about 150 ft and is composed primarily of red and gray shale and sandstone. The northernmost area of

Norphlet deposition, in southern Arkansas and northeastern Texas, is characterized by gravel with interbedded red and gray mudstone and is largely fluvial. Basinward, the Norphlet is believed to be composed of lagoonal deposits that are transitional with the lower Smackover; a minor diastem may separate the fluvial equivalents of these rocks from the limestone of the Smackover.

***Smackover Formation***

**Producing Parishes**
**Bossier, Webster**
**Claiborne, Lincoln, Union**

The Smackover Formation conformably overlies the Norphlet. It consists mainly of carbonate mud with pyrite and carbonaceous material deposited in a quiet, toxic environment and non-skeletal carbonate grains deposited in a shallow water environment (Hazzard et al., 1947; Bishop, 1968, 1971). It is reported that the deposition of these non-skeletal particles in the late Smackover sea is similar to those of the present Bahama Banks. Likewise, pellet-mud was deposited in warm, quiet, shallow, water followed by slight differential uplift causing turbulence in local areas, and deposition of mixed facies.

Dickinson's (1969) work was used successfully in predicting productive trends, and for reconstructing the environment of deposition of the upper Smackover section (late Jurassic) at North Haynesville field, Claiborne Parish, Louisiana. The oolitic limestone (mudstone, wackestone, packstone) and pelletoid "B" reservoir studied was believed to contain an estimated 16 million barrels of oil in place. Analysis of dry holes in North Haynesville field indicates that nondeposition or complete cementation of the reservoir facies is more important than present structure in limiting the productive area. However,

only those wells favorably located with respect to present structure, as well as to structure during deposition and diagenesis, are productive.

According to Moore and Druckman (1981), the upper Smackover is a blanket ooid grainstone 300 to 400 ft thick and covering approximately 4,000 sq mi in east Texas, southern Arkansas and northern Louisiana. Their work in burial diagenesis of the Smackover indicates that porosity is affected to a greater degree by burial diagenetic processes than by depositional environment processes. They indicate zones with porosity values ranging from 11 to 22%, and permeabilities of 1 to 100 millidarcys at the site of some of the larger upper Smackover discoveries of the 1960s, such as Walker Creek field, that eventually led to new exploration across the entire Smackover fairway.

Zimmerman's (1992) study of the sparsely drilled area in the northeast corner of Louisiana indicates that the extensively fractured intervals observed in Smackover conventional cores in the area can be attributed to wrench and normal faulting. Although located on the border of the North Louisiana Salt Basin, this area is an example of tectonic fracturing that may have future exploration and production potential in the Smackover interval.

In summary and regarding reservoir conditions of the Smackover in north Louisiana, depth to pay ranges from 8,600 to 11,600 ft with net pay of producing intervals ranging from 20 to 120 ft. The oolitic and pisolitic limestones tend to be tight with porosities of 11 to 22% and permeability less than 1 to 100 md. The hydrocarbons produced are generally 42º to 53º API gravity crudes and condensates.

***Haynesville-Buckner Formation***

**Producing Parishes**
**Bossier, Claiborne**

Forgotson and Forgotson (1976) described the Haynesville in southern Arkansas and northern Louisiana, as red shales and pink to white sandstones that grade laterally into the Gilmer Limestone in East Texas and basinward into black shale lithologically similar to the Bossier Shale. In some areas, the Haynesville or Gilmer Limestone (commonly called Cotton Valley Lime) rests unconformably on the Smackover Formation. The Buckner Member of the Haynesville (primarily red shale, sandstone, anhydrite, and limestone lenses) is transitional with the underlying Smackover limestone. According to Salvador (1987), the lower Buckner (Kimmeridgian) section reflects depositional environments that are less marine or shallower water marine than those of the underlying Oxfordian Smackover, because the Buckner consists of evaporitic deposits and associated red beds formed in hypersaline coastal lagoons or sabkhas. At North Haynesville field, most of the thick Buckner consists largely of red and greenish-gray mudstone and shale with varying amounts of nodular anhydrite and with a few thin beds of white to red, anhydritic sandstone (Bishop, 1971).

In Texas, Louisiana, and Arkansas, Dickinson (1968a, 1968b, 1969) divided the Buckner into two members, each of which is gradational with the Smackover in different areas. The lower is predominantly anhydrite and anhydritic mudstone, and was deposited in an evaporite basin north of a chain of salt-cored anticlines. The upper member consists largely of red and greenish-gray mudstone and shale with nodular anhydrite. Several zones of calcarenites similar to those of the Smackover are present in a general east-west trend area, and at least one of them, the "A" zone, extends regionally across most of

northern Louisiana. Dickinson stated that the lower member of the Buckner is time-equivalent to part of the upper member of the Smackover, but the upper Buckner grades basinward into the Bossier Formation. The Buckner calcarenite zones coalesce at the south edge of the Haynesville field to form a bank up to 600 ft thick, which extends regionally along the basinward edge of the shelf slope, a zone of active subsidence. Dickinson (1969) stated that the older zones of the Buckner calcarenite appear to be limited to the south flanks of Haynesville and Red Rock fields, and that the "A" zone is developed on a regional scale across North Louisiana and is known to extend from Texas nearly to Mississippi. The trends vary from east to west to northwest, with a beach deposit forming at the seaward edge of the shelf-slope break during the Buckner regression.

In summary, the Haynesville-Buckner consists of fine-grained sandstones, shales, bedded anhydrite, and oolitic limestone that were deposited in a shallow marine environment. Hydrocarbons were primarily sourced from the underlying Smackover Formation basinal deposits and are stratigraphically trapped in multiple, stacked, ooid shoal pinch-outs. With respect to the reservoirs, the depth to top of pay is from 9,400 to 10,750 ft. Porosity ranges from 9 to 16% and permeability from 50 to 400 md. Produced hydrocarbons consist of 42º API gravity oil, condensate, and gas.

**Upper Jurassic (Cotton Valley)**

***Cotton Valley Group***

**Producing Parishes**

**Caddo, Bossier, Webster, Claiborne, Lincoln, Union, Ouachita, De Soto, Bienville, Winn, Natchitoches, Jackson, Morehouse**

The Cotton Valley Group in southern Arkansas and northern Louisiana has been extensively studied (Crider, 1938; Imlay, 1943; Swain, 1944; Forgotson, 1954; Sloane, 1958; Mann and Thomas, 1964; Thomas and Mann, 1966; Collins, 1980; Coleman and Coleman, 1981; Eversull, 1985; Zimmerman, 2000). The Cotton Valley consists of the Schuler and Bossier formations and lies unconformably on the Louark Group. The uppermost Schuler Formation, predominantly composed of sandstone and siltstone, is unconformable to and oversteps the Bossier Formation (mainly shale) near the basin margins. Continuous deposition occurred in the deeper parts of the basin. The basal Cretaceous Coahuilan Series rests unconformably on the Schuler Formation of the Upper Jurassic Cotton Valley Group. Swain and Anderson (1993), in ascending order, divided the Cotton Valley Group into the Millerton, Shongaloo, and Dorcheat formations. They defined the Millerton as dominantly a siliciclastic shelf unit that was deposited over the Haynesville Formation and used it in place of the Bossier Shale. These authors described the Shongaloo Formation as typical foreshelf and shelf edge silty shales and sandstones, in part, calcareous. They assigned the name Dorcheat Formation to the uppermost unit below the Hosston Formation and used it in reference to the Schuler.

Kornfeld (1985) described the sandstones of the upper Cotton Valley Group of Mississippi, northern Louisiana, and eastern Texas as being deposited on a stable but subsiding shelf. The quartz-rich regressive sandstones are described as being deposited in a complex of deltaic and marine systems. The sediments of the Cotton Valley fluvial-deltaic systems were derived from Paleozoic and younger highlands to the north and

northwest. These sandstones accumulated on the shelf where they were subsequently reworked. Kornfeld (1985) stated that proximal destructive delta systems existed in northern Louisiana and northeastern Texas and that another system consisting of barrier beaches and bars was located centrally between them.

Environments of deposition located landward from the open Gulf to the south and paralleling the late Jurassic Gulf of Mexico coastline included a longshore barrier island in northern Louisiana and a coastal lagoon in southern Arkansas. Sands to the barrier island were supplied by a delta that was formed by the ancestral Mississippi River in northeastern Louisiana and adjacent Mississippi (Thomas and Mann, 1966). The description by these authors and others of the open and shallow marine systems together with the nearshore coastal features typify the lithofacies of the formations within the Cotton Valley Group. Updip in southern Arkansas, the uppermost Schuler Formation pinches out. Of interest are the thick downdip marine deposits in northern Louisiana that include the following formations: Bossier Shale, Terryville Sandstone, Hicos Shale, Knowles Limestone, and Schuler Formation. The sedimentary characteristics of the formations that comprise the group in northern Louisiana are summarized below.

***Bossier Shale* (*Millerton Formation*)**

The open marine basin deposits of the Bossier Shale are found in northern Louisiana and consist of dark-gray, fossiliferous, calcareous shale. A wedge of this marine shale pinches out updip in southernmost Arkansas. It attains a maximum thickness of 2,000 ft (610 m). The marine shale grades eastward into red shale and sandstone in northeastern Louisiana (Swain, 1944; Forgotson, 1954). The Haynesville Formation conformably underlies the Bossier; and where the Haynesville is absent, the Bossier rests on the

Smackover limestone. The Bossier grades upward into the overlying Terryville Formation.

***Terryville Sandstone***

The Terryville, which consists of regressive massive white quartzose sandstones, extends from Ouachita Parish westward through southern Caddo Parish, Louisiana (Mann and Thomas, 1964). It was deposited as an offshore sand barrier island that separated the open sea on the south from a coastal lagoon on the north (Forgotson, 1954; Sloane, 1958). The Terryville attains a maximum thickness of about 1,400 ft (426 m). Only a few thin, dark gray shale beds occur in this sandstone sequence. The Terryville interval consists of five sandstone tongues; each of the tongues is composed of one to five regionally extensive blanket sandstone beds, which are 10 to 50 ft (3-15 m) thick. Oyster beds occur at the pinch-out edges of some of the sandstones. The Terryville Sandstone interfingers with and grades northward into the overlying and laterally equivalent Hico Shale.

***Hico Shale***

In northern Louisiana, the Hico Shale consists mainly of dark gray shale and a few thin beds of silty limestone, siltstone, and sandstone. Locally, thin beds of carbonaceous and pyritic sandstone and shale are present. The dark shales of the Hico are believed to be a lagoonal facies that accumulated adjacent to the Terryville barrier island (Forgotson, 1954).

***Knowles Limestone***

The Knowles Limestone in Louisiana, which consists of alternating dark gray, argillaceous limestone and gray shale, is 300 to 400 ft thick (Mann and Thomas, 1964). Thin lenses of sandstone occur within, and locally supplant, some of the limestone units.

The limestones are 10 to 100 ft thick and are interbedded with shales that are 10 to 30 ft thick. Similar to the other underlying Cotton Valley units, the Knowles in Louisiana grades northward into terrestrial red beds of the Schuler Formation in Arkansas, and in some areas of Louisiana it is overlain conformably by the Cretaceous Hosston Formation.

***Schuler Formation (Dorcheat Formation)***

The Schuler Formation consists mainly of shale, but in Arkansas toward the pinch-out of the unit it contains increasing amounts of sandstone (Forgotson, 1954). In fact, near the pinch-out, the formation is entirely sandstone and pebble conglomerate. In southern Arkansas, there is a predominance of nearshore to nonmarine lenticular, fine-grained, red and gray sandstone and shale or mudstone. The lenticular red beds probably accumulated as coastal plain deposits on the coastal side of a lagoon. The red terrigenous siliciclastic sediments extend south in northeastern Louisiana and western Mississippi, where the Schuler is almost totally sandstone. According to Forgotson (1954), a large delta was responsible for the thickness and distribution of the sandstones in northeastern Louisiana and western Mississippi. The Hosston Formation overlies the Schuler Formation disconformably.

Approximately 45 reservoirs exist within the Cotton Valley Group. The optimum producing reservoirs consist of fine- to medium-grained, massive barrier bar sandstone and shallow marine oolitic limestone of the Terryville and Knowles formations, respectively. In northern Louisiana, depth to the top of the pay zones range from 3,600 to 14,500 ft. Net pay of the reservoirs ranges from 10 to 60 ft with porosities of 9 to 18% and permeabilities of 1 to 300 md. The produced hydrocarbons are typically 41º API gravity oil, condensate, and gas.

**Lower Cretaceous Coahuila (Hosston, Sligo)**

The Sligo and Hosston Formations belong to the Lower Cretaceous Coahuilan Series. The Pearsall, the basal formation of the Trinity Group, conformably overlies the Sligo. The Sligo, consisting of gray to black shale and limestone, grades transitionally downward into the red sandstones and shales of the Hosston. Basinward, both units thicken and the base of the Sligo occurs stratigraphically lower.

***Hosston Formation***

**Producing Parishes**
**Caddo, Bossier, Webster, Claiborne,**
**Union, Lincoln, De Soto, Bienville,**
**Red River, Natchitoches, Jackson,**
**Ouachita, Caldwell**

Deposition of predominantly fluvial-deltaic sediments continued during the early Cretaceous in the basin. During Hosston time this deposition included a large variety of lithologies from delta plain to shallow marine shelf environments. According to Rogers (1987), the Hosston Formation overlies the Dorcheat and is of early Cretaceous age. The Hosston Formation contains the early Cretaceous marker spore *Cicatricosisporites angicanalis*, and the Cretaceous dinoflagellate *Oligosphaeridium complex*. To the west in Texas, Blount et al. (1986) were able to identify the following five major lithofacies in the Hosston Formation of Trawick field, Nacogdoches County, Texas: (1) a clean, cross-bedded, tidal-channel facies; (2) a sandy, bioturbated, tidal-flat facies; (3) thin, rapidly deposited crevasse-splay deposits; (4) interdistributary bay sands, silts, and muds; and (5) partly reworked distal-deltaic sandstones. These workers observed distribution differences between the upper and lower Hosston. In the lower Hosston, the channel,

crevasse splay, and interdistributary bay facies were common, and in the upper Hosston a marginal marine delta-fringe system existed.

The predominant arenaceous siliciclastics of the Hosston range from claystones/shales, siltstones, very fine-grained sandstones to conglomerates resulting in prolific hydrocarbon reservoirs that can be found from Texas, across Northern Louisiana and into Mississippi (Beckman and Bloomer, 1953; Cullom et al., 1962; Gorrod, 1980; Saucier et al., 1985; Garner et al., 1987). The thickness of the Hosston varies from a few hundred ft to over 3,500 ft in Jackson Parish. Minor limestones and conglomerates, as well as some lignites, are also present in the Hosston (Granata, 1963; Saucier et al. 1985). In the Pine Island field, Caddo Parish, the non-marine beds of the Hosston are located between 3,900 and 5,900 ft in depth. Hosston reservoirs can be reached at drilling depths of less than 10,000 ft (3,000 m) over most of the productive trend in Texas and Louisiana. The thickness of the Hosston ranges from a few hundred feet near the zone of truncation in south Arkansas to over 3,500 ft in southern Jackson Parish, Louisiana (Cullom et al., 1962). Accompanying the change in thickness there is also a change in character of the formation from predominantly coarse red sandstones, often cherty, interbedded with red shales in south Arkansas, to finer grained white sandstones and siltstones interbedded with gray, green and red shales and oolitic limestones in the deeper parts of the North Louisiana Salt Basin.

In Texas, the Travis Peak Formation (Hosston equivalent) was deposited as a complex of fluvial and deltaic systems that rapidly prograded over a broad, shallow shelf more than 100 miles (160 km) wide. Aggradation resulted in braided stream deposits that were more than 2,000 ft (600 m) thick. The entire complex is considered a fluvial-deltaic

system that includes a variety of depositional environments associated with the transition from the continental braided stream deposits to shallow-marine carbonate shelf deposits of the overlying Sligo Formation.

Zimmerman and Goddard (2001), studying an area that includes parts of and extends to the south of the basin, reported there were four wells that completely penetrate the formation. The penetrations are located in a shallower shelf area along the eastern margin of the Sabine Uplift in Sabine and Natchitoches Parishes. These four wells provide facies control for the updip portion of the Hosston Formation. Farther downdip, deeper water facies were interpreted in the eight wells found to have penetrated the entire upper half of the Hosston interval. These eight wells, located in the deeper part of the study area, plus one additional well that penetrated the lower Hosston Formation in extreme southwest Mississippi, provide the main control for understanding deeper water Hosston deposition. It is noted that there are no known conventional cores available from any of the downdip wells, and the depositional environments are based on well-log interpretations. However, two wells, one updip in Red River Parish and one in Zwolle field, located in Sabine Parish, just southeast of the Sabine Uplift, encountered a shaly facies with Bossier-like lithology. Based on that data and a detailed facies interpretation, Zimmerman and Goddard (2001) concluded that depositional environments in the downdip area were deeper water and quite different from those found in the shallower updip Hosston.

In the past, in order to evaluate the hydrocarbon potential of the Hosston in unexplored areas, an attempt was made to predict what sort of environment might have existed for this formation in the deeper, sparsely drilled parts of the basin (Cullom et al., 1962). It was determined from sandstone-limestone percentage maps that some of the

better Hosston fields in north Louisiana were located in Bienville, Webster, Jackson, Caldwell, and Ouachita Parishes. The more favorable environments were then extrapolated to the southeast into Caldwell, Richland and Franklin Parishes, and with less certainty to the southwest into De Soto and Red River Parishes**.**

Based on these earlier studies, operators in north Louisiana and east Texas are now aware that the Hosston Formation has characteristically low porosity and permeability values and that both environment of deposition and diagenesis control variations in reservoir quality of these sandstones (Swain, 1944; Saucier, et al., 1985; Dutton and Finley, 1988). Late-stage diagenetic events include cementation by calcite and anhydrite as well as isolated occurrences of intergranular albite cementation. Channel sands of the lower Hosston maintain the highest consistent reservoir qualities. The oil and gas accumulations discovered to date are found predominantly in fine- to medium-grained sandstone reservoirs (approximately 40) from alluvial, fluvial-deltaic, and shallow marine shelf depositional environments. The porosities (10 to 26%) and permeabilities (10 to 250 md) observed in the gas prone reservoirs of Bassfield field in Mississippi, and fields in east Texas and northern Louisiana are the result of excessive compaction and cementation (Dutton and Finley, 1988; Mitchell-Tapping, 1981).

The Lower Cretaceous Travis Peak Formation of east Texas as well as its equivalent, the Hosston Formation of northern Louisiana and Mississippi, is a gas-bearing sandstone that has low permeability and requires hydraulic fracture treatment to produce gas at economic rates (Dutton and Finley, 1988; Dutton et al., 1990, 1993; Davies et al., 1991). Although a few thin zones near the top of the Travis Peak in east Texas have permeability

greater than 90 md, most of the Travis Peak has permeability of less than 0.1 md. Porosity in sandstones ranges from 3 to 17% but is mostly less than 8%.

Oil and gas accumulations in the Hosston are closely associated with salt-cored structures in east Texas and north Louisiana. It is an important source of oil and gas-distillate in many fields of north Louisiana and east Texas, with production generally coming from three zones, the upper 300 ft, the middle 300 ft and the basal 200 ft. The depths to the reservoirs in Caldwell, Richland and Franklin Parishes are estimated to range between 4,000 and 13,700 ft.

***Sligo Formation***

**Producing Parishes**
**Caddo, Bossier, Webster, Ouachita,**
**Claiborne, Lincoln, De Soto, Bienville,**
**Natchitoches, Winn**

The Hosston is transitional with the limestone and dark gray shale of the Sligo Formation. Early workers (Breedlove and Ogden, 1955; Nichols 1958; Murray, 1961) reported an early Cretaceous age for the Sligo and correlated this unit with the Nuevo Leon Stage of the Upper Coahuilan Series. These workers published thicknesses for the Sligo of less than 100 ft in south Arkansas and greater than 500 ft in central Louisiana. According to Hermann (1971), the Sligo in Rapides Parish of central Louisiana forms a large bioherm of least 450 ft thick. This main reef trends northerly through eastern Natchitoches, western Grant, and western Winn Parishes. The northern extent of the reef trend turns eastward through northern Winn, southern Jackson, and central Caldwell Parishes. The reef facies thins in Caldwell Parish.

Nichol’s (1958) description for the Sligo in the "Ark-La-Tex" region is as follows: gray to brown shales, limy shales and limestones, locally contain lentils of dark gray

oolitic argillaceous fossiliferous and sandy limestones and light to dark gray and brown fossiliferous shales. The oolitic to pseudo-oolitic limestones, where porous and well developed, are good petroleum reservoirs. Nichol (1958) considered the depositional sequence to be from a shallow water, neritic, or perhaps lagoonal, environment between a transitional, deltaic environment in south Arkansas and a biohermal reef trend in central Louisiana. There is some disagreement among petroleum geologists concerning the contact between the Sligo and overlying Pine Island Formation. Hermann (1971) picked the top of the Sligo at the top of the reef limestone.

Using paleontology, well data, and 2-D seismic, Forgotson and Forgotson (1975) considered the Sligo Formation a transgressive carbonate sequence with shelf edge and dolomitic reef-crest zones, trending approximately east-west through Vernon, Rapides, and Avoyelles Parishes. This Sligo trend is considered a reef complex, consisting of reef, fore-reef, back-reef, and inter-reef deposits. Forgotson and Forgotson (1975) showed the back-reef and patch-reef zones extending from the northern boundary of these parishes to approximately the southern boundary of De Soto, Red River, Bienville, Jackson, Ouachita, and Franklin Parishes. The limestone may be oolitic or pseudo-oolitic, and is productive in many areas where porosity is present. The distribution of the Sligo extends across east Texas, Louisiana, and Arkansas where it is mainly calcareous, but grades into a predominantly arenaceous facies in Mississippi. It is sometimes referred to as the Pettet Limestone; a term that refers to a productive, porous, pelletal-ooid limestone.

To date, the Sligo limestone has produced both gas and oil in Louisiana, Texas, Arkansas, and Mississippi. Throughout the region, the depth to top of limestone pay ranges from 3,000 to 8,000 ft. Net pay is generally between 10 and 160 ft. The Sligo

contains approximately 13 producing reservoirs in northern Louisiana. Porosity ranges from 16 to 20% and permeability from 9 to 100 md. The produced hydrocarbons are typically 25º to 46º API gravity oils, condensate, and gas.

Bailey's (1978) brief historical account of early drilling activity at Black Lake field in Natchitoches Parish gives insight as to the rather slow pace of Sligo development. The first well to show the existence of Sligo reefs was Hunt's Goodpine Lumber Co. #F-24, drilled in 1942. Later, between 1947 and 1949, the limits of the hydrocarbon trap were defined by four additional wells. The first well discovered 160 ft of Sligo reef, with 80 ft of water-wet porosity. The second well found no reef facies and no porosity in the Sligo. The third well penetrated 52 ft of wet reefal limestone about two miles south of the field and the fourth well found no reef and no porosity, only one mile north. Because of these rather poor results, it was not until 1958 that interest was renewed in the area and drilling began less than three miles west of the field. Again, no reef and no porosity were found. Then a well drilled some three miles east of original production, encountered almost 200 ft of Sligo reef, of which 130 ft was porous and water-wet. By this time, both downdip porosity and the updip permeability barriers were known to exist, and preliminary structure maps indicated the possibility of structural closure or nosing trend. In spite of the presence of the elements of a structural-stratigraphic trap, interest was again lost and Black Lake field remained undeveloped for several more years.

It was not until 1963 that a seismic survey, verified the existence of strong nosing in the Black Lake field area. The first drill test encountered water with a slight show of oil in the Sligo reef. The next well was lost because of drilling problems. At a distance of 100 ft away another hole was drilled and the perforated interval (7,990-8,000 ft) tested at

2.65-MMcf gas/day and 459 bbls of 45.8° API oil on an 11/64-inch choke, with a tubing pressure of 2,409 lb. and a gas/oil ratio of 5780 cf/bbl. Finally, in January 1966, commercial production in Black Lake field began after 24 years of drilling activity. Hermann (1971) mentions that after the successes of Black Lake field only minor production occurred in the Sligo in northern Louisiana.

**Lower Cretaceous Comanche/Trinity (Pine Island, James, Rodessa, Ferry Lake, Mooringsport)**

***Pearsall Formation***

According to Forgotson (1963), the Pearsall Formation is the lowest of the units of the Lower Cretaceous Trinity Stage. In southern Arkansas, north Louisiana, and east Texas, it is subdivided, in ascending order, into the basal Pine Island Shale, the James (Cow Creek) Limestone, and the Bexar Shale. In Louisiana, these members are nearshore, sandy facies along the updip margin of deposition and cannot be subdivided. The Rodessa, Ferry Lake, and Mooringsport formations overlie the Pearsall. The Rodessa and Mooringsport comprise separate platform sequences. Anhydrite beds occur throughout the Rodessa. The Ferry Lake Anhydrite reflects a regional episode and is used as a marker bed throughout the northern Gulf (Petty, 1995; Montgomery et al., 2002).

***Pine Island Formation***

**Producing Parishes**
**Lincoln, Ouachita**

The Pine Island consists predominantly of calcareous black shale with interbedded fine-grained sandstone and minor crystalline limestone layers associated with lagoonal to nearshore marine environments. The widespread nature of the marine shales of the Pine Island is interpreted by Yurewicz et al. (1993) as regional transgressive deposits. The

Pine Island shale, averaging 250 ft in thickness, is widely distributed in Arkansas and Louisiana and located in the subsurface between 4,000 and 7,000 ft. Minor production has been reported from its basal Causey, Hogg and Woodruff sandstone reservoirs (Breedlove et al., 1953; Crump, 1953; Whitfield, 1963). The first well drilled in the Pine Island found gas and salt water in a sandstone from 5,315 to 5,340 ft at the base of the formation, but the second in the Causey sandstone was the first commercial gas producer. Net pay of the reservoir sandstone ranges from 30 to 60 ft with porosity of 10 to 15% and permeability from 10 to 200 md. Hydrocarbons produced are typically 24º to 30º API gravity oil, condensate, and gas.

***James Formation***

**Producing Parishes**
**Bossier, Webster, Claiborne, Lincoln**
**De Soto, Bienville, Jackson**

The James Formation (late Aptian age) overlies the Pine Island Shale and was deposited in a moderately low energy open shelf environment. The James consists of burrowed argillaceous miliolid lime mudstone, wackestone, and packstone (Yurewicz et al., 1993). According to Forgotson (1957), the term “James limestone" was first applied in the year 1926 to a section of calcareous sandstone that was cored in Union Parish, Louisiana, from 3,827 to 3,917 ft. Forgotson (1957) described the James as sandy and chalky, fossiliferous limestone, fine- to medium-grained, and calcareous sandstone with gray shale interbeds. However, its lithology is quite variable throughout the region, changing westward to black marl and shale in northwest Louisiana and northeast Texas. In southwest Arkansas, the James consists of a fossiliferous, dense limestone and red and

gray shale. In southern North Louisiana and East Texas, it is characterized by porous, oolitic, and fossiliferous or fossiliferous-fragmental limestone.

Hermann (1976) described the James as reef-like deposits within an arcuate trend in Winn and Natchitoches Parishes, Louisiana. His description of the James is as follows: The principal limestone varieties within this trend are light-colored, pelletal-miliolid calcarenite, pelletal calcarenite, pelmicrite, and caprinid biosparite. On well logs the limestone is characterized by a leftward excursion of the spontaneous-potential curve giving the zone the massive look of a reef section as much as 300 ft (91 m) thick in one test well. However, the limestone appears to be nonreef in origin. Isopach studies have shown that the James is a detrital deposit that accumulated in low areas. The trend probably contains local patch-reef developments as indicated by the presence of a few caprinid zones, but it does not appear to be a true reef trend as generally defined. Southwest, south, and east of the main trend the James consists principally of interbedded gray argillaceous micrite and gray shale, and on the north and northwest it consists of some combination of interbedded gray micrite, oomicrite, oosparite, quartz sandstone, and gray shale.

The James Limestone produces from numerous fields from east Texas, through Louisiana to southern Mississippi. Production is mainly from rudist-coral-stromatoporoid reef facies on salt-related structural highs in the interior salt basins of east Texas, north Louisiana (Chatham field), and Mississippi (Hermann, 1976). When Chatham field was discovered in 1960, original estimates were 400 million bbl oil in place, of which at least 230 million bbl are recoverable. The few test wells that have cored the James massive-limestone interval indicate that porosity ranges from 10 to 15%, but is generally less than

10%. Calcite-lined vugs and intergranular openings are the main porosity types. Permeability likewise is generally low, commonly being less than 0.1 md but reaching as high as 100 md in small intervals. The hydrocarbons produced are light oils and condensates, as well as gas in porous limestone intervals. Because of the combination stratigraphic-structural anomalies present in the area, the James was considered an excellent exploration target (Hermann, 1976).

***Rodessa Formation***

**Producing Parishes**
**Caddeo, Bossier, Webster, Claiborne,**
**Lincoln, Bienvilole, De Soto, Red River**

The term Rodessa Formation includes the strata above the James Limestone and below the base of the Ferry Lake Anhydrite (Roberts and Lock, 1988). The type well for the formation is located in Rodessa Field, Caddo Parish, Louisiana (Forgotson, 1957). In the type well, the Rodessa interval is at depths of 5,320 to 5,805 ft. In this part of Louisiana, the Rodessa Formation consists of oolitic and crystalline limestones, lenticular fine-grained sandy limestone, anhydrite, coquinoid limestones and gray shales. Southward from the type area in northwest Louisiana, the limestones of the Rodessa have reduced porosity and grade into dense, crystalline limestones. The Rodessa siliciclastics were derived from the craton to the north. Ostracode assemblages in the Rodessa are typical of open-to-restricted shelf environmental conditions. Yurewicz et al. (1993) described the Rodessa in east Texas as typically skeletal–peloid-oncoid packstone that grades downdip into skeletal grainstone and packstone shoals and rudist and coral-red algae at the platform margin.

According to Roberts and Lock (1988), in 1982 a well in Sligo field, Boissier Parish was perforated through the intervals 4,360 to 4,366 ft and 4,442 to 4,446 ft with initial production of 68 bbls of 41.8 API gravity oil per day through a 14/64 choke. Between September 1982 and June 1987, total production was 38,951 bbls of oil and 28,846 Mcf casing head gas. Only 900 bbls were produced in the first six months of 1987. Of the two zones perforated, the upper is in miliolid packstone with up to 5 md permeability and 16% porosity (moldic and intercrystalline). The lower is dolomitized and has permeabilities of up to 15 md and porosities of up to 15%. The Rodessa also produces from a light-gray, porous, chalky, pseudo-oolitic, fossiliferous limestone with a few streaks of white, fine-grained sandstone in the western half of the field. This reservoir is about 25 ft thick, has a porosity of 20%, and produces from an area of approximately 19,000 acres.

Other Rodessa reservoirs are productive in northern Louisiana (Frizzel, 1987). Depth to the top of pay ranges from 3,700 to 6,000 ft. Net pay is generally 10 to 30 ft thick. Reservoir porosity ranges from 10 to 26% and permeability from 10 to 650 md. Hydrocarbons produced are typically 34º to 41º API gravity oil, condensate, and gas.

***Ferry Lake Anhydrite***

**Producing Parishes**
**Caddo, De Soto, Bossier**

The Lower Cretaceous Ferry Lake Anhydrite is one of the most distinctive, widespread sedimentary units within the Gulf Coastal Plain. The formation extends from east Texas across southern Arkansas, northern Louisiana, central Mississippi, and southern Alabama, and to south Florida where it has been correlated with anhydrite beds of the Punta Gorda Formation (Forgotson, 1957). The approximately 250 foot thick Ferry

Lake Anhydrite was deposited above the Rodessa in an extensive lagoonal sea. It is believed that the thickness of individual beds accumulating within the lagoon were controlled mainly by water depth, development of a restrictive barrier, subsidence, duration of each evaporative pulse, and areal salinity variation (Forgotson, 1957; Pittman, 1985). The Ferry Lake is described as consisting of white to gray, finely crystalline anhydrite that contains minor amounts of interbedded gray to black shale, dense limestone, and dolomite. The type well is the Gulf Refining Company's Gas Unit No. 1, in Jeems Bayou Field, Caddo Parish, Louisiana, with the top placed at 3,823 ft and the base 4,072 ft.

Only minor production has been reported to date from fractured intervals within the Ferry Lake Anhydrite from scattered fields within the interior salt basins. Kimball et al. (1989) described hydrocarbon production in Caddo-Pine Island field from the thin Haygood Limestone, found near the base of the Ferry Lake Anhydrite. The high resistivities of the anhydrite beds require the use of porosity logs such as sonic logs, micrologs, or neutron density logs, in order to adequately evaluate the formation. Where production has been found, pay depths range from 3,000 to 4,000 ft. Net pay is only 20 to 50 ft thick with minor porosity and low permeability.

***Mooringsport Formation***

**Producing Parishes**
**Caddo, Bossier, De Soto**
**Red River**

The Mooringsport Formation (early Albian age) consists of shallow marine carbonates that are predominantly crystalline and fossiliferous limestone interbedded with sandstone, red beds, anhydrite, and shale (Yurewicz et al., 1993). It is located above

the Ferry Lake Anhydrite in the Mooringsport field area of Caddo Parish, Louisiana. In the Union Producing Company's Noel Estate well No. 1-A, the Mooringsport occurs at a depth of 3,565 ft (Forgotson, 1957). McNamee (1969) included the Mooringsport and Upper Glen Rose formations as part of the Glen Rose Reef Complex in Texas and Louisiana. The Mooringsport (Rusk equivalent of Texas) has been extended into Mississippi. Adams (1985) placed the Mooringsport in the upper section of the Glen Rose Subgroup. He described six depositional environments in the Mooringsport, including basin, forereef, reef, bank margin, bank interior and restricted shelf. Adams (1985) reported that relatively rapid subsidence/sea level rise is responsible for the vertical growth of the Mooringsport reef complex of up to 1,600 ft thick.

In the areas where the Mooringsport produces in northern Louisiana, the depth to top of pay ranges from 3,000 to 5,000 ft with net pays of 10 to 30 ft. Porosity of 10 to 20% and permeability of 10 to 500 md are common. According to Baria (1981), in the deeper reservoirs (13,400 ft) in some areas of Waveland field, Mississippi, porosity and permeability are both related to primary intergranular and intraparticulate pore space in shoal or shallow bank deposits. In this field, porosity varies from 10 to 17%, and permeability averages about 7 md. In these reservoirs, fractures are an important factor controlling the prolonged and prolific production at Waveland field. The produced hydrocarbons are primarily gas and condensate.

**Lower Cretaceous Comanche (Fredericksburg/Washita-Paluxy, Walnut, Goodland)**

***Fredericksburg Group***

**<u>Producing Parishes</u>**
**Caddo, De Soto**

**Sabine, Franklin, Tensas**

Shallow water platform Fredericksburg deposition occurred over most of east Texas, but farther to the east in northern Louisiana the section is partially truncated (Granata, 1963). In northern Louisiana the Middle-Upper Albian Paluxy, Walnut and Goodland formations are considered part of the Fredericksburg Group. The younger Upper Albian–Lower Cenomanian Washita Group is truncated and, in some cases, cannot be differentiated from the Fredericksburg Group in areas of Louisiana. Early workers like Spofford (1945), placed the Paluxy at the base of Fredericksburg (Walnut clays) and observed from well study that the Paluxy trended northwest and southeast through Caddo Parish and northern De Soto Parish. To the west, the Goodland limestone, and the overlying Washita limestones and shales were also recognized in wells. Cullom et al. (1962) divided the Washita-Fredericksburg section into a lower Walnut Formation and an upper Goodland Formation. The former consists of dark shales and dense gray crystalline to earthy limestones found above the top of the Trinity and the latter unit consists of porous and non-porous light gray to tan crystalline, fossiliferous shallow water limestones and interbedded dark marine shales. The top of the Goodland is marked by the unconformity between beds of Comanchean and those of Gulfian age. According to these authors, post-Comanchean truncation on the south flank of the South Arkansas Uplift was cited as being responsible for the erosion of the beds of Washita age. Across the southern platform area, between 700 and 1,200 ft of Comanchean section is missing due to the uplift and truncation that accompanied the South Arkansas Uplift. Granata (1963) reported that the entire Washita Group is only present in a narrow band in east Texas that trends north into Arkansas but thins east and is no longer present at the north Louisiana

border. According to Granata (1963), the end of Comanchean time was characterized by uplift and erosion across east Texas, southern Arkansas, north Louisiana and across into west central portions of Mississippi. With the retreat of the seas in this region, workers estimate that up to 10,000 ft of sediments were removed by erosion in southwest Arkansas alone.

Minor hydrocarbon production occurs in Washita-Fredericksburg reservoirs. Depth to top of the pay ranges from 2,300 to 9,800 ft. The net pay of mostly gas prone carbonates is 10 to 30 ft thick. Although porosity can range from 10 to 30%, permeability tends to be low.

**Upper Cretaceous Gulf Series (Tuscaloosa, Austin, Taylor, Navarro)**

***Tuscaloosa Group***

**Producing Parishes**
**Bienville, Webster, Red River, Natchitoches,**
**Bossier, De Soto, Richland, Franklin,**
**Tensas, Concordia**

According to Granata (1963), deposition of Woodbine in Texas and Tuscaloosa in Louisiana began with the advance of the Gulfian seas over Lower Cretaceous Comanchean formations. From northwestern Louisiana and eastward, the Tuscaloosa thickens from 100 to almost 1,000 ft at the Mississippi border (Cullom et al., 1962). In northern Louisiana, the Upper Cretaceous consists of the Eagle Ford and Tuscaloosa Group, including Upper, Middle and Lower Tuscaloosa formations. The sequence consists mostly of red and gray shales, red and gray mudstones, gray siltstones, and fine- to medium-grained sandstones, that contain silt, ash, glauconite, mica and/or calcite. Conglomerates and/or pebbly sandstones and occasional thin, tan to gray fossiliferous limestones are also present.

Across northern Louisiana in the producing fields of Bienville, Richland, Franklin, Tensas and Concordia Parishes, the Tuscaloosa consists of fine- to coarse-grained quartz arenites and fossiliferous clays, ashy sands, red beds, gray shales, and minor chert gravels deposited in fluvial-deltaic to shallow marine environments. Generally, the Tuscaloosa is overlain by the shaly Eagle Ford Formation that averages approximately 100 ft in thickness (Lenert and Kidda, 1958; Morrow, 1958; Rogers, 1958). Production is from the basal sandstones of the lower Tuscaloosa where net porous sand ranges from 90 to 250 in thickness (Cullom et al., 1962). Depth to the top of the sandstone reservoirs across the region ranges from 2,400 to 9,700 ft. Production of 24º to 46º API gravity oil, condensate, and gas is derived from quality reservoirs with porosities of 25 to 30% and permeabilities ranging from 200 to 2,000 md.

***Austin Group***

**Producing Parishes**
**Caddo, Bossier, Webster,**
**Claiborne, Union**

The basal sediments of the Austin Group were deposited over a truncated surface of the Tuscaloosa Group (Forgotson, 1958a). In north Louisiana, the Austin Group includes the Brownstown and Tokio formations, with a thickness that ranges from zero on the Monroe Uplift to over 2,000 ft in Central Louisiana (Cullom et al., 1962). These shallow marine deposits consist mainly of medium- to coarse-grained glauconitic carbonaceous and argillaceous sandstone and alternating chalky, shaly and silty units. Carbonates that replace the sands and shales to the south typically are chalk or marl and have poor definition on well logs. Ogier (1963) described the Tokio Formation as consisting of coarse, gray and brown crossbedded quartz and dark gray lignitic fossiliferous clay. In

Caddo Parish, it attains a thickness of 620 ft on top of the Brownstown Formation. A number of reservoir quality sands exist within the Tokio and produce in Caddo, Bossier, and Webster Parishes. Located at depths of 2,400 to 3,100 ft, these reservoirs have porosities of 20 to 35% and permeabilities of 200 to 450 md. The overlying Brownstown Formation consists of dark gray calcareous clay or marl with sandy marl and fine-grained sand. The reservoir quality sands are reported to be located near the top of the formation in Caddo Parish (Ogier, 1963).

On the southern edge of the basin and overlying the Washita-Fredericksburg and parts of the older Cretaceous barrier reef system (Glen Rose), a band of Austin Chalk extends from Texas through Vernon Parish to the southwestern corner of Mississippi and beyond to the southeast. In this area of southernmost north Louisiana, approximately 50 miles south of the nearest shallow piercement salt dome in the North Louisiana Salt Basin, the Austin Chalk consists primarily of compacted argillaceous foraminiferal and coccolith limestone (biomicrite) with interbeds of marl and bentonitic marl. Hydrocarbon targets in the chalk include the fractured basal section of the Austin. The hydrocarbon bearing target section is approximately 180 to 400 ft in thickness and encountered at drill-depths of 12,500 to 17,500 ft (Zimmerman, 1998). According to Zimmerman (1998), the reservoirs within this Texas-Louisiana trend generally have a dual pore system which is derived from a microporous matrix and fractures that yield low porosity and low permeability reservoirs with high water content and less than 50% residual oil saturations. *In-situ* matrix porosities and permeabilities are generally less than 5% and 0.05 millidarcies, respectively. Reservoir development is through long lateral (horizontal) wellbores.

***Taylor Group***

**Producing Parishes**
**Caddo, Bossier, Webster, Claiborne, Bienville, De Soto, Red River, Sabine**

The Taylor Group averages 300 ft thick in north Louisiana and includes the Saratoga Chalk, Marlbrook Marl, Annona Chalk, and the more siliciclastic Ozan Formation (Cullom et al., 1962). These are primarily shallow marine deposits consisting of hard, gray glauconitic fossiliferous chalk, calcareous shale, marl, fine-grained sandstone and siltstone on the Sabine Uplift and in south Arkansas. In Vernon Parish, these deposits were probably deeper water limestones. In Sabine Parish, production of light oil and condensate from the Saratoga and Annona has been reported (Cameron, 1963; Woods, 1963). Where Taylor reservoirs produce in northern Louisiana they are located from 1,250 to 2,900 ft in depth. Production of light oil and condensate is derived from the deeper reservoirs with fracture porosity of 20 to 33% and permeability ranging from 100 to 1000 md. Farther to the north in Caddo Parish, the basal siliciclastic Ozan Formation is productive. The Ozan productive interval is called the Buckrange, located at 1,750 ft in the subsurface and averaging 30 ft thick. The reservoir consists of fine- to medium-grained calcareous and argillaceous sandstone interbedded with calcareous shale. According to Cullom et al. (1962), the greatest overall concentration of sands in the Ozan Formation is in southern Arkansas and northwest Louisiana, but coarse siliciclastics may be present to the south of the Sabine Uplift as well.

***Navarro Group***

**Producing Parishes**
**Caddo, Bossier, Claiborne, Union**

The uppermost sequence of the Gulfian Series is the Navarro Group consisting of the Nacotoch and Arkadelphia formations. The Nacatoch is a shallow marine deposit consisting predominantly of fine- to medium-grained unconsolidated quartz sandstone, sandy limestone, clay, marl, and shale. Sandstones tend to be glauconitic, ashy and argillaceous. The Arkadelphia also consists of shallow marine sediments, mainly light gray chalk/marl with calcareous, micaceous sandstone, and minor volcanic ash. The Navarro attains a maximum thickness of 600 ft in northwestern Louisiana. It thins southeasterly and gradually disappears in Natchitoches and Grant Parishes (Cullom et al., 1962). The Nacotoch is reported to have produced gas in shallow sandstones at depths of 960 ft in Caddo and Bossier Parishes. Where the Navarro produces, the reservoirs are located from 300 to 2,200 ft in depth. They have porosities of 20 to 28% and permeability of 200 to 2,500 md.

The Monroe Gas Rock Formation, originally described in the Monroe Gas field by Stroud and Shayes (1923), is a shallow marine deposit consisting of hard white and gray sandy chalk that produces in the Monroe Gas field in northeastern Louisiana. Other upper Cretaceous secondary reservoirs in the Monroe field area are the Arkadelphia, Nacatoch, and Ozan formations. Sourced through fracture systems from the Smackover, the Monroe Gas field is the largest gas field in Louisiana with a cumulative production of more than 7.3 trillion cubic feet of gas produced from the field since its discovery in 1916 (Zimmerman and Sassen, 1993). Its areal extent covers more than 365 square miles over a portion of a 25-township area within adjoining parts of 3 northeastern Louisiana Parishes: Union, Morehouse, and Ouachita. Depth to the top of the gas rock ranges from

2,000 to 2,500 ft with net pay of 10 to 70 ft. The porosity of the reservoir is from 5 to 25% and permeability can be as high as 500 md (Bebout et al., 1992).

**Tertiary Paleocene-Eocene (Midway, Wilcox)**

***Midway Group***

According to Murray (1955), the end of the Cretaceous is characterized by an interruption of deposition, accompanied by withdrawal of the seas, resulting in a widespread regional unconformity at the base of the Paleocene in the Coastal Plain province. Before the Cretaceous seas withdrew, they covered all of the Coastal Plain and much of the Central Interior of North America. Continued retreat of the early Tertiary seas in the Coastal Plain area is also evident because of appreciable quantities of later Midwayan, shallow-water, lignitic, arenaceous to argillaceous, marginal marine deposits. In outcrops from eastern Texas, Rainwater (1964) identified the Midway as including shallow marine to moderately deepwater environments consisting of prodeltaic marine silts and clays that are very carbonaceous and with marine fossils.

Alexander (1935) in a study of well cuttings from wells drilled in southwest Arkansas and northwest Louisiana was able to identify the Midway section based upon his correlations of ranges of foraminifera. The only microfossils observed by Alexander (1935) in the upper, silty, non-calcareous Midway shales of this region are small species of *Ammobaculites* and *Spiroplectammina*. Highly calcareous shales, commonly marly or chalky in character, and rich in microfauna, are usually encountered within a few feet, after the first hyaline foraminifera appear. Cores from the Midway in Bossier and Webster Parishes, Louisiana, were also used to recognize and describe the lower part of the Midway Group as predominantly calcareous, with true chalk occurring as lenses in

Arkansas and Louisiana. This study showed that the Midway Group ranges in thickness in southwest Arkansas and northwest Louisiana from about 400 to 600 ft, and that the basal, calcareous portion ranges in thickness from 40 to about 100 ft. The change from the calcareous, marly or chalky, shales of the lower Midway to the dark, steel-gray, finely laminated, silty shales or mudstones of the upper Midway, is apparently transitional (Alexander, 1935).

Murray (1955) stated that the contact between the Midway and the underlying Cretaceous strata in southern Arkansas is marked by a bed of white to gray ash, having a maximum observed thickness of about 6 ft. This bed of volcanic ash has been extensively used as a marker for the Midway-Cretaceous contact. In wells examined in southwestern Arkansas and northwestern Louisiana, this bentonite bed was observed to lie either at the top, or in the uppermost part of the lower, calcareous section of the Midway.

***Wilcox Group***

Because of prolific hydrocarbon production from numerous reservoirs in Texas, Louisiana and Mississippi, the Wilcox Group of Paleocene/Eocene age, has been extensively studied (Echols and Malkin, 1948; Fisher and McGowen, 1967; Galloway, 1968; McCulloh and Eversull, 1986; Sassen et al., 1988; Tye et al., 1988, 1991; Echols, 1991; Echols and Goddard, 1992, 1993; Glawe, et al., 1999). Sourced primarily from the northeast and northwest, the Wilcox in northern Louisiana reaches a thickness of 1,000 ft; and where production exists in Winn Parish, it is 2,200 ft thick. In Colgrade field, the reservoirs are at a depth of 1,500 ft with porosities of 15 to 35% and permeability of 200 to 600 md (Nelson, 1963). In Nanichtoches Parish, the Wilcox reservoirs are at a depth of 5,100 to 5,800 feet. Southeast of the North Louisiana Salt Basin, the Wilcox is oil

productive in east-central Louisiana and adjoining southwest Mississippi (Echols, 1991). Echols (1991) estimated that over one billion barrels of oil remains in place for this area. The reservoirs are unstructured deltaic facies. The North Louisiana Salt Basin is filled with about 3,600 ft of deltaic sediments of the Wilcox Group, which is subdivided into upper, middle, and lower intervals. Wilcox production has totaled about one billion barrels of oil since the initial Wilcox discovery in the early 1940's. The Wilcox is considered a thick sequence of complexly interbedded, continental to deltaic deposits that consist of seven principal component facies of a delta system, including the (1) bar-finger sand facies, (2) interdistributary bay mud-silt facies, (3) distributary channel sand facies, (4) prodelta mud facies, (5) distributary mouth bar-delta front sand facies, (6) interdistributary deltaic plain sand-mud-lignite facies, and (7) destructional phase sand-mud-lignite facies (Galloway, 1968). Tye et al. (1991) divided the Wilcox into five lithostratigraphic units on the basis of sedimentary processes and resistivity-log character, and mapped unit thicknesses and sand content in 22 parishes. Tye et al. (1991) showed the units varied from 115 to 1,000 ft in thickness and the sand content ranged from 25 to 60%.

**Tertiary Eocene, Oligocene, post-Oligocene (Claiborne, Jackson, Vicksburg)**

***Tertiary Strata***

The Eocene Claiborne Group overlies the Wilcox Group and outcrops in many parts of north-central Louisiana and in southern Arkansas. In ascending order the group consists of the following units: 1) Cane River, consisting mainly of glauconitic very fossiliferous clay; 2) Sparta, a predominantly sandy sequence with interbedded clay

lenses; 3) Cook Mountain, fossiliferous marine clay unit, and 4) Cockfield, composed mainly of fine-grained sands and silts (Andersen, 1960, 1993).

The Eocene Jackson Group outcrops in a line trending northeast from the southern part of Sabine Parish through Grant and La Salle Parishes. Therefore, in northern Louisiana, this group is absent at the surface where only Claiborne and Wilcox Groups are present. The Jackson consists of fossiliferous clay and limestone and thick clays.

The Oligocene Vicksburg and post-Oligocene strata form thin outcrop slivers that more or less parallel the older Jackson Group in Sabine, Natchitoches, Grant, La Salle and Catahoula Parishes. The Vicksburg consists of a basal crossbedded sand, a middle fossiliferous bentonic clay, and an upper marly clay unit. The Miocene strata consist of fine- to medium-grained sand overlain by a bentonitic clay and silt unit (Fleming) (Andersen, 1960, 1993). The depositional history in northern Louisiana is completed by a Pleistocene sedimentary sequence consisting of “terraces and valley trains” that can be observed mainly along the Red and Ouachita Rivers, and their tributaries, and as Recent alluvium that unconformably overlies the Tertiary deposits (Murray, 1948; Andersen, 1960, 1993).

This section was prepared by Donald Goddard with contributions by Ernest Mancini.

### *Burial History*

Understanding burial history is important to interpreting the geohistory of a basin. Burial history is critical to petroleum system identification and assists in determining the generation, expulsion and migration of hydrocarbons in the basin.

Study of the wells, regional cross sections (Figs. 3-13), and burial history profiles (Figs. 41-82) indicate that there are differences in the geohistory for various areas of the

North Louisiana Salt Basin. The structure maps constructed on top of the Cotton Valley (Fig. 14), on top of the Lower Cretaceous (Fig. 15) and on top of the Upper Cretaceous (Fig. 16) show the configuration of the basin. The cross sections and isopach maps of the interval from the top of the Smackover to the top of the Cotton Valley (Fig. 17) and of the interval from the top of the Cotton Valley to the top of the Lower Cretaceous (Fig. 18) show that the area updip or along the northern margin of the basin is characterized by a thinner stratigraphic section, and the area downdip or along the southern margin of the basin is characterized by a thicker stratigraphic section. The formation lithology maps illustrate lithologic changes in the various units (Figs. 21-40). Although an unconformity is present at the base of the Upper Cretaceous section throughout the basin (Figs. 3-13), this unconformity is particularly developed in Lower Cretaceous strata onlapping the Monroe Uplift as illustrated by the isopach map of the interval from the top of the Lower Cretaceous to the top of the Upper Cretaceous (Fig. 19), by the map that shows the erosional thickness of the total Lower Cretaceous section (Fig. 20), and by the cross sections.

### *Thermal Maturation History*

The thermal history of a basin is critical to petroleum identification and is a crucial element as to whether the basin has hydrocarbons in commercial quantities and as to whether these hydrocarbons are oil, natural gas or both. Thermal maturity modeling, which builds on burial history modeling, assists in this hydrocarbon determination. In the North Louisiana Salt Basin, Smackover oil has not been produced below 12,000 feet.

Study of the thermal maturation history profiles (Figs. 87-128) indicates that in the North Louisiana Salt Basin hydrocarbon generation and maturation trends are evident.

Maps of present day heat flow (Fig. 83), of lithospheric stretching beta factors (Fig. 84), and plots of vitrinite reflectance values (Figs. 85-86) were prepared to assist with this analysis. The generation of hydrocarbons from Smackover lime mudstone was initiated at 6,000 to 8,500 feet during the Early Cretaceous and continued into the Tertiary, using a transient heat flow model (Table 1). Organic carbon contents of up to 1.80% have been recorded from the Smackover for this basin. The dominant kerogen types in the Smackover are amorphous and microbial with herbaceous. These Smackover lime mudstone beds exhibit thermal alteration indices of $3^-$ to $3^+$. Hydrocarbon expulsion from Smackover source rocks commenced during the Early Cretaceous and continued into the Tertiary with peak expulsion chiefly in the Early to Late Cretaceous.

### *Basin Modeling and Petroleum System Identification*

Basin modeling is crucial to petroleum system identification. In basin modeling, regional hydrocarbon flow patterns generally are discerned from two-dimensional models. Petroleum system characterization assists in the recreation of the history of the hydrocarbons within a specific geologic system in a basin. Knowledge of the petroleum system can greatly facilitate the development of improved exploration strategies for hydrocarbons in a basin. From the basin modeling and petroleum system characterization, petroleum systems identified as potential for the North Louisiana Salt Basin have been identified for this study.

The burial and thermal maturation histories of the strata in this basin are consistent with its rift-related geohistory. Source rock analysis and geohistory, thermal maturity and hydrocarbon expulsion modeling indicate that lime mudstone of the Upper Jurassic Smackover Formation served as an effective regional petroleum source rock in the North

Louisiana Salt Basin. Lower Cretaceous lime mudstone was an effective local petroleum source rock in the South Florida Basin, and these rocks are possible source beds in the North Louisiana Salt Basin given the proper organic facies. Upper Jurassic strata were effective source rocks in Mexico and the East Texas Salt Basin; therefore, these strata are possible source beds in this basin given the proper organic facies. Upper Cretaceous marine shale probably is not a source bed in this basin given the thickness and organic facies of this unit. Lower Tertiary shale and lignite have been reported to have been source beds in south Louisiana and southwestern Mississippi, but these beds have not been subjected to favorable burial and thermal maturation histories required for petroleum generation in the North Louisiana Salt Basin.

### *Comparative Basin Evaluation*

The origin and evolution of the North Louisiana Salt Basin and Mississippi Interior Salt Basin are comparable, and Upper Jurassic Smackover lime mudstone beds are the main petroleum source rock in both of these basins (Table 1). There is a significant difference in the geohistories of these basins. This difference is the elevated heat flow the strata in the North Louisiana Salt Basin experienced in the Cretaceous. This event is primarily due to reactivation of upward movement, igneous activity, and erosion associated with the Monroe and Sabine Uplifts.

The difference is the heat flow values between the North Louisiana Salt Basin (1.25 HFU) and the Mississippi Interior Salt Basin (1.09 HFU) results in the generation of hydrocarbons being initiated at depths of 6,000 to 8,500 feet for the North Louisiana Salt Basin and hydrocarbon generation commencing at depths of 8,000 to 11,000 feet for the Mississippi Interior Salt Basin using a transient heat flow model (Table 1). This elevated

heat flow results in thermogenic gas generation being initiated at a depth of 12,000 feet for the North Louisiana Salt Basin compared to a depth of 16,500 feet for the Mississippi Interior Salt Basin.

### *Initial Resource Reservoir Assessment*

The assessment of the undiscovered and underdeveloped reservoirs of the North Louisiana Salt Basin was made based on the oil and gas production reported from the reservoirs in the North Louisiana Salt Basin and from the reservoirs in the Mississippi Interior Salt Basin (Table 2), and on the results from the basin analysis study of these basins. The potential undiscovered reservoirs in the North Louisiana Salt Basin are Triassic Eagle Mills sandstone and deeply buried Upper Jurassic sandstone and limestone. Potential underdeveloped reservoirs include Lower Cretaceous sandstone and limestone and Upper Cretaceous sandstone.

### *Smackover Petroleum System*

The Smackover petroleum system was characterized for the Mississippi Interior Salt Basin in Mancini et al. (2003) and in our 2006 DOE report on the resource assessment of the deep gas resource of the onshore interior salt basins for the North Louisiana Salt Basin (Mancini et al., 2006, 2008). The description of this petroleum system is summarized as follows. The underburden rocks include Paleozoic crystalline and sedimentary rocks, Upper Triassic to Lower Jurassic graben-fill red beds, Middle Jurassic evaporates, and Upper Jurassic siliciclastics, and the overburden strata consist of Upper Jurassic, Cretaceous, and Tertiary deposits (Mancini et al., 2003, 2008) (Fig. 328). Lower to middle lime mudstone beds of the Upper Jurassic Smackover Formation serve as the regional source rocks for the onshore salt basins (Oehler, 1984; Sassen et al.,

Table 2. Oil and gas production form the North Louisiana and Mississippi Interior Salt Basins.

| Reservoir | North Louisiana Salt Basin | | | | Mississippi Interior Salt Basin | | | |
|---|---|---|---|---|---|---|---|---|
| | Oil (bbls) | Gas (Mcf) | GOR (scf/bbl) | Reservoir Depth, m (ft) | Oil (bbls) | Gas (Mcf) | GOR (scf/bbl) | Formation Depth, m (ft) |
| Tertiary | | | | | | | | |
| Wilcox | 228,200 | 89,342 | 392 | 610-2134 (2,000-7,000) | 273,753,647 | 198,084,956 | 724 | 398-1,177 (1,307-3,863) |
| Upper Cretaceous | | | | | | | | |
| Selma/Jackson Gas Rock | | | | | 39,205,424 | 224,393,889 | 5,724 | 921-1,570 (3,022-5,150) |
| Arkadelphia/Monroe Gas Rock | 44,038 | 7,452,904,183 | 169,238,026 | 610-762 (2,000-2,500) | | | | |
| Nacatoch (Navarro) | 758,374,196 | 4,431,274,239 | 5,843 | 244-823 (800-2,700) | | | | |
| Ozan/Buckrange (Taylor) | 265,037,353 | 1,007,534,243 | 3,801 | 381-945 (1,250-3,100) | | | | |
| Tokio/Blossom (Austin) | 128,817,273 | 1,718,406,462 | 13,340 | 823-945 (2,700-3,100) | | | | |
| Eutaw | | | | | 301,449,711 | 1,754,506,272 | 5,820 | 945-2,448 (3,100-8,030) |
| Tuscaloosa/Eagle Ford | 3,971,873 | 75,601,381 | 19,034 | 945-2,819 (3,100-9,250) | | | | |
| Tuscaloosa | | | | | 637,040,878 | 1,824,392,781 | 2,598 | 1,084-2,602 (3,558-8,537) |
| Lower Cretaceous | | | | | | | | |
| Dantzler | | | | | 783,201 | 72,450,931 | 92,506 | 943-2,955 (3,095-9,695) |
| Washita-Fredericksburg | | | | | 56,943,318 | 255,821,157 | 4,493 | 1,446-2,955 (4,744-9,695) |
| Fredericksburg | 1,643,190 | 34,409,159 | 20,940 | 914-1829 (3,000-6,000) | | | | |
| Paluxy | 6,206,760 | 88,408,279 | 14,244 | 762-2,591 (2,500-8,500) | 56,544,588 | 568,991,732 | 10,063 | 1,730-3,706 (5,677-12,160) |
| Mooringsport/Ferry Lake | 312,309 | 1,171,999 | 3,753 | 914-1,524 (3,000-5,000) | 11,641,148 | 215,893,837 | 18,546 | 1,677-4,215 (5,502-13,830) |
| Rodessa | 198,858,232 | 5,615,080,804 | 28,237 | 1,250-1,829 (4,100-6,000) | 235,162,019 | 341,331,628 | 1,451 | 1,715-4,088 (5,628-13,413) |
| James | 12,409 | 2,869,335 | 231,230 | 1,433-1,829 (4,700-6,000) | 902,320 | 80,356,905 | 89,056 | 2,479-4,237 (8,133-13,900) |
| Pine Island | 8,745,072 | 545,229,418 | 62,347 | 1,219-2,134 (4,000-7,000) | 543,856 | 676,027 | 1,243 | 2,479-4,237 (8,133-13,900) |
| Sligo/Pettet | 140,715,109 | 3,557,065,945 | 25,278 | 1,524-2,743 (5,000-9,000) | | | | |
| Sligo | | | | | 30,927,220 | 157,859,597 | 5,104 | 2,543-4,478 (8,343-14,692) |
| Hosston | 12,896,970 | 1,641,948,296 | 127,313 | 1,524-3,658 (5,000-12,000) | 54,887,990 | 995,065,210 | 18,129 | 2,664-4,640 (8,740-15,223) |
| Upper Jurassic | | | | | | | | |
| Cotton Valley | 114,348,835 | 2,223,486,076 | 19,445 | 2,195-4,420 (7,200-14,500) | 106,461,276 | 146,163,240 | 1,373 | 1,437-5,502 (4,713-18,050) |
| Haynesville | 13,923,298 | 152,081,744 | 10,923 | 2,957-3,200 (9,700-10,500) | 6,421,491 | 349,786,844 | 54,471 | 1,990-6,367 (6,528-20,890) |
| Smackover | 33,800,601 | 271,765,406 | 8,040 | 3,048-3,810 (10,000-12,500) | 522,979,535 | 4,069,721,819 | 7,782 | 2,038-7,179 (6,685-23,553) |
| Norphlet | | | | | 12,664,335 | 331,269,443 | 26,158 | 2,209-7,500 (7,247-24,606) |
| Others | 25,388,311 | 130,564,541 | 5,143 | | 872,883,419 | 1,277,775,162 | 1,464 | |
| Total for Reservoirs | 1,713,324,029 | 28,949,890,852 | 16,897 | | 3,221,195,376 | 12,864,541,430 | 3,994 | |

Production data for Louisiana from the 2002 International Oil Scout Association Yearbook (unpublished), and production data for 2005 for Mississippi from Mississippi Oil and Gas Board. Reservoir depths for the North Louisiana Salt basin are from Goddard (2006), Quick look handbook onshore Louisiana petroleum producing formations (unppublished). Formation depths for the Mississippi Interior Salt basin are from from well logs in Mancini et al. (1999).

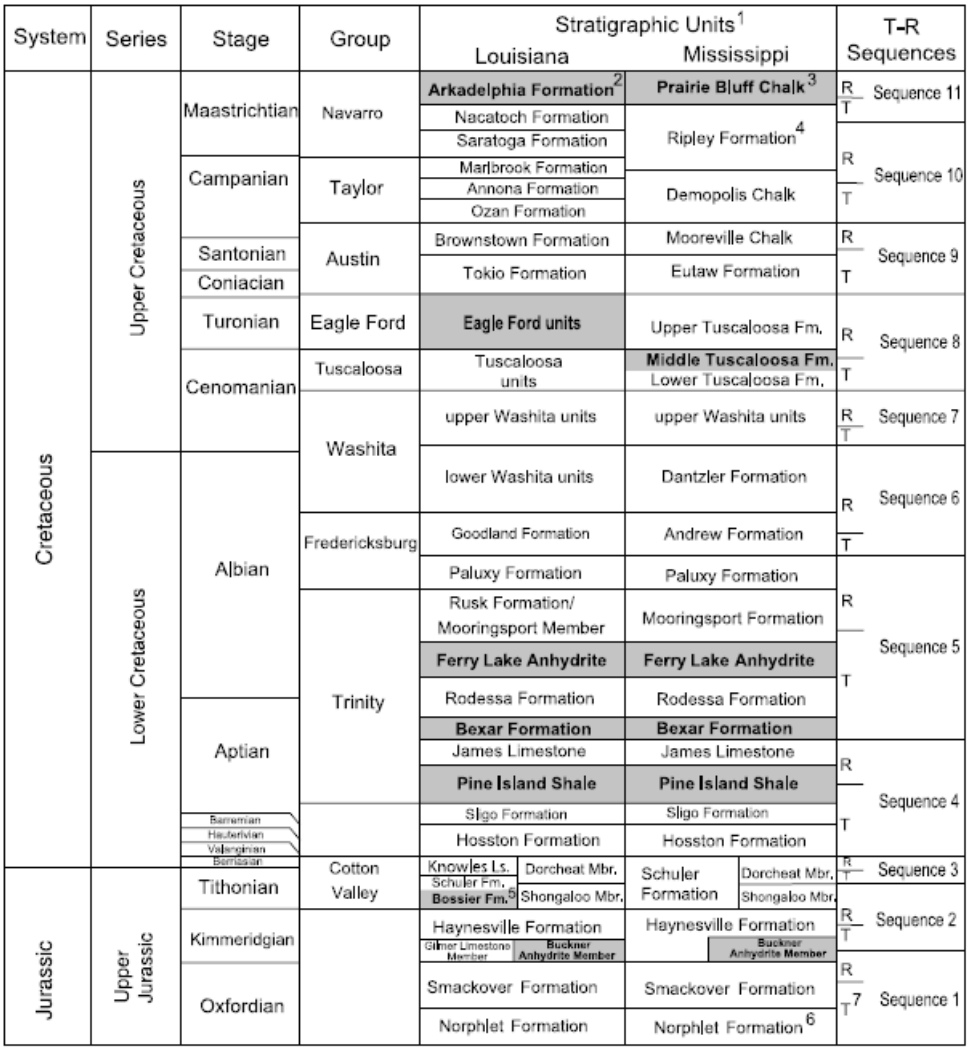


[1]Major petroleum seal rocks are shaded; Lower Tertiary Midway shale overlying Upper Cretaceous beds is a regional seal rock.
[2]Includes Monroe Gas Rock.
[3]Includes Jackson Gas Rock.
[4]Prairie Bluff, Ripley, Demopolis and Mooreville = Selma Group.
[5]Bossier Formation is basinal facies of lower Cotton Valley Group.
[6]Units below the Norphlet Formation, in descending order include the Middle Jurassic Louann Salt and Werner Anhydrite and the Upper Triassic to Lower Jurassic Eagle Mills Formation.
[7]T= Transgressive Systems Tract; R = Regressive Systems Tract.

Figure 328. Sequence-stratigraphic framework for the central and eastern Gulf coastal plain illustrating the transgressive and regressive (T-R) sequences recognized and the major petroleum seal rocks identified (modified from Mancini et al., 2006, 2008).

1987; Claypool and Mancini, 1989; Mancini et al., 2003, 2005, 2008). Present-day Smackover microbial and amorphous lime mudstone beds average less than 1% total organic carbon (Table 1). To adjust for the loss of organic carbon caused by the thermal maturation process, Li (2006) used the conversion of Daly and Edman (1987). The use of this conversion indicates that the original total organic carbon in the Smackover was reduced by 1.5 to 1.8 times during the thermal maturation process. Reservoir rocks include Upper Jurassic, Cretaceous, and Tertiary continental, coastal, nearshore, marine shelf, and deep-marine siliciclastics and nearshore marine, shelf, ramp, and reef carbonates (Mancini et al., 2003, 2008) (Fig. 328 and Table 3). Petroleum seal rocks consist of Upper Jurassic and Lower Cretaceous anhydrite and shale, Upper Cretaceous chalk and shale, and lower Tertiary shale (Mancini et al., 2003, 2008) (Fig. 328). Petroleum traps include structural, stratigraphic, and combination structural-stratigraphic. Salt related structures are common and consist of pillows and diapers (Hughes, 1968; Lobao and Pilger, 1985) (Figs. 329-332).

### *Bossier Petroleum System*

Upper Jurassic (Tithonian) to Lower Cretaceous (Berriasian) Bossier shale beds have been described as source rocks in the East Texas Salt Basin by Ridgley et al. (2006), and Hermann et al. (1993) reported that gas in the Ruston Field of north Louisiana was sourced by Cotton Valley shale beds. A preliminary evaluation of the Bossier in the North Louisiana Salt Basin indicated that these shale beds were possible source rocks in this basin given the proper organic facies and sufficient total organic carbon contents for they have experienced the required thermal conditions for thermogenic hydrocarbon

Table 3. Sedimentary and petrophysical characteristics of the reservoirs in the onshore interior salt basins, central and eastern Gulf Coastal Plain.

| Reservoir | Lithology [1] | Environment [2] | Porosity (%)[3] | Permeability (md) |
|---|---|---|---|---|
| Wilcox | SS | FD | 15–35 | 200– 600 |
| Arkadelphia/Monroe Gas Rock | CK | NS, MS | 5–25 | 1–500 |
| Selma/Jackson Gas Rock | CK | MS | 5–18 | 1– 500 |
| Nacatoch | SS | NS | 20–28 | 200–2,500 |
| Ozan | SS | NS | 20–33 | 100–1,000 |
| Tokio | SS | NS | 20–35 | 200–450 |
| Eutaw | SS | T, NS, MS | 13–39 | 1–5,470 |
| Tuscaloosa | SS | FD, C, MS | 25–30 | 200–2,000 |
| Dantzler | SS | FD | 25–30 | 50–150 |
| Fredericksburg | SS, LS | NS, MS, R | 10–30 | 1–150 |
| Paluxy | SS | F, NS, MS | 24–30 | 150–600 |
| Mooringsport | SS, LS | NS, MS, R | 10–20 | 10–500 |
| Rodessa | SS, LS | NS, MS, R | 10–26 | 10–650 |
| James | LS | NS, MS, R | 10–15 | 6–100 |
| Pine Island | SS | NS | 10–15 | 10–200 |
| Sligo | SS, LS | NS, MS, R | 16–20 | 9–100 |
| Hosston | SS | FD, NS, DM | 10–26 | 10–250 |
| Cotton Valley | SS, LS | FD, NS, R | 9–18 | 1–300 |
| Haynesville | SS, LS | F, NS, R | 9–16 | 50–400 |
| Smackover | LS | CR, R | 11–22 | 1–100 |
| Norphlet | SS | E, F | 3–20 | 1–891 |

[1] Lithology: SS = sandstone, LS = limestone, CK = chalk.

[2] Environment: E = eolian, F = fluvial, FD = fluvial-deltaic, C = coastal, T = tidal, NS = nearshore marine, MS = marine shelf, DM = deep marine, CR = carbonate ramp, R = reef.

[3] Reservoir porosity and permeability data are from published field studies files of the regulatory agencies and geological surveys, and Goddard (2006), Quick look handbook onshore Louisiana petroleum producing formations (unpublished).

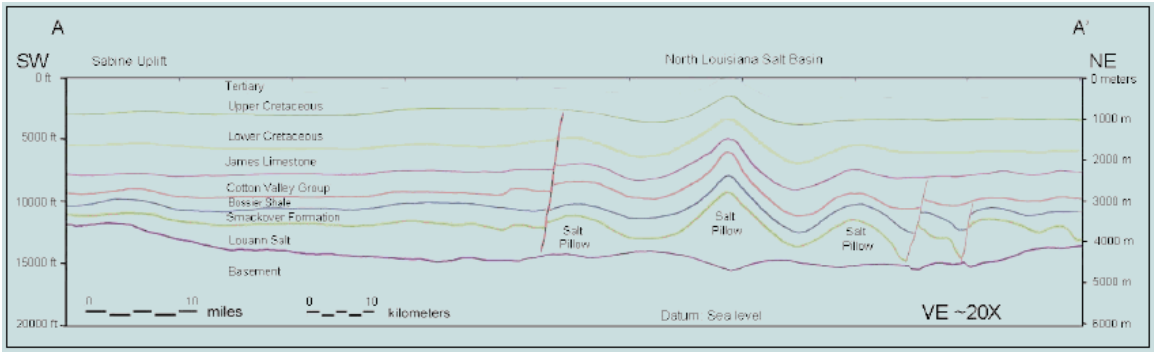


Figure 329**.** Cross section A–A'. Geologic model based on seismic and well log information. See Figure 1 for location of seismic line.

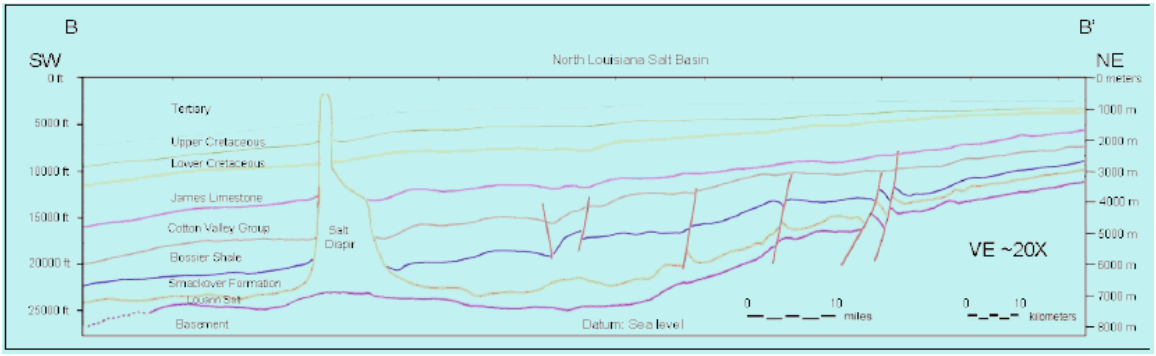


Figure 330. Cross section B-B'. Geologic model based on seismic and well log information. See Figure 1 for location of seismic line.

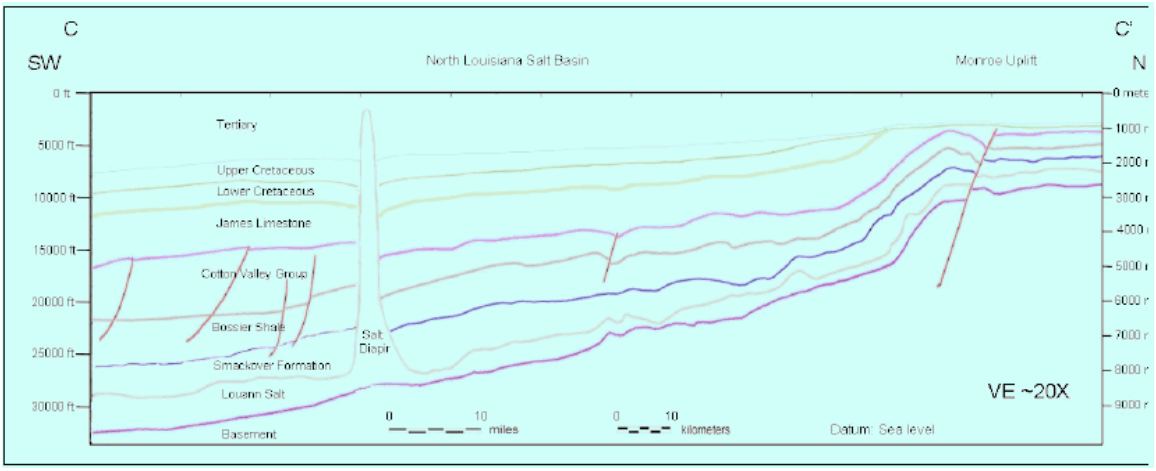


Figure 331. Cross section C-C'. Geologic model based on seismic and well log information. See Figure 1 for location of seismic line.

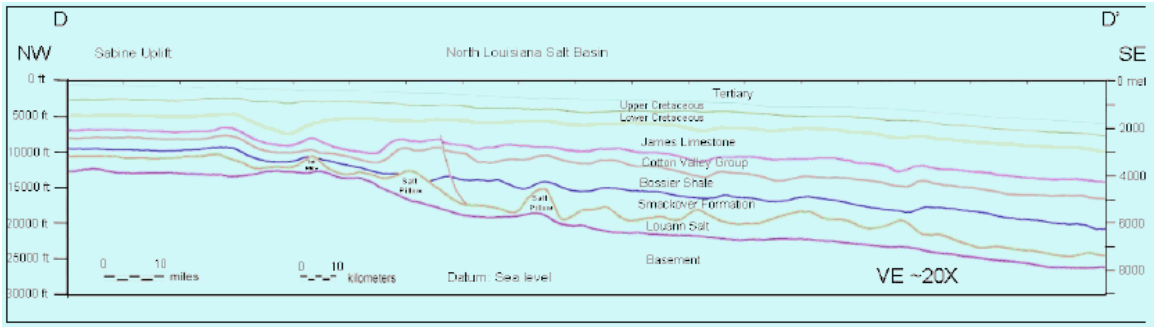


Figure 332. Cross section D-D'. Geologic model based on seismic and well log information. See Figure 1 for location of seismic line.

generation (Table 4). The following characterization of the Bossier shale beds is based on the geological studies (Tables 5-8 and Figs. 333-341) by Don Goddard and Marty Horn at LSU and geochemical analyses (Table 9 and Figs. 342-348) by Suhas Talukdar with Baseline Resolution, Inc. The Bossier shale beds are thermally mature and represent petroleum source rocks that generated and potentially expelled mostly gas and some oil. These shale beds at their present maturity level have mostly low to moderate total organic carbon contents and Type III kerogen. Original kerogen types in the immature stage, as assessed by kerogen petrography, were mainly gas-prone Type III and some oil and gas prone Type II/III. The principal macerals are partly oxidized, unstructured amorphous organic matter (liptinite) and vitrinite in varying proportions. Amorphous material was derived from degraded marine algal and humic matter (higher plant material). Visual kerogen data support the predominantly gas prone nature of the source rocks. Vitrinite reflectance (Ro) values (0.94 % to 2.62%) and thermal alteration indices (TAI) ($2^+$ to $3^+$) suggest that these source rocks entered the late oil window to main gas maturity window and thus have generated mostly gas with some oil. Thin section petrography of geochemically analyzed intervals documents the following rock types: muddy fine-grained sandstone, laminated fine-grained sandstone, sandy mudstone, and silty mudstone. These combined analytical results indicate that abundant woody organic material of continental origin was deposited in offshore areas in association with fine siliciclastic sediments in a marine prodelta environment during the Late Jurassic to Early Cretaceous. The thickness and widespread deposition of predominantly gas-prone source rocks within this basin and their high thermal maturity led to potential sourcing of mainly

Table 4. Organic geochemical analyses of potential Bossier source rocks, North Louisiana Salt Basin.

| Sample no. | Well | Parish | Depth (ft) | TOC (%) | Kerogen[1] | TAI | %$R_o$ | Tmax[2] (°C) | S1[3] (mg/g) | S2[4] (mg/g) | S3[5] (mg/g) | PI[6] | PC[7] | HI[8] | OI[9] |
|---|---|---|---|---|---|---|---|---|---|---|---|---|---|---|---|
| *17 | Davis Bros. | Jackson | 10,944 | 0.46 | H | 2.9 | 1.14 | 331 | 0.14 | 0.12 | 0.09 | 0.54 | 0.02 | 26 | 20 |
| *18 | Davis Bros. | Jackson | 12,956 | 0.43 | H | 3.0 | 1.22 | 304 | 0.10 | 0.08 | 0.22 | 0.56 | 0.01 | 19 | 51 |
| *19 | Davis Bros. | Jackson | 12,976 | 0.61 | H | 3.1 | 1.29 | 313 | 0.11 | 0.07 | 0.02 | 0.61 | 0.01 | 11 | 3 |
| *38 | CZ 5-7 | Winn | 15,608 | 0.28 | I | 3.7 | 1.80 | 307 | 0.02 | 0.04 | 0.00 | 0.33 | 0.00 | 14 | 0 |
| *39 | CZ 5-7 | Winn | 16,418 | 0.34 | I | 3.8 | 1.89 | 355 | 0.05 | 0.07 | 0.11 | 0.42 | 0.01 | 21 | 32 |
| *40 | CZ 5-7 | Winn | 16,431 | 0.34 | W/I | 3.8 | 1.89 | 329 | 0.06 | 0.10 | 0.37 | 0.38 | 0.01 | 29 | 109 |
| *41 | Pardee | Winn | 16,200 | 0.35 | Am/I | 3.7 | 1.80 | 322 | 0.21 | 0.29 | 0.29 | 0.42 | 0.04 | 83 | 83 |
| *42 | Pardee | Winn | 16,400 | 0.35 | Am/I | 3.7 | 1.80 | 328 | 0.19 | 0.16 | 0.16 | 0.54 | 0.03 | 46 | 46 |
| **71 | English #2 | Bossier | 11,136 | 0.55 | W/I | 2.7 | 1.00 | 515 | 0.08 | 0.23 | 0.24 | 0.26 | 0.03 | 42 | 44 |
| **72 | English #2 | Bossier | 11,168 | 0.91 | Am/H | 2.7 | 1.00 | 498 | 0.25 | 0.25 | 0.40 | 0.50 | 0.04 | 27 | 44 |
| **73 | First Bank #1 | Bossier | 11,108 | 0.35 | W/I | 2.9 | 1.14 | 482 | 0.06 | 0.11 | 0.17 | 0.34 | 0.01 | 31 | 49 |

1Kerogen: Am=amorphous, H=herbaceous, W=woody, I=inertinite, Lip=Liptinite, Vit=Vitrinite.
GeoChem Laboratories Inc. and Baseline Resolution Inc. use different classification of visual kerogen.
2Tmax=temperature index.
3S1=free hydrocarbon.
4S2=residual hydrocarbon potential.
5S3=$CO_2$ produced from kerogen pyrolysis.
6PI=S1/ (S1+S2).
7PC=0.083 (S1+S2).
8HI=hydrogen index.
9OI=oxygen index.
*All data by GeoChem Laboratories Inc..
**TOC, Kerogen type, and TAI data by GeoChem Laboratories Inc., Rock Pyrolysis data by Baseline Resolution Inc..
***All data by Baseline Resolution Inc..

Table 5. Cotton Valley-Bossier Group wells selected for analyses.

| (Ser#) & API# | OP/Well Name | (LA Parish) | Sample Depth (Ft) |
|---|---|---|---|
| 1) (107545) | PAN AM | (Union) | 9,347 |
| 171110003800 | Venzina | | 9,357 |
| | Green # 1 | | 9,372 |
| 4) (162291) | AMOCO | (Jackson) | 10,944 |
| 170492011000 | Davis Bros. | | 10,945 |
| | | | 10,948 |
| | | | 12,956 |
| | | | 12,976 |
| 6b) (166680) | EXXON | (Winn) | 16,195 |
| 171272085700 | Pardee | | 16,200 |
| | | | 16,400 |
| 7) (164798) | AMOCO CZ | (Winn) | 15,601 |
| 171272082000 | 5-7 | | 15,608 |
| | | | 16,413 |
| | | | 16,418 |
| | | | 16,431 |
| | | | 16,432 |

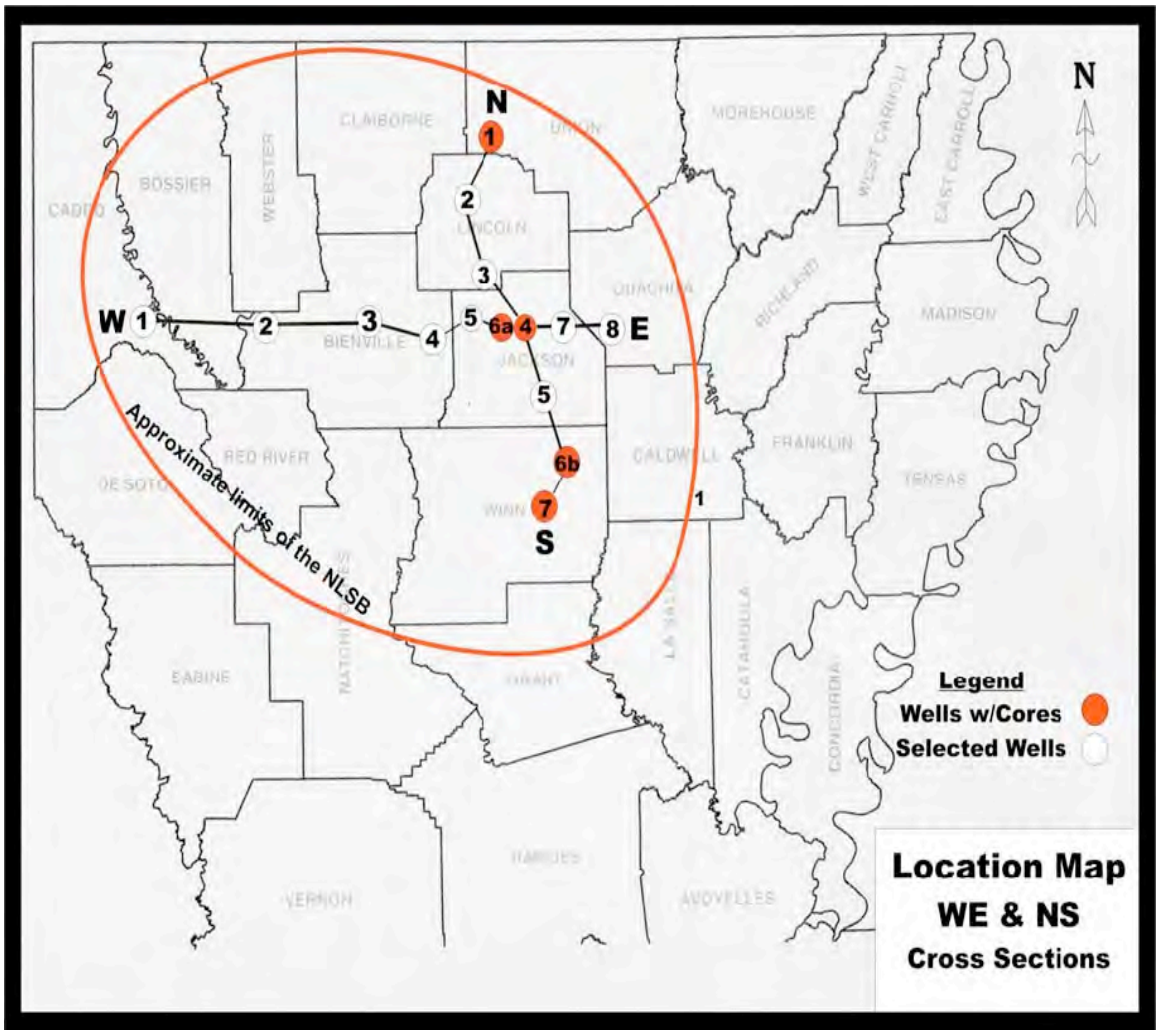


Figure 333. Regional map showing the north-south and west-east cross sections with cored (red) and selected wells (white) that penetrate the Cotton Valley – Bossier Group within the North Louisiana Salt Basin.

Table 6. Cotton Valley-Group samples in Vernon Field selected for analyses.

| Serial. #API | Operator | Well Name | Field | Sec | TWP | RGE | Parish | Sample Depth (Ft) |
|---|---|---|---|---|---|---|---|---|
| 1) 232316 1704920665 | Anadarko | Stewart Harrison 34 #2 | Vernon | 34 | 16N | 03W | Jackson | 11,805' |
| 2) 226742 1704920390 | Anadarko | Davis Bros 29 #2ALT | Vernon | 29 | 16N | 02W | Jackson | 14,035' 15,120' |
| 3) 224274 1704920332 | Anadarko | Fisher 16 #1ALT | Vernon | 16 | 16N | 02W | Jackson | 13,175' 13,770' |
| 4) 231813 1704920649 | Anadarko | Beasley 9 #2ALT | Vernon | 9 | 16N | 02W | Jackson | 11,348' |

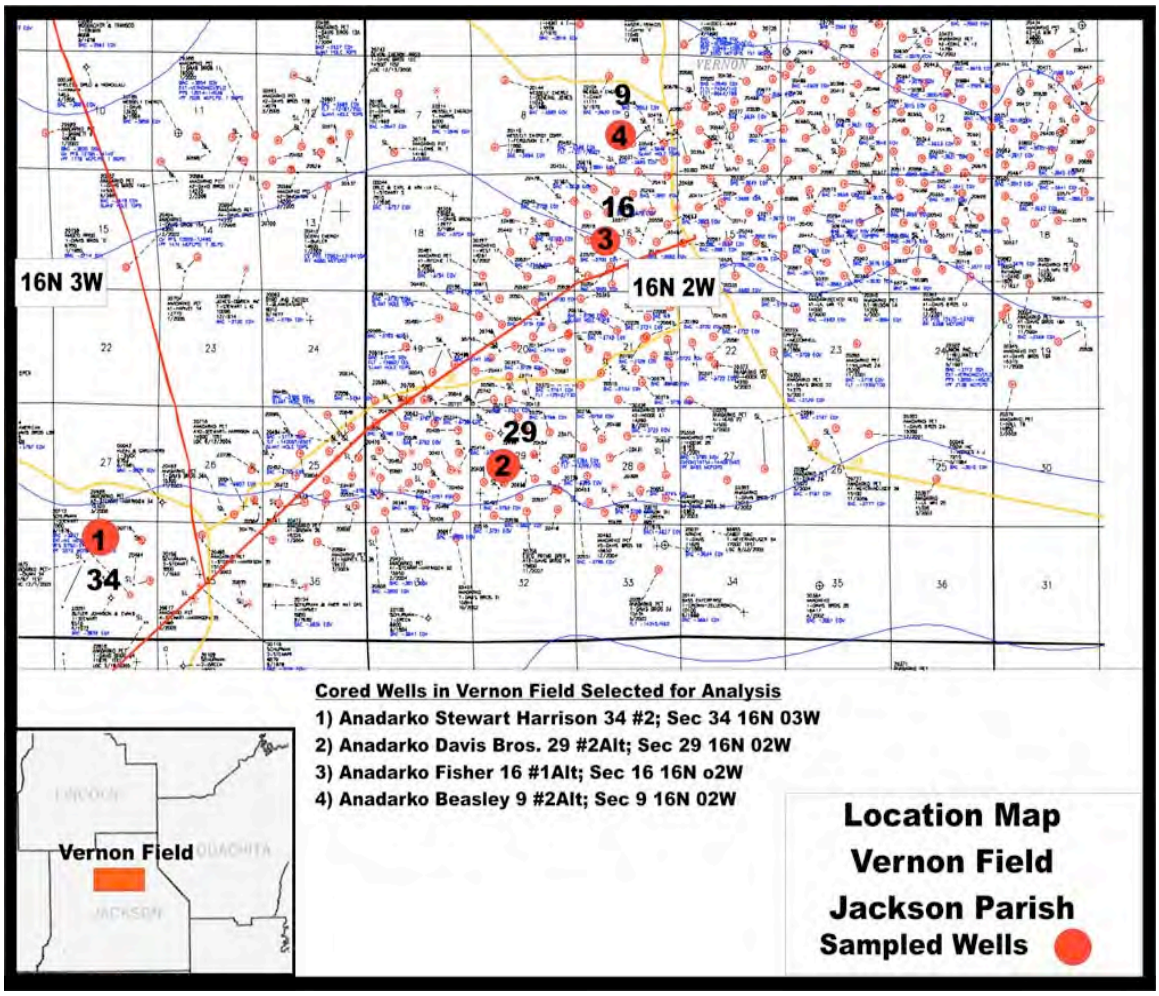


Figure 334. Map of Vernon Field, Jackson Parish with sampled wells highlighted in red.

Table 7. Wells used to construct the north-south stratigraphic cross section.

| Operator | Well | Field | Sec | Twp | Rge | Parish | TD(Ft) | Top Bossier (Ft.) | Base Bossier (Ft.) |
|---|---|---|---|---|---|---|---|---|---|
| 1) Pan Am | Venzina | wc (Bernice) | 22 | 21N | 03W | Union | 11,031 | 9,270 | 9,930 |
| 2) Chevron Oil | Eliza Lewis Dunn | Hico-Knowles | 31 | 20N | 03W | Lincoln | 12,197 | 9,925 | 10,495 |
| 3) Arkla Expor (Mobil) | Tomlinson #1 | Clay | 10 | 17N | 03W | Lincoln | 12,457 | 11,780 | na |
| 4) Anadarko Petr. | Fisher 16 #2ALT | Vernon | 16 | 16N | 02W | Jackson | 14,055 | 11,980 | 13,000 |
| 5) Cabot Oil & Gas | Knight et al 1 #1 | Clear Branch | 1 | 14N | 02W | Jackson | 15,918 | 12,785 | 14,890 |
| 6b) Exxon | Pardee #1 | East Sikes | 36 | 13N | 01W | Winn | 19,500 | 15,775 | 17,310 |
| 7) Amoco Prod | C Z.5-7 | Wildcat | 5 | 11N | 01W | Winn | 17,992 | 15,600 | na |

Table 8. Wells used to construct the west-east stratigraphic cross section

| Operator | Well | Field | Sec | Twp | Rge | Parish | TD(Ft) | Top Bossier (Ft.) | Base Bossier (Ft.) |
|---|---|---|---|---|---|---|---|---|---|
| 1) JW Operating | Cupples 18-12 ALT | Elm Grove | 3 | 16N | 13W | Caddo | 10,612 | 9,578 | 10,160 |
| 2) Tenneco Oil | Baker #1 | Lake Bistineau | 12 | 16N | 10W | Bienville | 11,123 | 8,495 | 9,120 |
| 3) Franks & Broyles | Bardin #1 | Bear Creek | 8 | 16N | 06W | Bienville | 12,550 | 11,770 | 12,365 |
| 4) J-W Operating | Davis Brothers 21-1 | Driscoll | 21 | 16N | 04W | Bienville | 16,900 | 12,120 | 12,930 |
| 5) Amoco Prod | Davis Bros 8-3 #1 | Vernon | 8 | 16N | 03W | Jackson | 13,250 | 11,970 | 12,725 |
| 6a) Anadarko Petr. | Fisher 16 #1ALT | Vernon | 16 | 16N | 02W | Jackson | 14,100 | 12,000 | 13,013 |
| 7) Cabot Oil & Gas | Weyerh Co. 15-1 | Vernon | 15 | 16N | 01W | Jackson | 13,778 | 11,895 | 12,930 |
| 8) Burlington Res. | Donner 13-1 | Cheniere Creek | 13 | 16N | 02E | Ouachita | 13,992 | 11,090 | 12,150 |

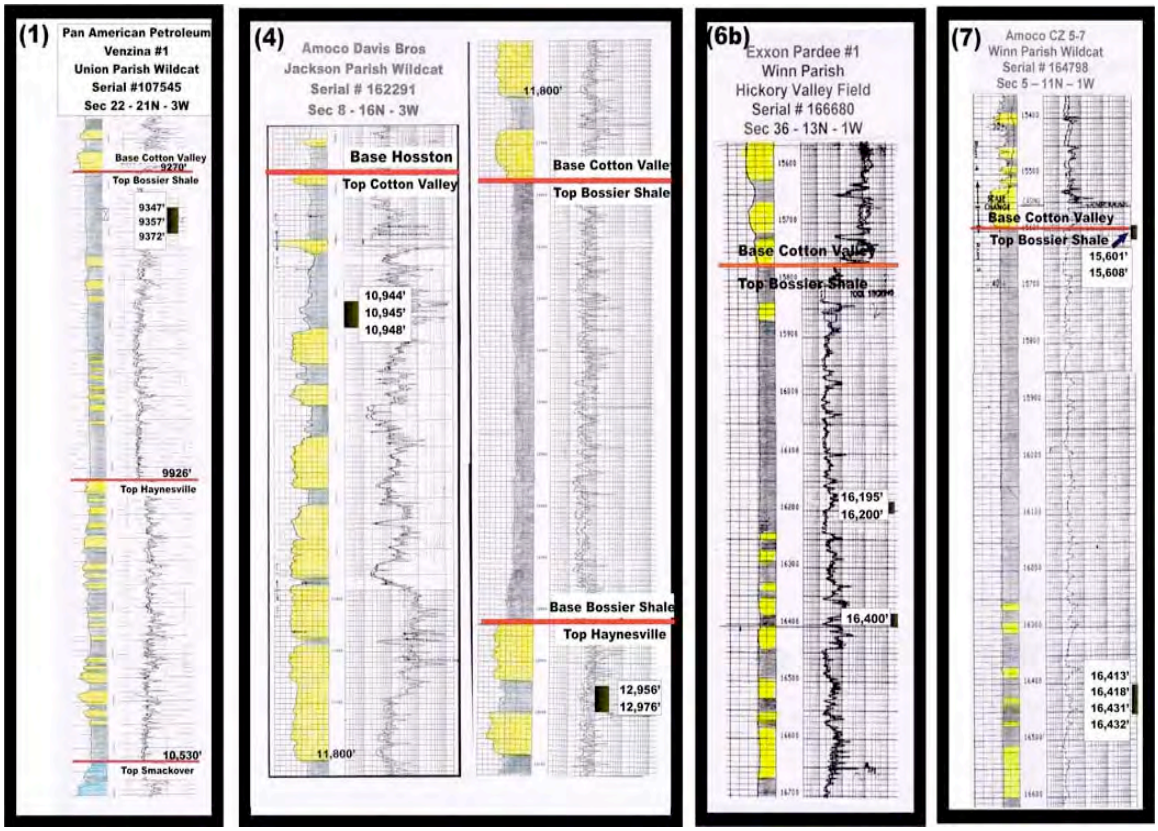


Figure 335. Electric logs from cored wells in the North Louisiana Salt Basin with major stratigraphic boundaries (Cotton Valley, Bossier & Haynesville) and depths for samples analyzed in the present study.

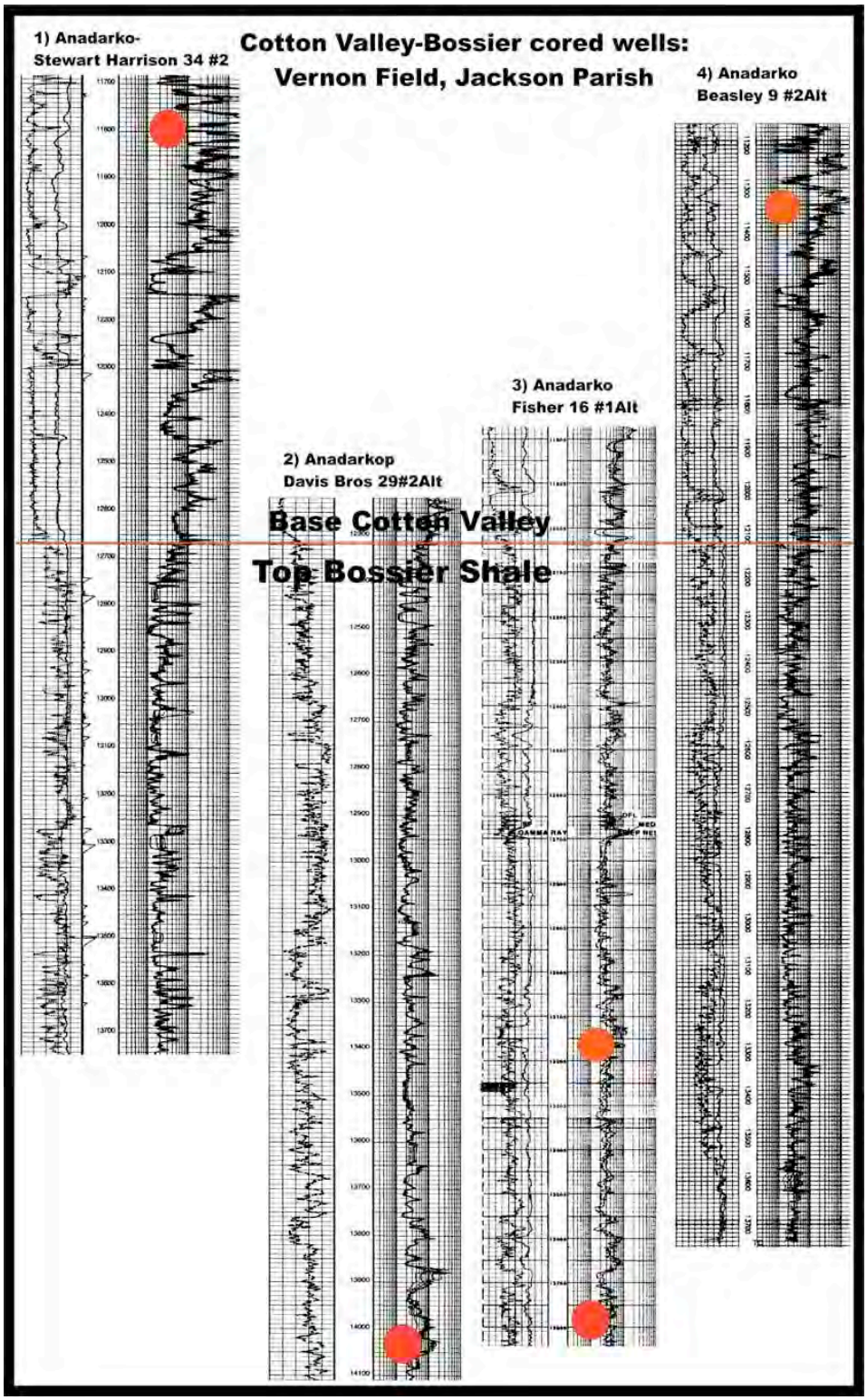


Figure 336. Electric logs for wells selected from Vernon Field, Jackson Parish showing depths where samples chosen for analysis. The Anadarko Davis Bros 29-2Alt sample at 15,120 ft depth is not shown at the scale of the electric logs.

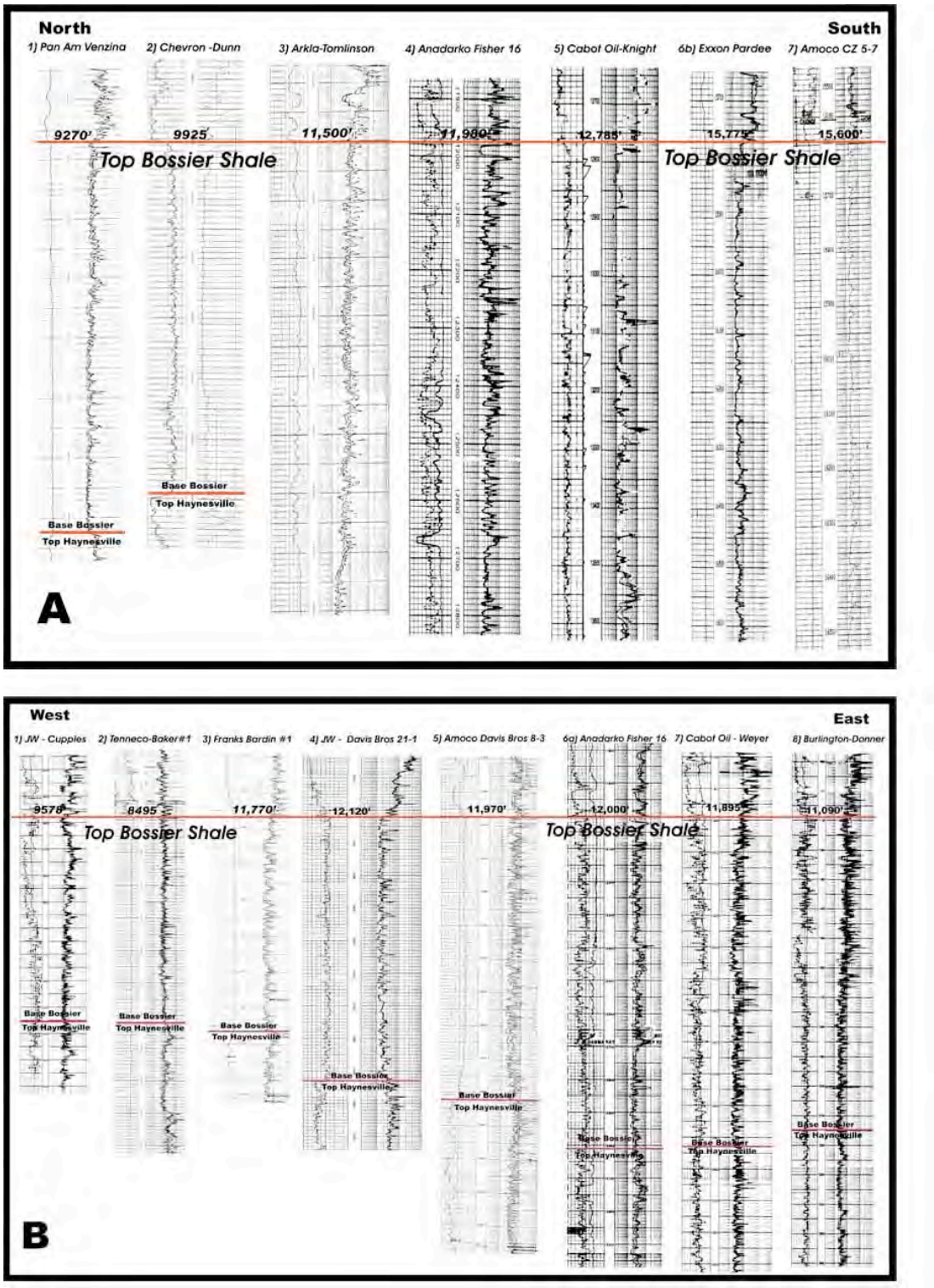


Figure 337. (A) North-south stratigraphic cross section showing the cored wells together with other wells that penetrate the Cotton Valley - Bossier Group, and (B) west-east stratigraphic cross section showing the cored wells together with other wells that penetrate the Cotton Valley - Bossier Group.

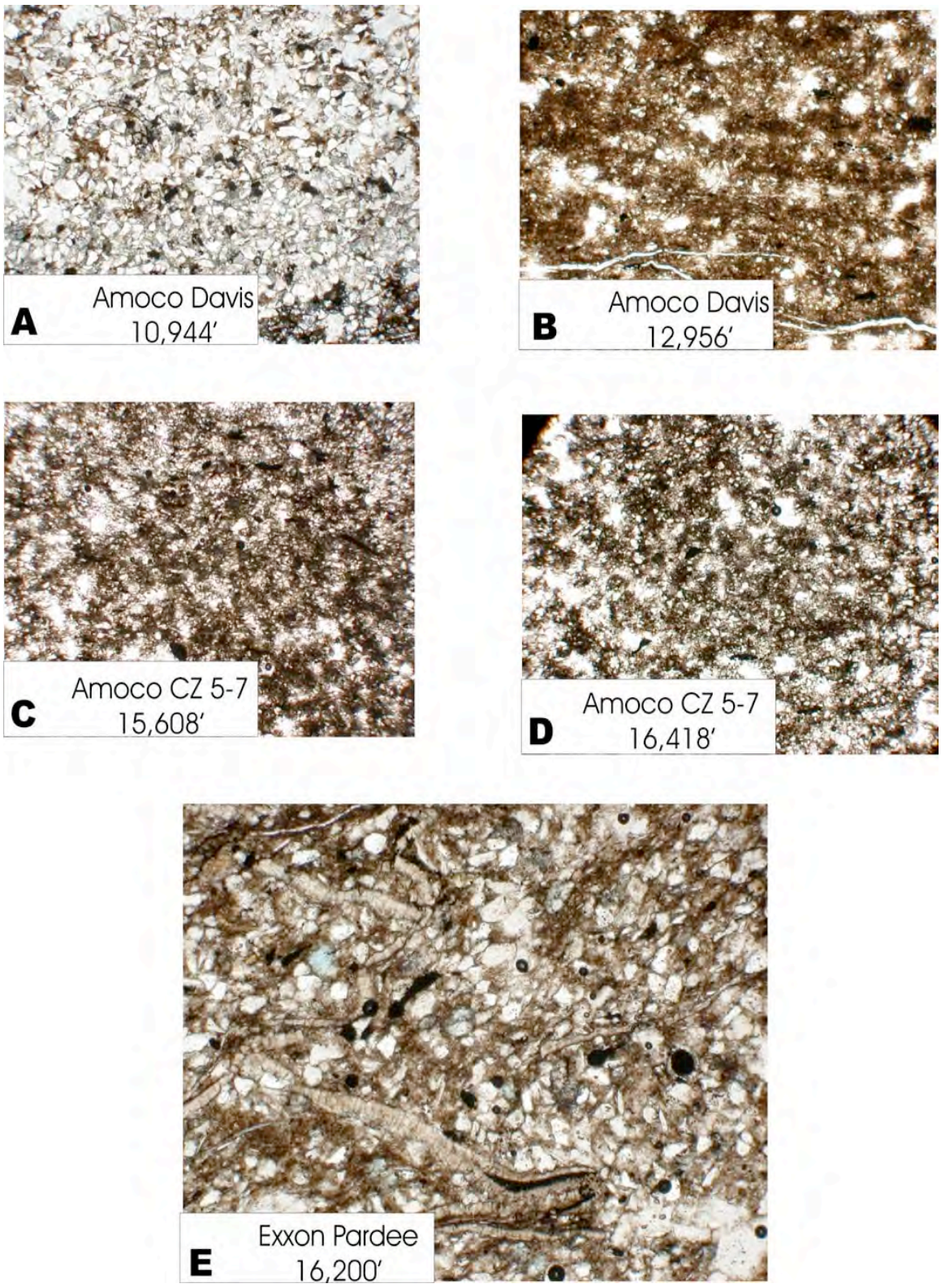


Figure 338. Thin section micrographs of the Cotton Valley – Bossier and Haynesville rocks that were described petrographically from the Amoco Davis well (A&B), Amoco CZ 5-7 (C&D), and Exxon Pardee wells (E).

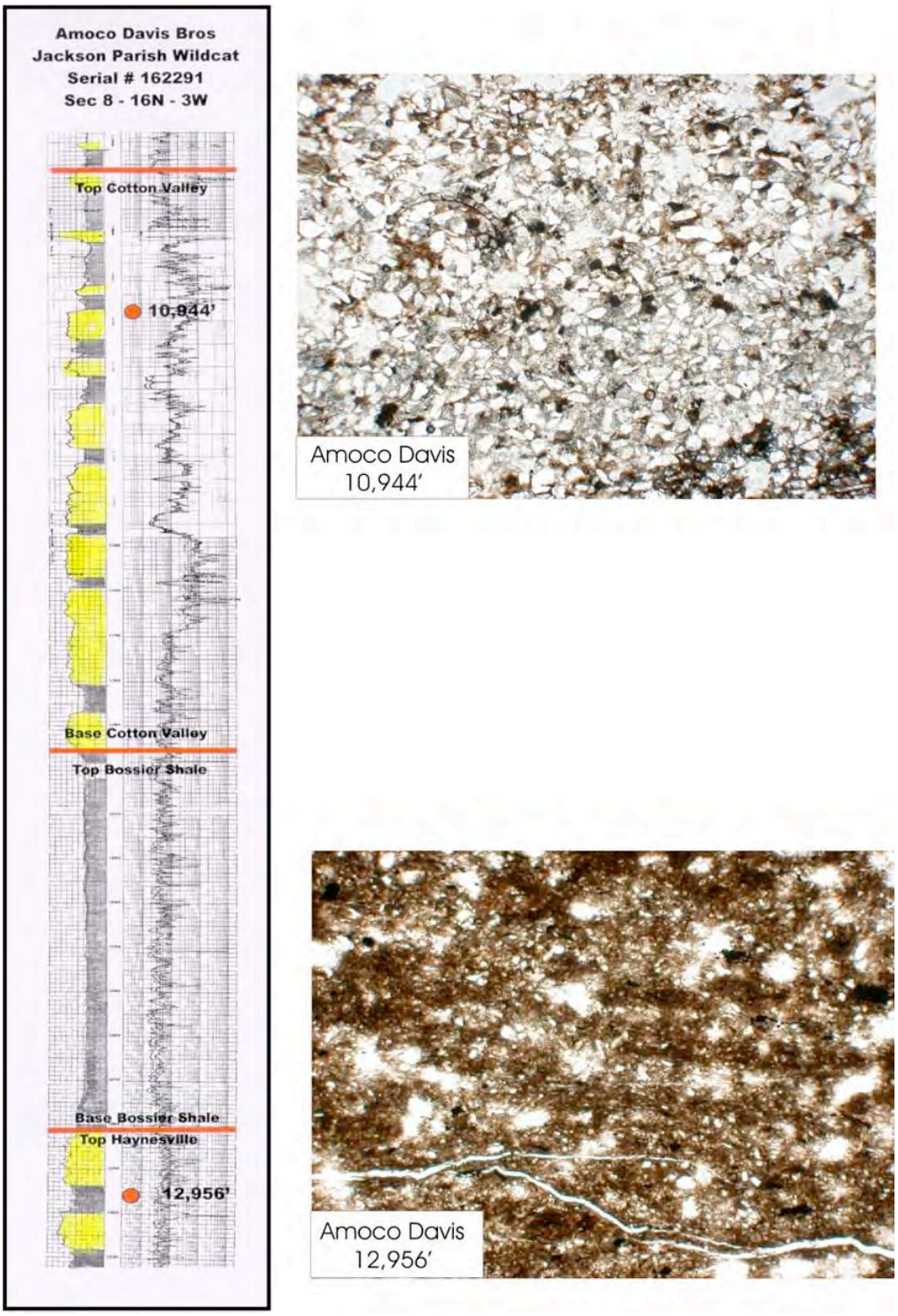


Figure 339. Amoco Davis well electric log in Jackson Parish showing sample depths within the Cotton Valley interval and within the Haynesville Formation accompanied by thin section micrographs.

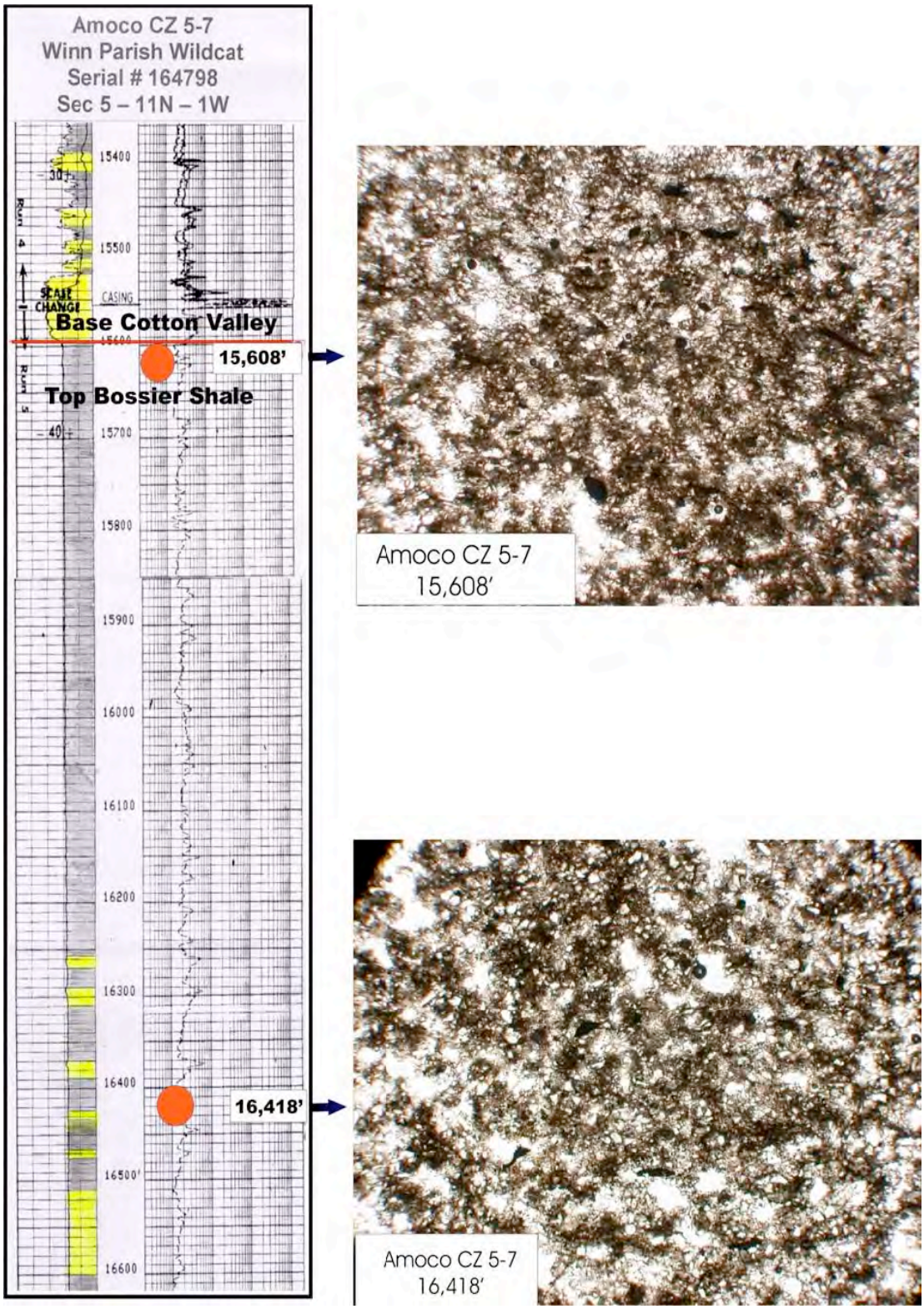


Figure 340. Amoco CZ 5-7 well electric log showing sample depths within the Bossier Shale with corresponding thin section micrographs.

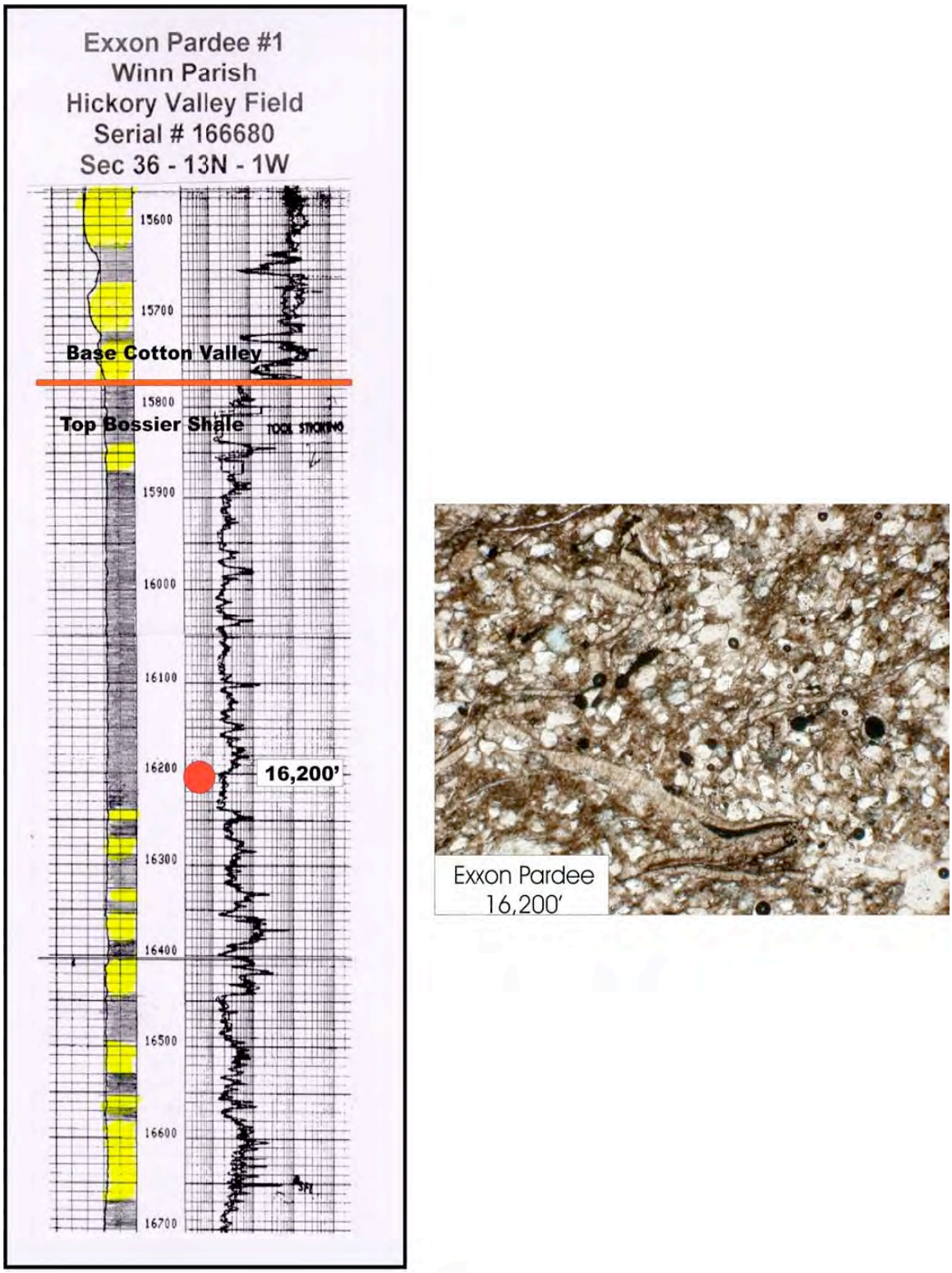


Figure 341. Exxon Pardee well electric log (Winn Parish) showing sample depths within the Bossier Shale and corresponding thin section micrograph.

Table 9. Total organic carbon, rock–eval pyrolysis and vitrinite reflectance analytical results.

| Cotton Valley-Bossier Group and Haynesville Cores Analyzed in North Louisiana Salt Basin | | | | | | | | | | | | | |
|---|---|---|---|---|---|---|---|---|---|---|---|---|---|
| Well | Rock Sample | Sample Depth (Ft) | TOC Wt. % | S1 mg/g | S2 mg/g | S3 mg/g | Tmax | HI | OI | S1/ TOC | PI | TAI | % Ro VITK |
| AMOCO DAVIS | Cotton V. | 10,944 | 0.46 | 0.14 | 0.12 | 0.09 | 331 | 26 | 20 | 30 | 0.54 | | |
| AMOCO DAVIS | Cotton V. | 10,945 | 0.25 | 0.04 | 0.04 | 0.12 | 442 | 17 | 46 | 17 | 0.49 | | |
| AMOCO DAVIS | Cotton V. | 10,948 | 0.11 | 0.02 | 0.04 | 0.11 | 424 | 35 | 98 | 18 | 0.33 | | |
| AMOCO DAVIS | Haynesville | 12,956 | 0.43 | 0.1 | 0.08 | 0.22 | 304 | 19 | 20 | 43 | 0.56 | 3.5-3.7 | 1.73 |
| AMOCO DAVIS | Haynesville | 12,976 | 0.61 | 0.11 | 0.07 | 0.02 | 313 | 11 | 3 | 18 | 0.61 | 3.5-3.7 | 1.77 |
| AMOCO CZ 5-7 | Bossier | 15,601 | 0.27 | 0.04 | 0.06 | 0.13 | 375 | 21 | 50 | 15 | 0.42 | | |
| AMOCO CZ 5-7 | Bossier | 15,608 | 0.28 | 0.02 | 0.04 | 0 | 307 | 14 | 0 | 7 | 0.33 | | |
| AMOCO CZ 5-7 | Bossier | 16,413 | 0.23 | 0.04 | 0.05 | 0.14 | 379 | 22 | 58 | 18 | 0.45 | | |
| AMOCO CZ 5-7 | Bossier | 16,418 | 0.34 | 0.05 | 0.07 | 0.11 | 355 | 21 | 32 | 15 | 0.42 | | |
| AMOCO CZ 5-7 | Bossier | 16,431 | 0.34 | 0.06 | 0.1 | 0.37 | 329 | 29 | 109 | 18 | 0.38 | 3.7-3.8 | 2.62 |
| AMOCO CZ 5-7 | Bossier | 16,432 | 0.28 | 0.05 | 0.09 | 0.15 | 375 | 31 | 55 | 18 | 0.37 | | |
| | | | | | | | | | | | | | |
| EXXON PARDEE | Bossier | 16,195 | 0.19 | 0.18 | 0.27 | 0.12 | 370 | 147 | 62 | 96 | 0.39 | | |
| EXXON PARDEE | Bossier | 16,200 | 0.35 | 0.21 | 0.29 | 0.29 | 322 | 83 | 83 | 60 | 0.42 | | |
| EXXON PARDEE | Bossier | 16,400 | 0.35 | 0.19 | 0.16 | 0.16 | 328 | 46 | 46 | 54 | 0.54 | 3.7-3.8 | 2.06 |
| | | | | | | | | | | | | | |
| PAN AM VENZINA | Bossier | 9347 | 0.5 | 0.06 | 0.26 | 0.44 | 442 | 52 | 88 | 12 | 0.19 | 2.8-3.0 | 0.91 |
| PAN AM VENZINA | Bossier | 9357 | 0.45 | 0.19 | 0.43 | 0.22 | 451 | 94 | 48 | 41 | 0.3 | 2.8-3.0 | 0.96 |
| PAN AM VENZINA | Bossier | 9372 | 0.39 | 0.1 | 0.24 | 0.32 | 449 | 62 | 83 | 26 | 0.29 | 2.8-3.0 | 0.96 |
| | | | | | | | | | | | | | |
| STWERTHARRISON | Cotton V. | 11,805 | 2.8 | 0.26 | 0.52 | 0.19 | 491 | 19 | 7 | 9 | 0.33 | | |
| FISHER 16-1 | Bossier | 13,175 | 0.51 | 0.17 | 0.09 | 0.57 | 406 | 18 | 112 | 33 | 0.65 | | |
| FISHER 16-1 | Bossier | 13,770 | 0.56 | 0.16 | 0.16 | 0.13 | 436 | 29 | 23 | 29 | 0.5 | | |
| DAVIS Bros 29-2 | Bossier | 14,035 | 0.68 | 0.87 | 0.44 | 0.49 | 359 | 65 | 72 | 128 | 0.66 | | |
| DAVIS Bros 29-2 | Bossier | 15,120 | 0.75 | 0.53 | 0.32 | 0.5 | 360 | 42 | 66 | 70 | 0.62 | | |
| BEASLEY 9-#2 | Cotton V. | 11,348 | 4.46 | 1.31 | 2.2 | 0.47 | 464 | 49 | 11 | 29 | 0.37 | | |

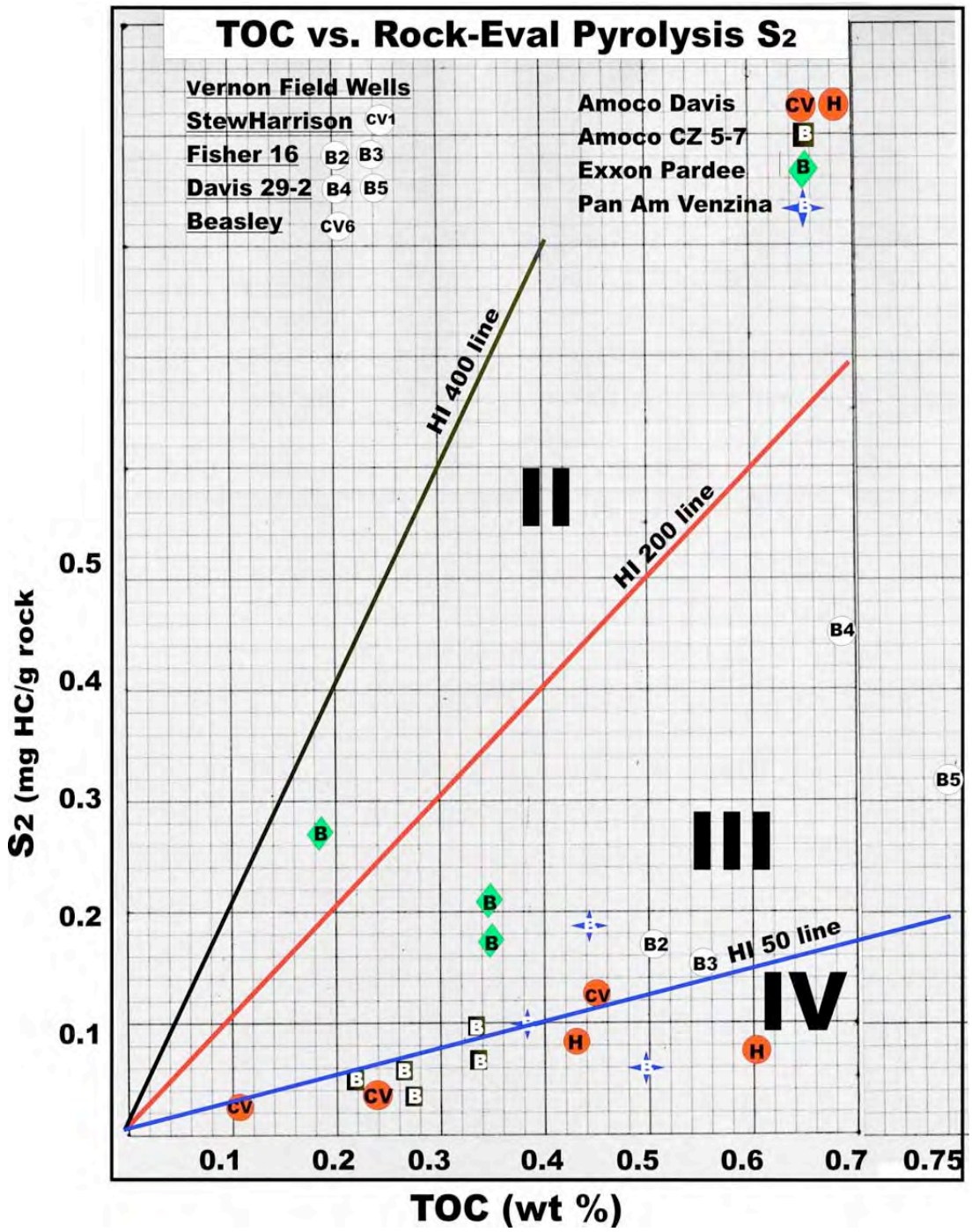


Figure 342. Diagram of $S_2$ versus TOC. The majority of the wells analyzed plot below the HI 200 line and lie in the III and IV fields, with TOCs ranging from 0.1 to 0.6 wt % (B=Bossier, CV=Cotton Valley, H=Haynesville).

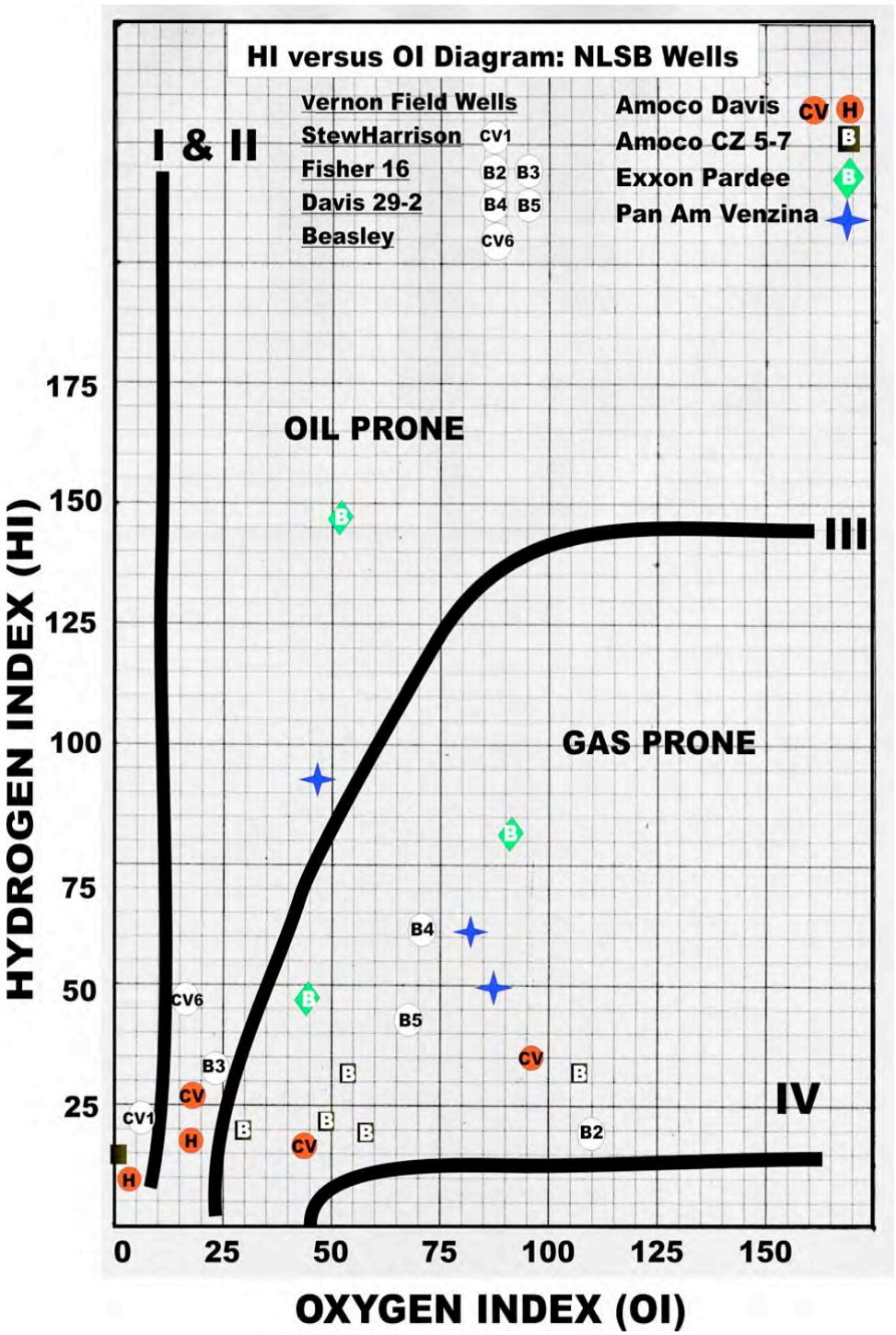


Figure 343. HI versus OI diagram. The majority of data plot between the III and IV fields, indicating they are mostly gas generative rocks. Haynesville and some Cotton Valley samples tend to be more oil prone (B=Bossier, CV=Cotton Valley, H= Haynesville).

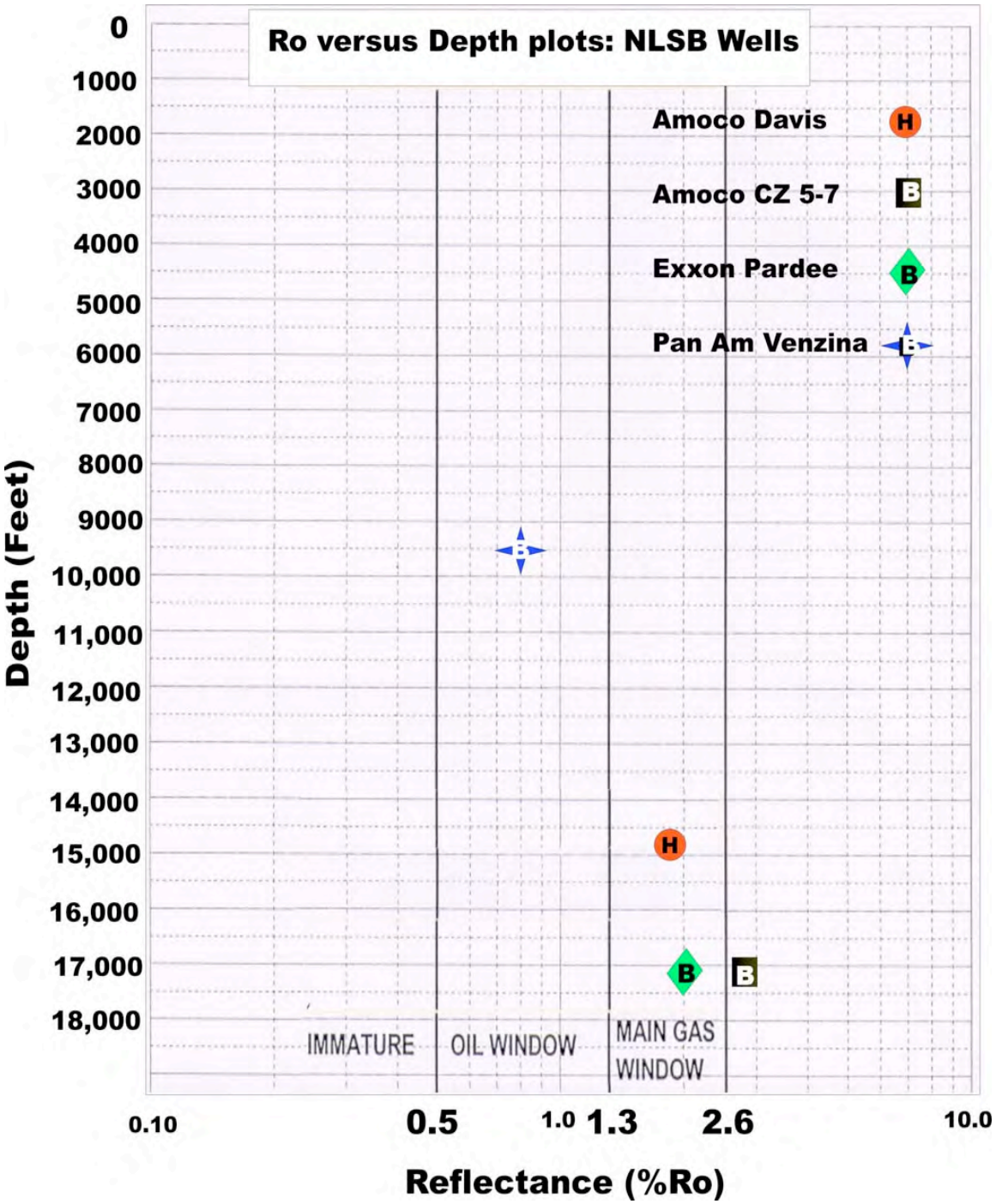


Figure 344. Ro versus depth plot. % Ro of the analyzed samples increases with depth, placing them within the main gas window (B=Bossier, H=Haynesville).

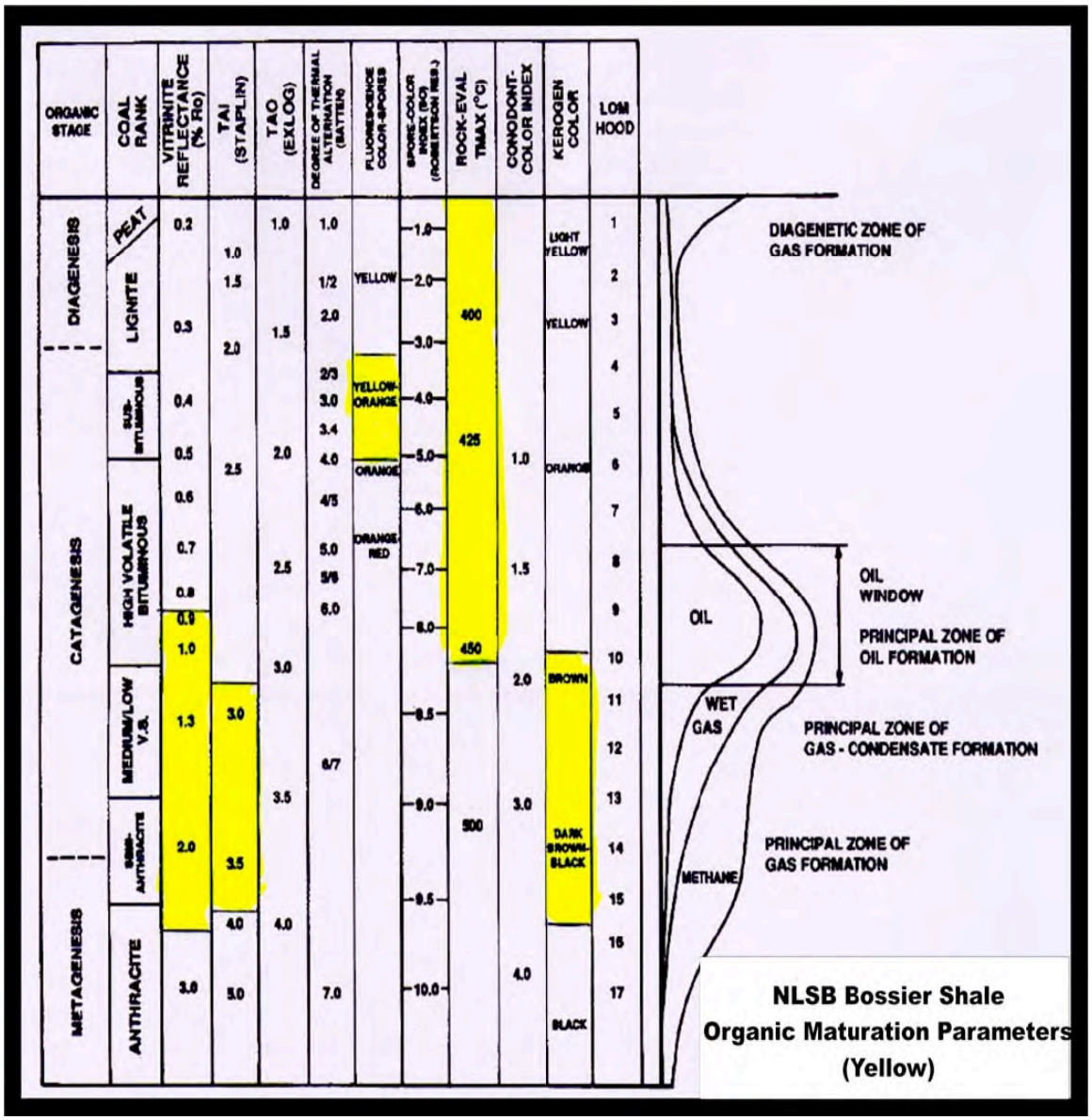


Figure 345. Rock-Eval pyrolysis analyses (Tmax), and organic maturation parameters (%Ro, TAI, kerogen coloration) obtained from visual kerogen analysis. Values obtained from the Cotton Valley – Bossier Group and Haynesville Formation samples (yellow) fall between the oil window and the principal zone of gas formation (modified after Senftle and Landis, 1991).

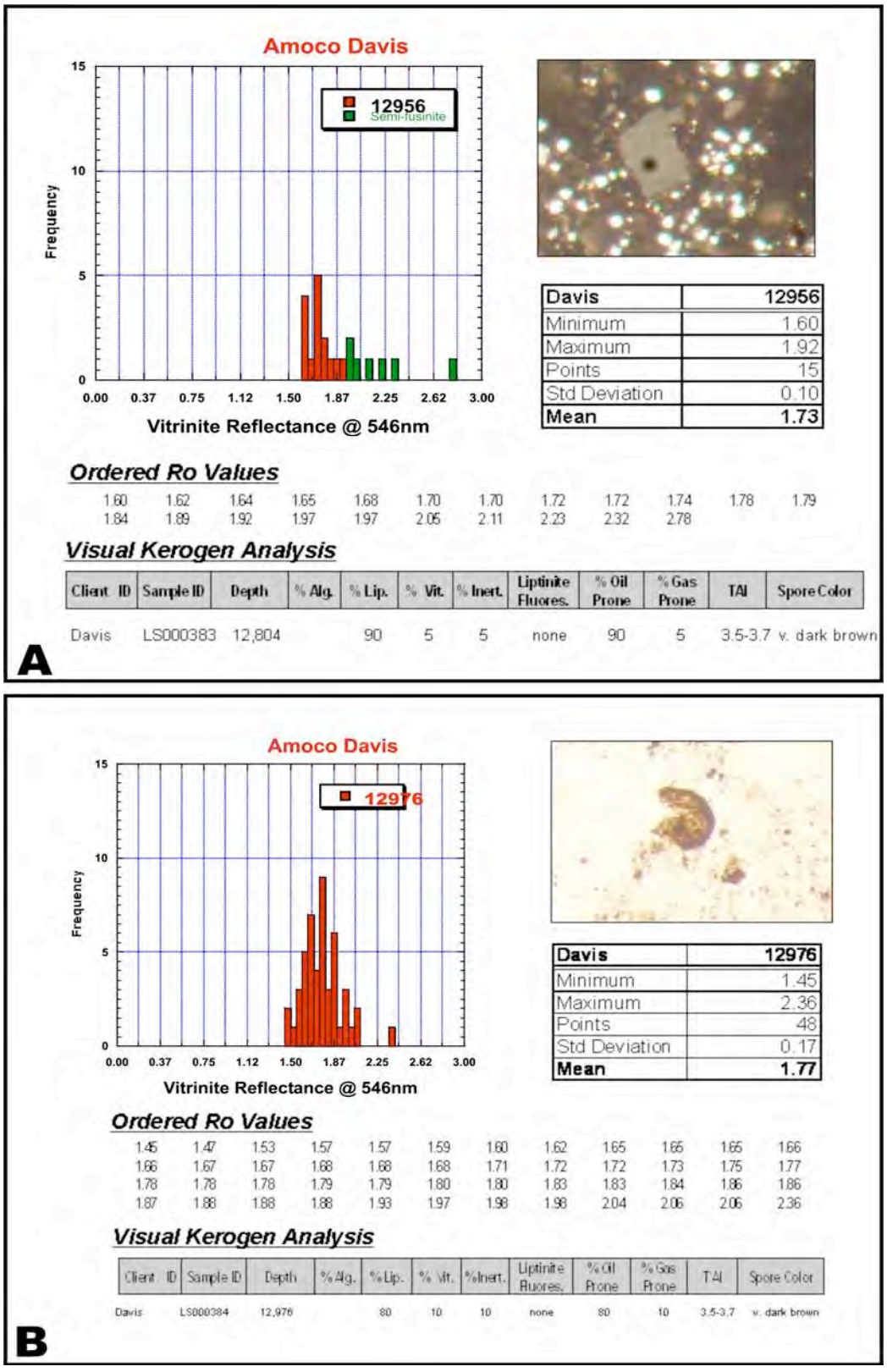


Figure 346. Visual kerogen analyses of Amoco Davis well sampled at 12,956 ft depth (A) and the Amoco Davis well at 12,976 ft depth (B).

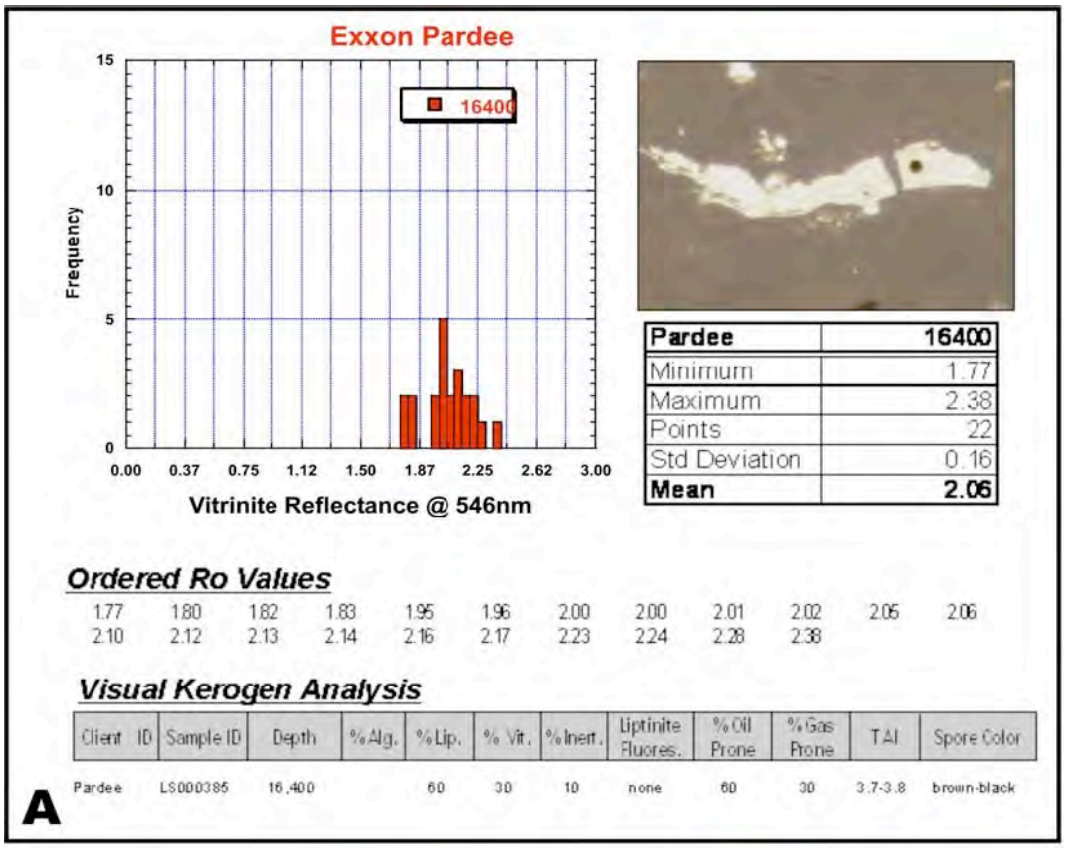


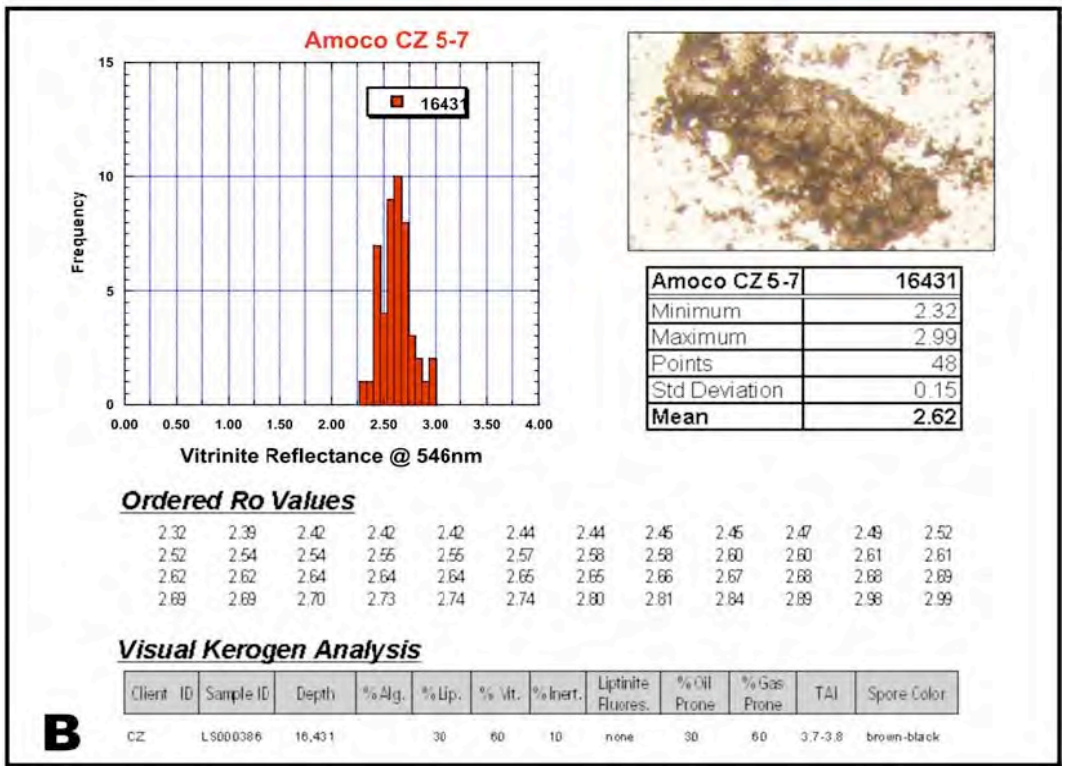


Figure 347. Visual kerogen analyses of Exxon Pardee well sampled at 16,400 depth (A) and the Amoco CZ 5-7 well at 16,431 depth (B).

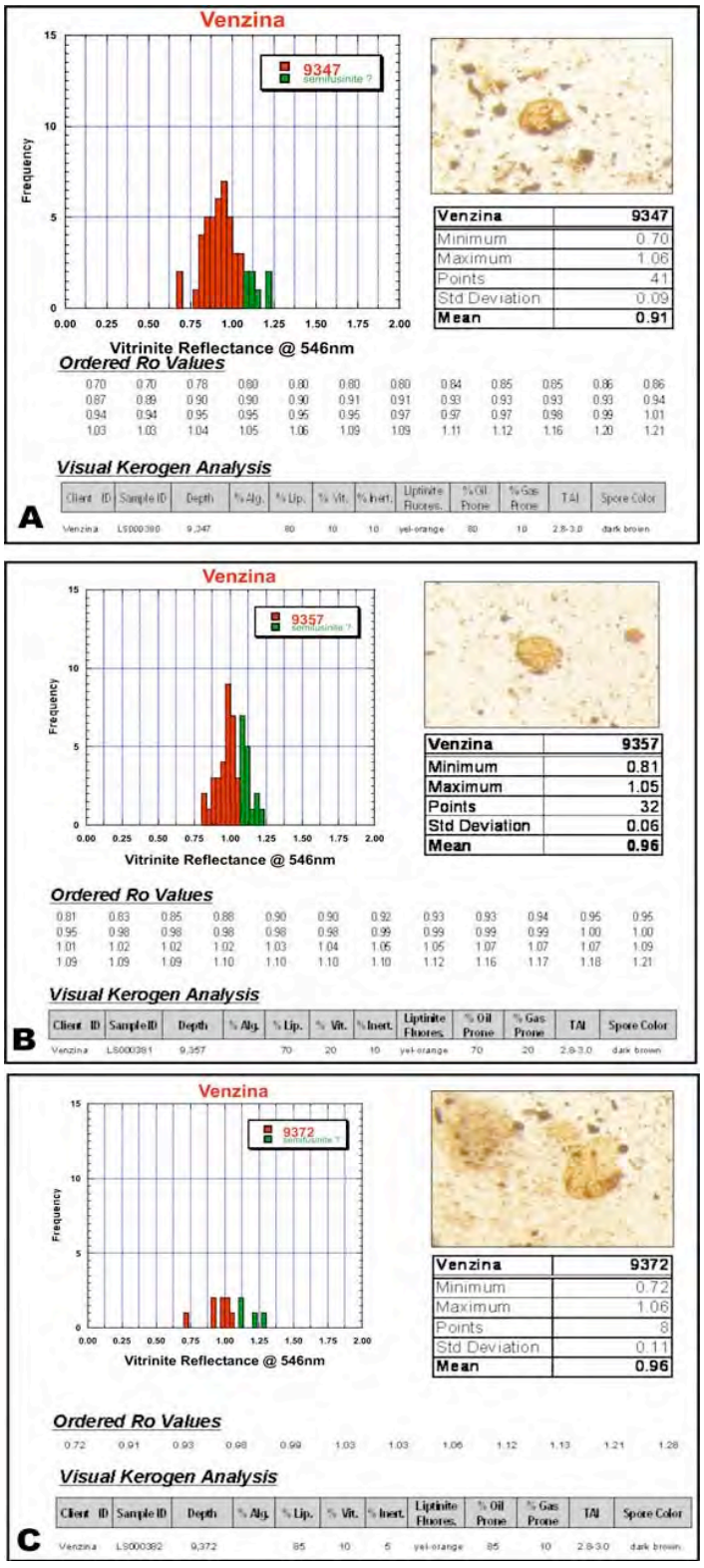


Figure 348. Visual kerogen analysis of the Pan Am Venzina well sampled at 9,347(A), 9,357'(B) and 9,372 (C) depths.

gas with some oil, not only within the Bossier shale, but also in overlying Upper Jurassic and Lower Cretaceous reservoirs, particularly in the Bossier and Cotton Valley.

The Bossier petroleum system includes essentially the same underburden and overburden rocks as the Smackover petroleum system. The petroleum source rocks are the Bossier shale beds. Generation of hydrocarbons was initiated in the late Early Cretaceous with the generation of secondary, non-associated thermogenic gas commencing in the Late Cretaceous (Figs. 349-351). Hydrocarbon expulsion appears minimal suggesting the Bossier has potential as a shale gas reservoir (Fig. 352). Sandstones within the Bossier and in the Cotton Valley Group also probably acted as reservoirs for the hydrocarbons that were expelled from the Bossier shale beds.

### *Hydrocarbon Flow Pathway Modeling*

Hydrocarbon flow pathway modeling indicates that Smackover hydrocarbons were first generated and expelled in the Early Cretaceous from the southern part of the North Louisiana Salt Basin and migrated north and updip into the areas of the Sabine Uplift, Monroe Uplift, and northern parts of the basin (Figs. 353-355). Hydrocarbons, essentially thermogenic gas, generated and expelled in the late Early Cretaceous from the Bossier followed the same flow pathways as Smackover hydrocarbons (Figs. 356-367). However, expulsion modeling (Fig. 352) indicates that much of the gas generated from the gas-prone Type III kerogen in this source rock was retained in the Bossier and was not expelled. The low total organic carbon content of the Bossier contributed to the accumulation of *in situ* thermogenic gas. The IES PetroMod® 2D software application was used for the hydrocarbon flow pathway modeling. No thermogenic hydrocarbon expulsion occurred in the immediate vicinity of the Monroe Uplift, and the main source

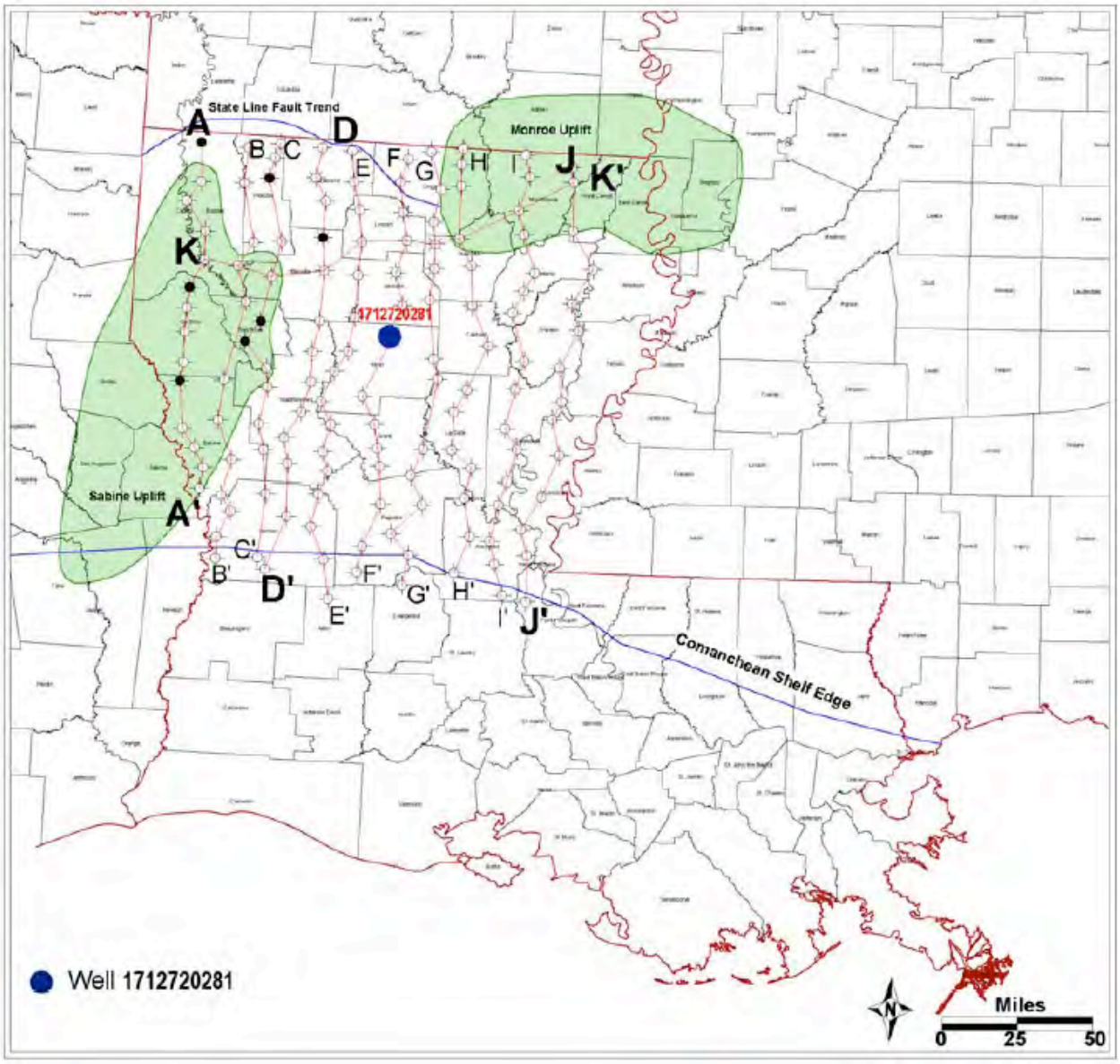


Figure 349. Index map showing location of the well studied to characterize source potential of the Bossier Formation.

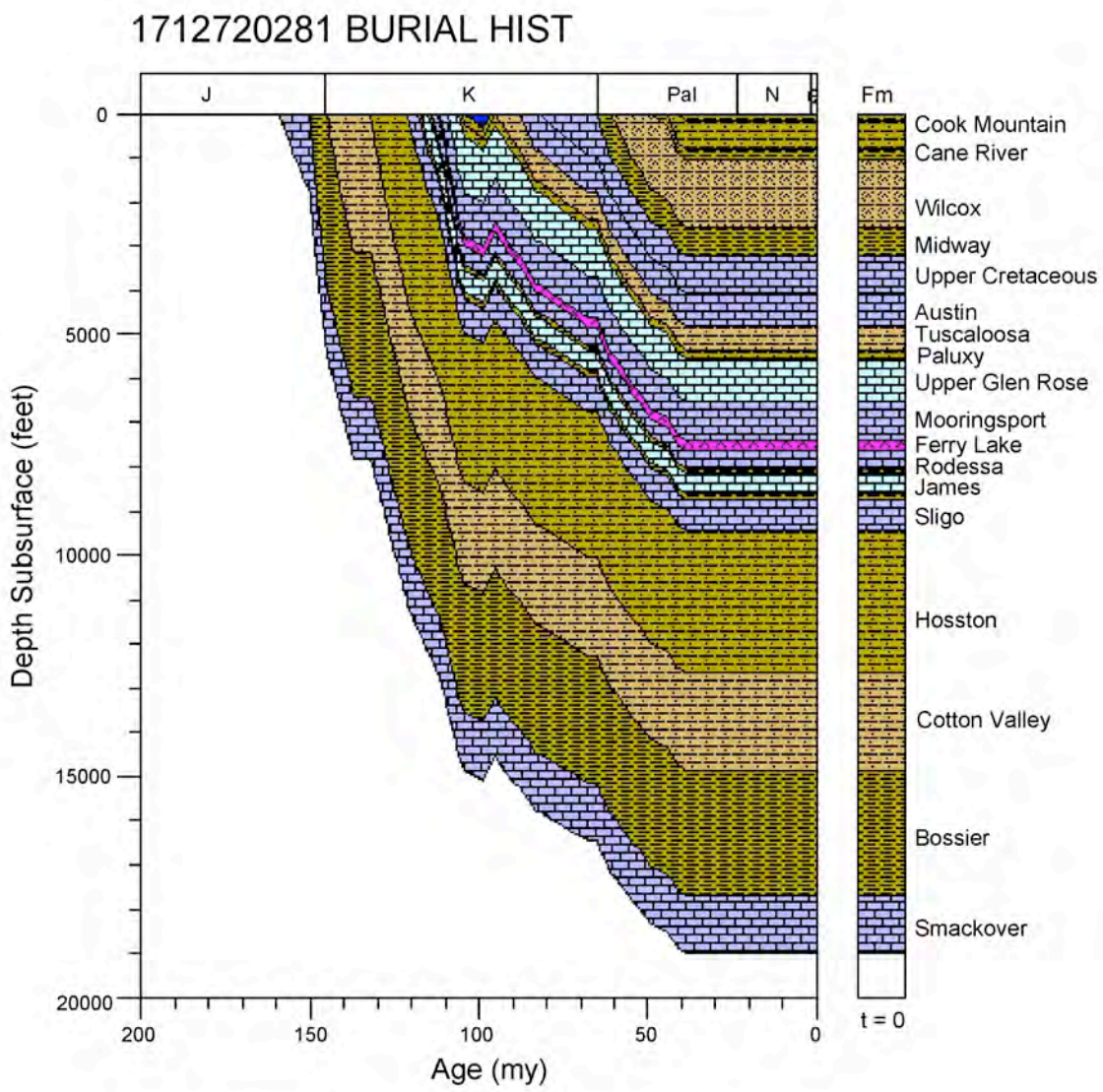


Figure 350. Burial history profile for well 1712720281, used in characterizating the Bossier Formation. See Figure 349 for location of well.

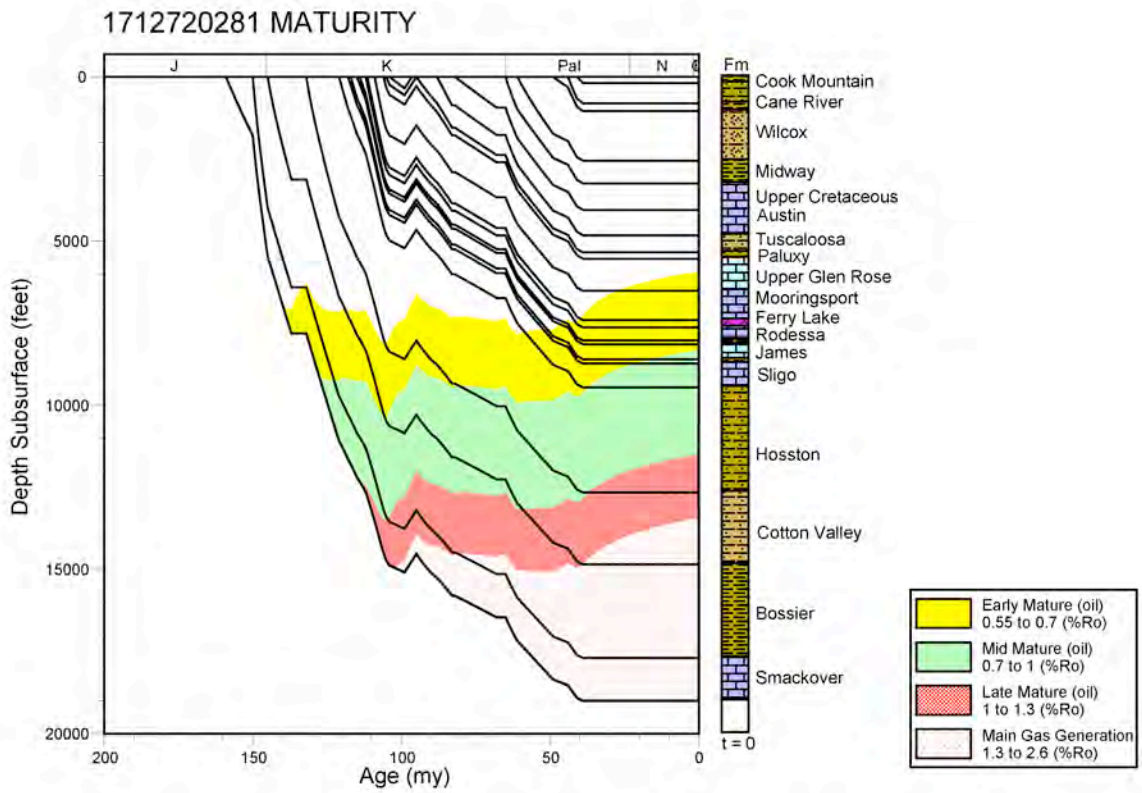


Figure 351. Thermal maturation profile for well 1712720281, North Louisiana Salt Basin.

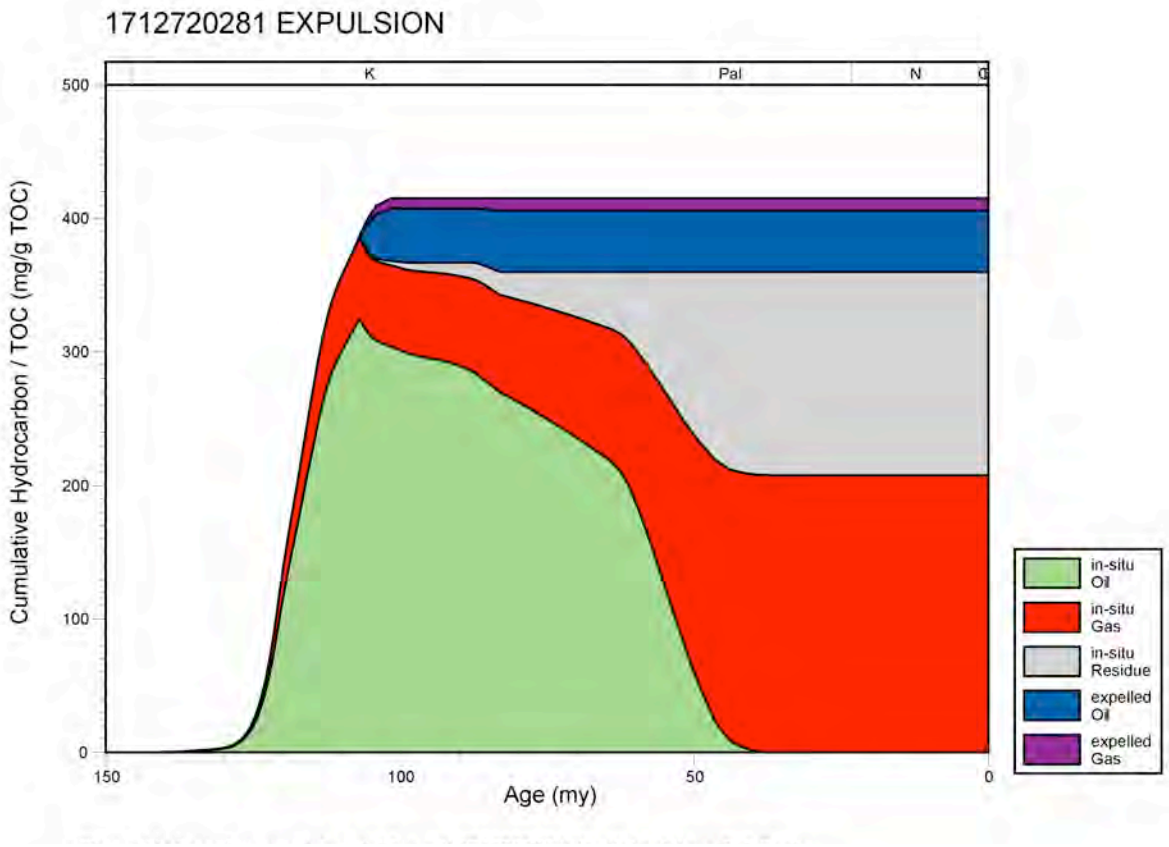


Figure 352. Hydrocarbon expulsion plot for well 1712720281, North Louisiana Salt Basin.

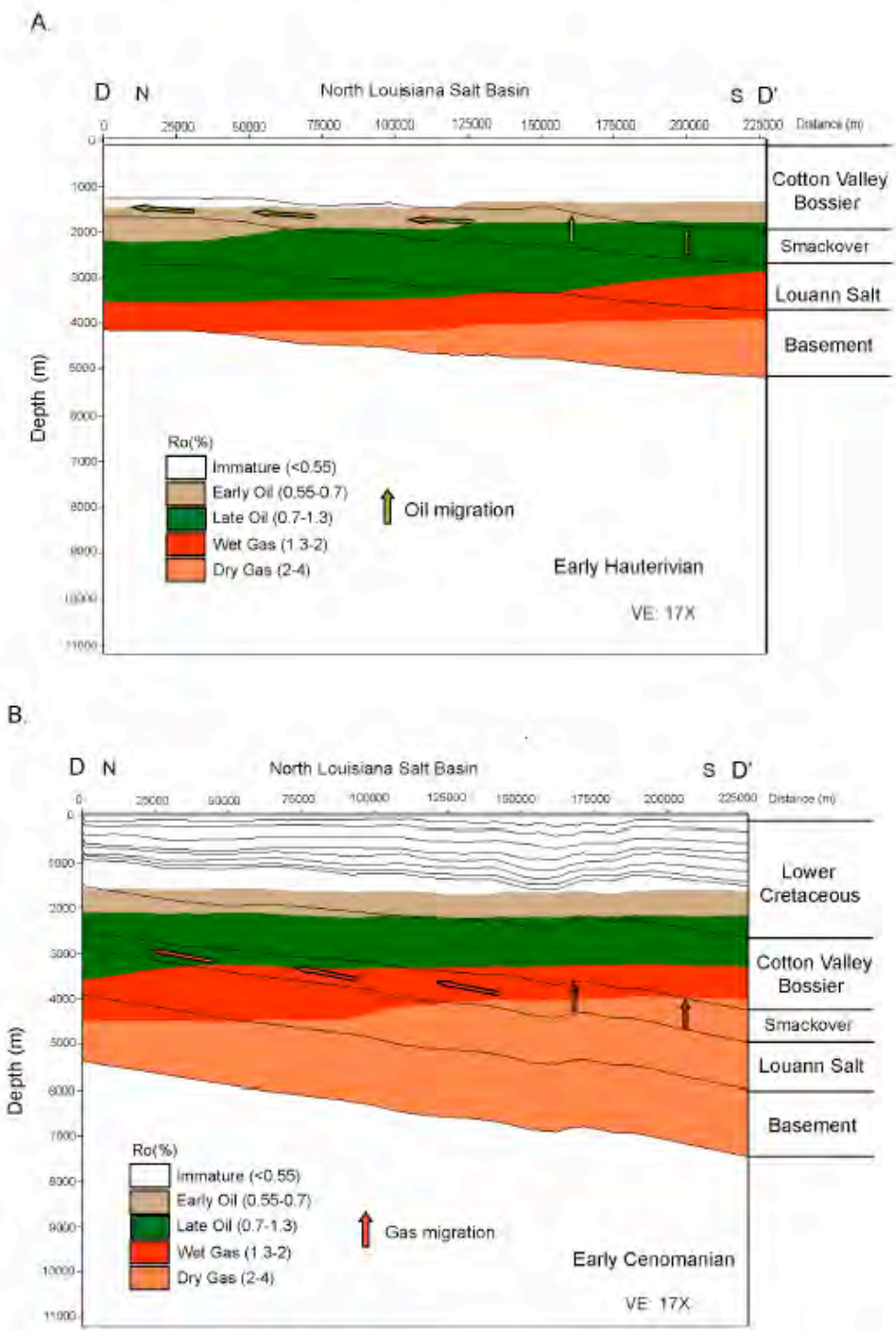


Figure 353. (A) Thermal-maturity and migration modeling at the initiation of oil expulsion during the Early Cretaceous in the southern part of the basin based on the geologic model constructed from cross section D-D'. (B) Thermal-maturity and migration modeling at peak dry-gas expulsion during the early Late Cretaceous in the southern part of the basin. See Figure 2 for the location of cross section D-D'.

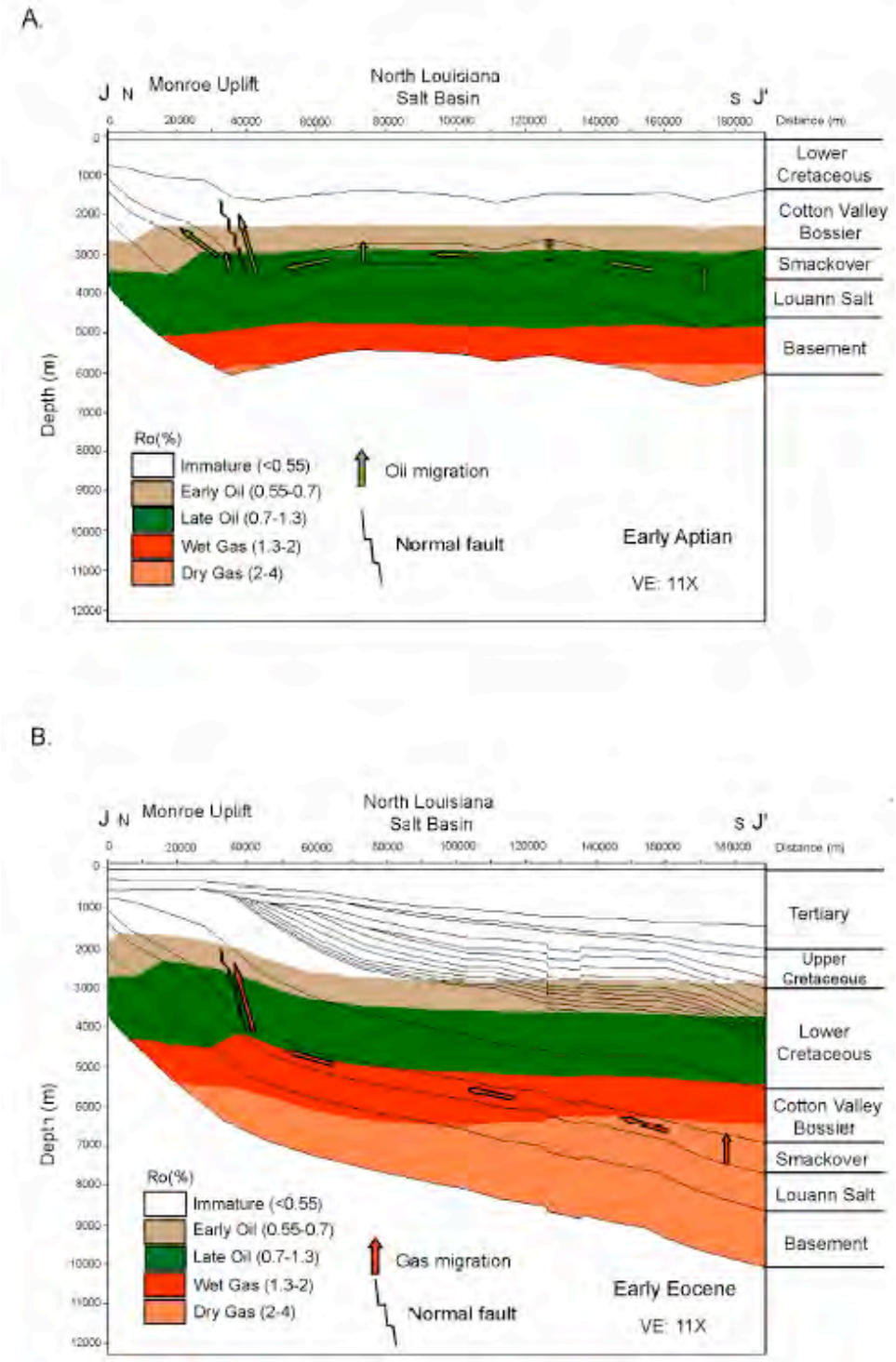


Figure 354. (A) Thermal-maturity and migration modeling at the initiation of oil expulsion during the Early Cretaceous in the southern part of the basin based on the geologic model constructed from cross section J-J'. (B) Thermal-maturity and migration into the Monroe uplift area during the early Eocene from the southern part of the basin. See Figure 2 for location of the cross section J-J'.

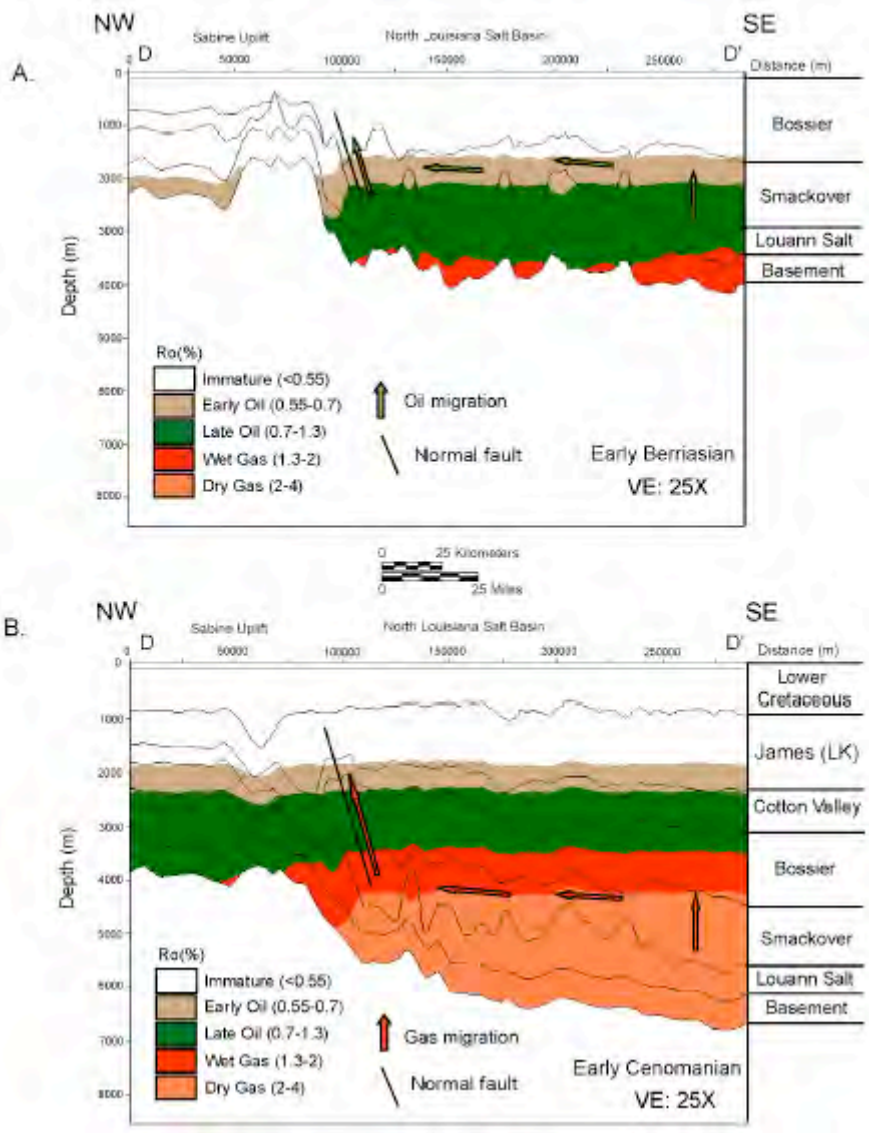


Figure 355. (A) Thermal-maturity and migration modeling at the time of oil expulsion during the Early Cretaceous in the southern part of the basin based on the geologic model constructed from seismic cross section D-D'. (B) Thermal-maturity and migration modeling at peak dry-gas expulsion during the early Late Cretaceous in the southern part of the basin. See Figure 1 for location of seismic cross section D-D'.

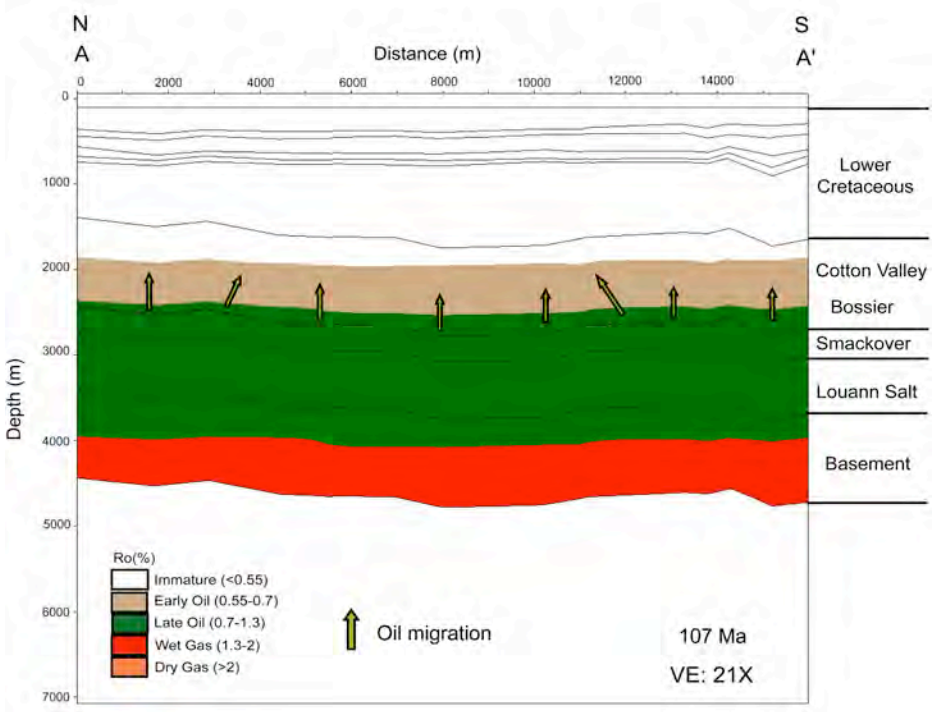


Figure 356. Cross section A-A' showing potential onset of oil expulsion from the Bossier in the Sabine Uplift area. See Figure 2 for location of cross section.

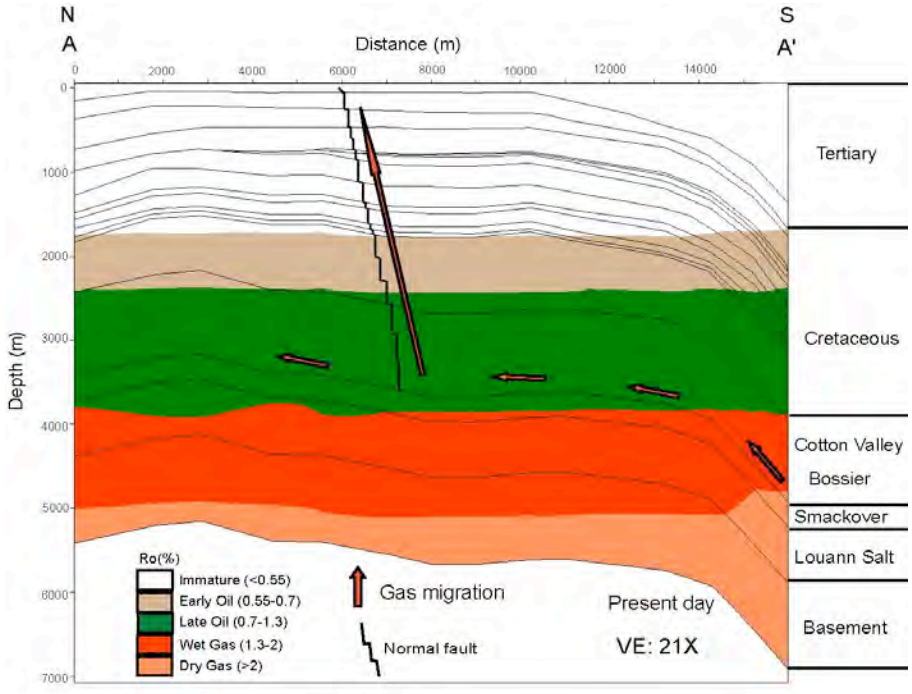


Figure 357. Cross section A-A' showing potential gas expulsion from the Bossier in the Sabine Uplift area. See Figure 2 for location of cross section.

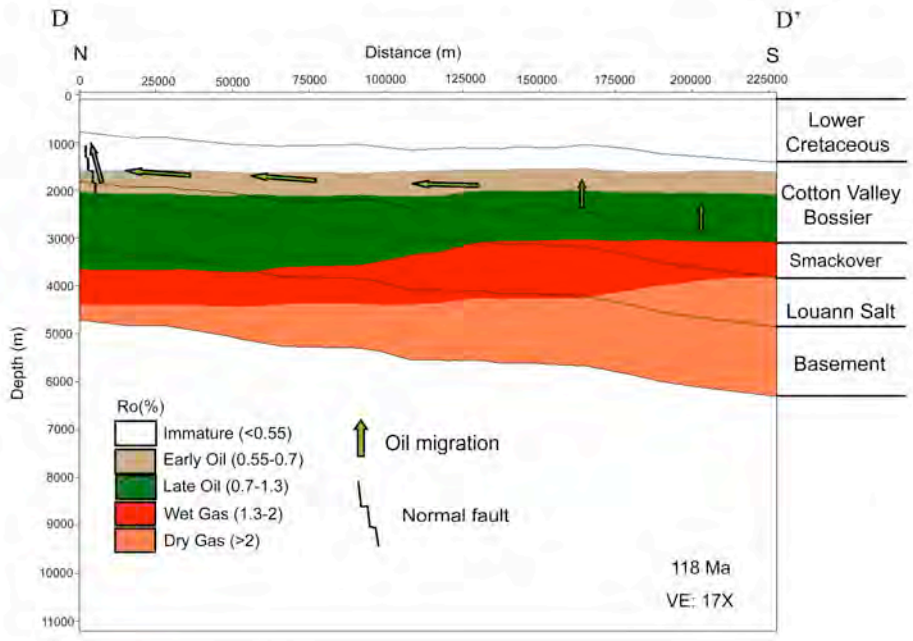


Figure 358. Cross section D-D' showing potential onset of oil expulsion from the Bossier in the North Louisiana Salt Basin. See Figure 2 for location of cross section.

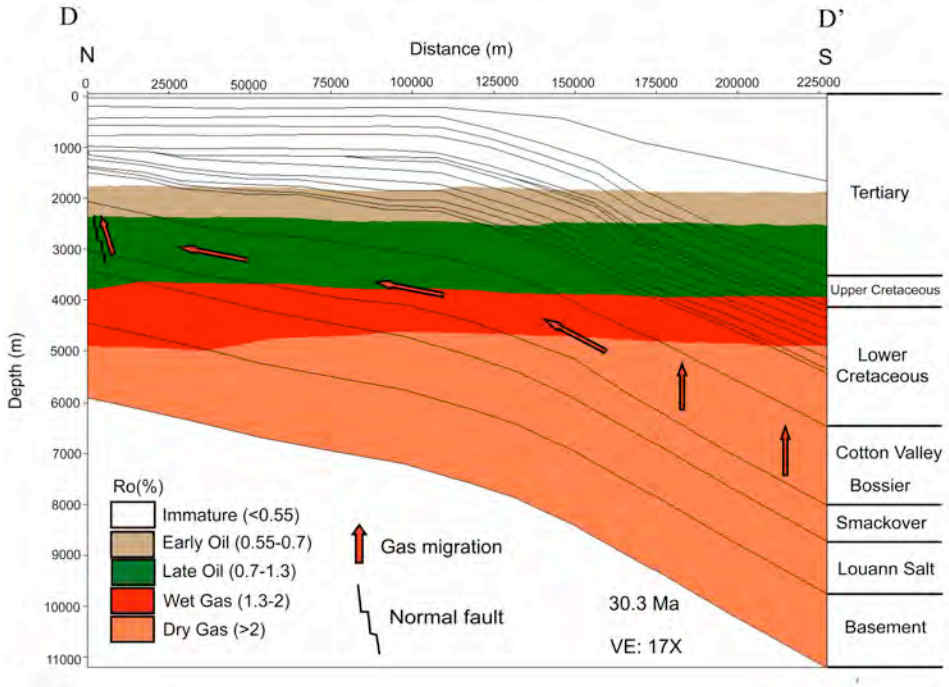


Figure 359. Cross section D-D' showing potential peak gas expulsion from the Bossier in the North Louisiana Salt Basin. See Figure 2 for location of cross section.

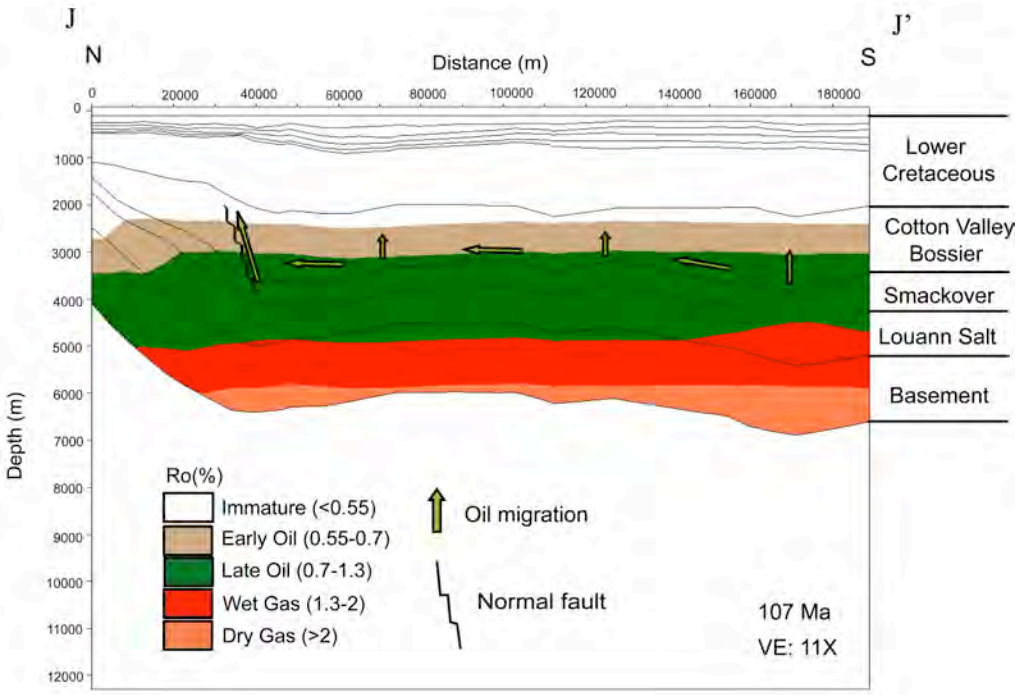


Figure 360. Cross section J-J' showing potential onset of oil expulsion from the Bossier south of the Monroe uplift. See Figure 2 for location of cross section.

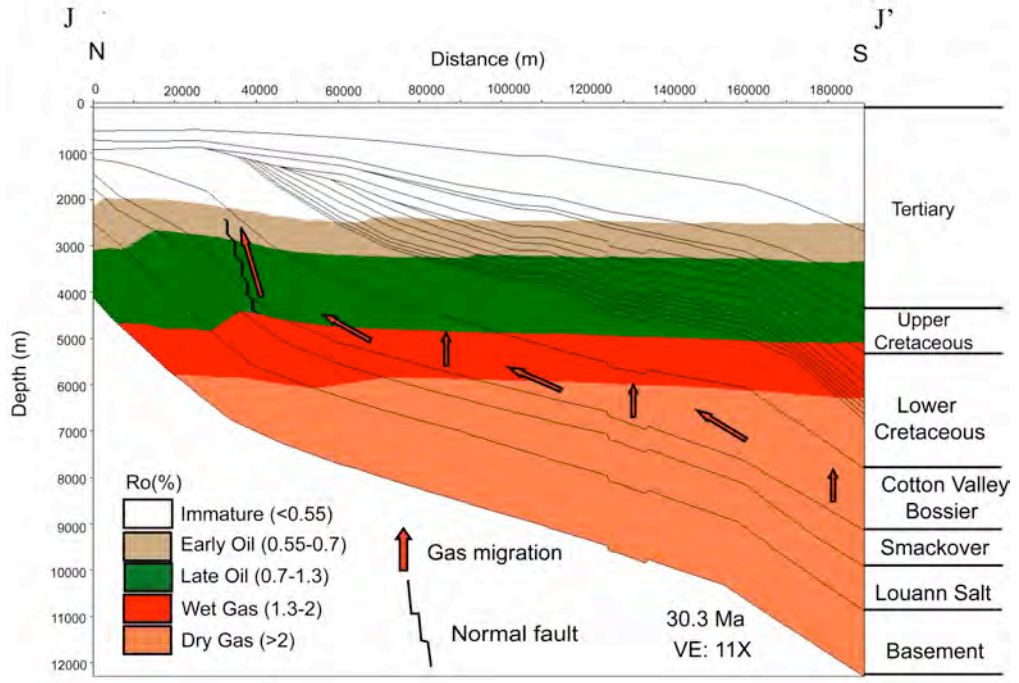


Figure 361. Cross section of J-J' showing potential peak gas expulsion from the Bossier south of the Monroe Uplift. See Figure 2 for location of cross section.

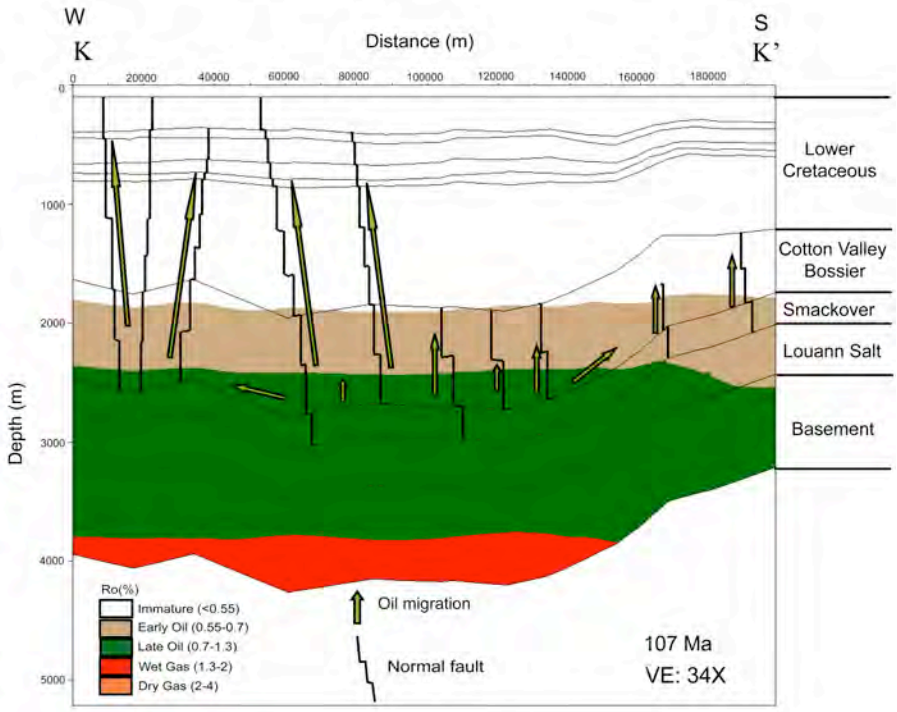


Figure 362. Cross section K-K' showing potential onset of oil expulsion from the Bossier in the northern part of the North Louisiana Salt Basin. See Figure 2 for location of cross section.

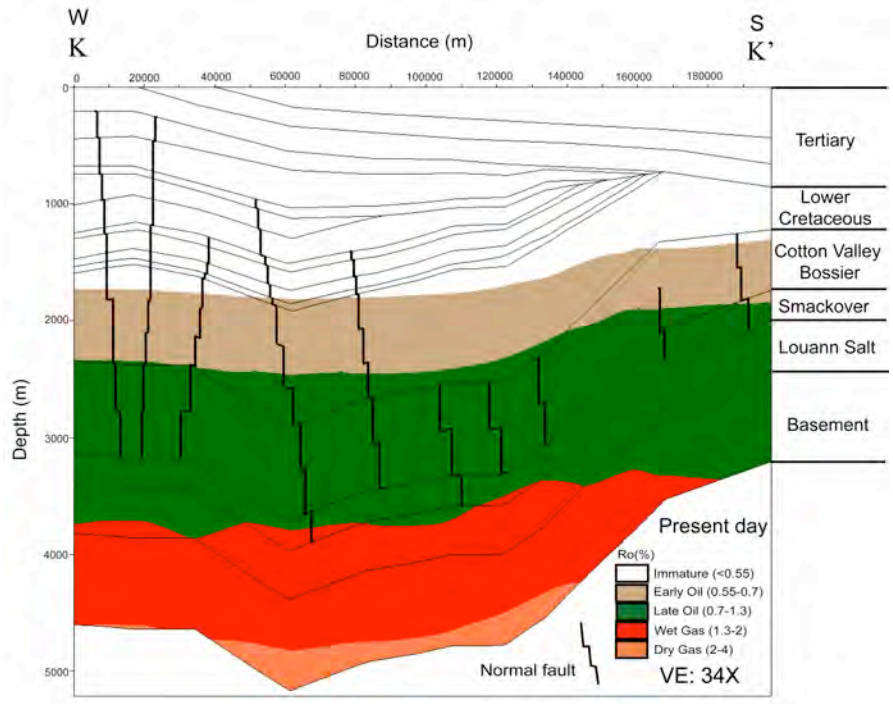


Figure 363. Cross section K-K' showing no gas expulsion to date from Bossier in the northern part of the North Louisiana Salt Basin. See Figure 2 for location of cross section.

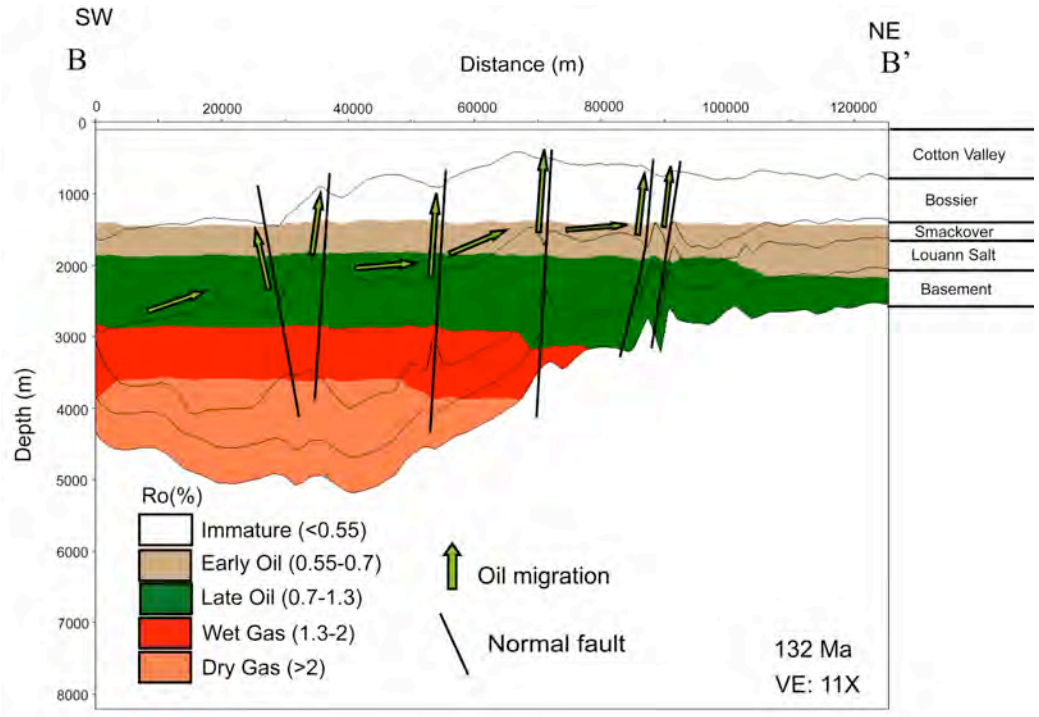


Figure 364. Seismic cross section B-B' showing potential onset of oil expulsion from the Bossier in the North Louisiana Salt Basin. See Figure 1 for location of cross section.

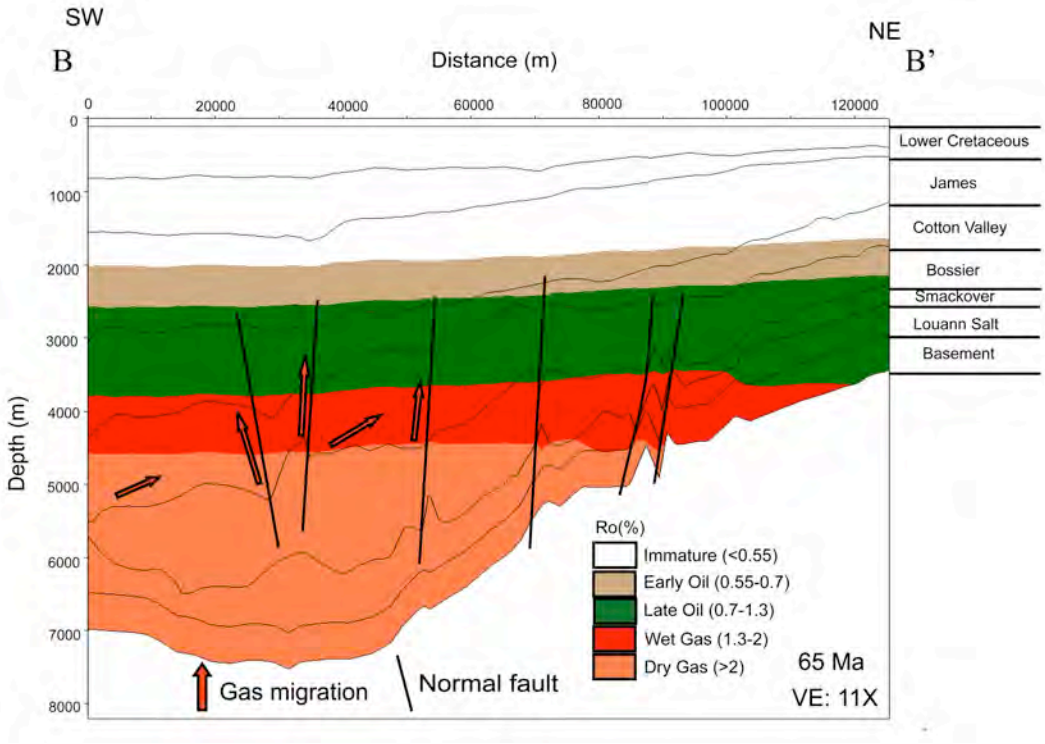


Figure 365. Seismic cross section B-B' showing potential onset of oil expulsion from the Bossier in the North Louisiana Salt Basin. See Figure 1 for location of cross section.

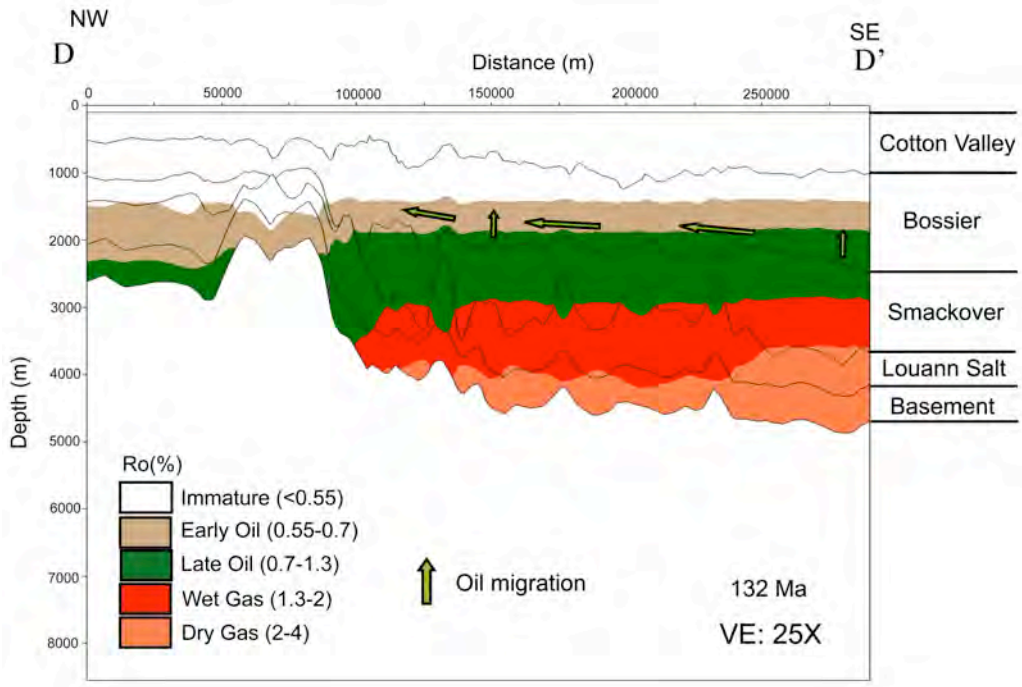


Figure 366. Seismic cross section D-D' showing potential onset of oil expulsion from the Bossier in the southern part of the North Louisiana Salt Basin. See Figure 1 for location of cross section.

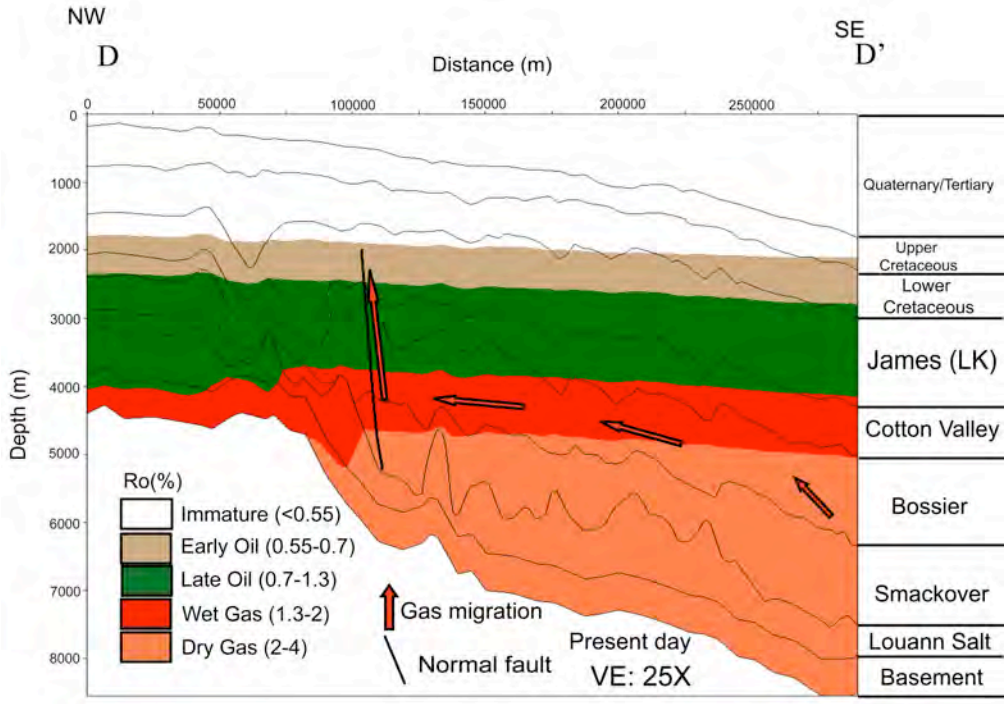


Figure 367. Seismic cross section D-D' showing potential peak gas expulsion from the Bossier in the southern part of the North Louisiana Salt Basin. See Figure 1 for location of cross section.

of secondary, non-associated thermogenic gas is generated from source beds in the southern part of the basin (Mancini et al., 2008). This modeling supports the conclusion of Zimmerman and Sassen (1993) that vertical as well as lateral migration is important in the North Louisiana Salt Basin.

### *Refined Resource Reservoir Assessment*

The refined assessment of the undiscovered and underdeveloped reservoirs based on basin analysis and petroleum system characterization and modeling indicates that the potential undiscovered reservoirs in the North Louisiana Salt Basin are subsalt Triassic Eagle Mills sandstone and deeply buried Upper Jurassic to Lower Cretaceous sandstone, shale, and limestone. Potential underdeveloped reservoirs include Lower Cretaceous sandstone and limestone and Upper Cretaceous sandstone. The potential Upper Cretaceous sandstone reservoirs are transgressive backstepping facies associated with a transgressive-regressive sequence (Fig. 328). These facies onlap onto the Monroe Uplift, resulting in a combination structural and stratigraphic trap (Figs. 11-13 and 331).

### *Technology Transfer*

Several presentations on the results of this work have been made at the annual meetings of the American Association of Petroleum Geologists and Gulf Coast Association of Geological Societies by Mancini, Li, Goddard, and Barnaby. Technology transfer workshops have been conducted in Shreveport, Louisiana; Jackson, Mississippi; and Tuscaloosa, Alabama and a fourth workshop is planned for Shreveport in September. Research results from this project have been published in the Bulletin of the American Association of Petroleum Geologists (1 paper by Mancini et al., 2008) and in the Transactions of the Gulf Coast Association of Geological Societies (5 papers-1 by

Mancini et al., 2005, 2 by Li, 2006, 1 by Barnaby, 2006, and 1 by Goddard et al. 2008, in press). These papers are as follows:

Barnaby, R., 2006, Modeling of the burial and thermal history, organic maturation, and oil expulsion of the North Louisiana petroleum system, Gulf Coast Association of Geological Societies Trans. 56: 23-25.

Goddard, D.A, Mancini, E.A., Horn, M.R., and Talukdar, S.C., 2008, Hydrocarbon generating potential: Jurassic Cotton Valley-Bossier Group, North Louisiana Salt Basin, Gulf Coast Association of Geological Societies Trans. 58 (in press).

Li, P., 2006a, Modeling of thermal maturity history of strata in the North Louisiana Salt Basin area, Gulf Coast Association of Geological Societies Trans. 56: 439-454.

Li, P., 2006b, Reconstruction of burial history of strata in the North Louisiana Salt Basin area, Gulf Coast Association of Geological Societies Trans. 56: 455-472.

Mancini, E.A., Li, P., Goddard, D.A., and Zimmerman, R.K., 2005, Petroleum source rocks of the onshore interior salt basins, north central and northeastern Gulf of Mexico, Gulf Coast Association of Geological Societies Trans. 55:486-504.

Mancini, E.A., Li., P., Ramirez, V.O., Goddard, D.A., and Talukdar, S.C., 2008, Mesozoic (Upper Jurassic-Lower Cretaceous) deep gas reservoir play, central and eastern Gulf Coastal Plain, USA, Am. Assoc. Petroleum Geologists Bull. 92:283-308.

## Work Planned

A technology transfer workshop is scheduled for Shreveport, Louisiana for September 25, 2008 on the final results of the project, including the Smackover and Bossier petroleum systems.

## RESULTS AND DISCUSSION

### Geologic History

The geologic history of the North Louisiana Salt Basin is directly linked to the evolution of the Gulf of Mexico basin (Wood and Walper, 1974). The Gulf of Mexico is a divergent margin basin dominated by extensional tectonics and wrench faulting (Pilger, 1981; Miller, 1982; Klitgord et al., 1984; Van Siclen, 1984; Pindell, 1985; Salvador, 1987; Winker and Buffler, 1988; Buffler, 1991). The origin of the Gulf of Mexico basin consists of phases of crustal extension and thinning, of rifting and sea-floor spreading, and of thermal subsidence (Nunn, 1984).

Sawyer et al. (1991) proposed the following as a model for the evolution of the Gulf of Mexico and related onshore interior salt basins based on the distribution of crust type. A Late Triassic-Early Jurassic early rifting phase is typified by half-grabens bounded by listric normal faults and filled with nonmarine red bed sediments and volcanics. A Middle Jurassic phase of rifting, crustal attenuation and the formation of transitional crust is characterized by a pattern of alternating basement paleotopographic highs and lows and the accumulation of thick salt deposits. A Late Jurassic phase of sea-floor spreading and oceanic crust formation is typified by an extensive marine transgression as a result of crustal cooling and subsidence. Subsidence continued into the Early Cretaceous and a carbonate shelf margin developed along the tectonic hinge zone of differential subsidence between thick transitional crust and thin transitional crust.

This depositional pattern was interrupted by a time of igneous activity and global sea-level fall during the Late Cretaceous (mid-Cenomanian) that produced a major drop in sea level and resulted in the exposure of the shallow Cretaceous platform margin that

rimmed the Gulf (Salvador, 1991a). This mid-Cenomanian unconformity is well developed in the North Louisiana Salt Basin.

The Mesozoic and Cenozoic sediments of the northern Gulf of Mexico accumulated as a seaward-dipping wedge in differentially subsiding basins (Martin, 1978). Basement cooling and subsidence resulted in an infilling of the accommodation space. Structural elements that affected the deposition of these sediments included basement features associated with plate movement and features formed due to the movement of Jurassic salt. The graben system that developed is a result of rifting, and its geometry is a reflection of the direction of plate separation (MacRae and Watkins, 1996). The Lower Cretaceous shelf margin corresponds to a major basement hinge. This feature dominated carbonate deposition throughout the Early Cretaceous.

The chief positive basement features that influenced the distribution and nature of Mesozoic deposits in the onshore central Gulf Coastal Plain area are the Sabine Uplift and Monroe Uplift. Paleotopography had a significant impact on the distribution of sediment, and positive areas within basins and along basin margins provided sources for Mesozoic terrigenous sediments (Mancini et al., 1985a). The North Louisiana Salt Basin, which is a major negative structural feature, is classified as the interior fracture portion of a margin sag basin using the classification of Kingston et al. (1983). This extensional basin was associated with early rifting linked with wrench faulting and was actively subsiding depocenters throughout the Mesozoic and into the Cenozoic.

Movement of the Jurassic Louann Salt has produced an array of structural features (Martin, 1978). Salt-related structures include diapirs, articlines, and extensional fault and half graben systems. Structural features resulting from halokinesis include the regional

peripheral fault trend and numerous salt domes and anticlines. The regional peripheral fault trend consists of a series of en echelon extensional faults and half grabens that are associated with salt movement. Structural deformation related to salt movement was initiated probably during the Late Jurassic (Dobson and Buffler, 1997).

Sedimentation in the northern Gulf of Mexico was associated with rifted continental margin tectonics. Syn-rift Triassic graben-fill red-beds of the Eagle Mills Formation were deposited locally as the oldest Mesozoic strata above pre-rift Paleozoic basement during the early stages of extension and rifting (Tolson et al., 1983; Dobson, 1990).

The syn-rift Middle Jurassic Werner Formation and Louann Salt are evaporite deposits that formed during the initial transgression of marine water into the Gulf of Mexico (Salvador, 1987). Basement structure influenced the distribution and thickness of Louann Salt, resulting in thick salt in the interior salt basins, and salt being absent over basement paleohighs (Wilson, 1975; Cagle and Khan 1983, Dobson, 1990; Dobson and Buffler, 1991). The updip limit of thick salt and the location of the extensional faults associated with the regional peripheral fault trend coincide with a basement hinge line and occur in the northern part of these salt basins and subbasins (Mancini and Benson, 1980; Dobson, 1990; Dobson and Buffler, 1991).

The distribution of the Late Jurassic post-rift deposits of the Norphlet, Smackover, Haynesville and Cotton Valley have been affected by basement paleotopography (Mancini and Benson, 1980; Dobson, 1990; Dobson and Buffler, 1991). The Norphlet Formation consists of alluvial fan and plain, fluvial and wadi, eolian sheet, dune and interdune and marine shoreface siliciclastic sediments (Mancini et al., 1985b; Dobson,

1990). The Smackover Formation, which was deposited on a ramp surface during the major Jurassic marine transgression in the Gulf, includes intertidal to subtidal laminated and microbial lime mudstone, subtidal peloidal wackestone and packstone, subtidal microbial boundstone, and subtidal to intertidal peloidal, ooid, oncoidal packstone and grainstone interbedded with fenestral lime mudstone (Mancini and Benson, 1980; Benson, 1988; Dobson, 1990). This transgression has been attributed to emplacement of oceanic crust in the Gulf and the resulting thermal subsidence due to crustal cooling (Nunn, 1984; Winker and Buffler, 1988). The Haynesville Formation consists of subaqueous to subaerial anhydrite, shelf to shoreline limestone, shale, and sandstone and eolian, fluvial, and alluvial sandstone (Tolson et al., 1983, Mann, 1988; Mancini et al., 1997). The Cotton Valley Group includes fluvial-deltaic and delta destructive sandstone and shale (Moore, 1983; Tolson, et al., 1983; Dobson, 1990). Deposition of the Early Cretaceous Knowles Limestone has been interpreted as the precursor to the development of the Lower Cretaceous carbonate shelf margin (Dobson, 1990).

The Early Cretaceous in the northern Gulf of Mexico consists of fluvial-deltaic to coastal siliciclastic sedimentation updip and the development of a broad carbonate shelf with a low-relief margin downdip at the boundary between thick transitional crust and thin transitional crust (Eaves, 1976; Winker and Buffler, 1988; McFarlan and Menes, 1991; Sawyer et al., 1991). The development of a carbonate shelf margin during the Early Cretaceous, which does not conform to the basement structure, is the result of a combination of a change in the slope of the basement that is marked by a crustal hinge zone and Jurassic sediment depositional patterns (Dobson, 1990; Sawyer et al., 1991). The hinge zone has formed as a result of differential subsidence across the crustal

boundary between thick transitional crust and thin transitional crust (Corso, 1987). Although Jurassic Norphlet, Smackover and Haynesville depositional patterns are greatly affected by basement paleotopography, sediments, such as the Lower Cretaceous Knowles Limestone, reflect an infilling of the basement low areas and a general progradation of the ramp margin (Dobson, 1990). This progradation has been interpreted by Dobson (1990) to produce a change from a carbonate ramp to a rimmed platform margin. The hiatus between the Cotton Valley Group-Knowles Limestone and the Hosston Formation is represented by most of the Valanginian Stage. This unconformity and hiatus are recognized throughout the Gulf Coast (McFarlan and Menes, 1991).

The Lower Cretaceous shelf margin was exposed during the early Late Cretaceous by a major lowering of sea level. This sea-level fall has been attributed to a combination of igneous activity and global sea-level fall (Salvador, 1991a). A Late Cretaceous marine transgression followed this regional erosional event, and this transgression in combination with the Laramide orogeny affected deposition from the Late Cretaceous to the Cenozoic (Salvador, 1991a). Throughout the Cenozoic, the western Gulf was the site of significant fluvial, deltaic and coastline siliciclastic sediment influx, while the eastern Gulf experienced principally carbonate deposition (Salvador, 1991a).

## Petroleum Systems

Three active petroleum source rocks have been reported from the onshore north central and northeastern Gulf of Mexico area. The Upper Jurassic (Oxfordian) Smackover lime mudstone beds have been described as serving as source rocks in the North Louisiana Salt Basin (Sassen et al., 1987). The Upper Cretaceous (Cenomanian-Turonian) Tuscaloosa marine shale beds have been reported as serving as source rocks in

Mississippi (Koons et al., 1974). The Lower Cretaceous (Albian) Sunniland lime mudstone beds have been described as serving as source rocks in south Florida (Palacas, 1978; Palacas et al., 1984). In addition, Sassen (1990) reported that lower Tertiary (Paleocene/Eocene) Midway, Wilcox, and Sparta shale beds are source rocks in southern Louisiana and that Paleocene/Eocene Wilcox lignite beds may be a petroleum source in southwestern Mississippi. Upper Jurassic (Tithonian) shale and carbonate beds are source rocks in Mexico (Mancini et al., 2001), and Upper Jurassic (Tithonian) to Lower Cretaceous (Berriasian) Bossier shale beds have been reported as source rocks in the East Texas Salt Basin (Ridgley et al., 2006).

From source rock and oil characterization studies and from burial and thermal maturation history modeling, Claypool and Mancini (1989), Mancini et al., (1999), and the results from this work, have shown that the Paleocene/Eocene shale and lignite beds have not been subjected to favorable burial and thermal maturation histories required for petroleum generation in the North Louisiana Salt Basin or Mississippi Interior Salt Basin. The Upper Cretaceous Tuscaloosa marine shale beds were an effective local petroleum source rock in parts of the Mississippi Interior Salt Basin but not in the North Louisiana Salt Basin. The uppermost Jurassic strata and the Lower Cretaceous lime mudstone and shale beds are possible source beds in parts of the North Louisiana Salt Basin and Mississippi Interior Salt Basin given the proper organic facies.

Based on this assessment of potential petroleum source rocks the Upper Jurassic Smackover lime mudstone beds were determined to be the principal petroleum source rock. Further, organic geochemical analyses, including $C_{15+}$ chromatograms and biomarker data of the oils produced from Upper Jurassic, Lower Cretaceous and Upper

Cretaceous reservoirs have shown that the oils produced from the Upper Jurassic, Lower Cretaceous and many of the Upper Cretaceous reservoirs were generated from organic matter that accumulated and was preserved in association with the Smackover lime mudstone beds (Koons et al., 1974; Claypool and Mancini, 1989; Mancini et al., 2001).

The organic rich and laminated Smackover lime mudstone beds are the petroleum source rocks for most of the oils (Oehler, 1984; Sassen et al., 1987; Claypool and Mancini, 1989; Mancini et al., 2003). Organic geochemical analyses of the Smackover source beds and of the oils indicate that the Jurassic oils and many of the Cretaceous oils originated from the organic matter associated with the Smackover lime mudstone beds.

Smackover samples from the lower and middle lime mudstone beds average 0.81% total organic carbon according to Claypool and Mancini (1989). Organic carbon contents of up to 1.54% for the North Louisiana Salt Basin and 9.30% for the Mississippi Interior Salt Basin have been reported by Sassen et al. (1987) and Sassen and Moore (1988). Because much of the Smackover has experienced advanced levels of thermal maturity, the total organic carbon values were higher in the past prior to the generation of crude oil (Sassen and Moore 1988).

The dominant kerogen types in the Smackover are algal (microbial) and microbial-derived amorphous (Oehler 1984; Sassen et al. 1987; Claypool and Mancini, 1989). In updip areas near the paleoshoreline, the Smackover includes herbaceous and woody kerogen (Wade et al. 1987). The dominant kerogen types in the North Louisiana Salt Basin are amorphous (microbial) and herbaceous. In the center areas of basins, Smackover samples exhibit thermal alteration indices of 2 to 4 (Oehler 1984; Sassen et al. 1987; Claypool and Mancini, 1989). These values represent an equivalent vitrinite

reflectance (Ro) of 0.55 to 4.0% (Sassen and Moore 1988). The thermal alteration indices for the North Louisiana Salt Basin are chiefly in the 3 range.

The generation of crude oil from the source rocks in the North Louisiana Salt Basin and Mississippi Interior Salt Basin has been interpreted to have been initiated at a level of thermal maturity of 0.55% Ro (435°C $T_{max}$; 2 TAI) and concluded at a level of thermal maturity of 1.5% Ro (470°C $T_{max}$; 3 TAI) (Nunn and Sassen 1986; Sassen and Moore 1988). This requires a depth of burial of 9,840 ft according to Driskill et al. (1988). Nunn and Sassen (1986) reported that the generation of crude oil was initiated at a depth of 11,500 ft. The generation of crude oil was determined to have been initiated from basinal Smackover lime mudstone beds in the Early Cretaceous, and the generation and migration of low to intermediate gravity crude oil is interpreted to have continued into Cenozoic time (Nunn and Sassen 1986; Driskill et al. 1988; Sassen and Moore 1988). Updip Smackover lime mudstone beds have been reported to have generated low gravity crude oil beginning in the Late Cretaceous or 20 my later than the basinal lime mudstone (Driskill et al. 1988). At a depth of burial of 16,400 to 19,700 ft, the basinal Smackover lime mudstone beds were determined to be over-mature for the generation of crude oil (Nunn and Sassen 1986; Driskill et al. 1988). The low to intermediate gravity crude oils that migrated into reservoirs were subjected to thermal cracking with increasing depth of burial and time (Sassen and Moore 1988; Claypool and Mancini 1989).

From burial history and thermal maturation history profiles for wells in the North Louisiana Salt Basin, hydrocarbon generation and maturation trends can be observed. In wells in much of the North Louisiana Salt Basin, the generation of hydrocarbons from Smackover lime mudstone was initiated at 6,000 to 8,500 ft during the Early Cretaceous

from the southern part of the basin and continued into the Tertiary. Present-day total organic carbon contents average 0.58% with original total organic contents probably averaging approximately 1%.

Hydrocarbon expulsion and migration from Smackover source rocks in the North Louisiana Salt Basin commenced during the Early Cretaceous and continued into the Tertiary with peak expulsion mainly in the Early to Late Cretaceous. The hydrocarbon expulsion profiles for the wells are in agreement with the thermal maturation profiles. The timing of commencement of oil expulsion is consistent with the tectonic, depositional, burial and thermal histories of the basin. Hydrocarbon flow pathway modeling supports an intermediate range migration process for Smackover crude oil. Smackover hydrocarbon migration into overlying strata was facilitated by vertical migration along faults. Evans (1987), Sassen (1990) and Zimmerman and Sassen (1993) also published information in support of combined intermediate range and vertical hydrocarbon migration in this area. Smackover hydrocarbons migrated into Upper Jurassic, Cretaceous, and lower Tertiary sandstone and carbonate reservoirs. Upper Jurassic and Lower Cretaceous anhydrite and shale, Upper Cretaceous chalk and shale, and lower Tertiary shale acted as effective petroleum seal rocks.

Hydrocarbons, mainly thermogenic gas, were generated from Upper Jurassic to Lower Cretaceous Bossier shale beds. The Type III kerogen in these beds is gas prone, and the total organic carbon content in this shale is low. These factors resulted in a saturation threshold that was not adequate to promote expulsion. Therefore, most of the gas generated probably was retained in the Bossier making this formation a potential gas shale reservoir.

## Comparative Basin Analysis

The origins of the North Louisiana and Mississippi Interior Salt Basins are comparable in that the geohistory of these basins is directly linked to the evolution of the Gulf of Mexico. These basins, which are major negative structural features, are classified as the interior fracture portion of a margin sag basin of Kingston et al. (1983). The timing of tectonic events and the nature of the structural styles control the type and size of petroleum traps formed and the volume of hydrocarbons contained within these traps. Halokinesis of Jurassic Louann Salt has produced a complex of structural features. The dominant structural styles are salt-supported anticlines, normal faults, and combination structural and stratigraphic features. Salt-supported anticlinal and domal structures include low-relief salt pillows, turtle structures, and deep and shallow piercement domes. Normal faulting is associated with the northern basin margin and listric down-to-the-basin faults (state-line fault complex) and faulted salt features. Combination structural and stratigraphic features include large regional domal structures, such as the Sabine and Monroe Uplifts.

The main difference in the geohistories of the North Louisiana and the Mississippi Interior Salt Basins is the elevated heat flow the strata in the North Louisiana Salt Basin experienced in the Cretaceous due primarily to the reactivation of upward movement, igneous activity, and erosion associated with the Monroe and Sabine Uplifts. The Jackson Dome in the Mississippi Interior Salt Basin is a similar phenomenon, but the effects of this igneous intrusion are on a much lower level geographically.

## Reservoir Assessment

Comparison of the geohistory and production history of the North Louisiana Salt Basin to those of the Mississippi Interior Salt Basin indicates that potential undiscovered and underdeveloped reservoirs are present in the North Louisiana Salt Basin. From an assessment of the undiscovered and underdeveloped reservoirs of the Mississippi Interior Salt Basin by Mancini et al. (2000), the Norphlet, Smackover, Haynesville, Cotton Valley, Hosston/Sligo, Rodessa/Mooringsport/Paluxy, Dantzler/Andrew/Fredericksburg-Washita, Tuscaloosa and Eutaw reservoirs were characterized as being productive throughout most of this basin. Reservoirs with a limited areal extent of production included the Selma Chalk, Wilcox sandstone, and James Limestone. Potential reservoirs in this basin were identified as subsalt Triassic Eagle Mills sandstone and Lower Cretaceous carbonates. Lower Cretaceous Hosston/Sligo, Rodessa/Mooringsport/Paluxy, and Dantzler/Fredericksburg-Washita sandstone facies and Upper Cretaceous Tuscaloosa and Eutaw sandstone facies were determined to be underdeveloped reservoirs having high potential for hydrocarbon productivity.

In the North Louisiana Salt Basin, the subsalt Triassic Eagle Mills sandstone and deeply buried Upper Jurassic sandstone, shale, and limestone facies of the Smackover, Haynesville, Bossier, and Cotton Valley are identified as potential undiscovered reservoirs. Upper Jurassic units account for 20% of the current oil production and 38% of the current gas production in the Mississippi Interior Salt Basin. The depositional and diagenetic histories of these strata in the North Louisiana Salt Basin are interpreted to be similar to those in the Mississippi Interior Salt Basin. These units currently account for some 10% of the oil production and some 10% of the gas production in the North

Louisiana Salt Basin. Potential underdeveloped reservoirs include Lower Cretaceous sandstone facies (Hosston, Paluxy) and limestone facies (Sligo, James, Rodessa, Mooringsport, and Fredericksburg) and Upper Cretaceous sandstone facies of the Austin (Tokio), Taylor (Ozan), and Navarro (Nacatoch) Groups.

## Exploration Strategies

Knowledge of the geohistory of the North Louisiana and Mississippi Interior Salt Basins and an understanding of the concepts of sequence stratigraphy (transgressive-regressive sequences) in association with information regarding lithofacies associations, diagenesis, and petroleum systems facilitates the design of new exploration strategies for these basins. For example, in the North Louisiana Salt Basin, secondary, non-associated thermogenic gas is expected to be preserved in Upper Jurassic and Lower Cretaceous deeply buried transgressive and regressive reservoirs. These potential reservoirs include Cotton Valley and Hosston sandstone facies, Bossier shale facies, and Smackover and Sligo carbonate facies at depths greater than 20,000 ft (Mancini et al., 2006, 2008). Porosity is predicted at this depth and to consist of a combination of depositional and diagenetic (fracture) types in Cotton Valley and Hosston shallow nearshore and deep marine sandstone facies. Porosity is predicted to be mainly diagenetic (vuggy and fracture) in Smackover and Sligo carbonate nearshore, marine shelf, ramp, and reef facies.

In addition, the knowledge of the geohistory of the North Louisiana Salt Basin and the use of transgressive-regressive sequences, as recognized in well log signatures and seismic reflection profiles, is of assistance in targeting combination structural and stratigraphic traps and specific reservoir facies in a transgressive-regressive sequence.

For example, Upper Cretaceous sandstone reservoirs are recognized as transgressive backstepping facies in transgressive-regressive sequences that onlap onto the Monroe Uplift that serves as a combination structural and stratigraphic trap. Also, an understanding of the Bossier petroleum system has resulted in the identification of the Bossier as a potential undiscovered shale gas reservoir in the North Louisiana Salt Basin.

## CONCLUSIONS

The principal research efforts of the project have been the determination of the tectonic, depositional, burial and thermal maturation histories of the North Louisiana Salt Basin, basin modeling (geohistory, thermal maturation, hydrocarbon expulsion, hydrocarbon flow pathway), petroleum system study (identification, characterization, modeling), comparative basin evaluation, and assessment of the undiscovered and underdeveloped reservoirs in the North Louisiana Salt Basin.

Existing information, including 2-D seismic sections, on the North Louisiana Salt Basin has been evaluated and an electronic database has been developed. Regional cross sections have been prepared. Structure, isopach, and formation lithology maps have been constructed on key surfaces and of key intervals, respectively. Seismic data, well logs, cross sections, subsurface maps and burial history, thermal maturation history and hydrocarbon expulsion profiles have been used in evaluating the tectonic history, depositional history, burial history and thermal maturation history of the basin.

The origin of the North Louisiana Salt Basin is comparable to the origin of the Mississippi Interior Salt Basin. The geohistory of these basins is directly linked to the evolution of the Gulf of Mexico. The timing of tectonic events and the nature of the structural styles control the type and size of petroleum traps formed and the volume of

hydrocarbons contained within these traps. The dominant structural styles are salt-supported anticlines, normal faults, and combination structural-stratigraphic features. Combination structural-stratigraphic features include large regional domal structures, such as the Sabine and Monroe Uplifts.

The main difference in the geohistories of the North Louisiana Salt Basin and the Mississippi Interior Salt Basin is the elevated heat flow the strata in the North Louisiana Salt Basin experienced in the Cretaceous due primarily to reactivation upward movement, igneous activity, and erosion associated with the Monroe and Sabine Uplifts. The Jackson Dome in the Mississippi Interior Salt Basin is a similar phenomenon, but the effects of this igneous intrusion are on a much lower level geographically.

The Upper Jurassic Smackover petroleum system is the principal petroleum system in these basins. The underburden, source, overburden, reservoir, and seal rocks associated with this petroleum system are a result of the rift-related geohistory. The generation of oil and gas from Smackover lime mudstone was initiated during the Early Cretaceous in the southern part of the basins and continued into the Tertiary. Hydrocarbon expulsion and migration commenced during the Early Cretaceous and continued into the Tertiary. Vertical and lateral migration is important to the productivity of these basins. In the North Louisiana Salt Basin, petroleum reservoirs include continental, coastal, and marine sandstone facies and nearshore marine, shelf, ramp, and reef carbonate facies. Seal rocks include Upper Jurassic and Lower Cretaceous anhydrite and shale, Upper Cretaceous chalk and shale, and lower Tertiary shale.

The Upper Jurassic to Lower Cretaceous Bossier petroleum system had the potential to generate gas from thermally mature shale containing Type III kerogen giving the Bossier high potential as a shale gas reservoir in the North Louisiana Salt Basin.

Potential undiscovered reservoirs in the North Louisiana Salt Basin are subsalt Triassic Eagle Mills sandstone and Upper Jurassic to Lower Cretaceous sandstone, shale, and limestone. Potential underdeveloped reservoirs include Lower Cretaceous sandstone and limestone and Upper Cretaceous sandstone.

Knowledge of basin geohistory and of the concepts of sequence stratigraphy and petroleum systems facilitates the design of new exploration strategies for the targeting of combination structural and stratigraphic traps and specific reservoir facies in a transgressive-regressive sequence. In the North Louisiana Salt Basin, Upper Cretaceous sandstone reservoirs are recognized as transgressive backstepping facies in transgressive-regressive sequences that onlap onto the Monroe Uplift that serves as a combination structural and stratigraphic trap, thermogenic gas is predicted to occur in Upper Jurassic to Lower Cretaceous transgressive and regressive deeply buried (>20,000 ft) porous sandstone and carbonate facies, and the Bossier Formation is identified as a potential shale gas reservoir as a result of petroleum system study.

## REFERENCES

Adams, G.S., 1985, Depositional history and diagenesis of the middle Glen Rose reef complex (lower Cretaceous), east Texas and Louisiana: Unpublished Master's Thesis, Louisiana State University, 200 p.

Alexander, C.I., 1935, Stratigraphy of Midway Group (Eocene) of southwest Arkansas and northwest Louisiana: AAPG Bulletin, v. 19, no. 5, p. 696-699.

Andersen, H.V., 1960, Geology of Sabine Parish, Louisiana Geological Survey, Geological Bulletin No. 34, 164 p.

Andersen, H.V., 1993, Geology of Natchitoches Parish: Louisiana Geological Survey, Geological Bulletin No. 44, 227 p.

Andrews, D.I., 1960, The Louann Salt and its relationship to Gulf Coast salt domes: GCAGS Trans., v. 10, p. 215-240.

Bailey, J., 1978, Black Lake Field Natchitoches Parish, Louisiana: a review, GCAGS Trans., v. 28, p. 11-24.

Baria, L.R., 1981, Waveland field: an analysis of facies, diagenesis, and hydrodynamics in the Mooringsport reservoirs: GCAGS Trans., v. 31, p. 19-30.

Benson, D.J., 1988, Depositional history of the Smackover Formation in Southwest Alabama: GCAGS Trans., v. 48, p. 197-205.

Bearden, B.L., Mancini, E.A., and Puckett, T.M., 2000, Salt anticline play in the Mississippi Interior Salt Basin: GCAGS Trans., v. 50, p. 261-268.

Bebout, D.G., and Garrett, C.M., et al., 1992, Upper Cretaceous Gas Rock—Louisiana and Mississippi: Atlas of Major Central and Eastern Gulf Coast Gas Reservoirs, Bureau of Economic Geology, University of Texas, p. 51.

Beckman, M.W., and Bloomer, P.A., 1953, Athens Field, Claiborne Parish, Louisiana: Shreveport Geological Society; Reference Report on Certain Oil and Gas Fields of North Louisiana, South Arkansas, Mississippi and Alabama, v. III, no. 2, p. 41-53.

Bishop, W.F., 1967, Age of pre-Smackover Formations, North Louisiana and South Arkansas: AAPG Bulletin v. 51, p. 244-250.

Bishop, W.F., 1968, Petrology of upper Smackover Limestone in North Haynesville Field, Claiborne Parish, Louisiana: AAPG Bulletin, v. 52, no. 1, p. 92-128.

Bishop, W.F., 1971, Geology of Upper Member of Buckner Formation, Haynesville Field area, Claiborne Parish, Louisiana: AAPG Bulletin, v. 55, p. 566-580.

Breedlove, R.L., Jones, J.P., and Jackson, A.M., 1953, Ruston Field, Lincoln Parish, Louisiana: Shreveport Geological Society; Reference Report on Certain Oil and Gas Fields of North Louisiana, South Arkansas, Mississippi and Alabama, v. III, no. 2, p. 87-94.

Breedlove, R.L, and Ogden, R.H., 1955, A study of the Crain trend of the Pettet Formation in the Bethany area of Texas and Louisiana: GCAGS Trans., v. 5, p. 221.

Buffler, R.T., 1991, Early evolution of the Gulf of Mexico basin, *in* D. Goldthwaite, ed., An Introduction to Central Gulf Coast geology, New Orleans, New Orleans Geological Society, p. 1-15.

Buffler, R.T., and Sawyer, D.S., 1985, Distribution of crust and early history, Gulf of Mexico basin: GCAGS Trans., v. 35, p. 333-344.

Cagle, J.W., and Khan, M.A., 1983, Smackover-Norphlet stratigraphy, South Wiggins Arch, Mississippi and Alabama: GCAGS Trans., v. 33, p. 23-29.

Cameron, L.G., 1963, Pendleton—Many—Ft. Jesup Field, Sabine Parish Louisiana: Shreveport Geological Society; Report on Selected North Louisiana and South Arkansas Oil and Gas Fields, v. V, p. 160-176.

Chapman, J.J., 1963, Deeper oil possibilities of South Arkansas and North Louisiana: AAPG Bulletin, v. 47, p. 1992-1996.

Claypool, G.E., and E.A. Mancini, 1989, Geochemical relationships of petroleum in Mesozoic reservoirs to carbonate source rocks of Jurassic Smackover Formation, southwestern Alabama, AAPG Bulletin, v. 73, p. 904-924.

Coleman, J.L., and Coleman, C.J. 1981, Stratigraphic, sedimentologic and diagenetic framework of the Jurassic Cotton Valley Terryville massive sandstone complex, North Louisiana: GCAGS Trans., v. 31, p. 71-80.

Collins, S.E., 1980, Jurassic Cotton Valley and Smackover reservoir trends, East Texas, North Louisiana, and South Arkansas: AAPG Bulletin, v. 64, p. 1004-1013.

Corso, W., 1987, Development of the Early Cretaceous northwest Florida carbonate platform: Unpublished Ph. D. dissertation, University of Texas, 136 p.

Crider, A.F., 1938, Geology of Bellevue oil field, Bossier Parish, Louisiana: AAPG Bulletin, v. 22, p. 1658-1681.

Crump, J.H., 1953, Hico Field, Lincoln Parish: Shreveport Geological Society; Reference Report on Certain Oil and Gas Fields of North Louisiana, South Arkansas, Mississippi and Alabama, v. III, p. 75-81.

Cullom, T., Granata, W., Gayer, S., Heffner, R., Pike, S., Hermann, L., Meyertons, C., and Sigler, G., 1962, The basin frontiers and limits for exploration in the Cretaceous System of central Louisiana: GCAGS Trans., v. 12, p. 97-115.

Davies D.K., Williams, B.P., and Vessell, R.K., 1991, Reservoir models for meandering and straight fluvial channels; examples from the Travis Peak Formation: GCAGS Trans., v. 41, p. 152-174.

Daly, A.R., and J.D. Edman. 1987, Loss of organic carbon from source rocks during thermal maturation (abs.): AAPG Bulletin, v. 71, p. 456.

Dawson, W.C., and Callender, C.A., 1991, Petrography and diagenesis of Eagle Mills sandstones, subsurface—northeast Texas and southwest Arkansas: AAPG Bulletin, v. 75, p. 558.

Dickinson, K.A., 1968a, Upper Jurassic stratigraphy of some adjacent parts of Texas, Louisiana, and Arkansas: USGS Prof. Paper 594-E, 25 p.

Dickinson, K.A., 1968b, Petrology of Buckner Member of Haynesville Formation in adjacent parts of Texas, Louisiana, and Arkansas: Jour. Sed. Petrology, v. 38, p. 555-557.

Dickinson, K.A., 1969, Upper Smackover carbonate rocks in northeastern Texas, and adjoining parts of Arkansas and Louisiana: GCAGS Trans., v. 19, p. 175-187.

Dobson, L.M., 1990, Seismic stratigraphy and geologic history of Jurassic rocks, northeastern Gulf of Mexico: Unpublished Master's Thesis, The University of Texas, Austin, 165 p.

Dobson, L.M., and R.T. Buffler, 1991, Basement rocks and structure, northeast Gulf of Mexico: AAPG Bulletin, v. 75, p. 1521.

Driskill, B.W., J.A. Nunn, R. Sassen, and R.H. Pilger, Jr., 1988, Tectonic subsidence, crustal thinning and petroleum generation in the Jurassic trend of Mississippi, Alabama and Florida: GCAGS Trans., v. 38, p. 257-265.

Dutton, S.P., Clift, S.J., Hamilton, D.S., Hamlin, H.S., and Hentz, T.F., 1993, Major low-permeability sandstone gas reservoirs in the continental United States: Bureau of Economic Geology, University of Texas/GRI Report of Investigations No. 211, 221 p.

Dutton, S.P, and Finley, R.J., 1988, Controls on reservoir quality in tight sandstones of the Travis Peak Formation, east Texas SPE Paper #15220.

Dutton, S.P., Laubach, S.E., Tye, R.S., Baumgardner, R.W., and Harrington, K.L., 1990, Geology of the Lower Cretaceous Travis Peak Formation, East Texas-depositional history, diagenesis, structure, and reservoir engineering implications: Bureau of Economic Geology, University of Texas/GRI Topical Report 90/0090, 170 p.

Eaves, E., 1976, Citronelle oil field, Mobile County, Alabama: AAPG Memoir 24, p. 259-275.

Echols, D.J., and Malkin, D., 1948, Wilcox (Eocene) stratigraphy, a key to production: AAPG Bulletin, v. 32, p. 11-33.

Echols, J.B., 1991, Sea level high stand shales and thin-stacked deltas, Paleocene Middle Wilcox of central Louisiana and Mississippi: GCAGS Trans., v. 41, p. 221-236.

Echols, J.B., and Goddard, D.A., 1992, Sea level fluctuations, Paleocene Middle Wilcox stratigraphy and hydrocarbon distribution in east-central Louisiana: GCAGS Trans., v. 42, p. 333-340.

Echols, J.B., and Goddard, D.A., 1993, Lower Wilcox reservoir characteristics: evidence for bypassed and subjacent hydrocarbon potential, east central Louisiana (abs): AAPG Bulletin, v. 77, no. 13, p. 96.

Evans, R., 1987, Pathways of migration of oil and gas in the south Mississippi Salt Basin: GCAGS Trans., v. 37, p. 75-76.

Eversull, L.G., 1985, Depositional systems and distribution of Cotton Valley blanket sandstones in northern Louisiana: GCAGS Trans., v. 35, p. 49-57.

Fisher, W.L., and McGowen, J.H., 1967, Depositional systems in the Wilcox Group of Texas and their relationship to occurrence of oil and gas: GCAGS Trans., v. 17, p. 105-125.

Forgotson, J.M., 1954, Regional stratigraphic analysis of Cotton Valley Group of Upper Gulf Coastal Plain: AAPG Bulletin, v. 38, p. 2476-2499.

Forgotson, J.M., 1957, Stratigraphy of Comanchean Cretaceous Trinity Group: AAPG Bulletin, v. 41, p. 2328-2363.

Forgotson, J.M., 1958, The basal sediments of the Austin Group and the stratigraphic position of the Tuscaloosa Formation of central Louisiana: GCAGS Trans., v. 8, p. 117-125.

Forgotson, J.M., 1963, Depositional history and paleotectonic framework of Comanchean Cretaceous Trinity Stage, Gulf Coast Area: AAPG Bulletin, v. 47, no. 1, p. 69-103.

Forgotson, J.M., Jr., and Forgotson, J.M., 1975, "Porosity pod": concept for successful stratigraphic exploration of fine-grained sandstones: AAPG Bulletin, v. 59, p. 1113-1125.

Forgotson, J.M., and Forgotson, J.M., Jr., 1976, Definition of Gilmer Limestone, Upper Jurassic formation, northeast Texas: AAPG Bulletin, v. 60, p. 1119-1123.

Frizzel, L.G., 1987, North Shongaloo—Red Rock Field, Hill Sand (Rodessa), Webster Parish, Louisiana: Shreveport Geological Society Report on Selected Oil and Gas Fields, ARK-LA-TEX and Mississippi, v. Vll, p. 80-84.

Galloway, W.E., 1968, Depositional systems of the Lower Wilcox Group, North-Central Gulf Coast Basin: GCAGS Trans., v. 18, p. 275-289.

Gamble, J.D., 1986, A study of the Jurassic sediments within a wildcat well, Madison Parish, Louisiana: Unpublished Master's Thesis, University of Southwestern Louisiana, 166 p.

Garner, N., Franks, C., and Livingston, J., 1987, Cotton Plant Field-Hosston, T13N-R2E, Caldwell Parish Louisiana: Shreveport Geol. Soc., Report on Selected Oil & Gas Fields, v. 7, p. 62-65.

Glawe, L.N., Young, L.M., and Roberts, H.H., 1999, Petrology, paleontology, and paleoenvironments of Wilds and Lower Nichols sands; Paleocene Wilcox units of Louisiana: GCAGS Trans., v. 49, p. 265-273.

Gorrod, H.M., 1980, Clear Branch Field-Hosston, T-14 & 15N, R-1 & 2W, Jackson Parish, Louisiana: Shreveport Geol. Soc., Report on Selected Oil & Gas Fields, v. 6, p. 58-62.

Granata, W.H., 1963, Cretaceous stratigraphy and structural development of the Sabine Uplift Area, Texas and Louisiana: Reference Report of the Shreveport Geological Society, v. 5, p. 50-96.

Hazzard, R.T., Spooner, W.C., and Blanpied, B.W., 1947, Notes on the stratigraphy of the formations which underlie the Smackover Limestone in south Arkansas, northeast Texas, and north Louisiana: Shreveport Geological Society 1945 Reference Report, v. 2, p. 483-503.

Herrmann, L.A., 1971, Lower Cretaceous Sligo reef trends in central Louisiana: GCAGS Trans., v. 21, p. 187-198.

Hermann, L.A., 1976, James Limestone in Winn and Natchitoches Parishes, Louisiana: AAPG Bulletin, v. 60, p. 1611.

Hermann, L.A., J.A. Lott, and R.E. Davenport, 1991, Ruston field-USA Gulf Coast Basin, Louisiana: AAPG Special Volume; Structural Traps V, p. 151-186.

Hughes, D.L., 1968, Salt tectonics as related to several Smackover fields along the northeast rim of the Gulf of Mexico basin: GCAGS Trans., v. 18, p. 320-330.

Imlay, R.W., 1942, Late Paleozoic age of Morehouse Formation of northeastern Louisiana: AAPG Bulletin, v. 29, p. 451-453.

Imlay, R.W., 1943, Jurassic formations of Gulf Region: AAPG Bulletin, v. 27, p. 1407-1533.

Johnson, O.H., Jr., 1961, The Monroe Uplift: GCAGS Trans., v. 8, p. 24-37.

Kidwell, A.L., 1951, Mesozoic igneous activity in the northern Gulf Coastal Plain: GCAGS Trans., v. 1, p. 182-199.

Kimball, C.E., Anderson, E.G., Sartin, A.A., and Young, L.M., 1989, Petrology and hydrocarbon potential of the Ferry Lake Anhydrite, Caddo Pine Island Field, Caddo Parish, Louisiana: GCAGS Trans., v. 39, p. 141-151.

Kingston, D.R., Dishroon, C.P., and Williams, P.A., 1983, Global basin classification system: AAPG Bull., v. 67, p. 2175-2193.

Klitgord, K.D., Popence, P., and Schouten, H., 1984, Florida: a Jurassic transform plate boundary: Jour. Geophysical Res., v. 89, p. 7753-7772.

Klitgord, K.D., and Schouten, H., 1980, Mesozoic evolution of the Atlantic, Caribbean, and Gulf of Mexico (abs.), *in* Pilger, R.H. Jr., ed., Proceedings of a Symposium, The origin of the Gulf of Mexico and the early opening of the Central North Atlantic Ocean: School of Geoscience, LSU, Baton Rouge, LA., p. 100-101.

Koons, C.B., J.G. Bond, and F.L. Peirce, 1974, Effects of depositional environment and postdepositional history on chemical composition of Lower Tuscaloosa oils: AAPG Bulletin, v. 58, p. 1272-1280.

Kornfeld, I.E., 1985, Depositional environments and hydrocarbon occurrence of Upper Jurassic Cotton Valley sandstones, Mississippi, Louisiana, and Texas**:** AAPG Bulletin, v. 69, p. 275.

Kupfer, D.A., Crowe, C.T., and Hessenbruch, J.M., 1976, North Louisiana Basin and salt movements (halokinetics): GCAGS Trans., v. 26, p. 94-110.

Lenert, H.A., and Kidda, M.K., 1958, Baskinton Field, Franklin Parish Louisiana: Shreveport Geological Society Reference Report of Certain Oil and Gas Fields, v. IV, p. 120-122.

Li, P., 2006, Modeling of thermal maturity history of strata in the North Louisiana Salt Basin area: GCAGS Trans., v. 56, p. 439-454.

Lobao, J.J., and Pilger, R.H., 1985, Early evolution of salt structures in the North Louisiana Salt Basin: GCAGS Trans., v. 35, p. 189-198.

Louisiana Geological Survey, 2000, Folio Series No. 8, stratigraphic charts of Louisiana.

Lowrie, A., Sullivan, N.M., Krotzer, C., Carter, J., Lerche, I., and Petersen, K., 1993, Tectonic and depositional model of the north Louisiana-south Arkansas basin: GCAGS Trans., v. 43, p. 231-238.

MacRae, G., and Watkins, J.S., 1996, Desoto Canyon Salt Basin: tectonic evolution and salts structural styles, *in* J.O. Jones, and R.L. Freed, eds., Structural Framework of the Northern Gulf of Mexico, A Special Publication of GCAGS, Austin, GCAGS, p. 53-61.

Mancini, E.A., M. Badali, T.M. Puckett, J.C. Llinas, and W.C. Parcell, 2001, Mesozoic carbonate petroleum systems in the northeastern Gulf of Mexico area, *in* Petroleum Systems of Deep-Water Basins: GCS-SEPM Foundation 21st Annual Research Conference, p. 423-451.

Mancini, E.A., and D.J. Benson, 1980, Regional stratigraphy of Upper Jurassic Smackover carbonates of southwest Alabama: GCAGS Trans., v. 30, p. 151-163.

Mancini, E.A., M.L. Epsman, and D.D. Stief, 1997, Characterization and evaluation of the Upper Jurassic Frisco City sandstone reservoir in southwestern Alabama utilizing Fullbore Formation MicroImager technology: GCAGS Trans., v. 47, p. 329-33.

Mancini, E.A., D.A. Goddard, R. Barnaby, and P. Aharon, 2006, Resource assessment of the in-place and potentially recoverable deep natural gas resource of the onshore interior salt basins, north central and northeastern Gulf of Mexico: U.S. Department of Energy Final Technical Report, Project Number DE-FC26-3NT41875, 173 p.

Mancini, E.A., P. Li, D.A. Goddard, V. Ramirez, and S.C. Talukdar, 2008, Mesozoic (Upper Jurassic-Lower Cretaceous) deep gas reservoir play, central and eastern Gulf coastal plain: AAPG Bulletin, v. 93, p. 283-308.

Mancini, E.A., P. Li, D.A. Goddard, and R.K. Zimmerman, 2005, Petroleum source rocks of the onshore interior salt basins, north central and northeastern Gulf of Mexico: GCAGS Trans., v. 55, 486-504.

Mancini, E.A., Mink, R.M., and Bearden, B.L., 1985a, Upper Jurassic Norphlet hydrocarbon potential along the regional peripheral fault trend in Mississippi, Alabama, and the Florida Panhandle: GCAGS Trans., v. 35, p. 225-232.

Mancini, E.A., Mink, R.M., Bearden, B.L., and Wilkerson, R.P., 1985b, Norphlet Formation (Upper Jurassic) of southwestern and offshore Alabama; environments of deposition and petroleum geology: AAPG Bull., v. 69, p. 881-898.

Mancini, E.A., Parcell, W.C., Puckett, T.M., and Benson, D.J., 2003, Upper Jurassic (Oxfordian) Smackover carbonate petroleum system characterization and modeling, Mississippi interior salt basin area, northeastern Gulf of Mexico, USA: Carbonates and Evaporites, v. 18, p. 125-150.

Mancini, E.A., Puckett, T.M., and Parcell, W.C., 1999, Modeling of the burial and thermal histories of strata in the Mississippi interior salt basin: GCAGS Trans., v. 49, p. 332-341.

Mancini, E.A., Puckett, T.M., Parcell, W.C., and Panetta, B., 1999, Basin analysis of the Mississippi interior salt basin and petroleum system modeling of the Jurassic Smackover Formation, Easter Gulf Coastal Plain; U.S. Department of Energy Topical Reports 1 and 2, Project DE-FG22-96BC14946, 425 p.

Mann, S.D., 1988, Subaqueous evaporites of the Buckner Member, Haynesville Formation, northeastern Mobile County, Alabama: GCAGS Trans., v. 38, p. 187-196.

Mann, C. J., and Thomas, W.A., 1964, Cotton Valley Group (Jurassic) nomenclature, Louisiana and Arkansas: GCAGS Trans., v. 14, p. 143-152.

Martin, R.G., 1978, Northern and eastern Gulf of Mexico continental margin: stratigraphic and structural framework: AAPG Studies in Geology, v. 7, p. 21-42.

McCulloh, R.P., and Eversull, L.G., 1986, Shale-filled channel system in the Wilcox Group (Paleocene-Eocene), north-central south Louisiana: GCAGS Trans., v. 36, p. 213-218.

McFarlan, E., Jr., and L.S. Menes, 1991, Lower Cretaceous, *in* A. Salvador, ed., The Gulf of Mexico Basin: Decade of North American Geology: Boulder, Geological Society of America, p. 181-204.

McNamee, D.F., 1969, The Glen Rose reef complex of east Texas and central Louisiana: GCAGS Trans., v. 19, p. 11-21.

Miller, J.A., 1982, Structural control of Jurassic sedimentation in Alabama and Florida: AAPG Bull., v. 66, p. 1289-1301.

Mink, R.M., Tew, B.H., Mann, S.D., Bearden, B.L., and Mancini, E.A., 1990, Norphlet and pre-Norphlet geologic framework of Alabama and panhandle Florida coastal waters area and adjacent federal waters area: Geological Survey of Alabama Bull. 140, 58 p.

Mitchell-Tapping, H.J., 1981, Petrophysical properties of the Sligo Formation of northern Louisiana and Arkansas: GCAGS. Trans., v. 31, p 155-166.

Montgomery, S.L., Petty, A.J., and Post, P.J., 2002, James Limestone, northeastern Gulf of Mexico: Refound opportunity in a Lower Cretaceous trend: AAPG Bulletin, v. 86, p. 381-398.

Moore, C.H., and Druckman, Y., 1981, Burial diagenesis and porosity evaluation, upper Jurassic Smackover, Arkansas and Louisiana: AAPG Bulletin, v. 65, p. 597-628.

Moore, T., 1983, Cotton Valley depositional systems of Mississippi: GCAGS Trans., v. 33, p. 163-167.

Morrow, E.H., 1958, Topy Creek Field, Bienville Parish, Louisiana: Shreveport Geological Society Reference Report of Certain Oil and Gas Fields, v. IV, p. 117-119.

Murray, G.E., 1948, Geology of Red River and Desoto Parishes, Louisiana Geological Survey, Geological Bulletin No. 25, 312 p.

Murray, G.E., 1955, Midway Stage, Sabine Stage, and Wilcox Group: AAPG Bulletin, v. 39, p. 671-696.

Murray, G.E., 1961, Geology of the Atlantic and Gulf coastal province of North America: New York, Harper and Bros., 692 p.

Nelson, N.E., 1963, Colgrade Field Winn Parish, Louisiana: GCAGS Trans., v. 13, p. 3-7.

Nichols, J.L., 1958, Sligo stratigraphy of North Louisiana, Arkansas and east Texas: Shreveport Geological Society Reference Report on Certain Oil and Gas Fields, v. IV, p. 124.

Nunn, J.A., 1984, Subsidence histories for the Jurassic sediments of the northern Gulf Coast: thermal-mechanical model: Third Annual Research Conf., Gulf Coast Section, SEPM Foundation, p. 309-322.

Nunn, J.A., and R. Sassen, 1986, The framework of hydrocarbon generation and migration, Gulf of Mexico continental slope: GCAGS Trans., v. 36, p. 257-262.

Nunn, J.A., Scardina, A.D., and Pilger, R.H., Jr., 1984, Thermal evolution of the north-central Gulf Coast: Tectonics, v. 7, p. 723-740.

Oehler, J.H., 1984, Carbonate source rocks in the Jurassic Smackover trend of Mississippi, Alabama, and Florida, *in* J.G. Palacas, ed., Petroleum Geochemistry and

Source Rock Potential of Carbonate Rocks, AAPG Studies in Geology, v. 18, p. 63-69.

Ogier, S.H., 1963, Stratigraphy of the Upper Cretaceous Tokio Formation, Caddo Parish, Louisiana: Shreveport Geological Society: Report on Selected North Louisiana and South Arkansas Oil and Gas Fields, v. V, p. 97-107.

Palacas, J.G., 1978, Preliminary assessment of organic carbon content and petroleum source rock potential of Cretaceous and Lower Tertiary carbonates, South Florida Basin: GCAGS Trans., v. 28, p. 357-381.

Palacas, J.G., D.E. Anders, and J.D. King, 1984, South Florida Basin—A prime example of carbonate source rocks for petroleum, *in* J.G. Palacas, ed., Petroleum Geochemistry and Source Rock Potential of Carbonate Rocks: AAPG Studies in Geology, v. 18, p. 71-96.

Parker, T.J., and McDowell, A.N., 1955, Model studies of salt-dome tectonics: AAPG Bulletin, no. 12, v. 39, p. 2384-2470.

Petty, A.J., 1995, Ferry Lake, Rodessa, and Punta Gorda Anhydrite bed correlation, Lower Cretaceous, offshore eastern Gulf of Mexico: GCAGS Trans., v. 45, p. 487-493.

Pilger, R.H., Jr., 1981, The opening of the Gulf of Mexico: implications for the tectonic evolution of the northern Gulf Coast: GCAGS Trans., v. 31, p. 377-381.

Pindell, J.L., 1985, Alleghenian reconstruction and subsequent evolution of the Gulf of Mexico, Bahamas, and Proto-Caribbean: Tectonics, v. 4, p. 1-39.

Pittman, J.G., 1983, Paleoenvironments of Lower Cretaceous DeQueen Formation of southwestern Arkansas: AAPG Bulletin, v. 67, p. 535.

Pitman, J.C., 1985, Correlation of beds within the Ferry Lake Anhydrite of the Gulf Coastal Plain: GCAGS Trans., v. 35, p. 251-260.

Rainwater, E.H., 1964, Transgressions and regressions in the Gulf Coast Tertiary: GCAGS Trans., v. 14, p. 217-230.

Ridgley, J.L., J.D. King, and M.L. Pawlewicz, 2006, Geochemistry of natural gas and condensates and source rock potential of the Jurassic Bossier Formation and adjacent formations, East Texas Salt Basin, *in* The Gulf Coast Mesozoic Sandstone Gas Province Symposium Volume: East Texas Geological Society Symposium, Tyler, Texas, p. 5-1 to 5-37.

Roberts, J.L., and Lock, B.E., 1988, The Rodessa Formation in Bossier Parish Louisiana: lithofacies analysis of a hydrocarbon productive shallow water clastic-carbonate sequence: GCAGS Trans., v. 38, p. 103-111.

Rogers, R.L., 1958, Killens Ferry Field, Franklin and Tensas Parishes, Louisiana: Shreveport Geological Society Reference Report of Certain Oil and Gas Fields, v. IV, p. 137-140.

Rogers, R.L., 1987, Palynological age determination for Dorcheat and Hosston Formations—Jurassic-Cretaceous Boundary in northern Louisiana: AAPG Bulletin, v. 71, p. 1121.

Salvador, A., 1987, Late Triassic-Jurassic paleography and origin of Gulf of Mexico basin: AAPG Bulletin, v. 71, p. 419-451

Salvador, A., 1991a, The Gulf of Mexico Basin: decade of North American geology, v. DNAG, v. J: Boulder, Colorado, GSA, 568 p.

Salvador, A., 1991b, Triassic-Jurassic, *in* A. Salvador, ed., The Gulf of Mexico Basin, Boulder, Colorado, GSA, p. 131-180.

Sassen, R., Tye, R.S., Chinn, E.W., and Lemoine, R.C., 1988, Origin of crude oil in the Wilcox trend of Louisiana and Mississippi: evidence of long-range migration: AAPG Bulletin, v. 72, p. 1122-1123.

Sassen, R., 1990, Lower Tertiary and Upper Cretaceous source rocks in Louisiana and Mississippi: implications to Gulf of Mexico crude oil: AAPG Bulletin, v. 74, p. 857-878.

Sassen, R., and C.H. Moore, 1988, Framework of hydrocarbon generation and destruction in eastern Smackover trend: AAPG Bulletin, v. 72, p. 649-663.

Sassen, R., C.H. Moore, and F.C. Meendsen, 1987, Distribution of hydrocarbon source potential in the Jurassic Smackover Formation: Organic Geochemistry, v. 11, p. 379-383.

Saucier, A.E., Finley, R.J., and Dutton, S.P., 1985, The Travis Peak (Hosston) Formation of east Texas and north Louisiana: SPE/DOE Paper #13850, Conference on Low Permeability Gas Reservoirs, Denver, Colorado. p. 15.

Sawyer, D.S., Buffler, R.T., and Pilger, Jr., R.H., 1991, The crust under the Gulf of Mexico, *in* A. Salvadore, ed., The Gulf of Mexico Basin: decade of North American Geology, Boulder, GSA, p. 53-72.

Scardina, A.D., 1982, Tectonic subsidence history of the North Louisiana Salt Basin: *in* LSU Publications in Geology and Geophysics, Gulf Coast Studies, v. 2, 34 p., Louisiana State University, Baton Rouge, LA.

Scott, K.R., Hayes, W.E., and Fietz, R.P., 1961, Geology of the Eagle Mills Formation: GCAGS Trans., v. 11, p. 1-14.

Senftle, J.T., and C.R. Landis, 1991, Vitrinite reflectance as a tool to assess thermal maturity, *in* R.K. Merrill, ed., Source and migration processes and evaluation techniques: AAPG Treatise of Petroleum Geology, p. 119-126.

Shearer, H.K., 1938, Developments in south Arkansas and north Louisiana in 1937: AAPG Bulletin, v. 22, p. 719-727.

Sloane, B.J., Jr., 1958, The subsurface Jurassic Bodcaw Sand in Louisiana: Louisiana Geological Survey Bulletin, 33 p.

Spofford, H.N., 1945, Holly Field, De Soto Parish, Louisiana: AAPG Bulletin, v. 29, p. 96-100.

Stroud, B.K., and Shayes, F.P., 1923, The Monroe Gas Field, Louisiana: AAPG Bulletin, v. 7, p. 565-574.

Swain, F.M., 1944, Stratigraphy of Cotton Valley beds of northern Gulf Coastal Plain: AAPG Bulletin, v. 28, p. 577-614.

Swain F.M., and Anderson, E.G., 1993, Stratigraphy and Ostracoda of the Cotton Valley Group, north central Louisiana: Louisiana Geological Survey, Geological Bulletin No. 45, 239 p.

Tew, B.H., Mink, R.M., Mann, S.D., Bearden, B.L., and Mancini, E.A., 1991, Geologic framework of Norphlet and pre-Norphlet strata of the onshore and offshore eastern Gulf of Mexico area: GCAGS Trans., v. 41, p. 590-600.

Thomas, W.A., and Mann, C.J., 1966, Late Jurassic depositional environments, Louisiana and Arkansas: AAPG Bulletin, v. 50, p. 178-182.

Tolson, J.S., C.W. Copeland, and B.L. Bearden, 1983, Stratigraphic profiles of Jurassic strata in the western part of the Alabama Coastal Plain: Geological Survey of Alabama Bulletin 122, 425 p.

Tye, R.S., Moslow, T.F., Kimbrell, W.C., and Wheeler, C.W., 1991, Lithostratigraphy and production characteristics of the Wilcox Group (Paleocene-Eocene) in central Louisiana: AAPG Bulletin, v. 75, v. 11, p. 1675-1713.

Tye, R.S., Wheeler, C.W., Kimbrell, W.C., and Moslow, T.F., 1988, Lithostratigraphic framework and production history of Wilcox in central Louisiana: AAPG Bulletin, v. 72, p. 255.

Van Siclen, D.C., 1984, Early opening of initially-closed Gulf of Mexico and central North Atlantic Ocean: GCAGS Trans., v. 34, p. 265-275.

Wade, W.J., R. Sassen, and E. Chinn, 1987, Stratigraphy and source potential of the Smackover Formation of the northern Manila embayment, southwest Alabama: GCAGS Trans., v. 37, p. 277-285.

Weeks, W.B., 1938, South Arkansas stratigraphy with emphasis on the older coastal plain beds: AAPG Bulletin, v. 22, p. 953-983.

Whitfield, M., 1963, A subsurface study of the Pine Island Formation of north central Louisiana: Shreveport Geological Society; Report on Selected North Louisiana and South Arkansas Oil and Gas Fields, v. V, p. 19-49.

Wilson, G.V., 1975, Early differential subsidence and configuration of the northern Gulf Coast basin in Southwest Alabama and Northwest Florida: GCAGS Trans., v. 25, p. 196-206.

Winker, C.D., and Buffler, R.T., 1988, Paleogeographic evolution of early deep-water Gulf of Mexico and margins, Jurassic to Middle Cretaceous (Comanchaean): AAPG Bulletin, v. 72, p. 318-346.

Wood, M.L., and Walper, J.L., 1974, The evolution of the interior Mesozoic basin and the Gulf of Mexico: GCAGS Trans., v. 24, p. 31-41.

Woods, D.J., 1963, Fractured chalk oil reservoirs, Sabine Parish, Louisiana: GCAGS Trans., v. 13, p. 127-138.

Yurewicz, D.A., Marler, T.B., Meyerholtz, K.A., and Siroky, F.X., 1993, Early Cretaceous carbonate platform, north rim of the Gulf of Mexico, Mississippi and Louisiana, *in* J. A. Toni Simo, R. W. Scott, and J. P. Masse, eds., Cretaceous carbonate platforms: AAPG Memoir 56, p. 81-96.

Zimmerman, R.K., 1992, Fractured Smackover Limestone in northeast Louisiana, implication for hydrocarbon exploitation: GCAGS Trans., v. 42, p. 401-412.

Zimmerman, R.K., 1995, Evidence and effects of wrench faulting, north central Gulf Coast region: GCAGS Trans., v. 45, p. 629-635.

Zimmerman, R.K., and R. Sassen, 1993, Hydrocarbon transfer pathways from Smackover source rocks to younger reservoir traps in the Monroe Gas Field, northeast Louisiana: Gulf Coast Association of Geological Societies Transactions, v. 43, p. 473-480.

Zimmerman, R.K., 1998, Chronology of oil generation in Louisiana's fractured Austin Chalk deep horizontal drilling trend: GCAGS Trans., v. 48, p. 517-525.

Zimmerman, R.K., 1999a, A potential Louisiana Haynesville-Cotton Valley pinnacle reef trend predicted from palinspastic reconstructions (abs.): AAPG Annual Convention Proceedings, San Antonio, Texas, p. A-160.

Zimmerman, R.K., 1999b, Potential oil generation capacity of the north Louisiana hydrocarbon system: GCAGS Trans., v. 49, p. 532-540.

Zimmerman, R.K., 2000, Predicting a north Louisiana Jurassic pinnacle reef trend from palinspastic reconstruction: Louisiana State University Basin Research Institute Bulletin, v. 9, p. 1-17.

Zimmerman, R.K., and Goddard, D. A., 2001, A north Louisiana gas-prone Hosston slope-basin sand trend: GCAGS Trans., v. 51, p. 423-432.

Zimmerman, R.K., and Sassen, R.A., 1993, Hydrocarbon migration pathways from Smackover source rocks to younger reservoir traps in the Monroe Gas Field, northeast Louisiana: GCAGS Trans., v. 43, p. 473-480.